Wolfgang Wagner
Hans-Joachim Kretzschmar

International Steam Tables

Properties of Water and Steam Based on the Industrial Formulation IAPWS-IF97

Tables, Algorithms, Diagrams, and CD-ROM Electronic Steam Tables

All of the equations of IAPWS-IF97 including a complete set of supplementary backward equations for fast calculations of heat cycles, boilers, and steam turbines

Second Edition

Springer

International Steam Tables

Second edition

Wolfgang Wagner · Hans-Joachim Kretzschmar

International Steam Tables

Properties of Water and Steam
Based on the Industrial Formulation IAPWS-IF97

Tables, Algorithms, Diagrams, and CD-ROM Electronic Steam Tables

All of the equations of IAPWS-IF97 including a complete set of supplementary backward equations for fast calculations of heat cycles, boilers, and steam turbines

Second edition

Springer

Dr. Wolfgang Wagner, Professor Emeritus
Ruhr-University Bochum
Faculty of Mechanical Engineering
Chair of Thermodynamics
Universitaetsstr. 150
44780 Bochum
Germany
Wagner@thermo.rub.de

Dr. Hans-Joachim Kretzschmar, Professor
Zittau/Goerlitz University of Applied Sciences
Faculty of Mechanical Engineering
Department of Technical Thermodynamics
Theodor-Koerner-Allee 16
02763 Zittau
Germany
hj.kretzschmar@hs-zigr.de

Originally published as a German-English edition

ISBN 978-3-540-21419-9 e-ISBN 978-3-540-74234-0

DOI 10.1007/978-3-540-74234-0

Library of Congress Control Number: 2007940182

Cover Design: WMXDesign GmbH, Heidelberg

Printed on acid-free paper

9 8 7 6 5 4 3 2 1

springer.com

Preface to the Second Edition

The international research regarding the thermophysical properties of water and steam has been coordinated by the International Association for the Properties of Water and Steam (IAPWS). IAPWS is responsible for the international standards for thermophysical properties. These standards and recommendations are given in the form of releases, guidelines, and advisory notes. One of the most important standards in this sense is the formulation for the thermodynamic properties of water and steam for industrial use.

In 1997, IAPWS adopted the “IAPWS Industrial Formulation 1997 for the Thermodynamic Properties of Water and Steam” for industrial use, called IAPWS-IF97 for short. The formulation IAPWS-IF97 replaced the previous industrial formulation IFC-67 published in 1967.

After the adoption of IAPWS-IF97 in 1997, further so-called backward equations were developed. These studies were coordinated by the IAPWS Task Group on Supplementary Backward Equations for IAPWS-IF97 chaired by one of the authors of this book (H.-J. K.). The final form of these equations is based on contributions by

J. R. Cooper	K. Knobloch	I. Stöcker
A. Dittmann	H.-J. Kretzschmar	R. Span
D. G. Friend	R. Mareš	W. Wagner
J. S. Gallagher	K. Miyagawa	I. Weber
A. H. Harvey	N. Okita	

In addition to these scientists, many other IAPWS colleagues, particularly the members of the working group “Industrial Calculations” (chairman up to 2001: B. Rukes, chairman from 2001 to 2003: K. Miyagawa, and chairman from 2004 onwards: Bill Parry) from 2002 onwards renamed in “Industrial Requirements and Solutions”, and the working group “Thermophysical Properties of Water and Steam” (chairman up to 2000: J. R. Cooper, chairman from 2000 to 2005: D. G. Friend, and chairman from 2005 onwards: H.-J. Kretzschmar), have contributed to the entire success of this IAPWS project; we appreciate their contribution very much. We are particularly grateful to the chairman of the evaluation task group, K. Miyagawa, for his exceptional efforts in testing these backward equations to ensure that they fulfill all requirements and checking the drafts of the several supplementary releases.

In 1998, Springer-Verlag published the book “Properties of Water and Steam” authored by W. Wagner and A. Kruse. This book described the industrial formulation IAPWS-IF97 as it was adopted by IAPWS in 1997. This new book is considered to be the second edition of the book published in 1998, although it has a different title and authorship and is only in English and no longer bilingual English/German. This second edition describes the industrial formulation in its current form, thus including all of the new so-called backward equations adopted by IAPWS between 2001 and 2005.

In addition to IAPWS-IF97, the industrial standard for the *thermodynamic* properties of water

and steam, the most recent equations for the *transport* properties dynamic viscosity and thermal conductivity are also presented. Moreover, equations for the surface tension, dielectric constant, and refractive index are given.

In contrast to the first edition, this second edition contains a number of extensions and new parts, namely:

- Incorporation of all "supplementary" backward equations.
- Inclusion of the uncertainty of the specific enthalpy into the uncertainty values of IAPWS-IF97 for the most important properties.
- Formulas to calculate all partial derivates of the eight most important thermodynamic properties.
- Additional properties in the steam tables.
- Incorporation of the new basic equation for the high-temperature region (1073.15 K to 2273.15 K) with pressures up to 50 MPa (previously up to 10 MPa).
- Pressure-temperature diagrams with isolines of all properties contained in the steam tables and further properties.
- A compact disc (CD) providing the interactive program "IAPWS-IF97 Electronic Steam Tables" for the calculation of all properties (contained in the book) dependent on freely selectable pressures and temperatures in the single-phase region and on pressure or temperature along the saturated-vapour and saturated-liquid lines. Those properties for which it is reasonable can also be calculated within the two-phase region for given values of pressure or temperature and vapour fraction.

We are very grateful to Dr. K. Knobloch who developed the supplementary backward equations in her dissertation. We would like to thank Mr. M. Kunick for calculating and formatting the tables as Microsoft Excel sheets for Part B. We are very grateful to Dr. I. Stöcker, Dr. K. Knobloch, Ms. M. Weidner, and Mr. S. Buchholz for their help in producing all of the pressure-temperature diagrams in Part C of the book. Our warmest thanks are dedicated to Dr. U. Overhoff for his assistance in preparing the "IAPWS-IF97 Electronic Steam Tables" on the CD in Part D and for several checkups, and to Dr. I. Stöcker for her help in producing the large size Mollier *h*-*s* and *T*-*s* diagrams, which are included as attachments to the book. We thank Mr. R. Preusche, Mr. M. Markward, and Mr. B. Salomo for reprogramming all of the equations presented in the book. We would also like to thank Mrs. B. Esch for typing the text of the manuscript and Mrs. R. Gölzenleuchter for producing all of the figures. Our thanks go to Dr. O. Kunz for his help in creating the electronic printing version of Part A of the manuscript. Finally, we are grateful to Dr. E. W. Lemmon and Mrs. R. Smith for carefully reading the manuscript and for a number of suggestions on improving the English style.

One of us (H.-J. Kretzschmar) is particularly grateful to the Saxon State Ministry for Science and Art for the financial support of the development of the supplementary backward equations at the Zittau/Görlitz University of Applied Sciences from 2001 to 2003.

Bochum and Zittau, November 2007

W. Wagner
H.-J. Kretzschmar

Preface to the First Edition

In 1997, the International Association for the Properties of Water and Steam (IAPWS) adopted a new formulation for the thermodynamic properties of water and steam for industrial use. This formulation is called "IAPWS Industrial Formulation 1997 for the Thermodynamic Properties of Water and Steam" and "IAPWS Industrial Formulation 1997" or "IAPWS-IF97" for short. The new formulation IAPWS-IF97 replaces the previous industrial formulation, IFC-67, that has formed the basis for power-plant calculations and other industrial applications since the late 1960's. IAPWS-IF97 improves significantly both the accuracy and the speed of the calculation of thermodynamic properties. The differences from IFC-67 will require many users, particularly boiler and turbine manufacturers but also power-station companies and corresponding engineering offices, to modify design and application codes. In addition to these applications, IAPWS-IF97 is also of importance for energy-engineering applications in chemical industry and in other branches of industry. Therefore, this book presents the individual equations of IAPWS-IF97 for calculating the thermodynamic properties of water and steam for industrial use.

The IAPWS Industrial Formulation 1997 was developed in an international research project. This development was coordinated by the IAPWS Task Group "New Industrial Formulation" chaired by one of the authors of this book (W. W.). The final form of IAPWS-IF97 is based on contributions and equations by

J. R. Cooper	R. Mareš	Y. Takaishi
A. Dittmann	K. Oguchi	I. Tanishita
J. Kijima	H. Sato	J. Trübenbach
H.-J. Kretzschmar	I. Stöcker	W. Wagner
A. Kruse	O. Šifner	Th. Willkommen.

Besides these "developers" many other IAPWS colleagues, particularly the members of the two working groups "Industrial Calculations" and "Thermophysical Properties of Water and Steam", contributed to the entire success of this comprehensive project; we appreciate their contribution very much. We are especially grateful to the chairmen of these two working groups, B. Rukes and J. R. Cooper. In addition, we would like to thank the members of the IAPWS Task Group "New Industrial Formulation - Evaluation" for testing IAPWS-IF97 regarding the fulfilment of requirements and checking the influence on real power-cycle calculations; concerning these important pieces of work we are particularly grateful to the chairman of this task group, K. Miyagawa, and his colleagues R. Spencer, R. B. McClintock, and H. W. Bradly for their exceptional efforts.

In addition to IAPWS-IF97, the industrial standard for the thermodynamic properties of water and steam, the most recent equations for the transport properties dynamic viscosity and thermal conductivity are also presented. Moreover, equations for the surface tension, static dielectric constant, and refractive index are given.

The text of this book is bilingual. Part A contains the description of the above mentioned equations for the thermophysical properties in English and Part B the corresponding description in German. Comprehensive tables of the most important thermophysical properties of water and steam are given in Part C in both languages.

The values in the tables of Part C were exclusively calculated from the corresponding equations summarized in Part A and Part B, respectively. These tables, which are mainly based on the new industrial formulation IAPWS-IF97, replace the tables “Properties of Water and Steam in SI-Units” prepared by E. Schmidt and edited by U. Grigull (Springer-Verlag Berlin Heidelberg New York, R. Oldenbourg München, Fourth, Enlarged Printing, 1989) which are based on the previous industrial formulation IFC-67.

We wish to express our warmest thanks to Mr. C. Bonsen for his help in handling the computer programs for calculating the transport properties and for producing all the tables. We would also like to thank Mrs. A.-M. Sieg for typing the text of the manuscript. We are particularly grateful to the Deutsche Forschungsgemeinschaft for their financial support of that part of the development of IAPWS-IF97 which was carried out at the Ruhr-University Bochum.

Bochum, February 1998

W. Wagner
A. Kruse

Contents

Nomenclature

Quantities

A	Function
a	Thermal diffusivity, $a = \lambda/(\rho c_p)$
a	Coefficient
B	Function
c_p	Specific isobaric heat capacity
$c^{\mathrm{o}}_{p,\mathrm{m}}$	Mean specific isobaric heat capacity in the ideal-gas state
c_v	Specific isochoric heat capacity
CTR	Computing-Time Ratio
f	Specific Helmholtz free energy, $f = u - Ts$
f^*	Fugacity
g	Specific Gibbs free energy, $g = h - Ts$
$\bar{g}$	$\bar{g}$-factor of Harris and Alder
h	Specific enthalpy
Δh_{v}	Specific enthalpy of vaporization, $\Delta h_{\mathrm{v}} = h'' - h'$
I	Exponent
i	Serial number; Exponent
J	Exponent
j	Serial number; Exponent
k	Boltzmann's constant
M	Molar mass
N_{A}	Avogadro's number
n	Refractive index
n	Coefficient
Pr	Prandtl number, $Pr = \eta\, c_p\, \lambda^{-1}$
p	Pressure
R	Specific gas constant
R_{m}	Molar gas constant
s	Specific entropy
Δs_{v}	Specific entropy of vaporization, $\Delta s_{\mathrm{v}} = s'' - s'$
T	Thermodynamic temperature[1]
t	Celsius temperature, $t/°\mathrm{C} = T/\mathrm{K} - 273.15$
u	Specific internal energy
v	Specific volume
w	Speed of sound

[1] All temperature values given in this book are temperatures according to the International Temperature Scale of 1990 (ITS-90)

x Vapour fraction
x Arbitrary state variable
y Arbitrary state variable
z Compression factor, $z = pv/(RT)$
z Arbitrary state variable
α Mean molecular polarizability of the isolated water molecule
α_p Relative pressure coefficient, $\alpha_p = p^{-1}(\partial p/\partial T)_v$
α_v Isobaric cubic expansion coefficient, $\alpha_v = v^{-1}(\partial v/\partial T)_p$
β Transformed pressure, Eq. (2.12a)
β_p Isothermal stress coefficient, $\beta_p = -p^{-1}(\partial p/\partial v)_T$
γ Dimensionless Gibbs free energy, $\gamma = g/(RT)$
Δ Difference in any quantity
δ Reduced density, $\delta = \rho/\rho^*$
δ_T Isothermal throttling coefficient, $\delta_T = (\partial h/\partial p)_T$
ε Dielectric constant
(relative static dielectric constant or relative static permittivity)
ε_0 Permittivity of vacuum (electric constant)
η Dynamic viscosity
η Reduced enthalpy, $\eta = h/h^*$
θ Reduced temperature, $\theta = T/T^*$
ϑ Transformed temperature, Eq. (2.12b)
κ Isentropic exponent, $\kappa = -vp^{-1}(\partial p/\partial v)_s$
κ_T Isothermal compressibility, $\kappa_T = -v^{-1}(\partial v/\partial p)_T$
λ Thermal conductivity
Λ Reduced thermal conductivity, $\Lambda = \lambda/\lambda^*$
$\bar{\lambda}$ Wavelength of light
$\bar{\Lambda}$ Reduced wavelength of light, $\bar{\Lambda} = \bar{\lambda}/\bar{\lambda}^*$
μ Joule-Thomson coefficient, $\mu = (\partial T/\partial p)_h$
μ Dipole moment of the isolated water molecule
ν Kinematic viscosity, $\nu = \eta\rho^{-1}$
π Reduced pressure, $\pi = p/p^*$
ρ Mass density
σ Surface tension
σ Reduced entropy, $\sigma = s/s^*$
τ Inverse reduced temperature, $\tau = T^*/T$
ϕ Dimensionless Helmholtz free energy, $\phi = f/(RT)$
Ψ Reduced dynamic viscosity, $\Psi = \eta/\eta^*$
ω Reduced volume, $\omega = v/v^*$

Superscripts

o Ideal-gas part; ideal gas
r Residual part
max Maximum value of a quantity
min Minimum value of a quantity

*	Reducing quantity
′	Saturated-liquid state
″	Saturated-vapour state

Subscripts

ad	Adiabat
b	Normal boiling point
c	Critical point
h	At constant specific enthalpy
ind	Industrial equation for λ
m	State on the melting line
m	Mean value
max	Maximum value of a quantity
p	At constant pressure
perm	Permissible
RMS	Root-mean-square value of a quantity, see below
ρ	At constant density
s	Saturation state
s	At constant specific entropy
sci	Scientific equation for λ
sub	State on the sublimation line
t	Triple point
T	At constant temperature
v	At constant specific volume

Root-mean-square value:

$$(\Delta x)_{\mathrm{RMS}} = \sqrt{\frac{1}{N}\sum_{n=1}^{N}(\Delta x_n)^2} \,,$$

where Δx_n can be either absolute or percentage differences of the corresponding property x; N is the number of Δx_n values (depending on the property, between 10 million and 100 million points are uniformly distributed over the respective range of validity)

Introduction

This book consists of five parts, Part A to Part E.

Part A presents the current internationally agreed upon equations for industrial calculations of the most relevant thermophysical properties of water and steam.

The current industrial standard for the *thermodynamic* properties, which replaced the former industrial standard IFC-67 [1], was adopted by the International Association for the Properties of Water and Steam (IAPWS) in 1997 under the name "IAPWS Industrial Formulation 1997 for the Thermodynamic Properties of Water and Steam" or simply IAPWS-IF97 for short. All relevant numerical details about the entire set of equations of IAPWS-IF97 are given in Chap. 2.

As a comprehensive supplement of the first edition of this book, this second edition contains all of the so-called backward equations of IAPWS-IF97 developed after 1997 and adopted by IAPWS between 2001 and 2005. In addition to the uncertainty values given in IAPWS-IF97 for the properties specific volume, specific isobaric heat capacity, speed of sound, and saturation pressure, now uncertainty values for the specific enthalpy and differences in specific enthalpy are given as well. Moreover, formulas are presented in this new work to calculate all partial derivatives from the equations of IAPWS-IF97 formed by any three combinations of the properties pressure, temperature, and the specific properties volume, enthalpy, internal energy, entropy, Gibbs free energy, and Helmholtz free energy. For the high-temperature region (1073.15 K to 2273.15 K), the new basic equation that covers this temperature range for pressures up to 50 MPa (previously 10 MPa) is presented.

In addition to the equations for the thermodynamic properties of water and steam, Chap. 3 of Part A summarizes current equations for industrial use for the *transport* properties dynamic viscosity and thermal conductivity and also presents correlation equations for the surface tension, dielectric constant, and refractive index.

Part B contains the tables of the most important properties of water and steam, which were calculated from the corresponding equations of Chaps. 2 and 3 in Part A. In comparison with the first edition, additional tables with values of the properties compression factor, isochoric heat capacity, isobaric expansion coefficient, and isothermal compressibility are given. The table for the ideal-gas state was extended by including the properties isochoric heat capacity, isentropic exponent, and mean isobaric heat capacity between 0 °C and the given temperature t.

Part C of this book presents pressure-temperature diagrams with isolines of all the properties tabulated in Part B and of further properties such as the specific internal energy, Joule-Thomson coefficient, and a number of partial derivatives.

Part D contains a CD providing the interactive program "IAPWS-IF97 Electronic Steam Tables" to calculate all of the properties contained in the book dependent on pressure and temperature. In this way, users can calculate "personal" steam tables for arbitrary values of pressure and temperature, as well as properties in the two-phase region as a function of pressure or temperature together with vapour-fraction. With the addition of this possibility, the size of the printed steam tables (Part B) was reduced in comparison with the first edition of this book.

Part E contains the two wall charts, a Molier h-s diagram and a T-s diagram.

Part A

Equations for the Calculation of the Thermophysical Properties of Water and Steam

1 Reference Constants

This chapter summarizes all reference constants needed for evaluating the equations given in Chaps. 2 and 3.

The specific gas constant of ordinary water,

$$R = 0.461\,526 \text{ kJ kg}^{-1}\text{ K}^{-1}, \tag{1.1}$$

results from the recommended value of the molar gas constant [2],

$$R_\mathrm{m} = 8.314\,51 \text{ kJ kmol}^{-1}\text{ K}^{-1}, \tag{1.2}$$

and from the molar mass of ordinary water,

$$M = 18.015\,257 \text{ kg kmol}^{-1} . \tag{1.3}$$

The value of the molar mass of ordinary water results from the molar mass of hydrogen, $M_\mathrm{H} = 1.007\,975\,97 \text{ g mol}^{-1}$ (based on the molar mass of the isotopes ^{1}H and ^{2}H given in [3] and the isotopic concentration corresponding to the molar fraction of ^{1}H equal to 0.999 85 and of ^{2}H equal to 0.000 15 [4]), and the molar mass of oxygen, $M_\mathrm{O} = 15.999\,304\,7 \text{ g mol}^{-1}$ (based on the molar mass of the isotopes ^{16}O, ^{17}O, and ^{18}O given in [3] and the isotopic concentrations corresponding to the molar fractions of ^{16}O, ^{17}O, and ^{18}O equal to 0.997 62, 0.000 38, and 0.002, respectively, considered to be characteristic for all natural occurrences of oxygen [4]).

The values of the critical parameters

$$T_\mathrm{c} = 647.096 \text{ K}, \tag{1.4}$$

$$p_\mathrm{c} = 22.064 \text{ MPa}, \text{ and} \tag{1.5}$$

$$\rho_\mathrm{c} = 322 \text{ kg m}^{-3} \tag{1.6}$$

are from the corresponding IAPWS release [5]. The triple-point temperature is

$$T_\mathrm{t} = 273.16 \text{ K} \tag{1.7}$$

according to the International Temperature Scale of 1990 (ITS-90) [6] and the triple-point pressure

$$p_\mathrm{t} = 611.657 \text{ Pa} \tag{1.8}$$

was determined by Guildner et al. [7]. According to the scientific standard for the thermodynamic properties of ordinary water, the IAPWS-95 formulation [8, 9], the temperature of the normal boiling point (at a pressure of 0.101 325 MPa (1 atm)) amounts to

$$T_\mathrm{b} = 373.124\,3 \text{ K} . \tag{1.9}$$

2 IAPWS Industrial Formulation 1997 for the Thermodynamic Properties of Water and Steam

At the IAPWS meeting in Erlangen, Germany in 1997, the "IAPWS Industrial Formulation 1997 for the Thermodynamic Properties of Water and Steam" was adopted as the new international industrial standard for the thermodynamic properties of water and steam. This new industrial standard is also called "IAPWS Industrial Formulation 1997" or "IAPWS-IF97" for short. The IAPWS-IF97 formulation replaced the previous industrial standard IFC-67 [1]. In comparison with IFC-67, IAPWS-IF97 significantly improves both the accuracy and the calculation speed of thermodynamic properties.

This chapter presents all of the information about the individual equations of IAPWS-IF97 necessary for calculating the thermodynamic properties of water and steam. It also includes the supplementary backward equations developed after 1997 and adopted by IAPWS between 2001 and 2005, and also a new basic equation for the high-temperature region 1073.15 K to 2273.15 K for pressures up to 50 MPa (previously 10 MPa). In contrast to the first edition of this book, the backward equations are not presented region by region, but all backward equations dependent on the same input variables are summarized in the same section. Section 2.4 presents formulas to calculate all of the partial derivatives $(\partial z/\partial x)_y$ from the equations of IAPWS-IF97, where the variables x, y, and z can represent any of the thermodynamic properties: pressure p, temperature T, and the specific properties volume v, enthalpy h, internal energy u, entropy s, Gibbs free energy g, or Helmholtz free energy f. In addition to the uncertainties of the equations of IAPWS-IF97 in the properties specific volume, specific isobaric heat capacity, speed of sound, and saturation pressure, Sec. 2.5 also contains uncertainty statements on the specific enthalpy and differences in specific enthalpy. Moreover, illustrations show the achieved consistency between the basic equations along the region boundaries.

Information about the development of the IAPWS-IF97 equations and details about their quality and calculation speed in comparison with the previous industrial standard IFC-67 are given in the international publication on IAPWS-IF97 [10]. Details about the development of the supplementary backward equations can be found in the articles [11-14].

2.1 Characteristic Features of IAPWS-IF97

This section gives general information about the structure of the industrial formulation IAPWS-IF97, including the entire range of validity, and makes some general statements about the quality of IAPWS-IF97 concerning accuracy and consistency along the region boundaries. In addition, statements on the calculation speed are made not only when the basic equations are used for calculations of properties that are not dependent on pressure and temperature, but also when the supplementary backward equations are used.

2.1.1 Structure of IAPWS-IF97

The IAPWS Industrial Formulation 1997 consists of a set of equations for different regions which cover the following range of validity:

$$273.15\ \mathrm{K}^2 \le T \le 1073.15\ \mathrm{K} \qquad 0 < p \le 100\ \mathrm{MPa}\ [15, 16]$$
$$1073.15\ \mathrm{K} < T \le 2273.15\ \mathrm{K} \qquad 0 < p \le 50\ \mathrm{MPa}\ [16]^3$$

Figure 2.1 shows the five regions which divide the entire range of validity of IAPWS-IF97; for the exact definition of the five regions see Sec. 2.2. Regions 1 and 2 are each covered by a fundamental equation for the specific Gibbs free energy $g(p,T)$, region 3 by a fundamental equation for the specific Helmholtz free energy $f(\rho,T)$, and region 4, the two-phase region (corresponding to the saturation curve in the p-T diagram), by a saturation-pressure equation $p_s(T)$. The high-temperature region 5 is also covered by a $g(p,T)$ equation. These five equations, shown in rectangular boxes in Fig. 2.1, form the so-called *basic equations*.

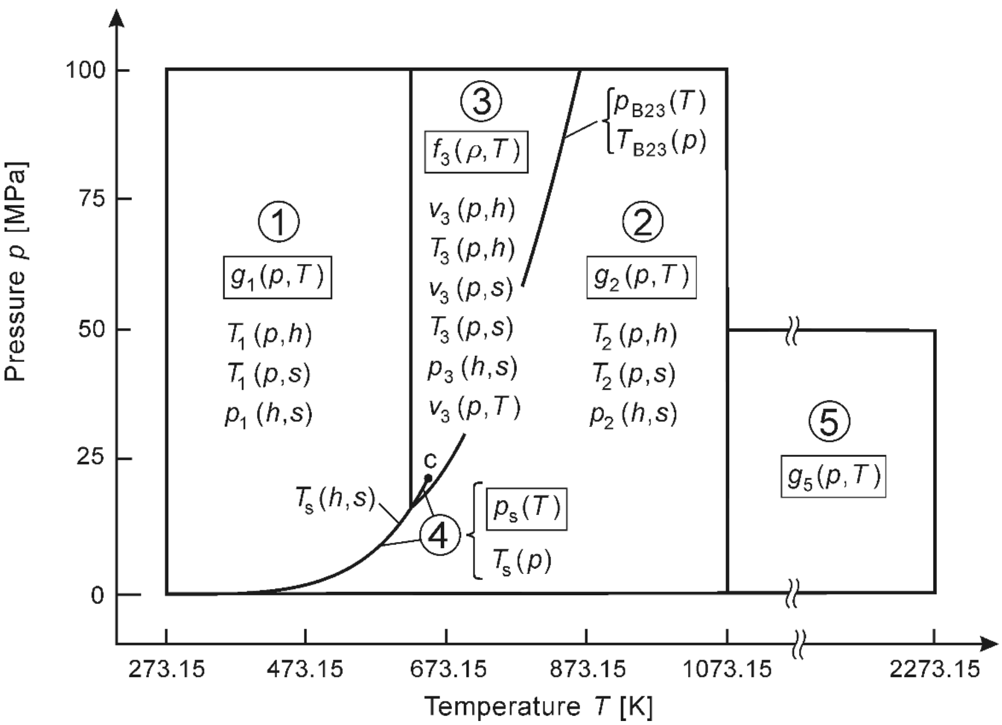

Fig. 2.1 Regions and equations of the industrial formulation IAPWS-IF97.

The industrial standard IAPWS-IF97 has been coupled to the scientific standard, the "IAPWS Formulation 1995 for the Thermodynamic Properties of Ordinary Water Substance for General

[2] In order to remain consistent with the previous industrial formulation IFC-67 [1], the range of validity of IAPWS-IF97 in temperature starts at 273.15 K (0 °C) rather than at the triple-point temperature T_t = 273.16 K (0.01 °C). Thus, when being thermodynamically exact, states in the temperature range 273.15 K ≤ T ≤ 273.16 K and at pressures $p_{sub}(T) \le p < p_m(T)$ are in the metastable region, where p_{sub} and p_m are the pressures along the sublimation and melting line [17], respectively.

[3] The revision of the release of 1997 [15] only relates to the extension of region 5 up to pressures of 50 MPa (previously 10 MPa).

and Scientific Use" [8, 9], hereafter abbreviated to IAPWS-95. This coupling was achieved by fitting the basic equations of regions 1 to 3 and 5 to values of the specific volume v, specific enthalpy h, specific isobaric heat capacity c_p, and speed of sound w calculated from IAPWS-95 [9]. Accordingly, the basic equation for region 4, the saturation-pressure equation, was fitted to the values of the saturation pressure p_s calculated from IAPWS-95.

In addition to these basic equations, so-called *backward equations* are provided for all regions except for region 5, where the backward equations are only valid for pressures $p \geq p_s(273.15\text{ K}) \approx 0.000\,611$ MPa. These backward equations were developed in the following combinations of variables: For regions 1 and 2 as equations of the form $T(p,h)$, $T(p,s)$, and $p(h,s)$, for region 3 as equations of the form $v(p,h)$, $T(p,h)$, $v(p,s)$, $T(p,s)$, $p(h,s)$, and $v(p,T)$, for the entire region 4 as a saturation-temperature equation $T_s(p)$, and for the technically most important part of region 4 ($s \geq s''(623.15\text{ K})$) as a saturation-temperature equation of the form $T_s(h,s)$. In Fig. 2.1, in addition to the (framed) basic equations, all of these types of backward equations are assigned to the corresponding region of IAPWS-IF97. The subscripts relate to the region for which the equation is valid.

These backward equations were developed in such a way that they are numerically very consistent with the corresponding basic equation. Thus, properties as functions of (p,h), (p,s), and (h,s) for regions 1 to 3, of (p) for the entire region 4, and of (h,s) for the technically most important part of region 4 can be calculated without any iteration. Due to the backward equation $v(p,T)$ for region 3, the specific volume can be calculated for this region without the necessity of its iteration from the basic equation $f_3(\rho,T)$. Consequently, properties such as $s(p,h)$ and $h(p,s)$ can be calculated directly from the corresponding backward equation or in combination with the corresponding basic equation, for example, $h(p,s)$ via the relation $h\big(p,T(p,s)\big)$. As a result of this special concept of the industrial standard IAPWS-IF97, all important combinations of properties can be calculated extremely quickly; more details are given in the next section and in Sec. 2.3.

2.1.2 Quality of IAPWS-IF97

The achieved overall quality of the industrial formulation IAPWS-IF97 is characterized by the following general results in the light of the three criteria accuracy, consistency between basic equations along region boundaries and between backward equations along subregion boundaries, and calculation speed.

The accuracy of IAPWS-IF97 is illustrated by the fact that for its entire range of validity only 0.2% of the calculated v values, 6% of the c_p values, 2% of the w values, and none of the p_s values are outside the uncertainty of the corresponding IAPWS-95 values [9]. When carrying out the same test with the previous industrial standard IFC-67, between 47% (for v) and 80% (for p_s) of the IFC-67 values were outside the uncertainty of the corresponding IAPWS-95 values. Based on all comparisons made [10] it can be concluded that IAPWS-IF97 is more than one order of magnitude more accurate than IFC-67. The estimated uncertainties of IAPWS-IF97 in the properties v, c_p, w, p_s, h, and Δh over the entire range of validity are given in Sec. 2.5. In addition to the representation of the properties for the stable homogeneous regions and at saturation, the corresponding IAPWS-IF97 equations also yield reasonable values for both the

metastable superheated-liquid region and the metastable subcooled-vapour region close to the saturated-liquid line and the saturated-vapour line, respectively.

Compared with IFC-67, an additional important jump in quality was achieved by the fact that IAPWS-IF97 clearly meets the requirements regarding the consistencies along the region boundaries, see Fig. 2.1. IAPWS-IF97 is clearly within the permitted inconsistencies according to the so-called Prague values [18]. This is also true for the "difficult" boundary between regions 2 and 3, along which the consistency requirements for the specific isobaric heat capacity are also met by the basic equations of regions 2 and 3. For IAPWS-IF97, the maximum inconsistency in c_p at this boundary amounts to 0.35% whereas the corresponding IFC-67 inconsistency was greater than 6%. Details of the achieved consistencies along the boundaries between regions 1 and 3, regions 2 and 3, and regions 2 and 5 are given in Sec. 2.5.

The third and probably the greatest advantage is the very large improvement in the calculation speed compared with IFC-67. Even when using only the backward equations that existed in 1997 when IAPWS-IF97 was adopted (the equations $T(p,h)$ and $T(p,s)$ for regions 1 and 2) for the most important regions 1, 2, and 4, where the computing time is particularly relevant, the calculation-speed factor of IAPWS-IF97 in comparison with IFC-67 amounts to 5.1. This value was determined by taking into account the frequencies of use of the most relevant property functions in these regions based on a survey of the international power-cycle companies and related industries. This means that for these important regions IAPWS-IF97 is more than 5 times faster than IFC-67 as long as the individual equations are properly programmed. Details about the accuracy, consistency along region boundaries, and calculation speed (in comparison with IFC-67) are given in the comprehensive article on IAPWS-IF97 [10]. These calculation-speed factors were determined in 1996 based on a computer running 16-bit DOS with a processor 486DX/33 MHz [10]. When repeating these comparisons with a modern Pentium 4/3.0 GHz PC and the operating system Windows XP, then IAPWS-IF97 is not only 5.1 times faster than IFC-67 but 8.3 times [19].

A comparison of the calculation speed within IAPWS-IF97 with and without using the backward equations shows that these equations bring an enormous increase in the calculation speed. When using the backward equations $T(p,s)$ and $T(p,h)$ for regions 1 and 2 (these backward equations were developed along with the basic equations of IAPWS-IF97), the calculation of properties in these regions as functions of (p,s) and (p,h) is between 11 and 38 times faster than calculating these properties by iteration from the respective basic equation.

A further essential step towards even shorter computing times was made by the supplementary backward equations developed after 1997. When using these equations, the calculation of properties dependent on (h,s) in regions 1 and 2 is more than 35 times faster than iterating the basic equations. For region 3, the calculation speed is increased by a factor of more than 10 for calculating properties as functions of (p,h), (p,s), and (h,s) with the help of the respective backward equations. The calculation of properties as a function of (p,T) using the backward equations $v(p,T)$ in combination with the basic equation $f_3(\rho,T)$ is 17 times faster than determining these properties only by iteration from the basic equation. In the part of the two-phase region 4 that is important for designing steam turbines, the calculation of the saturation properties p_s, T_s, and the vapour fraction x as a function of (h,s) from backward equations is 14 times faster than the determination of these properties by iteration with the corresponding basic equations. Thus, the new backward equations allow a significant increase in the calculation speed.

2.2 Basic Equations of IAPWS-IF97

This section contains all of the details relevant for using the basic equations of IAPWS-IF97. Figure 2.2 shows the assignment of the five basic equations to the corresponding regions. The boundaries of the regions can be taken directly from Fig. 2.2 except for the boundary between regions 2 and 3; this boundary is defined by the so-called B23-equation given in Sec. 2.2.1.

The boundary $T = 623.15$ K belongs to regions 1 and 3, the boundary corresponding to the p_{B23}-line (the T_{B23}-line is exactly the same line, see Eqs. (2.1) and (2.2)) belongs to regions 2 and 3, and the boundary $T = 1073.15$ K belongs to regions 2 and 5. Thus, the properties along these boundaries could be calculated from equations $g_1(p,T)$ or $f_3(\rho,T)$ on the boundary $T =$ 623.15 K, from equations $g_2(p,T)$ or $f_3(\rho,T)$ on the boundary $p_{B23}(T)$, and from equations $g_2(p,T)$ or $g_5(p,T)$ on the boundary $T = 1073.15$ K. In this way, on these boundaries one gets (slightly) different values from the g_1 and f_3 equations, from the g_2 and f_3 equations, and from the g_2 and g_5 equations. In order to avoid such ambiguities, the boundary $T = 623.15$ K is considered to belong to region 1, and the boundaries $p_{B23}(T)$ and $T = 1073.15$ K are considered to belong to region 2. Thus, the properties along these boundaries can be calculated unambiguously from the g_1 and g_2 equations, respectively.

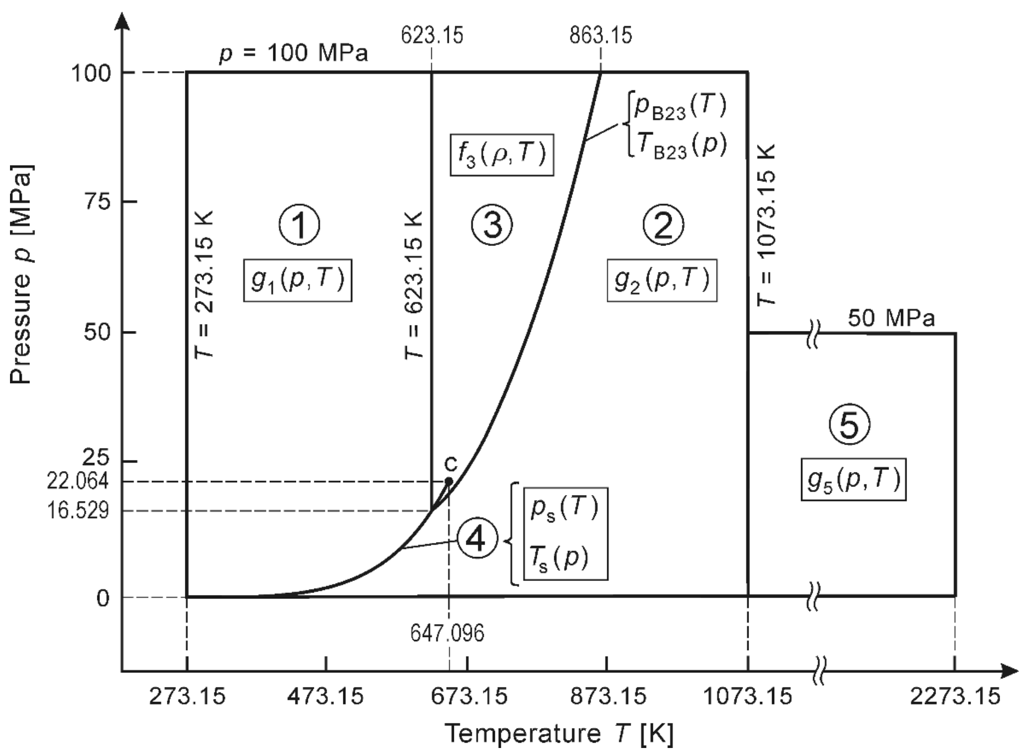

Fig. 2.2 The assignment of the basic equations to the five regions of IAPWS-IF97.

Although the saturation-temperature equation $T_s(p)$ is formally a backward equation, see Sec. 2.1.1 and [10, 15], it is nevertheless included in this section because it was derived from the same implicit quadratic equation for the saturation line, Eq. (2.12), as the saturation-pressure

equation $p_s(T)$, and is, in contrast to the "normal" backward equations given in Sec. 2.3, completely consistent with the $p_s(T)$ equation. Thus, from here onwards the saturation-temperature equation $T_s(p)$ is dealt with like a basic equation.

When using only the basic equations for the calculation of any thermodynamic property as a function of any of the most important combinations of input variables other than (p,T), e.g. (p,h), (p,s), and (h,s), due to the necessary iterations, the calculation is clearly slower than the calculation via the backward equations, but (within the iteration accuracy) consistent with all properties at the point fixed by the two input variables selected.

Uncertainty estimates of the most relevant properties, calculated from the IAPWS-IF97 basic equations, are summarized in Secs. 2.5.1 and 2.5.2. The inconsistencies between the corresponding basic equations along the boundaries between regions 1 and 3, regions 2 and 3, and regions 2 and 5 are given in Sec. 2.5.3.

Note. The user should be aware of these inconsistencies, in particular when calculating across and very near the region boundaries.

2.2.1 Auxiliary Equation for the Boundary between Regions 2 and 3

The boundary between regions 2 and 3, see Fig. 2.2, is defined by the following simple quadratic pressure-temperature relation (the B23-equation):

$$\frac{p_{B23}(T)}{p^*} = \pi(\theta) = n_1 + n_2\theta + n_3\theta^2 \quad , \tag{2.1}$$

where $\pi = p/p^*$ and $\theta = T/T^*$ with $p^* = 1$ MPa and $T^* = 1$ K. The coefficients n_1 to n_3 of Eq. (2.1) are listed in Table 2.1. Equation (2.1) roughly describes an isentropic line; the entropy values along this boundary line are between $s = 5.047$ kJ kg^{-1} K^{-1} and $s = 5.261$ kJ kg^{-1} K^{-1}.

Alternatively, Eq. (2.1) can be expressed explicitly in temperature as

$$\frac{T_{B23}(p)}{T^*} = \theta(\pi) = n_4 + \left[(\pi - n_5)/n_3\right]^{0.5} \tag{2.2}$$

with θ and π as defined for Eq. (2.1) and the coefficients n_3 to n_5 listed in Table 2.1. Equations (2.1) and (2.2) cover the range from 623.15 K at 16.5292 MPa up to 863.15 K at 100 MPa.

Table 2.1 Coefficients of the equations $p_{B23}(p)$ and $T_{B23}(T)$, Eqs. (2.1) and (2.2)

i	n_i	i	n_i
1	$0.348\,051\,856\,289\,69 \times 10^{3}$	4	$0.572\,544\,598\,627\,46 \times 10^{3}$
2	$-0.116\,718\,598\,799\,75 \times 10^{1}$	5	$0.139\,188\,397\,788\,70 \times 10^{2}$
3	$0.101\,929\,700\,393\,26 \times 10^{-2}$		

Computer-Program Verification. Eqs. (2.1) and (2.2) must meet the following T-p point:
$T = 0.623\,150\,000 \times 10^3$ K, $p = 0.165\,291\,642\,5 \times 10^2$ MPa.

2.2.2 Basic Equation for Region 1

This section contains all details relevant for using the basic equation for region 1 of IAPWS-IF97, see Fig. 2.2. Uncertainty estimates of the most relevant properties calculated from IAPWS-IF97 can be found in Sec. 2.5.

The basic equation for this region is a fundamental equation for the specific Gibbs free energy g. This equation is expressed in dimensionless form, $\gamma = g/(RT)$, and reads

$$\frac{g_1(p,T)}{RT} = \gamma(\pi,\tau) = \sum_{i=1}^{34} n_i (7.1-\pi)^{I_i} (\tau - 1.222)^{J_i} , \tag{2.3}$$

where $\pi = p/p^*$ and $\tau = T^*/T$ with $p^* = 16.53$ MPa and $T^* = 1386$ K; $R = 0.461\,526$ kJ kg^{-1} K^{-1} according to Eq. (1.1). The coefficients n_i and exponents I_i and J_i of Eq. (2.3) are listed in Table 2.2.

All thermodynamic properties can be derived from Eq. (2.3) by using the appropriate combinations of the dimensionless Gibbs free energy γ and its derivatives. The relations of the relevant thermodynamic properties to γ and its derivatives are summarized in Table 2.3. Moreover, with the information given in Sec. 2.4, particularly with the formulas of Sec. 2.4.1, all partial derivatives formed by the properties p, T, v, u, h, s, g, and f can be easily calculated. All required derivatives of the equation for the dimensionless Gibbs free energy γ, Eq. (2.3), are explicitly given in Table 2.4.

Since the 5th International Conference on the Properties of Steam in London in 1956, the specific internal energy and the specific entropy of the saturated liquid at the triple point have been set equal to zero:

$$u'_t = 0; \quad s'_t = 0. \tag{2.4}$$

In order to meet this condition at the temperature and pressure of the triple point, see Eqs. (1.7) and (1.8), the coefficients n_3 and n_4 in Eq. (2.3) have been adjusted accordingly, which results in a specific enthalpy of the saturated liquid at the triple point given by

$$h'_t = 0.000\,611\,783 \text{ kJ kg}^{-1} . \tag{2.5}$$

Table 2.2 Coefficients and exponents of the basic equation $g_1(p,T)$ in its dimensionless form, Eq. (2.3)

i	I_i	J_i	n_i	i	I_i	J_i	n_i
1	0	–2	0.146 329 712 131 67	18	2	3	−0.441 418 453 308 46 × 10^{-5}
2	0	–1	−0.845 481 871 691 14	19	2	17	−0.726 949 962 975 94 × 10^{-15}
3	0	0	−0.375 636 036 720 40 × 10^{1}	20	3	–4	−0.316 796 448 450 54 × 10^{-4}
4	0	1	0.338 551 691 683 85 × 10^{1}	21	3	0	−0.282 707 979 853 12 × 10^{-5}
5	0	2	−0.957 919 633 878 72	22	3	6	−0.852 051 281 201 03 × 10^{-9}
6	0	3	0.157 720 385 132 28	23	4	–5	−0.224 252 819 080 00 × 10^{-5}
7	0	4	−0.166 164 171 995 01 × 10^{-1}	24	4	–2	−0.651 712 228 956 01 × 10^{-6}
8	0	5	0.812 146 299 835 68 × 10^{-3}	25	4	10	−0.143 417 299 379 24 × 10^{-12}
9	1	–9	0.283 190 801 238 04 × 10^{-3}	26	5	–8	−0.405 169 968 601 17 × 10^{-6}
10	1	–7	−0.607 063 015 658 74 × 10^{-3}	27	8	–11	−0.127 343 017 416 41 × 10^{-8}
11	1	–1	−0.189 900 682 184 19 × 10^{-1}	28	8	–6	−0.174 248 712 306 34 × 10^{-9}
12	1	0	−0.325 297 487 705 05 × 10^{-1}	29	21	–29	−0.687 621 312 955 31 × 10^{-18}

Continued on next page.

Table 2.2 – Continued

i	I_i	J_i	n_i	i	I_i	J_i	n_i
13	1	1	$-0.218\,417\,171\,754\,14 \times 10^{-1}$	30	23	−31	$0.144\,783\,078\,285\,21 \times 10^{-19}$
14	1	3	$-0.528\,383\,579\,699\,30 \times 10^{-4}$	31	29	−38	$0.263\,357\,816\,627\,95 \times 10^{-22}$
15	2	−3	$-0.471\,843\,210\,732\,67 \times 10^{-3}$	32	30	−39	$-0.119\,476\,226\,400\,71 \times 10^{-22}$
16	2	0	$-0.300\,017\,807\,930\,26 \times 10^{-3}$	33	31	−40	$0.182\,280\,945\,814\,04 \times 10^{-23}$
17	2	1	$0.476\,613\,939\,069\,87 \times 10^{-4}$	34	32	−41	$-0.935\,370\,872\,924\,58 \times 10^{-25}$

Table 2.3 Relations of thermodynamic properties to the dimensionless Gibbs free energy γ and its derivatives when using Eq. (2.3)

Property	Relation
Specific volume $v = (\partial g/\partial p)_T$	$v(\pi,\tau)\dfrac{p}{RT} = \pi\gamma_\pi$
Specific enthalpy $h = g - T(\partial g/\partial T)_p$	$\dfrac{h(\pi,\tau)}{RT} = \tau\gamma_\tau$
Specific internal energy $u = g - T(\partial g/\partial T)_p - p(\partial g/\partial p)_T$	$\dfrac{u(\pi,\tau)}{RT} = \tau\gamma_\tau - \pi\gamma_\pi$
Specific entropy $s = -(\partial g/\partial T)_p$	$\dfrac{s(\pi,\tau)}{R} = \tau\gamma_\tau - \gamma$
Specific isobaric heat capacity $c_p = (\partial h/\partial T)_p$	$\dfrac{c_p(\pi,\tau)}{R} = -\tau^2\gamma_{\tau\tau}$
Specific isochoric heat capacity $c_v = (\partial u/\partial T)_v$	$\dfrac{c_v(\pi,\tau)}{R} = -\tau^2\gamma_{\tau\tau} + \dfrac{(\gamma_\pi - \tau\gamma_{\pi\tau})^2}{\gamma_{\pi\pi}}$
Speed of sound $w = v\left(-(\partial p/\partial v)_s\right)^{0.5}$	$\dfrac{w^2(\pi,\tau)}{RT} = \dfrac{\gamma_\pi^2}{\dfrac{(\gamma_\pi - \tau\gamma_{\pi\tau})^2}{\tau^2\gamma_{\tau\tau}} - \gamma_{\pi\pi}}$
Isobaric cubic expansion coefficient $\alpha_v = v^{-1}(\partial v/\partial T)_p$	$\alpha_v(\pi,\tau)T = 1 - \dfrac{\tau\gamma_{\pi\tau}}{\gamma_\pi}$
Isothermal compressibility $\kappa_T = -v^{-1}(\partial v/\partial p)_T$	$\kappa_T(\pi,\tau)p = -\dfrac{\pi\gamma_{\pi\pi}}{\gamma_\pi}$

$$\gamma_\pi = \left(\frac{\partial\gamma}{\partial\pi}\right)_\tau,\ \gamma_{\pi\pi} = \left(\frac{\partial^2\gamma}{\partial\pi^2}\right)_\tau,\ \gamma_\tau = \left(\frac{\partial\gamma}{\partial\tau}\right)_\pi,\ \gamma_{\tau\tau} = \left(\frac{\partial^2\gamma}{\partial\tau^2}\right)_\pi,\ \gamma_{\pi\tau} = \left(\frac{\partial^2\gamma}{\partial\pi\partial\tau}\right)$$

Table 2.4 The dimensionless Gibbs free energy γ, Eq. (2.3), and its derivatives

$$\gamma = \sum_{i=1}^{34} n_i (7.1-\pi)^{I_i} (\tau - 1.222)^{J_i} \qquad \gamma_\tau = \sum_{i=1}^{34} n_i (7.1-\pi)^{I_i} J_i (\tau - 1.222)^{J_i - 1}$$

$$\gamma_\pi = \sum_{i=1}^{34} -n_i I_i (7.1-\pi)^{I_i - 1} (\tau - 1.222)^{J_i} \qquad \gamma_{\tau\tau} = \sum_{i=1}^{34} n_i (7.1-\pi)^{I_i} J_i (J_i - 1)(\tau - 1.222)^{J_i - 2}$$

$$\gamma_{\pi\pi} = \sum_{i=1}^{34} n_i I_i (I_i - 1)(7.1-\pi)^{I_i - 2} (\tau - 1.222)^{J_i} \qquad \gamma_{\pi\tau} = \sum_{i=1}^{34} -n_i I_i (7.1-\pi)^{I_i - 1} J_i (\tau - 1.222)^{J_i - 1}$$

$$\gamma_\pi = \left(\frac{\partial \gamma}{\partial \pi}\right)_\tau, \; \gamma_{\pi\pi} = \left(\frac{\partial^2 \gamma}{\partial \pi^2}\right)_\tau, \; \gamma_\tau = \left(\frac{\partial \gamma}{\partial \tau}\right)_\pi, \; \gamma_{\tau\tau} = \left(\frac{\partial^2 \gamma}{\partial \tau^2}\right)_\pi, \; \gamma_{\pi\tau} = \left(\frac{\partial^2 \gamma}{\partial \pi \partial \tau}\right)$$

Range of Validity. Equation (2.3) covers region 1 of IAPWS-IF97 defined by the following range of temperature and pressure, see Fig. 2.2:

$$273.15\text{ K} \le T \le 623.15\text{ K} \qquad p_\mathrm{s}(T) \le p \le 100\text{ MPa}\,.$$

In addition to the properties in the stable single-phase liquid region, Eq. (2.3) also yields reasonable values in the metastable superheated-liquid region close to the saturated-liquid line.

Computer-Program Verification. To assist the user in computer-program verification of Eq. (2.3), Table 2.5 contains test values of the most relevant properties.

Table 2.5 Thermodynamic property values calculated from the basic equation $g_1(p,T)$, Eq. (2.3), for selected temperatures and pressures [a]

Property	$T = 300$ K $p = 3$ MPa	$T = 300$ K $p = 80$ MPa	$T = 500$ K $p = 3$ MPa
v [m^3 kg^{-1}]	$0.100\,215\,168 \times 10^{-2}$	$0.971\,180\,894 \times 10^{-3}$	$0.120\,241\,800 \times 10^{-2}$
h [kJ kg^{-1}]	$0.115\,331\,273 \times 10^{3}$	$0.184\,142\,828 \times 10^{3}$	$0.975\,542\,239 \times 10^{3}$
u [kJ kg^{-1}]	$0.112\,324\,818 \times 10^{3}$	$0.106\,448\,356 \times 10^{3}$	$0.971\,934\,985 \times 10^{3}$
s [kJ kg^{-1} K^{-1}]	$0.392\,294\,792$	$0.368\,563\,852$	$0.258\,041\,912 \times 10^{1}$
c_p [kJ kg^{-1} K^{-1}]	$0.417\,301\,218 \times 10^{1}$	$0.401\,008\,987 \times 10^{1}$	$0.465\,580\,682 \times 10^{1}$
c_v [kJ kg^{-1} K^{-1}]	$0.412\,120\,160 \times 10^{1}$	$0.391\,736\,606 \times 10^{1}$	$0.322\,139\,223 \times 10^{1}$
w [m s^{-1}]	$0.150\,773\,921 \times 10^{4}$	$0.163\,469\,054 \times 10^{4}$	$0.124\,071\,337 \times 10^{4}$
α_v [K^{-1}]	$0.277\,354\,533 \times 10^{-3}$	$0.344\,095\,843 \times 10^{-3}$	$0.164\,118\,128 \times 10^{-2}$
κ_T [MPa^{-1}]	$0.446\,382\,123 \times 10^{-3}$	$0.372\,039\,437 \times 10^{-3}$	$0.112\,892\,188 \times 10^{-2}$

[a] Programmed functions should be verified using 8 byte real values for all variables.

2.2.3 Basic Equation and Supplementary Equation for Region 2

This section contains all details relevant for using the basic equation of region 2 of IAPWS-IF97, see Fig. 2.2. The B23-equation for defining the boundary between regions 2 and 3 is given in Sec. 2.2.1. Uncertainty estimates of the most relevant properties calculated from IAPWS-IF97 can be found in Sec. 2.5.

2.2.3.1 Basic Equation

The basic equation for this region is a fundamental equation for the specific Gibbs free energy g. This equation is expressed in dimensionless form, $\gamma = g/(RT)$, and is separated into two parts, an ideal-gas part γ^{o} and a residual part γ^{r}, so that it reads

$$\frac{g_2(p,T)}{RT} = \gamma(\pi,\tau) = \gamma^{\mathrm{o}}(\pi,\tau) + \gamma^{\mathrm{r}}(\pi,\tau) \;, \tag{2.6}$$

where $\pi = p/p^*$ and $\tau = T^*/T$ with $R = 0.461\,526$ kJ kg^{-1} K^{-1} given by Eq. (1.1), and γ^{o} and γ^{r} according to Eqs. (2.7) and (2.8).

The equation for the dimensionless ideal-gas part γ^{o} of the basic equation $g_2(p,T)$ reads

$$\gamma^{\mathrm{o}}(\pi,\tau) = \ln\pi + \sum_{i=1}^{9} n_i^{\mathrm{o}}\, \tau^{J_i^{\mathrm{o}}} \;, \tag{2.7}$$

where $\pi = p/p^*$ and $\tau = T^*/T$ with $p^* = 1$ MPa and $T^* = 540$ K. The coefficients n_1^{o} and n_2^{o} were adjusted in such a way that the values for the specific internal energy and specific entropy, calculated from Eq. (2.6), correspond to Eq. (2.4). Table 2.6 contains the coefficients n_i^{o} and exponents J_i^{o} of Eq. (2.7).

Table 2.6 Coefficients and exponents of the ideal-gas part γ^{o}, Eq. (2.7)

i	J_i^{o}	n_i^{o}	i	J_i^{o}	n_i^{o}
1	0	$-0.969\,276\,865\,002\,17 \times 10^{1}$ [a]	6	–2	$0.142\,408\,191\,714\,44 \times 10^{1}$
2	1	$0.100\,866\,559\,680\,18 \times 10^{2}$ [a]	7	–1	$-0.438\,395\,113\,194\,50 \times 10^{1}$
3	–5	$-0.560\,879\,112\,830\,20 \times 10^{-2}$	8	2	$-0.284\,086\,324\,607\,72$
4	–4	$0.714\,527\,380\,814\,55 \times 10^{-1}$	9	3	$0.212\,684\,637\,533\,07 \times 10^{-1}$
5	–3	$-0.407\,104\,982\,239\,28$			

[a] If Eq. (2.7) is incorporated into Eq. (2.9), instead of the values for n_1^{o} and n_2^{o} given above, the following values for these two coefficients must be used: $n_1^{\mathrm{o}} = -\,0.969\,372\,683\,930\,49 \times 10^{1}$, $n_2^{\mathrm{o}} = 0.100\,872\,759\,700\,06 \times 10^{2}$.

The form of the dimensionless residual part γ^{r} of the basic equation $g_2(p,T)$ is as follows:

$$\gamma^{\mathrm{r}}(\pi,\tau) = \sum_{i=1}^{43} n_i\, \pi^{I_i} (\tau - 0.5)^{J_i} \;, \tag{2.8}$$

where $\pi = p/p^*$ and $\tau = T^*/T$ with $p^* = 1$ MPa and $T^* = 540$ K. The coefficients n_i and exponents I_i and J_i of Eq. (2.8) are listed in Table 2.7.

All thermodynamic properties can be derived from Eq. (2.6) by using the appropriate combinations of the ideal-gas part γ^{o}, Eq. (2.7), and the residual part γ^{r}, Eq. (2.8), of the dimensionless Gibbs free energy and their derivatives. The relations of the relevant thermodynamic properties to γ^{o} and γ^{r} and their derivatives are summarized in Table 2.8. Moreover, with the information given in Sec. 2.4, particularly with the formulas of Sec. 2.4.1, all partial derivatives formed by the properties p, T, v, u, h, s, g, and f can be very easily calculated. All required derivatives of the equations for γ^{o} and γ^{r} are explicitly given in Table 2.9 and Table 2.10, respectively.

Table 2.7 Coefficients and exponents of the residual part γ^{r}, Eq. (2.8)

i	I_i	J_i	n_i	i	I_i	J_i	n_i
1	1	0	$-0.177\,317\,424\,732\,13 \times 10^{-2}$	23	7	0	$-0.590\,595\,643\,242\,70 \times 10^{-17}$
2	1	1	$-0.178\,348\,622\,923\,58 \times 10^{-1}$	24	7	11	$-0.126\,218\,088\,991\,01 \times 10^{-5}$
3	1	2	$-0.459\,960\,136\,963\,65 \times 10^{-1}$	25	7	25	$-0.389\,468\,424\,357\,39 \times 10^{-1}$
4	1	3	$-0.575\,812\,590\,834\,32 \times 10^{-1}$	26	8	8	$0.112\,562\,113\,604\,59 \times 10^{-10}$
5	1	6	$-0.503\,252\,787\,279\,30 \times 10^{-1}$	27	8	36	$-0.823\,113\,408\,979\,98 \times 10^{1}$
6	2	1	$-0.330\,326\,416\,702\,03 \times 10^{-4}$	28	9	13	$0.198\,097\,128\,020\,88 \times 10^{-7}$
7	2	2	$-0.189\,489\,875\,163\,15 \times 10^{-3}$	29	10	4	$0.104\,069\,652\,101\,74 \times 10^{-18}$
8	2	4	$-0.393\,927\,772\,433\,55 \times 10^{-2}$	30	10	10	$-0.102\,347\,470\,959\,29 \times 10^{-12}$
9	2	7	$-0.437\,972\,956\,505\,73 \times 10^{-1}$	31	10	14	$-0.100\,181\,793\,795\,11 \times 10^{-8}$
10	2	36	$-0.266\,745\,479\,140\,87 \times 10^{-4}$	32	16	29	$-0.808\,829\,086\,469\,85 \times 10^{-10}$
11	3	0	$0.204\,817\,376\,923\,09 \times 10^{-7}$	33	16	50	$0.106\,930\,318\,794\,09$
12	3	1	$0.438\,706\,672\,844\,35 \times 10^{-6}$	34	18	57	$-0.336\,622\,505\,741\,71$
13	3	3	$-0.322\,776\,772\,385\,70 \times 10^{-4}$	35	20	20	$0.891\,858\,453\,554\,21 \times 10^{-24}$
14	3	6	$-0.150\,339\,245\,421\,48 \times 10^{-2}$	36	20	35	$0.306\,293\,168\,762\,32 \times 10^{-12}$
15	3	35	$-0.406\,682\,535\,626\,49 \times 10^{-1}$	37	20	48	$-0.420\,024\,676\,982\,08 \times 10^{-5}$
16	4	1	$-0.788\,473\,095\,593\,67 \times 10^{-9}$	38	21	21	$-0.590\,560\,296\,856\,39 \times 10^{-25}$
17	4	2	$0.127\,907\,178\,522\,85 \times 10^{-7}$	39	22	53	$0.378\,269\,476\,134\,57 \times 10^{-5}$
18	4	3	$0.482\,253\,727\,185\,07 \times 10^{-6}$	40	23	39	$-0.127\,686\,089\,346\,81 \times 10^{-14}$
19	5	7	$0.229\,220\,763\,376\,61 \times 10^{-5}$	41	24	26	$0.730\,876\,105\,950\,61 \times 10^{-28}$
20	6	3	$-0.167\,147\,664\,510\,61 \times 10^{-10}$	42	24	40	$0.554\,147\,153\,507\,78 \times 10^{-16}$
21	6	16	$-0.211\,714\,723\,213\,55 \times 10^{-2}$	43	24	58	$-0.943\,697\,072\,412\,10 \times 10^{-6}$
22	6	35	$-0.238\,957\,419\,341\,04 \times 10^{2}$				

Range of Validity. Equation (2.6) covers region 2 of IAPWS-IF97 defined by the following range of temperature and pressure, see Fig. 2.2:

$$
\begin{array}{llll}
273.15\ \mathrm{K} \le T \le 623.15\ \mathrm{K} & & 0 < p \le p_{\mathrm{s}}(T) \\
623.15\ \mathrm{K} < T \le 863.15\ \mathrm{K} & & 0 < p \le p_{\mathrm{B23}}(T) \\
863.15\ \mathrm{K} < T \le 1073.15\ \mathrm{K} & & 0 < p \le 100\ \mathrm{MPa},
\end{array}
$$

where $p_{\mathrm{s}}(T)$ is calculated from Eq. (2.13) and $p_{\mathrm{B23}}(T)$ from Eq. (2.1). In addition to the properties in the stable single-phase vapour region, Eq. (2.6) also yields reasonable values in the metastable-vapour region *for pressures above 10 MPa*. Equation (2.6) is not valid in the metastable-vapour region at pressures $p \le 10$ MPa; for this part of the metastable-vapour region see Sec. 2.2.3.2.

Table 2.8 Relations of thermodynamic properties to the ideal-gas part γ^{o} and the residual part γ^{r} of the dimensionless Gibbs free energy and their derivatives when using Eq. (2.6) or Eq. (2.9)

Property	Relation
Specific volume $v = (\partial g/\partial p)_T$	$v(\pi,\tau)\dfrac{p}{RT} = \pi\left(\gamma_\pi^{\mathrm{o}} + \gamma_\pi^{\mathrm{r}}\right)$
Specific enthalpy $h = g - T(\partial g/\partial T)_p$	$\dfrac{h(\pi,\tau)}{RT} = \tau\left(\gamma_\tau^{\mathrm{o}} + \gamma_\tau^{\mathrm{r}}\right)$
Specific internal energy $u = g - T(\partial g/\partial T)_p - p(\partial g/\partial p)_T$	$\dfrac{u(\pi,\tau)}{RT} = \tau\left(\gamma_\tau^{\mathrm{o}} + \gamma_\tau^{\mathrm{r}}\right) - \pi\left(\gamma_\pi^{\mathrm{o}} + \gamma_\pi^{\mathrm{r}}\right)$
Specific entropy $s = -(\partial g/\partial T)_p$	$\dfrac{s(\pi,\tau)}{R} = \tau\left(\gamma_\tau^{\mathrm{o}} + \gamma_\tau^{\mathrm{r}}\right) - \left(\gamma^{\mathrm{o}} + \gamma^{\mathrm{r}}\right)$
Specific isobaric heat capacity $c_p = (\partial h/\partial T)_p$	$\dfrac{c_p(\pi,\tau)}{R} = -\tau^2\left(\gamma_{\tau\tau}^{\mathrm{o}} + \gamma_{\tau\tau}^{\mathrm{r}}\right)$
Specific isochoric heat capacity $c_v = (\partial u/\partial T)_v$	$\dfrac{c_v(\pi,\tau)}{R} = -\tau^2\left(\gamma_{\tau\tau}^{\mathrm{o}} + \gamma_{\tau\tau}^{\mathrm{r}}\right) - \dfrac{\left(1 + \pi\gamma_\pi^{\mathrm{r}} - \tau\pi\gamma_{\pi\tau}^{\mathrm{r}}\right)^2}{1 - \pi^2\gamma_{\pi\pi}^{\mathrm{r}}}$
Speed of sound $w = v\left(-(\partial p/\partial v)_s\right)^{0.5}$	$\dfrac{w^2(\pi,\tau)}{RT} = \dfrac{1 + 2\pi\gamma_\pi^{\mathrm{r}} + \pi^2{\gamma_\pi^{\mathrm{r}}}^2}{\left(1 - \pi^2\gamma_{\pi\pi}^{\mathrm{r}}\right) + \dfrac{\left(1 + \pi\gamma_\pi^{\mathrm{r}} - \tau\pi\gamma_{\pi\tau}^{\mathrm{r}}\right)^2}{\tau^2\left(\gamma_{\tau\tau}^{\mathrm{o}} + \gamma_{\tau\tau}^{\mathrm{r}}\right)}}$
Isobaric cubic expansion coefficient $\alpha_v = v^{-1}(\partial v/\partial T)_p$	$\alpha_v(\pi,\tau)T = \dfrac{1 + \pi\gamma_\pi^{\mathrm{r}} - \tau\pi\gamma_{\pi\tau}^{\mathrm{r}}}{1 + \pi\gamma_\pi^{\mathrm{r}}}$
Isothermal compressibility $\kappa_T = -v^{-1}(\partial v/\partial p)_T$	$\kappa_T(\pi,\tau)p = \dfrac{1 - \pi^2\gamma_{\pi\pi}^{\mathrm{r}}}{1 + \pi\gamma_\pi^{\mathrm{r}}}$

$$\gamma_\pi^{\mathrm{r}} = \left(\frac{\partial\gamma^{\mathrm{r}}}{\partial\pi}\right)_\tau,\ \gamma_{\pi\pi}^{\mathrm{r}} = \left(\frac{\partial^2\gamma^{\mathrm{r}}}{\partial\pi^2}\right)_\tau,\ \gamma_\tau^{\mathrm{r}} = \left(\frac{\partial\gamma^{\mathrm{r}}}{\partial\tau}\right)_\pi,\ \gamma_{\tau\tau}^{\mathrm{r}} = \left(\frac{\partial^2\gamma^{\mathrm{r}}}{\partial\tau^2}\right)_\pi,\ \gamma_{\pi\tau}^{\mathrm{r}} = \left(\frac{\partial^2\gamma^{\mathrm{r}}}{\partial\pi\partial\tau}\right),\ \gamma_\tau^{\mathrm{o}} = \left(\frac{\partial\gamma^{\mathrm{o}}}{\partial\tau}\right)_\pi,\ \gamma_{\tau\tau}^{\mathrm{o}} = \left(\frac{\partial^2\gamma^{\mathrm{o}}}{\partial\tau^2}\right)_\pi$$

Table 2.9 The ideal-gas part γ^{o} of the dimensionless Gibbs free energy, Eq. (2.7), and its derivatives

$$\gamma^{\mathrm{o}} = \ln\pi + \sum_{i=1}^{9} n_i^{\mathrm{o}} \tau^{J_i^{\mathrm{o}}} \qquad \gamma_\tau^{\mathrm{o}} = \sum_{i=1}^{9} n_i^{\mathrm{o}} J_i^{\mathrm{o}} \tau^{J_i^{\mathrm{o}}-1}$$

$$\gamma_\pi^{\mathrm{o}} = \pi^{-1} \qquad \gamma_{\tau\tau}^{\mathrm{o}} = \sum_{i=1}^{9} n_i^{\mathrm{o}} J_i^{\mathrm{o}} \left(J_i^{\mathrm{o}}-1\right) \tau^{J_i^{\mathrm{o}}-2}$$

$$\gamma_{\pi\pi}^{\mathrm{o}} = -\pi^{-2} \qquad \gamma_{\pi\tau}^{\mathrm{o}} = 0$$

$$\gamma_\pi^{\mathrm{o}} = \left(\frac{\partial\gamma^{\mathrm{o}}}{\partial\pi}\right)_\tau,\ \gamma_{\pi\pi}^{\mathrm{o}} = \left(\frac{\partial^2\gamma^{\mathrm{o}}}{\partial\pi^2}\right)_\tau,\ \gamma_\tau^{\mathrm{o}} = \left(\frac{\partial\gamma^{\mathrm{o}}}{\partial\tau}\right)_\pi,\ \gamma_{\tau\tau}^{\mathrm{o}} = \left(\frac{\partial^2\gamma^{\mathrm{o}}}{\partial\tau^2}\right)_\pi,\ \gamma_{\pi\tau}^{\mathrm{o}} = \left(\frac{\partial^2\gamma^{\mathrm{o}}}{\partial\pi\partial\tau}\right)$$

Table 2.10 The residual part γ^{r} of the dimensionless Gibbs free energy, Eq. (2.8), and its derivatives

$$\gamma^{\mathrm{r}} = \sum_{i=1}^{43} n_i\, \pi^{I_i} (\tau-0.5)^{J_i} \qquad \gamma_\tau^{\mathrm{r}} = \sum_{i=1}^{43} n_i\, \pi^{I_i} J_i (\tau-0.5)^{J_i-1}$$

$$\gamma_\pi^{\mathrm{r}} = \sum_{i=1}^{43} n_i\, I_i\, \pi^{I_i-1} (\tau-0.5)^{J_i} \qquad \gamma_{\tau\tau}^{\mathrm{r}} = \sum_{i=1}^{43} n_i\, \pi^{I_i} J_i (J_i-1)(\tau-0.5)^{J_i-2}$$

$$\gamma_{\pi\pi}^{\mathrm{r}} = \sum_{i=1}^{43} n_i\, I_i (I_i-1) \pi^{I_i-2} (\tau-0.5)^{J_i} \qquad \gamma_{\pi\tau}^{\mathrm{r}} = \sum_{i=1}^{43} n_i\, I_i\, \pi^{I_i-1} J_i (\tau-0.5)^{J_i-1}$$

$$\gamma_\pi^{\mathrm{r}} = \left(\frac{\partial\gamma^{\mathrm{r}}}{\partial\pi}\right)_\tau,\ \gamma_{\pi\pi}^{\mathrm{r}} = \left(\frac{\partial^2\gamma^{\mathrm{r}}}{\partial\pi^2}\right)_\tau,\ \gamma_\tau^{\mathrm{r}} = \left(\frac{\partial\gamma^{\mathrm{r}}}{\partial\tau}\right)_\pi,\ \gamma_{\tau\tau}^{\mathrm{r}} = \left(\frac{\partial^2\gamma^{\mathrm{r}}}{\partial\tau^2}\right)_\pi,\ \gamma_{\pi\tau}^{\mathrm{r}} = \left(\frac{\partial^2\gamma^{\mathrm{r}}}{\partial\pi\partial\tau}\right)$$

Computer-Program Verification. To assist the user in computer-program verification of Eq. (2.6), Table 2.11 contains test values of the most relevant properties.

Table 2.11 Thermodynamic property values calculated from the basic equation $g_2(p,T)$, Eq. (2.6), for selected temperatures and pressures [a]

Property	T = 300 K p = 0.0035 MPa	T = 700 K p = 0.0035 MPa	T = 700 K p = 30 MPa
v [m^3 kg^{-1}]	$0.394\,913\,866 \times 10^{2}$	$0.923\,015\,898 \times 10^{2}$	$0.542\,946\,619 \times 10^{-2}$
h [kJ kg^{-1}]	$0.254\,991\,145 \times 10^{4}$	$0.333\,568\,375 \times 10^{4}$	$0.263\,149\,474 \times 10^{4}$
u [kJ kg^{-1}]	$0.241\,169\,160 \times 10^{4}$	$0.301\,262\,819 \times 10^{4}$	$0.246\,861\,076 \times 10^{4}$
s [kJ kg^{-1} K^{-1}]	$0.852\,238\,967 \times 10^{1}$	$0.101\,749\,996 \times 10^{2}$	$0.517\,540\,298 \times 10^{1}$
c_p [kJ kg^{-1} K^{-1}]	$0.191\,300\,162 \times 10^{1}$	$0.208\,141\,274 \times 10^{1}$	$0.103\,505\,092 \times 10^{2}$
c_v [kJ kg^{-1} K^{-1}]	$0.144\,132\,662 \times 10^{1}$	$0.161\,978\,333 \times 10^{1}$	$0.297\,553\,837 \times 10^{1}$
w [m s^{-1}]	$0.427\,920\,172 \times 10^{3}$	$0.644\,289\,068 \times 10^{3}$	$0.480\,386\,523 \times 10^{3}$
α_v [K^{-1}]	$0.337\,578\,289 \times 10^{-2}$	$0.142\,878\,736 \times 10^{-2}$	$0.126\,019\,688 \times 10^{-1}$
κ_T [MPa^{-1}]	$0.286\,239\,651 \times 10^{3}$	$0.285\,725\,461 \times 10^{3}$	$0.818\,411\,389 \times 10^{-1}$

[a] Programmed functions should be verified using 8 byte real values for all variables.

2.2.3.2 Supplementary Equation for the Metastable-Vapour Region

Such as the basic equation $g_2(p,T)$, Eq. (2.6), the supplementary equation for a part of the metastable-vapour region is given in the dimensionless form of the specific Gibbs free energy, $\gamma = g/(RT)$, consisting of an ideal-gas part γ^{o} and a residual part γ^{r}, so that

$$\frac{g_{2,\mathrm{meta}}(p,T)}{RT} = \gamma(\pi,\tau) = \gamma^{\mathrm{o}}(\pi,\tau) + \gamma^{\mathrm{r}}(\pi,\tau) \ , \tag{2.9}$$

where $\pi = p/p^*$ and $\tau = T^*/T$ with $R = 0.461\,526\ \mathrm{kJ\ kg^{-1}\ K^{-1}}$ given by Eq. (1.1), and γ^{o} and γ^{r} according to Eqs. (2.7) and (2.10).

The equation for the ideal-gas part γ^{o} is identical with Eq. (2.7) except for the values of the two coefficients n_1^{o} and n_2^{o}, see Table 2.6. To use Eq. (2.7) as a part of Eq. (2.9), the coefficients n_1^{o} and n_2^{o} were slightly readjusted to meet the high consistency requirement between Eqs. (2.9) and (2.6) for the properties *h* and *s* along the saturated-vapour line, see below.

The equation for the residual part γ^{r} of Eq. (2.9) reads

$$\gamma^{\mathrm{r}}(\pi,\tau) = \sum_{i=1}^{13} n_i\, \pi^{I_i} (\tau - 0.5)^{J_i} \ , \tag{2.10}$$

where $\pi = p/p^*$ and $\tau = T^*/T$ with $p^* = 1\ \mathrm{MPa}$ and $T^* = 540\ \mathrm{K}$. The coefficients n_i and exponents I_i and J_i of Eq. (2.10) are listed in Table 2.12. There are not any experimental data to which an equation can be fitted in the metastable-vapour region. Thus, Eq. (2.9) is only based on input values extrapolated from the stable single-phase region 2. These extrapolations were not performed with IAPWS-95 but with a special low-density gas equation [9].

Table 2.12 Coefficients and exponents of the residual part γ^{r}, Eq. (2.10)

i	I_i	J_i	n_i	i	I_i	J_i	n_i
1	1	0	$-0.733\,622\,601\,865\,06 \times 10^{-2}$	8	3	4	$-0.634\,980\,376\,573\,13 \times 10^{-2}$
2	1	2	$-0.882\,238\,319\,431\,46 \times 10^{-1}$	9	3	16	$-0.860\,430\,930\,285\,88 \times 10^{-1}$
3	1	5	$-0.723\,345\,552\,132\,45 \times 10^{-1}$	0	4	7	$0.753\,215\,815\,227\,70 \times 10^{-2}$
4	1	11	$-0.408\,131\,785\,344\,55 \times 10^{-2}$	11	4	10	$-0.792\,383\,754\,461\,39 \times 10^{-2}$
5	2	1	$0.200\,978\,033\,802\,07 \times 10^{-2}$	12	5	9	$-0.228\,881\,607\,784\,47 \times 10^{-3}$
6	2	7	$-0.530\,459\,218\,986\,42 \times 10^{-1}$	13	5	10	$-0.264\,565\,014\,828\,10 \times 10^{-2}$
7	2	16	$-0.761\,904\,090\,869\,70 \times 10^{-2}$				

All thermodynamic properties can be derived from Eq. (2.9) by using the appropriate combinations of the ideal-gas part γ^{o}, Eq. (2.7), and the residual part γ^{r}, Eq. (2.10), of the dimensionless Gibbs free energy and their derivatives. The relations of the relevant thermodynamic properties to γ^{o} and γ^{r} and their derivatives are summarized in Table 2.8. Moreover, with the information given in Sec. 2.4, particularly with the formulas given in Sec. 2.4.1, all of the partial derivatives of the properties *p*, *T*, *v*, *u*, *h*, *s*, *g*, and *f* can be calculated easily. All of the required derivatives for the equations for γ^{o} and γ^{r} are explicitly given in Table 2.9 and Table 2.13, respectively.

Range of Validity. Equation (2.9) is valid in the metastable-vapour region from the saturated-vapour line to the 5% equilibrium moisture line (corresponding to the vapour fraction $x = 0.95$,

determined from the equilibrium h' and h'' values) at pressures from the triple-point pressure, see Eq. (1.8), up to 10 MPa. The consistency of Eq. (2.9) with the basic equation $g_2(p,T)$, Eq. (2.6), along the saturated-vapour line is characterized by the following maximum inconsistencies in the properties v, h, c_p, s, g, and w:

$$|\Delta v|_{max} = 0.014\% \qquad |\Delta s|_{max} = 0.082 \text{ J kg}^{-1}\text{ K}^{-1}$$
$$|\Delta h|_{max} = 0.043 \text{ kJ kg}^{-1} \qquad |\Delta g|_{max} = 0.023 \text{ kJ kg}^{-1}$$
$$|\Delta c_p|_{max} = 0.78\% \qquad |\Delta w|_{max} = 0.051\%$$

These maximum inconsistencies are clearly smaller than the consistency requirements along the region boundaries corresponding to the so-called Prague values [18]. Along the 10 MPa isobar in the metastable-vapour region, the transition between Eq. (2.9) and Eq. (2.6) is not smooth, but for practical calculations the inconsistency is sufficiently small.

Computer-Program Verification. To assist the user in computer-program verification of Eq. (2.9), Table 2.14 contains test values of the most relevant properties.

Table 2.13 The residual part γ^r of the dimensionless Gibbs free energy, Eq. (2.10), and its derivatives

$$\gamma^r = \sum_{i=1}^{13} n_i\, \pi^{I_i} (\tau - 0.5)^{J_i} \qquad \gamma^r_\tau = \sum_{i=1}^{13} n_i\, \pi^{I_i} J_i (\tau - 0.5)^{J_i - 1}$$

$$\gamma^r_\pi = \sum_{i=1}^{13} n_i\, I_i\, \pi^{I_i - 1} (\tau - 0.5)^{J_i} \qquad \gamma^r_{\tau\tau} = \sum_{i=1}^{13} n_i\, \pi^{I_i} J_i (J_i - 1)(\tau - 0.5)^{J_i - 2}$$

$$\gamma^r_{\pi\pi} = \sum_{i=1}^{13} n_i\, I_i (I_i - 1) \pi^{I_i - 2} (\tau - 0.5)^{J_i} \qquad \gamma^r_{\pi\tau} = \sum_{i=1}^{13} n_i\, I_i\, \pi^{I_i - 1} J_i (\tau - 0.5)^{J_i - 1}$$

$$\gamma^r_\pi = \left(\frac{\partial \gamma^r}{\partial \pi}\right)_\tau,\ \gamma^r_{\pi\pi} = \left(\frac{\partial^2 \gamma^r}{\partial \pi^2}\right)_\tau,\ \gamma^r_\tau = \left(\frac{\partial \gamma^r}{\partial \tau}\right)_\pi,\ \gamma^r_{\tau\tau} = \left(\frac{\partial^2 \gamma^r}{\partial \tau^2}\right)_\pi,\ \gamma^r_{\pi\tau} = \left(\frac{\partial^2 \gamma^r}{\partial \pi \partial \tau}\right)$$

Table 2.14 Thermodynamic property values calculated from the $g_{2,\text{meta}}(p,T)$ equation, Eq. (2.9), for selected values of temperature and pressure [a]

Property	$T = 450$ K $p = 1$ MPa	$T = 440$ K $p = 1$ MPa	$T = 450$ K $p = 1.5$ MPa
v [m³ kg⁻¹]	0.192 516 540	0.186 212 297	0.121 685 206
h [kJ kg⁻¹]	0.276 881 115 × 10⁴	0.274 015 123 × 10⁴	0.272 134 539 × 10⁴
u [kJ kg⁻¹]	0.257 629 461 × 10⁴	0.255 393 894 × 10⁴	0.253 881 758 × 10⁴
s [kJ kg⁻¹ K⁻¹]	0.656 660 377 × 10¹	0.650 218 759 × 10¹	0.629 170 440 × 10¹
c_p [kJ kg⁻¹ K⁻¹]	0.276 349 265 × 10¹	0.298 166 443 × 10¹	0.362 795 578 × 10¹
c_v [kJ kg⁻¹ K⁻¹]	0.195 830 730 × 10¹	0.208 622 142 × 10¹	0.241 213 708 × 10¹
w [m s⁻¹]	0.498 408 101 × 10³	0.489 363 295 × 10³	0.481 941 819 × 10³
α_v [K⁻¹]	0.318 819 824 × 10⁻²	0.348 506 136 × 10⁻²	0.418 276 571 × 10⁻²
κ_T [MPa⁻¹]	0.109 364 239 × 10¹	0.111 133 230 × 10¹	0.787 967 952

[a] Programmed functions should be verified using 8 byte real values for all variables.

2.2.4 Basic Equation for Region 3

This section contains all details relevant for using the basic equation for region 3 of IAPWS-IF97, see Fig. 2.2. The B23-equation for defining the boundary between regions 2 and 3 is given in Sec. 2.2.1. Uncertainty estimates of the most relevant properties calculated from IAPWS-IF97 can be found in Sec. 2.5.

The basic equation for this region is a fundamental equation for the specific Helmholtz free energy f. This equation is expressed in dimensionless form, $\phi = f/(RT)$, and reads

$$\frac{f_3(\rho,T)}{RT} = \phi(\delta,\tau) = n_1 \ln\delta + \sum_{i=2}^{40} n_i\,\delta^{I_i}\tau^{J_i}\,, \tag{2.11}$$

where $\delta = \rho/\rho^*$ and $\tau = T^*/T$ with $\rho^* = \rho_c = 322\ \mathrm{kg\,m^{-3}}$, $T^* = T_c = 647.096\ \mathrm{K}$ and $R = 0.461\,526\ \mathrm{kJ\,kg^{-1}\,K^{-1}}$ according to Eqs. (1.6), (1.4), and (1.1). The coefficients n_i and exponents I_i and J_i of Eq. (2.11) are listed in Table 2.15.

Table 2.15 Coefficients and exponents of the basic equation $f_3(\rho,T)$ in its dimensionless form, Eq. (2.11)

i	I_i	J_i	n_i	i	I_i	J_i	n_i
1	–	–	$0.106\,580\,700\,285\,13 \times 10^{1}$	21	3	4	$-0.201\,899\,150\,235\,70 \times 10^{1}$
2	0	0	$-0.157\,328\,452\,902\,39 \times 10^{2}$	22	3	16	$-0.821\,476\,371\,739\,63 \times 10^{-2}$
3	0	1	$0.209\,443\,969\,743\,07 \times 10^{2}$	23	3	26	$-0.475\,960\,357\,349\,23$
4	0	2	$-0.768\,677\,078\,787\,16 \times 10^{1}$	24	4	0	$0.439\,840\,744\,735\,00 \times 10^{-1}$
5	0	7	$0.261\,859\,477\,879\,54 \times 10^{1}$	25	4	2	$-0.444\,764\,354\,287\,39$
6	0	10	$-0.280\,807\,811\,486\,20 \times 10^{1}$	26	4	4	$0.905\,720\,707\,197\,33$
7	0	12	$0.120\,533\,696\,965\,17 \times 10^{1}$	27	4	26	$0.705\,224\,500\,879\,67$
8	0	23	$-0.845\,668\,128\,125\,02 \times 10^{-2}$	28	5	1	$0.107\,705\,126\,263\,32$
9	1	2	$-0.126\,543\,154\,777\,14 \times 10^{1}$	29	5	3	$-0.329\,136\,232\,589\,54$
10	1	6	$-0.115\,244\,078\,066\,81 \times 10^{1}$	30	5	26	$-0.508\,710\,620\,411\,58$
11	1	15	$0.885\,210\,439\,843\,18$	31	6	0	$-0.221\,754\,008\,730\,96 \times 10^{-1}$
12	1	17	$-0.642\,077\,651\,816\,07$	32	6	2	$0.942\,607\,516\,650\,92 \times 10^{-1}$
13	2	0	$0.384\,934\,601\,866\,71$	33	6	26	$0.164\,362\,784\,479\,61$
14	2	2	$-0.852\,147\,088\,242\,06$	34	7	2	$-0.135\,033\,722\,413\,48 \times 10^{-1}$
15	2	6	$0.489\,722\,815\,418\,77 \times 10^{1}$	35	8	26	$-0.148\,343\,453\,524\,72 \times 10^{-1}$
16	2	7	$-0.305\,026\,172\,569\,65 \times 10^{1}$	36	9	2	$0.579\,229\,536\,280\,84 \times 10^{-3}$
17	2	22	$0.394\,205\,368\,791\,54 \times 10^{-1}$	37	9	26	$0.323\,089\,047\,037\,11 \times 10^{-2}$
18	2	26	$0.125\,584\,084\,243\,08$	38	10	0	$0.809\,648\,029\,962\,15 \times 10^{-4}$
19	3	0	$-0.279\,993\,296\,987\,10$	39	10	1	$-0.165\,576\,797\,950\,37 \times 10^{-3}$
20	3	2	$0.138\,997\,995\,694\,60 \times 10^{1}$	40	11	26	$-0.449\,238\,990\,618\,15 \times 10^{-4}$

In addition to representing the thermodynamic properties in the single-phase region along the saturation line for temperatures from 623.15 K to T_c = 647.096 K, Eq. (2.11) meets the phase-equilibrium condition for the coexisting vapour and liquid phase (equality of specific Gibbs free energy for both phases taken into account by the Maxwell criterion, see Table 2.16). Moreover, Eq. (2.11) reproduces exactly the critical parameters according to Eqs. (1.4) to (1.6) and yields zero for the first two pressure derivatives with respect to density at the critical point.

All thermodynamic properties can be derived from Eq. (2.11) by using the appropriate combinations of the dimensionless Helmholtz free energy ϕ and its derivatives. The relations of

the relevant thermodynamic properties to ϕ and its derivatives are summarized in Table 2.16. Moreover, with the information given in Sec. 2.4, particularly with the formulas of Sec. 2.4.2, all partial derivatives formed by the properties p, T, v, u, h, s, g, and f can be easily calculated. All required derivatives of the equation for the dimensionless Helmholtz free energy ϕ are explicitly given in Table 2.17.

Table 2.16 Relations of thermodynamic properties to the dimensionless Helmholtz free energy ϕ and its derivatives when using Eq. (2.11)

Property	Relation
Pressure $p=\rho^2(\partial f/\partial\rho)_T$	$\dfrac{p(\delta,\tau)}{\rho RT}=\delta\phi_\delta$
Specific enthalpy $h=f-T(\partial f/\partial T)_\rho+\rho(\partial f/\partial\rho)_T$	$\dfrac{h(\delta,\tau)}{RT}=\tau\phi_\tau+\delta\phi_\delta$
Specific internal energy $u=f-T(\partial f/\partial T)_\rho$	$\dfrac{u(\delta,\tau)}{RT}=\tau\phi_\tau$
Specific entropy $s=-(\partial f/\partial T)_\rho$	$\dfrac{s(\delta,\tau)}{R}=\tau\phi_\tau-\phi$
Specific isobaric heat capacity $c_p=(\partial h/\partial T)_p$	$\dfrac{c_p(\delta,\tau)}{R}=-\tau^2\phi_{\tau\tau}+\dfrac{(\delta\phi_\delta-\delta\tau\phi_{\delta\tau})^2}{2\delta\phi_\delta+\delta^2\phi_{\delta\delta}}$
Specific isochoric heat capacity $c_v=(\partial u/\partial T)_v$	$\dfrac{c_v(\delta,\tau)}{R}=-\tau^2\phi_{\tau\tau}$
Speed of sound $w=((\partial p/\partial\rho)_s)^{0.5}$	$\dfrac{w^2(\delta,\tau)}{RT}=2\,\delta\phi_\delta+\delta^2\phi_{\delta\delta}-\dfrac{(\delta\phi_\delta-\delta\tau\phi_{\delta\tau})^2}{\tau^2\phi_{\tau\tau}}$
Isobaric cubic expansion coefficient $\alpha_v=v^{-1}(\partial v/\partial T)_p$	$\alpha_v(\delta,\tau)T=\dfrac{\phi_\delta-\tau\phi_{\delta\tau}}{2\phi_\delta+\delta\phi_{\delta\delta}}$
Isothermal compressibility $\kappa_T=-v^{-1}(\partial v/\partial p)_T$	$\kappa_T(\delta,\tau)\rho RT=\dfrac{1}{2\delta\phi_\delta+\delta^2\phi_{\delta\delta}}$
Relative pressure coefficient $\alpha_p=p^{-1}(\partial p/\partial T)_v$	$\alpha_p(\delta,\tau)T=1-\dfrac{\tau\phi_{\delta\tau}}{\phi_\delta}$
Isothermal stress coefficient $\beta_p=-p^{-1}(\partial p/\partial v)_T$	$\dfrac{\beta_p(\delta,\tau)}{\rho}=2+\dfrac{\delta\phi_{\delta\delta}}{\phi_\delta}$
Phase-equilibrium condition (Maxwell criterion)	$\dfrac{p_\mathrm{s}}{RT\rho'}=\delta'\phi_\delta(\delta',\tau)$; $\dfrac{p_\mathrm{s}}{RT\rho''}=\delta''\phi_\delta(\delta'',\tau)$
	$\dfrac{p_\mathrm{s}}{RT}\left(\dfrac{1}{\rho''}-\dfrac{1}{\rho'}\right)=\phi(\delta',\tau)-\phi(\delta'',\tau)$

$$\phi_\delta=\left(\frac{\partial\phi}{\partial\delta}\right)_\tau,\ \phi_{\delta\delta}=\left(\frac{\partial^2\phi}{\partial\delta^2}\right)_\tau,\ \phi_\tau=\left(\frac{\partial\phi}{\partial\tau}\right)_\delta,\ \phi_{\tau\tau}=\left(\frac{\partial^2\phi}{\partial\tau^2}\right)_\delta,\ \phi_{\delta\tau}=\left(\frac{\partial^2\phi}{\partial\delta\partial\tau}\right)$$

Table 2.17 The dimensionless Helmholtz free energy ϕ, Eq. (2.11), and its derivatives

$$\phi = n_1 \ln \delta + \sum_{i=2}^{40} n_i \, \delta^{I_i} \, \tau^{J_i} \qquad \phi_\tau = \sum_{i=2}^{40} n_i \, \delta^{I_i} \, J_i \, \tau^{J_i - 1}$$

$$\phi_\delta = n_1 \delta^{-1} + \sum_{i=2}^{40} n_i \, I_i \, \delta^{I_i - 1} \, \tau^{J_i} \qquad \phi_{\tau\tau} = \sum_{i=2}^{40} n_i \, \delta^{I_i} \, J_i (J_i - 1) \, \tau^{J_i - 2}$$

$$\phi_{\delta\delta} = -n_1 \delta^{-2} + \sum_{i=2}^{40} n_i \, I_i (I_i - 1) \, \delta^{I_i - 2} \, \tau^{J_i} \qquad \phi_{\delta\tau} = \sum_{i=2}^{40} n_i \, I_i \, \delta^{I_i - 1} \, J_i \, \tau^{J_i - 1}$$

$$\phi_\delta = \left(\frac{\partial \phi}{\partial \delta}\right)_\tau , \; \phi_{\delta\delta} = \left(\frac{\partial^2 \phi}{\partial \delta^2}\right)_\tau , \; \phi_\tau = \left(\frac{\partial \phi}{\partial \tau}\right)_\delta , \; \phi_{\tau\tau} = \left(\frac{\partial^2 \phi}{\partial \tau^2}\right)_\delta , \; \phi_{\delta\tau} = \left(\frac{\partial^2 \phi}{\partial \delta \partial \tau}\right)$$

Range of Validity. Equation (2.11) covers region 3 of IAPWS-IF97 defined by the following range of temperature and pressure, see Fig. 2.2:

$$623.15\text{ K} \le T \le 863.15\text{ K} \qquad p_{\mathrm{B23}}(T) \le p \le 100\text{ MPa},$$

where $p_{\mathrm{B23}}(T)$ is calculated from Eq. (2.1). In addition to the properties in the stable single-phase region defined above, Eq. (2.11) also yields reasonable values in the metastable regions (superheated liquid and subcooled steam) close to the saturated-liquid and saturated-vapour lines.

As stated at the beginning of Sec. 2.2, the boundary between regions 1 and 2 is considered to belong to region 1 and the boundary between regions 2 and 3 is considered to belong to region 2. Thus, the properties along these boundaries are not determined from the basic equation of region 3, $f_3(\rho, T)$, Eq. (2.11), but the properties along the boundary between regions 1 and 3 are calculated from the basic equation $g_1(p, T)$, Eq. (2.3), and the properties along the boundary between regions 2 and 3 are determined from the basic equation $g_2(p, T)$, Eq. (2.6).

Computer-Program Verification. To assist the user in computer-program verification of Eq. (2.11), Table 2.18 contains test values of the most relevant properties.

Table 2.18 Thermodynamic property values calculated from the basic equation $f_3(\rho, T)$, Eq. (2.11), for selected temperatures and densities [a]

Property	T = 650 K ρ = 500 kg m^{-3}	T = 650 K ρ = 200 kg m^{-3}	T = 750 K ρ = 500 kg m^{-3}
p [MPa]	$0.255\,837\,018 \times 10^{2}$	$0.222\,930\,643 \times 10^{2}$	$0.783\,095\,639 \times 10^{2}$
h [kJ kg^{-1}]	$0.186\,343\,019 \times 10^{4}$	$0.237\,512\,401 \times 10^{4}$	$0.225\,868\,845 \times 10^{4}$
u [kJ kg^{-1}]	$0.181\,226\,279 \times 10^{4}$	$0.226\,365\,868 \times 10^{4}$	$0.210\,206\,932 \times 10^{4}$
s [kJ kg^{-1} K^{-1}]	$0.405\,427\,273 \times 10^{1}$	$0.485\,438\,792 \times 10^{1}$	$0.446\,971\,906 \times 10^{1}$
c_p [kJ kg^{-1} K^{-1}]	$0.138\,935\,717 \times 10^{2}$	$0.446\,579\,342 \times 10^{2}$	$0.634\,165\,359 \times 10^{1}$
c_v [kJ kg^{-1} K^{-1}]	$0.319\,131\,787 \times 10^{1}$	$0.404\,118\,076 \times 10^{1}$	$0.271\,701\,677 \times 10^{1}$
w [m s^{-1}]	$0.502\,005\,554 \times 10^{3}$	$0.383\,444\,594 \times 10^{3}$	$0.760\,696\,041 \times 10^{3}$
α_v [K^{-1}]	$0.168\,653\,107 \times 10^{-1}$	$0.685\,312\,229 \times 10^{-1}$	$0.441\,515\,098 \times 10^{-2}$
κ_T [MPa^{-1}]	$0.345\,506\,956 \times 10^{-1}$	$0.375\,798\,565$	$0.806\,710\,817 \times 10^{-2}$
α_p [K^{-1}]	$0.190\,798\,153 \times 10^{-1}$	$0.818\,019\,386 \times 10^{-2}$	$0.698\,896\,514 \times 10^{-2}$
β_p [kg m^{-3}]	$0.565\,652\,647 \times 10^{3}$	$0.238\,728\,962 \times 10^{2}$	$0.791\,475\,213 \times 10^{3}$

[a] Programmed functions should be verified using 8 byte real values for all variables.

2.2.5 Basic Equations for Region 4

This section contains all details relevant for using the equations for the two-phase region 4 of IAPWS-IF97 (corresponding to the saturation line in the p-T diagram), see Fig. 2.2. Uncertainty estimates of the saturation pressures calculated from IAPWS-IF97 can be found in Sec. 2.5.

The equation for describing the saturation line is an implicit quadratic equation, which can be solved directly with regard to both saturation pressure p_s and saturation temperature T_s. This equation reads

$$\beta^2\vartheta^2 + n_1\beta^2\vartheta + n_2\beta^2 + n_3\beta\vartheta^2 + n_4\beta\vartheta + n_5\beta + n_6\vartheta^2 + n_7\vartheta + n_8 = 0\,, \tag{2.12}$$

where
$$\beta = \left(p_s / p^*\right)^{0.25} \tag{2.12a}$$

and
$$\vartheta = \frac{T_s}{T^*} + \frac{n_9}{\left(T_s / T^*\right) - n_{10}} \tag{2.12b}$$

with $p^* = 1$ MPa and $T^* = 1$ K; for the coefficients n_1 to n_{10} see Table 2.19.

2.2.5.1 Saturation-Pressure Equation

The solution of Eq. (2.12) with regard to the saturation pressure p_s is as follows:

$$\frac{p_s}{p^*} = \left[\frac{2C}{-B + \left(B^2 - 4AC\right)^{0.5}}\right]^4, \tag{2.13}$$

where $p^* = 1$ MPa and

$$A = \vartheta^2 + n_1\vartheta + n_2$$
$$B = n_3\vartheta^2 + n_4\vartheta + n_5$$
$$C = n_6\vartheta^2 + n_7\vartheta + n_8$$

with ϑ according to Eq. (2.12b). The coefficients n_i of Eq. (2.13) are listed in Table 2.19.

Table 2.19 Coefficients of the basic equations for region 4, Eqs. (2.12) to (2.14)

i	n_i	i	n_i
1	$0.116\,705\,214\,527\,67 \times 10^4$	6	$0.149\,151\,086\,135\,30 \times 10^2$
2	$-0.724\,213\,167\,032\,06 \times 10^6$	7	$-0.482\,326\,573\,615\,91 \times 10^4$
3	$-0.170\,738\,469\,400\,92 \times 10^2$	8	$0.405\,113\,405\,420\,57 \times 10^6$
4	$0.120\,208\,247\,024\,70 \times 10^5$	9	$-0.238\,555\,575\,678\,49$
5	$-0.323\,255\,503\,223\,33 \times 10^7$	10	$0.650\,175\,348\,447\,98 \times 10^3$

Equations (2.12) to (2.14) reproduce exactly the p-T values at the triple point according to Eqs. (1.7) and (1.8), at the normal boiling point according to Eq. (1.9), and at the critical point according to Eqs. (1.4) and (1.5).

Range of Validity. Equation (2.13) is valid along the entire vapour-liquid saturation line from 273.15 K to the critical temperature T_c so that it covers the temperature range

$$273.15\text{ K} \le T \le 647.096\text{ K}\,.$$

Computer-Program Verification. To assist the user in computer-program verification of Eq. (2.13), Table 2.20 contains corresponding test values.

Table 2.20 Saturation-pressure values calculated from Eq. (2.13) for selected temperatures [a]

T [K]	p_s [MPa]
300	$0.353\,658\,941 \times 10^{-2}$
500	$0.263\,889\,776 \times 10^{1}$
600	$0.123\,443\,146 \times 10^{2}$

[a] Programmed functions should be verified using 8 byte real values for all variables.

2.2.5.2 Saturation-Temperature Equation

The solution of Eq. (2.12) with regard to the saturation temperature T_s reads

$$\frac{T_s}{T^*} = \frac{n_{10} + D - \left[\left(n_{10} + D\right)^2 - 4\left(n_9 + n_{10}D\right)\right]^{0.5}}{2} \ , \tag{2.14}$$

where $T^* = 1$ K and

$$D = \frac{2G}{-F - \left(F^2 - 4EG\right)^{0.5}}$$

with

$$E = \beta^2 + n_3\beta + n_6$$

$$F = n_1\beta^2 + n_4\beta + n_7$$

$$G = n_2\beta^2 + n_5\beta + n_8$$

and β according to Eq. (2.12a). The coefficients n_i of Eq. (2.14) are listed in Table 2.19.

Range of Validity. Equation (2.14) has the same range of validity as Eq. (2.13), which means that it covers the vapour-liquid saturation line according to the pressure range

$$611.212\,677 \text{ Pa} \le p \le 22.064 \text{ MPa} \ .$$

The value of 611.212 677 Pa corresponds to the saturation pressure at 273.15 K. Since the saturation-pressure equation, Eq. (2.13), and the saturation-temperature equation, Eq. (2.14), were derived from the same implicit equation, Eq. (2.12), for describing the saturation line, both Eq. (2.13) and Eq. (2.14) are numerically identical.

Computer-Program Verification. To assist the user in computer-program verification of Eq. (2.14), Table 2.21 contains corresponding test values.

Table 2.21 Saturation-temperature values calculated from Eq. (2.14) for selected pressures [a]

p [MPa]	T_s [K]
0.1	$0.372\,755\,919 \times 10^{3}$
1	$0.453\,035\,632 \times 10^{3}$
10	$0.584\,149\,488 \times 10^{3}$

[a] Programmed functions should be verified using 8 byte real values for all variables.

2.2.6 Basic Equation for Region 5

The high-temperature region (1073.15 K to 2273.15 K) was covered by a basic equation $g_5(p,T)$ that was valid for pressures up to 10 MPa [10, 15] until 2007. However, in order to enable users to calculate values of thermodynamic properties for designing future high-temperature power cycles and other processes for pressures above 10 MPa, a new basic equation $g_5(p,T)$ was developed that covers the high-temperature region 5 for pressures up to 50 MPa [20]. This equation was adopted at the IAPWS Meeting in 2007 [16].

This section contains the details relevant for using the basic equation for region 5 of IAPWS-IF97 that covers, as shown in Fig. 2.2, a pressure range up to 50 MPa.

The basic equation for this high-temperature region is a fundamental equation for the specific Gibbs free energy g. This equation is expressed in dimensionless form, $\gamma = g/(RT)$, and is separated into two parts, an ideal-gas part γ^{o} and a residual part γ^{r}, so that

$$\frac{g_5(p,T)}{RT} = \gamma(\pi,\tau) = \gamma^{\mathrm{o}}(\pi,\tau) + \gamma^{\mathrm{r}}(\pi,\tau) \ , \tag{2.15}$$

where $\pi = p/p^*$ and $\tau = T^*/T$ with $R = 0.461\,526$ kJ kg^{-1} K^{-1} given by Eq. (1.1), and γ^{o} and γ^{r} according to Eqs. (2.16) and (2.17).

The equation for the ideal-gas part γ^{o} of the dimensionless Gibbs free energy reads

$$\gamma^{\mathrm{o}}(\pi,\tau) = \ln\pi + \sum_{i=1}^{6} n_i^{\mathrm{o}}\,\tau^{J_i^{\mathrm{o}}} \ , \tag{2.16}$$

where $\pi = p/p^*$ and $\tau = T^*/T$ with $p^* = 1$ MPa and $T^* = 1000$ K. The coefficients n_1^{o} and n_2^{o} were adjusted in such a way that the values for the specific internal energy and specific entropy, calculated from Eq. (2.15), relate to Eq. (2.4). Table 2.22 contains the coefficients n_i^{o} and exponents J_i^{o} of Eq. (2.16). This equation was developed in connection with the development of the previous $g_5(p,T)$ equation [21].

Table 2.22 Coefficients and exponents of the ideal-gas part γ^{o}, Eq. (2.16)

i	J_i^{o}	n_i^{o}	i	J_i^{o}	n_i^{o}
1	0	$-0.131\,799\,836\,742\,01 \times 10^{2}$	4	-2	$0.369\,015\,349\,803\,33$
2	1	$0.685\,408\,416\,344\,34 \times 10^{1}$	5	-1	$-0.311\,613\,182\,139\,25 \times 10^{1}$
3	-3	$-0.248\,051\,489\,334\,66 \times 10^{-1}$	6	2	$-0.329\,616\,265\,389\,17$

The form of the residual part γ^{r} of the dimensionless Gibbs free energy is as follows:

$$\gamma^{\mathrm{r}}(\pi,\tau) = \sum_{i=1}^{6} n_i\,\pi^{I_i}\,\tau^{J_i} \ , \tag{2.17}$$

where $\pi = p/p^*$ and $\tau = T^*/T$ with $p^* = 1$ MPa and $T^* = 1000$ K. The coefficients n_i and exponents I_i and J_i of Eq. (2.17) are listed in Table 2.23.

All thermodynamic properties can be derived from Eq. (2.15) by using the appropriate combinations of the ideal-gas part γ^{o}, Eq. (2.16), and the residual part γ^{r}, Eq. (2.17), of the dimensionless Gibbs free energy and their derivatives. The relations of the relevant

thermodynamic properties to γ^{o} and γ^{r} and their derivatives are summarized in Table 2.24. Moreover, with the information given in Sec. 2.4, particularly with the formulas of Sec. 2.4.1, all of the partial derivatives of the properties p, T, v, u, h, s, g, and f can be calculated easily. All required derivatives of the equations for γ^{o} and γ^{r} are explicitly given in Table 2.25 and Table 2.26, respectively.

Table 2.23 Coefficients and exponents of the residual part γ^{r}, Eq. (2.17)

i	I_i	J_i	n_i	i	I_i	J_i	n_i
1	1	1	$0.157\,364\,048\,552\,59 \times 10^{-2}$	4	2	3	$0.224\,400\,374\,094\,85 \times 10^{-5}$
2	1	2	$0.901\,537\,616\,739\,44 \times 10^{-3}$	5	2	9	$-0.411\,632\,754\,534\,71 \times 10^{-5}$
3	1	3	$-0.502\,700\,776\,776\,48 \times 10^{-2}$	6	3	7	$0.379\,194\,548\,229\,55 \times 10^{-7}$

Table 2.24 Relations of thermodynamic properties to the ideal-gas part γ^{o} and the residual part γ^{r} of the dimensionless Gibbs free energy and their derivatives when using Eq. (2.15)

Property	Relation
Specific volume $v = (\partial g/\partial p)_T$	$v(\pi,\tau)\dfrac{p}{RT} = \pi\left(\gamma^{\mathrm{o}}_{\pi} + \gamma^{\mathrm{r}}_{\pi}\right)$
Specific enthalpy $h = g - T(\partial g/\partial T)_p$	$\dfrac{h(\pi,\tau)}{RT} = \tau\left(\gamma^{\mathrm{o}}_{\tau} + \gamma^{\mathrm{r}}_{\tau}\right)$
Specific internal energy $u = g - T(\partial g/\partial T)_p - p(\partial g/\partial p)_T$	$\dfrac{u(\pi,\tau)}{RT} = \tau\left(\gamma^{\mathrm{o}}_{\tau} + \gamma^{\mathrm{r}}_{\tau}\right) - \pi\left(\gamma^{\mathrm{o}}_{\pi} + \gamma^{\mathrm{r}}_{\pi}\right)$
Specific entropy $s = -(\partial g/\partial T)_p$	$\dfrac{s(\pi,\tau)}{R} = \tau\left(\gamma^{\mathrm{o}}_{\tau} + \gamma^{\mathrm{r}}_{\tau}\right) - \left(\gamma^{\mathrm{o}} + \gamma^{\mathrm{r}}\right)$
Specific isobaric heat capacity $c_p = (\partial h/\partial T)_p$	$\dfrac{c_p(\pi,\tau)}{R} = -\tau^2\left(\gamma^{\mathrm{o}}_{\tau\tau} + \gamma^{\mathrm{r}}_{\tau\tau}\right)$
Specific isochoric heat capacity $c_v = (\partial u/\partial T)_v$	$\dfrac{c_v(\pi,\tau)}{R} = -\tau^2\left(\gamma^{\mathrm{o}}_{\tau\tau} + \gamma^{\mathrm{r}}_{\tau\tau}\right) - \dfrac{\left(1+\pi\gamma^{\mathrm{r}}_{\pi} - \tau\pi\gamma^{\mathrm{r}}_{\pi\tau}\right)^2}{1-\pi^2\gamma^{\mathrm{r}}_{\pi\pi}}$
Speed of sound $w = v\left(-(\partial p/\partial v)_s\right)^{0.5}$	$\dfrac{w^2(\pi,\tau)}{RT} = \dfrac{1+2\pi\gamma^{\mathrm{r}}_{\pi} + \pi^2{\gamma^{\mathrm{r}}_{\pi}}^2}{\left(1-\pi^2\gamma^{\mathrm{r}}_{\pi\pi}\right) + \dfrac{\left(1+\pi\gamma^{\mathrm{r}}_{\pi} - \tau\pi\gamma^{\mathrm{r}}_{\pi\tau}\right)^2}{\tau^2\left(\gamma^{\mathrm{o}}_{\tau\tau} + \gamma^{\mathrm{r}}_{\tau\tau}\right)}}$
Isobaric cubic expansion coefficient $\alpha_v = v^{-1}(\partial v/\partial T)_p$	$\alpha_v(\pi,\tau)T = \dfrac{1+\pi\gamma^{\mathrm{r}}_{\pi} - \tau\pi\gamma^{\mathrm{r}}_{\pi\tau}}{1+\pi\gamma^{\mathrm{r}}_{\pi}}$
Isothermal compressibility $\kappa_T = -v^{-1}(\partial v/\partial p)_T$	$\kappa_T(\pi,\tau)p = \dfrac{1-\pi^2\gamma^{\mathrm{r}}_{\pi\pi}}{1+\pi\gamma^{\mathrm{r}}_{\pi}}$

$\gamma^{\mathrm{r}}_{\pi} = \left(\dfrac{\partial\gamma^{\mathrm{r}}}{\partial\pi}\right)_{\tau}$, $\gamma^{\mathrm{r}}_{\pi\pi} = \left(\dfrac{\partial^2\gamma^{\mathrm{r}}}{\partial\pi^2}\right)_{\tau}$, $\gamma^{\mathrm{r}}_{\tau} = \left(\dfrac{\partial\gamma^{\mathrm{r}}}{\partial\tau}\right)_{\pi}$, $\gamma^{\mathrm{r}}_{\tau\tau} = \left(\dfrac{\partial^2\gamma^{\mathrm{r}}}{\partial\tau^2}\right)_{\pi}$, $\gamma^{\mathrm{r}}_{\pi\tau} = \left(\dfrac{\partial^2\gamma^{\mathrm{r}}}{\partial\pi\partial\tau}\right)$, $\gamma^{\mathrm{o}}_{\tau} = \left(\dfrac{\partial\gamma^{\mathrm{o}}}{\partial\tau}\right)_{\pi}$, $\gamma^{\mathrm{o}}_{\tau\tau} = \left(\dfrac{\partial^2\gamma^{\mathrm{o}}}{\partial\tau^2}\right)_{\pi}$

Table 2.25 The ideal-gas part γ^{o} of the dimensionless Gibbs free energy, Eq. (2.16), and its derivatives

$\gamma^{\mathrm{o}} = \ln \pi + \sum_{i=1}^{6} n_i^{\mathrm{o}} \tau^{J_i^{\mathrm{o}}}$	$\gamma_{\tau}^{\mathrm{o}} = \sum_{i=1}^{6} n_i^{\mathrm{o}} J_i^{\mathrm{o}} \tau^{J_i^{\mathrm{o}}-1}$
$\gamma_{\pi}^{\mathrm{o}} = \pi^{-1}$	$\gamma_{\tau\tau}^{\mathrm{o}} = \sum_{i=1}^{6} n_i^{\mathrm{o}} J_i^{\mathrm{o}} \left(J_i^{\mathrm{o}}-1\right) \tau^{J_i^{\mathrm{o}}-2}$
$\gamma_{\pi\pi}^{\mathrm{o}} = -\pi^{-2}$	$\gamma_{\pi\tau}^{\mathrm{o}} = 0$

$\gamma_{\pi}^{\mathrm{o}} = \left(\frac{\partial \gamma^{\mathrm{o}}}{\partial \pi}\right)_{\tau}$, $\gamma_{\pi\pi}^{\mathrm{o}} = \left(\frac{\partial^2 \gamma^{\mathrm{o}}}{\partial \pi^2}\right)_{\tau}$, $\gamma_{\tau}^{\mathrm{o}} = \left(\frac{\partial \gamma^{\mathrm{o}}}{\partial \tau}\right)_{\pi}$, $\gamma_{\tau\tau}^{\mathrm{o}} = \left(\frac{\partial^2 \gamma^{\mathrm{o}}}{\partial \tau^2}\right)_{\pi}$, $\gamma_{\pi\tau}^{\mathrm{o}} = \left(\frac{\partial^2 \gamma^{\mathrm{o}}}{\partial \pi \partial \tau}\right)$

Table 2.26 The residual part γ^{r} of the dimensionless Gibbs free energy, Eq. (2.17), and its derivatives

$\gamma^{\mathrm{r}} = \sum_{i=1}^{6} n_i \pi^{I_i} \tau^{J_i}$	$\gamma_{\tau}^{\mathrm{r}} = \sum_{i=1}^{6} n_i \pi^{I_i} J_i \tau^{J_i-1}$
$\gamma_{\pi}^{\mathrm{r}} = \sum_{i=1}^{6} n_i I_i \pi^{I_i-1} \tau^{J_i}$	$\gamma_{\tau\tau}^{\mathrm{r}} = \sum_{i=1}^{6} n_i \pi^{I_i} J_i \left(J_i-1\right) \tau^{J_i-2}$
$\gamma_{\pi\pi}^{\mathrm{r}} = \sum_{i=1}^{6} n_i I_i \left(I_i-1\right) \pi^{I_i-2} \tau^{J_i}$	$\gamma_{\pi\tau}^{\mathrm{r}} = \sum_{i=1}^{6} n_i I_i \pi^{I_i-1} J_i \tau^{J_i-1}$

$\gamma_{\pi}^{\mathrm{r}} = \left(\frac{\partial \gamma^{\mathrm{r}}}{\partial \pi}\right)_{\tau}$, $\gamma_{\pi\pi}^{\mathrm{r}} = \left(\frac{\partial^2 \gamma^{\mathrm{r}}}{\partial \pi^2}\right)_{\tau}$, $\gamma_{\tau}^{\mathrm{r}} = \left(\frac{\partial \gamma^{\mathrm{r}}}{\partial \tau}\right)_{\pi}$, $\gamma_{\tau\tau}^{\mathrm{r}} = \left(\frac{\partial^2 \gamma^{\mathrm{r}}}{\partial \tau^2}\right)_{\pi}$, $\gamma_{\pi\tau}^{\mathrm{r}} = \left(\frac{\partial^2 \gamma^{\mathrm{r}}}{\partial \pi \partial \tau}\right)$

Range of Validity. Equation (2.15) covers region 5 of IAPWS-IF97 defined by the following temperature and pressure range, see Fig. 2.2:

$$1073.15 \text{ K} \le T \le 2273.15 \text{ K} \qquad 0 < p \le 50 \text{ MPa} .$$

In this range, Eq. (2.15) is only valid for pure undissociated water, any dissociation will have to be taken into account separately.

Computer-Program Verification. To assist the user in computer-program verification of Eq. (2.15), Table 2.27 contains test values of the most relevant properties.

Table 2.27 Thermodynamic property values calculated from the basic equation $g_5(p,T)$, Eq.(2.15), for selected temperatures and pressures [a]

Property	$T = 1500$ K $p = 0.5$ MPa	$T = 1500$ K $p = 30$ MPa	$T = 2000$ K $p = 30$ MPa
v [m^3 kg^{-1}]	$0.138\,455\,090 \times 10^{1}$	$0.230\,761\,299 \times 10^{-1}$	$0.311\,385\,219 \times 10^{-1}$
h [kJ kg^{-1}]	$0.521\,976\,855 \times 10^{4}$	$0.516\,723\,514 \times 10^{4}$	$0.657\,122\,604 \times 10^{4}$
u [kJ kg^{-1}]	$0.452\,749\,310 \times 10^{4}$	$0.447\,495\,124 \times 10^{4}$	$0.563\,707\,038 \times 10^{4}$
s [kJ kg^{-1} K^{-1}]	$0.965\,408\,875 \times 10^{1}$	$0.772\,970\,133 \times 10^{1}$	$0.853\,640\,523 \times 10^{1}$
c_p [kJ kg^{-1} K^{-1}]	$0.261\,609\,445 \times 10^{1}$	$0.272\,724\,317 \times 10^{1}$	$0.288\,569\,882 \times 10^{1}$
c_v [kJ kg^{-1} K^{-1}]	$0.215\,337\,784 \times 10^{1}$	$0.219\,274\,829 \times 10^{1}$	$0.239\,589\,436 \times 10^{1}$
w [m s^{-1}]	$0.917\,068\,690 \times 10^{3}$	$0.928\,548\,002 \times 10^{3}$	$0.106\,736\,948 \times 10^{4}$
α_v [K^{-1}]	$0.667\,539\,000 \times 10^{-3}$	$0.716\,950\,754 \times 10^{-3}$	$0.508\,830\,641 \times 10^{-3}$
κ_T [MPa^{-1}]	$0.200\,003\,859 \times 10^{1}$	$0.332\,881\,253 \times 10^{-1}$	$0.329\,193\,892 \times 10^{-1}$

[a] Programmed functions should be verified using 8 byte real values for all variables.

2.3 Backward Equations of IAPWS-IF97

This section contains details relevant for using all of the backward equations. However, these backward equations are not presented region by region, i.e. not all types of backward equations that are valid in the same region are described in one section, rather, all backward equations dependent on the same input variables are summarized in the same section. This is more practical for application of the different types of backward equations to the corresponding basic equations.

2.3.1 Survey and Important Annotations

A survey of all types of backward equations of the industrial formulation IAPWS-IF97 together with some general statements are given in this section. Important annotations on the use of the backward equations are summarized in Sec. 2.3.1.2.

2.3.1.1 Survey on All Types of Backward Equations

For industrial applications in the single-phase region of water and steam, property functions dependent on the input variables (p,T) are most important. For regions 1 and 2 more than 30% of all property calls relate to these input variables. However, for modelling steam power cycles and other applications, property functions of (p,h) and (p,s) are also quite necessary. From the basic equations, such property functions can only be calculated by iterations, which require intensive computing time. For very fast yet sufficiently accurate calculations of properties as functions of (p,h) and (p,s) for regions 1 and 2, backward equations in the form $T(p,h)$ and $T(p,s)$ were developed simultaneously with the basic equations of IAPWS-IF97 [10, 15].

Although properties as a function of (h,s) are not often used in process modelling, after the adoption of IAPWS-IF97 in 1997, IAPWS decided that backward equations in the form of $p(h,s)$ for regions 1 and 2 should supplement the other backward equations for these regions, because the determination of such property functions from the basic equations requires two-dimensional iterations, which are very time consuming. Therefore, backward equations in the form of $p(h,s)$ were developed [11, 22]. The combination of these equations with the other backward equations of regions 1 and 2 allows for the calculation of all properties as a function of (h,s) without iterations. Later, IAPWS also decided that it should be possible to calculate properties for region 3 as functions of (p,h), (p,s), (h,s), and even of (p,T) without iterations from the basic equation $f_3(\rho,T)$, Eq. (2.11). Therefore, backward equations of the form $T(p,h)$, $v(p,h)$, $T(p,s)$, $v(p,s)$ [12, 23], $p(h,s)$ [13, 24], and $v(p,T)$ [14, 25] were developed. Moreover, a saturation-temperature equation in the form $T_s(h,s)$ is also provided [13, 24] for the part of the two-phase region 4 that is important for steam-turbine calculations. Figure 2.3 shows the assignment of the existing backward equations to the various regions; all of these equations are described in this section. For region 5 there are no backward equations.

Before properties can be calculated for a given state point, the region in which the point is located must be determined. To minimize the computing time, one should also be able to perform the region determination without iterations. However, for the input variables (h,s), the region boundaries can only be calculated by iterating the corresponding basic equation. The same is true for the input variables (p,h) and (p,s) with regard to the boundary between the single-phase region 3 and the two-phase region 4. In order to avoid these iterative calculations, special equations for the region boundaries were developed and included in the IAPWS supplementary releases for the respective backward equations. These equations are called region-boundary equations in the following text.

The use of the backward equations and region-boundary equations enormously accelerates the calculation of properties dependent on the different combinations of input variables. The following sections, particularly Sec. 2.3.7, describe how much faster the calculations with the backward equations and region-boundary equations are in comparison with calculations from the basic equations through iteration.

All backward equations presented in this section[4] meet the requirements for very high consistency to the corresponding basic equation. The exact requirements for these numerical consistency values, set by IAPWS, are summarized in Sec. 2.3.2.

[4] The saturation-temperature equation $T_s(p)$ is not considered to be a backward equation and is therefore described in Sec. 2.2.5.2, see also the beginning of Sec. 2.2.

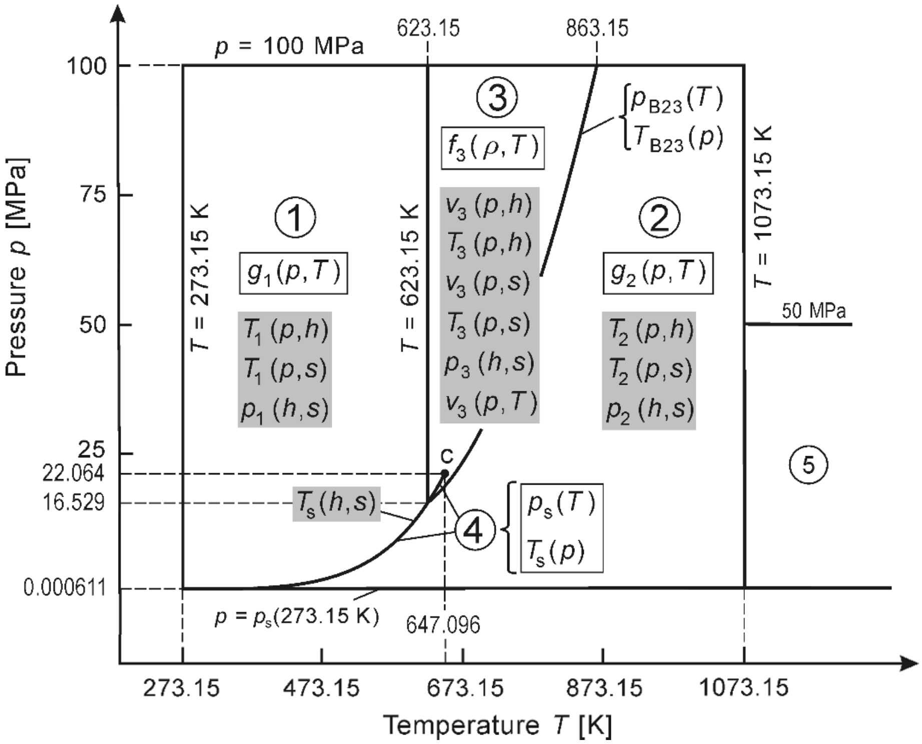

Fig. 2.3 All forms of backward equations (marked in grey) as assigned to the corresponding regions of IAPWS-IF97. The basic equations are shown in rectangular boxes.

2.3.1.2 Important Annotations on the Use of the Backward Equations

Although the backward equations clearly meet the very high numerical consistency requirements given in Sec. 2.3.2, the inconsistencies with respect to the basic equations are, of course, not zero. This fact has several consequences of which the user should be aware, for example:

- When calculating a property as a function of (p,h), (p,s), or (h,s), slightly different results are obtained depending on whether the backward equations are used or if the properties are directly calculated from the basic equation $g(p,T)$ by iteration. These differences are described in detail in the sections for the respective backward equations.
- When calculating properties with the help of backward equations for a given state point extremely close to a region boundary, attention should be paid to the existence of (very small) inconsistencies between backward equations and basic equations, and between region-boundary equations and basic equations. Due to these inconsistencies, the calculations could indicate that the state point is in the adjacent region, but (of course) extremely close to the region boundary. The user should be aware of these effects in order to avoid possible numerical problems by taking suitable measures in the program code. For this purpose, values for the numerical inconsistencies of the backward and region-boundary equations will be given in the respective sections.

- The backward equations and region-boundary equations should never be used to calculate derivatives of a property.
- When properties are to be determined by iteration of the basic equations (because the input variables are not the independent variables of the equation), then these iterations may only be carried out with the basic equations alone, not in combination with any backward or region boundary equation.

These inconsistencies are unavoidable when using backward equations and are therefore an agreed-upon feature of IAPWS-IF97. However, these inconsistencies are insignificant enough to have nearly no practical relevance for any technical application. Thus, because of their great advantage due to shorter computing times, the backward equations should be used whenever possible. For such applications, however, where these minor inconsistencies are indeed not acceptable, the calculations should be performed with the basic equations through the use of iteration. Even in this case the inconsistency is not zero, but depends on the selected convergence criterion of the iteration. For example, the convergence criterion has to be less than 10^{-5} in $\Delta T/T$ to achieve a smaller inconsistency than that with the backward equations. However, even for such direct iterations with the basic equations, the backward equations are still very useful because they provide very good starting values for the iterations.

2.3.2 Requirements for the Numerical Consistencies between Backward Equations, Backward Functions, and Basic Equations

The use of the backward equations of the forms $T(p,h)$, $v(p,h)$, $T(p,s)$, $v(p,s)$, $p(h,s)$, $v(p,T)$, and the backward functions[5] $T(h,s)$ and $v(h,s)$ in combination with the corresponding basic equations of the forms $g(p,T)$ and $f(\rho,T)$, see Fig. 2.3, enormously accelerates the calculation of the thermodynamic properties dependent on the input variables (p,h), (p,s), (h,s) for regions 1 to 3, (p,T) for region 3, and (h,s) for a part of region 4. These "fast" calculations are particularly important for heat cycle, turbine and boiler calculations. However, the main precondition for the effective use of such backward equations and backward functions in combination with the corresponding basic equations is that these equations must be numerically very consistent with each other. The final requirements for these numerical consistencies were set by IAPWS based on comprehensive test calculations that were carried out by the international power-cycle industry for several characteristic power cycles. These numerical consistency requirements for the backward equations and backward functions in temperature, pressure and specific volume, assigned to the corresponding region of IAPWS-IF97, are summarized in Fig. 2.4 and described in the following text.

[5] For the explanation of the term "backward function" see the beginning of Sec. 2.3.5.

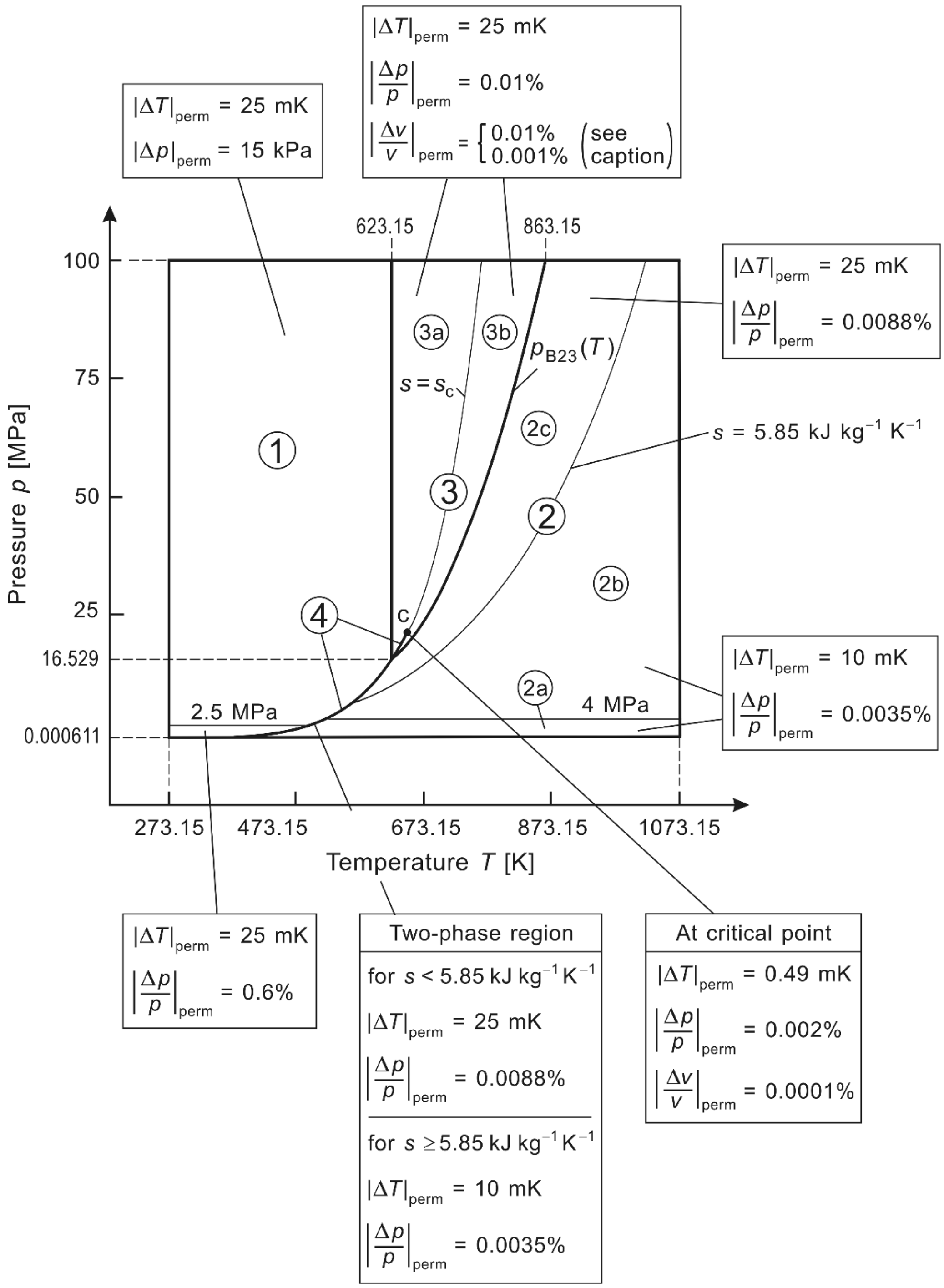

Fig. 2.4 Permissible values for numerical inconsistencies $|\Delta T|_{\text{perm}}$ in calculated temperatures, $|\Delta p/p|_{\text{perm}}$ or $|\Delta p|_{\text{perm}}$ in calculated pressures, and $|\Delta v/v|_{\text{perm}}$ in calculated specific volumes between the backward equations/functions and the corresponding basic equation assigned to the corresponding regions of IAPWS-IF97. For region 3: The value $|\Delta v/v|_{\text{perm}} = 0.01\%$ relates to the backward equations/functions with the input variables (p,h), (p,s), and (h,s). The value $|\Delta v/v|_{\text{perm}} = 0.001\%$ relates to the backward equations $v(p,T)$, for which region 3 is divided into many subregions not shown in this figure; details are given in Sec. 2.3.6.3.

Numerical Consistency Requirements in Temperature. The permissible inconsistency between the temperature calculated from the backward equations and the temperature calculated by iteration from the corresponding basic equations/functions was set to ± 25 mK for the range of specific entropies less than 5.85 $\mathrm{kJ\,kg^{-1}\,K^{-1}}$ and to ± 10 mK for the range of specific entropies greater than or equal to this value. This means that the value $|\Delta T|_{\mathrm{perm}} = 25$ mK is valid in regions 1, 3, and in the part of region 2 with $s < 5.85\ \mathrm{kJ\,kg^{-1}\,K^{-1}}$. This part of region 2 corresponds to subregion 2c, which will be explained in the following sections, e.g. Sec. 2.3.3.3a. The value $|\Delta T|_{\mathrm{perm}} = 10$ mK is valid in the part of region 2 with $s \geq 5.85\ \mathrm{kJ\,kg^{-1}\,K^{-1}}$ corresponding to subregions 2a and 2b.

In order to avoid numerical problems at the critical point, the value 647.096 K for the critical temperature should be represented by the backward equations/functions for all six figures. Therefore, the permissible inconsistency value was set to $|\Delta T|_{\mathrm{perm}} = 0.49$ mK. This value has to be met by the backward equations/functions of the adjacent subregions 3a and 3b.

In the part of the two-phase region 4 with $s \geq s''(623.15\ \mathrm{K})$, which is important for steam turbine calculations, see Fig. 2.21, the permissible numerical inconsistency in temperature was set to $|\Delta T|_{\mathrm{perm}} = 10$ mK for $s \geq 5.85\ \mathrm{kJ\,kg^{-1}\,K^{-1}}$ and $|\Delta T|_{\mathrm{perm}} = 25$ mK for $s < 5.85\ \mathrm{kJ\,kg^{-1}\,K^{-1}}$.

Numerical Consistency Requirements in Pressure. In region 1, the permissible inconsistency between the pressure calculated from the backward equations/functions and the pressure calculated by iteration from the corresponding basic equation was set to $\pm 0.6\%$ for pressures less than or equal to 2.5 MPa and to ± 15 kPa for pressures greater than this value. For region 2 with $s < 5.85\ \mathrm{kJ\,kg^{-1}\,K^{-1}}$, corresponding to subregion 2c, the permissible numerical inconsistency in the calculated pressure amounts to $|\Delta p/p|_{\mathrm{perm}} = 0.0088\%$. For region 2 with $s \geq 5.85\ \mathrm{kJ\,kg^{-1}\,K^{-1}}$, corresponding to subregions 2a and 2b, the permissible inconsistency in pressure is $|\Delta p/p|_{\mathrm{perm}} = 0.0035\%$. For region 3 consisting of subregions 3a and 3b, it is $|\Delta p/p|_{\mathrm{perm}} = 0.01\%$.

At the critical point, the value 22.064 MPa for the critical pressure should be represented by the backward equations for all five figures. Therefore, the permissible inconsistency value was set to $|\Delta p/p|_{\mathrm{perm}} = 0.002\%$. The backward equations in the adjacent subregions 3a and 3b have to fulfil this requirement.

In the part of the two-phase region 4 with $s \geq s''(623.15\ \mathrm{K})$, which is important for steam turbine calculations, see Fig. 2.21, the permissible numerical inconsistency in pressure amounts to $|\Delta p/p|_{\mathrm{perm}} = 0.0035\%$ for $s \geq 5.85\ \mathrm{kJ\,kg^{-1}\,K^{-1}}$ and $|\Delta p/p|_{\mathrm{perm}} = 0.0088\%$ for $s < 5.85\ \mathrm{kJ\,kg^{-1}\,K^{-1}}$.

Numerical Consistency Requirements in Specific Volume. Backward equations/functions for specific volume are required in region 3 because the corresponding basic equation is defined as a function of the input variables density (the reciprocal value of specific volume) and temperature. The permissible difference between the specific volume calculated from the backward equations/functions and the specific volume calculated by iteration from the basic equation was determined to $\pm 0.01\%$ for the input variables (p,h), (p,s), and (h,s).

The functional dependence of the specific volume on pressure and temperature in region 3, see Fig.2.3, represents a special case for which $|\Delta v/v|_{\mathrm{perm}} = 0.001\%$. The permissible numerical inconsistencies for other properties will be given in Sec. 2.3.6.1. At the critical point, the value $v_{\mathrm{c}} = 0.003\,105\,59\ \mathrm{m^3\,kg^{-1}}$ should be represented by the backward equations/functions

for all six significant figures. Therefore, the permissible inconsistency value was set to $|\Delta v/v|_{\mathrm{perm}}$ = 0.0001%. The backward equations/functions in the adjacent subregions 3a and 3b have to meet this requirement.

Summary of the Permissible Inconsistencies. The permissible inconsistencies in temperature, pressure and specific volume between the backward equations/functions and the corresponding basic equation, presented in detail above, are summarized in Table 2.28.

Table 2.28 Permissible numerical inconsistencies $|\Delta T|_{\mathrm{perm}}$ in calculated temperatures, $|\Delta p/p|_{\mathrm{perm}}$ or $|\Delta p|_{\mathrm{perm}}$ in calculated pressures, and $|\Delta v/v|_{\mathrm{perm}}$ in calculated specific volumes between the backward equations/functions and the corresponding basic equation

Region		Subregion	$\|\Delta T\|_{\mathrm{perm}}$	$\|\Delta p/p\|_{\mathrm{perm}}$ or $\|\Delta p\|_{\mathrm{perm}}$	$\|\Delta v/v\|_{\mathrm{perm}}$
1			25 mK	$p \le 2.5$ MPa 0.6%	
				$p > 2.5$ MPa 15 kPa	
2	$s < 5.85$ kJ kg^{-1} K^{-1}	2c	25 mK	0.0088%	
	$s \ge 5.85$ kJ kg^{-1} K^{-1}	2a, 2b	10 mK	0.0035%	
3		3a, 3b	25 mK	0.001%	0.01% [a] 0.001% [b]
4	$s < 5.85$ kJ kg^{-1} K^{-1}		25 mK	0.0088%	
	$s \ge 5.85$ kJ kg^{-1} K^{-1}		10 mK	0.0035%	
Critical point		3a, 3b	0.49 mK	0.002%	0.0001%

[a] This value relates to the input variables (p,h), (p,s), and (h,s).
[b] This value relates to the input variables (p,T).

For example, the permissible inconsistency $|\Delta T|_{\mathrm{perm}}$ = 25 mK in region 1 means that the temperature value determined from the backward equations $T_1(p,h)$, $T_1(p,s)$ and the backward function $T_1(h,s)$ must agree within ±25 mK with the temperature value determined by iteration from the basic equation $g_1(p,T)$ for the same input values. The permissible value $|\Delta p/p|_{\mathrm{perm}}$ = 0.6% means that the difference between the pressure calculated from the backward equation $p_1(h,s)$ and the pressure determined by iteration from the basic equation $g_1(p,T)$ must be not greater than 0.6%.

2.3.3 Backward Equations as a Function of the Input Variables (p,h)

In this section, all of the backward equations as a function of (p,h) are summarized. These are the backward equations $T(p,h)$ for regions 1 to 3 and the backward equations $v(p,h)$ for region 3. When these equations are combined with the basic equations for regions 1 to 4, all other properties that are dependent on (p,h) can be calculated without iteration in the four regions.

The backward equations for regions 1 and 2 were developed and adopted together with the basic equations of IAPWS-IF97 [10, 15], whereas the backward equations for region 3 were developed later [12] and adopted by IAPWS in 2003 and in an expanded form in 2004 [23].

2.3.3.1 Regions and Region Boundaries in the Variables (p,h)

Figure 2.5 shows the regions and region boundaries in a pressure-enthalpy diagram along with the assignment of the backward equations $T(p,h)$ and $v(p,h)$ to regions 1 to 3. In order to avoid any iteration in practical calculations with IAPWS-IF97, the region boundaries must also be determinable without iterations. Therefore, a saturation-pressure equation as a function of enthalpy, $p_{s,3}(h)$, for the saturated-liquid and saturated-vapour lines between region 3 and region 4 was developed [12, 23] and is given as Eq. (2.18).

When property calculations with IAPWS-IF97 are carried out with the variables (p,h) as input variables, all tests to determine whether the given (p,h) point is within the range of regions 1 to 4 of IAPWS-IF97 and, if so, in which region, must be performed with respect to these input variables. To make such tests easier, the following subsections describe which equations are used to calculate the h values for given p values (or vice versa) along the respective region boundaries. These explanations are based on Fig. 2.5. Thus, Fig. 2.5 along with the description of the region boundaries given in Secs. 2.3.3.1a to 2.3.3.1c can be regarded as definitions of regions 1 to 4 of IAPWS-IF97 for the variables p and h.

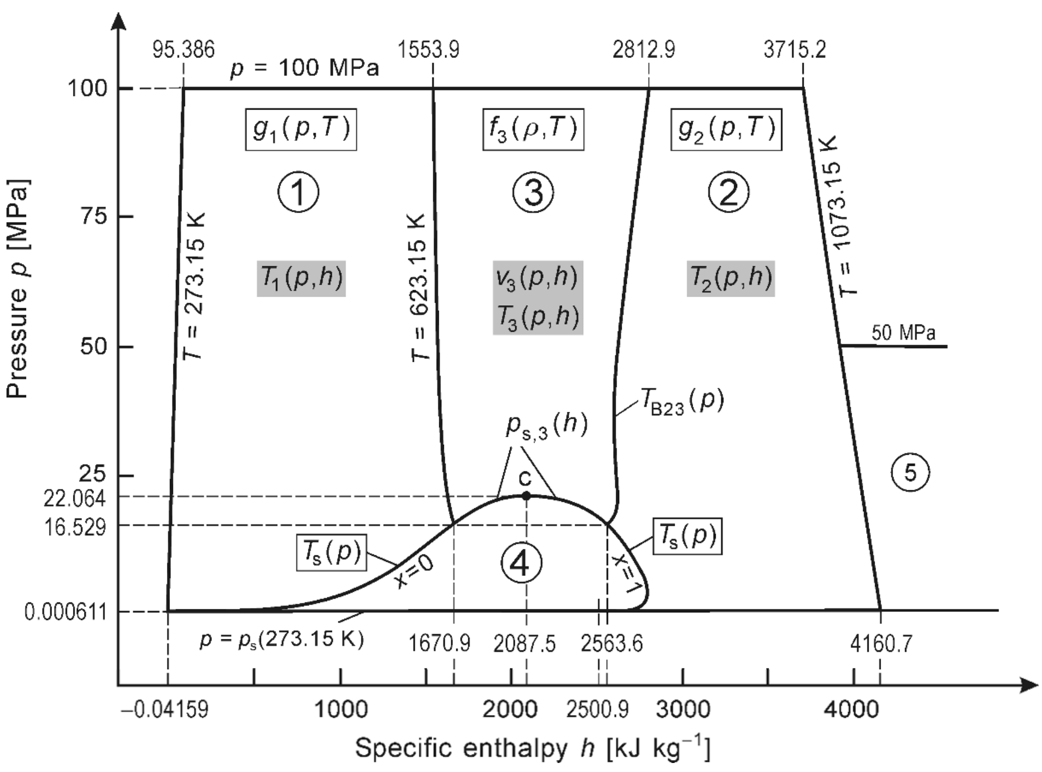

Fig. 2.5 Regions and region boundaries of IAPWS-IF97 for the variables (p,h). Assignment of the backward equations $T(p,h)$ and $v(p,h)$ to these regions (without showing how regions 2 and 3 will be divided into subregions). The p and h values given at the corner points of the region boundaries are rounded values.

a) Outer Boundaries of Regions 1 to 4

The description of the boundaries starts at the left-hand side of Fig. 2.5 with the isotherm $T = 273.15$ K and proceeds clockwise.

The Isotherm T = 273.15 K. This isotherm corresponds to the lowest temperature limit of IAPWS-IF97 and covers the pressure range given by

$$p_s(273.15\ \mathrm{K}) \le p \le 100\ \mathrm{MPa},$$

where p_s is calculated from the saturation-pressure equation $p_s(T)$, Eq. (2.13). Along this isotherm, the h value for the given p value is calculated from the basic equation of region 1, $g_1(p, T)$, Eq. (2.3), with $T = 273.15$ K. If the specific enthalpy h of a given (p,h) point is less than $h_1(p, 273.15\ \mathrm{K})$, then the (p,h) point is outside the range of validity of IAPWS-IF97, see Fig. 2.5.

The Isobar p = 100 MPa. This isobar is the upper pressure limit of the range of validity of IAPWS-IF97 (except for region 5). If the given pressure p is greater than 100 MPa, then the (p,h) point is outside the range of validity of IAPWS-IF97.

The Isotherm T = 1073.15 K. This isotherm corresponds to the upper temperature limit of IAPWS-IF97 (except for region 5) and covers the range of pressure

$$p_s(273.15\ \mathrm{K}) \le p \le 100\ \mathrm{MPa},$$

where p_s is calculated from the equation $p_s(T)$, Eq. (2.13). On this isotherm, the h value for the given p value is obtained from the basic equation of region 2, $g_2(p, T)$, Eq. (2.6), with $T =$ 1073.15 K. If the specific enthalpy h of the given (p,h) point is greater than $h_2(p, 1073.15\ \mathrm{K})$ for the given pressure p, then the (p,h) point is outside the range of IAPWS-IF97 for which the backward equations exist, see Fig. 2.5.

The Isobar p = p_s(273.15 K) = 0.000 611 212 677 MPa. This saturation pressure p_s is calculated from the equation $p_s(T)$, Eq. (2.13), and is the lower pressure limit of the range of validity of the IAPWS-IF97 backward equations. If the given pressure p is lower than $p = 0.000\,611\,212\,677$ MPa, then the (p,h) point is outside the range of validity of the backward equations, see Fig. 2.5.

b) Boundary between the Single-Phase Regions 1 to 3 and the Two-Phase Region 4

According to Fig. 2.5, the boundary between the single-phase regions 1 to 3 and the two-phase region 4 is given by the saturated-liquid line ($x = 0$) and the saturated-vapour line ($x = 1$).

Boundary between Regions 1 and 4. The part of the saturated-liquid line ($x = 0$) that forms the boundary between regions 1 and 4 covers a range of pressures given by

$$p_s(273.15\ \mathrm{K}) \le p \le p_s(623.15\ \mathrm{K}),$$

see Fig. 2.5; the p_s values are calculated from the equation $p_s(T)$, Eq. (2.13). Along this boundary, the h value for the given p value is determined from the basic equation $g_1(p, T)$, Eq. (2.3), where $T = T_s$ is obtained from the saturation-temperature equation $T_s(p)$, Eq. (2.14). The given enthalpy value can then be compared with the calculated value for h.

Boundary between Regions 3 and 4. The part of the saturated-liquid line and the saturated-vapour line that forms the boundary between regions 3 and 4 is given by the enthalpy range

$$h'(623.15\ \mathrm{K}) \le h \le h''(623.15\ \mathrm{K})$$
$$\text{with } h'(623.15\ \mathrm{K}) = h_1(p_s(623.15\ \mathrm{K}), 623.15\ \mathrm{K})$$
$$\text{and } h''(623.15\ \mathrm{K}) = h_2(p_s(623.15\ \mathrm{K}), 623.15\ \mathrm{K}),$$

where p_s is calculated from Eq. (2.13). In this relation, h_1 is calculated from the basic equation $g_1(p, T)$, Eq. (2.3), with $p = p_s(T)$ and $T = 623.15$ K. The enthalpy h_2 is obtained from the basic equation $g_2(p, T)$, Eq. (2.6), for $p = p_s(T)$ and $T = 623.15$ K. The reason for calculating the enthalpies h_1 and h_2 at these corner points from the basic equations for regions 1 and 2, $g_1(p, T)$ and $g_2(p, T)$, Eqs. (2.3) and (2.6), and not from the basic equation for region 3, $f_3(\rho, T)$, Eq. (2.11), is given at the beginning of Sec. 2.3.3.1c. Along this boundary, the p value for the given h value is calculated from the saturation-pressure equation as a function of enthalpy, $p_{s,3}(h)$, which is given in Sec. 2.3.3.1d as Eq. (2.18). The given pressure value can then be compared with the calculated value for p.

Boundary between Regions 2 and 4. The part of the saturated-vapour line ($x = 1$) that forms the boundary with region 2 covers the pressure range

$$p_s(273.15\ \mathrm{K}) \le p \le p_s(623.15\ \mathrm{K}),$$

see Fig. 2.5; the p_s values are calculated from the equation $p_s(T)$, Eq. (2.13). Along this boundary, the h value for the given p value is determined from the basic equation $g_2(p, T)$, Eq. (2.6), where $T = T_s$ is obtained from the saturation-temperature equation $T_s(p)$, Eq. (2.14). The given enthalpy value can then be compared with the calculated value for h.

c) Boundaries between the Single-Phase Regions

The boundaries between regions 1 and 3 ($T = 623.15$ K) and between regions 2 and 3 (T_{B23}-line) belong to both adjacent regions, see Figs. 2.2 and 2.5. However, in order to avoid to having two different values along these boundaries, the boundary between regions 1 and 3 is considered to belong to region 1 and the boundary between regions 2 and 3 is considered to belong to region 2. Thus, the properties along the boundary between regions 1 and 3 are calculated from the equations for region 1 and the properties along the boundary between regions 2 and 3 are determined from the equations for region 2. The calculations can be performed directly in this way; neither iteration nor additional use of any backward equation is required.

Boundary between Regions 1 and 3. The boundary that corresponds to the isotherm $T = 623.15$ K covers the pressure range

$$p_s(623.15\ \mathrm{K}) \le p \le 100\ \mathrm{MPa},$$

see Fig. 2.5; p_s is calculated from Eq. (2.13). Along this boundary, the h value for the given p value is determined from the basic equation $g_1(p, T)$, Eq. (2.3), with $T = 623.15$ K. The given enthalpy value can then be compared with the calculated value for h.

Boundary between Regions 2 and 3. This boundary, namely the T_{B23}-line, covers the pressure range

$$p_s(623.15\ \mathrm{K}) \le p \le 100\ \mathrm{MPa},$$

see Fig. 2.5; p_s is obtained from Eq. (2.13). Along this boundary, the h value for the given p value is calculated from the basic equation $g_2(p, T)$, Eq. (2.6), with $T = T_{B23}$ determined from the equation $T_{B23}(p)$, Eq. (2.2). The given enthalpy value can then be compared with the calculated value for h.

d) The Boundary Equation $p_{s,3}(h)$

The boundary equation $p_{s,3}(h)$ has the following dimensionless form:

$$\frac{p_{s,3}(h)}{p^*} = \pi(\eta) = \sum_{i=1}^{14} n_i (\eta - 1.02)^{I_i} (\eta - 0.608)^{J_i} \quad , \tag{2.18}$$

where $\pi = p/p^*$ and $\eta = h/h^*$ with $p^* = 22$ MPa and $h^* = 2600$ kJ kg^{-1}. The coefficients n_i and exponents I_i and J_i of Eq. (2.18) are listed in Table 2.29.

Table 2.29 Coefficients and exponents of the boundary equation $p_{s,3}(h)$ in its dimensionless form, Eq. (2.18)

i	I_i	J_i	n_i	i	I_i	J_i	n_i
1	0	0	0.600 073 641 753 024	8	8	24	$0.252\,304\,969\,384\,128 \times 10^{18}$
2	1	1	$-0.936\,203\,654\,849\,857 \times 10^{1}$	9	14	16	$-0.389\,718\,771\,997\,719 \times 10^{19}$
3	1	3	$0.246\,590\,798\,594\,147 \times 10^{2}$	10	20	16	$-0.333\,775\,713\,645\,296 \times 10^{23}$
4	1	4	$-0.107\,014\,222\,858\,224 \times 10^{3}$	11	22	3	$0.356\,499\,469\,636\,328 \times 10^{11}$
5	1	36	$-0.915\,821\,315\,805\,768 \times 10^{14}$	12	24	18	$-0.148\,547\,544\,720\,641 \times 10^{27}$
6	5	3	$-0.862\,332\,011\,700\,662 \times 10^{4}$	13	28	8	$0.330\,611\,514\,838\,798 \times 10^{19}$
7	7	0	$-0.235\,837\,344\,740\,032 \times 10^{2}$	14	36	24	$0.813\,641\,294\,467\,829 \times 10^{38}$

The equation $p_{s,3}(h)$, Eq. (2.18), describes the saturated-liquid line and the saturated-vapour line including the critical point in the following enthalpy range, see Fig. 2.5:

$$h'(623.15\text{ K}) \le h \le h''(623.15\text{ K}),$$
$$\text{where } h'(623.15\text{ K}) = h_1(p_s(623.15\text{ K}), 623.15\text{ K}) = 1.670\,858\,218\text{ kJ kg}^{-1}$$
$$\text{and } h''(623.15\text{ K}) = h_2(p_s(623.15\text{ K}), 623.15\text{ K}) = 2.563\,592\,004\text{ kJ kg}^{-1}.$$

Computer-Program Verification. To assist the user in computer-program verification of Eq. (2.18), Table 2.30 contains test values for calculated pressures.

Table 2.30 Pressure values calculated from the boundary equation $p_{s,3}(h)$, Eq. (2.18), for selected specific enthalpies [a]

Equation	h [kJ kg^{-1}]	p [MPa]
	1700	$1.724\,175\,718 \times 10^{1}$
$p_{s,3}(h)$, Eq. (2.18)	2000	$2.193\,442\,957 \times 10^{1}$
	2400	$2.018\,090\,839 \times 10^{1}$

[a] Programmed functions should be verified using 8 byte real values for all variables.

Note. For points extremely close to the boundary between the single-phase region 3 and the two-phase region 4, the following procedure is recommended. When calculating the pressure with the $p_{s,3}(h)$ equation, Eq. (2.18), its numerical inconsistency of 0.00043% in pressure with respect to the basic equation $p_s(T)$, Eq. (2.13), has to be considered. Due to this minor inconsistency the result of the calculated pressure should be corrected to $p_{s,3} = p_{s,3}(h)(1 - \Delta p/p)$, where $\Delta p/p = 4.3 \times 10^{-6}$. This procedure ensures that (p,h) points extremely close to the two-phase region are correctly assigned to the single-phase region and not falsely to the two-phase region.

2.3.3.2 Backward Equation T(p,h) for Region 1

Figure 2.6 shows the assignment of the backward equation $T_1(p,h)$ to region 1 in a *p-h* diagram. The boundaries of region 1 in *p-h* coordinates are described in Secs. 2.3.3.1a to 2.3.3.1c.

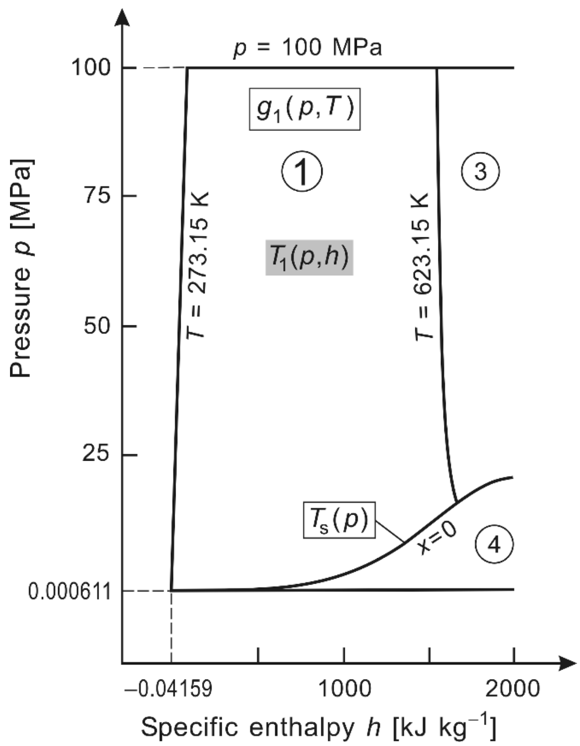

Fig. 2.6 Assignment of the backward equation $T_1(p,h)$ to region 1 in a *p-h* diagram. The *p* and *h* values at the corner points of region 1 are given in Fig. 2.5.

The backward equation $T_1(p,h)$ for region 1 has the following dimensionless form:

$$\frac{T_1(p,h)}{T^*} = \theta(\pi,\eta) = \sum_{i=1}^{20} n_i \, \pi^{I_i} (\eta+1)^{J_i} \quad , \tag{2.19}$$

where $\theta = T/T^*$, $\pi = p/p^*$, and $\eta = h/h^*$ with $T^* = 1\ \mathrm{K}$, $p^* = 1$ MPa, and $h^* = 2500\ \mathrm{kJ\ kg^{-1}}$. The coefficients n_i and exponents I_i and J_i of Eq. (2.19) are listed in Table 2.31.

Table 2.31 Coefficients and exponents of the backward equation $T_1(p,h)$ in its dimensionless form, Eq. (2.19)

i	I_i	J_i	n_i	i	I_i	J_i	n_i
1	0	0	$-0.238\,724\,899\,245\,21 \times 10^{3}$	11	1	4	$-0.659\,647\,494\,236\,38 \times 10^{1}$
2	0	1	$0.404\,211\,886\,379\,45 \times 10^{3}$	12	1	10	$0.939\,654\,008\,783\,63 \times 10^{-2}$
3	0	2	$0.113\,497\,468\,817\,18 \times 10^{3}$	13	1	32	$0.115\,736\,475\,053\,40 \times 10^{-6}$
4	0	6	$-0.584\,576\,160\,480\,39 \times 10^{1}$	14	2	10	$-0.258\,586\,412\,820\,73 \times 10^{-4}$
5	0	22	$-0.152\,854\,824\,131\,40 \times 10^{-3}$	15	2	32	$-0.406\,443\,630\,847\,99 \times 10^{-8}$
6	0	32	$-0.108\,667\,076\,953\,77 \times 10^{-5}$	16	3	10	$0.664\,561\,861\,916\,35 \times 10^{-7}$
7	1	0	$-0.133\,917\,448\,726\,02 \times 10^{2}$	17	3	32	$0.806\,707\,341\,030\,27 \times 10^{-10}$
8	1	1	$0.432\,110\,391\,835\,59 \times 10^{2}$	18	4	32	$-0.934\,777\,712\,139\,47 \times 10^{-12}$
9	1	2	$-0.540\,100\,671\,705\,06 \times 10^{2}$	19	5	32	$0.582\,654\,420\,206\,01 \times 10^{-14}$
10	1	3	$0.305\,358\,922\,039\,16 \times 10^{2}$	20	6	32	$-0.150\,201\,859\,535\,03 \times 10^{-16}$

Range of Validity. The range of validity of the backward equation $T_1(p,h)$, Eq. (2.19), can be derived from the graphical representation of region 1 in Fig. 2.5. The determination of the h values for given p values along the region boundaries is described in Secs. 2.3.3.1a to 2.3.3.1c.

Computer-Program Verification. To assist the user in computer-program verification of Eq. (2.19), Table 2.32 contains corresponding test values.

Numerical Consistency. The numerical inconsistency between the backward equation $T_1(p,h)$, Eq. (2.19), and the basic equation $g_1(p,T)$, Eq. (2.3), in comparison with the permissible inconsistency, given in Sec. 2.3.2, is listed in Table 2.33.

Note. When calculating properties in the range $p \le p_s(623.15\text{ K})$ and extremely close to the saturated-liquid line, Eq. (2.19) might yield temperatures $T_1(p,h) > T_s(p)$ due to the minor inconsistencies. In this case, the result of Eq. (2.19) must be corrected to $T_1 = T_s(p)$, where the saturation temperature $T_s(p)$ is calculated for the given pressure from Eq. (2.14).

Table 2.32 Temperature values calculated from the backward equation $T_1(p,h)$, Eq. (2.19), for selected pressures and specific enthalpies [a]

p [MPa]	h [kJ kg^{-1}]	T [K]
3	500	$0.391\,798\,509 \times 10^3$
80	500	$0.378\,108\,626 \times 10^3$
80	1500	$0.611\,041\,229 \times 10^3$

[a] Programmed functions should be verified using 8 byte real values for all variables.

Table 2.33 Maximum and root-mean-square inconsistency in temperature between the backward equation $T_1(p,h)$, Eq. (2.19), and the basic equation $g_1(p,T)$, Eq. (2.3), in comparison with the permissible inconsistency

Inconsistencies in temperature [mK]		
$\lvert\Delta T\rvert_{\text{perm}}$	$\lvert\Delta T\rvert_{\max}$	$(\Delta T)_{\text{RMS}}$
25	23.6	13.4

Computing Time. The calculation of temperature as a function of (p,h) with the backward equation $T_1(p,h)$, Eq. (2.19), is about 25 times faster than when using only the basic equation $g_1(p,T)$, Eq. (2.3), [19]. In this comparison, the basic equation was applied in combination with a one-dimensional Newton iteration with convergence tolerances corresponding to the consistency requirement that were set for the backward equation.

2.3.3.3 Backward Equations $T(p,h)$ for Region 2

The boundaries of region 2 in p-h coordinates are described in Secs. 2.3.3.1a to 2.3.3.1c. Due to the demand for very high numerical consistency between the basic equation $g_2(p,T)$, Eq. (2.6), and a backward equation $T(p,h)$ for region 2, given in Sec. 2.3.2, region 2 is divided into three subregions.

a) Division of Region 2 into Subregions 2a, 2b, and 2c

Figure 2.7 shows how region 2 is divided into three subregions for the backward equations $T(p,h)$. The boundary between subregions 2a and 2b is the isobar $p = 4$ MPa, and the boundary between subregions 2b and 2c is described by the equation $h_{2bc}(p)$, Eq. (2.21).

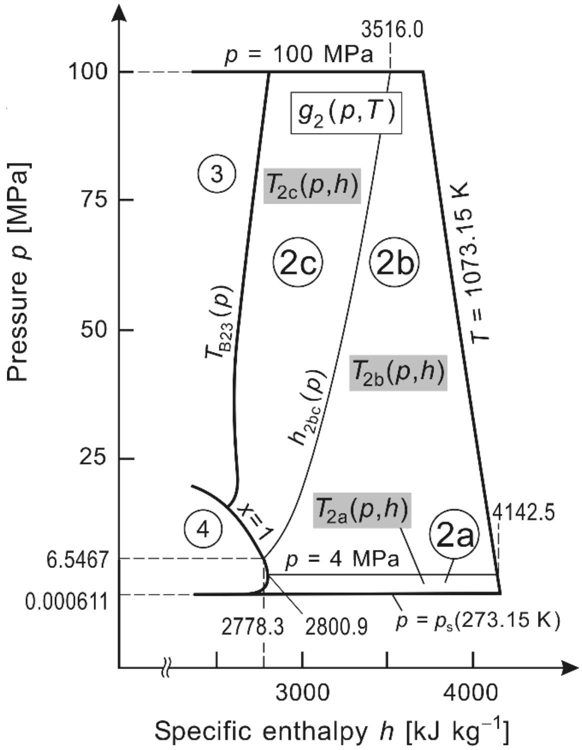

Fig. 2.7 Division of region 2 into subregions 2a, 2b, and 2c and the assignment of the backward equations $T(p,h)$ to these subregions. The p and h values at the corner points of region 2 are given in Fig. 2.5.

The equation for the boundary between subregions 2b and 2c is a simple quadratic pressure-enthalpy relation which reads

$$\frac{p_{2\mathrm{bc}}(h)}{p^*} = \pi(\eta) = n_1 + n_2\eta + n_3\eta^2 \quad , \tag{2.20}$$

where $\pi = p/p^*$ and $\eta = h/h^*$ with $p^* = 1$ MPa and $h^* = 1$ kJ kg^{-1}. The coefficients n_1 to n_3 of Eq. (2.20) are listed in Table 2.34. Equation (2.20) approximately describes the isentropic line $s = 5.85$ kJ kg^{-1} K^{-1}; the entropy values corresponding to this p-h relation are between $s = 5.81$ kJ kg^{-1} K^{-1} and $s = 5.85$ kJ kg^{-1} K^{-1}. If the subregion determination is not carried out via the function $p(h)$ but via $h(p)$, Eq. (2.21) can be used, which is the enthalpy-explicit form of Eq. (2.20), namely

$$\frac{h_{2\mathrm{bc}}(p)}{h^*} = \eta(\pi) = n_4 + \left[(\pi - n_5)/n_3\right]^{0.5} \tag{2.21}$$

with η and π according to Eq. (2.20) and the coefficients n_3 to n_5 listed in Table 2.34. Equations (2.20) and (2.21) define the boundary line between subregions 2b and 2c from the saturation state at $p_s = 6.546\,699\,678$ MPa and $h'' = 2778.265\,753$ kJ kg^{-1} to $p = 100$ MPa and $h = 3516.004\,323$ kJ kg^{-1}. Thus, the h value for the given p value along the boundary between subregions 2b and 2c can be directly calculated from the equation $h_{2\mathrm{bc}}(p)$, Eq. (2.21). The given enthalpy value can then be compared with the calculated value for h.

Note. To be in accordance with the statements given in [11, 22], the boundary between subregions 2a and 2b is considered to belong to subregion 2a and the boundary between subregions 2b and 2c is considered to belong to subregion 2b.

Table 2.34 Coefficients of the subregion-boundary equations $p_{2bc}(h)$ and $h_{2bc}(p)$ in their dimensionless forms, Eqs. (2.20) and (2.21)

i	n_i	i	n_i
1	$0.905\,842\,785\,147\,23 \times 10^{3}$	4	$0.265\,265\,719\,084\,28 \times 10^{4}$
2	$-0.679\,557\,863\,992\,41$	5	$0.452\,575\,789\,059\,48 \times 10^{1}$
3	$0.128\,090\,027\,301\,36 \times 10^{-3}$		

Computer-Program Verification. For computer-program verification, Eqs. (2.20) and (2.21) must meet the following *p*-*h* point: $p = 0.100\,000\,000 \times 10^{3}$ MPa , $h = 0.351\,600\,432\,3 \times 10^{4}$ kJ kg^{-1}.

b) The Backward Equations T(p,h) for Subregions 2a, 2b, and 2c

The backward equation $T_{2a}(p,h)$ for **subregion 2a** in its dimensionless form reads

$$\frac{T_{2a}(p,h)}{T^*} = \theta(\pi,\eta) = \sum_{i=1}^{34} n_i\, \pi^{I_i} (\eta - 2.1)^{J_i} \ , \tag{2.22}$$

where $\theta = T/T^*$, $\pi = p/p^*$, and $\eta = h/h^*$ with $T^* = 1$ K, $p^* = 1$ MPa, and $h^* = 2000$ kJ kg^{-1}. The coefficients n_i and exponents I_i and J_i of Eq. (2.22) are listed in Table 2.35.

The backward equation $T_{2b}(p,h)$ for **subregion 2b** in its dimensionless form reads

$$\frac{T_{2b}(p,h)}{T^*} = \theta(\pi,\eta) = \sum_{i=1}^{38} n_i (\pi - 2)^{I_i} (\eta - 2.6)^{J_i} \ , \tag{2.23}$$

where $\theta = T/T^*$, $\pi = p/p^*$, and $\eta = h/h^*$ with $T^* = 1$ K, $p^* = 1$ MPa, and $h^* = 2000$ kJ kg^{-1}. The coefficients n_i and exponents I_i and J_i of Eq. (2.23) are listed in Table 2.36.

The backward equation $T_{2c}(p,h)$ for **subregion 2c** in its dimensionless form reads

$$\frac{T_{2c}(p,h)}{T^*} = \theta(\pi,\eta) = \sum_{i=1}^{23} n_i (\pi + 25)^{I_i} (\eta - 1.8)^{J_i} \ , \tag{2.24}$$

where $\theta = T/T^*$, $\pi = p/p^*$, and $\eta = h/h^*$ with $T^* = 1$ K, $p^* = 1$ MPa, and $h^* = 2000$ kJ kg^{-1}. The coefficients n_i and exponents I_i and J_i of Eq. (2.24) are listed in Table 2.37.

Table 2.35 Coefficients and exponents of the backward equation $T_{2a}(p,h)$ for subregion 2a in its dimensionless form, Eq. (2.22)

i	I_i	J_i	n_i	i	I_i	J_i	n_i
1	0	0	$0.108\,989\,523\,182\,88 \times 10^{4}$	18	2	7	$0.116\,708\,730\,771\,07 \times 10^{2}$
2	0	1	$0.849\,516\,544\,955\,35 \times 10^{3}$	19	2	36	$0.128\,127\,984\,040\,46 \times 10^{9}$
3	0	2	$-0.107\,817\,480\,918\,26 \times 10^{3}$	20	2	38	$-0.985\,549\,096\,232\,76 \times 10^{9}$
4	0	3	$0.331\,536\,548\,012\,63 \times 10^{2}$	21	2	40	$0.282\,245\,469\,730\,02 \times 10^{10}$
5	0	7	$-0.742\,320\,167\,902\,48 \times 10^{1}$	22	2	42	$-0.359\,489\,714\,107\,03 \times 10^{10}$
6	0	20	$0.117\,650\,487\,243\,56 \times 10^{2}$	23	2	44	$0.172\,273\,499\,131\,97 \times 10^{10}$
7	1	0	$0.184\,457\,493\,557\,90 \times 10^{1}$	24	3	24	$-0.135\,513\,342\,407\,75 \times 10^{5}$
8	1	1	$-0.417\,927\,005\,496\,24 \times 10^{1}$	25	3	44	$0.128\,487\,346\,646\,50 \times 10^{8}$
9	1	2	$0.624\,781\,969\,358\,12 \times 10^{1}$	26	4	12	$0.138\,657\,242\,832\,26 \times 10^{1}$

Continued on next page.

Table 2.35 – Continued

i	I_i	J_i	n_i	i	I_i	J_i	n_i
10	1	3	$-0.173\,445\,631\,081\,14 \times 10^{2}$	27	4	32	$0.235\,988\,325\,565\,14 \times 10^{6}$
11	1	7	$-0.200\,581\,768\,620\,96 \times 10^{3}$	28	4	44	$-0.131\,052\,365\,450\,54 \times 10^{8}$
12	1	9	$0.271\,960\,654\,737\,96 \times 10^{3}$	29	5	32	$0.739\,998\,354\,747\,66 \times 10^{4}$
13	1	11	$-0.455\,113\,182\,858\,18 \times 10^{3}$	30	5	36	$-0.551\,966\,970\,300\,60 \times 10^{6}$
14	1	18	$0.309\,196\,886\,047\,55 \times 10^{4}$	31	5	42	$0.371\,540\,859\,962\,33 \times 10^{7}$
15	1	44	$0.252\,266\,403\,578\,72 \times 10^{6}$	32	6	34	$0.191\,277\,292\,396\,60 \times 10^{5}$
16	2	0	$-0.617\,074\,228\,683\,39 \times 10^{-2}$	33	6	44	$-0.415\,351\,648\,356\,34 \times 10^{6}$
17	2	2	$-0.310\,780\,466\,295\,83$	34	7	28	$-0.624\,598\,551\,925\,07 \times 10^{2}$

Table 2.36 Coefficients and exponents of the backward equation $T_{2b}(p,h)$ for subregion 2b in its dimensionless form, Eq. (2.23)

i	I_i	J_i	n_i	i	I_i	J_i	n_i
1	0	0	$0.148\,950\,410\,795\,16 \times 10^{4}$	20	2	40	$0.712\,803\,519\,595\,51 \times 10^{-4}$
2	0	1	$0.743\,077\,983\,140\,34 \times 10^{3}$	21	3	1	$0.110\,328\,317\,899\,99 \times 10^{-3}$
3	0	2	$-0.977\,083\,187\,978\,37 \times 10^{2}$	22	3	2	$0.189\,552\,483\,879\,02 \times 10^{-3}$
4	0	12	$0.247\,424\,647\,056\,74 \times 10^{1}$	23	3	12	$0.308\,915\,411\,605\,37 \times 10^{-2}$
5	0	18	$-0.632\,813\,200\,160\,26$	24	3	24	$0.135\,555\,045\,549\,49 \times 10^{-2}$
6	0	24	$0.113\,859\,521\,296\,58 \times 10^{1}$	25	4	2	$0.286\,402\,374\,774\,56 \times 10^{-6}$
7	0	28	$-0.478\,118\,636\,486\,25$	26	4	12	$-0.107\,798\,573\,575\,12 \times 10^{-4}$
8	0	40	$0.852\,081\,234\,315\,44 \times 10^{-2}$	27	4	18	$-0.764\,627\,124\,548\,14 \times 10^{-4}$
9	1	0	$0.937\,471\,473\,779\,32$	28	4	24	$0.140\,523\,928\,183\,16 \times 10^{-4}$
10	1	2	$0.335\,931\,186\,049\,16 \times 10^{1}$	29	4	28	$-0.310\,838\,143\,314\,34 \times 10^{-4}$
11	1	6	$0.338\,093\,556\,014\,54 \times 10^{1}$	30	4	40	$-0.103\,027\,382\,121\,03 \times 10^{-5}$
12	1	12	$0.168\,445\,396\,719\,04$	31	5	18	$0.282\,172\,816\,350\,40 \times 10^{-6}$
13	1	18	$0.738\,757\,452\,366\,95$	32	5	24	$0.127\,049\,022\,719\,45 \times 10^{-5}$
14	1	24	$-0.471\,287\,374\,361\,86$	33	5	40	$0.738\,033\,534\,682\,92 \times 10^{-7}$
15	1	28	$0.150\,202\,731\,397\,07$	34	6	28	$-0.110\,301\,392\,389\,09 \times 10^{-7}$
16	1	40	$-0.217\,641\,142\,197\,50 \times 10^{-2}$	35	7	2	$-0.814\,563\,652\,078\,33 \times 10^{-13}$
17	2	2	$-0.218\,107\,553\,247\,61 \times 10^{-1}$	36	7	28	$-0.251\,805\,456\,829\,62 \times 10^{-10}$
18	2	8	$-0.108\,297\,844\,036\,77$	37	9	1	$-0.175\,652\,339\,694\,07 \times 10^{-17}$
19	2	18	$-0.463\,333\,246\,358\,12 \times 10^{-1}$	38	9	40	$0.869\,341\,563\,441\,63 \times 10^{-14}$

Table 2.37 Coefficients and exponents of the backward equation $T_{2c}(p,h)$ for subregion 2c in its dimensionless form, Eq. (2.24)

i	I_i	J_i	n_i	i	I_i	J_i	n_i
1	−7	0	$-0.323\,683\,985\,552\,42 \times 10^{13}$	13	1	4	$0.379\,660\,012\,724\,86 \times 10^{1}$
2	−7	4	$0.732\,633\,509\,021\,81 \times 10^{13}$	14	1	8	$-0.108\,429\,848\,800\,77 \times 10^{2}$
3	−6	0	$0.358\,250\,899\,454\,47 \times 10^{12}$	15	2	4	$-0.453\,641\,726\,766\,60 \times 10^{-1}$
4	−6	2	$-0.583\,401\,318\,515\,90 \times 10^{12}$	16	6	0	$0.145\,591\,156\,586\,98 \times 10^{-12}$
5	−5	0	$-0.107\,830\,682\,174\,70 \times 10^{11}$	17	6	1	$0.112\,615\,974\,072\,30 \times 10^{-11}$
6	−5	2	$0.208\,255\,445\,631\,71 \times 10^{11}$	18	6	4	$-0.178\,049\,822\,406\,86 \times 10^{-10}$
7	−2	0	$0.610\,747\,835\,645\,16 \times 10^{6}$	19	6	10	$0.123\,245\,796\,908\,32 \times 10^{-6}$
8	−2	1	$0.859\,777\,225\,355\,80 \times 10^{6}$	20	6	12	$-0.116\,069\,211\,309\,84 \times 10^{-5}$
9	−1	0	$-0.257\,457\,236\,041\,70 \times 10^{5}$	21	6	16	$0.278\,463\,670\,885\,54 \times 10^{-4}$
10	−1	2	$0.310\,810\,884\,227\,14 \times 10^{5}$	22	6	20	$-0.592\,700\,384\,741\,76 \times 10^{-3}$
11	0	0	$0.120\,823\,158\,659\,36 \times 10^{4}$	23	6	22	$0.129\,185\,829\,918\,78 \times 10^{-2}$
12	0	1	$0.482\,197\,551\,092\,55 \times 10^{3}$				

Ranges of Validity. The ranges of validity of the backward equations $T_{2a}(p,h)$, $T_{2b}(p,h)$, and $T_{2c}(p,h)$, Eqs. (2.22) to (2.24), can be derived from the graphical representation of region 2 in Fig. 2.5 and of subregions 2a, 2b, and 2c in Fig. 2.7. The determination of the h values for given p values along the region boundaries is described in Secs. 2.3.3.1a to 2.3.3.1c and along the subregion boundaries in Sec. 2.3.3.3a.

Computer-Program Verification. To assist the user in computer-program verification of Eqs. (2.22) to (2.24), Table 2.38 contains corresponding test values.

Numerical Consistencies. The numerical inconsistencies between the backward equations $T_{2a}(p,h)$, $T_{2b}(p,h)$, and $T_{2c}(p,h)$, Eqs. (2.22) to (2.24), and the basic equation $g_2(p,T)$, Eq. (2.6), in comparison with the permissible inconsistencies, given in Sec. 2.3.2, are listed in Table 2.39.

Note. When calculating properties in the range $p \le p_s(623.15\text{ K})$ and extremely close to the saturated-vapour line, Eqs. (2.22) to (2.24) might yield temperatures $T_{2a}(p,h) < T_s(p)$, $T_{2b}(p,h) < T_s(p)$, and $T_{2c}(p,h) < T_s(p)$, respectively, due to the minor inconsistencies. In these cases, the results of Eqs. (2.22) to (2.24) must be corrected to $T_{2a} = T_s(p)$, $T_{2b} = T_s(p)$, and $T_{2c} = T_s(p)$, respectively, where the saturation temperature $T_s(p)$ is calculated for the given pressure from Eq. (2.14).

Table 2.38 Temperature values calculated from the backward equations $T_{2a}(p,h)$, $T_{2b}(p,h)$, and $T_{2c}(p,h)$, Eqs. (2.22) to (2.24), for selected pressures and specific enthalpies [a]

Equation	p [MPa]	h [kJ kg^{-1}]	T [K]
$T_{2a}(p,h)$, Eq. (2.22)	0.001	3000	$0.534\,433\,241 \times 10^3$
	3	3000	$0.575\,373\,370 \times 10^3$
	3	4000	$0.101\,077\,577 \times 10^4$
$T_{2b}(p,h)$, Eq. (2.23)	5	3500	$0.801\,299\,102 \times 10^3$
	5	4000	$0.101\,531\,583 \times 10^4$
	25	3500	$0.875\,279\,054 \times 10^3$
$T_{2c}(p,h)$, Eq. (2.24)	40	2700	$0.743\,056\,411 \times 10^3$
	60	2700	$0.791\,137\,067 \times 10^3$
	60	3200	$0.882\,756\,860 \times 10^3$

[a] Programmed functions should be verified using 8 byte real values for all variables.

Table 2.39 Maximum and root-mean-square inconsistencies in temperature between the backward equations $T_{2a}(p,h)$, $T_{2b}(p,h)$, and $T_{2c}(p,h)$, Eqs. (2.22) to (2.24), and the basic equation $g_2(p,T)$, Eq. (2.6), in comparison with the permissible inconsistencies

Subregion	Equation	Inconsistencies in temperature [mK]		
		$\lvert\Delta T\rvert_{\text{perm}}$	$\lvert\Delta T\rvert_{\text{max}}$	$(\Delta T)_{\text{RMS}}$
2a	$T_{2a}(p,h)$, Eq. (2.22)	10	9.3	2.9
2b	$T_{2b}(p,h)$, Eq. (2.23)	10	9.6	3.9
2c	$T_{2c}(p,h)$, Eq. (2.24)	25	23.7	10.4

c) Computing Time when Using the Backward Equations T(p,h) in Comparison with the Basic Equation

The calculation of temperature as a function of (p, h) with the backward equations $T_{2a}(p, h)$, $T_{2b}(p, h)$, or $T_{2c}(p, h)$, Eqs. (2.22) to (2.24), is about 11 times faster than when using only the basic equation $g_2(p, T)$, Eq. (2.6), [19]. In this comparison, the basic equation was applied in combination with a one-dimensional Newton iteration with convergence tolerances corresponding to the consistency requirements that were set for the backward equations.

2.3.3.4 Backward Equations $v(p,h)$ and $T(p,h)$ for Region 3

The boundaries of region 3 in p-h coordinates are described in Secs. 2.3.3.1a to 2.3.3.1c.

a) Division of Region 3 into Subregions 3a and 3b

Due to the demand for very high numerical consistency between the backward equations for this region and the basic equation $f_3(\rho, T)$, Eq. (2.11), as given in Sec. 2.3.2, region 3 is divided into two subregions as illustrated in Fig. 2.8.

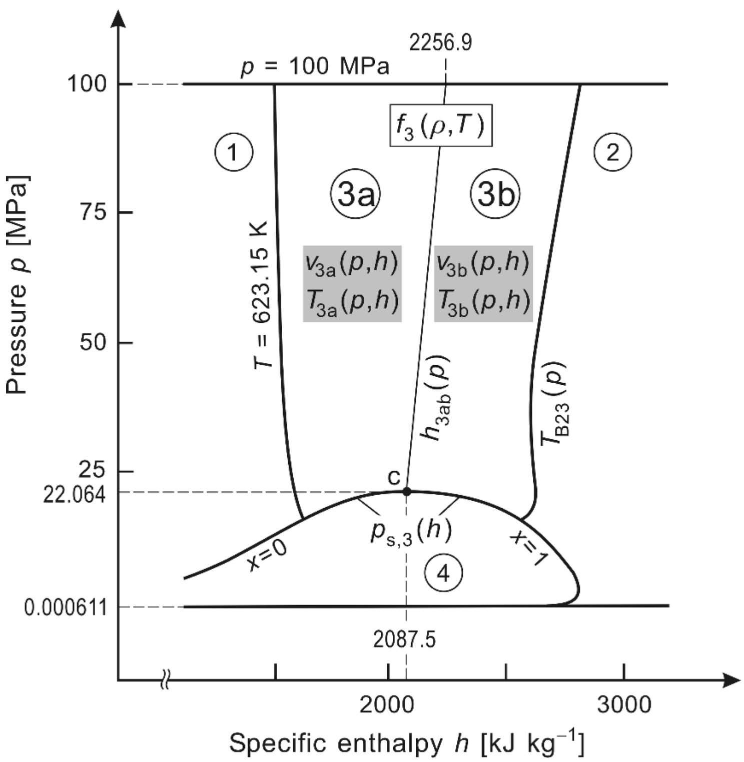

Fig. 2.8 Division of region 3 into subregions 3a and 3b, and the assignment of the backward equations $v(p,h)$ and $T(p,h)$ to these subregions. The p and h values at the corner points of region 3 are given in Fig. 2.5.

The boundary between subregions 3a and 3b is defined by the equation $h_{3ab}(p)$, which reads in its dimensionless form

$$\frac{h_{3ab}(p)}{h^*} = \eta(\pi) = n_1 + n_2\pi + n_3\pi^2 + n_4\pi^3 \,, \tag{2.25}$$

where $\eta = h/h^*$ and $\pi = p/p^*$ with $h^* = 1\ \mathrm{kJ\,kg^{-1}}$ and $p^* = 1$ MPa. The coefficients n_1 to n_4 of Eq. (2.25) are listed in Table 2.40. The equation $h_{3ab}(p)$ describes this subregion boundary from the critical point ($p_c = 22.064$ MPa, $h_c = 2087.546\,845\ \mathrm{kJ\,kg^{-1}}$) to 100 MPa at $h = 2256.927\,860\ \mathrm{kJ\,kg^{-1}}$. Equation (2.25) approximates the critical isentropic line $s = s_c$, Eq. (2.35), where the maximum deviation from this line amounts to $0.000\,66\ \mathrm{kJ\,kg^{-1}\,K^{-1}}$. The given enthalpy value can then be compared with the calculated value for h.

Table 2.40 Coefficients of the subregion-boundary equation $h_{3ab}(p)$ in its dimensionless form, Eq. (2.25), for defining the boundary between subregions 3a and 3b

i	n_i	i	n_i
1	$0.201\,464\,004\,206\,875 \times 10^{4}$	3	$-0.219\,921\,901\,054\,187 \times 10^{-1}$
2	$0.374\,696\,550\,136\,983 \times 10^{1}$	4	$0.875\,131\,686\,009\,950 \times 10^{-4}$

Note. The boundary between subregions 3a and 3b is considered to belong to subregion 3a [12, 23].

Computer-Program Verification. For computer-program verification, Eq. (2.25) yields the following p-h point: $p = 25$ MPa, $h_{3ab}(p) = 2.095\,936\,454 \times 10^3\ \mathrm{kJ\ kg^{-1}}$.

b) Backward Equations v(p,h) for Subregions 3a and 3b

The backward equation $v_{3a}(p,h)$ for **subregion 3a** has the following dimensionless form:

$$\frac{v_{3a}(p,h)}{v^*} = \omega(\pi,\eta) = \sum_{i=1}^{32} n_i\,(\pi + 0.128)^{I_i}\,(\eta - 0.727)^{J_i}\ , \tag{2.26}$$

where $\omega = v/v^*$, $\pi = p/p^*$, and $\eta = h/h^*$ with $v^* = 0.0028\ \mathrm{m^3\ kg^{-1}}$, $p^* = 100$ MPa, and $h^* = 2100\ \mathrm{kJ\ kg^{-1}}$. The coefficients n_i and exponents I_i and J_i of Eq. (2.26) are listed in Table 2.41.

The backward equation $v_{3b}(p,h)$ for **subregion 3b** has the following dimensionless form:

$$\frac{v_{3b}(p,h)}{v^*} = \omega(\pi,\eta) = \sum_{i=1}^{30} n_i\,(\pi + 0.0661)^{I_i}\,(\eta - 0.720)^{J_i}\ , \tag{2.27}$$

where $\omega = v/v^*$, $\pi = p/p^*$, and $\eta = h/h^*$ with $v^* = 0.0088\ \mathrm{m^3\ kg^{-1}}$, $p^* = 100$ MPa, and $h^* = 2800\ \mathrm{kJ\ kg^{-1}}$. The coefficients n_i and exponents I_i and J_i of Eq. (2.27) are listed in Table 2.42.

Table 2.41 Coefficients and exponents of the backward equation $v_{3a}(p,h)$ for subregion 3a in its dimensionless form, Eq. (2.26)

i	I_i	J_i	n_i	i	I_i	J_i	n_i
1	−12	6	$0.529\,944\,062\,966\,028 \times 10^{-2}$	17	−2	16	$0.568\,366\,875\,815\,960 \times 10^{4}$
2	−12	8	$-0.170\,099\,690\,234\,461$	18	−1	0	$0.808\,169\,540\,124\,668 \times 10^{-2}$
3	−12	12	$0.111\,323\,814\,312\,927 \times 10^{2}$	19	−1	1	$0.172\,416\,341\,519\,307$
4	−12	18	$-0.217\,898\,123\,145\,125 \times 10^{4}$	20	−1	2	$0.104\,270\,175\,292\,927 \times 10^{1}$
5	−10	4	$-0.506\,061\,827\,980\,875 \times 10^{-3}$	21	−1	3	$-0.297\,691\,372\,792\,847$
6	−10	7	$0.556\,495\,239\,685\,324$	22	0	0	$0.560\,394\,465\,163\,593$
7	−10	10	$-0.943\,672\,726\,094\,016 \times 10^{1}$	23	0	1	$0.275\,234\,661\,176\,914$
8	−8	5	$-0.297\,856\,807\,561\,527$	24	1	0	$-0.148\,347\,894\,866\,012$
9	−8	12	$0.939\,353\,943\,717\,186 \times 10^{2}$	25	1	1	$-0.651\,142\,513\,478\,515 \times 10^{-1}$

Continued on next page.

Table 2.41 – Continued

i	I_i	J_i	n_i	i	I_i	J_i	n_i
10	−6	3	$0.192\,944\,939\,465\,981 \times 10^{-1}$	26	1	2	$-0.292\,468\,715\,386\,302 \times 10^{1}$
11	−6	4	$0.421\,740\,664\,704\,763$	27	2	0	$0.664\,876\,096\,952\,665 \times 10^{-1}$
12	−6	22	$-0.368\,914\,126\,282\,330 \times 10^{7}$	28	2	2	$0.352\,335\,014\,263\,844 \times 10^{1}$
13	−4	2	$-0.737\,566\,847\,600\,639 \times 10^{-2}$	29	3	0	$-0.146\,340\,792\,313\,332 \times 10^{-1}$
14	−4	3	$-0.354\,753\,242\,424\,366$	30	4	2	$-0.224\,503\,486\,668\,184 \times 10^{1}$
15	−3	7	$-0.199\,768\,169\,338\,727 \times 10^{1}$	31	5	2	$0.110\,533\,464\,706\,142 \times 10^{1}$
16	−2	3	$0.115\,456\,297\,059\,049 \times 10^{1}$	32	8	2	$-0.408\,757\,344\,495\,612 \times 10^{-1}$

Table 2.42 Coefficients and exponents of the backward equation $v_{3b}(p,h)$ for subregion 3b in its dimensionless form, Eq. (2.27)

i	I_i	J_i	n_i	i	I_i	J_i	n_i
1	−12	0	$-0.225\,196\,934\,336\,318 \times 10^{-8}$	16	−4	6	$-0.321\,087\,965\,668\,917 \times 10^{1}$
2	−12	1	$0.140\,674\,363\,313\,486 \times 10^{-7}$	17	−4	10	$0.607\,567\,815\,637\,771 \times 10^{3}$
3	−8	0	$0.233\,784\,085\,280\,560 \times 10^{-5}$	18	−3	0	$0.557\,686\,450\,685\,932 \times 10^{-3}$
4	−8	1	$-0.331\,833\,715\,229\,001 \times 10^{-4}$	19	−3	2	$0.187\,499\,040\,029\,550$
5	−8	3	$0.107\,956\,778\,514\,318 \times 10^{-2}$	20	−2	1	$0.905\,368\,030\,448\,107 \times 10^{-2}$
6	−8	6	$-0.271\,382\,067\,378\,863$	21	−2	2	$0.285\,417\,173\,048\,685$
7	−8	7	$0.107\,202\,262\,490\,333 \times 10^{1}$	22	−1	0	$0.329\,924\,030\,996\,098 \times 10^{-1}$
8	−8	8	$-0.853\,821\,329\,075\,382$	23	−1	1	$0.239\,897\,419\,685\,483$
9	−6	0	$-0.215\,214\,194\,340\,526 \times 10^{-4}$	24	−1	4	$0.482\,754\,995\,951\,394 \times 10^{1}$
10	−6	1	$0.769\,656\,088\,222\,730 \times 10^{-3}$	25	−1	5	$-0.118\,035\,753\,702\,231 \times 10^{2}$
11	−6	2	$-0.431\,136\,580\,433\,864 \times 10^{-2}$	26	0	0	$0.169\,490\,044\,091\,791$
12	−6	5	$0.453\,342\,167\,309\,331$	27	1	0	$-0.179\,967\,222\,507\,787 \times 10^{-1}$
13	−6	6	$-0.507\,749\,535\,873\,652$	28	1	1	$0.371\,810\,116\,332\,674 \times 10^{-1}$
14	−6	10	$-0.100\,475\,154\,528\,389 \times 10^{3}$	29	2	2	$-0.536\,288\,335\,065\,096 \times 10^{-1}$
15	−4	3	$-0.219\,201\,924\,648\,793$	30	2	6	$0.160\,697\,101\,092\,520 \times 10^{1}$

Ranges of Validity. The ranges of validity of the backward equations $v_{3a}(p,h)$ and $v_{3b}(p,h)$, Eqs. (2.26) and (2.27), can be derived from the graphical representation of region 3 in Fig. 2.5 and of subregions 3a and 3b in Fig. 2.8. The determination of the h values for given p values along the region boundaries is described in Secs. 2.3.3.1a to 2.3.3.1c and along the subregion boundary in Sec. 2.3.3.4a.

Computer-Program Verification. To assist the user in computer-program verification of Eqs. (2.26) and (2.27), Table 2.43 contains test values for calculated specific volumes.

Table 2.43 Values of the specific volume calculated from the backward equations $v_{3a}(p,h)$ and $v_{3b}(p,h)$, Eqs. (2.26) and (2.27), for selected pressures and specific enthalpies [a]

Equation	p [MPa]	h [kJ kg^{-1}]	v [m^3 kg^{-1}]
$v_{3a}(p,h)$, Eq. (2.26)	20	1700	$1.749\,903\,962 \times 10^{-3}$
	50	2000	$1.908\,139\,035 \times 10^{-3}$
	100	2100	$1.676\,229\,776 \times 10^{-3}$
$v_{3b}(p,h)$, Eq. (2.27)	20	2500	$6.670\,547\,043 \times 10^{-3}$
	50	2400	$2.801\,244\,590 \times 10^{-3}$
	100	2700	$2.404\,234\,998 \times 10^{-3}$

[a] Programmed functions should be verified using 8 byte real values for all variables.

Numerical Consistencies. The numerical inconsistencies between the backward equations $v_{3a}(p,h)$ and $v_{3b}(p,h)$, Eqs. (2.26) and (2.27), and the basic equation $f_3(\rho,T)$, Eq. (2.11), are listed in Table 2.44 in comparison with the permissible inconsistencies given in Sec. 2.3.2. These inconsistencies are less than the permissible values. This is also true when the backward equations are used in combination with the boundary equation $p_{s,3}(h)$, Eq. (2.18). The critical volume $v_c = 1/\rho_c = (1/322)\ \mathrm{m^3\,kg^{-1}} = 0.003\,105\,59\ \mathrm{m^3\,kg^{-1}}$ is calculated by the two $v(p,h)$ equations for the given six significant figures. The maximum inconsistency in specific volume between the two backward equations, Eq. (2.26) and Eq. (2.27), along the subregion boundary $h_{3ab}(p)$, Eq. (2.25), amounts to 0.000 15%, which is within the permissible inconsistency given in Sec. 2.3.2.

Table 2.44 Maximum and root-mean-square inconsistencies in specific volume between the backward equations $v_{3a}(p,h)$ and $v_{3b}(p,h)$, Eqs. (2.26) and (2.27), and the basic equation $f_3(\rho,T)$, Eq. (2.11), in comparison with the permissible inconsistencies

Subregion	Equation	Inconsistencies in specific volume [%]		
		$\lvert\Delta v/v\rvert_{\mathrm{perm}}$	$\lvert\Delta v/v\rvert_{\mathrm{max}}$	$(\Delta v/v)_{\mathrm{RMS}}$
3a	$v_{3a}(p,h)$, Eq. (2.26)	0.01	0.0080	0.0032
3b	$v_{3b}(p,h)$, Eq. (2.27)	0.01	0.0095	0.0042

Computing Time. A statement about the computing time is given in Sec. 2.3.3.4d.

c) Backward Equations $T(p,h)$ for Subregions 3a and 3b

The backward equation $T_{3a}(p,h)$ for **subregion 3a** has the following dimensionless form:

$$\frac{T_{3a}(p,h)}{T^*} = \theta(\pi,\eta) = \sum_{i=1}^{31} n_i\,(\pi + 0.240)^{I_i}\,(\eta - 0.615)^{J_i}\ , \tag{2.28}$$

where $\theta = T/T^*$, $\pi = p/p^*$, and $\eta = h/h^*$ with $T^* = 760$ K, $p^* = 100$ MPa, and $h^* = 2300\ \mathrm{kJ\,kg^{-1}}$. The coefficients n_i and exponents I_i and J_i of Eq. (2.28) are listed in Table 2.45.

The backward equation $T_{3b}(p,h)$ for **subregion 3b** has the following dimensionless form:

$$\frac{T_{3b}(p,h)}{T^*} = \theta(\pi,\eta) = \sum_{i=1}^{33} n_i\,(\pi + 0.298)^{I_i}\,(\eta - 0.720)^{J_i}\ , \tag{2.29}$$

where $\theta = T/T^*$, $\pi = p/p^*$, and $\eta = h/h^*$ with $T^* = 860$ K, $p^* = 100$ MPa, and $h^* = 2800\ \mathrm{kJ\,kg^{-1}}$. The coefficients n_i and exponents I_i and J_i of Eq. (2.29) are listed in Table 2.46.

Table 2.45 Coefficients and exponents of the backward equation $T_{3a}(p,h)$ for subregion 3a in its dimensionless form, Eq. (2.28)

i	I_i	J_i	n_i	i	I_i	J_i	n_i
1	−12	0	$-0.133\,645\,667\,811\,215 \times 10^{-6}$	17	−3	0	$-0.384\,460\,997\,596\,657 \times 10^{-5}$
2	−12	1	$0.455\,912\,656\,802\,978 \times 10^{-5}$	18	−2	1	$0.337\,423\,807\,911\,655 \times 10^{-2}$
3	−12	2	$-0.146\,294\,640\,700\,979 \times 10^{-4}$	19	−2	3	$-0.551\,624\,873\,066\,791$
4	−12	6	$0.639\,341\,312\,970\,080 \times 10^{-2}$	20	−2	4	$0.729\,202\,277\,107\,470$
5	−12	14	$0.372\,783\,927\,268\,847 \times 10^{3}$	21	−1	0	$-0.992\,522\,757\,376\,041 \times 10^{-2}$
6	−12	16	$-0.718\,654\,377\,460\,447 \times 10^{4}$	22	−1	2	$-0.119\,308\,831\,407\,288$
7	−12	20	$0.573\,494\,752\,103\,400 \times 10^{6}$	23	0	0	$0.793\,929\,190\,615\,421$
8	−12	22	$-0.267\,569\,329\,111\,439 \times 10^{7}$	24	0	1	$0.454\,270\,731\,799\,386$
9	−10	1	$-0.334\,066\,283\,302\,614 \times 10^{-4}$	25	1	1	$0.209\,998\,591\,259\,910$
10	−10	5	$-0.245\,479\,214\,069\,597 \times 10^{-1}$	26	3	0	$-0.642\,109\,823\,904\,738 \times 10^{-2}$
11	−10	12	$0.478\,087\,847\,764\,996 \times 10^{2}$	27	3	1	$-0.235\,155\,868\,604\,540 \times 10^{-1}$
12	−8	0	$0.764\,664\,131\,818\,904 \times 10^{-5}$	28	4	0	$0.252\,233\,108\,341\,612 \times 10^{-2}$
13	−8	2	$0.128\,350\,627\,676\,972 \times 10^{-2}$	29	4	3	$-0.764\,885\,133\,368\,119 \times 10^{-2}$
14	−8	4	$0.171\,219\,081\,377\,331 \times 10^{-1}$	30	10	4	$0.136\,176\,427\,574\,291 \times 10^{-1}$
15	−8	10	$-0.851\,007\,304\,583\,213 \times 10^{1}$	31	12	5	$-0.133\,027\,883\,575\,669 \times 10^{-1}$
16	−5	2	$-0.136\,513\,461\,629\,781 \times 10^{-1}$				

Table 2.46 Coefficients and exponents of the backward equation $T_{3b}(p,h)$ for subregion 3b in its dimensionless form, Eq. (2.29)

i	I_i	J_i	n_i	i	I_i	J_i	n_i
1	−12	0	$0.323\,254\,573\,644\,920 \times 10^{-4}$	18	−3	5	$-0.307\,622\,221\,350\,501 \times 10^{1}$
2	−12	1	$-0.127\,575\,556\,587\,181 \times 10^{-3}$	19	−2	0	$-0.574\,011\,959\,864\,879 \times 10^{-1}$
3	−10	0	$-0.475\,851\,877\,356\,068 \times 10^{-3}$	20	−2	4	$0.503\,471\,360\,939\,849 \times 10^{1}$
4	−10	1	$0.156\,183\,014\,181\,602 \times 10^{-2}$	21	−1	2	$-0.925\,081\,888\,584\,834$
5	−10	5	$0.105\,724\,860\,113\,781$	22	−1	4	$0.391\,733\,882\,917\,546 \times 10^{1}$
6	−10	10	$-0.858\,514\,221\,132\,534 \times 10^{2}$	23	−1	6	$-0.773\,146\,007\,130\,190 \times 10^{2}$
7	−10	12	$0.724\,140\,095\,480\,911 \times 10^{3}$	24	−1	10	$0.949\,308\,762\,098\,587 \times 10^{4}$
8	−8	0	$0.296\,475\,810\,273\,257 \times 10^{-2}$	25	−1	14	$-0.141\,043\,719\,679\,409 \times 10^{7}$
9	−8	1	$-0.592\,721\,983\,365\,988 \times 10^{-2}$	26	−1	16	$0.849\,166\,230\,819\,026 \times 10^{7}$
10	−8	2	$-0.126\,305\,422\,818\,666 \times 10^{-1}$	27	0	0	$0.861\,095\,729\,446\,704$
11	−8	4	$-0.115\,716\,196\,364\,853$	28	0	2	$0.323\,346\,442\,811\,720$
12	−8	10	$0.849\,000\,969\,739\,595 \times 10^{2}$	29	1	1	$0.873\,281\,936\,020\,439$
13	−6	0	$-0.108\,602\,260\,086\,615 \times 10^{-1}$	30	3	1	$-0.436\,653\,048\,526\,683$
14	−6	1	$0.154\,304\,475\,328\,851 \times 10^{-1}$	31	5	1	$0.286\,596\,714\,529\,479$
15	−6	2	$0.750\,455\,441\,524\,466 \times 10^{-1}$	32	6	1	$-0.131\,778\,331\,276\,228$
16	−4	0	$0.252\,520\,973\,612\,982 \times 10^{-1}$	33	8	1	$0.676\,682\,064\,330\,275 \times 10^{-2}$
17	−4	1	$-0.602\,507\,901\,232\,996 \times 10^{-1}$				

Ranges of Validity. The ranges of validity of the backward equations $T_{3a}(p,h)$ and $T_{3b}(p,h)$, Eqs. (2.28) and (2.29), can be derived from the graphical representation of region 3 in Fig. 2.5 and of subregions 3a and 3b in Fig. 2.8. The determination of the h values for given p values along the region boundaries and the subregion boundary is described in Secs. 2.3.3.1a to 2.3.3.1c and in Sec. 2.3.3.4a.

Computer-Program Verification. To assist the user in computer-program verification of Eqs. (2.28) and (2.29), Table 2.47 contains test values for calculated temperatures.

Table 2.47 Temperature values calculated from the backward equations $T_{3a}(p,h)$ and $T_{3b}(p,h)$, Eqs. (2.28) and (2.29), for selected pressures and specific enthalpies [a]

Equation	p [MPa]	h [kJ kg^{-1}]	T [K]
$T_{3a}(p,h)$, Eq. (2.28)	20	1700	$6.293\,083\,892 \times 10^2$
	50	2000	$6.905\,718\,338 \times 10^2$
	100	2100	$7.336\,163\,014 \times 10^2$
$T_{3b}(p,h)$, Eq. (2.29)	20	2500	$6.418\,418\,053 \times 10^2$
	50	2400	$7.351\,848\,618 \times 10^2$
	100	2700	$8.420\,460\,876 \times 10^2$

[a] Programmed functions should be verified using 8 byte real values for all variables.

Numerical Consistencies. The numerical inconsistencies between the backward equations $T_{3a}(p,h)$ and $T_{3b}(p,h)$, Eqs. (2.28) and (2.29), and the basic equation $f_3(\rho,T)$, Eq. (2.11), are listed in Table 2.48 in comparison with the permissible inconsistencies given in Sec. 2.3.2. These inconsistencies are less than the permissible values. This is also true when the backward equations are used in combination with the boundary equation $p_{s,3}(h)$, Eq. (2.18). The critical temperature $T_c = 647.096$ K is calculated using the two $T(p,h)$ equations for all six figures. The maximum temperature difference between the two backward equations, Eq. (2.28) and Eq. (2.29), along the subregion boundary $h_{3ab}(p)$, Eq. (2.25), amounts to 0.37 mK. All of these inconsistency values are within the permissible values given in Sec. 2.3.2.

Note. When calculating properties in the range $p \le p_c$ and extremely close to the saturation lines, Eq. (2.28) might yield temperatures $T_{3a}(p,h) > T_s(p)$ and Eq. (2.29) might yield temperatures $T_{3b}(p,h) < T_s(p)$ due to the minor inconsistencies. In these cases, the results of Eqs. (2.28) and (2.29) must be corrected to $T_{3a} = T_s(p)$ and $T_{3b} = T_s(p)$, respectively, where the saturation temperature $T_s(p)$ is calculated from Eq. (2.14) for the given pressure.

Table 2.48 Maximum and root-mean-square inconsistencies in temperature between the backward equations $T_{3a}(p,h)$ and $T_{3b}(p,h)$, Eqs. (2.28) and (2.29), and the basic equation $f_3(\rho,T)$, Eq. (2.11), in comparison with the permissible values

		Inconsistencies in temperature [mK]		
Subregion	Equation	$\lvert\Delta T\rvert_{\text{perm}}$	$\lvert\Delta T\rvert_{\max}$	$(\Delta T)_{\text{RMS}}$
3a	$T_{3a}(p,h)$, Eq. (2.28)	25	23.6	10.5
3b	$T_{3b}(p,h)$, Eq. (2.29)	25	19.6	9.6

d) Computing Time when Using the Backward Equations $T(p,h)$ and $v(p,h)$ in Comparison with the Basic Equation

The calculation of specific volume and temperature as a function of (p,h) with the backward equations $v_{3a}(p,h)$ and $T_{3a}(p,h)$, Eqs. (2.26) and (2.28), or $v_{3b}(p,h)$ and $T_{3b}(p,h)$, Eqs. (2.27) and (2.29), is about 14 times faster than when using only the basic equation $f_3(\rho,T)$, Eq. (2.11), [19]. In this comparison, the basic equation was applied in combination with a two-dimensional Newton iteration with convergence tolerances corresponding to the consistency requirements that were set for the backward equations.

2.3.4 Backward Equations as a Function of the Input Variables (p,s)

In this section, all of the backward equations as a function of (p,s) are summarized. These are the backward equations $T(p,s)$ for regions 1 to 3 and the backward equations $v(p,s)$ for region 3. When these equations are combined with the basic equations for regions 1 to 4, all properties that are dependent on (p,s) can be calculated without iteration in the four regions.

The backward equations for regions 1 and 2 were developed and adopted together with the basic equations of IAPWS-IF97 [10, 15], whereas the backward equations for region 3 were developed later [12] and adopted by IAPWS in 2003 and in an expanded form in 2004 [23].

2.3.4.1 Regions and Region Boundaries in the Variables (p,s)

Figure 2.9 shows the regions and region boundaries in a pressure-entropy diagram along with the assignment of the backward equations $T(p,s)$ and $v(p,s)$ to regions 1 to 3. In order to avoid any iteration in practical calculations with IAPWS-IF97, the region boundaries must also be determinable without iteration. Therefore, a saturation-pressure equation as a function of entropy, $p_{s,3}(s)$, for the saturated-liquid and saturated-vapour lines between regions 3 and 4, was developed [12, 23], and is given as Eq. (2.30).

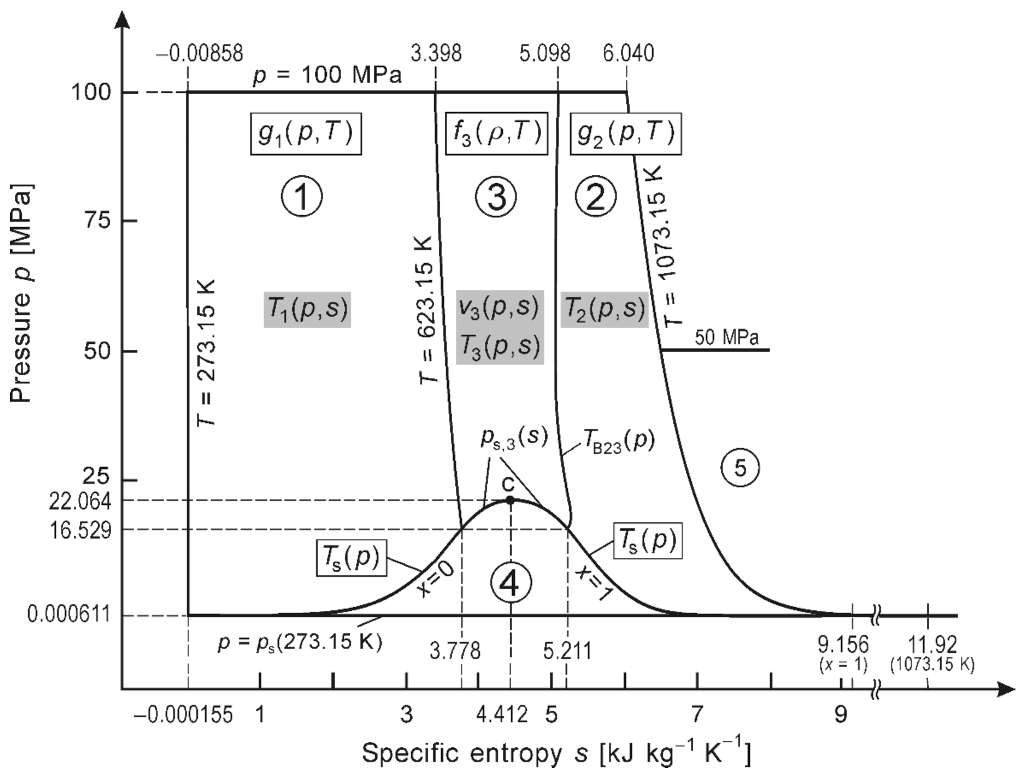

Fig. 2.9 Regions and region boundaries of IAPWS-IF97 for the variables (p,s). Assignment of the backward equations $T(p,s)$ and $v(p,s)$ to these regions, (without showing how regions 2 and 3 will be divided into subregions). The p and s values at the corner points of the region boundaries are rounded values.

When property calculations with IAPWS-IF97 are carried out with the variables (p,s) as input variables, all tests to determine whether the given (p,s) point is within the range of regions 1 to 4 of IAPWS-IF97 and, if so, in which region, must be performed with respect to these input variables. To make such tests easier, the following subsections show which equations are used to calculate the s values for given p values (or vice versa) along the respective region boundaries. These explanations are based on Fig. 2.9. Thus, Fig. 2.9 along with the description of the region boundaries given in Secs. 2.3.4.1a to 2.3.4.1c can be regarded as definitions of regions 1 to 4 of IAPWS-IF97 in the variables p and s.

a) Outer Boundaries of Regions 1 to 4

The description of the boundaries starts at the left-hand side of Fig. 2.9 with the isotherm $T = 273.15$ K and proceeds clockwise.

The Isotherm T = 273.15 K. This isotherm corresponds to the lowest temperature limit of IAPWS-IF97 and covers the pressure range given by

$$p_s(273.15\text{ K}) \le p \le 100\text{ MPa},$$

where p_s is calculated from the saturation-pressure equation $p_s(T)$, Eq. (2.13). Along this isotherm, the s value for the given p value is calculated from the basic equation of region 1, $g_1(p, T)$, Eq. (2.3), with $T = 273.15$ K. If the specific entropy s of a given (p,s) point is less than $s_1(p, 273.15\text{ K})$, then the (p,s) point is outside the range of validity of IAPWS-IF97, see Fig. 2.9.

The Isobar p = 100 MPa. This isobar is the upper pressure limit of the range of validity of IAPWS-IF97 (except for region 5). If the given pressure p is greater than 100 MPa, then the (p,s) point is outside the range of validity of IAPWS-IF97.

The Isotherm T = 1073.15 K. This isotherm corresponds to the upper temperature limit of IAPWS-IF97 (except for region 5) and covers the range of pressure

$$p_s(273.15\text{ K}) \le p \le 100\text{ MPa},$$

where p_s is calculated from the equation $p_s(T)$, Eq. (2.13). On this isotherm, the s value for the given p value is calculated from the basic equation of region 2, $g_2(p, T)$, Eq. (2.6), with $T = 1073.15$ K. If the specific entropy s of the given (p,s) point is greater than $s_2(p, 1073.15\text{ K})$ for the given pressure p, then the (p,s) point is outside the range of IAPWS-IF97 for which the backward equations exist, see Fig. 2.9.

The Isobar p = p_s(273.15 K) = 0.000 611 212 677 MPa. This saturation pressure p_s is calculated from the equation $p_s(T)$, Eq. (2.13), and is the lower pressure limit of the range of validity of the IAPWS-IF97 backward equations. If the given pressure p is lower than $p = 0.000\,611\,212\,677$ MPa, then the (p,s) point is outside the range of validity of the backward equations, see Fig. 2.9.

b) Boundary between the Single-Phase Regions 1 to 3 and the Two-Phase Region 4

According to Fig. 2.9, the boundary between the single-phase regions 1 to 3 and the two-phase region 4 is given by the saturated-liquid line ($x = 0$) and the saturated-vapour line ($x = 1$).

Boundary between Regions 1 and 4. The part of the saturated-liquid line ($x = 0$) that forms the boundary between regions 1 and 4 covers a range of pressures given by

$$p_s(273.15\text{ K}) \le p \le p_s(623.15\text{ K}),$$

see Fig. 2.9; the p_s values are calculated from the equation $p_s(T)$, Eq. (2.13). Along this

boundary, the s value for the given p value is calculated from the basic equation $g_1(p,T)$, Eq. (2.3), where $T = T_s$ results from the saturation-temperature equation $T_s(p)$, Eq. (2.14). The given entropy value can then be compared with the calculated value for s.

Boundary between Regions 3 and 4. The part of the saturated-liquid line and the saturated-vapour line that forms the boundary between regions 3 and 4 is given by the entropy range

$$s'(623.15\ \mathrm{K}) \le s \le s''(623.15\ \mathrm{K})$$
$$\text{with } s'(623.15\ \mathrm{K}) = s_1(p_s(623.15\ \mathrm{K}), 623.15\ \mathrm{K})$$
$$\text{and } s''(623.15\ \mathrm{K}) = s_2(p_s(623.15\ \mathrm{K}), 623.15\ \mathrm{K}),$$

where p_s is calculated from Eq. (2.13). In this relation, s_1 is calculated from the basic equation $g_1(p,T)$, Eq. (2.3), with $p = p_s(T)$ and $T = 623.15$ K. The entropy s_2 results from the basic equation $g_2(p,T)$, Eq. (2.6), for $p = p_s(T)$ and $T = 623.15$ K. The reason for calculating the entropies s_1 and s_2 at these corner points from the basic equations of regions 1 and 2, $g_1(p,T)$ and $g_2(p,T)$, Eqs. (2.3) and (2.6), and not from the basic equation for region 3, $f_3(\rho,T)$, Eq. (2.11), is given at the beginning of Sec. 2.3.4.1c. Along this boundary, the p value for the given s value is calculated from the special saturation-pressure equation as a function of entropy, $p_{s,3}(s)$, which is given in Sec. 2.3.4.1d as Eq. (2.30). The given pressure value can then be compared with the calculated value for p.

Boundary between Regions 2 and 4. The part of the saturated-vapour line ($x = 1$) that forms the boundary between regions 2 and 4 covers the pressure range

$$p_s(273.15\ \mathrm{K}) \le p \le p_s(623.15\ \mathrm{K}),$$

see Fig. 2.9; the p_s values are calculated from the equation $p_s(T)$, Eq. (2.13). Along this boundary, the s value for the given p value is determined from the basic equation $g_2(p,T)$, Eq. (2.6), where $T = T_s$ is obtained from the saturation-temperature equation $T_s(p)$, Eq. (2.14). The given entropy value can then be compared with the calculated value for s.

c) Boundaries between the Single-Phase Regions

The boundaries between regions 1 and 3 ($T = 623.15$ K) and between regions 2 and 3 (T_{B23}-line) belong to both adjacent regions, see Figs. 2.2 and 2.9. However, in order to avoid having different values along these boundaries, the boundary between regions 1 and 2 is considered to belong to region 1 and the boundary between regions 2 and 3 is considered to belong to region 2. Thus, the properties along the boundary between regions 1 and 3 are calculated from the equations for region 1 and the properties along the boundary between regions 2 and 3 are determined from the equations for region 2. In this way, the calculations can be performed directly, neither iteration nor additional use of any backward equation is required.

Boundary between Regions 1 and 3. The boundary that corresponds to the isotherm $T = 623.15$ K covers the pressure range

$$p_s(623.15\ \mathrm{K}) \le p \le 100\ \mathrm{MPa},$$

see Fig. 2.9; p_s is calculated from Eq. (2.13). Along this boundary, the s value for the given p value results from the basic equation $g_1(p,T)$, Eq. (2.3), with $T = 623.15$ K. The given entropy value can then be compared with the calculated value for s.

Boundary between Regions 2 and 3. This boundary, namely the T_{B23}-line, covers the pressure range

$$p_s(623.15\ \mathrm{K}) \le p \le 100\ \mathrm{MPa},$$

see Fig. 2.9; p_s is determined from Eq. (2.13). Along this boundary, the s value for the given p value is calculated from the basic equation $g_2(p, T)$, Eq. (2.6), with $T = T_{B23}$ determined from the equation $T_{B23}(p)$, Eq. (2.2). The given entropy value can then be compared with the calculated value for s.

d) The Boundary Equation $p_{s,3}(s)$

The boundary equation $p_{s,3}(s)$ has the following dimensionless form:

$$\frac{p_{s,3}(s)}{p^*} = \pi(\sigma) = \sum_{i=1}^{10} n_i\,(\sigma - 1.03)^{I_i}\,(\sigma - 0.699)^{J_i}\ , \qquad (2.30)$$

where $\pi = p/p^*$ and $\sigma = s/s^*$ with $p^* = 22$ MPa and $s^* = 5.2$ kJ kg^{-1} K^{-1}. The coefficients n_i and exponents I_i and J_i of Eq. (2.30) are listed in Table 2.49.

Table 2.49 Coefficients and exponents of the boundary equation $p_{s,3}(s)$ in its dimensionless form, Eq. (2.30)

i	I_i	J_i	n_i	i	I_i	J_i	n_i
1	0	0	0.639 767 553 612 785	6	12	14	$-0.378\,829\,107\,169\,011 \times 10^{18}$
2	1	1	$-0.129\,727\,445\,396\,014 \times 10^{2}$	7	16	36	$-0.955\,586\,736\,431\,328 \times 10^{35}$
3	1	32	$-0.224\,595\,125\,848\,403 \times 10^{16}$	8	24	10	$0.187\,269\,814\,676\,188 \times 10^{24}$
4	4	7	$0.177\,466\,741\,801\,846 \times 10^{7}$	9	28	0	$0.119\,254\,746\,466\,473 \times 10^{12}$
5	12	4	$0.717\,079\,349\,571\,538 \times 10^{10}$	10	32	18	$0.110\,649\,277\,244\,882 \times 10^{37}$

The equation $p_{s,3}(s)$, Eq. (2.30), describes the saturated-liquid line and the saturated-vapour line including the critical point in the following entropy range (see Fig. 2.9):

$$s'(623.15\ \mathrm{K}) \le s \le s''(623.15\ \mathrm{K}),$$

where $s'(623.15\ \mathrm{K}) = s_1(p_s(623.15\ \mathrm{K}), 623.15\ \mathrm{K}) = 3.778\,281\,340$ kJ kg^{-1} K^{-1}
and $s''(623.15\ \mathrm{K}) = s_2(p_s(623.15\ \mathrm{K}), 623.15\ \mathrm{K}) = 5.210\,887\,825$ kJ kg^{-1} K^{-1}.

Computer-Program Verification. To assist the user in computer-program verification of Eq. (2.30), Table 2.50 contains test values for calculated pressures.

Table 2.50 Pressure values calculated from the boundary equation $p_{s,3}(s)$, Eq. (2.30), for selected specific entropies [a]

Equation	s [kJ kg^{-1}K^{-1}]	p [MPa]
	3.8	$1.687\,755\,057 \times 10^{1}$
$p_{s,3}(s)$, Eq. (2.30)	4.2	$2.164\,451\,789 \times 10^{1}$
	5.2	$1.668\,968\,482 \times 10^{1}$

[a] Programmed functions should be verified using 8 byte real values for all variables.

Note. For points extremely close to the boundary between the single-phase region 3 and the two-phase region 4, the following procedure is recommended. When calculating the pressure with the $p_{s,3}(s)$ equation, Eq. (2.30), its numerical inconsistency of 0.00033% in pressure with respect to the basic equation $p_s(T)$, Eq. (2.13), has to be considered. Due to this minor inconsistency the result of the calculated pressure should be corrected to $p_{s,3} = p_{s,3}(s)(1-\Delta p/p)$, where $\Delta p/p = 3.3 \times 10^{-6}$. This procedure ensures that (p,s) points extremely close to the two-phase region are correctly assigned to the single-phase region and not falsely to the two-phase region.

2.3.4.2 Backward Equation T (p,s) for Region 1

Figure 2.10 shows the assignment of the backward equation $T_1(p,s)$ to region 1 in a *p-s* diagram. The boundaries of region 1 in *p-s* coordinates are described in Secs. 2.3.4.1a to 2.3.4.1c. A statement about the computing speed with this backward equation can be found at the end of this section.

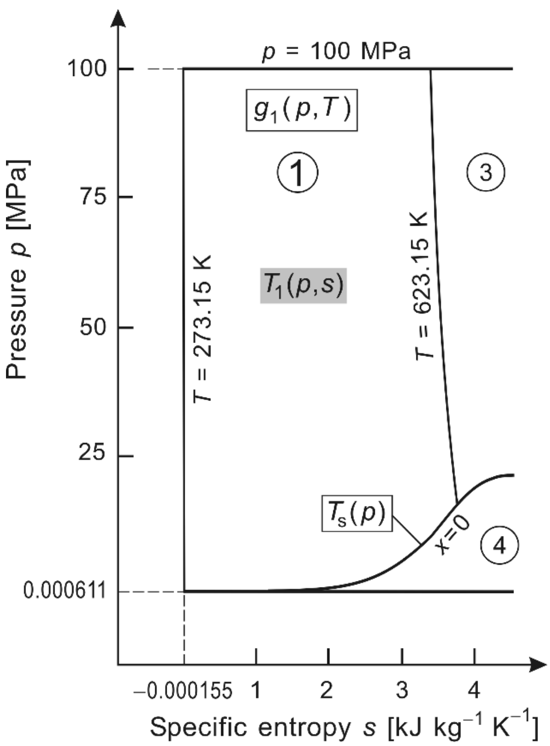

Fig. 2.10 Assignment of the backward equation $T_1(p,s)$ to region 1 in a *p-s* diagram. The *p* and *s* values at the corner points of region 1 are given in Fig. 2.9.

The backward equation $T_1(p,s)$ for region 1 has the following dimensionless form:

$$\frac{T_1(p,s)}{T^*} = \theta(\pi,\sigma) = \sum_{i=1}^{20} n_i \, \pi^{I_i} (\sigma + 2)^{J_i} \ , \tag{2.31}$$

where $\theta = T/T^*$, $\pi = p/p^*$, and $\sigma = s/s^*$ with $T^* = 1\ \mathrm{K}$, $p^* = 1$ MPa, and $s^* = 1$ kJ kg^{-1} K^{-1}. The coefficients n_i and exponents I_i and J_i of Eq. (2.31) are listed in Table 2.51.

Table 2.51 Coefficients and exponents of the backward equation $T_1(p,s)$ in its dimensionless form, Eq. (2.31)

i	I_i	J_i	n_i	i	I_i	J_i	n_i
1	0	0	$0.174\,782\,680\,583\,07 \times 10^{3}$	11	1	12	$0.356\,721\,106\,073\,66 \times 10^{-9}$
2	0	1	$0.348\,069\,308\,928\,73 \times 10^{2}$	12	1	31	$0.173\,324\,969\,948\,95 \times 10^{-23}$
3	0	2	$0.652\,925\,849\,784\,55 \times 10^{1}$	13	2	0	$0.566\,089\,006\,548\,37 \times 10^{-3}$
4	0	3	$0.330\,399\,817\,754\,89$	14	2	1	$-0.326\,354\,831\,397\,17 \times 10^{-3}$
5	0	11	$-0.192\,813\,829\,231\,96 \times 10^{-6}$	15	2	2	$0.447\,782\,866\,906\,32 \times 10^{-4}$
6	0	31	$-0.249\,091\,972\,445\,73 \times 10^{-22}$	16	2	9	$-0.513\,221\,569\,085\,07 \times 10^{-9}$
7	1	0	$-0.261\,076\,364\,893\,32$	17	2	31	$-0.425\,226\,570\,422\,07 \times 10^{-25}$
8	1	1	$0.225\,929\,659\,815\,86$	18	3	10	$0.264\,004\,413\,606\,89 \times 10^{-12}$
9	1	2	$-0.642\,564\,633\,952\,26 \times 10^{-1}$	19	3	32	$0.781\,246\,004\,597\,23 \times 10^{-28}$
10	1	3	$0.788\,762\,892\,705\,26 \times 10^{-2}$	20	4	32	$-0.307\,321\,999\,036\,68 \times 10^{-30}$

Range of Validity. The range of validity of the backward equation $T_1(p,s)$, Eq. (2.31), can be derived from the graphical representation of region 1 in Fig. 2.9. The determination of the (p,s) values along the region boundaries is described in Secs. 2.3.4.1a to 2.3.4.1c.

Computer-Program Verification. To assist the user in computer-program verification of Eq. (2.31), Table 2.52 contains corresponding test values.

Numerical Consistency. The numerical inconsistency between the backward equation $T_1(p,s)$, Eq. (2.31), and the basic equation $g_1(p,T)$, Eq. (2.3), in comparison with the permissible inconsistency, given in Sec. 2.3.2, is listed in Table 2.53.

Note. When calculating properties in the range $p \le p_s(623.15\text{ K})$ and extremely close to the saturated-liquid line, Eq. (2.31) might yield temperatures $T_1(p,s) > T_s(p)$ due to the minor inconsistencies. In this case, the result of Eq. (2.31) must be corrected to $T_1 = T_s(p)$, where the saturation temperature $T_s(p)$ is calculated for the given pressure from Eq. (2.14).

Table 2.52 Temperature values calculated from the backward equation $T_1(p,s)$, Eq. (2.31), for selected pressures and specific entropies [a]

p [MPa]	s [kJ kg^{-1} K^{-1}]	T [K]
3	0.5	$0.307\,842\,258 \times 10^{3}$
80	0.5	$0.309\,979\,785 \times 10^{3}$
80	3	$0.565\,899\,909 \times 10^{3}$

[a] Programmed functions should be verified using 8 byte real values for all variables.

Table 2.53 Maximum and root-mean-square inconsistency in temperature between the backward equation $T_1(p,s)$, Eq. (2.31), and the basic equation $g_1(p,T)$, Eq. (2.3), in comparison with the permissible inconsistency

Inconsistencies in temperature [mK]		
$\lvert\Delta T\rvert_{\text{perm}}$	$\lvert\Delta T\rvert_{\text{max}}$	$(\Delta T)_{\text{RMS}}$
25	21.8	5.8

Computing Time. The calculation of temperature as a function of (p,s) with the backward equation $T_1(p,s)$, Eq. (2.31), is about 38 times faster than when using only the basic equation $g_1(p,T)$, Eq. (2.3), [19]. In this comparison, the basic equation was applied in combination with a one-dimensional Newton iteration with convergence tolerances corresponding to the consistency requirement that were set for the backward equation.

2.3.4.3 Backward Equations $T(p,s)$ for Region 2

The boundaries of region 2 in p-s coordinates are described in Secs. 2.3.4.1a to 2.3.4.1c. Due to the demand for very high numerical consistency between the basic equation $g_2(p,T)$, Eq. (2.6), and a backward equation $T(p,s)$ for region 2, see Sec. 2.3.2, region 2 is divided into three subregions.

a) Division of Region 2 into Subregions 2a, 2b, and 2c

Figure 2.11 shows how region 2 is divided into three subregions for the backward equations $T(p,s)$. The boundary between subregions 2a and 2b is the isobar p = 4 MPa, and the boundary between subregions 2b and 2c is given by the isentropic line $s = s_{2bc}$ = 5.85 kJ kg^{-1} K^{-1}.

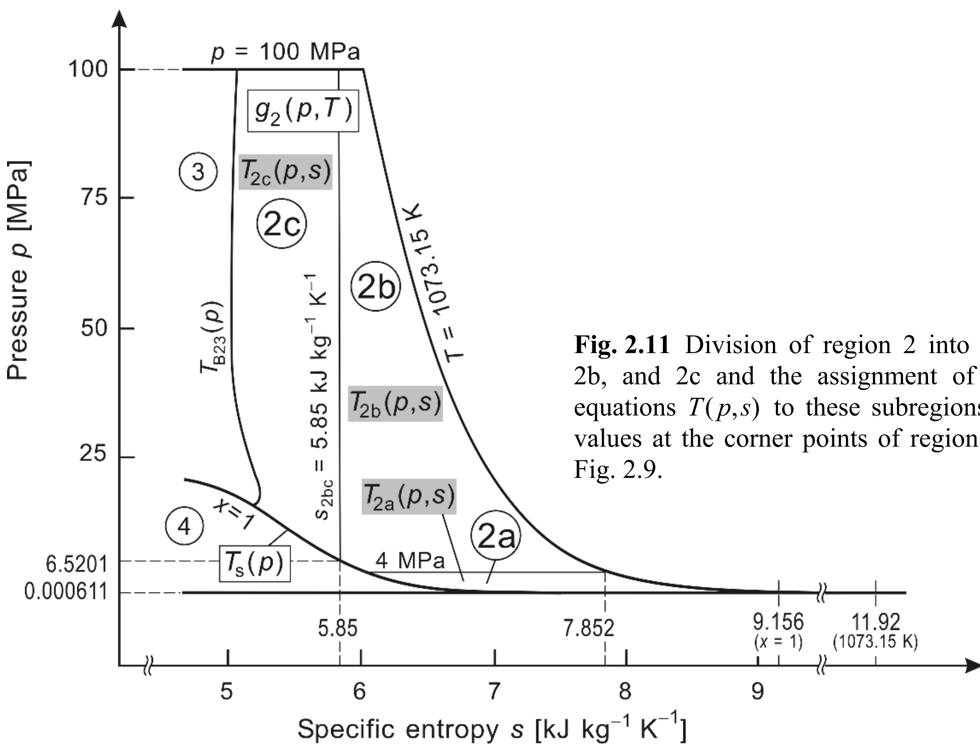

Fig. 2.11 Division of region 2 into subregions 2a, 2b, and 2c and the assignment of the backward equations $T(p,s)$ to these subregions. The p and s values at the corner points of region 2 are given in Fig. 2.9.

Note. To be in accordance with the statements given in [11, 22], the boundary between subregions 2a and 2b is considered to belong to subregion 2a and the boundary between subregions 2b and 2c is considered to belong to subregion 2b.

b) The Backward Equations $T(p, s)$ for Subregions 2a, 2b, and 2c

The backward equation $T_{2a}(p,s)$ for **subregion 2a** in its dimensionless form reads

$$\frac{T_{2a}(p,s)}{T^*} = \theta(\pi,\sigma) = \sum_{i=1}^{46} n_i \, \pi^{I_i} (\sigma - 2)^{J_i} \,, \tag{2.32}$$

where $\theta = T/T^*$, $\pi = p/p^*$, and $\sigma = s/s^*$ with $T^* = 1$ K, $p^* = 1$ MPa, and $s^* = 2$ kJ kg^{-1} K^{-1}. The coefficients n_i and exponents I_i and J_i of Eq. (2.32) are listed in Table 2.54.

The backward equation $T_{2b}(p,s)$ for **subregion 2b** in its dimensionless form reads

$$\frac{T_{2b}(p,s)}{T^*} = \theta(\pi,\sigma) = \sum_{i=1}^{44} n_i \, \pi^{I_i} (10-\sigma)^{J_i} \, , \tag{2.33}$$

where $\theta = T/T^*$, $\pi = p/p^*$, and $\sigma = s/s^*$ with $T^* = 1\,\mathrm{K}$, $p^* = 1\,\mathrm{MPa}$, and $s^* = 0.7853\,\mathrm{kJ\,kg^{-1}K^{-1}}$. The coefficients n_i and exponents I_i and J_i of Eq. (2.33) are listed in Table 2.55.

The backward equation $T_{2c}(p,s)$ for **subregion 2c** in its dimensionless form reads

$$\frac{T_{2c}(p,s)}{T^*} = \theta(\pi,\sigma) = \sum_{i=1}^{30} n_i \, \pi^{I_i} (2-\sigma)^{J_i} \, , \tag{2.34}$$

where $\theta = T/T^*$, $\pi = p/p^*$, and $\sigma = s/s^*$ with $T^* = 1\,\mathrm{K}$, $p^* = 1\,\mathrm{MPa}$, and $s^* = 2.9251\,\mathrm{kJ\,kg^{-1}\,K^{-1}}$. The coefficients n_i and exponents I_i and J_i of Eq. (2.34) are listed in Table 2.56.

Table 2.54 Coefficients and exponents of the backward equation $T_{2a}(p,s)$ for subregion 2a in its dimensionless form, Eq. (2.32)

i	I_i	J_i	n_i	i	I_i	J_i	n_i
1	−1.5	−24	$-0.392\,359\,838\,619\,84 \times 10^{6}$	24	−0.25	−11	$-0.597\,806\,388\,727\,18 \times 10^{4}$
2	−1.5	−23	$0.515\,265\,738\,272\,70 \times 10^{6}$	25	−0.25	−6	$-0.704\,014\,639\,268\,62 \times 10^{3}$
3	−1.5	−19	$0.404\,824\,431\,610\,48 \times 10^{5}$	26	0.25	1	$0.338\,367\,841\,075\,53 \times 10^{3}$
4	−1.5	−13	$-0.321\,937\,909\,239\,02 \times 10^{3}$	27	0.25	4	$0.208\,627\,866\,351\,87 \times 10^{2}$
5	−1.5	−11	$0.969\,614\,242\,186\,94 \times 10^{2}$	28	0.25	8	$0.338\,341\,726\,561\,96 \times 10^{-1}$
6	−1.5	−10	$-0.228\,678\,463\,717\,73 \times 10^{2}$	29	0.25	11	$-0.431\,244\,284\,148\,93 \times 10^{-4}$
7	−1.25	−19	$-0.449\,429\,141\,243\,57 \times 10^{6}$	30	0.5	0	$0.166\,537\,913\,564\,12 \times 10^{3}$
8	−1.25	−15	$-0.501\,183\,360\,201\,66 \times 10^{4}$	31	0.5	1	$-0.139\,862\,920\,558\,98 \times 10^{3}$
9	−1.25	−6	$0.356\,844\,635\,600\,15$	32	0.5	5	$-0.788\,495\,479\,998\,72$
10	−1.0	−26	$0.442\,353\,358\,481\,90 \times 10^{5}$	33	0.5	6	$0.721\,324\,117\,538\,72 \times 10^{-1}$
11	−1.0	−21	$-0.136\,733\,888\,117\,08 \times 10^{5}$	34	0.5	10	$-0.597\,548\,393\,982\,83 \times 10^{-2}$
12	−1.0	−17	$0.421\,632\,602\,078\,64 \times 10^{6}$	35	0.5	14	$-0.121\,413\,589\,539\,04 \times 10^{-4}$
13	−1.0	−16	$0.225\,169\,258\,374\,75 \times 10^{5}$	36	0.5	16	$0.232\,270\,967\,338\,71 \times 10^{-6}$
14	−1.0	−9	$0.474\,421\,448\,656\,46 \times 10^{3}$	37	0.75	0	$-0.105\,384\,635\,661\,94 \times 10^{2}$
15	−1.0	−8	$-0.149\,311\,307\,976\,47 \times 10^{3}$	38	0.75	4	$0.207\,189\,254\,965\,02 \times 10^{1}$
16	−0.75	−15	$-0.197\,811\,263\,204\,52 \times 10^{6}$	39	0.75	9	$-0.721\,931\,552\,604\,27 \times 10^{-1}$
17	−0.75	−14	$-0.235\,543\,994\,707\,60 \times 10^{5}$	40	0.75	17	$0.207\,498\,870\,811\,20 \times 10^{-6}$
18	−0.5	−26	$-0.190\,706\,163\,020\,76 \times 10^{5}$	41	1.0	7	$-0.183\,406\,579\,113\,79 \times 10^{-1}$
19	−0.5	−13	$0.553\,756\,698\,831\,64 \times 10^{5}$	42	1.0	18	$0.290\,362\,723\,486\,96 \times 10^{-6}$
20	−0.5	−9	$0.382\,936\,914\,373\,63 \times 10^{4}$	43	1.25	3	$0.210\,375\,278\,936\,19$
21	−0.5	−7	$-0.603\,918\,605\,805\,67 \times 10^{3}$	44	1.25	15	$0.256\,812\,397\,299\,99 \times 10^{-3}$
22	−0.25	−27	$0.193\,631\,026\,203\,31 \times 10^{4}$	45	1.5	5	$-0.127\,990\,029\,337\,81 \times 10^{-1}$
23	−0.25	−25	$0.426\,606\,436\,986\,10 \times 10^{4}$	46	1.5	18	$-0.821\,981\,026\,520\,18 \times 10^{-5}$

Table 2.55 Coefficients and exponents of the backward equation $T_{2b}(p,s)$ for subregion 2b in its dimensionless form, Eq. (2.33)

i	I_i	J_i	n_i	i	I_i	J_i	n_i
1	−6	0	$0.316\,876\,650\,834\,97 \times 10^{6}$	23	0	2	$0.417\,273\,471\,596\,10 \times 10^{2}$
2	−6	11	$0.208\,641\,758\,818\,58 \times 10^{2}$	24	0	4	$0.219\,325\,494\,345\,32 \times 10^{1}$
3	−5	0	$-0.398\,593\,998\,035\,99 \times 10^{6}$	25	0	5	$-0.103\,200\,500\,090\,77 \times 10^{1}$
4	−5	11	$-0.218\,160\,585\,188\,77 \times 10^{2}$	26	0	6	$0.358\,829\,435\,167\,03$
5	−4	0	$0.223\,697\,851\,942\,42 \times 10^{6}$	27	0	9	$0.525\,114\,537\,260\,66 \times 10^{-2}$
6	−4	1	$-0.278\,417\,034\,458\,17 \times 10^{4}$	28	1	0	$0.128\,389\,164\,507\,05 \times 10^{2}$
7	−4	11	$0.992\,074\,360\,714\,80 \times 10^{1}$	29	1	1	$-0.286\,424\,372\,193\,81 \times 10^{1}$
8	−3	0	$-0.751\,975\,122\,991\,57 \times 10^{5}$	30	1	2	$0.569\,126\,836\,648\,55$
9	−3	1	$0.297\,086\,059\,511\,58 \times 10^{4}$	31	1	3	$-0.999\,629\,545\,849\,31 \times 10^{-1}$
10	−3	11	$-0.344\,068\,785\,485\,26 \times 10^{1}$	32	1	7	$-0.326\,320\,377\,784\,59 \times 10^{-2}$
11	−3	12	$0.388\,155\,642\,491\,15$	33	1	8	$0.233\,209\,225\,767\,23 \times 10^{-3}$
12	−2	0	$0.175\,112\,950\,857\,50 \times 10^{5}$	34	2	0	$-0.153\,348\,098\,574\,50$
13	−2	1	$-0.142\,371\,128\,544\,49 \times 10^{4}$	35	2	1	$0.290\,722\,882\,399\,02 \times 10^{-1}$
14	−2	6	$0.109\,438\,033\,641\,67 \times 10^{1}$	36	2	5	$0.375\,347\,027\,411\,67 \times 10^{-3}$
15	−2	10	$0.899\,716\,193\,084\,95$	37	3	0	$0.172\,966\,917\,024\,11 \times 10^{-2}$
16	−1	0	$-0.337\,597\,400\,989\,58 \times 10^{4}$	38	3	1	$-0.385\,560\,508\,445\,04 \times 10^{-3}$
17	−1	1	$0.471\,628\,858\,183\,55 \times 10^{3}$	39	3	3	$-0.350\,177\,122\,926\,08 \times 10^{-4}$
18	−1	5	$-0.191\,882\,419\,936\,79 \times 10^{1}$	40	4	0	$-0.145\,663\,936\,314\,92 \times 10^{-4}$
19	−1	8	$0.410\,785\,804\,921\,96$	41	4	1	$0.564\,208\,572\,672\,69 \times 10^{-5}$
20	−1	9	$-0.334\,653\,781\,720\,97$	42	5	0	$0.412\,861\,500\,746\,05 \times 10^{-7}$
21	0	0	$0.138\,700\,347\,775\,05 \times 10^{4}$	43	5	1	$-0.206\,846\,711\,188\,24 \times 10^{-7}$
22	0	1	$-0.406\,633\,261\,958\,38 \times 10^{3}$	44	5	2	$0.164\,093\,936\,747\,25 \times 10^{-8}$

Table 2.56 Coefficients and exponents of the backward equation $T_{2c}(p,s)$ for subregion 2c in its dimensionless form, Eq. (2.34)

i	I_i	J_i	n_i	i	I_i	J_i	n_i
1	−2	0	$0.909\,685\,010\,053\,65 \times 10^{3}$	16	3	1	$-0.145\,970\,082\,847\,53 \times 10^{-1}$
2	−2	1	$0.240\,456\,670\,884\,20 \times 10^{4}$	17	3	5	$0.566\,311\,756\,310\,27 \times 10^{-2}$
3	−1	0	$-0.591\,623\,263\,871\,30 \times 10^{3}$	18	4	0	$-0.761\,558\,645\,845\,77 \times 10^{-4}$
4	0	0	$0.541\,454\,041\,280\,74 \times 10^{3}$	19	4	1	$0.224\,403\,429\,193\,32 \times 10^{-3}$
5	0	1	$-0.270\,983\,084\,111\,92 \times 10^{3}$	20	4	4	$-0.125\,610\,950\,134\,13 \times 10^{-4}$
6	0	2	$0.979\,765\,250\,979\,26 \times 10^{3}$	21	5	0	$0.633\,231\,326\,609\,34 \times 10^{-6}$
7	0	3	$-0.469\,667\,729\,594\,35 \times 10^{3}$	22	5	1	$-0.205\,419\,896\,753\,75 \times 10^{-5}$
8	1	0	$0.143\,992\,746\,047\,23 \times 10^{2}$	23	5	2	$0.364\,053\,703\,900\,82 \times 10^{-7}$
9	1	1	$-0.191\,042\,042\,304\,29 \times 10^{2}$	24	6	0	$-0.297\,598\,977\,892\,15 \times 10^{-8}$
10	1	3	$0.532\,991\,671\,119\,71 \times 10^{1}$	25	6	1	$0.101\,366\,185\,297\,63 \times 10^{-7}$
11	1	4	$-0.212\,529\,753\,759\,34 \times 10^{2}$	26	7	0	$0.599\,257\,196\,923\,51 \times 10^{-11}$
12	2	0	$-0.311\,473\,344\,137\,60$	27	7	1	$-0.206\,778\,701\,051\,64 \times 10^{-10}$
13	2	1	$0.603\,348\,408\,946\,23$	28	7	3	$-0.208\,742\,781\,818\,86 \times 10^{-10}$
14	2	2	$-0.427\,648\,397\,025\,09 \times 10^{-1}$	29	7	4	$0.101\,621\,668\,250\,89 \times 10^{-9}$
15	3	0	$0.581\,855\,972\,552\,59 \times 10^{-2}$	30	7	5	$-0.164\,298\,282\,813\,47 \times 10^{-9}$

Ranges of Validity. The ranges of validity of the backward equations $T_{2a}(p,s)$, $T_{2b}(p,s)$, and $T_{2c}(p,s)$, Eqs. (2.32) to (2.34), can be derived from the graphical representation of region 2 in Fig. 2.9 and of subregions 2a, 2b, and 2c in Fig. 2.11. The determination of the (p,s) values along the region boundaries is described in Secs. 2.3.4.1a to 2.3.4.1c and along the subregion boundaries in Sec. 2.3.4.3a.

Computer-Program Verification. To assist the user in computer-program verification of Eqs. (2.32) to (2.34), Table 2.57 contains corresponding test values.

Numerical Consistencies. The numerical inconsistencies between the backward equations $T_{2a}(p,s)$, $T_{2b}(p,s)$, and $T_{2c}(p,s)$, Eqs. (2.32) to (2.34), and the basic equation $g_2(p,T)$, Eq. (2.6), in comparison with the permissible inconsistencies, given in Sec. 2.3.2, are listed in Table 2.58.

Note. When calculating properties in the range $p \le p_s(623.15\text{ K})$ and extremely close to the saturated-vapour line, Eqs. (2.32) to (2.34) might yield temperatures $T_{2a}(p,s) < T_s(p)$, $T_{2b}(p,s) < T_s(p)$, and $T_{2c}(p,s) < T_s(p)$, respectively, due to the minor inconsistencies. In this case, the results of Eqs. (2.32) to (2.34) must be corrected to $T_{2a} = T_s(p)$, $T_{2b} = T_s(p)$, and $T_{2c} = T_s(p)$, respectively, where the saturation temperature $T_s(p)$ is calculated for the given pressure from Eq. (2.14).

Table 2.57 Temperature values calculated from the backward equations $T_{2a}(p,s)$, $T_{2b}(p,s)$, and $T_{2c}(p,s)$, Eqs. (2.32) to (2.34), for selected pressures and specific entropies [a]

Equation	p [MPa]	s [kJ kg^{-1}K^{-1}]	T [K]
	0.1	7.5	0.399 517 097 × 10^3
$T_{2a}(p,s)$, Eq. (2.32)	0.1	8	0.514 127 081 × 10^3
	2.5	8	0.103 984 917 × 10^4
	8	6	0.600 484 040 × 10^3
$T_{2b}(p,s)$, Eq. (2.33)	8	7.5	0.106 495 556 × 10^4
	90	6	0.103 801 126 × 10^4
	20	5.75	0.697 992 849 × 10^3
$T_{2c}(p,s)$, Eq. (2.34)	80	5.25	0.854 011 484 × 10^3
	80	5.75	0.949 017 998 × 10^3

[a] Programmed functions should be verified using 8 byte real values for all variables.

Table 2.58 Maximum and root-mean-square inconsistencies in temperature between the backward equations $T_{2a}(p,s)$, $T_{2b}(p,s)$, and $T_{2c}(p,s)$, Eqs. (2.32) to (2.34), and the basic equation $g_2(p,T)$, Eq. (2.6), in comparison with the permissible inconsistencies

		Inconsistencies in temperature [mK]		
Subregion	Equation	$\lvert\Delta T\rvert_{\mathrm{perm}}$	$\lvert\Delta T\rvert_{\max}$	$(\Delta T)_{\mathrm{RMS}}$
2a	$T_{2a}(p,s)$, Eq. (2.32)	10	8.8	1.2
2b	$T_{2b}(p,s)$, Eq. (2.33)	10	6.5	2.8
2c	$T_{2c}(p,s)$, Eq. (2.34)	25	19.0	8.3

c) Computing Time when Using the Backward Equations *T*(*p*,*s*) in Comparison with the Basic Equation

The calculation of temperature as a function of (p,s) with the backward equations $T_{2a}(p,s)$, $T_{2b}(p,s)$, or $T_{2c}(p,s)$, Eqs. (2.32) to (2.34), is about 14 times faster than when using only the basic equation $g_2(p,T)$, Eq. (2.6), [19]. In this comparison, the basic equation was applied in combination with a one-dimensional Newton iteration with convergence tolerances corresponding to the consistency requirements that were set for the backward equations.

2.3.4.4 Backward Equations $v(p,s)$ and $T(p,s)$ for Region 3

The boundaries of region 3 in *p-s* coordinates are described in Secs. 2.3.4.1a to 2.3.4.1c.

a) Division of Region 3 into Subregions 3a and 3b

Due to the demand for very high numerical consistency between the backward equations and the basic equation $f_3(\rho,T)$, Eq. (2.11), as given in Sec. 2.3.2, region 3 is divided into two subregions as illustrated in Fig. 2.12.

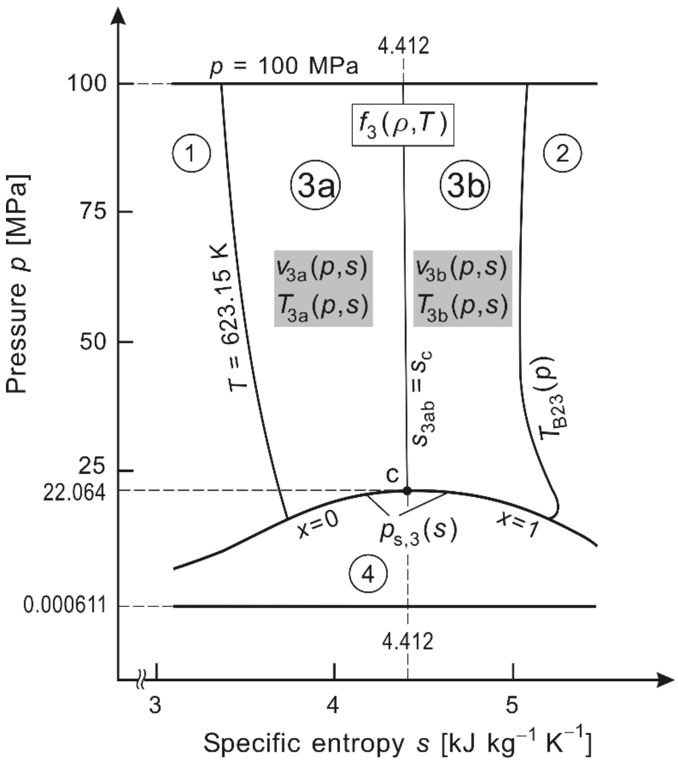

Fig. 2.12 Division of region 3 into subregions 3a and 3b, and the assignment of backward equations $v(p,s)$ and $T(p,s)$ to these subregions. The p and s values at the corner points of region 3 are given in Fig. 2.9.

The boundary between subregions 3a and 3b is defined by the critical isentropic line

$$s_{3ab} = s_c = 4.412\,021\,482\,234\,76 \text{ kJ kg}^{-1}\text{ K}^{-1}, \tag{2.35}$$

where this value was calculated from the basic equation of region 3, $f_3(\rho,T)$, Eq. (2.11), for $\rho = \rho_c$ and $T = T_c$ according to Eqs. (1.6) and (1.4).

Note. The boundary between subregions 3a and 3b is considered to belong to subregion 3a [12, 23].

b) Backward Equations $v(p,s)$ for Subregions 3a and 3b

The backward equation $v_{3a}(p,s)$ for **subregion 3a** reads in its dimensionless form

$$\frac{v_{3a}(p,s)}{v^*} = \omega(\pi,\sigma) = \sum_{i=1}^{28} n_i\,(\pi+0.187)^{I_i}\,(\sigma-0.755)^{J_i} \;, \tag{2.36}$$

where $\omega = v/v^*$, $\pi = p/p^*$, and $\sigma = s/s^*$ with $v^* = 0.0028\ \text{m}^3\,\text{kg}^{-1}$, $p^* = 100$ MPa, and

$s^* = 4.4\ \mathrm{kJ\ kg^{-1}\ K^{-1}}$. The coefficients n_i and exponents I_i and J_i of Eq. (2.36) are listed in Table 2.59.

The backward equation $v_{3b}(p,s)$ for **subregion 3b** reads in its dimensionless form

$$\frac{v_{3b}(p,s)}{v^*} = \omega(\pi,\sigma) = \sum_{i=1}^{31} n_i (\pi + 0.298)^{I_i} (\sigma - 0.816)^{J_i} \ , \tag{2.37}$$

where $\omega = v/v^*$, $\pi = p/p^*$, and $\sigma = s/s^*$ with $v^* = 0.0088\ \mathrm{m^3\ kg^{-1}}$, $p^* = 100\ \mathrm{MPa}$, and $s^* = 5.3\ \mathrm{kJ\ kg^{-1}\ K^{-1}}$. The coefficients n_i and exponents I_i and J_i of Eq. (2.37) are listed in Table 2.60.

Table 2.59 Coefficients and exponents of the backward equation $v_{3a}(p,s)$ for subregion 3a in its dimensionless form, Eq. (2.36)

i	I_i	J_i	n_i	i	I_i	J_i	n_i
1	−12	10	$0.795\,544\,074\,093\,975 \times 10^{2}$	15	−3	2	$-0.118\,008\,384\,666\,987$
2	−12	12	$-0.238\,261\,242\,984\,590 \times 10^{4}$	16	−3	4	$0.253\,798\,642\,355\,900 \times 10^{1}$
3	−12	14	$0.176\,813\,100\,617\,787 \times 10^{5}$	17	−2	3	$0.965\,127\,704\,669\,424$
4	−10	4	$-0.110\,524\,727\,080\,379 \times 10^{-2}$	18	−2	8	$-0.282\,172\,420\,532\,826 \times 10^{2}$
5	−10	8	$-0.153\,213\,833\,655\,326 \times 10^{2}$	19	−1	1	$0.203\,224\,612\,353\,823$
6	−10	10	$0.297\,544\,599\,376\,982 \times 10^{3}$	20	−1	2	$0.110\,648\,186\,063\,513 \times 10^{1}$
7	−10	20	$-0.350\,315\,206\,871\,242 \times 10^{8}$	21	0	0	$0.526\,127\,948\,451\,280$
8	−8	5	$0.277\,513\,761\,062\,119$	22	0	1	$0.277\,000\,018\,736\,321$
9	−8	6	$-0.523\,964\,271\,036\,888$	23	0	3	$0.108\,153\,340\,501\,132 \times 10^{1}$
10	−8	14	$-0.148\,011\,182\,995\,403 \times 10^{6}$	24	1	0	$-0.744\,127\,885\,357\,893 \times 10^{-1}$
11	−8	16	$0.160\,014\,899\,374\,266 \times 10^{7}$	25	2	0	$0.164\,094\,443\,541\,384 \times 10^{-1}$
12	−6	28	$0.170\,802\,322\,663\,427 \times 10^{13}$	26	4	2	$-0.680\,468\,275\,301\,065 \times 10^{-1}$
13	−5	1	$0.246\,866\,996\,006\,494 \times 10^{-3}$	27	5	2	$0.257\,988\,576\,101\,640 \times 10^{-1}$
14	−4	5	$0.165\,326\,084\,797\,980 \times 10^{1}$	28	6	0	$-0.145\,749\,861\,944\,416 \times 10^{-3}$

Table 2.60 Coefficients and exponents of the backward equation $v_{3b}(p,s)$ for subregion 3b in its dimensionless form, Eq. (2.37)

i	I_i	J_i	n_i	i	I_i	J_i	n_i
1	−12	0	$0.591\,599\,780\,322\,238 \times 10^{-4}$	17	−4	2	$-0.121\,613\,320\,606\,788 \times 10^{2}$
2	−12	1	$-0.185\,465\,997\,137\,856 \times 10^{-2}$	18	−4	3	$0.167\,637\,540\,957\,944 \times 10^{1}$
3	−12	2	$0.104\,190\,510\,480\,013 \times 10^{-1}$	19	−3	1	$-0.744\,135\,838\,773\,463 \times 10^{1}$
4	−12	3	$0.598\,647\,302\,038\,590 \times 10^{-2}$	20	−2	0	$0.378\,168\,091\,437\,659 \times 10^{-1}$
5	−12	5	$-0.771\,391\,189\,901\,699$	21	−2	1	$0.401\,432\,203\,027\,688 \times 10^{1}$
6	−12	6	$0.172\,549\,765\,557\,036 \times 10^{1}$	22	−2	2	$0.160\,279\,837\,479\,185 \times 10^{2}$
7	−10	0	$-0.467\,076\,079\,846\,526 \times 10^{-3}$	23	−2	3	$0.317\,848\,779\,347\,728 \times 10^{1}$
8	−10	1	$0.134\,533\,823\,384\,439 \times 10^{-1}$	24	−2	4	$-0.358\,362\,310\,304\,853 \times 10^{1}$
9	−10	2	$-0.808\,094\,336\,805\,495 \times 10^{-1}$	25	−2	12	$-0.115\,995\,260\,446\,827 \times 10^{7}$
10	−10	4	$0.508\,139\,374\,365\,767$	26	0	0	$0.199\,256\,573\,577\,909$
11	−8	0	$0.128\,584\,643\,361\,683 \times 10^{-2}$	27	0	1	$-0.122\,270\,624\,794\,624$
12	−5	1	$-0.163\,899\,353\,915\,435 \times 10^{1}$	28	0	2	$-0.191\,449\,143\,716\,586 \times 10^{2}$
13	−5	2	$0.586\,938\,199\,318\,063 \times 10^{1}$	29	1	0	$-0.150\,448\,002\,905\,284 \times 10^{-1}$
14	−5	3	$-0.292\,466\,667\,918\,613 \times 10^{1}$	30	1	2	$0.146\,407\,900\,162\,154 \times 10^{2}$
15	−4	0	$-0.614\,076\,301\,499\,537 \times 10^{-2}$	31	2	2	$-0.327\,477\,787\,188\,230 \times 10^{1}$
16	−4	1	$0.576\,199\,014\,049\,172 \times 10^{1}$				

Ranges of Validity. The ranges of validity of the backward equations $v_{3a}(p,s)$ and $v_{3b}(p,s)$, Eqs. (2.36) and (2.37), can be derived from the graphical representation of region 3 in Fig. 2.9 and of subregions 3a and 3b in Fig. 2.12. The determination of the (p,s) values along the region boundaries is described in Secs. 2.3.4.1a to 2.3.4.1c and along the subregion boundary in Sec. 2.3.4.4a.

Computer-Program Verification. To assist the user in computer-program verification of Eqs. (2.36) and (2.37), Table 2.61 contains test values for calculated specific volumes.

Table 2.61 Values of the specific volume calculated from the backward equations $v_{3a}(p,s)$ and $v_{3b}(p,s)$, Eqs. (2.36) and (2.37), for selected pressures and specific entropies [a]

Equation	p [MPa]	s [kJ kg^{-1} K^{-1}]	v [m^3 kg^{-1}]
	20	3.8	$1.733\,791\,463 \times 10^{-3}$
$v_{3a}(p,s)$, Eq. (2.36)	50	3.6	$1.469\,680\,170 \times 10^{-3}$
	100	4.0	$1.555\,893\,131 \times 10^{-3}$
	20	5.0	$6.262\,101\,987 \times 10^{-3}$
$v_{3b}(p,s)$, Eq. (2.37)	50	4.5	$2.332\,634\,294 \times 10^{-3}$
	100	5.0	$2.449\,610\,757 \times 10^{-3}$

[a] Programmed functions should be verified using 8 byte real values for all variables.

Numerical Consistencies. The numerical inconsistencies between the backward equations $v_{3a}(p,s)$ and $v_{3b}(p,s)$, Eqs. (2.36) and (2.37), and the basic equation $f_3(\rho,T)$, Eq. (2.11), are listed in Table 2.62 in comparison with the permissible inconsistencies, given in Sec. 2.3.2. These inconsistencies are less than the permissible values. This is also true when the backward equations are used in combination with the boundary equation $p_{s,3}(s)$, Eq. (2.30). The critical volume $v_c = 1/\rho_c = (1/322)\ \mathrm{m^3\,kg^{-1}} = 0.003\,105\,59\ \mathrm{m^3\,kg^{-1}}$ is met by the two $v(p,s)$ equations for the given six significant figures. The maximum inconsistency in specific volume between the two backward equations, Eq. (2.36) and Eq. (2.37), along the subregion boundary $s_{3ab} = s_c$, Eq. (2.35), amounts to 0.000 46%.

Table 2.62 Maximum and root-mean-square inconsistencies in specific volume between the backward equations $v_{3a}(p,s)$ and $v_{3b}(p,s)$, Eqs. (2.36), and (2.37) and the basic equation $f_3(\rho,T)$, Eq. (2.11), in comparison with the permissible inconsistencies

Subregion	Equation	Inconsistencies in specific volume [%] $\lvert\Delta v/v\rvert_{perm}$	$\lvert\Delta v/v\rvert_{max}$	$(\Delta v/v)_{RMS}$
3a	$v_{3a}(p,s)$, Eq. (2.36)	0.01	0.0096	0.0052
3b	$v_{3b}(p,s)$, Eq. (2.37)	0.01	0.0077	0.0037

Computing Time. A statement about the computing time is given in Sec. 2.3.4.4d.

c) Backward Equations T(p,s) for Subregions 3a and 3b

The backward equation $T_{3a}(p,s)$ for **subregion 3a** reads in its dimensionless form

$$\frac{T_{3a}(p,s)}{T^*} = \theta(\pi,\sigma) = \sum_{i=1}^{33} n_i (\pi + 0.240)^{I_i} (\sigma - 0.703)^{J_i} \quad , \tag{2.38}$$

where, $\theta = T/T^*$, $\pi = p/p^*$, and $\sigma = s/s^*$ with $T^* = 760\ \mathrm{K}$, $p^* = 100\ \mathrm{MPa}$, and $s^* = 4.4\ \mathrm{kJ\ kg^{-1}\ K^{-1}}$. The coefficients n_i and exponents I_i and J_i of Eq. (2.38) are listed in Table 2.63.

The backward equation $T_{3b}(p,s)$ for **subregion 3b** reads in its dimensionless form

$$\frac{T_{3b}(p,s)}{T^*} = \theta(\pi,\sigma) = \sum_{i=1}^{28} n_i (\pi + 0.760)^{I_i} (\sigma - 0.818)^{J_i} \quad , \tag{2.39}$$

where $\theta = T/T^*$, $\pi = p/p^*$, and $\sigma = s/s^*$ with $T^* = 860\ \mathrm{K}$, $p^* = 100\ \mathrm{MPa}$, and $s^* = 5.3\ \mathrm{kJ\ kg^{-1}\ K^{-1}}$. The coefficients n_i and exponents I_i and J_i of Eq. (2.39) are listed in Table 2.64.

Table 2.63 Coefficients and exponents of the backward equation $T_{3a}(p,s)$ for subregion 3a in its dimensionless form, Eq. (2.38)

i	I_i	J_i	n_i	i	I_i	J_i	n_i
1	–12	28	$0.150\,042\,008\,263\,875 \times 10^{10}$	18	–4	10	$-0.368\,275\,545\,889\,071 \times 10^{3}$
2	–12	32	$-0.159\,397\,258\,480\,424 \times 10^{12}$	19	–4	36	$0.664\,768\,904\,779\,177 \times 10^{16}$
3	–10	4	$0.502\,181\,140\,217\,975 \times 10^{-3}$	20	–2	1	$0.449\,359\,251\,958\,880 \times 10^{-1}$
4	–10	10	$-0.672\,057\,767\,855\,466 \times 10^{2}$	21	–2	4	$-0.422\,897\,836\,099\,655 \times 10^{1}$
5	–10	12	$0.145\,058\,545\,404\,456 \times 10^{4}$	22	–1	1	$-0.240\,614\,376\,434\,179$
6	–10	14	$-0.823\,889\,534\,888\,890 \times 10^{4}$	23	–1	6	$-0.474\,341\,365\,254\,924 \times 10^{1}$
7	–8	5	$-0.154\,852\,214\,233\,853$	24	0	0	$0.724\,093\,999\,126\,110$
8	–8	7	$0.112\,305\,046\,746\,695 \times 10^{2}$	25	0	1	$0.923\,874\,349\,695\,897$
9	–8	8	$-0.297\,000\,213\,482\,822 \times 10^{2}$	26	0	4	$0.399\,043\,655\,281\,015 \times 10^{1}$
10	–8	28	$0.438\,565\,132\,635\,495 \times 10^{11}$	27	1	0	$0.384\,066\,651\,868\,009 \times 10^{-1}$
11	–6	2	$0.137\,837\,838\,635\,464 \times 10^{-2}$	28	2	0	$-0.359\,344\,365\,571\,848 \times 10^{-2}$
12	–6	6	$-0.297\,478\,527\,157\,462 \times 10^{1}$	29	2	3	$-0.735\,196\,448\,821\,653$
13	–6	32	$0.971\,777\,947\,349\,413 \times 10^{13}$	30	3	2	$0.188\,367\,048\,396\,131$
14	–5	0	$-0.571\,527\,767\,052\,398 \times 10^{-4}$	31	8	0	$0.141\,064\,266\,818\,704 \times 10^{-3}$
15	–5	14	$0.288\,307\,949\,778\,420 \times 10^{5}$	32	8	1	$-0.257\,418\,501\,496\,337 \times 10^{-2}$
16	–5	32	$-0.744\,428\,289\,262\,703 \times 10^{14}$	33	10	2	$0.123\,220\,024\,851\,555 \times 10^{-2}$
17	–4	6	$0.128\,017\,324\,848\,921 \times 10^{2}$				

Table 2.64 Coefficients and exponents of the backward equation $T_{3\mathrm{b}}(p,s)$ for subregion 3b in its dimensionless form, Eq. (2.39)

i	I_i	J_i	n_i	i	I_i	J_i	n_i
1	−12	1	0.527 111 701 601 660	15	−5	6	$0.880\,531\,517\,490\,555 \times 10^{3}$
2	−12	3	$-0.401\,317\,830\,052\,742 \times 10^{2}$	16	−4	12	$0.265\,015\,592\,794\,626 \times 10^{7}$
3	−12	4	$0.153\,020\,073\,134\,484 \times 10^{3}$	17	−3	1	−0.359 287 150 025 783
4	−12	7	$-0.224\,799\,398\,218\,827 \times 10^{4}$	18	−3	6	$-0.656\,991\,567\,673\,753 \times 10^{3}$
5	−8	0	−0.193 993 484 669 048	19	−2	2	$0.241\,768\,149\,185\,367 \times 10^{1}$
6	−8	1	$-0.140\,467\,557\,893\,768 \times 10^{1}$	20	0	0	0.856 873 461 222 588
7	−8	3	$0.426\,799\,878\,114\,024 \times 10^{2}$	21	2	1	0.655 143 675 313 458
8	−6	0	0.752 810 643 416 743	22	3	1	−0.213 535 213 206 406
9	−6	2	$0.226\,657\,238\,616\,417 \times 10^{2}$	23	4	0	$0.562\,974\,957\,606\,348 \times 10^{-2}$
10	−6	4	$-0.622\,873\,556\,909\,932 \times 10^{3}$	24	5	24	$-0.316\,955\,725\,450\,471 \times 10^{15}$
11	−5	0	−0.660 823 667 935 396	25	6	0	$-0.699\,997\,000\,152\,457 \times 10^{-3}$
12	−5	1	0.841 267 087 271 658	26	8	3	$0.119\,845\,803\,210\,767 \times 10^{-1}$
13	−5	2	$-0.253\,717\,501\,764\,397 \times 10^{2}$	27	12	1	$0.193\,848\,122\,022\,095 \times 10^{-4}$
14	−5	4	$0.485\,708\,963\,532\,948 \times 10^{3}$	28	14	2	$-0.215\,095\,749\,182\,309 \times 10^{-4}$

Ranges of Validity. The ranges of validity of the backward equations $T_{3\mathrm{a}}(p,s)$ and $T_{3\mathrm{b}}(p,s)$, Eqs. (2.38) and (2.39), can be derived from the graphical representation of region 3 in Fig. 2.9 and of subregions 3a and 3b in Fig. 2.12. The determination of the (p,s) values along the region boundaries is described in Secs. 2.3.4.1a to 2.3.4.1c and along the subregion boundary in Sec. 2.3.4.4a.

Computer-Program Verification. To assist the user in computer-program verification of Eqs. (2.38) and (2.39), Table 2.65 contains test values for calculated temperatures.

Table 2.65 Temperature values calculated from the backward equations $T_{3\mathrm{a}}(p,s)$ and $T_{3\mathrm{b}}(p,s)$, Eqs. (2.38) and (2.39), for selected pressures and specific entropies [a]

Equation	p [MPa]	s [kJ kg^{-1}K^{-1}]	T [K]
	20	3.8	$6.282\,959\,869 \times 10^{2}$
$T_{3\mathrm{a}}(p,s)$, Eq. (2.38)	50	3.6	$6.297\,158\,726 \times 10^{2}$
	100	4.0	$7.056\,880\,237 \times 10^{2}$
	20	5.0	$6.401\,176\,443 \times 10^{2}$
$T_{3\mathrm{b}}(p,s)$, Eq. (2.39)	50	4.5	$7.163\,687\,517 \times 10^{2}$
	100	5.0	$8.474\,332\,825 \times 10^{2}$

[a] Programmed functions should be verified using 8 byte real values for all variables.

Numerical Consistencies. The numerical inconsistencies between Eqs. (2.38) and (2.39) and the basic equation $f_3(\rho,T)$, Eq. (2.11), in comparison with the permissible inconsistencies, given in Sec. 2.3.2, are listed in Table 2.66. These inconsistencies are less than the permissible values. This is also true when the backward equations are used in combination with the boundary equation $p_{\mathrm{s},3}(s)$, Eq. (2.30). The critical temperature T_c = 647.096 K is calculated by the two $T(p,s)$ equations for all six figures. The maximum inconsistency in temperature between the two backward equations, Eq. (2.38) and Eq. (2.39), along the boundary $s_{3\mathrm{ab}} = s_\mathrm{c}$,

Eq. (2.35), amounts to 0.093 mK, which is within the permissible inconsistency given in Sec. 2.3.2.

Table 2.66 Maximum and root-mean-square inconsistencies in temperature between the backward equations $T_{3\,\mathrm{a}}(p,s)$ and $T_{3\,\mathrm{b}}(p,s)$, Eqs. (2.38) and (2.39), and the basic equation $f_3(\rho,T)$, Eq. (2.11), in comparison with the permissible values

Subregion	Equation	Inconsistencies in temperature [mK] $\lvert\Delta T\rvert_{\mathrm{perm}}$	$\lvert\Delta T\rvert_{\mathrm{max}}$	$(\Delta T)_{\mathrm{RMS}}$
3a	$T_{3\,\mathrm{a}}(p,s)$, Eq. (2.38)	25	24.8	11.2
3b	$T_{3\,\mathrm{b}}(p,s)$, Eq. (2.39)	25	22.1	10.1

Note. When calculating properties in the range $p \le p_{\mathrm{c}}$ and extremely close to the saturation lines, Eq. (2.38) might yield temperatures $T_{3\mathrm{a}}(p,s) > T_{\mathrm{s}}(p)$ and Eq. (2.39) might yield temperatures $T_{3\mathrm{b}}(p,s) < T_{\mathrm{s}}(p)$ due to the minor inconsistencies. In these cases, the results of Eqs. (2.38) and (2.39) must be corrected to $T_{3\mathrm{a}} = T_{\mathrm{s}}(p)$ and $T_{3\mathrm{b}} = T_{\mathrm{s}}(p)$, respectively, where the saturation temperature $T_{\mathrm{s}}(p)$ is calculated from Eq. (2.14) for the given pressure.

d) Computing Time when Using the Backward Equations $T(p,s)$ and $v(p,s)$ in Comparison with the Basic Equation

The calculation of specific volume and temperature as a function of (p,s) with the backward equations $v_{3\mathrm{a}}(p,s)$ and $T_{3\mathrm{a}}(p,s)$, Eqs. (2.36) and (2.38), or $v_{3\mathrm{b}}(p,s)$ and $T_{3\mathrm{b}}(p,s)$, Eqs. (2.37) and (2.39), is about 14 times faster than when using only the basic equation $f_3(\rho,T)$, Eq. (2.11), [19]. In this comparison, the basic equation has to be applied in combination with a two-dimensional Newton iteration with convergence tolerances corresponding to the consistency requirements that were set for the backward equations.

2.3.5 Backward Equations and Backward Functions Dependent on the Input Variables (h,s)

In this section, all backward equations as a function of the variables (h,s) are summarized. These are the backward equations $p(h,s)$ for regions 1 to 3 and the backward equation $T_{\mathrm{s}}(h,s)$ for the technically important part of region 4, the two-phase region.

For the calculation of thermodynamic properties as a function of the input variables (p,h) and (p,s) without iteration from the basic equations $g(p,T)$ of regions 1 and 2, only one variable, namely the temperature, had to be provided by a backward equation. This was achieved by the backward equations $T(p,h)$ and $T(p,s)$ as given in Secs. 2.3.3 and 2.3.4. However, when thermodynamic properties as a function of the input variables (h,s) need to be calculated from the basic equations $g(p,T)$ without iteration, the backward equations $p(h,s)$ yield only one of the two input variables of the g equation, namely the pressure; the second one, the temperature, is still missing. Although direct backward equations of the form $T(h,s)$ for the single-phase regions 1 to 3 have not been developed, the temperature belonging to the input variables (h,s) can be determined by combining the respective backward equation $p(h,s)$ with the corresponding backward equation $T(p,h)$.[6] Such a combination of two backward equations, e.g. in the form $T(h,s) = T(p(h,s),h)$, is called a *backward function* in the following text. For given values of (h,s), property calculations in region 3 from the basic equation $f_3(\rho,T)$,

[6] The alternative use of the backward equation $T(p,s)$ leads to worse numerical consistency.

Eq. (2.11), require, in addition to temperature (see above), the determination of the density $\rho = 1/v$. The value of the specific volume v can be obtained without iteration from the backward function $v(p(h,s),s)$, which is a combination of the two backward equations $p(h,s)$ and $v(p,s)$[7]. Another example is the calculation of the saturation pressure p_s as a function of (h,s) in the part of the two-phase region 4 that is important for steam-turbine calculations. In this region, $p_s(h,s)$ can be calculated without iteration from the backward function $p_s(T_s(h,s))$ formed by the combination of the backward equation $T_s(h,s)$, Eq. (2.61), with the saturation-pressure equation $p_s(T)$, Eq. (2.13).

The first backward equations that were developed after the adoption of IAPWS-IF97 were the equations $p(h,s)$ for regions 1 and 2 [11]; these equations were adopted by IAPWS in 2001 [22]. Later, the corresponding backward equations for region 3 including all region-boundary equations were developed [13] and adopted by IAPWS in 2004 [24].

Figure 2.13 shows in an *h*-*s* diagram the assignment of the backward equations $p(h,s)$ to the single-phase regions 1 to 3 and $T_s(h,s)$ to region 4 for $s \geq s''(623.15\text{ K})$. In Sec. 2.3.5.1, the calculation of h values along the region boundaries for given values of s is described and the region-boundary equations themselves are given in Sec. 2.3.5.2.

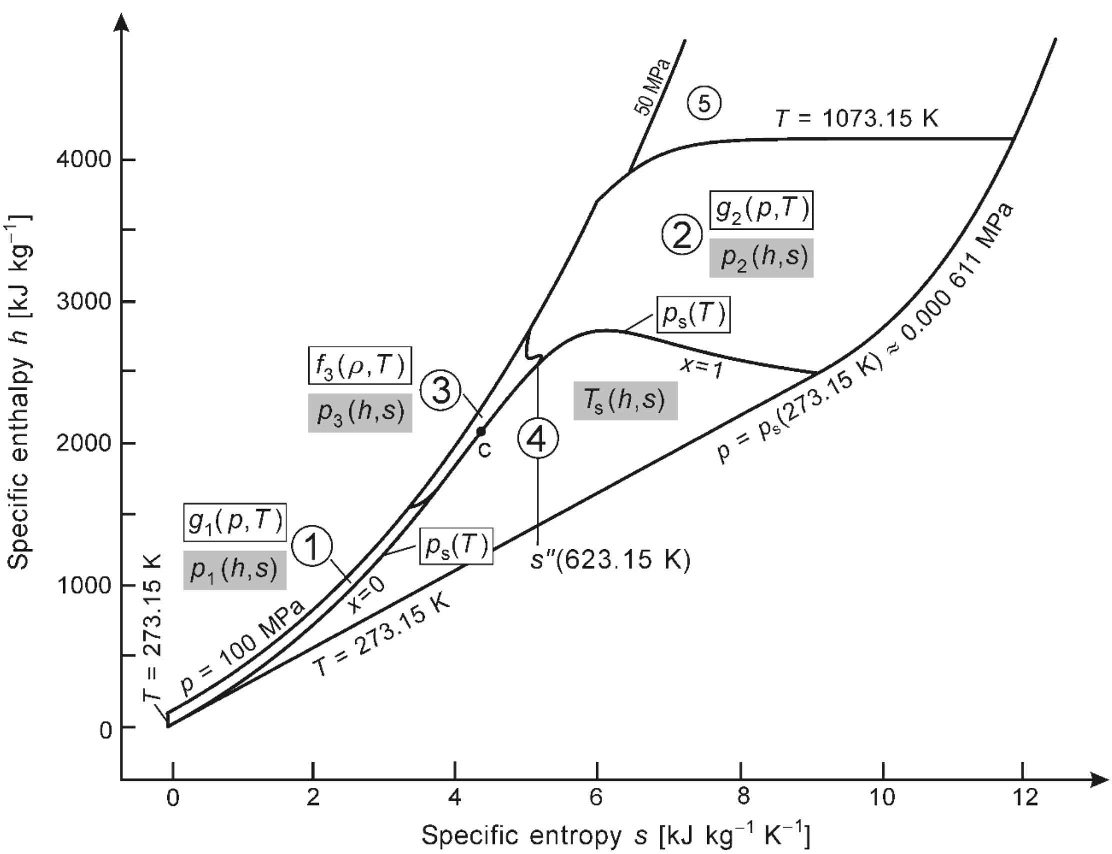

Fig. 2.13 Assignment of the backward equations $p(h,s)$ to the single-phase regions 1 to 3 and $T_s(h,s)$ to that part of the two-phase region 4 with $s \geq s''(623.15\text{ K})$. For this overview, it is not shown how regions 2 and 3 will be divided into subregions.

[7] The alternative use of the backward equation $v(p,h)$ leads to worse numerical consistency.

2.3.5.1 Regions and Region Boundaries in the Variables (h,s)

When property calculations with IAPWS-IF97 for regions 1 to 4 are carried out with the variables (h,s) as input variables, the regions are defined by describing how to calculate the h values for given s values along the outer region boundaries and the boundaries between the regions of IAPWS-IF97. Thus, all tests to determine whether a given (h,s) point is within the range of regions 1 to 4 of IAPWS-IF97 and, if so, in which region, must be performed with respect to these input variables. To be able to carry out such tests without any iteration, the h values along the region boundaries for given values of s must be calculable without iteration. Therefore, for all boundaries *between* the various regions, special region-boundary equations of the form $h(s)$ and $T(h,s)$, were developed [13] and adopted by IAPWS in 2004 [24], see Fig. 2.14. All of these region-boundary equations are given in Sec. 2.3.5.2. There are no special region-boundary equations for the outer region boundaries formed by the two isobars $p = 100$ MPa and $p = p_s(273.15\text{ K}) \approx 0.000\,611$ MPa and by the two isotherms $T = 273.15$ K and $T = 1073.15$ K, see Fig. 2.14.

Based on Fig. 2.14, the following subsections summarize which equations should be used to calculate h values along the various region boundaries for given values of s. For the two isotherms $T = 273.15$ K and $T = 1073.15$ K, for which the enthalpy calculations cannot be carried out without iterations, a special procedure is presented to perform the necessary tests without calculating the enthalpies along these boundaries.

Note. When calculating properties with the help of backward equations for a given state point extremely close to a region boundary, attention should be paid to the existence of (very minor) inconsistencies between backward equations and basic equations, and between region-boundary equations and basic equations. Due to these inconsistencies, the calculations could indicate that the state point is in the adjacent region, but (of course) extremely close to the region boundary. The user should be aware of these effects in order to avoid possible numerical problems by taking suitable measures in the program code. For this purpose, corresponding notes on how to proceed in such cases are given in the respective sections.

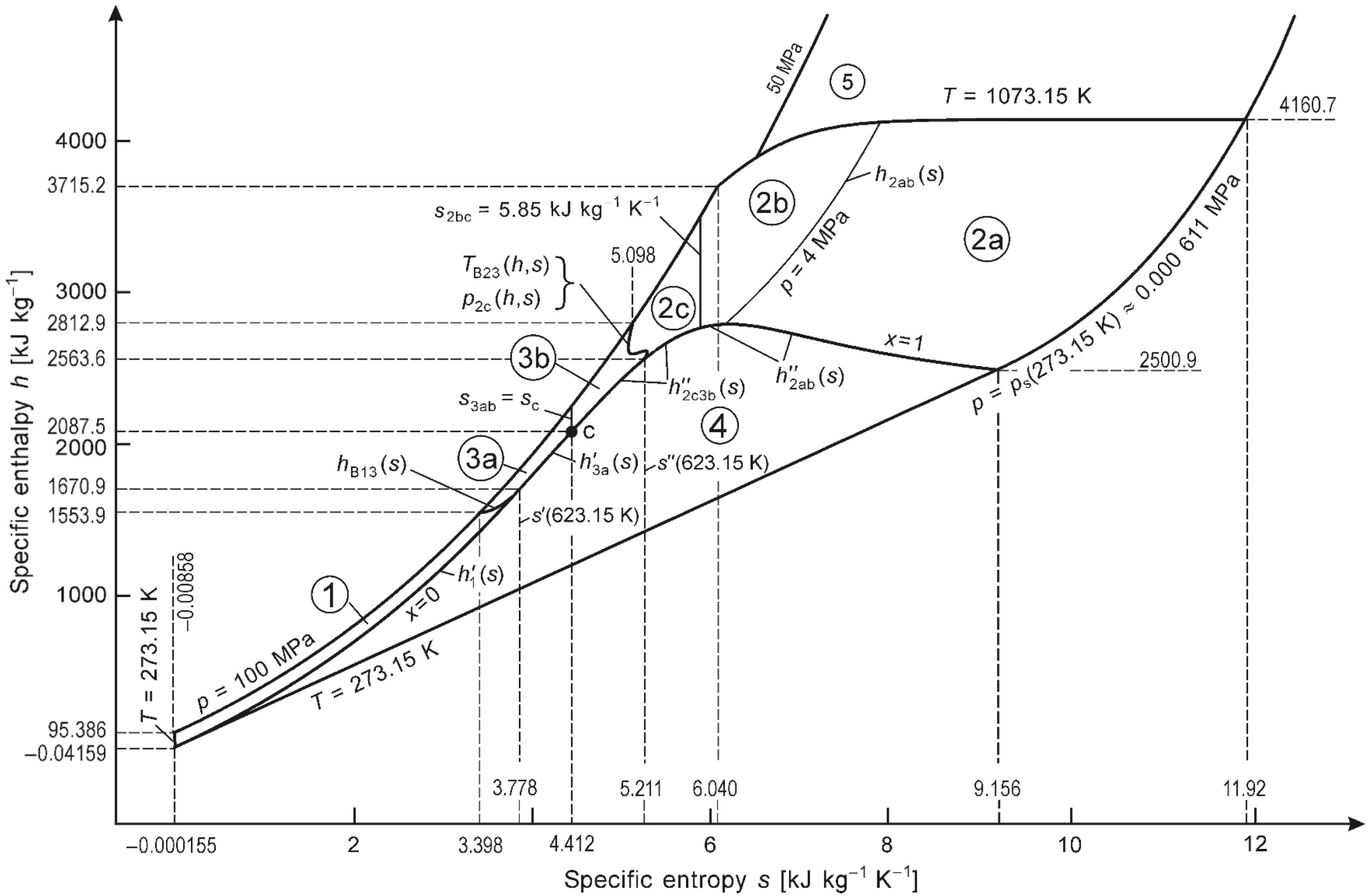

Fig. 2.14 Assignment of the region-boundary equations $h_{B13}(s)$, the combination of $T_{B23}(h,s)$ and $p_{2c}(h,s)$, $h'_1(s)$, $h'_{3a}(s)$, $h''_{2c3b}(s)$, and $h''_{2ab}(s)$ to the corresponding region boundaries. The h and s values at the corner points of the region boundaries are rounded values.

a) Outer Boundaries of Regions 1 to 4

The description of the boundaries starts at the left-hand side of Fig. 2.14 with the isotherm $T = 273.15$ K and proceeds clockwise.

The Isotherm T = 273.15 K. This isotherm is the lowest temperature limit of region 1 and also of IAPWS-IF97. Figure 2.15 shows the h-s region around the isotherm $T = 273.15$ K in greater detail. In the range between the saturated-liquid line ($x = 0$) and the isobar $p = 100$ MPa, this isotherm covers the ranges of specific enthalpy and specific entropy given by

$$h_1(p_s(273.15\text{ K}), 273.15\text{ K}) \le h \le h_1(100\text{ MPa}, 273.15\text{ K}),$$
$$s_1(100\text{ MPa}, 273.15\text{ K}) \le s \le s_{max}(T = 273.15\text{ K})$$
$$\text{with } s_{max}(T = 273.15\text{ K}) = 4.751\,610\,0567\times10^{-4}\text{ kJ kg}^{-1}\text{ K}^{-1}.$$

The value of p_s is calculated from the $p_s(T)$ equation, Eq. (2.13); s_{max} was determined from the basic equation of region 1, $g_1(p,T)$, Eq. (2.3), by iteration.

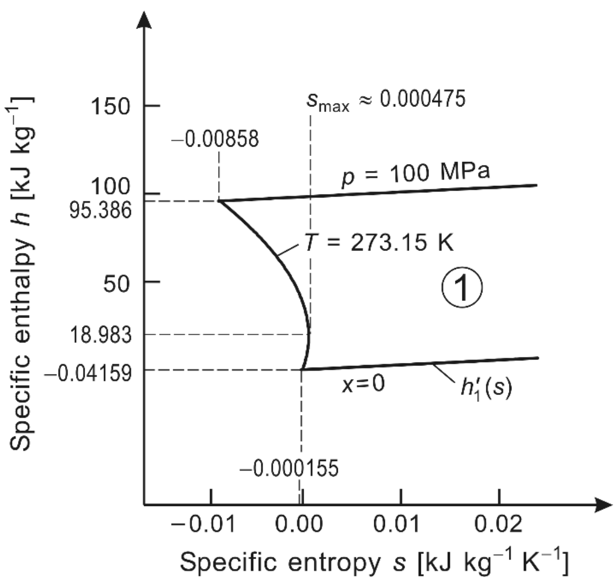

Fig. 2.15 Enlarged section of the h-s diagram of Fig. 2.14 very near the isotherm $T = 273.15$ K.

Along the isotherm $T = 273.15$ K, the h values for given s values can only be determined by iteration with the basic equation $g_1(p,T)$, Eq. (2.3), because there is no backward equation $p(T,s)$ that could provide the missing pressure. Thus, if values of h are needed along the isotherm $T = 273.15$ K, iterations with Eq. (2.3) cannot be avoided. It can be determined, however, without iteration, whether any given (h,s) point has a temperature $T \ge 273.15$ K, using the following method. For given values of h and s, the corresponding temperature is calculated from the backward function $T = T_1(p_1(h,s),h)$[8] and compared with the boundary temperature $T = 273.15$ K. The value p_1 is determined from the backward equation $p_1(h,s)$, Eq. (2.46), and T_1 is calculated from the backward equation $T_1(p,h)$, Eq. (2.19). The extrapolation capability of the two backward equations into the entropy range down to $s = s_1(100\text{ MPa}, 273.15\text{ K})$ was successfully tested.

[8] The alternative use of the backward equation $T_1(p,s)$ leads to worse numerical consistency.

Note. For (h,s) points extremely close to the boundary $T = 273.15\text{ K}$, the following procedure is recommended. When calculating the temperature $T = T_1(p_1(h,s),h)$ as described above, the numerical inconsistency of the combined backward equations $p_1(h,s)$ and $T_1(p,h)$ with respect to the basic equation $g_1(p,T)$ has to be considered. Due to this minor inconsistency the result of the calculated temperature should be corrected to $T = T_1(p_1(h,s),h) + \Delta T$, where ΔT = 24 mK according to the maximum inconsistency given in Table 2.80. This procedure ensures that (h,s) points extremely close to T = 273.15 K are correctly assigned to the range of validity of IAPWS-IF97.

The Isobar p = 100 MPa. Figure 2.14 shows that the 100 MPa isobar is the upper pressure limit for regions 1 to 4 of IAPWS-IF97 and covers the entropy range

$$s_1(100\text{ MPa, }273.15\text{ K}) \le s \le s_2(100\text{ MPa, }1073.15\text{ K}),$$

where s_1 is obtained from the basic equation of region 1, $g_1(p,T)$, Eq. (2.3), and s_2 from the basic equation of region 2, $g_2(p,T)$, Eq. (2.6).

Figure 2.9 shows that, in the range of region 1, the 100 MPa isobar covers the entropy range

$$s_1(100\text{ MPa, }273.15\text{ K}) \le s \le s_1(100\text{ MPa, }623.15\text{ K}),$$

where s_1 is calculated as given above. For this entropy range, the h value for the given s value is determined from the basic equation $g_1(p,T)$, Eq. (2.3), with p = 100 MPa and $T = T_1$ calculated from the backward equation $T_1(p,s)$, Eq. (2.31), with p = 100 MPa. The given enthalpy value can then be compared with the calculated value for h.

According to Secs. 2.3.3.4a and 2.3.4.4a and Figs. 2.8, 2.12, and 2.14, region 3 is divided into subregions 3a and 3b. Along this isobar, subregion 3a covers the entropy range

$$s_1(100\text{ MPa, }623.15\text{ K}) \le s \le s_\mathrm{c}$$
$$\text{with } s_\mathrm{c} = 4.412\,021\,482\,234\,76\text{ kJ kg}^{-1}\text{ K}^{-1}$$

according to Eq. (2.35) and where s_1 is determined from the basic equation $g_1(p,T)$, Eq. (2.3). For this entropy range, the h value for the given s value is calculated from the basic equation of region 3, $f_3(\rho,T)$, Eq. (2.11), with $\rho = 1/v_{3a}$ and $T = T_{3a}$, where v_{3a} and T_{3a} are calculated from the backward equations $v_{3a}(p,s)$ and $T_{3a}(p,s)$, Eqs. (2.36) and (2.38), with p = 100 MPa. The given enthalpy value can then be compared with the calculated value for h.

The entropy range of subregion 3b along the isobar p = 100 MPa is given by the relation

$$s_\mathrm{c} \le s \le s_2(100\text{ MPa, }863.15\text{ K})$$

with s_c as given in Eq. (2.35) and s_2 determined from the basic equation of region 2, $g_2(p,T)$, Eq. (2.6), for p = 100 MPa and T = 863.15 K, the highest temperature on the B23-line that is described by the equation $T_{\mathrm{B23}}(p)$, Eq. (2.2). For this entropy range, the h value for the given s value is obtained from the basic equation $f_3(\rho,T)$, Eq. (2.11), with $\rho = 1/v_{3b}$ and $T = T_{3b}$, where v_{3b} and T_{3b} are determined from the backward equations $v_{3b}(p,s)$ and $T_{3b}(p,s)$, Eqs. (2.37) and (2.39), for p = 100 MPa. The given enthalpy value can then be compared with the calculated value for h.

As described in Secs. 2.3.3.3a and 2.3.4.3a and illustrated in Figs. 2.7, 2.11, and 2.14, region 2 is divided into subregions 2a, 2b, and 2c. Along the isobar p = 100 MPa, region 2c covers the entropy range

$$s_2(100\text{ MPa, }863.15\text{ K}) < s \le s_{2\mathrm{bc}} = 5.85\text{ kJ kg}^{-1}\text{ K}^{-1},$$

where $T = 863.15$ K in accordance with the $T_{B23}(p)$ equation, Eq. (2.2), for $p = 100$ MPa. The calculation of s_2 is the same as described above for subregion 3b. For this entropy range, the h value for the given s value is obtained from the basic equation $g_2(p,T)$, Eq. (2.6), with $p = 100$ MPa and $T = T_{2c}$ determined from the backward equation $T_{2c}(p,s)$, Eq. (2.34), with $p = 100$ MPa. The given enthalpy value can then be compared with the calculated value for h.

According to Fig. 2.14, the uppermost part of the isobar $p = 100$ MPa is given by the entropy range

$$s_{2bc} \le s \le s_2(100 \text{ MPa}, 1073.15 \text{ K})$$

with $s_{2bc} = 5.85 \text{ kJ kg}^{-1} \text{ K}^{-1}$ and s_2 calculated from the basic equation $g_2(p,T)$, Eq. (2.6). The h value for the given s value is obtained from the equation $g_2(p,T)$ with $p = 100$ MPa and $T = T_{2b}$ determined from the backward equation $T_{2b}(p,s)$, Eq. (2.33), for $p = 100$ MPa. The given enthalpy value can then be compared with the calculated value for h.

Note. For such (h,s) points extremely close to the boundary $p = 100$ MPa, the following procedure is recommended. When calculating the enthalpy at the boundary $p = 100$ MPa as described above, the numerical inconsistencies of the backward equations $T_1(p,s)$, $v_{3a}(p,s)$ and $T_{3a}(p,s)$, $v_{3b}(p,s)$ and $T_{3b}(p,s)$, $T_{2c}(p,s)$, and $T_{2b}(p,s)$ with respect to the basic equations $g_1(p,T)$, $f_3(\rho,T)$, and $g_2(p,T)$ have to be considered. Due to these minor inconsistencies the results for the calculated temperatures and specific volumes should be corrected according to the maximum inconsistencies given in Tables 2.53, 2.62, 2.66, and 2.58 as follows:

$T = T_1(p,s) - \Delta T$, where $\Delta T = 21.8$ mK,
$v = v_{3a}(p,s)\,(1 + \Delta v/v)$, where $\Delta v/v = 9.6 \times 10^{-5}$,
$T = T_{3a}(p,s) - \Delta T$, where $\Delta T = 24.8$ mK,
$v = v_{3b}(p,s)\,(1 + \Delta v/v)$, where $\Delta v/v = 7.7 \times 10^{-5}$,
$T = T_{3b}(p,s) - \Delta T$, where $\Delta T = 22.1$ mK,
$T = T_{2c}(p,s) - \Delta T$, where $\Delta T = 19.0$ mK, and
$T = T_{2b}(p,s) - \Delta T$, where $\Delta T = 6.5$ mK.

This procedure ensures that (h,s) points given extremely close to the boundary $p = 100$ MPa are correctly assigned to the range of validity of IAPWS-IF97.

The Isotherm T = 1073.15 K. Figure 2.14 shows that the 1073.15 K isotherm corresponds to the upper temperature limit of region 2 and thus for all of regions 1 to 4 of IAPWS-IF97 and covers the entropy range

$$s_2(100 \text{ MPa}, 1073.15 \text{ K}) \le s \le s_2(p_s(273.15 \text{ K}), 1073.15 \text{ K}),$$

where the values of specific entropy s_2 can be calculated simply from the basic equation $g_2(p,T)$, Eq. (2.6). Along this isotherm the h values for given s values can only be calculated by iteration with the basic equation $g_2(p,T)$, Eq. (2.6), because there is no backward equation $p(T,s)$ that can provide the missing pressure. Thus, if h values are needed along this isotherm, iterations with Eq. (2.6) cannot be avoided. It can be determined, however, without iteration, whether any given (h,s) point has a temperature $T \ge 273.15$ K, using the following method.

The (h,s) point is first checked to find out whether it meets the condition $h \le h_{max}$, where $h_{max} = h_2(p_s(273.15 \text{ K}), 1073.15 \text{ K})$ is the highest specific enthalpy value for all of regions 1 to 4 of IAPWS-IF97 and occurs at $p = p_s(273.15 \text{ K})$ and $T = 1073.15$ K, see Fig. 2.14. If this enthalpy condition is not met, the (h,s) point is outside regions 1 to 4 of IAPWS-IF97 and no further test is necessary. If $h \le h_{max}$ is fulfilled, the backward equations $p_{2a}(h,s)$, $p_{2b}(h,s)$,

$T_{2a}(p,h)$, and $T_{2b}(p,h)$ may be used to calculate the temperature for the given (h,s) point. Then, this temperature can be compared with the boundary temperature $T = 1073.15$ K as follows.

In the entropy range

$$s_2(100 \text{ MPa}, 1073.15 \text{ K}) \le s < s_2(4 \text{ MPa}, 1073.15 \text{ K}),$$

for given values of h and s, the corresponding temperature can be calculated from the backward function $T = T_{2b}(p_{2b}(h,s),h)$[9] and compared with the boundary temperature $T = 1073.15$ K. The value p_{2b} is determined from the backward equation $p_{2b}(h,s)$, Eq. (2.50), and T_{2b} is calculated from the backward equation $T_{2b}(p,h)$, Eq. (2.23).

In the entropy range

$$s_2(4 \text{ MPa}, 1073.15 \text{ K}) \le s \le s_2(p_s(273.15 \text{ K}), 1073.15 \text{ K}),$$

for given values of h and s, the corresponding temperature can be calculated from the backward function $T = T_{2a}(p_{2a}(h,s),h)$[10] and compared with the boundary temperature $T = 1073.15$ K. The value p_{2a} is determined from the backward equation $p_{2a}(h,s)$, Eq. (2.49), and T_{2a} is calculated from the backward equation $T_{2a}(p,h)$, Eq. (2.22).

The extrapolation capability of the backward equations into the enthalpy range up to h_{max} was successfully tested.

Note. For (h,s) points extremely close to the boundary $T = 1073.15$ K, the following procedure is recommended. When calculating the temperature $T = T_{2a}(p_{2a}(h,s),h)$ or $T = T_{2b}(p_{2b}(h,s),h)$ as described above, the numerical inconsistencies of the combined backward equations $p_{2a}(h,s)$ and $T_{2a}(p,h)$ and of $p_{2b}(h,s)$ and $T_{2b}(p,h)$ with the basic equation $g_2(p,T)$ have to be considered. Due to these minor inconsistencies the results of the calculated temperatures should be corrected to $T = T_{2a}(p_{2a}(h,s),h) - \Delta T$, where $\Delta T = 9.7$ mK, or $T = T_{2b}(p_{2b}(h,s),h) - \Delta T$, where $\Delta T = 9.8$ mK according to the maximum inconsistencies given in Table 2.87. This procedure ensures that (h,s) points extremely close to $T = 1073.15$ K are correctly assigned to the range of validity of IAPWS-IF97.

The Isobar $p = p_s(273.15 \text{ K}) = 0.000\,611\,212\,677$ MPa. Figure 2.14 shows that this isobar is the lower pressure limit of the IAPWS-IF97 backward equations. Within regions 1 to 4 of IAPWS-IF97, this isobar covers the entropy range entirely:

$$s_1(p_s(273.15 \text{ K}), 273.15 \text{ K}) \le s \le s_2(p_s(273.15 \text{ K}), 1073.15 \text{ K}),$$

where s_1 is determined from the basic equation $g_1(p,T)$, Eq. (2.3), and s_2 is obtained from the basic equation $g_2(p,T)$, Eq. (2.6).

As can be seen in Fig. 2.14, the entropy range in which this isobar limits region 2a is defined by

$$s''(273.15 \text{ K}) \le s \le s_2(p_s(273.15 \text{ K}), 1073.15 \text{ K})$$
$$\text{with } s''(273.15 \text{ K}) = s_2(p_s(273.15 \text{ K}), 273.15 \text{ K}),$$

where the specific entropies s_2 are calculated from the basic equation $g_2(p,T)$, Eq. (2.6), and $p = p_s(T)$ according to Eq. (2.13) with $T = 273.15$ K. For this entropy range, the h value for the given s value is determined from the basic equation $g_2(p,T)$ with $T = T_{2a}$ calculated from the

[9] The alternative use of the backward equation $T_{2b}(p,s)$ leads to worse numerical consistency.
[10] The alternative use of the backward equation $T_{2a}(p,s)$ leads to worse numerical consistency.

backward equation $T_{2a}(p,s)$, Eq. (2.32), with $p = p_s(273.15\ \text{K})$. The given enthalpy value can then be compared with the calculated h value.

The isobar $p = p_s(273.15\ \text{K})$ also forms the lower pressure limit of the two-phase region 4 over the entropy range

$$s'(273.15\ \text{K}) \le s \le s''(273.15\ \text{K})$$
$$\text{with } s'(273.15\ \text{K}) = s_1(p_s(273.15\ \text{K}), 273.15\ \text{K})$$
$$\text{and } s''(273.15\ \text{K}) = s_2(p_s(273.15\ \text{K}), 273.15\ \text{K}),$$

where s_1 is calculated from the basic equation $g_1(p,T)$, Eq. (2.3), s_2 from the basic equation $g_2(p,T)$, Eq. (2.6), and p_s is obtained from Eq. (2.13). For this entropy range, the h value for the given s value is calculated by the relation

$$h = h' + \frac{s - s'}{s'' - s'}\left(h'' - h'\right).$$

In this relation, $h' = h_1(p_s(273.15\ \text{K}), 273.15\ \text{K})$ and $s' = s_1(p_s(273.15\ \text{K}), 273.15\ \text{K})$ are calculated from the basic equation $g_1(p,T)$, Eq. (2.3), and $h'' = h_2(p_s(273.15\ \text{K}), 273.15\ \text{K})$ and $s'' = s_2(p_s(273.15\ \text{K}), 273.15\ \text{K})$ are determined from the basic equation $g_2(p,T)$, Eq. (2.6), where $p = p_s(T)$ is obtained from Eq. (2.13). The given enthalpy value can then be compared with the calculated value for h.

Note. For (h,s) points in the range $s''(273.15\ \text{K}) \le s \le s_2(p_s(273.15\ \text{K}), 1073.15\ \text{K})$ extremely close to the boundary $p = 0.000\,611\,212\,677$ MPa, the following procedure is recommended. When calculating the enthalpy at the boundary $p = 0.000\,611\,212\,677$ MPa as described above, the numerical inconsistency between the backward equation $T_{2a}(p,s)$ and the basic equation $g_2(p,T)$ has to be considered. Due to this minor inconsistency the result of the calculated temperature should be corrected to $T = T_{2a}(p,s) + \Delta T$, where $\Delta T = 8.8$ mK according to the maximum inconsistency given in Table 2.58. This procedure ensures that (h,s) points extremely close to $p = 0.000\,611\,212\,677$ MPa are correctly assigned to the range of validity of IAPWS-IF97 backward equations.

b) The Boundary between the Single-Phase Regions 1 to 3 and the Two-Phase Region 4

According to Fig. 2.14, this boundary, corresponding to the saturated-liquid and saturated-vapour lines, is described by the equations $h'_1(s)$, $h'_{3a}(s)$, $h''_{2c3b}(s)$, and $h''_{2ab}(s)$ given in Secs. 2.3.5.2a and 2.3.5.2b.

The part of the saturated-liquid line ($x = 0$) that adjoins region 1 covers the entropy range

$$s'(273.15\ \text{K}) \le s \le s'(623.15\ \text{K})$$
$$\text{with } s'(273.15\ \text{K}) = s_1(p_s(273.15\ \text{K}), 273.15\ \text{K})$$
$$\text{and } s'(623.15\ \text{K}) = s_1(p_s(623.15\ \text{K}), 623.15\ \text{K}),$$

where the two values s_1 are calculated from the basic equation $g_1(p,T)$, Eq. (2.3), and $p = p_s(T)$ is determined from Eq. (2.13). Along this part of the boundary, the h value for the given s value is calculated from the equation $h'_1(s)$, Eq. (2.40). The given enthalpy value can then be compared with the calculated value for h.

The part of the saturated-liquid line ($x = 0$) that adjoins subregion 3a is given by the entropy range

$$s'(623.15\ \text{K}) \le s \le s_c,$$
$$\text{with } s'(623.15\ \text{K}) = s_1(p_s(623.15\ \text{K}), 623.15\ \text{K})$$

and the value of s_c is given in Eq. (2.35); p_s is determined from Eq. (2.13). Along this part of the boundary, the h value for the given s value is calculated from the equation $h'_{3a}(s)$, Eq. (2.41). The given enthalpy value can then be compared with the calculated value for h.

The part of the saturated-vapour line ($x = 1$) extending from the critical point to the subregion boundary s_{2bc} covers the entropy range

$$s_c \leq s < s_{2bc}$$

with s_c according to Eq. (2.35) and $s_{2bc} = 5.85\ \mathrm{kJ\ kg^{-1}\ K^{-1}}$. Along this part of the boundary, the h value for the given s value is calculated from the equation $h''_{2c3b}(s)$, Eq. (2.43). The given enthalpy value can the be compared with then calculated value for h.

The rest of the saturated-vapour line ($x = 1$) is within the entropy range

$$s_{2bc} \leq s \leq s''(273.15\ \mathrm{K}),$$
$$\text{with } s''(273.15\ \mathrm{K}) = s_2(p_s(273.15\ \mathrm{K}), 273.15\ \mathrm{K}),$$

where $s_{2bc} = 5.85\ \mathrm{kJ\ kg^{-1}\ K^{-1}}$ and s_2 is obtained from the basic equation $g_2(p,T)$, Eq. (2.6), with $p = p_s(T)$ according to Eq. (2.13). Along this part of the boundary, the h value for the given s value is determined from the equation $h''_{2ab}(s)$, Eq. (2.42). The given enthalpy value can then be compared with the calculated value for h.

Note. The entire boundary between the single-phase regions 1 to 3 and the two-phase region 4 is considered to belong to both single-phase regions and the two-phase region.

c) Boundaries between the Single-Phase Regions

As shown in Fig. 2.14, the boundaries between the single-phase regions are the boundaries between regions 1 and 3, and between regions 2 and 3. According to the statement made at the beginning of Sec. 2.2, see also Figs. 2.2 and 2.5, the boundary between regions 1 and 3 ($T = 623.15$ K) is considered to belong to region 1 and the boundary between regions 2 and 3 (T_{B23}-line) is considered to belong to region 2. Thus, the properties along the boundary between regions 1 and 3 are calculated from the equations for region 1 and the properties along the boundary between regions 2 and 3 are determined from the equations for region 2.

Boundary between Regions 1 and 3. This boundary covers the entropy range

$$s_1(100\ \mathrm{MPa}, 623.15\ \mathrm{K}) \leq s \leq s'(623.15\ \mathrm{K})$$
$$\text{with } s'(623.15\ \mathrm{K}) = s_1(p_s(623.15\ \mathrm{K}), 623.15\ \mathrm{K}),$$

where s_1 is determined from the basic equation $g_1(p,T)$, Eq. (2.3), and $p_s(T)$ from Eq. (2.13). Along this boundary, the h value for the given s value is calculated from the equation $h_{B13}(s)$, Eq. (2.44). The given enthalpy value can then be compared with the calculated value for h.

Boundary between Regions 2 and 3. This boundary is defined by a *combination* of the region-boundary equation $T_{B23}(h,s)$ and the backward equation $p_{2c}(h,s)$ that are given as Eqs. (2.45) and (2.51). The reason why two equations are used for the description of the boundary between regions 2 and 3 is explained below.

In the variables (p,T), (p,h), and (p,s), the region boundary B23 is defined simply by the B23-equation in the forms of $p_{B23}(T)$ and $T_{B23}(p)$, Eqs. (2.1) and (2.2), which is also shown in Figs. 2.2, 2.5, and 2.9. However, the definition of this boundary in the variables (h,s) is more complex. Since the equation $p_{B23}(T)$ has an S-shape in the h-s plane as illustrated in Fig. 2.16, it is not possible to develop equations of the form $h_{B23}(s)$ or $s_{B23}(h)$ for this boundary; such

functions would not be single-valued. Therefore, the special region-boundary equation $T_{B23}(h,s)$, Eq. (2.45), for a small region around the B23-boundary was developed [13].

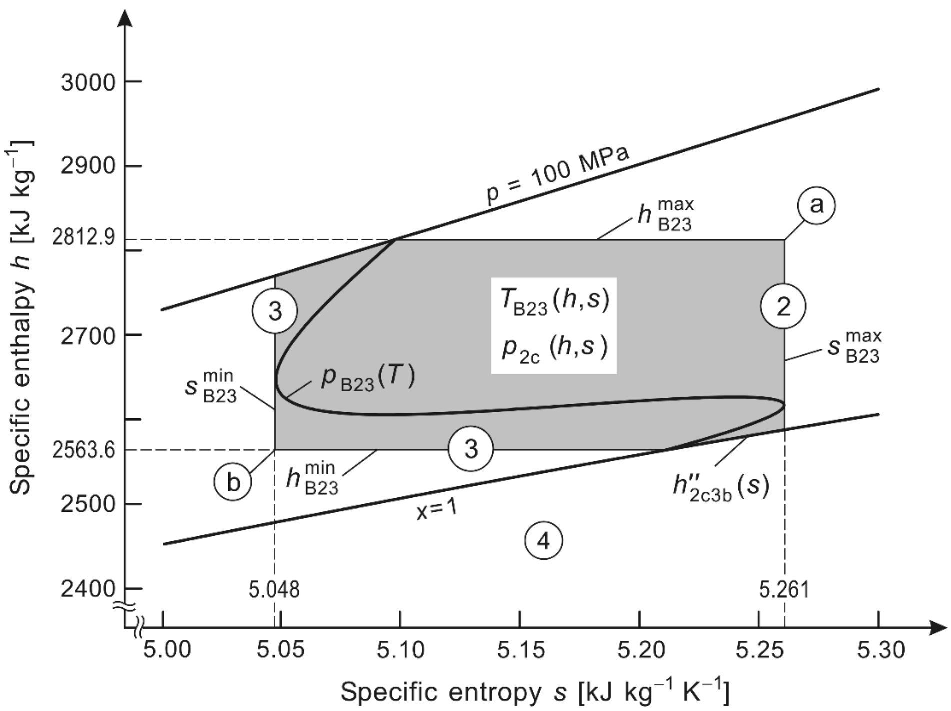

Fig. 2.16 Plot of the equation $p_{B23}(T)$, Eq. (2.1), and the range of validity (grey area) of the equation $T_{B23}(h,s)$, Eq. (2.45), in an h-s diagram. To be exact, region 2 means subregion 2c and region 3 means subregion 3b. The corner points a and b are needed to show their place in Fig. 2.17.

The range of validity of the equation $T_{B23}(h,s)$, which corresponds to the grey area in Fig. 2.16, extends from the saturated-vapour line ($x = 1$) up to 100 MPa over the entropy range

$$s_{B23}^{min} \le s \le s_{B23}^{max},$$

$$\text{where } s_{B23}^{min} = 5.048\,096\,828 \text{ kJ kg}^{-1}\text{ K}^{-1}$$

$$\text{and } s_{B23}^{max} = 5.260\,578\,707 \text{ kJ kg}^{-1}\text{ K}^{-1},$$

and in the enthalpy range

$$h_{B23}^{min} \le h \le h_{B23}^{max},$$

$$\text{where } h_{B23}^{min} = h''(623.15\text{ K}) = h_2(p_s(623.15\text{ K}), 623.15\text{ K}) = 2.563\,592\,004 \times 10^3 \text{ kJ kg}^{-1}$$

$$\text{and } h_{B23}^{max} = h_2(100\text{ MPa}, 863.15\text{ K}) = 2.812\,942\,061 \times 10^3 \text{ kJ kg}^{-1}.$$

The entropy values of s_{B23}^{min} and s_{B23}^{max} were calculated from the basic equation $g_2(p,T)$, Eq. (2.6), in combination with the equation $p_{B23}(T)$, Eq. (2.1), via iteration. The two h_2 values were obtained directly from the equation $g_2(p,T)$ with $p = p_s$ that was determined from the equation $p_s(T)$, Eq. (2.13), for $T = 623.15$ K.

With this background, the test for whether a given (h,s) point is located in region 2 or region 3 is carried out as follows:

If the two conditions

$$s_{\mathrm{B23}}^{\min} \le s \le s_{\mathrm{B23}}^{\max} \quad \text{and} \quad h_{\mathrm{B23}}^{\min} \le h \le h_{\mathrm{B23}}^{\max}$$

are met, then the (h, s) point is in the grey area of Fig. 2.16. In this case, the region-boundary equation $T_{\mathrm{B23}}(h, s)$ along with the backward equation $p_{2\mathrm{c}}(h, s)$, Eq. (2.51), determine in which region the given (h, s) point is located.

If the (h, s) point fulfils the condition

$$p_{2\mathrm{c}}(h, s) \le p_{\mathrm{B23}}(T_{\mathrm{B23}}(h, s)),$$

then the (h, s) point is in region 2, otherwise it is in region 3.

In these tests, the values of $s_{\mathrm{B23}}^{\min}$, $s_{\mathrm{B23}}^{\max}$, $h_{\mathrm{B23}}^{\min}$, and $h_{\mathrm{B23}}^{\max}$ are given above, $p_{2\mathrm{c}}(h, s)$ is obtained from Eq. (2.51), $T_{\mathrm{B23}}(h, s)$ from Eq. (2.45), and $p_{\mathrm{B23}}(T)$ from Eq. (2.1) with $T = T_{\mathrm{B23}}$. Checks were made to ensure that the backward equation $p_{2\mathrm{c}}(h, s)$ can be reasonably extrapolated into region 3 for $s \ge s_{\mathrm{B23}}^{\min}$ and $h \ge h_{\mathrm{B23}}^{\min}$. For further information, Fig. 2.17 shows the range of validity of the region-boundary equation $T_{\mathrm{B23}}(h, s)$, Eq. (2.45), in a p-T diagram.

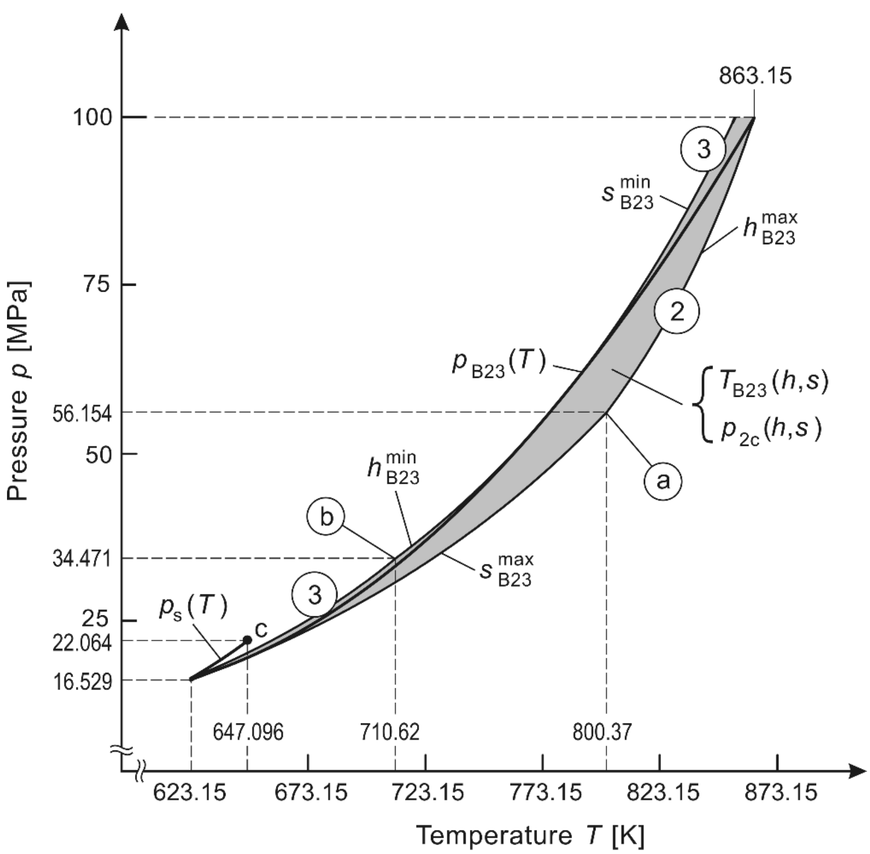

Fig. 2.17 Illustration of the B23-equation $p_{\mathrm{B23}}(T)$, Eq. (2.1), and the range of validity of the boundary equation $T_{\mathrm{B23}}(h, s)$, Eq. (2.45), in a p-T diagram. To be exact, region 2 means subregion 2c and region 3 means subregion 3b.

Note. For (h,s) points extremely close to the boundary between regions 2 and 3, the following procedure is recommended. When calculating pressures with the equations $p_{\mathrm{B23}}(T_{\mathrm{B23}}(h,s))$ and $p_{\mathrm{2c}}(h,s)$, the numerical inconsistency of 0.0045% in pressure of the used equations $T_{\mathrm{B23}}(h,s)$, Eq. (2.45), and $p_{\mathrm{2c}}(h,s)$, Eq. (2.51), with the B23-equation $p_{\mathrm{B23}}(T)$, Eq. (2.1), have to be considered. Due to this minor inconsistency the result of the calculated pressure p_{B23} should be corrected to $p_{\mathrm{B23}} = p_{\mathrm{B23}}(T_{\mathrm{B23}}(h,s))\ (1 + \Delta p/p)$, where $\Delta p/p = 4.5 \times 10^{-5}$. This procedure ensures that (p,h) points extremely close to the region boundary $p_{\mathrm{B23}}(T)$ are correctly assigned to region 2 and not falsely to region 3.

2.3.5.2 Equations for Region Boundaries in the Variables (h,s)

In this section, all of the equations that describe the region boundaries in the variables (h,s) are summarized. The equations for the saturated-liquid line, for the saturated-vapour line, and for the two boundaries between the single-phase regions are given in separate subsections.

When the backward equations and functions depending on (h,s) are used in combination with such boundary equations, their inconsistencies with the respective basic equation are less than the permissible values, as given in Sec. 2.3.2. Therefore, the use of these special region-boundary equations determines the region in which a given (h,s) point is located without computing-time consuming iterations with the basic equations of regions 1 to 4.

a) Boundary Equations $h'(s)$ for the Saturated-Liquid Line

In order to meet the requirements for numerical consistency given in Sec. 2.3.2, the saturated-liquid line ($x = 0$) is covered by two equations of the form $h'(s)$.

The equation $h'_1(s)$ describes the saturated-liquid line over the entire range adjoining the single-phase region 1. As shown in Fig. 2.14, the equation $h'_1(s)$ covers the temperature range from 273.15 K to 623.15 K with the entropy range given by:

$$s'(273.15\ \mathrm{K}) \le s \le s'(623.15\ \mathrm{K})$$
$$\text{with } s'(273.15\ \mathrm{K}) = s_1(p_\mathrm{s}(273.15\ \mathrm{K}), 273.15\ \mathrm{K}) = -1.545\,495\,919 \times 10^{-4}\ \mathrm{kJ\,kg^{-1}\,K^{-1}}$$
$$\text{and } s'(623.15\ \mathrm{K}) = s_1(p_\mathrm{s}(623.15\ \mathrm{K}), 623.15\ \mathrm{K}) = 3.778\,281\,340\ \mathrm{kJ\,kg^{-1}\,K^{-1}},$$

where the two values for s_1 were calculated from the basic equation $g_1(p,T)$, Eq. (2.3), with $p = p_\mathrm{s}(T)$ from Eq. (2.13).

The boundary equation $h'_1(s)$ has the following dimensionless form:

$$\frac{h'_1(s)}{h^*} = \eta'(\sigma) = \sum_{i=1}^{27} n_i (\sigma - 1.09)^{I_i} \left(\sigma + 0.366 \times 10^{-4}\right)^{J_i}, \tag{2.40}$$

where $\eta = h/h^*$ and $\sigma = s/s^*$ with $h^* = 1\,700\ \mathrm{kJ\,kg^{-1}}$ and $s^* = 3.8\ \mathrm{kJ\,kg^{-1}\,K^{-1}}$. The coefficients n_i and exponents I_i and J_i of Eq. (2.40) are listed in Table 2.67.

The equation $h'_{3\mathrm{a}}(s)$ describes the saturated-liquid line in the range adjoining the single-phase region 3a. Figure 2.14 shows that this equation covers the entropy range

$$s'(623.15\ \mathrm{K}) \le s \le s_\mathrm{c}$$
$$\text{with } s'(623.15\ \mathrm{K}) = 3.778\,281\,340\ \mathrm{kJ\,kg^{-1}\,K^{-1}}$$
$$\text{and } s_\mathrm{c} = 4.412\,021\,482\,234\,76\ \mathrm{kJ\,kg^{-1}\,K^{-1}}$$

according to Eq. (2.35), the procedure of calculating the value for $s'(623.15\ \mathrm{K})$ is given above.

The boundary equation $h'_{3a}(s)$ has the following dimensionless form:

$$\frac{h'_{3a}(s)}{h^*} = \eta'(\sigma) = \sum_{i=1}^{19} n_i (\sigma - 1.09)^{I_i} \left(\sigma + 0.366 \times 10^{-4}\right)^{J_i} , \tag{2.41}$$

where $\eta = h/h^*$ and $\sigma = s/s^*$ with $h^* = 1\,700$ kJ kg^{-1} and $s^* = 3.8$ kJ kg^{-1} K^{-1}. The coefficients n_i and exponents I_i and J_i of Eq. (2.41) are listed in Table 2.68.

The equation $h'_1(s)$, Eq. (2.40), meets exactly the enthalpy value $h'(273.15\text{ K}) = h_1(p_s(273.15\text{ K}), 273.15\text{ K}) = -4.158\,782\,623 \times 10^{-2}$ kJ kg^{-1} that was determined from the basic equation $g_1(p,T)$, Eq. (2.3), where $p_s(273.15\text{ K})$ is obtained from Eq. (2.13). The equation $h'_{3a}(s)$, Eq. (2.41) yields exactly the enthalpy value at the critical point $h_c = 2.087\,546\,845 \times 10^3$ kJ kg^{-1} calculated from the basic equation $f_3(\rho,T)$, Eq. (2.11), for $\rho = \rho_c$ and $T = T_c$ according to Eqs. (1.6) and (1.4).

Table 2.67 Coefficients and exponents of the boundary equation $h'_1(s)$ in its dimensionless form, Eq. (2.40)

i	I_i	J_i	n_i	i	I_i	J_i	n_i
1	0	14	0.332 171 191 705 237	15	8	4	$0.194\,486\,637\,751\,291 \times 10^{2}$
2	0	36	$0.611\,217\,706\,323\,496 \times 10^{-3}$	16	12	2	$-0.357\,915\,139\,457\,043 \times 10^{1}$
3	1	3	$-0.882\,092\,478\,906\,822 \times 10^{1}$	17	12	4	$-0.335\,369\,414\,148\,819 \times 10^{1}$
4	1	16	−0.455 628 192 543 250	18	14	1	−0.664 426 796 332 460
5	2	0	$-0.263\,483\,840\,850\,452 \times 10^{-4}$	19	14	22	$0.323\,321\,885\,383\,934 \times 10^{5}$
6	2	5	$-0.223\,949\,661\,148\,062 \times 10^{2}$	20	16	10	$0.331\,766\,744\,667\,084 \times 10^{4}$
7	3	4	$-0.428\,398\,660\,164\,013 \times 10^{1}$	21	20	12	$-0.223\,501\,257\,931\,087 \times 10^{5}$
8	3	36	−0.616 679 338 856 916	22	20	28	$0.573\,953\,875\,852\,936 \times 10^{7}$
9	4	4	$-0.146\,823\,031\,104\,040 \times 10^{2}$	23	22	8	$0.173\,226\,193\,407\,919 \times 10^{3}$
10	4	16	$0.284\,523\,138\,727\,299 \times 10^{3}$	24	24	3	$-0.363\,968\,822\,121\,321 \times 10^{-1}$
11	4	24	$-0.113\,398\,503\,195\,444 \times 10^{3}$	25	28	0	$0.834\,596\,332\,878\,346 \times 10^{-6}$
12	5	18	$0.115\,671\,380\,760\,859 \times 10^{4}$	26	32	6	$0.503\,611\,916\,682\,674 \times 10^{1}$
13	5	24	$0.395\,551\,267\,359\,325 \times 10^{3}$	27	32	8	$0.655\,444\,787\,064\,505 \times 10^{2}$
14	7	1	$-0.154\,891\,257\,229\,285 \times 10^{1}$				

Table 2.68 Coefficients and exponents of the boundary equation $h'_{3a}(s)$ in its dimensionless form, Eq. (2.41)

i	I_i	J_i	n_i	i	I_i	J_i	n_i
1	0	1	0.822 673 364 673 336	11	6	4	0.191 413 958 471 069
2	0	4	0.181 977 213 534 479	12	7	2	$0.581\,062\,241\,093\,136 \times 10^{-1}$
3	0	10	$-0.112\,000\,260\,313\,624 \times 10^{-1}$	13	7	28	$-0.165\,505\,498\,701\,029 \times 10^{4}$
4	0	16	$-0.746\,778\,287\,048\,033 \times 10^{-3}$	14	7	32	$0.158\,870\,443\,421\,201 \times 10^{4}$
5	2	1	−0.179 046 263 257 381	15	10	14	$-0.850\,623\,535\,172\,818 \times 10^{2}$
6	3	36	$0.424\,220\,110\,836\,657 \times 10^{-1}$	16	10	32	$-0.317\,714\,386\,511\,207 \times 10^{5}$
7	4	3	−0.341 355 823 438 768	17	10	36	$-0.945\,890\,406\,632\,871 \times 10^{5}$
8	4	16	$-0.209\,881\,740\,853\,565 \times 10^{1}$	18	32	0	$-0.139\,273\,847\,088\,690 \times 10^{-5}$
9	5	20	$-0.822\,477\,343\,323\,596 \times 10^{1}$	19	32	6	0.631 052 532 240 980
10	5	36	$-0.499\,684\,082\,076\,008 \times 10^{1}$				

Computer-Program Verification. To assist the user in computer-program verification of Eqs. (2.40) and (2.41), Table 2.69 contains test values for calculated enthalpies.

Table 2.69 Values of the specific enthalpy calculated from Eqs. (2.40) and (2.41) for selected specific entropies [a]

Equation	s [kJ kg^{-1} K^{-1}]	h [kJ kg^{-1}]
$h'_1(s)$, Eq. (2.40)	1.0	$3.085\,509\,647 \times 10^2$
	2.0	$7.006\,304\,472 \times 10^2$
	3.0	$1.198\,359\,754 \times 10^3$
$h'_{3a}(s)$, Eq. (2.41)	3.8	$1.685\,025\,565 \times 10^3$
	4.0	$1.816\,891\,476 \times 10^3$
	4.2	$1.949\,352\,563 \times 10^3$

[a] Programmed functions should be verified using 8 byte real values for all variables.

Note. For (h,s) points extremely close to the saturated-liquid line, the following procedure is recommended. When calculating specific enthalpies with equations $h'_1(s)$, Eq. (2.40), and $h'_{3a}(s)$, Eq. (2.41), their numerical inconsistencies of 0.0034 kJ kg^{-1} and 0.0045 kJ kg^{-1} in specific enthalpy with respect to the basic equations $g_1(p,T)$, Eq. (2.3), and $f_3(\rho,T)$, Eq. (2.11), have to be considered. Due to these minor inconsistencies, the results of the calculated enthalpies should be corrected to $h'_1 = h'_1(s) - \Delta h$, where Δh = 0.0034 kJ kg^{-1} and $h'_{3a} = h'_{3a}(s) - \Delta h$, where Δh = 0.0045 kJ kg^{-1}. This procedure ensures that (h,s) points extremely close to the saturated-liquid line will be correctly assigned to the single-phase region and not falsely to the two-phase region.

b) Boundary Equations $h''(s)$ for the Saturated-Vapour Line

The equation $h''_{2ab}(s)$ describes the saturated-vapour line in the range adjoining the single-phase subregions 2a and 2b. Figure 2.14 shows that this equation covers the entropy range

$$s_{2bc} = 5.85 \text{ kJ kg}^{-1}\text{ K}^{-1} \le s \le s''(273.15 \text{ K}),$$
$$\text{with } s''(273.15\text{ K}) = s_2(p_s(273.15\text{ K}), 273.15\text{ K}) = 9.155\,759\,395 \text{ kJ kg}^{-1}\text{ K}^{-1},$$

where s_2 was calculated from the basic equation $g_2(p,T)$, Eq. (2.6), with $p = p_s(T)$ from Eq. (2.13).

The boundary equation $h''_{2ab}(s)$ has the following dimensionless form:

$$\frac{h''_{2ab}(s)}{h^*} = \eta''(\sigma) = \exp\left[\sum_{i=1}^{30} n_i \left(\sigma_1^{-1} - 0.513\right)^{I_i} \left(\sigma_2 - 0.524\right)^{J_i}\right], \tag{2.42}$$

where $\eta = h/h^*$, $\sigma_1 = s/s_1^*$, and $\sigma_2 = s/s_2^*$ with $h^* = 2800$ kJ kg^{-1}, $s_1^* = 5.21$ kJ kg^{-1} K^{-1}, and $s_2^* = 9.2$ kJ kg^{-1} K^{-1}. The coefficients n_i and exponents I_i and J_i of Eq. (2.42) are listed in Table 2.70.

The equation $h''_{2c3b}(s)$ describes the saturated-vapour line in the range adjoining the single-phase subregions 2c and 3b. Figure 2.14 shows that this equation covers the entropy range

$$s_c \le s \le s_{2bc} = 5.85 \text{ kJ kg}^{-1}\text{ K}^{-1},$$
$$\text{where } s_c = 4.412\,021\,482\,234\,76 \text{ kJ kg}^{-1}\text{ K}^{-1}$$

according to Eq. (2.35).

The boundary equation $h''_{2c3b}(s)$ has the following dimensionless form:

$$\frac{h''_{2c3b}(s)}{h^*} = \eta''(\sigma) = \left[\sum_{i=1}^{16} n_i (\sigma - 1.02)^{I_i} (\sigma - 0.726)^{J_i} \right]^4 , \tag{2.43}$$

where $\eta = h/h^*$ and $\sigma = s/s^*$ with $h^* = 2\,800\ \mathrm{kJ\ kg^{-1}}$ and $s^* = 5.9\ \mathrm{kJ\ kg^{-1}\ K^{-1}}$. The coefficients n_i and exponents I_i and J_i of Eq. (2.43) are listed in Table 2.71.

The equation $h''_{2ab}(s)$, Eq. (2.42), exactly meets the enthalpy value $h''(273.15\ \mathrm{K}) = h_2(p_s(273.15\ \mathrm{K}),\ 273.15\ \mathrm{K}) = 2.500\,892\,618 \times 10^3\ \mathrm{kJ\ kg^{-1}}$ that was calculated from the basic equation $g_2(p,T)$, Eq. (2.6), where $p = p_s(T)$ is obtained from Eq. (2.13). The equation $h''_{2c3b}(s)$, Eq. (2.43), yields exactly the enthalpy value at the critical point $h_c = 2.087\,546\,845 \times 10^3\ \mathrm{kJ\ kg^{-1}}$ that was calculated from the basic equation $f_3(\rho, T)$, Eq. (2.11), for $\rho = \rho_c = 322\ \mathrm{kg\ m^{-3}}$ and $T = T_c = 647.096\ \mathrm{K}$ according to Eqs. (1.6) and (1.4).

Table 2.70 Coefficients and exponents of the boundary equation $h''_{2ab}(s)$ in its dimensionless form, Eq. (2.42)

i	I_i	J_i	n_i	i	I_i	J_i	n_i
1	1	8	$-0.524\,581\,170\,928\,788 \times 10^{3}$	16	28	8	$0.660\,788\,766\,938\,091 \times 10^{16}$
2	1	24	$-0.926\,947\,218\,142\,218 \times 10^{7}$	17	28	12	$0.166\,320\,055\,886\,021 \times 10^{23}$
3	2	4	$-0.237\,385\,107\,491\,666 \times 10^{3}$	18	28	20	$-0.218\,003\,784\,381\,501 \times 10^{30}$
4	2	32	$0.210\,770\,155\,812\,776 \times 10^{11}$	19	28	22	$-0.787\,276\,140\,295\,618 \times 10^{30}$
5	4	1	$-0.239\,494\,562\,010\,986 \times 10^{2}$	20	28	24	$0.151\,062\,329\,700\,346 \times 10^{32}$
6	4	2	$0.221\,802\,480\,294\,197 \times 10^{3}$	21	32	2	$0.795\,732\,170\,300\,541 \times 10^{7}$
7	7	7	$-0.510\,472\,533\,393\,438 \times 10^{7}$	22	32	7	$0.131\,957\,647\,355\,347 \times 10^{16}$
8	8	5	$0.124\,981\,396\,109\,147 \times 10^{7}$	23	32	12	$-0.325\,097\,068\,299\,140 \times 10^{24}$
9	8	12	$0.200\,008\,436\,996\,201 \times 10^{10}$	24	32	14	$-0.418\,600\,611\,419\,248 \times 10^{26}$
10	10	1	$-0.815\,158\,509\,791\,035 \times 10^{3}$	25	32	24	$0.297\,478\,906\,557\,467 \times 10^{35}$
11	12	0	$-0.157\,612\,685\,637\,523 \times 10^{3}$	26	36	10	$-0.953\,588\,761\,745\,473 \times 10^{20}$
12	12	7	$-0.114\,200\,422\,332\,791 \times 10^{11}$	27	36	12	$0.166\,957\,699\,620\,939 \times 10^{25}$
13	18	10	$0.662\,364\,680\,776\,872 \times 10^{16}$	28	36	20	$-0.175\,407\,764\,869\,978 \times 10^{33}$
14	20	12	$-0.227\,622\,818\,296\,144 \times 10^{19}$	29	36	22	$0.347\,581\,490\,626\,396 \times 10^{35}$
15	24	32	$-0.171\,048\,081\,348\,406 \times 10^{32}$	30	36	28	$-0.710\,971\,318\,427\,851 \times 10^{39}$

Table 2.71 Coefficients and exponents of the boundary equation $h'_{2c3b}(s)$ in its dimensionless form, Eq. (2.43)

i	I_i	J_i	n_i	i	I_i	J_i	n_i
1	0	0	$0.104\,351\,280\,732\,769 \times 10^{1}$	9	8	2	$0.743\,957\,464\,645\,363 \times 10^{4}$
2	0	3	$-0.227\,807\,912\,708\,513 \times 10^{1}$	10	8	20	$-0.356\,896\,445\,355\,761 \times 10^{20}$
3	0	4	$0.180\,535\,256\,723\,202 \times 10^{1}$	11	12	32	$0.167\,590\,585\,186\,801 \times 10^{32}$
4	1	0	$0.420\,440\,834\,792\,042$	12	16	36	$-0.355\,028\,625\,419\,105 \times 10^{38}$
5	1	12	$-0.105\,721\,244\,834\,660 \times 10^{6}$	13	22	2	$0.396\,611\,982\,166\,538 \times 10^{12}$
6	5	36	$0.436\,911\,607\,493\,884 \times 10^{25}$	14	22	32	$-0.414\,716\,268\,484\,468 \times 10^{41}$
7	6	12	$-0.328\,032\,702\,839\,753 \times 10^{12}$	15	24	7	$0.359\,080\,103\,867\,382 \times 10^{19}$
8	7	16	$-0.678\,686\,760\,804\,270 \times 10^{16}$	16	36	20	$-0.116\,994\,334\,851\,995 \times 10^{41}$

Computer-Program Verification. To assist the user in computer-program verification of Eqs. (2.42) and (2.43), Table 2.72 contains test values for calculated enthalpies.

Table 2.72 Values of the specific enthalpy calculated from Eqs. (2.42) and (2.43) for selected specific entropies [a]

Equation	s [kJ kg^{-1} K^{-1}]	h [kJ kg^{-1}]
$h''_{2ab}(s)$, Eq. (2.42)	7.0	$2.723\,729\,985 \times 10^3$
	8.0	$2.599\,047\,210 \times 10^3$
	9.0	$2.511\,861\,477 \times 10^3$
$h''_{2c3b}(s)$, Eq. (2.43)	5.5	$2.687\,693\,850 \times 10^3$
	5.0	$2.451\,623\,609 \times 10^3$
	4.5	$2.144\,360\,448 \times 10^3$

[a] Programmed functions should be verified using 8 byte real values for all variables.

Note. For (h,s) points extremely close to the saturated-vapour line, the following procedure is recommended. When calculating specific enthalpies with equations $h''_{2ab}(s)$, Eq. (2.42), and $h''_{2c3b}(s)$, Eq. (2.43), their minor numerical inconsistencies Δh with respect to the basic equations $g_2(p,T)$, Eq. (2.6), and $f_3(\rho,T)$, Eq. (2.11), have to be considered. Thus, the results of Eq. (2.42) should be corrected to $h''_{2ab} = h''_{2ab}(s) - \Delta h$, where $\Delta h = 0.0012$ kJ kg^{-1} and the results of Eq. (2.43) should be corrected to $h''_{2c3b} = h''_{2c3b}(s) - \Delta h$, where $\Delta h = 0.0058$ kJ kg^{-1} for $s''(623.15\ \text{K}) \le s < s_{2bc} = 5.85$ kJ kg^{-1} K^{-1} and $\Delta h = 0.0073$ kJ kg^{-1} for $s_c \le s < s''(623.15\ \text{K})$. This procedure ensures that (h, s) points extremely close to the saturated-vapour line will be correctly assigned to the single-phase region and not falsely to the two-phase region.

c) Equation $h_{B13}(s)$ for the Boundary between Regions 1 and 3

The equation $h_{B13}(s)$ describes the enthalpy as a function of entropy for the isotherm $T = 623.15$ K from the saturated-liquid line up to 100 MPa. Figure 2.14 shows that this equation covers the entropy range

$$s_1(100\ \text{MPa}, 623.15\ \text{K}) \le s \le s'(623.15\ \text{K})$$
$$\text{with } s_1(100\ \text{MPa}, 623.15\ \text{K}) = 3.397\,782\,955\ \text{kJ kg}^{-1}\ \text{K}^{-1}$$
$$\text{and } s'(623.15\ \text{K}) = s_1(p_s(623.15\ \text{K}), 623.15\ \text{K}) = 3.778\,281\,340\ \text{kJ kg}^{-1}\ \text{K}^{-1},$$

where the two values for s_1 were calculated from the basic equation $g_1(p,T)$, Eq. (2.3)[11], and p_s from Eq. (2.13).

The boundary equation $h_{B13}(s)$ has the following dimensionless form:

$$\frac{h_{B13}(s)}{h^*} = \eta(\sigma) = \sum_{i=1}^{6} n_i\,(\sigma - 0.884)^{I_i}\,(\sigma - 0.864)^{J_i}\ , \tag{2.44}$$

where $\eta = h/h^*$ and $\sigma = s/s^*$ with $h^* = 1\,700$ kJ kg^{-1} and $s^* = 3.8$ kJ kg^{-1} K^{-1}. The coefficients n_i and exponents I_i and J_i of Eq. (2.44) are listed in Table 2.73. Equation (2.44) describes the isotherm $T = 623.15$ K with maximum deviations in temperature of 3.2 mK.

[11] See the statement at the beginning of Sec. 2.3.5.1c.

Table 2.73 Coefficients and exponents of the boundary equation $h_{B13}(s)$ in its dimensionless form, Eq. (2.44)

i	I_i	J_i	n_i
1	0	0	0.913 965 547 600 543
2	1	−2	−0.430 944 856 041 991 × 10^−4
3	1	2	0.603 235 694 765 419 × 10^2
4	3	−12	0.117 518 273 082 168 × 10^−17
5	5	−4	0.220 000 904 781 292
6	6	−3	−0.690 815 545 851 641 × 10^2

Computer-Program Verification. To assist the user in computer-program verification of Eq. (2.44), Table 2.74 contains test values for calculated enthalpies.

Table 2.74 Values of the specific enthalpy calculated from Eq. (2.44) for selected specific entropies [a]

Equation	s [kJ kg^{-1} K^{-1}]	h [kJ kg^{-1}]
	3.7	1.632 525 047 × 10^3
$h_{B13}(s)$, Eq. (2.44)	3.6	1.593 027 214 × 10^3
	3.5	1.566 104 611 × 10^3

[a] Programmed functions should be verified using 8 byte real values for all variables.

Note. For (h,s) points extremely close to the boundary between regions 1 and 3, the following procedure is recommended. When calculating specific enthalpies with the equation $h_{B13}(s)$, Eq. (2.44), its numerical inconsistency of 0.018 kJ kg^{-1} in specific enthalpy with respect to the basic equation $g_1(p,T)$, Eq. (2.3), has to be considered. Due to this minor inconsistency the result of Eq. (2.44) should be corrected to $h_{B13} = h_{B13}(s) + \Delta h$, where $\Delta h = 0.018$ kJ kg^{-1}. This procedure ensures that (h,s) points extremely close to the region boundary are correctly assigned to region 1 and not falsely to region 3.

d) Equation $T_{B23}(h,s)$ for the Boundary between Regions 2 and 3

The equation $T_{B23}(h,s)$ has the following dimensionless form:

$$\frac{T_{B23}(h,s)}{T^*} = \theta(\eta,\sigma) = \sum_{i=1}^{25} n_i (\eta - 0.727)^{I_i} (\sigma - 0.864)^{J_i} , \qquad (2.45)$$

where $\theta = T/T^*$, $\eta = h/h^*$, and $\sigma = s/s^*$ with $T^* = 900$ K, $h^* = 3000$ kJ kg^{-1}, and $s^* = 5.3$ kJ kg^{-1} K^{-1}. The coefficients n_i and exponents I_i and J_i of Eq. (2.45) are listed in Table 2.75. The range of validity of Eq. (2.45) and the procedure for its application are described in Sec. 2.3.5.1c, subpoint "Boundary Between Regions 2 and 3."

Table 2.75 Coefficients and exponents of the boundary equation $T_{B23}(h,s)$ in its dimensionless form, Eq. (2.45)

i	I_i	J_i	n_i	i	I_i	J_i	n_i
1	−12	10	$0.629\,096\,260\,829\,810 \times 10^{-3}$	14	3	−2	$0.149\,276\,502\,463\,272$
2	−10	8	$-0.823\,453\,502\,583\,165 \times 10^{-3}$	15	3	−1	$0.698\,733\,471\,798\,484$
3	−8	3	$0.515\,446\,951\,519\,474 \times 10^{-7}$	16	5	−5	$-0.252\,207\,040\,114\,321 \times 10^{-1}$
4	−4	4	$-0.117\,565\,945\,784\,945 \times 10^{1}$	17	6	−6	$0.147\,151\,930\,985\,213 \times 10^{-1}$
5	−3	3	$0.348\,519\,684\,726\,192 \times 10^{1}$	18	6	−3	$-0.108\,618\,917\,681\,849 \times 10^{1}$
6	−2	−6	$-0.507\,837\,382\,408\,313 \times 10^{-11}$	19	8	−8	$-0.936\,875\,039\,816\,322 \times 10^{-3}$
7	−2	2	$-0.284\,637\,670\,005\,479 \times 10^{1}$	20	8	−2	$0.819\,877\,897\,570\,217 \times 10^{2}$
8	−2	3	$-0.236\,092\,263\,939\,673 \times 10^{1}$	21	8	−1	$-0.182\,041\,861\,521\,835 \times 10^{3}$
9	−2	4	$0.601\,492\,324\,973\,779 \times 10^{1}$	22	12	−12	$0.261\,907\,376\,402\,688 \times 10^{-5}$
10	0	0	$0.148\,039\,650\,824\,546 \times 10^{1}$	23	12	−1	$-0.291\,626\,417\,025\,961 \times 10^{5}$
11	1	−3	$0.360\,075\,182\,221\,907 \times 10^{-3}$	24	14	−12	$0.140\,660\,774\,926\,165 \times 10^{-4}$
12	1	−2	$-0.126\,700\,045\,009\,952 \times 10^{-1}$	25	14	1	$0.783\,237\,062\,349\,385 \times 10^{7}$
13	1	10	$-0.122\,184\,332\,521\,413 \times 10^{7}$				

Computer-Program Verification. To assist the user in computer-program verification of Eq. (2.45), Table 2.76 contains test values for calculated temperatures.

Table 2.76 Temperature values calculated from Eq. (2.45) for selected specific enthalpies and specific entropies [a]

Equation	h [kJ kg^{-1}]	s [kJ kg^{-1} K^{-1}]	T [K]
	2600	5.1	$7.135\,259\,364 \times 10^{2}$
$T_{B23}(h,s)$, Eq. (2.45)	2700	5.15	$7.685\,345\,532 \times 10^{2}$
	2800	5.2	$8.176\,202\,120 \times 10^{2}$

[a] Programmed functions should be verified using 8 byte real values for all variables.

Use of the Equation $T_{B23}(h,s)$, Eq. (2.45). Equation $T_{B23}(h,s)$ should only be used to determine the region for a given (h,s) point within the range of validity of Eq. (2.45) given above and by the grey area in Fig. 2.16. The procedure for such a determination by combining the equation $T_{B23}(h,s)$ with the backward equation of region 2c, $p_{2c}(h,s)$, Eq. (2.51), is described in Sec. 2.3.5.1c.

Numerical consistency. The differences between the backward equation $p_{2c}(h,s)$, Eq. (2.51), and the equation $T_{B23}(h,s)$, Eq. (2.45), combined with the equation $p_{B23}(T)$, Eq. (2.1) are small enough that the region of a given (h,s) point can be determined with sufficient accuracy. The maximum percentage inconsistency between the pressures calculated from equations $p_{B23}(T_{B23}(h,s))$ and $p_{2c}(h,s)$ at the B23-boundary amounts to 0.0045%. For a given (h,s) point extremely close to this boundary, the note at the end of Sec. 2.3.5.1c describes how to proceed.

2.3.5.3 Backward Equation $p(h,s)$ and Backward Function $T(h,s)$ for Region 1

When properties as a function of (h,s) are required from the basic equation of region 1, $g_1(p,T)$, Eq. (2.3), without iteration, both variables p and T must be calculable as a function of (h,s). As mentioned at the beginning of Sec. 2.3.5, the relation $p(h,s)$ is provided as a direct backward equation and the relation $T(h,s)$ is given as a backward function. This backward function $T(h,s)$ is a combination of the two backward equations $p(h,s)$ and $T(p,h)$[12] in the form $T(p(h,s),h)$. A statement about the computing time with the backward equation and backward function can be found at the end of this section.

a) Backward Equation $p(h,s)$ for Region 1

Figure 2.18 shows the assignment of the backward equation $p_1(h,s)$ to region 1 in an h-s diagram. The boundaries of region 1 in h-s coordinates are described in Secs. 2.3.5.1a to 2.3.5.1c.

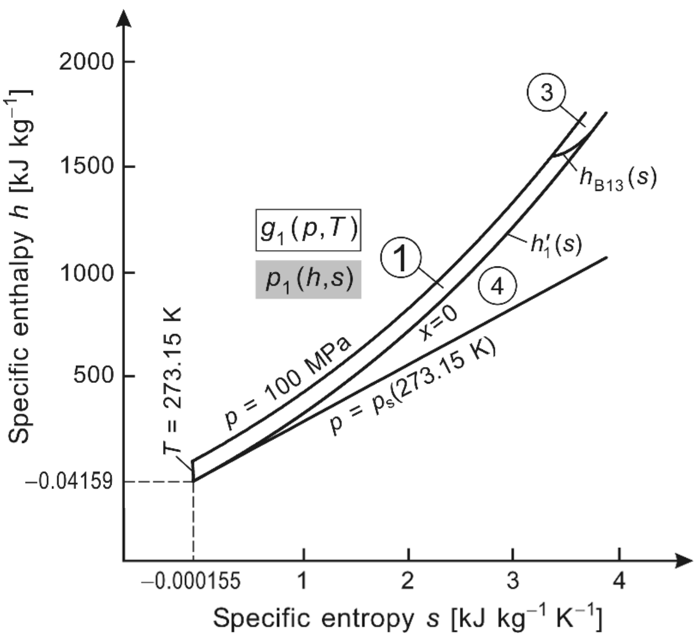

Fig. 2.18 Assignment of the backward equation $p_1(h,s)$ to region 1 in an h-s diagram. The h and s values at the corner points of region 1 are given in Fig. 2.14.

The backward equation $p_1(h,s)$ for region 1 in its dimensionless form reads:

$$\frac{p_1(h,s)}{p^*} = \pi(\eta,\sigma) = \sum_{i=1}^{19} n_i\,(\eta+0.05)^{I_i}\,(\sigma+0.05)^{J_i} \;, \tag{2.46}$$

where $\pi = p/p^*$, $\eta = h/h^*$, and $\sigma = s/s^*$ with $p^* = 100\ \mathrm{MPa}$, $h^* = 3400\ \mathrm{kJ\,kg^{-1}}$, and $s^* = 7.6\ \mathrm{kJ\,kg^{-1}\,K^{-1}}$. The coefficients n_i and exponents I_i and J_i of Eq. (2.46) are listed in Table 2.77.

[12] The alternative use of the backward equation $T(p,s)$ leads to worse numerical consistency.

Table 2.77 Coefficients and exponents of the backward equation $p_1(h,s)$ in its dimensionless form, Eq. (2.46)

i	I_i	J_i	n_i	i	I_i	J_i	n_i
1	0	0	$-0.691\,997\,014\,660\,582$	11	1	4	$-0.319\,947\,848\,334\,300 \times 10^3$
2	0	1	$-0.183\,612\,548\,787\,560 \times 10^2$	12	1	6	$-0.928\,354\,307\,043\,320 \times 10^3$
3	0	2	$-0.928\,332\,409\,297\,335 \times 10$	13	2	0	$0.303\,634\,537\,455\,249 \times 10^2$
4	0	4	$0.659\,639\,569\,909\,906 \times 10^2$	14	2	1	$-0.650\,540\,422\,444\,146 \times 10^2$
5	0	5	$-0.162\,060\,388\,912\,024 \times 10^2$	15	2	10	$-0.430\,991\,316\,516\,130 \times 10^4$
6	0	6	$0.450\,620\,017\,338\,667 \times 10^3$	16	3	4	$-0.747\,512\,324\,096\,068 \times 10^3$
7	0	8	$0.854\,680\,678\,224\,170 \times 10^3$	17	4	1	$0.730\,000\,345\,529\,245 \times 10^3$
8	0	14	$0.607\,523\,214\,001\,162 \times 10^4$	18	4	4	$0.114\,284\,032\,569\,021 \times 10^4$
9	1	0	$0.326\,487\,682\,621\,856 \times 10^2$	19	5	0	$-0.436\,407\,041\,874\,559 \times 10^3$
10	1	1	$-0.269\,408\,844\,582\,931 \times 10^2$				

Range of Validity. The range of validity of the backward equation $p_1(h,s)$, Eq. (2.46), can be derived from the graphical representation of region 1 in Fig. 2.14. The determination of h values for given s values along the region boundaries is described in Secs. 2.3.5.1a to 2.3.5.1c.

Computer-Program Verification. To assist the user in computer-program verification of Eq. (2.46), Table 2.78 contains the corresponding test values.

Numerical Consistency. The numerical inconsistencies between the backward equation $p_1(h,s)$, Eq. (2.46), and the basic equation $g_1(p,T)$, Eq. (2.3), in comparison with the permissible inconsistencies, given in Sec. 2.3.2, are listed in Table 2.79. These inconsistencies are less than the permissible values. This is also true when the backward equation is used in combination with the corresponding boundary equations given in Sec. 2.3.5.2.

Table 2.78 Pressure values calculated from the backward equation $p_1(h,s)$, Eq. (2.46), for selected specific enthalpies and specific entropies [a]

h [kJ kg^{-1}]	s [kJ kg^{-1} K^{-1}]	p [MPa]
0.001	0	$9.800\,980\,612 \times 10^{-4}$
90	0	$9.192\,954\,727 \times 10^1$
1500	3.4	$5.868\,294\,423 \times 10^1$

[a] Programmed functions should be verified using 8 byte real values for all variables.

Table 2.79 Maximum and root-mean-square inconsistencies in pressure between the backward equation $p_1(h,s)$, Eq. (2.46), and the basic equation $g_1(p,T)$, Eq. (2.3), in comparison with the permissible inconsistencies

	Inconsistencies in pressure		
	$\lvert\Delta p\rvert_{\mathrm{perm}}$	$\lvert\Delta p\rvert_{\max}$	$(\Delta p)_{\mathrm{RMS}}$
$p \le 2.5$ MPa	0.60%	0.55%	0.11%
$p > 2.5$ MPa	15 kPa	14 kPa	6 kPa

Computing Time. A statement about the computing time is given in Sec. 2.3.5.3c.

b) Backward Function $T(h,s)$ for Region 1

The backward equation $p_1(h,s)$, Eq. (2.46), in combination with the backward equation $T_1(p,h)$[13], Eq. (2.19), forms the backward function

$$T_1(h,s) = T_1(p_1(h,s),h), \tag{2.47}$$

where p_1 is calculated from Eq. (2.46) and $T_1(p_1,h)$ is determined from Eq. (2.19).

Range of Validity: The backward function $T_1(h,s)$, Eq. (2.47), has the same range of validity as the backward equation $p_1(h,s)$, Eq. (2.46).

Numerical Consistency. The numerical inconsistency between the backward function $T_1(h,s)$, Eq. (2.47), and the basic equation $g_1(p,T)$, Eq. (2.3), in comparison with the permissible inconsistency, given in Sec. 2.3.2, is listed in Table 2.80. This inconsistency is less than the permissible values. This is also true when the backward function in combination with the corresponding boundary equations given in Sec. 2.3.5.2 is used.

Note: When calculating properties extremely close to the saturated-liquid line, the backward function, Eq. (2.47), might yield temperatures $T_1(h,s) > T_s(p_1(h,s))$ due to minor inconsistencies; $p_1(h,s)$ is calculated from Eq. (2.46) and $T_s(p_1)$ from Eq. (2.14). In this case, the result of Eq. (2.47) should be corrected to $T_1 = T_s(p_1)$.

An analogous procedure is recommended for (h,s) points extremely close to the boundary $T = 623.15$ K between regions 1 and 3. Due to minor inconsistencies, the backward function, Eq. (2.47), might yield temperatures $T_1(h,s) > 623.15$ K. In this case, the result of Eq. (2.47) should be corrected to $T_1 = 623.15$ K.

Table 2.80 Maximum and root-mean-square inconsistency in temperature between the backward function $T_1(h,s)$, Eq. (2.47), and the basic equation $g_1(p,T)$, Eq. (2.3), in comparison with the permissible inconsistency

Inconsistencies in temperature [mK]		
$\lvert\Delta T\rvert_{perm}$	$\lvert\Delta T\rvert_{max}$	$(\Delta T)_{RMS}$
25	24.0	13.4

c) Computing Time when Using the Backward Equation $p_1(h,s)$ together with the Backward Function $T_1(h,s)$ in Comparison with the Basic Equation

The calculation of pressure and temperature as a function of (h,s) by using the backward equation $p_1(h,s)$, Eq. (2.46), together with the backward function $T_1(h,s)$, Eq. (2.47), is about 35 times faster than when using only the basic equation $g_1(p,T)$, Eq. (2.3), [19]. In this comparison, the basic equation was applied in combination with a two-dimensional Newton iteration with convergence tolerances corresponding to the consistency requirements that were set for the backward equation.

[13] The alternative use of the backward equation $T_1(p,s)$ leads to worse numerical consistency.

2.3.5.4 Backward Equations $p(h,s)$ and Backward Functions $T(h,s)$ for Region 2

When properties as a function of (h,s) need to be calculated from the basic equation of region 2, $g_2(p,T)$, Eq. (2.6), without iteration, both variables p and T must be calculable as a function of (h,s). As mentioned at the beginning of Sec. 2.3.5, the relations $p(h,s)$ are provided as direct backward equations and the relations $T(h,s)$ are given as backward functions. These backward functions $T(h,s)$ are a combination of the two backward equations $p(h,s)$ and $T(p,h)$[14] in the form $T(p(h,s),h)$.

a) Division of Region 2 into Subregions 2a, 2b, and 2c

Figure 2.19 shows how region 2 is divided into the three subregions 2a, 2b, and 2c for a backward equation $p(h,s)$ as was done in Secs. 2.3.3.3a and 2.3.4.3a for the backward equations $T(p,h)$ and $T(p,s)$ for region 2.

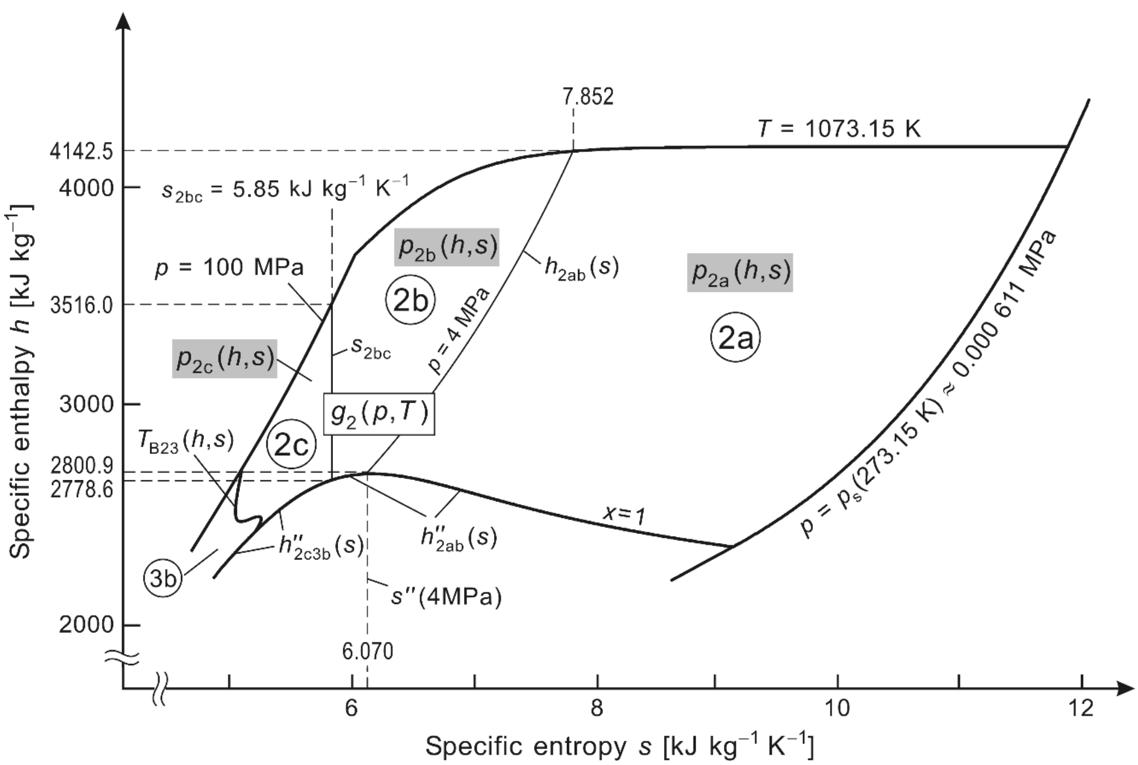

Fig. 2.19 Division of region 2 into subregions 2a, 2b, and 2c and the assignment of the backward equations $p(h,s)$ to these subregions. The h and s values at the corner points of region 2 are given in Fig. 2.14.

Boundary between Subregions 2a and 2b. This boundary corresponds to the isobar $p = 4$ MPa. In order to determine without iteration in which of the two subregions a given (h,s)

[14] The alternative use of the backward equation $T(p,s)$ leads to worse numerical consistency.

point is located, the boundary equation $h_{2ab}(s)$ was developed [11, 22]. This equation that describes the isobar $p = 4$ MPa for the variables (h,s) reads:

$$\frac{h_{2ab}(s)}{h^*} = \eta(\sigma) = n_1 + n_2\,\sigma + n_3\,\sigma^2 + n_4\,\sigma^3 \;, \tag{2.48}$$

where $\eta = h/h^*$ and $\sigma = s/s^*$ with $h^* = 1$ kJ kg^{-1} and $s^* = 1$ kJ kg^{-1} K^{-1}. The coefficients n_1 to n_4 of Eq. (2.48) are listed in Table 2.81.

Figure 2.19 shows that Eq. (2.48) covers the entropy range

$$s''(4\text{ MPa}) = s_2(4\text{ MPa}, T_s(4\text{ MPa})) \le s \le s_2(4\text{ MPa}, 1073.15\text{ K}),$$

where the two values for s_2 are calculated from the basic equation $g_2(p,T)$, Eq. (2.6), with T_s obtained from the equation $T_s(p)$, Eq. (2.14). Thus, the h values for given s values along the boundary between subregions 2a and 2b can be directly calculated from the equation $h_{2ab}(s)$, Eq. (2.48). This equation describes the isobar $p = 4$ MPa with maximum differences in pressure of 22 kPa. The given enthalpy value can then be compared with the calculated value for h.

Note. To be in accordance with the statements given in [11, 22], the boundary between subregions 2a and 2b is counted as belonging to subregion 2a.

Table 2.81 Coefficients of the equation $h_{2ab}(s)$ in its dimensionless form, Eq. (2.48), for defining the boundary between subregions 2a and 2b

i	n_i	i	n_i
1	$-0.349\,898\,083\,432\,139 \times 10^4$	3	$-0.421\,073\,558\,227\,969 \times 10^3$
2	$0.257\,560\,716\,905\,876 \times 10^4$	4	$0.276\,349\,063\,799\,944 \times 10^2$

Computer-Program Verification. For $s = 7$ kJ kg^{-1} K^{-1}, Eq. (2.48) yields $h_{2ab} = 3376.437\,884$ kJ kg^{-1}.

Boundary between Subregions 2b and 2c. This boundary corresponds to the isentropic line $s = s_{2bc} = 5.85$ kJ kg^{-1} K^{-1}. Therefore, a given (h,s) point can be directly assigned to subregion 2b or subregion 2c.

Note. To be in accordance with the statements given in [11, 22], the boundary between subregions 2b and 2c is considered to belong to subregion 2b.

b) The Backward Equations p(h,s) for Subregions 2a, 2b, and 2c

The backward equation $p_{2a}(h,s)$ for **subregion 2a** in its dimensionless form reads:

$$\frac{p_{2a}(h,s)}{p^*} = \pi(\eta,\sigma) = \left[\sum_{i=1}^{29} n_i\,(\eta - 0.5)^{I_i}\,(\sigma - 1.2)^{J_i}\right]^4 , \tag{2.49}$$

where $\pi = p/p^*$, $\eta = h/h^*$, and $\sigma = s/s^*$ with $p^* = 4$ MPa, $h^* = 4200$ kJ kg^{-1}, and $s^* = 12$ kJ kg^{-1} K^{-1}. The coefficients n_i and exponents I_i and J_i of Eq. (2.49) are listed in Table 2.82.

The backward equation $p_{2b}(h,s)$ for **subregion 2b** in its dimensionless form reads:

$$\frac{p_{2b}(h,s)}{p^*} = \pi(\eta,\sigma) = \left[\sum_{i=1}^{33} n_i (\eta - 0.6)^{I_i} (\sigma - 1.01)^{J_i}\right]^4 , \tag{2.50}$$

where $\pi = p/p^*$, $\eta = h/h^*$, and $\sigma = s/s^*$ with $p^* = 100$ MPa, $h^* = 4100\ \mathrm{kJ\ kg^{-1}}$, and $s^* = 7.9\ \mathrm{kJ\ kg^{-1}\ K^{-1}}$. The coefficients n_i and exponents I_i and J_i of Eq. (2.50) are listed in Table 2.83.

The backward equation $p_{2c}(h,s)$ for **subregion 2c** in its dimensionless form reads:

$$\frac{p_{2c}(h,s)}{p^*} = \pi(\eta,\sigma) = \left[\sum_{i=1}^{31} n_i (\eta - 0.7)^{I_i} (\sigma - 1.1)^{J_i}\right]^4 , \tag{2.51}$$

where $\pi = p/p^*$, $\eta = h/h^*$, and $\sigma = s/s^*$ with $p^* = 100$ MPa, $h^* = 3500\ \mathrm{kJ\ kg^{-1}}$, and $s^* = 5.9\ \mathrm{kJ\ kg^{-1}\ K^{-1}}$. The coefficients n_i and exponents I_i and J_i of Eq. (2.51) are listed in Table 2.84.

Table 2.82 Coefficients and exponents of the backward equation $p_{2a}(h,s)$ for subregion 2a in its dimensionless form, Eq. (2.49)

i	I_i	J_i	n_i	i	I_i	J_i	n_i
1	0	1	$-0.182\,575\,361\,923\,032 \times 10^{-1}$	16	1	22	$0.431\,757\,846\,408\,006 \times 10^{4}$
2	0	3	$-0.125\,229\,548\,799\,536$	17	2	3	$0.112\,894\,040\,802\,650 \times 10^{1}$
3	0	6	$0.592\,290\,437\,320\,145$	18	2	16	$0.197\,409\,186\,206\,319 \times 10^{4}$
4	0	16	$0.604\,769\,706\,185\,122 \times 10^{1}$	19	2	20	$0.151\,612\,444\,706\,087 \times 10^{4}$
5	0	20	$0.238\,624\,965\,444\,474 \times 10^{3}$	20	3	0	$0.141\,324\,451\,421\,235 \times 10^{-1}$
6	0	22	$-0.298\,639\,090\,222\,922 \times 10^{3}$	21	3	2	$0.585\,501\,282\,219\,601$
7	1	0	$0.512\,250\,813\,040\,750 \times 10^{-1}$	22	3	3	$-0.297\,258\,075\,863\,012 \times 10^{1}$
8	1	1	$-0.437\,266\,515\,606\,486$	23	3	6	$0.594\,567\,314\,847\,319 \times 10^{1}$
9	1	2	$0.413\,336\,902\,999\,504$	24	3	16	$-0.623\,656\,565\,798\,905 \times 10^{4}$
10	1	3	$-0.516\,468\,254\,574\,773 \times 10^{1}$	25	4	16	$0.965\,986\,235\,133\,332 \times 10^{4}$
11	1	5	$-0.557\,014\,838\,445\,711 \times 10^{1}$	26	5	3	$0.681\,500\,934\,948\,134 \times 10^{1}$
12	1	6	$0.128\,555\,037\,824\,478 \times 10^{2}$	27	5	16	$-0.633\,207\,286\,824\,489 \times 10^{4}$
13	1	10	$0.114\,144\,108\,953\,290 \times 10^{2}$	28	6	3	$-0.558\,919\,224\,465\,760 \times 10^{1}$
14	1	16	$-0.119\,504\,225\,652\,714 \times 10^{3}$	29	7	1	$0.400\,645\,798\,472\,063 \times 10^{-1}$
15	1	20	$-0.284\,777\,985\,961\,560 \times 10^{4}$				

Table 2.83 Coefficients and exponents of the backward equation $p_{2b}(h,s)$ for subregion 2b in its dimensionless form, Eq. (2.50)

i	I_i	J_i	n_i	i	I_i	J_i	n_i
1	0	0	$0.801\,496\,989\,929\,495 \times 10^{-1}$	18	3	12	$0.336\,972\,380\,095\,287 \times 10^{8}$
2	0	1	$-0.543\,862\,807\,146\,111$	19	4	1	$-0.586\,634\,196\,762\,720 \times 10^{3}$
3	0	2	$0.337\,455\,597\,421\,283$	20	4	16	$-0.221\,403\,224\,769\,889 \times 10^{11}$
4	0	4	$0.890\,555\,451\,157\,450 \times 10^{1}$	21	5	1	$0.171\,606\,668\,708\,389 \times 10^{4}$
5	0	8	$0.313\,840\,736\,431\,485 \times 10^{3}$	22	5	12	$-0.570\,817\,595\,806\,302 \times 10^{9}$
6	1	0	$0.797\,367\,065\,977\,789$	23	6	1	$-0.312\,109\,693\,178\,482 \times 10^{4}$
7	1	1	$-0.121\,616\,973\,556\,240 \times 10^{1}$	24	6	8	$-0.207\,841\,384\,633\,010 \times 10^{7}$

Continued on next page.

Table 2.83 – Continued

i	I_i	J_i	n_i	i	I_i	J_i	n_i
8	1	2	$0.872\,803\,386\,937\,477 \times 10^{1}$	25	6	18	$0.305\,605\,946\,157\,786 \times 10^{13}$
9	1	3	$-0.169\,769\,781\,757\,602 \times 10^{2}$	26	7	1	$0.322\,157\,004\,314\,333 \times 10^{4}$
10	1	5	$-0.186\,552\,827\,328\,416 \times 10^{3}$	27	7	16	$0.326\,810\,259\,797\,295 \times 10^{12}$
11	1	12	$0.951\,159\,274\,344\,237 \times 10^{5}$	28	8	1	$-0.144\,104\,158\,934\,487 \times 10^{4}$
12	2	1	$-0.189\,168\,510\,120\,494 \times 10^{2}$	29	8	3	$0.410\,694\,867\,802\,691 \times 10^{3}$
13	2	6	$-0.433\,407\,037\,194\,840 \times 10^{4}$	30	8	14	$0.109\,077\,066\,873\,024 \times 10^{12}$
14	2	18	$0.543\,212\,633\,012\,715 \times 10^{9}$	31	8	18	$-0.247\,964\,654\,258\,893 \times 10^{14}$
15	3	0	$0.144\,793\,408\,386\,013$	32	12	10	$0.188\,801\,906\,865\,134 \times 10^{10}$
16	3	1	$0.128\,024\,559\,637\,516 \times 10^{3}$	33	14	16	$-0.123\,651\,009\,018\,773 \times 10^{15}$
17	3	7	$-0.672\,309\,534\,071\,268 \times 10^{5}$				

Table 2.84 Coefficients and exponents of the backward equation $p_{2c}(h,s)$ for subregion 2c in its dimensionless form, Eq. (2.51)

i	I_i	J_i	n_i	i	I_i	J_i	n_i
1	0	0	$0.112\,225\,607\,199\,012$	17	3	0	$0.772\,465\,073\,604\,171$
2	0	1	$-0.339\,005\,953\,606\,712 \times 10^{1}$	18	3	5	$0.463\,929\,973\,837\,746 \times 10^{5}$
3	0	2	$-0.320\,503\,911\,730\,094 \times 10^{2}$	19	3	8	$-0.137\,317\,885\,134\,128 \times 10^{8}$
4	0	3	$-0.197\,597\,305\,104\,900 \times 10^{3}$	20	3	16	$0.170\,470\,392\,630\,512 \times 10^{13}$
5	0	4	$-0.407\,693\,861\,553\,446 \times 10^{3}$	21	3	18	$-0.251\,104\,628\,187\,308 \times 10^{14}$
6	0	8	$0.132\,943\,775\,222\,331 \times 10^{5}$	22	4	18	$0.317\,748\,830\,835\,520 \times 10^{14}$
7	1	0	$0.170\,846\,839\,774\,007 \times 10^{1}$	23	5	1	$0.538\,685\,623\,675\,312 \times 10^{2}$
8	1	2	$0.373\,694\,198\,142\,245 \times 10^{2}$	24	5	4	$-0.553\,089\,094\,625\,169 \times 10^{5}$
9	1	5	$0.358\,144\,365\,815\,434 \times 10^{4}$	25	5	6	$-0.102\,861\,522\,421\,405 \times 10^{7}$
10	1	8	$0.423\,014\,446\,424\,664 \times 10^{6}$	26	5	14	$0.204\,249\,418\,756\,234 \times 10^{13}$
11	1	14	$-0.751\,071\,025\,760\,063 \times 10^{9}$	27	6	8	$0.273\,918\,446\,626\,977 \times 10^{9}$
12	2	2	$0.523\,446\,127\,607\,898 \times 10^{2}$	28	6	18	$-0.263\,963\,146\,312\,685 \times 10^{16}$
13	2	3	$-0.228\,351\,290\,812\,417 \times 10^{3}$	29	10	7	$-0.107\,890\,854\,108\,088 \times 10^{10}$
14	2	7	$-0.960\,652\,417\,056\,937 \times 10^{6}$	30	12	7	$-0.296\,492\,620\,980\,124 \times 10^{11}$
15	2	10	$-0.807\,059\,292\,526\,074 \times 10^{8}$	31	16	10	$-0.111\,754\,907\,323\,424 \times 10^{16}$
16	2	18	$0.162\,698\,017\,225\,669 \times 10^{13}$				

Ranges of Validity. The ranges of validity of the backward equations $p_{2a}(h,s)$, $p_{2b}(h,s)$, and $p_{2c}(h,s)$, Eqs. (2.49) to (2.51), can be derived from the graphical representation of region 2 in Fig. 2.14 and of subregions 2a, 2b, and 2c in Fig. 2.19. The determination of h values for given s values along the region boundaries is described in Secs. 2.3.5.1a to 2.3.5.1c and along the subregion boundaries in Sec. 2.3.5.4a.

Computer-Program Verification. To assist the user in computer-program verification of Eqs. (2.49) to (2.51), Table 2.85 contains the corresponding test values.

Numerical Consistencies. The numerical inconsistencies between the backward equations $p_{2a}(h,s)$, $p_{2b}(h,s)$, and $p_{2c}(h,s)$, Eqs. (2.49) to (2.51), and the basic equation $g_2(p,T)$, Eq. (2.6), in comparison with the permissible inconsistencies, given in Sec. 2.3.2, are listed in Table 2.86. These inconsistencies are less than the permissible values. This is also true when the backward equations are used in combination with the corresponding boundary equations given in Sec. 2.3.5.2.

Table 2.85 Pressure values calculated from the backward equations $p_{2a}(h,s)$, $p_{2b}(h,s)$, and $p_{2c}(h,s)$, Eqs. (2.49) to (2.51), for selected specific enthalpies and specific entropies [a]

Equation	h [kJ kg^{-1}]	s [kJ kg^{-1} K^{-1}]	p [MPa]
$p_{2a}(h,s)$, Eq. (2.49)	2800	6.5	1.371 012 767
	2800	9.5	$1.879\,743\,844 \times 10^{-3}$
	4100	9.5	$1.024\,788\,997 \times 10^{-1}$
$p_{2b}(h,s)$, Eq. (2.50)	2800	6	4.793 911 442
	3600	6	$8.395\,519\,209 \times 10^{1}$
	3600	7	7.527 161 441
$p_{2c}(h,s)$, Eq. (2.51)	2800	5.1	$9.439\,202\,060 \times 10^{1}$
	2800	5.8	8.414 574 124
	3400	5.8	$8.376\,903\,879 \times 10^{1}$

[a] Programmed functions should be verified using 8 byte real values for all variables.

Table 2.86 Maximum and root-mean-square inconsistencies in pressure between the backward equations $p_{2a}(h,s)$, $p_{2b}(h,s)$, and $p_{2c}(h,s)$, Eqs. (2.49) to (2.51), and the basic equation $g_2(p,T)$, Eq. (2.6), in comparison with the permissible inconsistencies

		Inconsistencies in pressure [%]		
Subregion	Equation	$\|\Delta p/p\|_{\mathrm{perm}}$	$\|\Delta p/p\|_{\mathrm{max}}$	$(\Delta p/p)_{\mathrm{RMS}}$
2a	$p_{2a}(h,s)$, Eq. (2.49)	0.0035	0.0029	0.0013
2b	$p_{2b}(h,s)$, Eq. (2.50)	0.0035	0.0034	0.0005
2c	$p_{2c}(h,s)$, Eq. (2.51)	0.0088	0.0063	0.0010

Computing Time. A statement about the computing time is given in Sec. 2.3.5.4d.

c) Backward Functions $T(h,s)$ for Subregions 2a, 2b, and 2c

The backward function $T_{2a}(h,s)$ for **subregion 2a** is formed by combining the backward equation $p_{2a}(h,s)$ with the backward equation $T_{2a}(p,h)$[15] in the form

$$T_{2a}(h,s) = T_{2a}(p_{2a}(h,s),h), \tag{2.52}$$

where p_{2a} is calculated from Eq. (2.49) and then $T_{2a}(p_{2a},h)$ is obtained from Eq. (2.22).

The backward function $T_{2b}(h,s)$ for **subregion 2b** is formed by combining the backward equation $p_{2b}(h,s)$ with the backward equation $T_{2b}(p,h)$[15] in the form

$$T_{2b}(h,s) = T_{2b}(p_{2b}(h,s),h), \tag{2.53}$$

where p_{2b} is calculated from Eq. (2.50) and then $T_{2b}(p_{2b},h)$ is determined from Eq. (2.23).

The backward function $T_{2c}(h,s)$ for **subregion 2c** is formed by combining the backward equation $p_{2c}(h,s)$ with the backward equation $T_{2c}(p,h)$[15] in the form

$$T_{2c}(h,s) = T_{2c}(p_{2c}(h,s),h), \tag{2.54}$$

where p_{2c} is calculated from Eq. (2.51) and then $T_{2c}(p_{2c},h)$ is obtained from Eq. (2.24).

[15] The alternative use of the backward equations $T_{2a}(p,s)$, $T_{2b}(p,s)$, and $T_{2c}(p,s)$ leads to worse numerical consistency.

Ranges of Validity. The backward functions $T_{2a}(h,s)$, $T_{2b}(h,s)$, and $T_{2c}(h,s)$, Eqs. (2.52) to (2.54), have the same ranges of validity as the corresponding backward equations $p_{2a}(h,s)$, $p_{2b}(h,s)$, and $p_{2c}(h,s)$, Eqs. (2.49) to (2.51).

Numerical Consistencies. The numerical inconsistencies between the backward functions $T_{2a}(h,s)$, $T_{2b}(h,s)$, and $T_{2c}(h,s)$, Eqs. (2.52) to (2.54), and the basic equation $g_2(p,T)$, Eq. (2.6), in comparison with the permissible inconsistencies, given in Sec. 2.3.2, are listed in Table 2.87. These inconsistencies are less than the permissible values. This is also true when the backward functions are used in combination with the corresponding boundary equations given in Sec. 2.3.5.2.

Note: When calculating properties extremely close to the saturated-vapour line, due to minor inconsistencies, the backward functions, Eqs. (2.52) to (2.54), might yield temperatures $T_{2a}(h,s) < T_s(p_{2a}(h,s))$, $T_{2b}(h,s) < T_s(p_{2b}(h,s))$, and $T_{2c}(h,s) < T_s(p_{2c}(h,s))$, where $p_{2a}(h,s)$, $p_{2b}(h,s)$, and $p_{2c}(h,s)$ are calculated from Eqs. (2.49) to (2.51), and $T_s(p_{2a})$, $T_s(p_{2b})$, and $T_s(p_{2c})$ from Eq. (2.14). In this case, the results of Eqs. (2.52) to (2.54) should be corrected to $T_{2a} = T_s(p_{2a})$, $T_{2b} = T_s(p_{2b})$, and $T_{2c} = T_s(p_{2c})$.

An analogous procedure is recommended for (h,s) points extremely close to the B23-boundary. Due to the minor inconsistencies, the backward function, Eq. (2.54), might yield temperatures $T_{2c}(h,s) < T_{B23}(p_{2c}(h,s))$, where $T_{B23}(p)$ is calculated from Eq. (2.2). In this case the result of Eq. (2.54) should be corrected to $T_{2c} = T_{B23}(p_{2c}(h,s))$.

Table 2.87 Maximum and root-mean-square inconsistencies in temperature between the backward functions $T_{2a}(h,s)$, $T_{2b}(h,s)$, and $T_{2c}(h,s)$, Eqs. (2.52) to (2.54), and the basic equation $g_2(p,T)$, Eq. (2.6), in comparison with the permissible inconsistencies

Subregion	Equation	Inconsistencies in temperature [mK] $\lvert\Delta T\rvert_{perm}$	$\lvert\Delta T\rvert_{max}$	$(\Delta T)_{RMS}$
2a	$T_{2a}(h,s)$, Eq. (2.52)	10	9.7	3.0
2b	$T_{2b}(h,s)$, Eq. (2.53)	10	9.8	4.0
2c	$T_{2c}(h,s)$, Eq. (2.54)	25	24.9	10.3

d) Computing Time when Using the Backward Functions $T_2(h,s)$ together with the Backward Equations $p_2(h,s)$ in Comparison with the Basic Equation

The calculation of pressure and temperature as a function of (h,s) using the backward equations $p_{2a}(h,s)$, $p_{2b}(h,s)$, or $p_{2c}(h,s)$, Eqs. (2.49) to (2.51), in combination with the corresponding backward function $T_{2a}(h,s)$, $T_{2b}(h,s)$, or $T_{2c}(h,s)$, Eqs. (2.52) to (2.54), is about 46 times faster than when using only the basic equation $g_2(p,T)$, Eq. (2.6), [19]. In this comparison, the basic equation was applied in combination with a two-dimensional Newton iteration with convergence tolerances corresponding to the consistency requirements that were set for the backward equations.

2.3.5.5 Backward Equations $p(h,s)$ and Backward Functions $v(h,s)$ and $T(h,s)$ for Region 3

When properties as a function of (h,s) are required from the basic equation of region 3, $f_3(\rho,T)$, Eq. (2.11), without iteration, both variables $\rho = 1/v$ and T must be calculable as a

function of (h,s). As mentioned at the beginning of Sec. 2.3.5, first the relations $p(h,s)$ are provided as direct backward equations, then the relations $v(h,s)$ and $T(h,s)$ are given as backward functions. The backward functions $v(h,s)$ are a combination of the two backward equations $p(h,s)$ and $v(p,s)$[16] in the form $v(p(h,s),s)$. The backward functions $T(h,s)$ are a combination of the two backward equations $p(h,s)$ and $T(p,h)$[17] in the form $T(p(h,s),h)$.

a) Division of Region 3 into Subregions 3a and 3b

Due to the very high demands for numerical consistency between the backward equations of this region and the basic equation $f_3(\rho,T)$, Eq. (2.11), given in Sec. 2.3.2, region 3 is divided into two subregions as was done in Secs. 2.3.3.4 and 2.3.4.4 for the backward equations $T(p,h)$ and $T(p,s)$. This division is illustrated in Fig. 2.20.

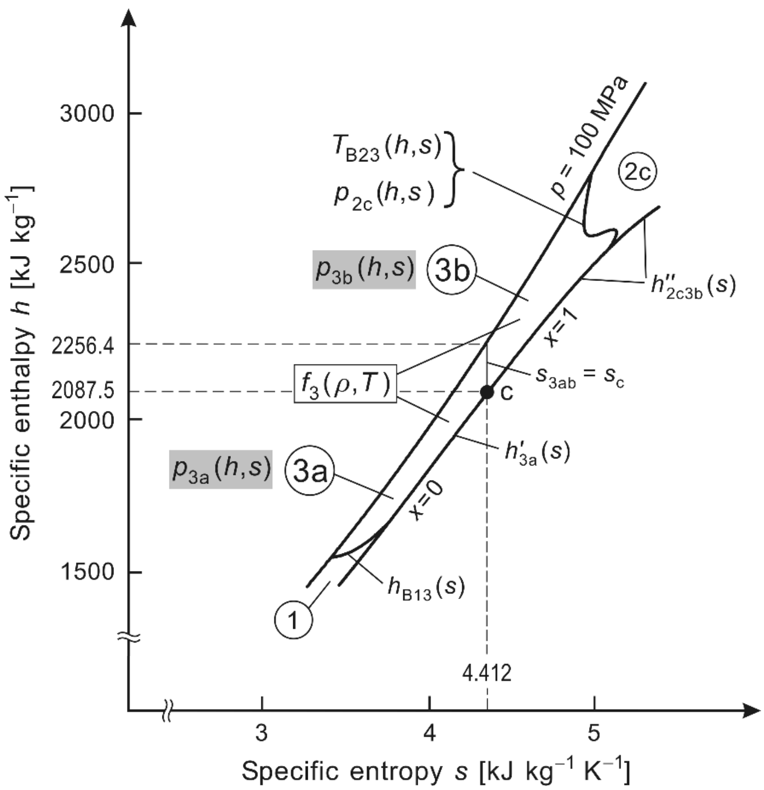

Fig. 2.20 Division of region 3 into subregions 3a and 3b, and the assignment of backward equations $p_{3a}(h,s)$ and $p_{3b}(h,s)$ to these subregions. The h and s values at the corner points of region 3 are given in Fig. 2.14.

The boundary between subregions 3a and 3b is defined by the critical isentropic line $s_{3ab} = s_c = 4.412\,021\,482\,234\,76$ kJ kg^{-1} K^{-1} according to Eq. (2.35).

Note. The boundary between subregions 3a and 3b is considered to belong to subregion 3a [13, 24].

---

[16] The alternative use of the backward equation $v(p,h)$ leads to worse numerical consistency.

[17] The alternative use of the backward equation $T(p,s)$ leads to worse numerical consistency.

b) Backward Equations p(h,s) for Subregions 3a and 3b

The backward equation $p_{3a}(h,s)$ for **subregion 3a** has the following dimensionless form:

$$\frac{p_{3a}(h,s)}{p^*} = \pi(\eta,\sigma) = \sum_{i=1}^{33} n_i\,(\eta - 1.01)^{I_i}\,(\sigma - 0.75)^{J_i}\ , \tag{2.55}$$

where $\pi = p/p^*$, $\eta = h/h^*$, and $\sigma = s/s^*$ with $p^* = 99\ \mathrm{MPa}$, $h^* = 2300\ \mathrm{kJ\,kg^{-1}}$, and $s^* = 4.4\ \mathrm{kJ\,kg^{-1}\,K^{-1}}$. The coefficients n_i and exponents I_i and J_i of Eq. (2.55) are listed in Table 2.88.

The backward equation $p_{3b}(h,s)$ for **subregion 3b** has the following dimensionless form:

$$\frac{p_{3b}(h,s)}{p^*} = \pi(\eta,\sigma) = \left[\sum_{i=1}^{35} n_i(\eta - 0.681)^{I_i}(\sigma - 0.792)^{J_i}\right]^{-1}\ , \tag{2.56}$$

where $\pi = p/p^*$, $\eta = h/h^*$, and $\sigma = s/s^*$ with $p^* = 16.6\ \mathrm{MPa}$, $h^* = 2800\ \mathrm{kJ\,kg^{-1}}$, and $s^* = 5.3\ \mathrm{kJ\,kg^{-1}\,K^{-1}}$. The coefficients n_i and exponents I_i and J_i of Eq. (2.56) are listed in Table 2.89.

Table 2.88 Coefficients and exponents of the backward equation $p_{3a}(h,s)$ for subregion 3a in its dimensionless form, Eq. (2.55)

i	I_i	J_i	n_i	i	I_i	J_i	n_i
1	0	0	$0.770\,889\,828\,326\,934 \times 10^{1}$	18	5	28	$0.538\,069\,315\,091\,534 \times 10^{20}$
2	0	1	$-0.260\,835\,009\,128\,688 \times 10^{2}$	19	6	28	$0.143\,619\,827\,291\,346 \times 10^{22}$
3	0	5	$0.267\,416\,218\,930\,389 \times 10^{3}$	20	7	24	$0.364\,985\,866\,165\,994 \times 10^{20}$
4	1	0	$0.172\,221\,089\,496\,844 \times 10^{2}$	21	8	1	$-0.254\,741\,561\,156\,775 \times 10^{4}$
5	1	3	$-0.293\,542\,332\,145\,970 \times 10^{3}$	22	10	32	$0.240\,120\,197\,096\,563 \times 10^{28}$
6	1	4	$0.614\,135\,601\,882\,478 \times 10^{3}$	23	10	36	$-0.393\,847\,464\,679\,496 \times 10^{30}$
7	1	8	$-0.610\,562\,757\,725\,674 \times 10^{5}$	24	14	22	$0.147\,073\,407\,024\,852 \times 10^{25}$
8	1	14	$-0.651\,272\,251\,118\,219 \times 10^{8}$	25	18	28	$-0.426\,391\,250\,432\,059 \times 10^{32}$
9	2	6	$0.735\,919\,313\,521\,937 \times 10^{5}$	26	20	36	$0.194\,509\,340\,621\,077 \times 10^{39}$
10	2	16	$-0.116\,646\,505\,914\,191 \times 10^{11}$	27	22	16	$0.666\,212\,132\,114\,896 \times 10^{24}$
11	3	0	$0.355\,267\,086\,434\,461 \times 10^{2}$	28	22	28	$0.706\,777\,016\,552\,858 \times 10^{34}$
12	3	2	$-0.596\,144\,543\,825\,955 \times 10^{3}$	29	24	36	$0.175\,563\,621\,975\,576 \times 10^{42}$
13	3	3	$-0.475\,842\,430\,145\,708 \times 10^{3}$	30	28	16	$0.108\,408\,607\,429\,124 \times 10^{29}$
14	4	0	$0.696\,781\,965\,359\,503 \times 10^{2}$	31	28	36	$0.730\,872\,705\,175\,151 \times 10^{44}$
15	4	1	$0.335\,674\,250\,377\,312 \times 10^{3}$	32	32	10	$0.159\,145\,847\,398\,870 \times 10^{25}$
16	4	4	$0.250\,526\,809\,130\,882 \times 10^{5}$	33	32	28	$0.377\,121\,605\,943\,324 \times 10^{41}$
17	4	5	$0.146\,997\,380\,630\,766 \times 10^{6}$				

Table 2.89 Coefficients and exponents of the backward equation $p_{3b}(h,s)$ for subregion 3b in its dimensionless form, Eq. (2.56)

i	I_i	J_i	n_i	i	I_i	J_i	n_i
1	−12	2	$0.125\,244\,360\,717\,979 \times 10^{-12}$	19	−4	8	$0.355\,073\,647\,696\,481 \times 10^{4}$
2	−12	10	$-0.126\,599\,322\,553\,713 \times 10^{-1}$	20	−3	1	$-0.115\,303\,107\,290\,162 \times 10^{-3}$
3	−12	12	$0.506\,878\,030\,140\,626 \times 10^{1}$	21	−3	3	$-0.175\,092\,403\,171\,802 \times 10^{1}$
4	−12	14	$0.317\,847\,171\,154\,202 \times 10^{2}$	22	−3	5	$0.257\,981\,687\,748\,160 \times 10^{3}$
5	−12	20	$-0.391\,041\,161\,399\,932 \times 10^{6}$	23	−3	6	$-0.727\,048\,374\,179\,467 \times 10^{3}$

Continued on next page.

Table 2.89 – Continued

i	I_i	J_i	n_i	i	I_i	J_i	n_i
6	−10	2	$-0.975\,733\,406\,392\,044 \times 10^{-10}$	24	−2	0	$0.121\,644\,822\,609\,198 \times 10^{-3}$
7	−10	10	$-0.186\,312\,419\,488\,279 \times 10^{2}$	25	−2	1	$0.393\,137\,871\,762\,692 \times 10^{-1}$
8	−10	14	$0.510\,973\,543\,414\,101 \times 10^{3}$	26	−1	0	$0.704\,181\,005\,909\,296 \times 10^{-2}$
9	−10	18	$0.373\,847\,005\,822\,362 \times 10^{6}$	27	0	3	$-0.829\,108\,200\,698\,110 \times 10^{2}$
10	−8	2	$0.299\,804\,024\,666\,572 \times 10^{-7}$	28	2	0	$-0.265\,178\,818\,131\,250$
11	−8	8	$0.200\,544\,393\,820\,342 \times 10^{2}$	29	2	1	$0.137\,531\,682\,453\,991 \times 10^{2}$
12	−6	2	$-0.498\,030\,487\,662\,829 \times 10^{-5}$	30	5	0	$-0.522\,394\,090\,753\,046 \times 10^{2}$
13	−6	6	$-0.102\,301\,806\,360\,030 \times 10^{2}$	31	6	1	$0.240\,556\,298\,941\,048 \times 10^{4}$
14	−6	7	$0.552\,819\,126\,990\,325 \times 10^{2}$	32	8	1	$-0.227\,361\,631\,268\,929 \times 10^{5}$
15	−6	8	$-0.206\,211\,367\,510\,878 \times 10^{3}$	33	10	1	$0.890\,746\,343\,932\,567 \times 10^{5}$
16	−5	10	$-0.794\,012\,232\,324\,823 \times 10^{4}$	34	14	3	$-0.239\,234\,565\,822\,486 \times 10^{8}$
17	−4	4	$0.782\,248\,472\,028\,153 \times 10^{1}$	35	14	7	$0.568\,795\,808\,129\,714 \times 10^{10}$
18	−4	5	$-0.586\,544\,326\,902\,468 \times 10^{2}$				

Ranges of Validity. The ranges of validity of the backward equations $p_{3a}(h,s)$ and $p_{3b}(h,s)$, Eqs. (2.55) and (2.56), can be derived from the graphical representation of region 3 in Fig. 2.14 and of subregions 3a and 3b in Fig. 2.20. The determination of h values for given s values along the region boundaries is described in Secs. 2.3.5.1a to 2.3.5.1c and along the subregion boundary in Sec. 2.3.5.5a.

Computer-Program Verification. To assist the user in computer-program verification of Eqs. (2.55) and (2.56), Table 2.90 contains test values for calculated pressures.

Table 2.90 Pressure values calculated from the backward equations $p_{3a}(h,s)$ and $p_{3b}(h,s)$, Eqs. (2.55) and (2.56), for selected specific enthalpies and specific entropies [a]

Equation	h [kJ kg^{-1}]	s [kJ kg^{-1} K^{-1}]	p [MPa]
$p_{3a}(h,s)$, Eq. (2.55)	1700	3.8	$2.555\,703\,246 \times 10^{1}$
	2000	4.2	$4.540\,873\,468 \times 10^{1}$
	2100	4.3	$6.078\,123\,340 \times 10^{1}$
$p_{3b}(h,s)$, Eq. (2.56)	2400	4.7	$6.363\,924\,887 \times 10^{1}$
	2600	5.1	$3.434\,999\,263 \times 10^{1}$
	2700	5.0	$8.839\,043\,281 \times 10^{1}$

[a] Programmed functions should be verified using 8 byte real values for all variables.

Numerical Consistencies. The numerical inconsistencies between the backward equations $p_{3a}(h,s)$ and $p_{3b}(h,s)$, Eqs. (2.55) and (2.56), and the basic equation $f_3(\rho,T)$, Eq. (2.11), in comparison with the permissible inconsistencies, given in Sec. 2.3.2, are listed in Table 2.91. These inconsistencies are less than the permissible values. This is also true when the backward equations in combination with the corresponding boundary equations given in Sec. 2.3.5.2 are used. The critical pressure $p_c = 22.064$ MPa is met by the two $p(h,s)$ equations for all five figures. The maximum inconsistency in pressure between the two backward equations, Eq. (2.55) and Eq. (2.56), along the boundary $s_{3ab} = s_c$, Eq. (2.35), amounts to 0.00074%, which is smaller than the permissible inconsistency.

Table 2.91 Maximum and root-mean-square inconsistencies in pressure between the backward equations $p_{3a}(h,s)$ and $p_{3b}(h,s)$, Eqs. (2.55) and (2.56), and the basic equation $f_3(\rho,T)$, Eq. (2.11), in comparison with the permissible inconsistencies

Subregion	Equation	Inconsistencies in pressure [%] $\|\Delta p/p\|_{perm}$	$\|\Delta p/p\|_{max}$	$(\Delta p/p)_{RMS}$
3a	$p_{3a}(h,s)$, Eq. (2.55)	0.01	0.0070	0.0030
3b	$p_{3b}(h,s)$, Eq. (2.56)	0.01	0.0084	0.0036

Computing Time. A statement about the computing time is given in Sec. 2.3.5.5e.

c) Backward Functions $v(h,s)$ for Subregions 3a and 3b

The backward function $v_{3a}(h,s)$ for **subregion 3a** is formed by combining the backward equation $p_{3a}(h,s)$ with the backward equation $v_{3a}(p,s)$[18] in the form

$$v_{3a}(h,s) = v_{3a}(p_{3a}(h,s),s), \tag{2.57}$$

where p_{3a} is calculated from Eq. (2.55) and then $v_{3a}(p_{3a},s)$ is obtained from Eq. (2.36).

The backward function $v_{3b}(h,s)$ for **subregion 3b** is formed by combining the backward equation $p_{3b}(h,s)$ with the backward equation $v_{3b}(p,s)$[18] in the form

$$v_{3b}(h,s) = v_{3b}(p_{3b}(h,s),s), \tag{2.58}$$

where p_{3b} is calculated from Eq. (2.56) and then $v_{3b}(p_{3b},s)$ is determined from Eq. (2.37).

Ranges of Validity. The backward functions $v_{3a}(h,s)$ and $v_{3b}(h,s)$, Eqs. (2.57) and (2.58), have the same ranges of validity as the corresponding backward equations $p_{3a}(h,s)$ and $p_{3b}(h,s)$, Eqs. (2.55) and (2.56).

Numerical Consistencies. The numerical inconsistencies between the backward functions $v_{3a}(h,s)$ and $v_{3b}(h,s)$, Eqs. (2.57) and (2.58), and the basic equation $f_3(\rho,T)$, Eq. (2.11), are listed in Table 2.92 in comparison with the permissible inconsistencies, given in Sec. 2.3.2. These inconsistencies are less than the permissible values. This is also true when the backward functions are used in combination with the corresponding boundary equations given in Sec. 2.3.5.2. The critical temperature $T_c = 647.096$ K is calculated by the two $T(h,s)$ functions for all six figures. The maximum inconsistency in specific volume between the two backward functions, Eqs. (2.57) and (2.58), along the subregion boundary $s_{3ab} = s_c$, Eq. (2.35), amounts to 0.000 28%.

Table 2.92 Maximum and root-mean-square inconsistencies in specific volume between the backward functions $v_{3a}(h,s)$ and $v_{3b}(h,s)$, Eqs. (2.57) and (2.58), and the basic equation $f_3(\rho,T)$, Eq. (2.11), in comparison with the permissible inconsistencies

Subregion	Equation	Inconsistencies in specific volume [%] $\|\Delta v/v\|_{perm}$	$\|\Delta v/v\|_{max}$	$(\Delta v/v)_{RMS}$
3a	$v_{3a}(h,s)$, Eq. (2.57)	0.01	0.0097	0.0053
3b	$v_{3b}(h,s)$, Eq. (2.58)	0.01	0.0095	0.0043

Computing Time. A statement about the computing time is given in Sec. 2.3.5.5e.

[18] The alternative use of the backward equations $v_{3a}(p,h)$ and $v_{3b}(p,h)$ leads to worse numerical consistency.

d) Backward Functions T(h,s) for Subregions 3a and 3b

The backward function $T_{3a}(h,s)$ for **subregion 3a** is formed by combining the backward equation $p_{3a}(h,s)$ with the backward equation $T_{3a}(p,h)$[19] in the form

$$T_{3a}(h,s) = T_{3a}(p_{3a}(h,s),h), \tag{2.59}$$

where p_{3a} is calculated from Eq. (2.55) and then $T_{3a}(p_{3a},h)$ is obtained from Eq. (2.28).

The backward function $T_{3b}(h,s)$ for **subregion 3b** is formed by combining the backward equation $p_{3b}(h,s)$ with the backward equation $T_{3b}(p,h)$[20] in the form

$$T_{3b}(h,s) = T_{3b}(p_{3b}(h,s),h), \tag{2.60}$$

where p_{3b} is calculated from Eq. (2.56) and then $T_{3b}(p_{3b},h)$ is determined from Eq. (2.29).

Ranges of Validity. The backward functions $T_{3a}(h,s)$ and $T_{3b}(h,s)$, Eqs. (2.59) and (2.60), have the same ranges of validity as the corresponding backward equations $p_{3a}(h,s)$ and $p_{3b}(h,s)$, Eqs. (2.55) and (2.56).

Numerical Consistencies. The numerical inconsistencies between the backward functions $T_{3a}(h,s)$ and $T_{3b}(h,s)$, Eqs. (2.59) and (2.60), and the basic equation $f_3(\rho,T)$, Eq. (2.11), in comparison with the permissible inconsistencies, given in Sec. 2.3.2, are listed in Table 2.93. These inconsistencies are less than the permissible values. This is also true when the backward functions are used in combination with the corresponding boundary equations given in Sec. 2.3.5.2. The critical volume $v_c = 1/\rho_c = (1/322)\ \mathrm{m^3\,kg^{-1}} = 0.003\,105\,59\ \mathrm{m^3\,kg^{-1}}$ is calculated by the two $v(h,s)$ functions for the given six significant figures. The maximum inconsistency in temperature between the two backward functions, Eq. (2.59) and (2.60), along the subregion boundary $s = s_c$ amounts to 0.68 mK, for details see [24].

Note. When calculating properties in the range $s \le s_c$ and extremely close to the saturated-liquid line, due to minor inconsistencies, Eq. (2.59) might yield temperatures $T_{3a}(h,s) > T_s(p_{3a}(h,s))$, where $p_{3a}(h,s)$ is calculated from Eq. (2.55) and $T_s(p_{3a})$ from Eq. (2.14). In this case, the result of Eq. (2.59) must be corrected to $T_{3a} = T_s(p_{3a})$. If the given specific entropy s is greater than s_c and the properties to be calculated are located extremely close to the saturated-vapour line, due to minor inconsistencies, Eq. (2.60) might yield temperatures $T_{3b}(h,s) < T_s(p_{3b}(h,s))$, where $p_{3b}(h,s)$ is calculated from Eq. (2.56) and $T_s(p_{3b})$ from Eq. (2.14). In this case, the result of Eq. (2.60) must be corrected to $T_{3b} = T_s(p_{3b})$.

Table 2.93 Maximum and root-mean-square inconsistencies in temperature between the backward functions $T_{3a}(h,s)$ and $T_{3b}(h,s)$, Eqs. (2.59) and (2.60), and the basic equation $f_3(\rho,T)$, Eq. (2.11), in comparison with the permissible inconsistencies

		Inconsistencies in temperature [mK]		
Subregion	Equation	$\lvert\Delta T\rvert_{\mathrm{perm}}$	$\lvert\Delta T\rvert_{\max}$	$(\Delta T)_{\mathrm{RMS}}$
3a	$T_{3a}(h,s)$, Eq. (2.59)	25	23.7	10.5
3b	$T_{3b}(h,s)$, Eq. (2.60)	25	22.4	9.9

[19] The alternative use of the backward equation $T_{3a}(p,s)$ leads to worse numerical consistency.

[20] The alternative use of the backward equation $T_{3b}(p,s)$ leads to worse numerical consistency.

e) Computing Time when Using the Backward Functions $v_3(h,s)$ and $T_3(h,s)$ together with the Backward Equations $p_3(h,s)$ in Comparison with the Basic Equation

The calculation of specific volume and temperature as a function of (h,s) with the backward functions $v_{3a}(h,s)$ and $T_{3a}(h,s)$, Eqs. (2.57) and (2.59), or $v_{3b}(h,s)$ and $T_{3b}(h,s)$ Eqs. (2.58) and (2.60), in combination with the corresponding backward equations $p_{3a}(h,s)$ or $p_{3b}(h,s)$, Eqs. (2.55) and (2.56), is about 10 times faster than that using only the basic equation $f_3(\rho,T)$, Eq. (2.11), [19]. In this comparison, the basic equation was applied in combination with a two-dimensional Newton iteration with convergence tolerances corresponding to the consistency requirements that were set for the backward equations.

2.3.5.6 Backward Equation $T_s(h,s)$ and Backward Functions $p_s(h,s)$ and $x(h,s)$ for the Technically Important Part of the Two-Phase Region 4

When modelling power cycles and, in particular, steam turbines, thermodynamic properties as a function of the variables (h,s) are also required in the two-phase (wet-steam) region. The important region for steam turbine calculations is the range $s \geq s''(623.15\ \mathrm{K})$, where the saturation temperature is less than or equal to 623.15 K; this region is marked in Fig. 2.21. In the p-T diagram, this part of the two-phase region is located between regions 1 and 2, see Fig. 2.3. In this region, the calculation of saturation properties from given values of h and s requires iterations with the basic equations $g_1(p,T)$, Eq. (2.3), and $g_2(p,T)$, Eq. (2.6), and the saturation-pressure equation $p_s(T)$, Eq. (2.13). In order to avoid such iterations, this subsection provides the backward equation $T_s(h,s)$ and the backward functions $p_s(h,s)$ and $x(h,s)$ for this technically important part of the two-phase region.

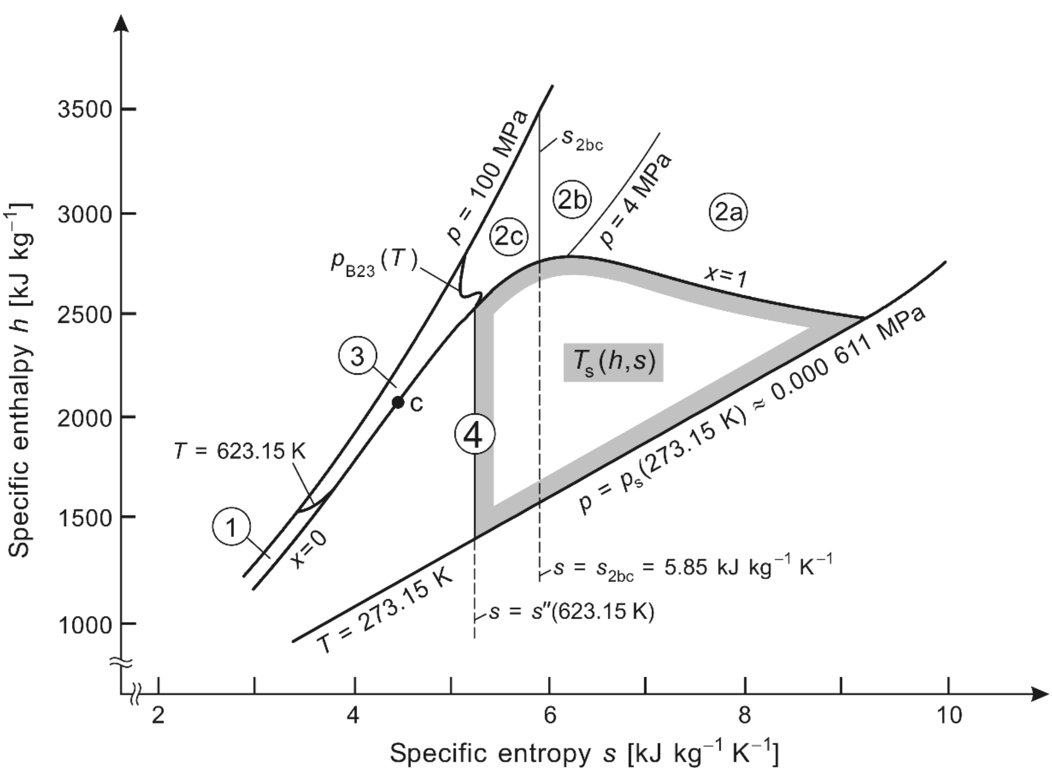

Fig. 2.21 Range of validity of the backward equation $T_s(h,s)$ and assignment of this range to the other regions and subregions of IAPWS-IF97.

a) Backward Equation $T_s(h,s)$

The backward equation $T_s(h,s)$ for the technically important part of the two-phase region 4 has the following dimensionless form:

$$\frac{T_s(h,s)}{T^*} = \theta_s(\eta,\sigma) = \sum_{i=1}^{36} n_i(\eta - 0.119)^{I_i}(\sigma - 1.07)^{J_i}, \tag{2.61}$$

where $\theta_s = T_s/T^*$, $\eta = h/h^*$, and $\sigma = s/s^*$ with $T^* = 550\,\mathrm{K}$, $h^* = 2800\,\mathrm{kJ\,kg^{-1}}$, and $s^* = 9.2\,\mathrm{kJ\,kg^{-1}\,K^{-1}}$. The coefficients n_i and exponents I_i and J_i of Eq. (2.61) are listed in Table 2.94.

Table 2.94 Coefficients and exponents of the equation $T_s(h,s)$ in its dimensionless form, Eq. (2.61)

i	I_i	J_i	n_i	i	I_i	J_i	n_i
1	0	0	0.179 882 673 606 601	19	5	4	$0.125\,028\,363\,714\,877 \times 10^{1}$
2	0	3	−0.267 507 455 199 603	20	5	16	$0.101\,316\,840\,309\,509 \times 10^{4}$
3	0	12	$0.116\,276\,722\,612\,600 \times 10^{1}$	21	6	6	$-0.151\,791\,558\,000\,712 \times 10^{1}$
4	1	0	0.147 545 428 713 616	22	6	8	$0.524\,277\,865\,990\,866 \times 10^{2}$
5	1	1	−0.512 871 635 973 248	23	6	22	$0.230\,495\,545\,563\,912 \times 10^{5}$
6	1	2	0.421 333 567 697 984	24	8	1	$0.249\,459\,806\,365\,456 \times 10^{-1}$
7	1	5	0.563 749 522 189 870	25	10	20	$0.210\,796\,467\,412\,137 \times 10^{7}$
8	2	0	0.429 274 443 819 153	26	10	36	$0.366\,836\,848\,613\,065 \times 10^{9}$
9	2	5	$-0.335\,704\,552\,142\,140 \times 10^{1}$	27	12	24	$-0.144\,814\,105\,365\,163 \times 10^{9}$
10	2	8	$0.108\,890\,916\,499\,278 \times 10^{2}$	28	14	1	$-0.179\,276\,373\,003\,590 \times 10^{-2}$
11	3	0	−0.248 483 390 456 012	29	14	28	$0.489\,955\,602\,100\,459 \times 10^{10}$
12	3	2	0.304 153 221 906 390	30	16	12	$0.471\,262\,212\,070\,518 \times 10^{3}$
13	3	3	−0.494 819 763 939 905	31	16	32	$-0.829\,294\,390\,198\,652 \times 10^{11}$
14	3	4	$0.107\,551\,674\,933\,261 \times 10^{1}$	32	18	14	$-0.171\,545\,662\,263\,191 \times 10^{4}$
15	4	0	$0.733\,888\,415\,457\,688 \times 10^{-1}$	33	18	22	$0.355\,777\,682\,973\,575 \times 10^{7}$
16	4	1	$0.140\,170\,545\,411\,085 \times 10^{-1}$	34	18	36	$0.586\,062\,760\,258\,436 \times 10^{12}$
17	5	1	−0.106 110 975 998 808	35	20	24	$-0.129\,887\,635\,078\,195 \times 10^{8}$
18	5	2	$0.168\,324\,361\,811\,875 \times 10^{-1}$	36	28	36	$0.317\,247\,449\,371\,057 \times 10^{11}$

Range of Validity. The range of validity of the backward equation $T_s(h,s)$ is the part of the two-phase region with $s \geq s''(623.15\,\mathrm{K}) = 5.210\,887\,825\,\mathrm{kJ\,kg^{-1}\,K^{-1}}$ as shown in Fig. 2.21. The corresponding temperature range is $273.15\,\mathrm{K} \leq T \leq 623.15\,\mathrm{K}$.

Computer-Program Verification. To assist the user in computer-program verification of Eq. (2.61), Table 2.95 contains test values for calculated temperatures.

Table 2.95 Temperature values calculated from the backward equation $T_s(h,s)$, Eq. (2.61), for selected specific enthalpies and specific entropies [a]

Equation	h [kJ kg^{-1}]	s [kJ kg^{-1} K^{-1}]	T [K]
	1800	5.3	$3.468\,475\,498 \times 10^{2}$
$T_s(h,s)$, Eq. (2.61)	2400	6.0	$4.251\,373\,305 \times 10^{2}$
	2500	5.5	$5.225\,579\,013 \times 10^{2}$

[a] Programmed functions should be verified using 8 byte real values for all variables.

Numerical Consistency. The numerical inconsistency between the backward equation $T_s(h,s)$, Eq. (2.61), and the basic equations $g_1(p,T)$, $g_2(p,T)$, and $p_s(T)$, Eqs. (2.3), (2.6), and (2.13), in comparison with the permissible inconsistencies, given in Sec. 2.3.2, are listed in Table 2.96. These consistency investigations were carried out as follows: First, values of the saturation temperature T_s and the vapour fraction x were given. For these T_s values, the saturation pressure p_s was calculated from Eq. (2.13). Then, from the basic equation $g_1(p_s, T_s)$, Eq. (2.3), h' and s' were determined, and the basic equation $g_2(p_s, T_s)$, Eq. (2.6), yielded h'' and s''. With these values and the given values of x, the properties h and s in the two-phase region were calculated. For these values of h and s, the saturation temperature T_s was determined from the backward equation $T_s(h,s)$, Eq. (2.61). The difference between this T_s value and the starting value corresponds to the inconsistency in saturation temperature.

Table 2.96 shows that the inconsistencies are significantly less than the permissible values. This is also true when the backward equation in combination with the corresponding boundary equations given in Sec. 2.3.5.2 is used.

Table 2.96 Maximum and root-mean-square inconsistencies in saturation temperature between the backward equation $T_s(h,s)$, Eq. (2.61), and the basic equations $g_1(p,T)$, $g_2(p,T)$, and $p_s(T)$, Eqs. (2.3), (2.6), and (2.13), in comparison with the permissible inconsistencies

	Inconsistencies in temperature [mK]		
Entropy range	$\lvert\Delta T_s\rvert_{perm}$	$\lvert\Delta T_s\rvert_{max}$	$(\Delta T_s)_{RMS}$
$s \geq 5.85\ \mathrm{kJ\ kg^{-1}\ K^{-1}}$	10	0.67	0.33
$s < 5.85\ \mathrm{kJ\ kg^{-1}\ K^{-1}}$	25	0.86	0.45

Computing Time. A statement about the computing time is given in Sec. 2.3.5.6d.

b) Backward Function $p_s(h,s)$

The backward function $p_s(h,s)$ for the technically important part of the two-phase region 4 is formed by combining the backward equation $T_s(h,s)$ with the saturation-pressure equation $p_s(T)$ in the form

$$p_s(h,s) = p_s(T_s(h,s)), \tag{2.62}$$

where T_s is calculated from Eq. (2.61) and then $p_s(T_s)$ is determined from Eq. (2.13).

Range of Validity. The backward function $p_s(h,s)$, Eq. (2.62), is valid in the same range as the backward equation $T_s(h,s)$, Eq. (2.61).

Numerical Consistency. The numerical inconsistency between the backward function $p_s(h,s)$, Eq. (2.62), and the basic equations $g_1(p,T)$, $g_2(p,T)$, and $p_s(T)$, Eqs. (2.3), (2.6), and (2.13), in comparison with the permissible inconsistencies, given in Sec. 2.3.2, are listed in Table 2.97. These consistency investigations were performed analogously as described above for the backward equation $T_s(h,s)$, Eq. (2.61). Here, however, values for the saturation pressure p_s were compared instead of the values for the saturation temperature T_s.

Table 2.97 shows that the inconsistencies are less than the permissible values. This is also true when the backward function is used in combination with the corresponding boundary equations given in Sec. 2.3.5.2.

Table 2.97 Maximum and root-mean-square inconsistencies in saturation pressure between the backward function $p_s(h,s)$, Eq. (2.62), and the basic equations $g_1(p,T)$, $g_2(p,T)$, and $p_s(T)$, Eqs. (2.3), (2.6), and (2.13), in comparison with the permissible inconsistencies.

Entropy range	Inconsistencies in pressure [%] $\lvert\Delta p_s/p_s\rvert_{perm}$	$\lvert\Delta p_s/p_s\rvert_{max}$	$(\Delta p_s/p_s)_{RMS}$
$s \geq 5.85$ kJ kg^{-1} K^{-1}	0.0035	0.0029	0.0012
$s < 5.85$ kJ kg^{-1} K^{-1}	0.0088	0.0034	0.0013

Computing Time. A statement about the computing time is given in Sec. 2.3.5.6d.

c) Backward Function x (h,s)

For the formulation of the vapour fraction as a function of (h,s), $x = x(h,s)$, one can start with the relation[21]

$$x = \frac{h - h'}{h'' - h'}. \tag{2.63}$$

When calculating h' and h'' from the basic equations $g_1(p,T)$ and $g_2(p,T)$ with $T = T_s(h,s)$ and $p = p_s(T_s)$, the backward function for the vapour fraction dependent on (h,s) is obtained in the form

$$x(h,s) = \frac{\left(h - h'\left(p_s\left(T_s(h,s)\right), T_s(h,s)\right)\right)}{h''\left(p_s\left(T_s(h,s)\right), T_s(h,s)\right) - h'\left(p_s\left(T_s(h,s)\right), T_s(h,s)\right)}. \tag{2.64}$$

For the given values of h and s the saturation temperature T_s is calculated from the backward equation $T_s(h,s)$, Eq. (2.61). Then, for this temperature T_s, the saturation pressure p_s is determined from the equation $p_s(T)$, Eq. (2.13). Finally, with these p_s and T_s values, h' is calculated from the basic equation $g_1(p,T)$, Eq. (2.3), and h'' is obtained from the basic equation $g_2(p,T)$, Eq. (2.6), for $p = p_s$ and $T = T_s$.

Range of Validity. The backward function $x(h,s)$, Eq. (2.64), is valid within the same range as the backward equation $T_s(h,s)$, Eq. (2.61).

Numerical Consistency. The numerical inconsistencies between the vapour fraction x calculated from Eq. (2.64) via the backward equation $T_s(h,s)$ and the vapour fraction x calculated iteratively from the basic equations $g_1(p,T)$, Eq. (2.3), $g_2(p,T)$, Eq. (2.6), and $p_s(T)$, Eq. (2.13), are listed in Table 2.98. The inconsistencies in x calculated in these two ways are less than 10^{-5}, i.e. the value of the vapour fraction x calculated from the backward function, Eq. (2.64), agrees within five decimal figures with the x value determined from the basic equation via iterations.

When the backward function is used in combination with the corresponding boundary equations, given in Sec. 2.3.5.2, the inconsistency remains within 10^{-5}.

[21] The use of the relation $x = (s-s')/(s''-s')$ as a starting point for the derivation of the backward function $x(h,s)$ leads to worse numerical consistency.

Table 2.98 Maximum and root-mean-square inconsistencies in vapour fraction x between calculations with the backward function $x(h,s)$, Eq. (2.64), and iterating the basic equations $g_1(p,T)$, Eq. (2.3), $g_2(p,T)$, Eq. (2.6), and $p_s(T)$, Eq. (2.13).

Entropy range	Inconsistencies in vapour fraction $\|\Delta x\|_{max}$	$(\Delta x)_{RMS}$
$s \geq 5.85$ kJ kg^{-1} K^{-1}	0.64×10^{-6}	0.25×10^{-6}
$s < 5.85$ kJ kg^{-1} K^{-1}	4.40×10^{-6}	0.57×10^{-6}

Note. When calculating properties extremely close to the saturated-vapour line, due to minor inconsistencies, the backward function, Eq. (2.64), might yield vapour fractions $x(h,s) > 1$. In this case, the result of Eq. (2.64) should be corrected to $x = 1$.

d) Computing Time when Using the Backward Equation $T_s(h,s)$ together with the Backward Functions $p_s(h,s)$ and $x(h,s)$

The calculation of temperature, pressure, and vapour fraction in the technically important part of the two-phase region 4 with the backward equation $T_s(h,s)$, Eq. (2.61), together with the corresponding backward functions $p_s(h,s)$, Eq. (2.62), and $x(h,s)$, Eq. (2.64) in combination with the basic equations $g_1(p,T)$, Eq. (2.3), $g_2(p,T)$, Eq. (2.6), and $p_s(T)$, Eq. (2.13), is about 14 times faster than when using only the basic equations [19]. In this comparison, the basic equations were applied in combination with a two-dimensional Newton iteration with convergence tolerances corresponding to the consistency requirements that were given for the backward equations in Sec. 2.3.2.

2.3.6 Backward Equations Dependent on the Input Variables (p,T) for Region 3

The basic equation $f_3(\rho,T)$, Eq. (2.11), is used in region 3. This basic equation along with the backward equations $v(p,h)$, $T(p,h)$, $v(p,s)$, $T(p,s)$, and $p(h,s)$, given in Secs. 2.3.3 to 2.3.5, can be used to calculate all thermodynamic properties as a function of (p,h), (p,s) and (h,s) without any iteration. However, in modelling modern steam power cycles, in particular in boiler calculations, properties as a function of the variables (p,T) are required for region 3. Such calculations from the basic equation $f_3(\rho,T)$, Eq. (2.11), are cumbersome because they require iterations of v for given values of p and T using the relation $p(v,T)$ with $v = 1/\rho$ derived from Eq. (2.11) as given in the first line of Table 2.16.

In order to avoid such iterations, this section provides backward equations $v_3(p,T)$ for region 3 as given in Fig. 2.22. With the specific volume v calculated from the backward equations $v_3(p,T)$, all other properties in region 3 can be calculated without iteration from the basic equation $f_3(\rho,T)$, Eq. (2.11), with $\rho = 1/v_3$.

For process calculations, the numerical consistency requirements for the backward equations $v_3(p,T)$ are very strict. Since the specific volume on the v-p-T surface has a complicated structure including an infinite slope at the critical point, region 3 had to be divided into 26 subregions. The first 20 subregions and their associated backward equations, described in Sec. 2.3.6.4, cover nearly the entire region 3 and fully meet the consistency requirements given in Sec. 2.3.6.1. For a small area very near the critical point, it was not possible to meet the consistency requirements completely. This near-critical region is covered with reasonable consistency by six subregions with auxiliary equations that are described in Sec. 2.3.6.5.

This set of recently-developed backward and auxiliary equations [14] was adopted by IAPWS in 2005 [25].

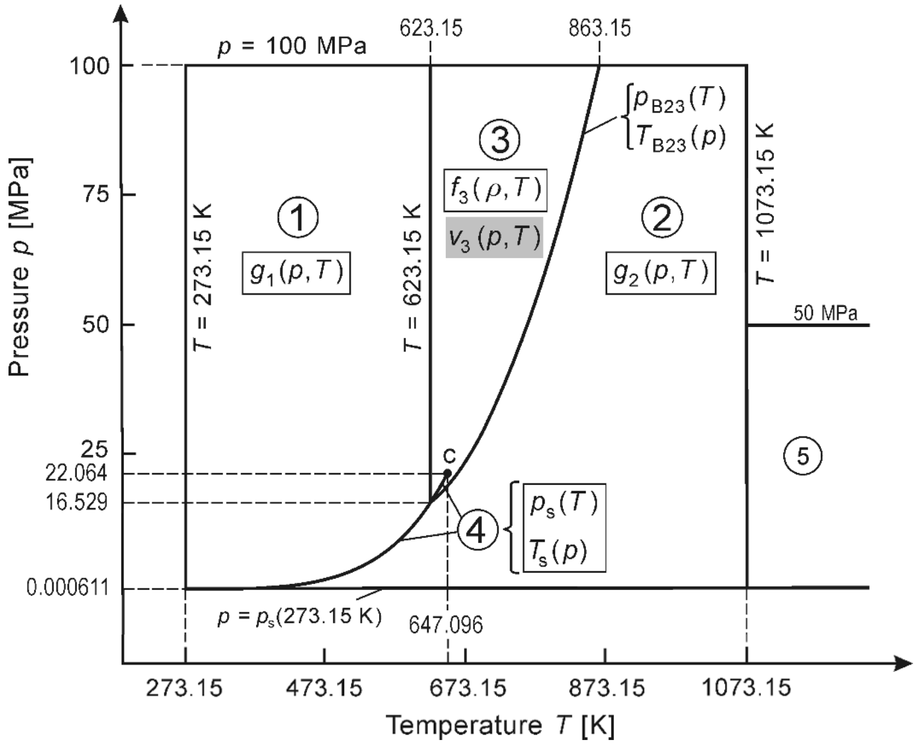

Fig. 2.22 Assignment of backward equations $v_3(p,T)$ to region 3 in a p-T diagram. For this overview, it is not shown how region 3 will be divided into subregions.

2.3.6.1 Numerical Consistency Requirements

In region 3, any property calculation from the basic equation $f_3(\rho,T)$, Eq. (2.11), for given values of p and T requires the determination of the density ρ ($\rho = 1/v$) by iteration. Based on experience with process calculations in this region, the numerical uncertainty in the calculation of the specific volume by iteration should be not greater than 0.001%. Likewise, the uncertainty in the subsequent determination of the specific enthalpy and specific entropy should be less than 0.001%, and for the specific isobaric heat capacity and speed of sound it should not be greater than 0.01%. These requirements must also be fulfilled when v is calculated directly from the backward equations $v_3(p,T)$, rather than calculated by iterating the basic equation $f_3(\rho,T)$, Eq. (2.11). The consistency requirements for all of these properties are summarized in Table 2.99. In order to achieve these very minor inconsistencies simultaneously for all of the properties, the inconsistencies in v between the backward equations $v_3(p,T)$ and the basic equation $f_3(\rho,T)$ had to be at least 0.001%, and for some parts of region 3 even smaller.

In the near-critical region, there are no defined numerical consistency requirements for the auxiliary equations, but the inconsistencies should be as small as possible.

Table 2.99 Permissible numerical inconsistencies in the properties v, h, s, c_p, and w when v is calculated one time via iteration with the basic equation $f_3(\rho, T)$, Eq. (2.11), for given inputs of p and T, and the other time directly from the respective backward equation $v_3(p,T)$. Based on these two (slightly different) v values, the properties h, s, c_p, and w are obtained from the basic equation $f_3(\rho, T)$ with $\rho = 1/v$ [a]

Permissible inconsistencies [%]				
$\lvert \Delta v/v \rvert_{\text{perm}}$	$\lvert \Delta h/h \rvert_{\text{perm}}$	$\lvert \Delta s/s \rvert_{\text{perm}}$	$\lvert \Delta c_p/c_p \rvert_{\text{perm}}$	$\lvert \Delta w/w \rvert_{\text{perm}}$
0.001	0.001	0.001	0.01	0.01

[a] The values for v are calculated from the backward equations $v_3(p,T)$.

2.3.6.2 Range of Validity of the Backward and Auxiliary Equations

The range of validity of the entire set of the backward equations $v_3(p,T)$ corresponds to region 3 of IAPWS-IF97, which is defined by the following range of temperature and pressure:

$$623.15\text{ K} \le T \le 863.15\text{ K} \qquad p_{\text{B23}}(T) \le p \le 100\text{ MPa}$$

with $p_{\text{B23}}(T)$ according to the B23-equation, Eq. (2.1), as shown in Fig. 2.23.

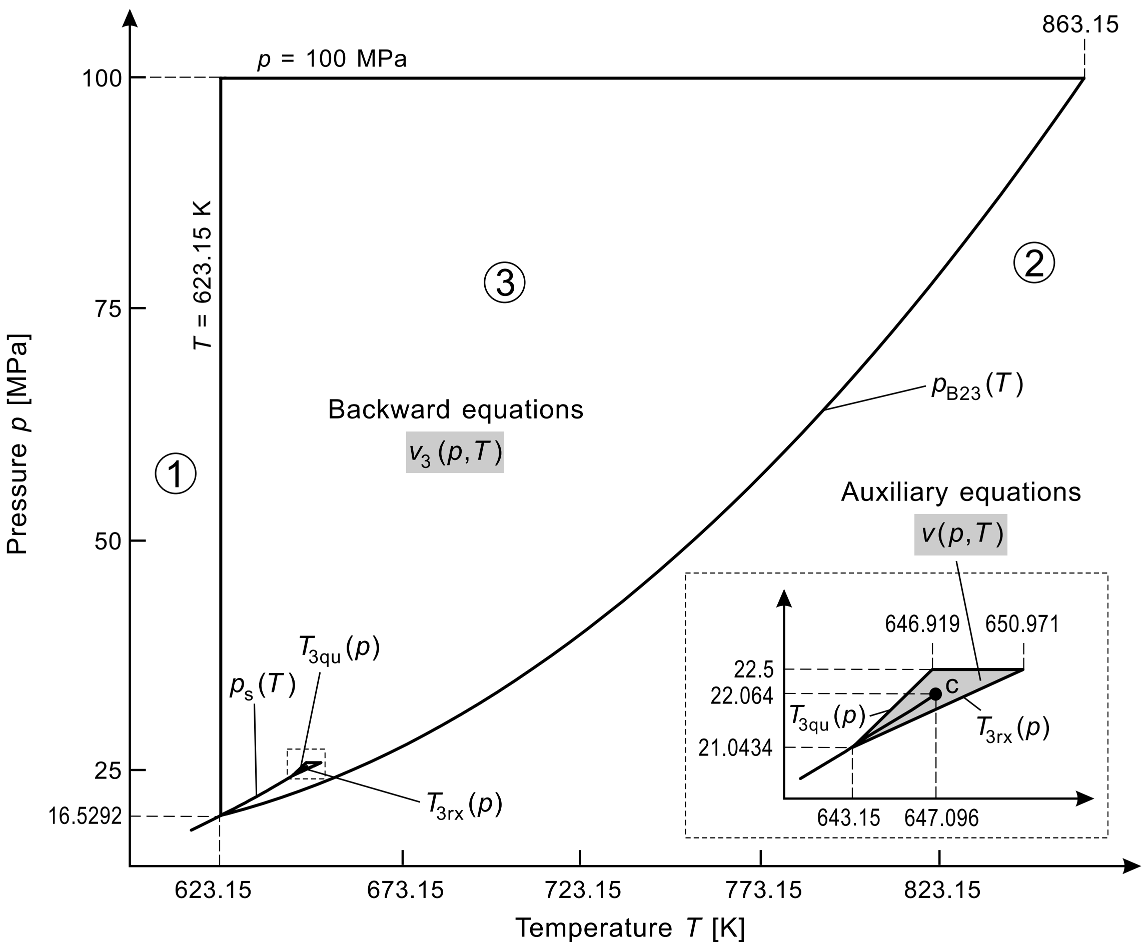

Fig. 2.23 Range of validity of the backward equations $v_3(p,T)$ covering all of region 3 except for the near-critical region. The near-critical region is enlarged and marked in grey in the lower right part of the figure, where this region is covered by the auxiliary equations $v(p,T)$. This near-critical region includes a temperature range from 643.15 K to 650.971 K at pressures from 21.0434 MPa to 22.5 MPa. Figure 2.26 shows this small region in more detail.

Achieving the numerical consistency requirement of 0.001% for $v_3(p,T)$ proved to be infeasible using simple functional forms in the region

$$p_s(643.15\ \mathrm{K}) \le p \le 22.5\ \mathrm{MPa} \qquad T_{3qu}(p) \le T \le T_{3rx}(p),$$

$$\text{where } p_s(643.15\ \mathrm{K}) = 21.034\,367\,32\ \mathrm{MPa}.$$

This region is marked in grey in Fig. 2.23, which also shows the temperature and pressure range of the boundary equations $T_{3qu}(p)$ and $T_{3rx}(p)$; the boundary equations themselves are given in Sec. 2.3.6.3 and $p_s(643.15\ \mathrm{K})$ is calculated from Eq. (2.13). The reason for excluding the near-critical region (grey area in Fig. 2.23) from the range of validity of the backward equations $v_3(p,T)$ is based on the complex structure of this region on the v-p-T surface with the infinite slope $(\partial v/\partial p)_T$ at the critical point. In order to not exclude the near-critical region completely from the equations $v(p,T)$, Sec. 2.3.6.5 contains equations for this small region very close to the critical point. These equations exhibit clearly larger inconsistencies with the basic equation $f_3(\rho,T)$ and are called auxiliary equations in the following.

2.3.6.3 Division of Region 3 into Subregions 3a to 3t and the Subregion-Boundary Equations

Preliminary investigations showed that it was not possible to meet the numerical consistency requirements with only a few subregions [14, 25]. Therefore, the main part of region 3 was divided into 20 subregions, 3a to 3t, as illustrated in Figs. 2.24 and 2.25.

The following subscripts mark the subregion boundaries that separate the adjacent subregions:

3ab:	Boundary between subregions 3a/3b and 3d/3e
3cd:	Boundary between subregions 3c/3d, 3c/3g, and 3c/3l
3ef:	Boundary between subregions 3e/3f, 3h/3i, and 3n/o
3gh:	Boundary between subregions 3g/3h and 3l/3m
3ij:	Boundary between subregions 3i/3j and 3p/3j
3jk:	Boundary between subregions 3j/3k and 3r/3k
3mn:	Boundary between subregions 3m/3n
3op:	Boundary between subregions 3o/3p
3qu:	Boundary between subregions 3q/3u
3rx:	Boundary between subregions 3r/3x
3uv:	Boundary between subregions 3u/3v
3wx:	Boundary between subregions 3w/3x
B23:	Boundary between regions 2/3

These subregion boundaries are also shown in Figs. 2.24 and 2.25.

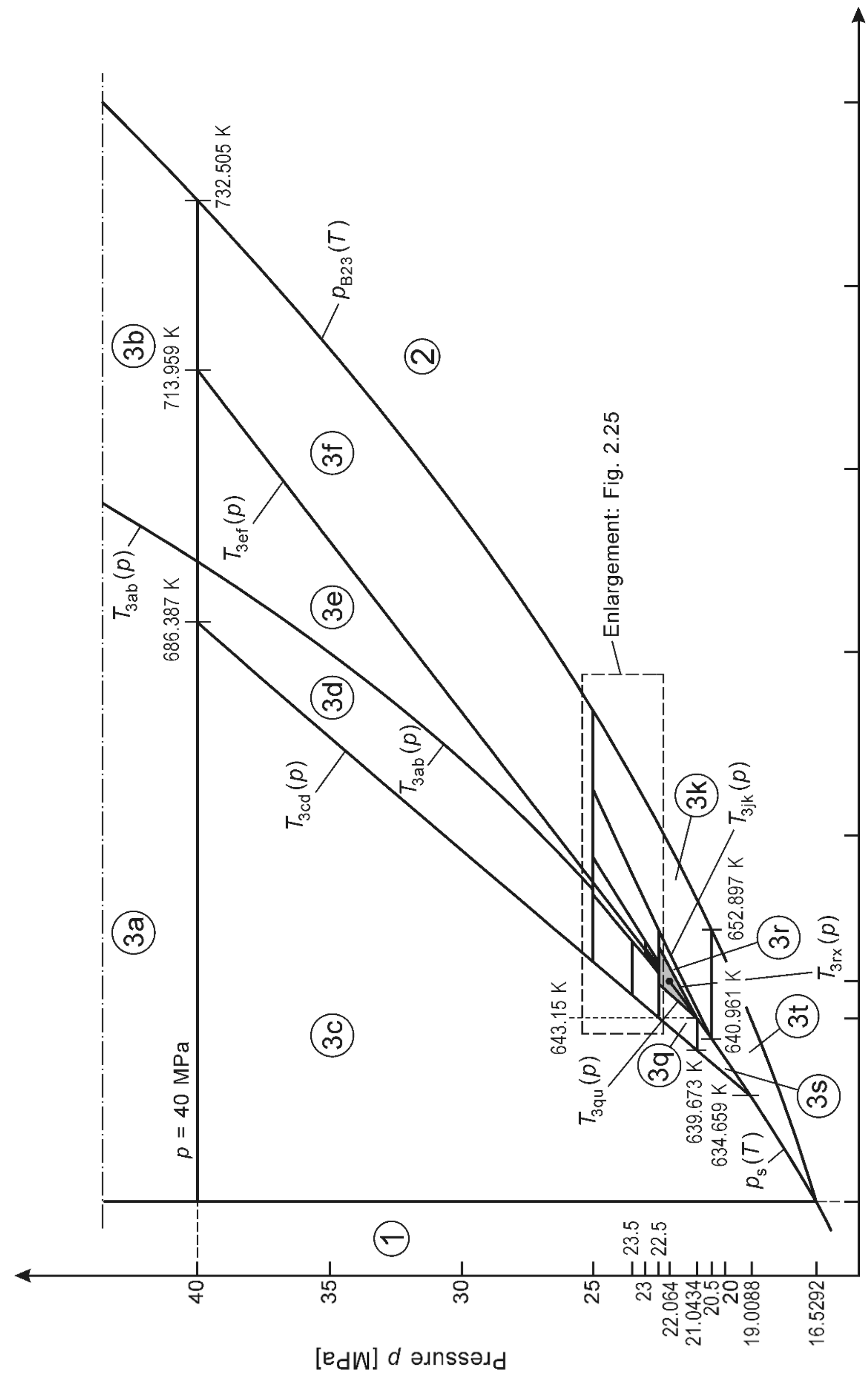

Fig. 2.24 Division of region 3 into subregions for the backward equations $v_3(p,T)$. The subregions 3a and 3b extend up to 100 MPa.

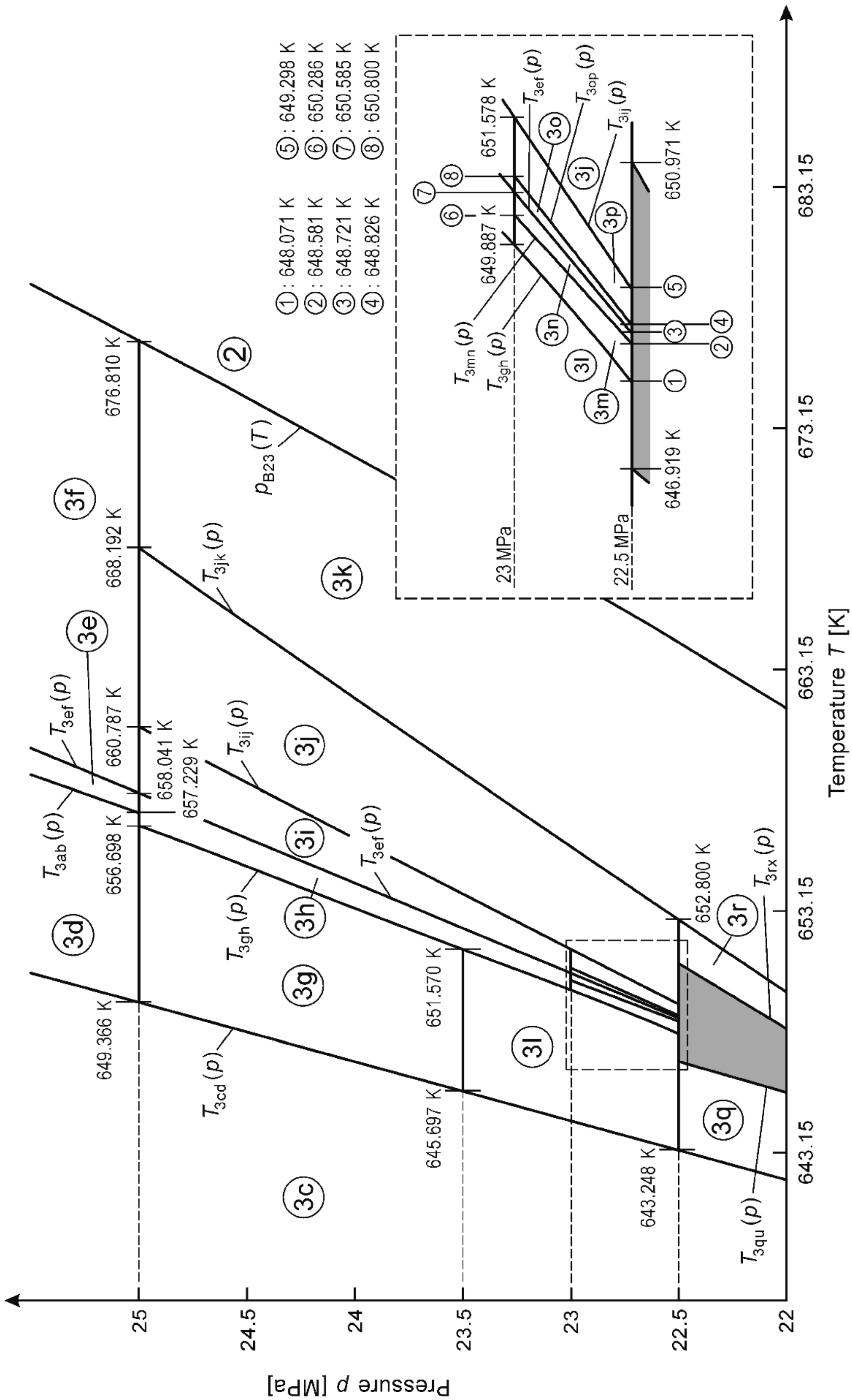

Fig. 2.25 Enlargement of Fig. 2.24 for subregions 3c to 3r for the corresponding backward equations $v_3(p, T)$.

The subregion-boundary equations, except for the equations $T_{3ab}(p)$, $T_{3ef}(p)$, and $T_{3op}(p)$, have the following dimensionless form:

$$\frac{T(p)}{T^*} = \theta(\pi) = \sum_{i=1}^{N} n_i\, \pi^{I_i} \ , \tag{2.65}$$

where $\theta = T/T^*$ and $\pi = p/p^*$ with $T^* = 1$ K and $p^* = 1$ MPa.

The equations $T_{3ab}(p)$ and $T_{3op}(p)$ have the form:

$$\frac{T(p)}{T^*} = \theta(\pi) = \sum_{i=1}^{N} n_i\, (\ln \pi)^{I_i} \ , \tag{2.66}$$

and $T_{3ef}(p)$ has the form:

$$\frac{T_{3ef}(p)}{T^*} = \theta(\pi) = \left.\frac{\mathrm{d}\theta}{\mathrm{d}\pi}\right|_{\mathrm{c}} (\pi - 22.064) + 647.096\,, \tag{2.67}$$

where the derivative of the saturation-temperature equation, Eq. (2.14), at the critical point is $\mathrm{d}\theta/\mathrm{d}\pi|_{\mathrm{c}} = 3.727\,888\,004$.

The coefficients n_i and exponents I_i of these subregion-boundary equations are listed in Table 2.100.

Table 2.100 Coefficients n_i and exponents I_i of the subregion-boundary equations, except for the equation $T_{3ef}(p)$.

Equation	i	I_i	n_i	i	I_i	n_i
$T_{3ab}(p)$	1	0	$0.154\,793\,642\,129\,415 \times 10^{4}$	4	−1	$-0.191\,887\,498\,864\,292 \times 10^{4}$
	2	1	$-0.187\,661\,219\,490\,113 \times 10^{3}$	5	−2	$0.918\,419\,702\,359\,447 \times 10^{3}$
	3	2	$0.213\,144\,632\,222\,113 \times 10^{2}$			
$T_{3cd}(p)$	1	0	$0.585\,276\,966\,696\,349 \times 10^{3}$	3	2	$-0.127\,283\,549\,295\,878 \times 10^{-1}$
	2	1	$0.278\,233\,532\,206\,915 \times 10^{1}$	4	3	$0.159\,090\,746\,562\,729 \times 10^{-3}$
$T_{3gh}(p)$	1	0	$-0.249\,284\,240\,900\,418 \times 10^{5}$	4	3	$0.751\,608\,051\,114\,157 \times 10^{1}$
	2	1	$0.428\,143\,584\,791\,546 \times 10^{4}$	5	4	$-0.787\,105\,249\,910\,383 \times 10^{-1}$
	3	2	$-0.269\,029\,173\,140\,130 \times 10^{3}$			
$T_{3ij}(p)$	1	0	$0.584\,814\,781\,649\,163 \times 10^{3}$	4	3	$-0.587\,071\,076\,864\,459 \times 10^{-2}$
	2	1	$-0.616\,179\,320\,924\,617$	5	4	$0.515\,308\,185\,433\,082 \times 10^{-4}$
	3	2	$0.260\,763\,050\,899\,562$			
$T_{3jk}(p)$	1	0	$0.617\,229\,772\,068\,439 \times 10^{3}$	4	3	$-0.157\,391\,839\,848\,015 \times 10^{-1}$
	2	1	$-0.770\,600\,270\,141\,675 \times 10^{1}$	5	4	$0.137\,897\,492\,684\,194 \times 10^{-3}$
	3	2	$0.697\,072\,596\,851\,896$			
$T_{3mn}(p)$	1	0	$0.535\,339\,483\,742\,384 \times 10^{3}$	3	2	$-0.158\,365\,725\,441\,648$
	2	1	$0.761\,978\,122\,720\,128 \times 10^{1}$	4	3	$0.192\,871\,054\,508\,108 \times 10^{-2}$
$T_{3op}(p)$	1	0	$0.969\,461\,372\,400\,213 \times 10^{3}$	4	−1	$0.773\,845\,935\,768\,222 \times 10^{3}$
	2	1	$-0.332\,500\,170\,441\,278 \times 10^{3}$	5	−2	$-0.152\,313\,732\,937\,084 \times 10^{4}$
	3	2	$0.642\,859\,598\,466\,067 \times 10^{2}$			
$T_{3qu}(p)$	1	0	$0.565\,603\,648\,239\,126 \times 10^{3}$	3	2	$-0.102\,020\,639\,611\,016$
	2	1	$0.529\,062\,258\,221\,222 \times 10^{1}$	4	3	$0.122\,240\,301\,070\,145 \times 10^{-2}$
$T_{3rx}(p)$	1	0	$0.584\,561\,202\,520\,006 \times 10^{3}$	3	2	$0.243\,293\,362\,700\,452$
	2	1	$-0.102\,961\,025\,163\,669 \times 10^{1}$	4	3	$-0.294\,905\,044\,740\,799 \times 10^{-2}$

With the help of the ranges of pressure and temperature given in Table 2.101, any (p, T) point can be assigned to the corresponding subregions 3a to 3t as given in Figs (2.24) and (2.25); the subregion-boundary equations $T_{3\mathrm{ab}}(p)$ to $T_{3\mathrm{rx}}(p)$ are defined in Eqs. (2.65) to (2.67) in combination with Table 2.100.

Table 2.101 Pressure ranges and corresponding subregion-boundary equations for determining the correct subregion, 3a to 3t, for the backward equations $v_3(p, T)$

Pressure range	Sub-region	Temperature range	Sub-region	Temperature range
40 MPa $< p \le$ 100 MPa	3a	$T \le T_{3\mathrm{ab}}(p)$	3b	$T > T_{3\mathrm{ab}}(p)$
25 MPa $< p \le$ 40 MPa	3c 3d	$T \le T_{3\mathrm{cd}}(p)$ $T_{3\mathrm{cd}}(p) < T \le T_{3\mathrm{ab}}(p)$	3e 3f	$T_{3\mathrm{ab}}(p) < T \le T_{3\mathrm{ef}}(p)$ $T > T_{3\mathrm{ef}}(p)$
23.5 MPa $< p \le$ 25 MPa	3c 3g 3h	$T \le T_{3\mathrm{cd}}(p)$ $T_{3\mathrm{cd}}(p) < T \le T_{3\mathrm{gh}}(p)$ $T_{3\mathrm{gh}}(p) < T \le T_{3\mathrm{ef}}(p)$	3i 3j 3k	$T_{3\mathrm{ef}}(p) < T \le T_{3\mathrm{ij}}(p)$ $T_{3\mathrm{ij}}(p) < T \le T_{3\mathrm{jk}}(p)$ $T > T_{3\mathrm{jk}}(p)$
23 MPa $< p \le$ 23.5 MPa	3c 3l 3h	$T \le T_{3\mathrm{cd}}(p)$ $T_{3\mathrm{cd}}(p) < T \le T_{3\mathrm{gh}}(p)$ $T_{3\mathrm{gh}}(p) < T \le T_{3\mathrm{ef}}(p)$	3i 3j 3k	$T_{3\mathrm{ef}}(p) < T \le T_{3\mathrm{ij}}(p)$ $T_{3\mathrm{ij}}(p) < T \le T_{3\mathrm{jk}}(p)$ $T > T_{3\mathrm{jk}}(p)$
22.5 MPa $< p \le$ 23 MPa	3c 3l 3m 3n	$T \le T_{3\mathrm{cd}}(p)$ $T_{3\mathrm{cd}}(p) < T \le T_{3\mathrm{gh}}(p)$ $T_{3\mathrm{gh}}(p) < T \le T_{3\mathrm{mn}}(p)$ $T_{3\mathrm{mn}}(p) < T \le T_{3\mathrm{ef}}(p)$	3o 3p 3j 3k	$T_{3\mathrm{ef}}(p) < T \le T_{3\mathrm{op}}(p)$ $T_{3\mathrm{op}}(p) < T \le T_{3\mathrm{ij}}(p)$ $T_{3\mathrm{ij}}(p) < T \le T_{3\mathrm{jk}}(p)$ $T > T_{3\mathrm{jk}}(p)$
p_s(643.15 K)[a] $< p \le$ 22.5 MPa	3c 3q	$T \le T_{3\mathrm{cd}}(p)$ $T_{3\mathrm{cd}}(p) < T \le T_{3\mathrm{qu}}(p)$	3r 3k	$T_{3\mathrm{rx}}(p) < T \le T_{3\mathrm{jk}}(p)$ $T > T_{3\mathrm{jk}}(p)$
20.5 MPa$< p \le p_\mathrm{s}$(643.15 K)[a]	3c 3s	$T \le T_{3\mathrm{cd}}(p)$ $T_{3\mathrm{cd}}(p) < T \le T_\mathrm{s}(p)$	3r 3k	$T_\mathrm{s}(p) \le T \le T_{3\mathrm{jk}}(p)$ $T > T_{3\mathrm{jk}}(p)$
$p_{3\mathrm{cd}}$[b] $< p \le$ 20.5 MPa	3c 3s	$T \le T_{3\mathrm{cd}}(p)$ $T_{3\mathrm{cd}}(p) < T \le T_\mathrm{s}(p)$	3t	$T \ge T_\mathrm{s}(p)$
p_s(623.15 K)[c] $< p \le p_{3\mathrm{cd}}$[b]	3c	$T \le T_\mathrm{s}(p)$	3t	$T \ge T_\mathrm{s}(p)$

[a] p_s(643.15 K) = 21.043 367 32 MPa.
[b] $p_{3\mathrm{cd}}$ = 19.008 811 89 MPa.
[c] p_s(623.15 K) = 16.529 164 25 MPa.

The **equation** $\boldsymbol{T_{3\mathrm{ab}}(p)}$ approximates the critical isentrope from 25 MPa to 100 MPa and divides subregions 3a from 3b and 3d from 3e.

The **equation** $\boldsymbol{T_{3\mathrm{cd}}(p)}$ ranges from $p_{3\mathrm{cd}}$ = 19.008 811 89 MPa to 40 MPa. The pressure $p_{3\mathrm{cd}}$ corresponds to the pressure p for which $T_\mathrm{s}(p) = T_{3\mathrm{cd}}(p)$, where $T_\mathrm{s}(p)$ is the saturation-temperature equation, Eq. (2.14). The equation $T_{3\mathrm{cd}}(p)$ divides subregion 3c from subregions 3d, 3g, 3l, 3q, and 3s.

The subregion-boundary **equation** $\boldsymbol{T_{3\mathrm{ef}}(p)}$ is a straight line from 22.064 MPa to 40 MPa with the slope of the saturation-temperature line, Eq. (2.14), at the critical point. This equation divides subregion 3e from 3f, 3h from 3i, and 3n from 3o.

The **equation** $\boldsymbol{T_{3\mathrm{gh}}(p)}$ ranges from 22.5 MPa to 25 MPa and divides subregion 3g from subregion 3h and 3l from 3h and 3m.

The **equation $T_{3ij}(p)$** approximates the isochore $v = 0.0041\ \mathrm{m^3\ kg^{-1}}$ from 22.5 MPa to 25 MPa and divides subregion 3j from subregions 3i and 3p.

The **equation $T_{3jk}(p)$** approximates the isochore $v = v''(20.5\ \mathrm{MPa})$ from 20.5 MPa to 25 MPa. This equation divides subregion 3k from subregions 3j and 3r.

The **equation $T_{3mn}(p)$** approximates the isochore $v = 0.0028\ \mathrm{m^3\ kg^{-1}}$ from 22.5 MPa to 23 MPa and describes the boundary between subregion 3m and 3n.

The **equation $T_{3op}(p)$** approximates the isochore $v = 0.0034\ \mathrm{m^3\ kg^{-1}}$ from 22.5 MPa to 23 MPa. It divides subregion 3o from 3p.

The **equation $T_{3qu}(p)$** approximates the isochore $v = v'(643.15\ \mathrm{K})$ from $p = p_s(643.15\ \mathrm{K}) =$ 21.043 367 32 MPa to 22.5 MPa. This equation describes the boundary between subregion 3q and subregion 3u in the range covered by the auxiliary equation as shown in Fig. 2.26.

The **equation $T_{3rx}(p)$** approximates the isochore $v = v''(643.15\ \mathrm{K})$ from $p = p_s(643.15\ \mathrm{K}) =$ 21.043 367 32 MPa to 22.5 MPa. The equation $T_{3rx}(p)$ describes the boundary between subregion 3r and 3x for the auxiliary equations as illustrated in Fig. 2.26.

Computer-Program Verification. To assist the user in computer-program verification of the equations for the subregion boundaries, Table 2.102 contains test values for calculated temperatures.

Table 2.102 Temperature values calculated from the subregion-boundary equations for selected pressures [a]

Equation	p [MPa]	T [K]	Equation	p [MPa]	T [K]
$T_{3ab}(p)$	40	$6.930\,341\,408 \times 10^2$	$T_{3jk}(p)$	23	$6.558\,338\,344 \times 10^2$
$T_{3cd}(p)$	25	$6.493\,659\,208 \times 10^2$	$T_{3mn}(p)$	22.8	$6.496\,054\,133 \times 10^2$
$T_{3ef}(p)$	40	$7.139\,593\,992 \times 10^2$	$T_{3op}(p)$	22.8	$6.500\,106\,943 \times 10^2$
$T_{3gh}(p)$	23	$6.498\,873\,759 \times 10^2$	$T_{3qu}(p)$	22	$6.456\,355\,027 \times 10^2$
$T_{3ij}(p)$	23	$6.515\,778\,091 \times 10^2$	$T_{3rx}(p)$	22	$6.482\,622\,754 \times 10^2$

[a] Programmed functions should be verified using 8 byte real values for all variables.

2.3.6.4 Backward Equations $v(p,T)$ for Subregions 3a to 3t

This section presents the backward equations $v(p,T)$ for subregions 3a to 3t, explains how to use these equations, and makes statements on the numerical consistencies.

a) Backward Equations $v(p,T)$

The backward equations $v(p,T)$ for subregions 3a to 3t, except for 3n, have the following dimensionless form:

$$\frac{v(p,T)}{v^*} = \omega(\pi,\theta) = \left[\sum_{i=1}^{N} n_i \left[(\pi - a)^c\right]^{I_i} \left[(\theta - b)^d\right]^{J_i}\right]^e . \tag{2.68}$$

The equation for subregion 3n has the form:

$$\frac{v_{3n}(p,T)}{v^*} = \omega(\pi,\theta) = \exp\left[\sum_{i=1}^{N} n_i (\pi - a)^{I_i} (\theta - b)^{J_i}\right], \tag{2.69}$$

where $\omega = v/v^*$, $\pi = p/p^*$, and $\theta = T/T^*$. The reducing quantities v^*, p^*, and T^*, the number of coefficients N, the non-linear parameters a and b, and the exponents c, d, and e are listed in

Table 2.103. The coefficients n_i and exponents I_i and J_i of these equations are given in Tables 2.106 to 2.125, which are collected in Sec. 2.3.6.4e.

Table 2.103 Reducing quantities v^*, p^*, and T^*, the number of coefficients *N*, the non-linear parameters *a* and *b*, and exponents *c*, *d*, and *e* of the backward equations $v(p,T)$ of subregions 3a to 3t

Subregion	v^* [m^3 kg^{-1}]	p^* [MPa]	T^* [K]	N	a	b	c	d	e
3a	0.0024	100	760	30	0.085	0.817	1	1	1
3b	0.0041	100	860	32	0.280	0.779	1	1	1
3c	0.0022	40	690	35	0.259	0.903	1	1	1
3d	0.0029	40	690	38	0.559	0.939	1	1	4
3e	0.0032	40	710	29	0.587	0.918	1	1	1
3f	0.0064	40	730	42	0.587	0.891	0.5	1	4
3g	0.0027	25	660	38	0.872	0.971	1	1	4
3h	0.0032	25	660	29	0.898	0.983	1	1	4
3i	0.0041	25	660	42	0.910	0.984	0.5	1	4
3j	0.0054	25	670	29	0.875	0.964	0.5	1	4
3k	0.0077	25	680	34	0.802	0.935	1	1	1
3l	0.0026	24	650	43	0.908	0.989	1	1	4
3m	0.0028	23	650	40	1.000	0.997	1	0.25	1
3n	0.0031	23	650	39	0.976	0.997	-	-	-
3o	0.0034	23	650	24	0.974	0.996	0.5	1	1
3p	0.0041	23	650	27	0.972	0.997	0.5	1	1
3q	0.0022	23	650	24	0.848	0.983	1	1	4
3r	0.0054	23	650	27	0.874	0.982	1	1	1
3s	0.0022	21	640	29	0.886	0.990	1	1	4
3t	0.0088	20	650	33	0.803	1.020	1	1	1

Computer-Program Verification. To assist the user in computer-program verification of the backward equations $v(p,T)$, Eqs. (2.68) and (2.69), for subregions 3a to 3t, Table 2.104 contains test values for calculated specific volumes.

Table 2.104 Values of the specific volume calculated from the backward equations $v(p,T)$ of subregions 3a to 3t for selected values of pressure and temperature [a]

Equation	p [MPa]	T [K]	v[m^3 kg^{-1}]	Equation	p [MPa]	T [K]	v[m^3 kg^{-1}]
$v_{3a}(p,T)$	50	630	$1.470\,853\,100 \times 10^{-3}$	$v_{3k}(p,T)$	23	660	$6.109\,525\,997 \times 10^{-3}$
	80	670	$1.503\,831\,359 \times 10^{-3}$		24	670	$6.427\,325\,645 \times 10^{-3}$
$v_{3b}(p,T)$	50	710	$2.204\,728\,587 \times 10^{-3}$	$v_{3l}(p,T)$	22.6	646	$2.117\,860\,851 \times 10^{-3}$
	80	750	$1.973\,692\,940 \times 10^{-3}$		23	646	$2.062\,374\,674 \times 10^{-3}$
$v_{3c}(p,T)$	20	630	$1.761\,696\,406 \times 10^{-3}$	$v_{3m}(p,T)$	22.6	648.6	$2.533\,063\,780 \times 10^{-3}$
	30	650	$1.819\,560\,617 \times 10^{-3}$		22.8	649.3	$2.572\,971\,781 \times 10^{-3}$
$v_{3d}(p,T)$	26	656	$2.245\,587\,720 \times 10^{-3}$	$v_{3n}(p,T)$	22.6	649.0	$2.923\,432\,711 \times 10^{-3}$
	30	670	$2.506\,897\,702 \times 10^{-3}$		22.8	649.7	$2.913\,311\,494 \times 10^{-3}$
$v_{3e}(p,T)$	26	661	$2.970\,225\,962 \times 10^{-3}$	$v_{3o}(p,T)$	22.6	649.1	$3.131\,208\,996 \times 10^{-3}$
	30	675	$3.004\,627\,086 \times 10^{-3}$		22.8	649.9	$3.221\,160\,278 \times 10^{-3}$

Continued on next page.

Table 2.104 – Continued

Equation	p [MPa]	T [K]	$v\,[\mathrm{m^3\,kg^{-1}}]$	Equation	p [MPa]	T [K]	$v\,[\mathrm{m^3\,kg^{-1}}]$
$v_{3f}(p,T)$	26	671	$5.019\,029\,401\times10^{-3}$	$v_{3p}(p,T)$	22.6	649.4	$3.715\,596\,186\times10^{-3}$
	30	690	$4.656\,470\,142\times10^{-3}$		22.8	650.2	$3.664\,754\,790\times10^{-3}$
$v_{3g}(p,T)$	23.6	649	$2.163\,198\,378\times10^{-3}$	$v_{3q}(p,T)$	21.1	640	$1.970\,999\,272\times10^{-3}$
	24	650	$2.166\,044\,161\times10^{-3}$		21.8	643	$2.043\,919\,161\times10^{-3}$
$v_{3h}(p,T)$	23.6	652	$2.651\,081\,407\times10^{-3}$	$v_{3r}(p,T)$	21.1	644	$5.251\,009\,921\times10^{-3}$
	24	654	$2.967\,802\,335\times10^{-3}$		21.8	648	$5.256\,844\,741\times10^{-3}$
$v_{3i}(p,T)$	23.6	653	$3.273\,916\,816\times10^{-3}$	$v_{3s}(p,T)$	19.1	635	$1.932\,829\,079\times10^{-3}$
	24	655	$3.550\,329\,864\times10^{-3}$		20	638	$1.985\,387\,227\times10^{-3}$
$v_{3j}(p,T)$	23.5	655	$4.545\,001\,142\times10^{-3}$	$v_{3t}(p,T)$	17	626	$8.483\,262\,001\times10^{-3}$
	24	660	$5.100\,267\,704\times10^{-3}$		20	640	$6.227\,528\,101\times10^{-3}$

[a] Programmed functions should be verified using 8 byte real values for all variables.

b) Calculation of Properties with the Help of the Backward Equations $v(p,T)$

The backward equations $v_{3a}(p,T)$ to $v_{3t}(p,T)$, described in Sec. 2.3.6.4a along with the basic equation $f_3(\rho,T)$, Eq. (2.11), make it possible to determine all thermodynamic properties, e.g. specific enthalpy, specific entropy, specific isobaric heat capacity, and speed of sound, for given values of pressure p and temperature T in region 3 without iteration.

The following steps should be taken:

- Identify the subregion (3a to 3t) for the given values of the pressure p and temperature T following the instructions in Sec. 2.3.6.3 in conjunction with Table 2.101 and Figs. 2.24 and 2.25. Then calculate the specific volume v for the subregion using the corresponding backward equation $v(p,T)$, Eq. (2.68) or Eq. (2.69).
- Calculate the desired thermodynamic property for the previously calculated specific volume v and the given temperature T using the relation of this property to the basic equation $f_3(\rho,T)$, Eq. (2.11), where $\rho = 1/v$ is determined from the corresponding backward equation, Eq. (2.68) or Eq. (2.69).

c) Numerical Consistencies

The numerical inconsistencies between the backward equations $v(p,T)$, Eqs. (2.68) and (2.69), and the basic equation $f_3(\rho,T)$, Eq. (2.11), are listed in Table 2.105 in comparison with the permissible inconsistencies given in Table 2.99 in Sec. 2.3.6.1. In addition to the inconsistencies in specific volume v itself, the effect of these inconsistencies with regard to the inconsistencies in specific enthalpy, specific entropy, specific isobaric heat capacity, and speed of sound are also given; the calculation of these properties based on the calculation of v from the backward equations $v(p,T)$, Eqs. (2.68) and (2.69), is described in paragraph b) above.

Table 2.105 Maximum and root-mean-square inconsistencies in v, h, s, c_p, and w when these properties are calculated from the basic equation $f_3(\rho, T)$, Eq. (2.11), after ρ was determined by iteration and when $\rho = 1/v$ was calculated directly from the backward equations $v(p, T)$ of regions 3a to 3t

Sub-region	Inconsistencies in v, h, s, c_p, and w [%]									
	$\lvert\Delta v/v\rvert$		$\lvert\Delta h/h\rvert$		$\lvert\Delta s/s\rvert$		$\lvert\Delta c_p/c_p\rvert$		$\lvert\Delta w/w\rvert$	
	max	RMS	max	RMS	max	RMS	max	RMS	max	RMS
3a	0.00061	0.00031	0.00018	0.00008	0.00026	0.00011	0.0016	0.0006	0.0015	0.0006
3b	0.00064	0.00035	0.00017	0.00008	0.00016	0.00008	0.0012	0.0003	0.0008	0.0003
3c	0.00080	0.00038	0.00026	0.00012	0.00025	0.00011	0.0059	0.0016	0.0023	0.0010
3d	0.00059	0.00025	0.00018	0.00008	0.00014	0.00006	0.0035	0.0010	0.0012	0.0004
3e	0.00072	0.00033	0.00018	0.00009	0.00014	0.00007	0.0017	0.0005	0.0006	0.0002
3f	0.00068	0.00020	0.00018	0.00005	0.00013	0.00004	0.0015	0.0003	0.0002	0.0001
3g	0.00047	0.00016	0.00014	0.00005	0.00011	0.00004	0.0032	0.0011	0.0010	0.0003
3h	0.00085	0.00044	0.00022	0.00012	0.00017	0.00009	0.0066	0.0018	0.0006	0.0002
3i	0.00067	0.00028	0.00018	0.00008	0.00013	0.00006	0.0019	0.0006	0.0002	0.0001
3j	0.00034	0.00019	0.00009	0.00005	0.00007	0.00004	0.0020	0.0006	0.0002	0.0001
3k	0.00034	0.00012	0.00008	0.00003	0.00007	0.00002	0.0018	0.0003	0.0002	0.0001
3l	0.00033	0.00019	0.00010	0.00006	0.00008	0.00005	0.0035	0.0015	0.0008	0.0004
3m	0.00057	0.00031	0.00015	0.00009	0.00011	0.00006	0.0062	0.0030	0.0006	0.0002
3n	0.00064	0.00029	0.00017	0.00008	0.00012	0.00006	0.0050	0.0013	0.0002	0.0001
3o	0.00031	0.00015	0.00008	0.00004	0.00006	0.00003	0.0007	0.0002	0.0001	0.0001
3p	0.00044	0.00022	0.00012	0.00006	0.00009	0.00005	0.0026	0.0010	0.0002	0.0001
3q	0.00036	0.00018	0.00012	0.00006	0.00009	0.00005	0.0040	0.0016	0.0010	0.0005
3r	0.00037	0.00007	0.00010	0.00002	0.00008	0.00002	0.0030	0.0004	0.0002	0.0001
3s	0.00030	0.00016	0.00010	0.00005	0.00007	0.00004	0.0033	0.0015	0.0009	0.0005
3t	0.00095	0.00045	0.00022	0.00010	0.00018	0.00008	0.0046	0.0015	0.0004	0.0002
Permis-sible values	0.001		0.001		0.001		0.01		0.01	

Table 2.105 shows that the numerical inconsistencies in specific volume v, specific enthalpy h, and specific entropy s are less than 0.001% when v is calculated one time from the backward equations $v(p,T)$ given in Sec. 2.3.6.4a and the other time from the basic equation $f_3(\rho,T)$, Eq. (2.11). The corresponding inconsistencies in the specific isobaric heat capacity c_p and in the speed of sound w are less than 0.01%. Thus, all inconsistencies are less than the permissible values. This means that the calculation with the backward equations agrees within five significant figures for v, h, and s and within four significant figures for c_p and w with the calculation using the basic equations only.

Comprehensive tests have shown that the maximum inconsistencies between the backward equations $v(p,T)$ of adjacent subregions are less than 0.001%. Moreover, the inconsistencies in h, s, c_p, and w along subregion boundaries, when these properties are calculated one time with the help of the backward equations $v(p,T)$ and the other time with the basic equation $f_3(\rho,T)$ alone, are also less than the permissible values given in Table 2.99; this is valid for subregion

boundaries, isobars and lines defined by the subregion-boundary equations according to Eqs. (2.65) to (2.67).

d) Computing Time when Using the Backward Equations $v_3(p,T)$ in Comparison with the Basic Equation

A very important motivation for the development of the backward equations $v_3(p,T)$ was reducing the computing time for the calculation of thermodynamic properties for the given variables (p,T) in region 3. When only the basic equation $f_3(\rho,T)$, Eq. (2.11), is used, time consuming iterations are required, whereas when the basic equation is used in combination with the backward equations $v_3(p,T)$, all iterations are avoided. Then, the calculation speed is about 17 times faster than that using only the basic equation [19]. In this comparison, the basic equation has to be applied in combination with a one-dimensional Newton iteration with convergence tolerances corresponding to the consistency requirements for the backward equations given in Sec. 2.3.6.1.

e) Coefficients and Exponents of the Backward Equations $v(p,T)$ for Subregion 3a to 3t

This section contains Tables 2.106 to 2.125 with the coefficients and exponents of the backward equations $v_{3a}(p,T)$ to $v_{3t}(p,T)$ for subregions 3a to 3t according to Eqs. (2.68) and (2.69).

Table 2.106 Coefficients and exponents of the backward equation $v_{3a}(p,T)$ for subregion 3a

i	I_i	J_i	n_i	i	I_i	J_i	n_i
1	−12	5	$0.110\,879\,558\,823\,853 \times 10^{-2}$	16	−3	1	$-0.122\,494\,831\,387\,441 \times 10^{-1}$
2	−12	10	$0.572\,616\,740\,810\,616 \times 10^{3}$	17	−3	3	$0.179\,357\,604\,019\,989 \times 10^{1}$
3	−12	12	$-0.767\,051\,948\,380\,852 \times 10^{5}$	18	−3	6	$0.442\,729\,521\,058\,314 \times 10^{2}$
4	−10	5	$-0.253\,321\,069\,529\,674 \times 10^{-1}$	19	−2	0	$-0.593\,223\,489\,018\,342 \times 10^{-2}$
5	−10	10	$0.628\,008\,049\,345\,689 \times 10^{4}$	20	−2	2	$0.453\,186\,261\,685\,774$
6	−10	12	$0.234\,105\,654\,131\,876 \times 10^{6}$	21	−2	3	$0.135\,825\,703\,129\,140 \times 10^{1}$
7	−8	5	$0.216\,867\,826\,045\,856$	22	−1	0	$0.408\,748\,415\,856\,745 \times 10^{-1}$
8	−8	8	$-0.156\,237\,904\,341\,963 \times 10^{3}$	23	−1	1	$0.474\,686\,397\,863\,312$
9	−8	10	$-0.269\,893\,956\,176\,613 \times 10^{5}$	24	−1	2	$0.118\,646\,814\,997\,915 \times 10^{1}$
10	−6	1	$-0.180\,407\,100\,085\,505 \times 10^{-3}$	25	0	0	$0.546\,987\,265\,727\,549$
11	−5	1	$0.116\,732\,227\,668\,261 \times 10^{-2}$	26	0	1	$0.195\,266\,770\,452\,643$
12	−5	5	$0.266\,987\,040\,856\,040 \times 10^{2}$	27	1	0	$-0.502\,268\,790\,869\,663 \times 10^{-1}$
13	−5	10	$0.282\,776\,617\,243\,286 \times 10^{5}$	28	1	2	$-0.369\,645\,308\,193\,377$
14	−4	8	$-0.242\,431\,520\,029\,523 \times 10^{4}$	29	2	0	$0.633\,828\,037\,528\,420 \times 10^{-2}$
15	−3	0	$0.435\,217\,323\,022\,733 \times 10^{-3}$	30	2	2	$0.797\,441\,793\,901\,017 \times 10^{-1}$

Table 2.107 Coefficients and exponents of the backward equation $v_{3b}(p,T)$ for subregion 3b

i	I_i	J_i	n_i	i	I_i	J_i	n_i
1	−12	10	$-0.827\,670\,470\,003\,621\times10^{-1}$	17	−3	2	$-0.416\,375\,290\,166\,236\times10^{-1}$
2	−12	12	$0.416\,887\,126\,010\,565\times10^{2}$	18	−3	3	$-0.413\,754\,957\,011\,042\times10^{2}$
3	−10	8	$0.483\,651\,982\,197\,059\times10^{-1}$	19	−3	5	$-0.506\,673\,295\,721\,637\times10^{2}$
4	−10	14	$-0.291\,032\,084\,950\,276\times10^{5}$	20	−2	0	$-0.572\,212\,965\,569\,023\times10^{-3}$
5	−8	8	$-0.111\,422\,582\,236\,948\times10^{3}$	21	−2	2	$0.608\,817\,368\,401\,785\times10^{1}$
6	−6	5	$-0.202\,300\,083\,904\,014\times10^{-1}$	22	−2	5	$0.239\,600\,660\,256\,161\times10^{2}$
7	−6	6	$0.294\,002\,509\,338\,515\times10^{3}$	23	−1	0	$0.122\,261\,479\,925\,384\times10^{-1}$
8	−6	8	$0.140\,244\,997\,609\,658\times10^{3}$	24	−1	2	$0.216\,356\,057\,692\,938\times10^{1}$
9	−5	5	$-0.344\,384\,158\,811\,459\times10^{3}$	25	0	0	$0.398\,198\,903\,368\,642$
10	−5	8	$0.361\,182\,452\,612\,149\times10^{3}$	26	0	1	$-0.116\,892\,827\,834\,085$
11	−5	10	$-0.140\,699\,677\,420\,738\times10^{4}$	27	1	0	$-0.102\,845\,919\,373\,532$
12	−4	2	$-0.202\,023\,902\,676\,481\times10^{-2}$	28	1	2	$-0.492\,676\,637\,589\,284$
13	−4	4	$0.171\,346\,792\,457\,471\times10^{3}$	29	2	0	$0.655\,540\,456\,406\,790\times10^{-1}$
14	−4	5	$-0.425\,597\,804\,058\,632\times10^{1}$	30	3	2	$-0.240\,462\,535\,078\,530$
15	−3	0	$0.691\,346\,085\,000\,334\times10^{-5}$	31	4	0	$-0.269\,798\,180\,310\,075\times10^{-1}$
16	−3	1	$0.151\,140\,509\,678\,925\times10^{-2}$	32	4	1	$0.128\,369\,435\,967\,012$

Table 2.108 Coefficients and exponents of the backward equation $v_{3c}(p,T)$ for subregion 3c

i	I_i	J_i	n_i	i	I_i	J_i	n_i
1	−12	6	$0.311\,967\,788\,763\,030\times10^{1}$	19	−2	4	$0.234\,604\,891\,591\,616\times10^{3}$
2	−12	8	$0.276\,713\,458\,847\,564\times10^{5}$	20	−2	5	$0.377\,515\,668\,966\,951\times10^{4}$
3	−12	10	$0.322\,583\,103\,403\,269\times10^{8}$	21	−1	0	$0.158\,646\,812\,591\,361\times10^{-1}$
4	−10	6	$-0.342\,416\,065\,095\,363\times10^{3}$	22	−1	1	$0.707\,906\,336\,241\,843$
5	−10	8	$-0.899\,732\,529\,907\,377\times10^{6}$	23	−1	2	$0.126\,016\,225\,146\,570\times10^{2}$
6	−10	10	$-0.793\,892\,049\,821\,251\times10^{8}$	24	0	0	$0.736\,143\,655\,772\,152$
7	−8	5	$0.953\,193\,003\,217\,388\times10^{2}$	25	0	1	$0.676\,544\,268\,999\,101$
8	−8	6	$0.229\,784\,742\,345\,072\times10^{4}$	26	0	2	$-0.178\,100\,588\,189\,137\times10^{2}$
9	−8	7	$0.175\,336\,675\,322\,499\times10^{6}$	27	1	0	$-0.156\,531\,975\,531\,713$
10	−6	8	$0.791\,214\,365\,222\,792\times10^{7}$	28	1	2	$0.117\,707\,430\,048\,158\times10^{2}$
11	−5	1	$0.319\,933\,345\,844\,209\times10^{-4}$	29	2	0	$0.840\,143\,653\,860\,447\times10^{-1}$
12	−5	4	$-0.659\,508\,863\,555\,767\times10^{2}$	30	2	1	$-0.186\,442\,467\,471\,949$
13	−5	7	$-0.833\,426\,563\,212\,851\times10^{6}$	31	2	3	$-0.440\,170\,203\,949\,645\times10^{2}$
14	−4	2	$0.645\,734\,680\,583\,292\times10^{-1}$	32	2	7	$0.123\,290\,423\,502\,494\times10^{7}$
15	−4	8	$-0.382\,031\,020\,570\,813\times10^{7}$	33	3	0	$-0.240\,650\,039\,730\,845\times10^{-1}$
16	−3	0	$0.406\,398\,848\,470\,079\times10^{-4}$	34	3	7	$-0.107\,077\,716\,660\,869\times10^{7}$
17	−3	3	$0.310\,327\,498\,492\,008\times10^{2}$	35	8	1	$0.438\,319\,858\,566\,475\times10^{-1}$
18	−2	0	$-0.892\,996\,718\,483\,724\times10^{-3}$				

Table 2.109 Coefficients and exponents of the backward equation $v_{3d}(p,T)$ for subregion 3d

i	I_i	J_i	n_i	i	I_i	J_i	n_i
1	−12	4	$-0.452\,484\,847\,171\,645 \times 10^{-9}$	20	−5	1	$-0.436\,701\,347\,922\,356 \times 10^{-5}$
2	−12	6	$0.315\,210\,389\,538\,801 \times 10^{-4}$	21	−5	2	$-0.404\,213\,852\,833\,996 \times 10^{-3}$
3	−12	7	$-0.214\,991\,352\,047\,545 \times 10^{-2}$	22	−5	5	$-0.348\,153\,203\,414\,663 \times 10^{3}$
4	−12	10	$0.508\,058\,874\,808\,345 \times 10^{3}$	23	−5	7	$-0.385\,294\,213\,555\,289 \times 10^{6}$
5	−12	12	$-0.127\,123\,036\,845\,932 \times 10^{8}$	24	−4	0	$0.135\,203\,700\,099\,403 \times 10^{-6}$
6	−12	16	$0.115\,371\,133\,120\,497 \times 10^{13}$	25	−4	1	$0.134\,648\,383\,271\,089 \times 10^{-3}$
7	−10	0	$-0.197\,805\,728\,776\,273 \times 10^{-15}$	26	−4	7	$0.125\,031\,835\,351\,736 \times 10^{6}$
8	−10	2	$0.241\,554\,806\,033\,972 \times 10^{-10}$	27	−3	2	$0.968\,123\,678\,455\,841 \times 10^{-1}$
9	−10	4	$-0.156\,481\,703\,640\,525 \times 10^{-5}$	28	−3	4	$0.225\,660\,517\,512\,438 \times 10^{3}$
10	−10	6	$0.277\,211\,346\,836\,625 \times 10^{-2}$	29	−2	0	$-0.190\,102\,435\,341\,872 \times 10^{-3}$
11	−10	8	$-0.203\,578\,994\,462\,286 \times 10^{2}$	30	−2	1	$-0.299\,628\,410\,819\,229 \times 10^{-1}$
12	−10	10	$0.144\,369\,489\,909\,053 \times 10^{7}$	31	−1	0	$0.500\,833\,915\,372\,121 \times 10^{-2}$
13	−10	14	$-0.411\,254\,217\,946\,539 \times 10^{11}$	32	−1	1	$0.387\,842\,482\,998\,411$
14	−8	3	$0.623\,449\,786\,243\,773 \times 10^{-5}$	33	−1	5	$-0.138\,535\,367\,777\,182 \times 10^{4}$
15	−8	7	$-0.221\,774\,281\,146\,038 \times 10^{2}$	34	0	0	$0.870\,745\,245\,971\,773$
16	−8	8	$-0.689\,315\,087\,933\,158 \times 10^{5}$	35	0	2	$0.171\,946\,252\,068\,742 \times 10^{1}$
17	−8	10	$-0.195\,419\,525\,060\,713 \times 10^{8}$	36	1	0	$-0.326\,650\,121\,426\,383 \times 10^{-1}$
18	−6	6	$0.316\,373\,510\,564\,015 \times 10^{4}$	37	1	6	$0.498\,044\,171\,727\,877 \times 10^{4}$
19	−6	8	$0.224\,040\,754\,426\,988 \times 10^{7}$	38	3	0	$0.551\,478\,022\,765\,087 \times 10^{-2}$

Table 2.110 Coefficients and exponents of the backward equation $v_{3e}(p,T)$ for subregion 3e

i	I_i	J_i	n_i	i	I_i	J_i	n_i
1	−12	14	$0.715\,815\,808\,404\,721 \times 10^{9}$	16	−3	6	$0.475\,992\,667\,717\,124 \times 10^{5}$
2	−12	16	$-0.114\,328\,360\,753\,449 \times 10^{12}$	17	−3	7	$-0.266\,627\,750\,390\,341 \times 10^{6}$
3	−10	3	$0.376\,531\,002\,015\,720 \times 10^{-11}$	18	−2	0	$-0.153\,314\,954\,386\,524 \times 10^{-3}$
4	−10	6	$-0.903\,983\,668\,691\,157 \times 10^{-4}$	19	−2	1	$0.305\,638\,404\,828\,265$
5	−10	10	$0.665\,695\,908\,836\,252 \times 10^{6}$	20	−2	3	$0.123\,654\,999\,499\,486 \times 10^{3}$
6	−10	14	$0.535\,364\,174\,960\,127 \times 10^{10}$	21	−2	4	$-0.104\,390\,794\,213\,011 \times 10^{4}$
7	−10	16	$0.794\,977\,402\,335\,603 \times 10^{11}$	22	−1	0	$-0.157\,496\,516\,174\,308 \times 10^{-1}$
8	−8	7	$0.922\,230\,563\,421\,437 \times 10^{2}$	23	0	0	$0.685\,331\,118\,940\,253$
9	−8	8	$-0.142\,586\,073\,991\,215 \times 10^{6}$	24	0	1	$0.178\,373\,462\,873\,903 \times 10^{1}$
10	−8	10	$-0.111\,796\,381\,424\,162 \times 10^{7}$	25	1	0	$-0.544\,674\,124\,878\,910$
11	−6	6	$0.896\,121\,629\,640\,760 \times 10^{4}$	26	1	4	$0.204\,529\,931\,318\,843 \times 10^{4}$
12	−5	6	$-0.669\,989\,239\,070\,491 \times 10^{4}$	27	1	6	$-0.228\,342\,359\,328\,752 \times 10^{5}$
13	−4	2	$0.451\,242\,538\,486\,834 \times 10^{-2}$	28	2	0	$0.413\,197\,481\,515\,899$
14	−4	4	$-0.339\,731\,325\,977\,713 \times 10^{2}$	29	2	2	$-0.341\,931\,835\,910\,405 \times 10^{2}$
15	−3	2	$-0.120\,523\,111\,552\,278 \times 10^{1}$				

Table 2.111 Coefficients and exponents of the backward equation $v_{3f}(p,T)$ for subregion 3f

i	I_i	J_i	n_i	i	I_i	J_i	n_i
1	0	−3	$-0.251\,756\,547\,792\,325 \times 10^{-7}$	22	10	−6	$0.470\,942\,606\,221\,652 \times 10^{-5}$
2	0	−2	$0.601\,307\,193\,668\,763 \times 10^{-5}$	23	12	−10	$0.195\,049\,710\,391\,712 \times 10^{-12}$
3	0	−1	$-0.100\,615\,977\,450\,049 \times 10^{-2}$	24	12	−8	$-0.911\,627\,886\,266\,077 \times 10^{-8}$
4	0	0	$0.999\,969\,140\,252\,192$	25	12	−4	$0.604\,374\,640\,201\,265 \times 10^{-3}$
5	0	1	$0.214\,107\,759\,236\,486 \times 10^{1}$	26	14	−12	$-0.225\,132\,933\,900\,136 \times 10^{-15}$
6	0	2	$-0.165\,175\,571\,959\,086 \times 10^{2}$	27	14	−10	$0.610\,916\,973\,582\,981 \times 10^{-11}$
7	1	−1	$-0.141\,987\,303\,638\,727 \times 10^{-2}$	28	14	−8	$-0.303\,063\,908\,043\,404 \times 10^{-6}$
8	1	1	$0.269\,251\,915\,156\,554 \times 10^{1}$	29	14	−6	$-0.137\,796\,070\,798\,409 \times 10^{-4}$
9	1	2	$0.349\,741\,815\,858\,722 \times 10^{2}$	30	14	−4	$-0.919\,296\,736\,666\,106 \times 10^{-3}$
10	1	3	$-0.300\,208\,695\,771\,783 \times 10^{2}$	31	16	−10	$0.639\,288\,223\,132\,545 \times 10^{-9}$
11	2	0	$-0.131\,546\,288\,252\,539 \times 10^{1}$	32	16	−8	$0.753\,259\,479\,898\,699 \times 10^{-6}$
12	2	1	$-0.839\,091\,277\,286\,169 \times 10^{1}$	33	18	−12	$-0.400\,321\,478\,682\,929 \times 10^{-12}$
13	3	−5	$0.181\,545\,608\,337\,015 \times 10^{-9}$	34	18	−10	$0.756\,140\,294\,351\,614 \times 10^{-8}$
14	3	−2	$-0.591\,099\,206\,478\,909 \times 10^{-3}$	35	20	−12	$-0.912\,082\,054\,034\,891 \times 10^{-11}$
15	3	0	$0.152\,115\,067\,087\,106 \times 10^{1}$	36	20	−10	$-0.237\,612\,381\,140\,539 \times 10^{-7}$
16	4	−3	$0.252\,956\,470\,663\,225 \times 10^{-4}$	37	20	−6	$0.269\,586\,010\,591\,874 \times 10^{-4}$
17	5	−8	$0.100\,726\,265\,203\,786 \times 10^{-14}$	38	22	−12	$-0.732\,828\,135\,157\,839 \times 10^{-10}$
18	5	1	$-0.149\,774\,533\,860\,650 \times 10^{1}$	39	24	−12	$0.241\,995\,578\,306\,660 \times 10^{-9}$
19	6	−6	$-0.793\,940\,970\,562\,969 \times 10^{-9}$	40	24	−4	$-0.405\,735\,532\,730\,322 \times 10^{-3}$
20	7	−4	$-0.150\,290\,891\,264\,717 \times 10^{-3}$	41	28	−12	$0.189\,424\,143\,498\,011 \times 10^{-9}$
21	7	1	$0.151\,205\,531\,275\,133 \times 10^{1}$	42	32	−12	$-0.486\,632\,965\,074\,563 \times 10^{-9}$

Table 2.112 Coefficients and exponents of the backward equation $v_{3g}(p,T)$ for subregion 3g

i	I_i	J_i	n_i	i	I_i	J_i	n_i
1	−12	7	$0.412\,209\,020\,652\,996 \times 10^{-4}$	20	−2	3	$-0.910\,782\,540\,134\,681 \times 10^{2}$
2	−12	12	$-0.114\,987\,238\,280\,587 \times 10^{7}$	21	−2	5	$0.135\,033\,227\,281\,565 \times 10^{6}$
3	−12	14	$0.948\,180\,885\,032\,080 \times 10^{10}$	22	−2	14	$-0.712\,949\,383\,408\,211 \times 10^{19}$
4	−12	18	$-0.195\,788\,865\,718\,971 \times 10^{18}$	23	−2	24	$-0.104\,578\,785\,289\,542 \times 10^{37}$
5	−12	22	$0.496\,250\,704\,871\,300 \times 10^{25}$	24	−1	2	$0.304\,331\,584\,444\,093 \times 10^{2}$
6	−12	24	$-0.105\,549\,884\,548\,496 \times 10^{29}$	25	−1	8	$0.593\,250\,797\,959\,445 \times 10^{10}$
7	−10	14	$-0.758\,642\,165\,988\,278 \times 10^{12}$	26	−1	18	$-0.364\,174\,062\,110\,798 \times 10^{28}$
8	−10	20	$-0.922\,172\,769\,596\,101 \times 10^{23}$	27	0	0	$0.921\,791\,403\,532\,461$
9	−10	24	$0.725\,379\,072\,059\,348 \times 10^{30}$	28	0	1	$-0.337\,693\,609\,657\,471$
10	−8	7	$-0.617\,718\,249\,205\,859 \times 10^{2}$	29	0	2	$-0.724\,644\,143\,758\,508 \times 10^{2}$
11	−8	8	$0.107\,555\,033\,344\,858 \times 10^{5}$	30	1	0	$-0.110\,480\,239\,272\,601$
12	−8	10	$-0.379\,545\,802\,336\,487 \times 10^{8}$	31	1	1	$0.536\,516\,031\,875\,059 \times 10^{1}$
13	−8	12	$0.228\,646\,846\,221\,831 \times 10^{12}$	32	1	3	$-0.291\,441\,872\,156\,205 \times 10^{4}$
14	−6	8	$-0.499\,741\,093\,010\,619 \times 10^{7}$	33	3	24	$0.616\,338\,176\,535\,305 \times 10^{40}$
15	−6	22	$-0.280\,214\,310\,054\,101 \times 10^{31}$	34	5	22	$-0.120\,889\,175\,861\,180 \times 10^{39}$
16	−5	7	$0.104\,915\,406\,769\,586 \times 10^{7}$	35	6	12	$0.818\,396\,024\,524\,612 \times 10^{23}$
17	−5	20	$0.613\,754\,229\,168\,619 \times 10^{28}$	36	8	3	$0.940\,781\,944\,835\,829 \times 10^{9}$
18	−4	22	$0.802\,056\,715\,528\,378 \times 10^{32}$	37	10	0	$-0.367\,279\,669\,545\,448 \times 10^{5}$
19	−3	7	$-0.298\,617\,819\,828\,065 \times 10^{8}$	38	10	6	$-0.837\,513\,931\,798\,655 \times 10^{16}$

Table 2.113 Coefficients and exponents of the backward equation $v_{3h}(p,T)$ for subregion 3h

i	I_i	J_i	n_i	i	I_i	J_i	n_i
1	−12	8	$0.561\,379\,678\,887\,577 \times 10^{-1}$	16	−6	8	$-0.656\,174\,421\,999\,594 \times 10^{7}$
2	−12	12	$0.774\,135\,421\,587\,083 \times 10^{10}$	17	−5	2	$0.156\,362\,212\,977\,396 \times 10^{-4}$
3	−10	4	$0.111\,482\,975\,877\,938 \times 10^{-8}$	18	−5	3	$-0.212\,946\,257\,021\,400 \times 10^{1}$
4	−10	6	$-0.143\,987\,128\,208\,183 \times 10^{-2}$	19	−5	4	$0.135\,249\,306\,374\,858 \times 10^{2}$
5	−10	8	$0.193\,696\,558\,764\,920 \times 10^{4}$	20	−4	2	$0.177\,189\,164\,145\,813$
6	−10	10	$-0.605\,971\,823\,585\,005 \times 10^{9}$	21	−4	4	$0.139\,499\,167\,345\,464 \times 10^{4}$
7	−10	14	$0.171\,951\,568\,124\,337 \times 10^{14}$	22	−3	1	$-0.703\,670\,932\,036\,388 \times 10^{-2}$
8	−10	16	$-0.185\,461\,154\,985\,145 \times 10^{17}$	23	−3	2	$-0.152\,011\,044\,389\,648$
9	−8	0	$0.387\,851\,168\,078\,010 \times 10^{-16}$	24	−2	0	$0.981\,916\,922\,991\,113 \times 10^{-4}$
10	−8	1	$-0.395\,464\,327\,846\,105 \times 10^{-13}$	25	−1	0	$0.147\,199\,658\,618\,076 \times 10^{-2}$
11	−8	6	$-0.170\,875\,935\,679\,023 \times 10^{3}$	26	−1	2	$0.202\,618\,487\,025\,578 \times 10^{2}$
12	−8	7	$-0.212\,010\,620\,701\,220 \times 10^{4}$	27	0	0	$0.899\,345\,518\,944\,240$
13	−8	8	$0.177\,683\,337\,348\,191 \times 10^{8}$	28	1	0	$-0.211\,346\,402\,240\,858$
14	−6	4	$0.110\,177\,443\,629\,575 \times 10^{2}$	29	1	2	$0.249\,971\,752\,957\,491 \times 10^{2}$
15	−6	6	$-0.234\,396\,091\,693\,313 \times 10^{6}$				

Table 2.114 Coefficients and exponents of the backward equation $v_{3i}(p,T)$ for subregion 3i

i	I_i	J_i	n_i	i	I_i	J_i	n_i
1	0	0	$0.106\,905\,684\,359\,136 \times 10^{1}$	22	12	−12	$0.164\,395\,334\,345\,040 \times 10^{-23}$
2	0	1	$-0.148\,620\,857\,922\,333 \times 10^{1}$	23	12	−6	$-0.339\,823\,323\,754\,373 \times 10^{-5}$
3	0	10	$0.259\,862\,256\,980\,408 \times 10^{15}$	24	12	−4	$-0.135\,268\,639\,905\,021 \times 10^{-1}$
4	1	−4	$-0.446\,352\,055\,678\,749 \times 10^{-11}$	25	14	−10	$-0.723\,252\,514\,211\,625 \times 10^{-14}$
5	1	−2	$-0.566\,620\,757\,170\,032 \times 10^{-6}$	26	14	−8	$0.184\,386\,437\,538\,366 \times 10^{-8}$
6	1	−1	$-0.235\,302\,885\,736\,849 \times 10^{-2}$	27	14	−4	$-0.463\,959\,533\,752\,385 \times 10^{-1}$
7	1	0	$-0.269\,226\,321\,968\,839$	28	14	5	$-0.992\,263\,100\,376\,750 \times 10^{14}$
8	2	0	$0.922\,024\,992\,944\,392 \times 10^{1}$	29	18	−12	$0.688\,169\,154\,439\,335 \times 10^{-16}$
9	3	−5	$0.357\,633\,505\,503\,772 \times 10^{-11}$	30	18	−10	$-0.222\,620\,998\,452\,197 \times 10^{-10}$
10	3	0	$-0.173\,942\,565\,562\,222 \times 10^{2}$	31	18	−8	$-0.540\,843\,018\,624\,083 \times 10^{-7}$
11	4	−3	$0.700\,681\,785\,556\,229 \times 10^{-5}$	32	18	−6	$0.345\,570\,606\,200\,257 \times 10^{-2}$
12	4	−2	$-0.267\,050\,351\,075\,768 \times 10^{-3}$	33	18	2	$0.422\,275\,800\,304\,086 \times 10^{11}$
13	4	−1	$-0.231\,779\,669\,675\,624 \times 10^{1}$	34	20	−12	$-0.126\,974\,478\,770\,487 \times 10^{-14}$
14	5	−6	$-0.753\,533\,046\,979\,752 \times 10^{-12}$	35	20	−10	$0.927\,237\,985\,153\,679 \times 10^{-9}$
15	5	−1	$0.481\,337\,131\,452\,891 \times 10^{1}$	36	22	−12	$0.612\,670\,812\,016\,489 \times 10^{-13}$
16	5	12	$-0.223\,286\,270\,422\,356 \times 10^{22}$	37	24	−12	$-0.722\,693\,924\,063\,497 \times 10^{-11}$
17	7	−4	$-0.118\,746\,004\,987\,383 \times 10^{-4}$	38	24	−8	$-0.383\,669\,502\,636\,822 \times 10^{-3}$
18	7	−3	$0.646\,412\,934\,136\,496 \times 10^{-2}$	39	32	−10	$0.374\,684\,572\,410\,204 \times 10^{-3}$
19	8	−6	$-0.410\,588\,536\,330\,937 \times 10^{-9}$	40	32	−5	$-0.931\,976\,897\,511\,086 \times 10^{5}$
20	8	10	$0.422\,739\,537\,057\,241 \times 10^{20}$	41	36	−10	$-0.247\,690\,616\,026\,922 \times 10^{-1}$
21	10	−8	$0.313\,698\,180\,473\,812 \times 10^{-12}$	42	36	−8	$0.658\,110\,546\,759\,474 \times 10^{2}$

Table 2.115 Coefficients and exponents of the backward equation $v_{3j}(p, T)$ for subregion 3j

i	I_i	J_i	n_i	i	I_i	J_i	n_i
1	0	−1	$-0.111\,371\,317\,395\,540 \times 10^{-3}$	16	10	−6	$-0.960\,754\,116\,701\,669 \times 10^{-8}$
2	0	0	$0.100\,342\,892\,423\,685 \times 10^{1}$	17	12	−8	$-0.510\,572\,269\,720\,488 \times 10^{-10}$
3	0	1	$0.530\,615\,581\,928\,979 \times 10^{1}$	18	12	−3	$0.767\,373\,781\,404\,211 \times 10^{-2}$
4	1	−2	$0.179\,058\,760\,078\,792 \times 10^{-5}$	19	14	−10	$0.663\,855\,469\,485\,254 \times 10^{-14}$
5	1	−1	$-0.728\,541\,958\,464\,774 \times 10^{-3}$	20	14	−8	$-0.717\,590\,735\,526\,745 \times 10^{-9}$
6	1	1	$-0.187\,576\,133\,371\,704 \times 10^{2}$	21	14	−5	$0.146\,564\,542\,926\,508 \times 10^{-4}$
7	2	−1	$0.199\,060\,874\,071\,849 \times 10^{-2}$	22	16	−10	$0.309\,029\,474\,277\,013 \times 10^{-11}$
8	2	1	$0.243\,574\,755\,377\,290 \times 10^{2}$	23	18	−12	$-0.464\,216\,300\,971\,708 \times 10^{-15}$
9	3	−2	$-0.177\,040\,785\,499\,444 \times 10^{-3}$	24	20	−12	$-0.390\,499\,637\,961\,161 \times 10^{-13}$
10	4	−2	$-0.259\,680\,385\,227\,130 \times 10^{-2}$	25	20	−10	$-0.236\,716\,126\,781\,431 \times 10^{-9}$
11	4	2	$-0.198\,704\,578\,406\,823 \times 10^{3}$	26	24	−12	$0.454\,652\,854\,268\,717 \times 10^{-11}$
12	5	−3	$0.738\,627\,790\,224\,287 \times 10^{-4}$	27	24	−6	$-0.422\,271\,787\,482\,497 \times 10^{-2}$
13	5	−2	$-0.236\,264\,692\,844\,138 \times 10^{-2}$	28	28	−12	$0.283\,911\,742\,354\,706 \times 10^{-10}$
14	5	0	$-0.161\,023\,121\,314\,333 \times 10^{1}$	29	28	−5	$0.270\,929\,002\,720\,228 \times 10^{1}$
15	6	3	$0.622\,322\,971\,786\,473 \times 10^{4}$				

Table 2.116 Coefficients and exponents of the backward equation $v_{3k}(p, T)$ for subregion 3k

i	I_i	J_i	n_i	i	I_i	J_i	n_i
1	−2	10	$-0.401\,215\,699\,576\,099 \times 10^{9}$	18	1	2	$-0.194\,646\,110\,037\,079 \times 10^{3}$
2	−2	12	$0.484\,501\,478\,318\,406 \times 10^{11}$	19	2	−8	$0.808\,354\,639\,772\,825 \times 10^{-15}$
3	−1	−5	$0.394\,721\,471\,363\,678 \times 10^{-14}$	20	2	−6	$-0.180\,845\,209\,145\,470 \times 10^{-10}$
4	−1	6	$0.372\,629\,967\,374\,147 \times 10^{5}$	21	2	−3	$-0.696\,664\,158\,132\,412 \times 10^{-5}$
5	0	−12	$-0.369\,794\,374\,168\,666 \times 10^{-29}$	22	2	−2	$-0.181\,057\,560\,300\,994 \times 10^{-2}$
6	0	−6	$-0.380\,436\,407\,012\,452 \times 10^{-14}$	23	2	0	$0.255\,830\,298\,579\,027 \times 10^{1}$
7	0	−2	$0.475\,361\,629\,970\,233 \times 10^{-6}$	24	2	4	$0.328\,913\,873\,658\,481 \times 10^{4}$
8	0	−1	$-0.879\,148\,916\,140\,706 \times 10^{-3}$	25	5	−12	$-0.173\,270\,241\,249\,904 \times 10^{-18}$
9	0	0	$0.844\,317\,863\,844\,331$	26	5	−6	$-0.661\,876\,792\,558\,034 \times 10^{-6}$
10	0	1	$0.122\,433\,162\,656\,600 \times 10^{2}$	27	5	−3	$-0.395\,688\,923\,421\,250 \times 10^{-2}$
11	0	2	$-0.104\,529\,634\,830\,279 \times 10^{3}$	28	6	−12	$0.604\,203\,299\,819\,132 \times 10^{-17}$
12	0	3	$0.589\,702\,771\,277\,429 \times 10^{3}$	29	6	−10	$-0.400\,879\,935\,920\,517 \times 10^{-13}$
13	0	14	$-0.291\,026\,851\,164\,444 \times 10^{14}$	30	6	−8	$0.160\,751\,107\,464\,958 \times 10^{-8}$
14	1	−3	$0.170\,343\,072\,841\,850 \times 10^{-5}$	31	6	−5	$0.383\,719\,409\,025\,556 \times 10^{-4}$
15	1	−2	$-0.277\,617\,606\,975\,748 \times 10^{-3}$	32	8	−12	$-0.649\,565\,446\,702\,457 \times 10^{-14}$
16	1	0	$-0.344\,709\,605\,486\,686 \times 10^{1}$	33	10	−12	$-0.149\,095\,328\,506\,000 \times 10^{-11}$
17	1	1	$0.221\,333\,862\,447\,095 \times 10^{2}$	34	12	−10	$0.541\,449\,377\,329\,581 \times 10^{-8}$

Table 2.117 Coefficients and exponents of the backward equation $v_{3l}(p,T)$ for subregion 3l

i	I_i	J_i	n_i	i	I_i	J_i	n_i
1	−12	14	$0.260\,702\,058\,647\,537\times10^{10}$	23	−3	20	$-0.695\,953\,622\,348\,829\times10^{33}$
2	−12	16	$-0.188\,277\,213\,604\,704\times10^{15}$	24	−2	2	$0.110\,609\,027\,472\,280$
3	−12	18	$0.554\,923\,870\,289\,667\times10^{19}$	25	−2	3	$0.721\,559\,163\,361\,354\times10^{2}$
4	−12	20	$-0.758\,966\,946\,387\,758\times10^{23}$	26	−2	10	$-0.306\,367\,307\,532\,219\times10^{15}$
5	−12	22	$0.413\,865\,186\,848\,908\times10^{27}$	27	−1	0	$0.265\,839\,618\,885\,530\times10^{-4}$
6	−10	14	$-0.815\,038\,000\,738\,060\times10^{12}$	28	−1	1	$0.253\,392\,392\,889\,754\times10^{-1}$
7	−10	24	$-0.381\,458\,260\,489\,955\times10^{33}$	29	−1	3	$-0.214\,443\,041\,836\,579\times10^{3}$
8	−8	6	$-0.123\,239\,564\,600\,519\times10^{-1}$	30	0	0	$0.937\,846\,601\,489\,667$
9	−8	10	$0.226\,095\,631\,437\,174\times10^{8}$	31	0	1	$0.223\,184\,043\,101\,700\times10^{1}$
10	−8	12	$-0.495\,017\,809\,506\,720\times10^{12}$	32	0	2	$0.338\,401\,222\,509\,191\times10^{2}$
11	−8	14	$0.529\,482\,996\,422\,863\times10^{16}$	33	0	12	$0.494\,237\,237\,179\,718\times10^{21}$
12	−8	18	$-0.444\,359\,478\,746\,295\times10^{23}$	34	1	0	$-0.198\,068\,404\,154\,428$
13	−8	24	$0.521\,635\,864\,527\,315\times10^{35}$	35	1	16	$-0.141\,415\,349\,881\,140\times10^{31}$
14	−8	36	$-0.487\,095\,672\,740\,742\times10^{55}$	36	2	1	$-0.993\,862\,421\,613\,651\times10^{2}$
15	−6	8	$-0.714\,430\,209\,937\,547\times10^{6}$	37	4	0	$0.125\,070\,534\,142\,731\times10^{3}$
16	−5	4	$0.127\,868\,634\,615\,495$	38	5	0	$-0.996\,473\,529\,004\,439\times10^{3}$
17	−5	5	$-0.100\,752\,127\,917\,598\times10^{2}$	39	5	1	$0.473\,137\,909\,872\,765\times10^{5}$
18	−4	7	$0.777\,451\,437\,960\,990\times10^{7}$	40	6	14	$0.116\,662\,121\,219\,322\times10^{33}$
19	−4	16	$-0.108\,105\,480\,796\,471\times10^{25}$	41	10	4	$-0.315\,874\,976\,271\,533\times10^{16}$
20	−3	1	$-0.357\,578\,581\,169\,659\times10^{-5}$	42	10	12	$-0.445\,703\,369\,196\,945\times10^{33}$
21	−3	3	$-0.212\,857\,169\,423\,484\times10^{1}$	43	14	10	$0.642\,794\,932\,373\,694\times10^{33}$
22	−3	18	$0.270\,706\,111\,085\,238\times10^{30}$				

Table 2.118 Coefficients and exponents of the backward equation $v_{3m}(p,T)$ for subregion 3m

i	I_i	J_i	n_i	i	I_i	J_i	n_i
1	0	0	$0.811\,384\,363\,481\,847$	21	28	20	$0.368\,193\,926\,183\,570\times10^{60}$
2	3	0	$-0.568\,199\,310\,990\,094\times10^{4}$	22	2	22	$0.170\,215\,539\,458\,936\times10^{18}$
3	8	0	$-0.178\,657\,198\,172\,556\times10^{11}$	23	16	22	$0.639\,234\,909\,918\,741\times10^{42}$
4	20	2	$0.795\,537\,657\,613\,427\times10^{32}$	24	0	24	$-0.821\,698\,160\,721\,956\times10^{15}$
5	1	5	$-0.814\,568\,209\,346\,872\times10^{5}$	25	5	24	$-0.795\,260\,241\,872\,306\times10^{24}$
6	3	5	$-0.659\,774\,567\,602\,874\times10^{8}$	26	0	28	$0.233\,415\,869\,478\,510\times10^{18}$
7	4	5	$-0.152\,861\,148\,659\,302\times10^{11}$	27	3	28	$-0.600\,079\,934\,586\,803\times10^{23}$
8	5	5	$-0.560\,165\,667\,510\,446\times10^{12}$	28	4	28	$0.594\,584\,382\,273\,384\times10^{25}$
9	1	6	$0.458\,384\,828\,593\,949\times10^{6}$	29	12	28	$0.189\,461\,279\,349\,492\times10^{40}$
10	6	6	$-0.385\,754\,000\,383\,848\times10^{14}$	30	16	28	$-0.810\,093\,428\,842\,645\times10^{46}$
11	2	7	$0.453\,735\,800\,004\,273\times10^{8}$	31	1	32	$0.188\,813\,911\,076\,809\times10^{22}$
12	4	8	$0.939\,454\,935\,735\,563\times10^{12}$	32	8	32	$0.111\,052\,244\,098\,768\times10^{36}$
13	14	8	$0.266\,572\,856\,432\,938\times10^{28}$	33	14	32	$0.291\,133\,958\,602\,503\times10^{46}$
14	2	10	$-0.547\,578\,313\,899\,097\times10^{10}$	34	0	36	$-0.329\,421\,923\,951\,460\times10^{22}$
15	5	10	$0.200\,725\,701\,112\,386\times10^{15}$	35	2	36	$-0.137\,570\,282\,536\,696\times10^{26}$
16	3	12	$0.185\,007\,245\,563\,239\times10^{13}$	36	3	36	$0.181\,508\,996\,303\,902\times10^{28}$
17	0	14	$0.185\,135\,446\,828\,337\times10^{9}$	37	4	36	$-0.346\,865\,122\,768\,353\times10^{30}$
18	1	14	$-0.170\,451\,090\,076\,385\times10^{12}$	38	8	36	$-0.211\,961\,148\,774\,260\times10^{38}$
19	1	18	$0.157\,890\,366\,037\,614\times10^{15}$	39	14	36	$-0.128\,617\,899\,887\,675\times10^{49}$
20	1	20	$-0.202\,530\,509\,748\,774\times10^{16}$	40	24	36	$0.479\,817\,895\,699\,239\times10^{65}$

Table 2.119 Coefficients and exponents of the backward equation $v_{3n}(p,T)$ for subregion 3n

i	I_i	J_i	n_i	i	I_i	J_i	n_i
1	0	−12	$0.280\,967\,799\,943\,151 \times 10^{-38}$	21	3	−6	$0.705\,412\,100\,773\,699 \times 10^{-11}$
2	3	−12	$0.614\,869\,006\,573\,609 \times 10^{-30}$	22	4	−6	$0.258\,585\,887\,897\,486 \times 10^{-8}$
3	4	−12	$0.582\,238\,667\,048\,942 \times 10^{-27}$	23	2	−5	$-0.493\,111\,362\,030\,162 \times 10^{-10}$
4	6	−12	$0.390\,628\,369\,238\,462 \times 10^{-22}$	24	4	−5	$-0.158\,649\,699\,894\,543 \times 10^{-5}$
5	7	−12	$0.821\,445\,758\,255\,119 \times 10^{-20}$	25	7	−5	$-0.525\,037\,427\,886\,100$
6	10	−12	$0.402\,137\,961\,842\,776 \times 10^{-14}$	26	4	−4	$0.220\,019\,901\,729\,615 \times 10^{-2}$
7	12	−12	$0.651\,718\,171\,878\,301 \times 10^{-12}$	27	3	−3	$-0.643\,064\,132\,636\,925 \times 10^{-2}$
8	14	−12	$-0.211\,773\,355\,803\,058 \times 10^{-7}$	28	5	−3	$0.629\,154\,149\,015\,048 \times 10^{2}$
9	18	−12	$0.264\,953\,354\,380\,072 \times 10^{-2}$	29	6	−3	$0.135\,147\,318\,617\,061 \times 10^{3}$
10	0	−10	$-0.135\,031\,446\,451\,331 \times 10^{-31}$	30	0	−2	$0.240\,560\,808\,321\,713 \times 10^{-6}$
11	3	−10	$-0.607\,246\,643\,970\,893 \times 10^{-23}$	31	0	−1	$-0.890\,763\,306\,701\,305 \times 10^{-3}$
12	5	−10	$-0.402\,352\,115\,234\,494 \times 10^{-18}$	32	3	−1	$-0.440\,209\,599\,407\,714 \times 10^{4}$
13	6	−10	$-0.744\,938\,506\,925\,544 \times 10^{-16}$	33	1	0	$-0.302\,807\,107\,747\,776 \times 10^{3}$
14	8	−10	$0.189\,917\,206\,526\,237 \times 10^{-12}$	34	0	1	$0.159\,158\,748\,314\,599 \times 10^{4}$
15	12	−10	$0.364\,975\,183\,508\,473 \times 10^{-5}$	35	1	1	$0.232\,534\,272\,709\,876 \times 10^{6}$
16	0	−8	$0.177\,274\,872\,361\,946 \times 10^{-25}$	36	0	2	$-0.792\,681\,207\,132\,600 \times 10^{6}$
17	3	−8	$-0.334\,952\,758\,812\,999 \times 10^{-18}$	37	1	4	$-0.869\,871\,364\,662\,769 \times 10^{11}$
18	7	−8	$-0.421\,537\,726\,098\,389 \times 10^{-8}$	38	0	5	$0.354\,542\,769\,185\,671 \times 10^{12}$
19	12	−8	$-0.391\,048\,167\,929\,649 \times 10^{-1}$	39	1	6	$0.400\,849\,240\,129\,329 \times 10^{15}$
20	2	−6	$0.541\,276\,911\,564\,176 \times 10^{-13}$				

Table 2.120 Coefficients and exponents of the backward equation $v_{3o}(p,T)$ for subregion 3o

i	I_i	J_i	n_i	i	I_i	J_i	n_i
1	0	−12	$0.128\,746\,023\,979\,718 \times 10^{-34}$	13	6	−8	$0.814\,897\,605\,805\,513 \times 10^{-14}$
2	0	−4	$-0.735\,234\,770\,382\,342 \times 10^{-11}$	14	7	−12	$0.425\,596\,631\,351\,839 \times 10^{-25}$
3	0	−1	$0.289\,078\,692\,149\,150 \times 10^{-2}$	15	8	−10	$-0.387\,449\,113\,787\,755 \times 10^{-17}$
4	2	−1	$0.244\,482\,731\,907\,223$	16	8	−8	$0.139\,814\,747\,930\,240 \times 10^{-12}$
5	3	−10	$0.141\,733\,492\,030\,985 \times 10^{-23}$	17	8	−4	$-0.171\,849\,638\,951\,521 \times 10^{-2}$
6	4	−12	$-0.354\,533\,853\,059\,476 \times 10^{-28}$	18	10	−12	$0.641\,890\,529\,513\,296 \times 10^{-21}$
7	4	−8	$-0.594\,539\,202\,901\,431 \times 10^{-17}$	19	10	−8	$0.118\,960\,578\,072\,018 \times 10^{-10}$
8	4	−5	$-0.585\,188\,401\,782\,779 \times 10^{-8}$	20	14	−12	$-0.155\,282\,762\,571\,611 \times 10^{-17}$
9	4	−4	$0.201\,377\,325\,411\,803 \times 10^{-5}$	21	14	−8	$0.233\,907\,907\,347\,507 \times 10^{-7}$
10	4	−1	$0.138\,647\,388\,209\,306 \times 10^{1}$	22	20	−12	$-0.174\,093\,247\,766\,213 \times 10^{-12}$
11	5	−4	$-0.173\,959\,365\,084\,772 \times 10^{-4}$	23	20	−10	$0.377\,682\,649\,089\,149 \times 10^{-8}$
12	5	−3	$0.137\,680\,878\,349\,369 \times 10^{-2}$	24	24	−12	$-0.516\,720\,236\,575\,302 \times 10^{-10}$

Table 2.121 Coefficients and exponents of the backward equation $v_{3p}(p,T)$ for subregion 3p

i	I_i	J_i	n_i	i	I_i	J_i	n_i
1	0	−1	$-0.982\,825\,342\,010\,366 \times 10^{-4}$	15	12	−12	$0.343\,480\,022\,104\,968 \times 10^{-25}$
2	0	0	$0.105\,145\,700\,850\,612 \times 10^{1}$	16	12	−6	$0.816\,256\,095\,947\,021 \times 10^{-5}$
3	0	1	$0.116\,033\,094\,095\,084 \times 10^{3}$	17	12	−5	$0.294\,985\,697\,916\,798 \times 10^{-2}$
4	0	2	$0.324\,664\,750\,281\,543 \times 10^{4}$	18	14	−10	$0.711\,730\,466\,276\,584 \times 10^{-16}$
5	1	1	$-0.123\,592\,348\,610\,137 \times 10^{4}$	19	14	−8	$0.400\,954\,763\,806\,941 \times 10^{-9}$
6	2	−1	$-0.561\,403\,450\,013\,495 \times 10^{-1}$	20	14	−3	$0.107\,766\,027\,032\,853 \times 10^{2}$
7	3	−3	$0.856\,677\,401\,640\,869 \times 10^{-7}$	21	16	−8	$-0.409\,449\,599\,138\,182 \times 10^{-6}$
8	3	0	$0.236\,313\,425\,393\,924 \times 10^{3}$	22	18	−8	$-0.729\,121\,307\,758\,902 \times 10^{-5}$
9	4	−2	$0.972\,503\,292\,350\,109 \times 10^{-2}$	23	20	−10	$0.677\,107\,970\,938\,909 \times 10^{-8}$
10	6	−2	$-0.103\,001\,994\,531\,927 \times 10^{1}$	24	22	−10	$0.602\,745\,973\,022\,975 \times 10^{-7}$
11	7	−5	$-0.149\,653\,706\,199\,162 \times 10^{-8}$	25	24	−12	$-0.382\,323\,011\,855\,257 \times 10^{-10}$
12	7	−4	$-0.215\,743\,778\,861\,592 \times 10^{-4}$	26	24	−8	$0.179\,946\,628\,317\,437 \times 10^{-2}$
13	8	−2	$-0.834\,452\,198\,291\,445 \times 10^{1}$	27	36	−12	$-0.345\,042\,834\,640\,005 \times 10^{-3}$
14	10	−3	$0.586\,602\,660\,564\,988$				

Table 2.122 Coefficients and exponents of the backward equation $v_{3q}(p,T)$ for subregion 3q

i	I_i	J_i	n_i	i	I_i	J_i	n_i
1	−12	10	$-0.820\,433\,843\,259\,950 \times 10^{5}$	13	−3	3	$0.232\,808\,472\,983\,776 \times 10^{3}$
2	−12	12	$0.473\,271\,518\,461\,586 \times 10^{11}$	14	−2	0	$-0.142\,808\,220\,416\,837 \times 10^{-4}$
3	−10	6	$-0.805\,950\,021\,005\,413 \times 10^{-1}$	15	−2	1	$-0.643\,596\,060\,678\,456 \times 10^{-2}$
4	−10	7	$0.328\,600\,025\,435\,980 \times 10^{2}$	16	−2	2	$-0.428\,577\,227\,475\,614 \times 10^{1}$
5	−10	8	$-0.356\,617\,029\,982\,490 \times 10^{4}$	17	−2	4	$0.225\,689\,939\,161\,918 \times 10^{4}$
6	−10	10	$-0.172\,985\,781\,433\,335 \times 10^{10}$	18	−1	0	$0.100\,355\,651\,721\,510 \times 10^{-2}$
7	−8	8	$0.351\,769\,232\,729\,192 \times 10^{8}$	19	−1	1	$0.333\,491\,455\,143\,516$
8	−6	6	$-0.775\,489\,259\,985\,144 \times 10^{6}$	20	−1	2	$0.109\,697\,576\,888\,873 \times 10^{1}$
9	−5	2	$0.710\,346\,691\,966\,018 \times 10^{-4}$	21	0	0	$0.961\,917\,379\,376\,452$
10	−5	5	$0.993\,499\,883\,820\,274 \times 10^{5}$	22	1	0	$-0.838\,165\,632\,204\,598 \times 10^{-1}$
11	−4	3	$-0.642\,094\,171\,904\,570$	23	1	1	$0.247\,795\,908\,411\,492 \times 10^{1}$
12	−4	4	$-0.612\,842\,816\,820\,083 \times 10^{4}$	24	1	3	$-0.319\,114\,969\,006\,533 \times 10^{4}$

Table 2.123 Coefficients and exponents of the backward equation $v_{3r}(p,T)$ for subregion 3r

i	I_i	J_i	n_i	i	I_i	J_i	n_i
1	−8	6	$0.144\,165\,955\,660\,863 \times 10^{-2}$	15	8	−10	$0.399\,988\,795\,693\,162 \times 10^{-12}$
2	−8	14	$-0.701\,438\,599\,628\,258 \times 10^{13}$	16	8	−8	$-0.536\,479\,560\,201\,811 \times 10^{-6}$
3	−3	−3	$-0.830\,946\,716\,459\,219 \times 10^{-16}$	17	8	−5	$0.159\,536\,722\,411\,202 \times 10^{-1}$
4	−3	3	$0.261\,975\,135\,368\,109$	18	10	−12	$0.270\,303\,248\,860\,217 \times 10^{-14}$
5	−3	4	$0.393\,097\,214\,706\,245 \times 10^{3}$	19	10	−10	$0.244\,247\,453\,858\,506 \times 10^{-7}$
6	−3	5	$-0.104\,334\,030\,654\,021 \times 10^{5}$	20	10	−8	$-0.983\,430\,636\,716\,454 \times 10^{-5}$
7	−3	8	$0.490\,112\,654\,154\,211 \times 10^{9}$	21	10	−6	$0.663\,513\,144\,224\,454 \times 10^{-1}$
8	0	−1	$-0.147\,104\,222\,772\,069 \times 10^{-3}$	22	10	−5	$-0.993\,456\,957\,845\,006 \times 10^{1}$
9	0	0	$0.103\,602\,748\,043\,408 \times 10^{1}$	23	10	−4	$0.546\,491\,323\,528\,491 \times 10^{3}$
10	0	1	$0.305\,308\,890\,065\,089 \times 10^{1}$	24	10	−3	$-0.143\,365\,406\,393\,758 \times 10^{5}$
11	0	5	$-0.399\,745\,276\,971\,264 \times 10^{7}$	25	10	−2	$0.150\,764\,974\,125\,511 \times 10^{6}$
12	3	−6	$0.569\,233\,719\,593\,750 \times 10^{-11}$	26	12	−12	$-0.337\,209\,709\,340\,105 \times 10^{-9}$
13	3	−2	$-0.464\,923\,504\,407\,778 \times 10^{-1}$	27	14	−12	$0.377\,501\,980\,025\,469 \times 10^{-8}$
14	8	−12	$-0.535\,400\,396\,512\,906 \times 10^{-17}$				

Table 2.124 Coefficients and exponents of the backward equation $v_{3s}(p,T)$ for subregion 3s

i	I_i	J_i	n_i	i	I_i	J_i	n_i
1	−12	20	$-0.532\,466\,612\,140\,254 \times 10^{23}$	16	0	0	$0.965\,961\,650\,599\,775$
2	−12	24	$0.100\,415\,480\,000\,824 \times 10^{32}$	17	0	1	$0.294\,885\,696\,802\,488 \times 10^{1}$
3	−10	22	$-0.191\,540\,001\,821\,367 \times 10^{30}$	18	0	4	$-0.653\,915\,627\,346\,115 \times 10^{5}$
4	−8	14	$0.105\,618\,377\,808\,847 \times 10^{17}$	19	0	28	$0.604\,012\,200\,163\,444 \times 10^{50}$
5	−6	36	$0.202\,281\,884\,477\,061 \times 10^{59}$	20	1	0	$-0.198\,339\,358\,557\,937$
6	−5	8	$0.884\,585\,472\,596\,134 \times 10^{8}$	21	1	32	$-0.175\,984\,090\,163\,501 \times 10^{58}$
7	−5	16	$0.166\,540\,181\,638\,363 \times 10^{23}$	22	3	0	$0.356\,314\,881\,403\,987 \times 10^{1}$
8	−4	6	$-0.313\,563\,197\,669\,111 \times 10^{6}$	23	3	1	$-0.575\,991\,255\,144\,384 \times 10^{3}$
9	−4	32	$-0.185\,662\,327\,545\,324 \times 10^{54}$	24	3	2	$0.456\,213\,415\,338\,071 \times 10^{5}$
10	−3	3	$-0.624\,942\,093\,918\,942 \times 10^{-1}$	25	4	3	$-0.109\,174\,044\,987\,829 \times 10^{8}$
11	−3	8	$-0.504\,160\,724\,132\,590 \times 10^{10}$	26	4	18	$0.437\,796\,099\,975\,134 \times 10^{34}$
12	−2	4	$0.187\,514\,491\,833\,092 \times 10^{5}$	27	4	24	$-0.616\,552\,611\,135\,792 \times 10^{46}$
13	−1	1	$0.121\,399\,979\,993\,217 \times 10^{-2}$	28	5	4	$0.193\,568\,768\,917\,797 \times 10^{10}$
14	−1	2	$0.188\,317\,043\,049\,455 \times 10^{1}$	29	14	24	$0.950\,898\,170\,425\,042 \times 10^{54}$
15	−1	3	$-0.167\,073\,503\,962\,060 \times 10^{4}$				

Table 2.125 Coefficients and exponents of the backward equation $v_{3t}(p,T)$ for subregion 3t

i	I_i	J_i	n_i	i	I_i	J_i	n_i
1	0	0	$0.155\,287\,249\,586\,268 \times 10^{1}$	18	7	36	$-0.341\,552\,040\,860\,644 \times 10^{51}$
2	0	1	$0.664\,235\,115\,009\,031 \times 10^{1}$	19	10	10	$-0.527\,251\,339\,709\,047 \times 10^{21}$
3	0	4	$-0.289\,366\,236\,727\,210 \times 10^{4}$	20	10	12	$0.245\,375\,640\,937\,055 \times 10^{24}$
4	0	12	$-0.385\,923\,202\,309\,848 \times 10^{13}$	21	10	14	$-0.168\,776\,617\,209\,269 \times 10^{27}$
5	1	0	$-0.291\,002\,915\,783\,761 \times 10^{1}$	22	10	16	$0.358\,958\,955\,867\,578 \times 10^{29}$
6	1	10	$-0.829\,088\,246\,858\,083 \times 10^{12}$	23	10	22	$-0.656\,475\,280\,339\,411 \times 10^{36}$
7	2	0	$0.176\,814\,899\,675\,218 \times 10^{1}$	24	18	18	$0.355\,286\,045\,512\,301 \times 10^{39}$
8	2	6	$-0.534\,686\,695\,713\,469 \times 10^{9}$	25	20	32	$0.569\,021\,454\,413\,270 \times 10^{58}$
9	2	14	$0.160\,464\,608\,687\,834 \times 10^{18}$	26	22	22	$-0.700\,584\,546\,433\,113 \times 10^{48}$
10	3	3	$0.196\,435\,366\,560\,186 \times 10^{6}$	27	22	36	$-0.705\,772\,623\,326\,374 \times 10^{65}$
11	3	8	$0.156\,637\,427\,541\,729 \times 10^{13}$	28	24	24	$0.166\,861\,176\,200\,148 \times 10^{53}$
12	4	0	$-0.178\,154\,560\,260\,006 \times 10^{1}$	29	28	28	$-0.300\,475\,129\,680\,486 \times 10^{61}$
13	4	10	$-0.229\,746\,237\,623\,692 \times 10^{16}$	30	32	22	$-0.668\,481\,295\,196\,808 \times 10^{51}$
14	7	3	$0.385\,659\,001\,648\,006 \times 10^{8}$	31	32	32	$0.428\,432\,338\,620\,678 \times 10^{69}$
15	7	4	$0.110\,554\,446\,790\,543 \times 10^{10}$	32	32	36	$-0.444\,227\,367\,758\,304 \times 10^{72}$
16	7	7	$-0.677\,073\,830\,687\,349 \times 10^{14}$	33	36	36	$-0.281\,396\,013\,562\,745 \times 10^{77}$
17	7	20	$-0.327\,910\,592\,086\,523 \times 10^{31}$				

2.3.6.5 Auxiliary Equations $v(p,T)$ for the Near-Critical Region

This section contains the entire numerical information about the auxiliary equations $v(p,T)$ for the near-critical region.

a) Range of Validity of the Auxiliary Equations, Division of the Near-Critical Region into Subregions, and Subregion-Boundary Equations

The auxiliary equations $v(p,T)$ for subregions 3u to 3z are valid in the temperature and pressure range given by

$$T_{3\mathrm{qu}}(p) \le T \le T_{3\mathrm{rx}}(p) \quad \text{and} \quad p_\mathrm{s}(643.15\ \mathrm{K}) \le p \le 22.5\ \mathrm{MPa},$$
$$\text{where } p_\mathrm{s}(643.15\ \mathrm{K}) = 21.043\,367\,32\ \mathrm{MPa}$$

as given in Fig. 2.26.

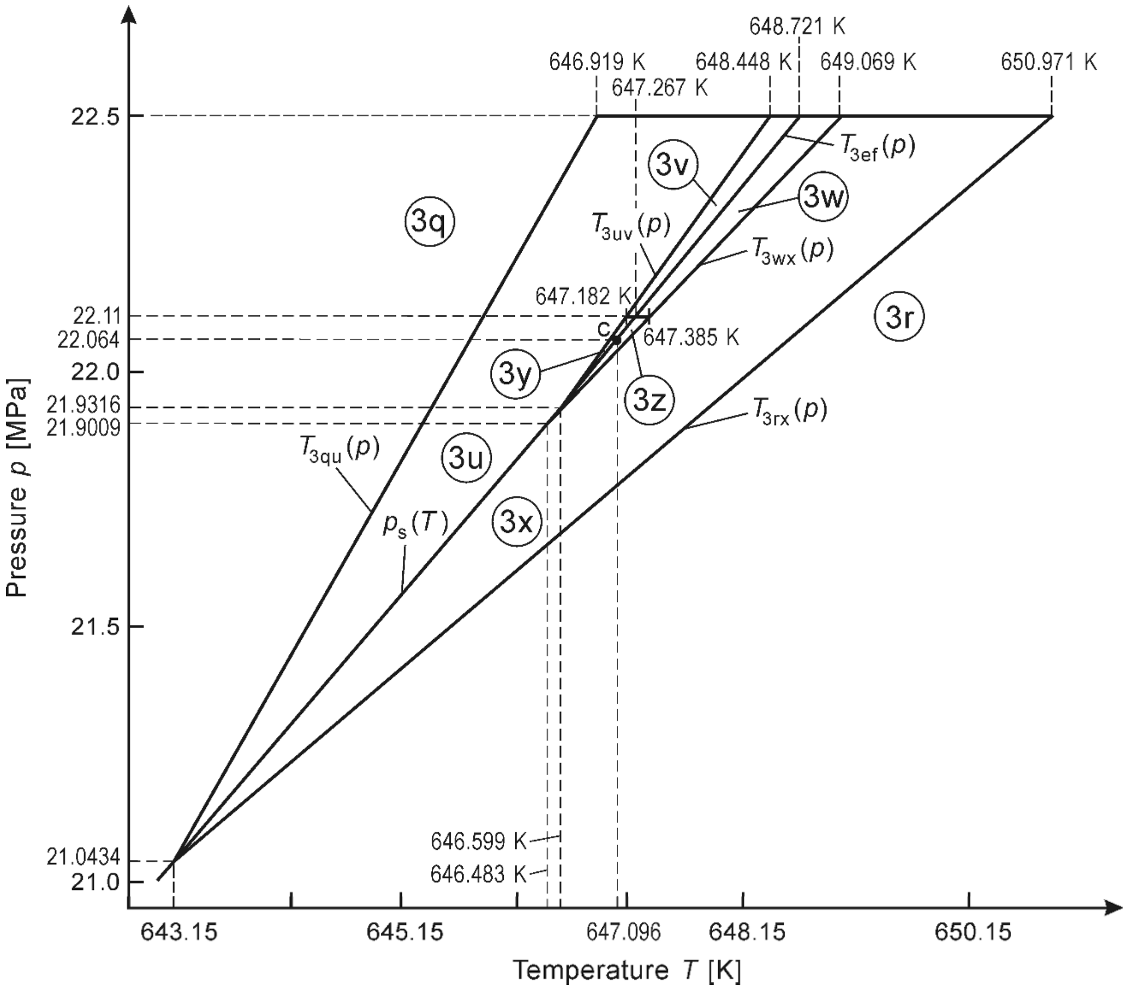

Fig. 2.26 Division of the near-critical region into subregions 3u to 3z for the auxiliary equations $v(p,T)$.

The subregion-boundary equation $T_{3uv}(p)$ has the form of Eq. (2.65) and the equation $T_{3wx}(p)$ has the form of Eq. (2.66). The coefficients n_i and the exponents I_i of these two subregion-boundary equations are listed in Table 2.126. The numerical information on the subregion-boundary equation $T_{3ef}(p)$ is given in Sec. 2.3.6.3.

Table 2.126 Coefficients and exponents of the subregion-boundary equations $T_{3uv}(p)$ and $T_{3wx}(p)$

Equation	i	I_i	n_i	i	I_i	n_i
$T_{3uv}(p)$	1	0	$0.528\,199\,646\,263\,062 \times 10^{3}$	3	2	$-0.222\,814\,134\,903\,755$
	2	1	$0.890\,579\,602\,135\,307 \times 10^{1}$	4	3	$0.286\,791\,682\,263\,697 \times 10^{-2}$
$T_{3wx}(p)$	1	0	$0.728\,052\,609\,145\,380 \times 10^{1}$	4	−1	$0.329\,196\,213\,998\,375 \times 10^{3}$
	2	1	$0.973\,505\,869\,861\,952 \times 10^{2}$	5	−2	$0.873\,371\,668\,682\,417 \times 10^{3}$
	3	2	$0.147\,370\,491\,183\,191 \times 10^{2}$			

The description of the use of the subregion-boundary equations is summarized in Table 2.127, where the subregion boundaries are shown in Fig. 2.26.

Table 2.127 Pressure ranges and corresponding subregion-boundary equations for determining the correct subregion, 3u to 3z, for the auxiliary equations $v(p,T)$

Subcritical pressure region $(p \le p_c)$

Temperature range	Pressure range	Sub-region	Temperature range
$T \le T_s(p)$ (liquid)	$p_s(0.00264\ \mathrm{m^3\,kg^{-1}})^a < p \le 22.064\ \mathrm{MPa}$	3u	$T_{3qu}(p) < T \le T_{3uv}(p)$
		3y	$T_{3uv}(p) < T$
	$p_s(643.15\ \mathrm{K}) < p \le p_s(0.00264\ \mathrm{m^3\,kg^{-1}})^a$	3u	$T_{3qu}(p) < T$
$T \ge T_s(p)$ (vapour)	$p_s(0.00385\ \mathrm{m^3\,kg^{-1}})^b < p \le 22.064\ \mathrm{MPa}$	3z	$T \le T_{3wx}(p)$
		3x	$T_{3wx}(p) < T \le T_{3rx}(p)$
	$p_s(643.15\ \mathrm{K}) < p \le p_s(0.00385\ \mathrm{m^3\,kg^{-1}})^b$	3x	$T \le T_{3rx}(p)$

Supercritical pressure region $(p > p_c)$

Pressure range	Sub-region	Temperature range	Sub-region	Temperature range
$22.064\ \mathrm{MPa} < p \le 22.11\ \mathrm{MPa}$	3u	$T_{3qu}(p) < T \le T_{3uv}(p)$	3y	$T_{3uv}(p) < T \le T_{3ef}(p)$
	3z	$T_{3ef}(p) < T \le T_{3wx}(p)$	3x	$T_{3wx}(p) < T \le T_{3rx}(p)$
$22.11\ \mathrm{MPa} < p \le 22.5\ \mathrm{MPa}$	3u	$T_{3qu}(p) < T \le T_{3uv}(p)$	3v	$T_{3uv}(p) < T \le T_{3ef}(p)$
	3w	$T_{3ef}(p) < T \le T_{3wx}(p)$	3x	$T_{3wx}(p) < T \le T_{3rx}(p)$

[a] $p_s(0.00264\ \mathrm{m^3\,kg^{-1}}) = 21.931\,615\,51\ \mathrm{MPa}$.

[b] $p_s(0.00385\ \mathrm{m^3\,kg^{-1}}) = 21.900\,962\,65\ \mathrm{MPa}$.

The **equation $T_{3uv}(p)$** approximates the isochore $v = 0.00264\ \mathrm{m^3\,kg^{-1}}$ from $p = p_s(0.00264\ \mathrm{m^3\,kg^{-1}}) = 21.931\,615\,51\ \mathrm{MPa}$ to $p = 22.5\ \mathrm{MPa}$. This equation divides subregion 3u from subregions 3v and 3y.

The **equation $T_{3wx}(p)$** approximates the isochore $v = 0.00385\ \mathrm{m^3\,kg^{-1}}$ from $p = p_s(0.00385\ \mathrm{m^3\,kg^{-1}}) = 21.900\,962\,65\ \mathrm{MPa}$ to $p = 22.5\ \mathrm{MPa}$ and divides subregion 3x from subregions 3w and 3z.

The **equations $T_{3qu}(p)$, $T_{3ef}(p)$, and $T_{3rx}(p)$** are described in Sec. 2.3.6.3.

Computer-Program Verification. To assist the user in computer-program verification of the equations $T_{3uv}(p)$ and $T_{3wx}(p)$ for the subregion boundaries, Table 2.128 contains test values for calculated temperatures.

Table 2.128 Temperature values calculated from the subregion-boundary equations $T_{3uv}(p)$ and $T_{3wx}(p)$ for selected pressures [a]

Equation	p [MPa]	T [K]
$T_{3uv}(p)$	22.3	$6.477\,996\,121 \times 10^2$
$T_{3wx}(p)$	22.3	$6.482\,049\,480 \times 10^2$

[a] Programmed functions should be verified using 8 byte real values for all variables.

b) Auxiliary Equations $v(p,T)$ for Subregions 3u to 3z

The auxiliary equations $v(p,T)$ for subregions 3u to 3z have the dimensionless form of Eq. (2.68). The reducing quantities v^*, p^*, and T^*, the number of coefficients N, the non-linear parameters a and b, and the exponents c, d, and e are listed in Table 2.129. The coefficients n_i and exponents I_i and J_i are given in Tables 2.132 to 2.137 that are given in Sec. 2.3.6.5c.

Table 2.129 Reducing quantities v^*, p^*, and T^*, number of coefficients N, non-linear parameters a and b, and exponents c, d, and e of the auxiliary equations $v(p,T)$, Eq. (2.68), of subregions 3u to 3z

Subregion	v^*[m^3 kg^{-1}]	p^*[MPa]	T^*[K]	N	a	b	c	d	e
3u	0.0026	23	650	38	0.902	0.988	1	1	1
3v	0.0031	23	650	39	0.960	0.995	1	1	1
3w	0.0039	23	650	35	0.959	0.995	1	1	4
3x	0.0049	23	650	36	0.910	0.988	1	1	1
3y	0.0031	22	650	20	0.996	0.994	1	1	4
3z	0.0038	22	650	23	0.993	0.994	1	1	4

Computer-Program Verification. To assist the user in computer-program verification of the auxiliary equations $v(p,T)$, Eq. (2.68), for subregions 3u to 3z, Table 2.130 contains test values for calculated specific volumes.

Table 2.130 Values of the specific volume calculated from the auxiliary equations $v(p,T)$, Eq. (2.68), for subregions 3u to 3z [a]

Equation	p[MPa]	T[K]	v [m^3 kg^{-1}]	Equation	p[MPa]	T[K]	v [m^3 kg^{-1}]
$v_{3u}(p,T)$	21.5	644.6	$2.268\,366\,647 \times 10^{-3}$	$v_{3x}(p,T)$	22.11	648.0	$4.528\,072\,649 \times 10^{-3}$
	22.0	646.1	$2.296\,350\,553 \times 10^{-3}$		22.3	649.0	$4.556\,905\,799 \times 10^{-3}$
$v_{3v}(p,T)$	22.5	648.6	$2.832\,373\,260 \times 10^{-3}$	$v_{3y}(p,T)$	22.0	646.84	$2.698\,354\,719 \times 10^{-3}$
	22.3	647.9	$2.811\,424\,405 \times 10^{-3}$		22.064	647.05	$2.717\,655\,648 \times 10^{-3}$
$v_{3w}(p,T)$	22.15	647.5	$3.694\,032\,281 \times 10^{-3}$	$v_{3z}(p,T)$	22.0	646.89	$3.798\,732\,962 \times 10^{-3}$
	22.3	648.1	$3.622\,226\,305 \times 10^{-3}$		22.064	647.15	$3.701\,940\,010 \times 10^{-3}$

[a] Programmed functions should be verified using 8 byte real values for all variables.

Numerical Consistencies. The numerical inconsistencies between the auxiliary equations $v(p,T)$, Eq. (2.68), for subregions 3u to 3z and the basic equation $f_3(\rho,T)$, Eq. (2.11), are listed in Table 2.131. This table shows that the maximum inconsistencies in specific volume between these equations are less than 0.1%. Only in a small region at pressures between 21.9 MPa and 22.11 MPa, see Fig. 2.26, do the maximum inconsistencies between the auxiliary equations and the basic equation $f_3(\rho,T)$ approach nearly 2%.

Table 2.131 Maximum and root-mean-square inconsistencies in specific volume between the auxiliary equations $v(p,T)$ for subregions 3u to 3z and the basic equation $f_3(\rho,T)$, Eq. (2.11)

Subregion	$\lvert\Delta v/v\rvert$ [%] max	RMS	Subregion	$\lvert\Delta v/v\rvert$ [%] max	RMS
3u	0.097	0.058	3x	0.090	0.050
3v	0.082	0.040	3y	1.77	1.04
3w	0.065	0.023	3z	1.80	0.921

The maximum inconsistencies in specific volume between the auxiliary equations $v(p,T)$ of adjacent subregions along subregion boundaries are as follows: Along subregion boundaries that are isobars, the inconsistencies are less than 0.1% for all subregions except for the subregion boundaries between subregions 3v/3y and 3w/3z, where the inconsistencies amount to 1.7%. Along subregion boundaries defined by the subregion-boundary equations given in Sec. 2.3.6.5a, the inconsistencies are also less than 0.1% except for the boundaries between subregions 3u/3v and 3u/3y (equation $T_{3\mathrm{uv}}(p)$), 3y/3z (equation $T_{3\mathrm{ef}}(p)$), and 3z/3x (equation $T_{3\mathrm{wx}}(p)$), where the inconsistencies amount to 0.14%, 1.8%, 3.5%, and 1.8%, respectively. Further details are given in Tables 15 and 16 of the IAPWS supplementary release [25].

Calculation of Properties with the Help of the Auxiliary Equations $v(p,T)$. In order to calculate the thermodynamic properties in the range very close to the critical point with the help of the auxiliary equations $v(p,T)$ for regions 3u to 3t, the description given in Sec. 2.3.6.4b for the backward equations $v(p,T)$ can be applied analogously to the auxiliary equations $v(p,T)$.

Application of the Auxiliary Equations $v(p,T)$. In comparison with the backward equations $v(p,T)$, the corresponding numerical consistency of the auxiliary equations $v(p,T)$ for the range very close to the critical point is clearly worse. Nevertheless, for many applications, this consistency is satisfactory.

c) Coefficients and Exponents of the Auxiliary Equations $v(p,T)$ for Subregions 3u to 3z

This section contains Tables 2.132 to 2.137 with the coefficients and exponents of the auxiliary equations $v(p,T)$ for subregions 3u to 3z given in Sec. 2.3.6.5b.

Table 2.132 Coefficients and exponents of the auxiliary equation $v_{3\mathrm{u}}(p,T)$ for subregion 3u

i	I_i	J_i	n_i	i	I_i	J_i	n_i
1	−12	14	$0.122\,088\,349\,258\,355 \times 10^{18}$	19	1	−2	$0.105\,581\,745\,346\,187 \times 10^{-2}$
2	−10	10	$0.104\,216\,468\,608\,488 \times 10^{10}$	21	2	5	$-0.651\,903\,203\,602\,581 \times 10^{15}$
3	−10	12	$-0.882\,666\,931\,564\,652 \times 10^{16}$	22	2	10	$-0.160\,116\,813\,274\,676 \times 10^{25}$
4	−10	14	$0.259\,929\,510\,849\,499 \times 10^{20}$	23	3	−5	$-0.510\,254\,294\,237\,837 \times 10^{-8}$
5	−8	10	$0.222\,612\,779\,142\,211 \times 10^{15}$	24	5	−4	$-0.152\,355\,388\,953\,402$
6	−8	12	$-0.878\,473\,585\,050\,085 \times 10^{18}$	25	5	2	$0.677\,143\,292\,290\,144 \times 10^{12}$
7	−8	14	$-0.314\,432\,577\,551\,552 \times 10^{22}$	26	5	3	$0.276\,378\,438\,378\,930 \times 10^{15}$
8	−6	8	$-0.216\,934\,916\,996\,285 \times 10^{13}$	27	6	−5	$0.116\,862\,983\,141\,686 \times 10^{-1}$
9	−6	12	$0.159\,079\,648\,196\,849 \times 10^{21}$	28	6	2	$-0.301\,426\,947\,980\,171 \times 10^{14}$
10	−5	4	$-0.339\,567\,617\,303\,423 \times 10^{3}$	29	8	−8	$0.169\,719\,813\,884\,840 \times 10^{-7}$
11	−5	8	$0.884\,387\,651\,337\,836 \times 10^{13}$	30	8	8	$0.104\,674\,840\,020\,929 \times 10^{27}$
12	−5	12	$-0.843\,405\,926\,846\,418 \times 10^{21}$	31	10	−4	$-0.108\,016\,904\,560\,140 \times 10^{5}$
13	−3	2	$0.114\,178\,193\,518\,022 \times 10^{2}$	32	12	−12	$-0.990\,623\,601\,934\,295 \times 10^{-12}$
14	−1	−1	$-0.122\,708\,229\,235\,641 \times 10^{-3}$	33	12	−4	$0.536\,116\,483\,602\,738 \times 10^{7}$

Continued on next page.

Table 2.132 – Continued

i	I_i	J_i	n_i	i	I_i	J_i	n_i
15	−1	1	$-0.106\,201\,671\,767\,107 \times 10^{3}$	34	12	4	$0.226\,145\,963\,747\,881 \times 10^{22}$
16	−1	12	$0.903\,443\,213\,959\,313 \times 10^{25}$	35	14	−12	$-0.488\,731\,565\,776\,210 \times 10^{-9}$
17	−1	14	$-0.693\,996\,270\,370\,852 \times 10^{28}$	36	14	−10	$0.151\,001\,548\,880\,670 \times 10^{-4}$
18	0	−3	$0.648\,916\,718\,965\,575 \times 10^{-8}$	37	14	−6	$-0.227\,700\,464\,643\,920 \times 10^{5}$
19	0	1	$0.718\,957\,567\,127\,851 \times 10^{4}$	38	14	6	$-0.781\,754\,507\,698\,846 \times 10^{28}$

Table 2.133 Coefficients and exponents of the auxiliary equation $v_{3\mathrm{v}}(p,T)$ for subregion 3v

i	I_i	J_i	n_i	i	I_i	J_i	n_i
1	−10	−8	$-0.415\,652\,812\,061\,591 \times 10^{-54}$	21	−3	12	$0.742\,705\,723\,302\,738 \times 10^{27}$
2	−8	−12	$0.177\,441\,742\,924\,043 \times 10^{-60}$	22	−2	2	$-0.517\,429\,682\,450\,605 \times 10^{2}$
3	−6	−12	$-0.357\,078\,668\,203\,377 \times 10^{-54}$	23	−2	4	$0.820\,612\,048\,645\,469 \times 10^{7}$
4	−6	−3	$0.359\,252\,213\,604\,114 \times 10^{-25}$	24	−1	−2	$-0.188\,214\,882\,341\,448 \times 10^{-8}$
5	−6	5	$-0.259\,123\,736\,380\,269 \times 10^{2}$	25	−1	0	$0.184\,587\,261\,114\,837 \times 10^{-1}$
6	−6	6	$0.594\,619\,766\,193\,460 \times 10^{5}$	26	0	−2	$-0.135\,830\,407\,782\,663 \times 10^{-5}$
7	−6	8	$-0.624\,184\,007\,103\,158 \times 10^{11}$	27	0	6	$-0.723\,681\,885\,626\,348 \times 10^{17}$
8	−6	10	$0.313\,080\,299\,915\,944 \times 10^{17}$	28	0	10	$-0.223\,449\,194\,054\,124 \times 10^{27}$
9	−5	1	$0.105\,006\,446\,192\,036 \times 10^{-8}$	29	1	−12	$-0.111\,526\,741\,826\,431 \times 10^{-34}$
10	−5	2	$-0.192\,824\,336\,984\,852 \times 10^{-5}$	30	1	−10	$0.276\,032\,601\,145\,151 \times 10^{-28}$
11	−5	6	$0.654\,144\,373\,749\,937 \times 10^{6}$	31	3	3	$0.134\,856\,491\,567\,853 \times 10^{15}$
12	−5	8	$0.513\,117\,462\,865\,044 \times 10^{13}$	32	4	−6	$0.652\,440\,293\,345\,860 \times 10^{-9}$
13	−5	10	$-0.697\,595\,750\,347\,391 \times 10^{19}$	33	4	3	$0.510\,655\,119\,774\,360 \times 10^{17}$
14	−5	14	$-0.103\,977\,184\,454\,767 \times 10^{29}$	34	4	10	$-0.468\,138\,358\,908\,732 \times 10^{32}$
15	−4	−12	$0.119\,563\,135\,540\,666 \times 10^{-47}$	35	5	2	$-0.760\,667\,491\,183\,279 \times 10^{16}$
16	−4	−10	$-0.436\,677\,034\,051\,655 \times 10^{-41}$	36	8	−12	$-0.417\,247\,986\,986\,821 \times 10^{-18}$
17	−4	−6	$0.926\,990\,036\,530\,639 \times 10^{-29}$	37	10	−2	$0.312\,545\,677\,756\,104 \times 10^{14}$
18	−4	10	$0.587\,793\,105\,620\,748 \times 10^{21}$	38	12	−3	$-0.100\,375\,333\,864\,186 \times 10^{15}$
19	−3	−3	$0.280\,375\,725\,094\,731 \times 10^{-17}$	39	14	1	$0.247\,761\,392\,329\,058 \times 10^{27}$
20	−3	10	$-0.192\,359\,972\,440\,634 \times 10^{23}$				

Table 2.134 Coefficients and exponents of the auxiliary equation $v_{3\mathrm{w}}(p,T)$ for subregion 3w

i	I_i	J_i	n_i	i	I_i	J_i	n_i
1	−12	8	$-0.586\,219\,133\,817\,016 \times 10^{-7}$	19	−1	−8	$0.237\,416\,732\,616\,644 \times 10^{-26}$
2	−12	14	$-0.894\,460\,355\,005\,526 \times 10^{11}$	20	−1	−4	$0.271\,700\,235\,739\,893 \times 10^{-14}$
3	−10	−1	$0.531\,168\,037\,519\,774 \times 10^{-30}$	21	−1	1	$-0.907\,886\,213\,483\,600 \times 10^{2}$
4	−10	8	$0.109\,892\,402\,329\,239$	22	0	−12	$-0.171\,242\,509\,570\,207 \times 10^{-36}$
5	−8	6	$-0.575\,368\,389\,425\,212 \times 10^{-1}$	23	0	1	$0.156\,792\,067\,854\,621 \times 10^{3}$
6	−8	8	$0.228\,276\,853\,990\,249 \times 10^{5}$	24	1	−1	$0.923\,261\,357\,901\,470$
7	−8	14	$-0.158\,548\,609\,655\,002 \times 10^{19}$	25	2	−1	$-0.597\,865\,988\,422\,577 \times 10^{1}$
8	−6	−4	$0.329\,865\,748\,576\,503 \times 10^{-27}$	26	2	2	$0.321\,988\,767\,636\,389 \times 10^{7}$
9	−6	−3	$-0.634\,987\,981\,190\,669 \times 10^{-24}$	27	3	−12	$-0.399\,441\,390\,042\,203 \times 10^{-29}$
10	−6	2	$0.615\,762\,068\,640\,611 \times 10^{-8}$	28	3	−5	$0.493\,429\,086\,046\,981 \times 10^{-7}$
11	−6	8	$-0.961\,109\,240\,985\,747 \times 10^{8}$	29	5	−10	$0.812\,036\,983\,370\,565 \times 10^{-19}$
12	−5	−10	$-0.406\,274\,286\,652\,625 \times 10^{-44}$	30	5	−8	$-0.207\,610\,284\,654\,137 \times 10^{-11}$
13	−4	−1	$-0.471\,103\,725\,498\,077 \times 10^{-12}$	31	5	−6	$-0.340\,821\,291\,419\,719 \times 10^{-6}$
14	−4	3	$0.725\,937\,724\,828\,145$	32	8	−12	$0.542\,000\,573\,372\,233 \times 10^{-17}$
15	−3	−10	$0.187\,768\,525\,763\,682 \times 10^{-38}$	33	8	−10	$-0.856\,711\,586\,510\,214 \times 10^{-12}$
16	−3	3	$-0.103\,308\,436\,323\,771 \times 10^{4}$	34	10	−12	$0.266\,170\,454\,405\,981 \times 10^{-13}$
17	−2	1	$-0.662\,552\,816\,342\,168 \times 10^{-1}$	35	10	−8	$0.858\,133\,791\,857\,099 \times 10^{-5}$
18	−2	2	$0.579\,514\,041\,765\,710 \times 10^{3}$				

Table 2.135 Coefficients and exponents of the auxiliary equation $v_{3x}(p, T)$ for subregion 3x

i	I_i	J_i	n_i	i	I_i	J_i	n_i
1	−8	14	$0.377\,373\,741\,298\,151 \times 10^{19}$	19	4	3	$0.397\,949\,001\,553\,184 \times 10^{14}$
2	−6	10	$-0.507\,100\,883\,722\,913 \times 10^{13}$	20	5	−6	$0.100\,824\,008\,584\,757 \times 10^{-6}$
3	−5	10	$-0.103\,363\,225\,598\,860 \times 10^{16}$	21	5	−2	$0.162\,234\,569\,738\,433 \times 10^{5}$
4	−4	1	$0.184\,790\,814\,320\,773 \times 10^{-5}$	22	5	1	$-0.432\,355\,225\,319\,745 \times 10^{11}$
5	−4	2	$-0.924\,729\,378\,390\,945 \times 10^{-3}$	23	6	1	$-0.592\,874\,245\,598\,610 \times 10^{12}$
6	−4	14	$-0.425\,999\,562\,292\,738 \times 10^{24}$	24	8	−6	$0.133\,061\,647\,281\,106 \times 10^{1}$
7	−3	−2	$-0.462\,307\,771\,873\,973 \times 10^{-12}$	25	8	−3	$0.157\,338\,197\,797\,544 \times 10^{7}$
8	−3	12	$0.107\,319\,065\,855\,767 \times 10^{22}$	26	8	1	$0.258\,189\,614\,270\,853 \times 10^{14}$
9	−1	5	$0.648\,662\,492\,280\,682 \times 10^{11}$	27	8	8	$0.262\,413\,209\,706\,358 \times 10^{25}$
10	0	0	$0.244\,200\,600\,688\,281 \times 10^{1}$	28	10	−8	$-0.920\,011\,937\,431\,142 \times 10^{-1}$
11	0	4	$-0.851\,535\,733\,484\,258 \times 10^{10}$	29	12	−10	$0.220\,213\,765\,905\,426 \times 10^{-2}$
12	0	10	$0.169\,894\,481\,433\,592 \times 10^{22}$	30	12	−8	$-0.110\,433\,759\,109\,547 \times 10^{2}$
13	1	−10	$0.215\,780\,222\,509\,020 \times 10^{-26}$	31	12	−5	$0.847\,004\,870\,612\,087 \times 10^{7}$
14	1	−1	$-0.320\,850\,551\,367\,334$	32	12	−4	$-0.592\,910\,695\,762\,536 \times 10^{9}$
15	2	6	$-0.382\,642\,448\,458\,610 \times 10^{17}$	33	14	−12	$-0.183\,027\,173\,269\,660 \times 10^{-4}$
16	3	−12	$-0.275\,386\,077\,674\,421 \times 10^{-28}$	34	14	−10	$0.181\,339\,603\,516\,302$
17	3	0	$-0.563\,199\,253\,391\,666 \times 10^{6}$	35	14	−8	$-0.119\,228\,759\,669\,889 \times 10^{4}$
18	3	8	$-0.326\,068\,646\,279\,314 \times 10^{21}$	36	14	−6	$0.430\,867\,658\,061\,468 \times 10^{7}$

Table 2.136 Coefficients and exponents of the auxiliary equation $v_{3y}(p, T)$ for subregion 3y

i	I_i	J_i	n_i	i	I_i	J_i	n_i
1	0	−3	$-0.525\,597\,995\,024\,633 \times 10^{-9}$	11	3	4	$0.705\,106\,224\,399\,834 \times 10^{21}$
2	0	1	$0.583\,441\,305\,228\,407 \times 10^{4}$	12	3	8	$-0.266\,713\,136\,106\,469 \times 10^{31}$
3	0	5	$-0.134\,778\,968\,457\,925 \times 10^{17}$	13	4	−6	$-0.145\,370\,512\,554\,562 \times 10^{-7}$
4	0	8	$0.118\,973\,500\,934\,212 \times 10^{26}$	14	4	6	$0.149\,333\,917\,053\,130 \times 10^{28}$
5	1	8	$-0.159\,096\,490\,904\,708 \times 10^{27}$	15	5	−2	$-0.149\,795\,620\,287\,641 \times 10^{8}$
6	2	−4	$-0.315\,839\,902\,302\,021 \times 10^{-6}$	16	5	1	$-0.381\,881\,906\,271\,100 \times 10^{16}$
7	2	−1	$0.496\,212\,197\,158\,239 \times 10^{3}$	17	8	−8	$0.724\,660\,165\,585\,797 \times 10^{-4}$
8	2	4	$0.327\,777\,227\,273\,171 \times 10^{19}$	18	8	−2	$-0.937\,808\,169\,550\,193 \times 10^{14}$
9	2	5	$-0.527\,114\,657\,850\,696 \times 10^{22}$	19	10	−5	$0.514\,411\,468\,376\,383 \times 10^{10}$
10	3	−8	$0.210\,017\,506\,281\,863 \times 10^{-16}$	20	12	−8	$-0.828\,198\,594\,040\,141 \times 10^{5}$

Table 2.137 Coefficients and exponents of the auxiliary equation $v_{3z}(p, T)$ for subregion 3z

i	I_i	J_i	n_i	i	I_i	J_i	n_i
1	−8	3	$0.244\,007\,892\,290\,650 \times 10^{-10}$	13	0	3	$0.328\,380\,587\,890\,663 \times 10^{12}$
2	−6	6	$-0.463\,057\,430\,331\,242 \times 10^{7}$	14	1	1	$-0.625\,004\,791\,171\,543 \times 10^{8}$
3	−5	6	$0.728\,803\,274\,777\,712 \times 10^{10}$	15	2	6	$0.803\,197\,957\,462\,023 \times 10^{21}$
4	−5	8	$0.327\,776\,302\,858\,856 \times 10^{16}$	16	3	−6	$-0.204\,397\,011\,338\,353 \times 10^{-10}$
5	−4	5	$-0.110\,598\,170\,118\,409 \times 10^{10}$	17	3	−2	$-0.378\,391\,047\,055\,938 \times 10^{4}$
6	−4	6	$-0.323\,899\,915\,729\,957 \times 10^{13}$	18	6	−6	$0.972\,876\,545\,938\,620 \times 10^{-2}$
7	−4	8	$0.923\,814\,007\,023\,245 \times 10^{16}$	19	6	−5	$0.154\,355\,721\,681\,459 \times 10^{2}$
8	−3	−2	$0.842\,250\,080\,413\,712 \times 10^{-12}$	20	6	−4	$-0.373\,962\,862\,928\,643 \times 10^{4}$
9	−3	5	$0.663\,221\,436\,245\,506 \times 10^{12}$	21	6	−1	$-0.682\,859\,011\,374\,572 \times 10^{11}$
10	−3	6	$-0.167\,170\,186\,672\,139 \times 10^{15}$	22	8	−8	$-0.248\,488\,015\,614\,543 \times 10^{-3}$
11	−2	2	$0.253\,749\,358\,701\,391 \times 10^{4}$	23	8	−4	$0.394\,536\,049\,497\,068 \times 10^{7}$
12	−1	−6	$-0.819\,731\,559\,610\,523 \times 10^{-20}$				

2.3.7 Summarizing Statements on the Calculation Speed when Using Backward and Region-Boundary Equations

The decisive argument for the development of backward equations and region-boundary equations was the reduction of computing time needed to calculate thermodynamic properties in process modelling. When using only the basic equations described in Sec. 2.2, time-consuming iterations such as one- or two-dimensional Newton methods are required for calculating properties as a function of the input variables that are not the independent variables of the basic equations. This section summarizes statements on the computing speed when using backward equations and region-boundary equations in comparison with iterative calculations using only the basic equations.

The test calculations were carried out for IAPWS by Miyagawa [19] with a Pentium 4/3.0 GHz PC using the Microsoft Windows XP operating system. The algorithms were programmed in Fortran 77 and compiled using Microsoft PowerStation 4.0 with default options.

The computing time was measured by means of a test program similar to the benchmark program NIFBENCH [15] developed by IAPWS for the determination of the calculation speed of IAPWS-IF97 in comparison with the previous industrial formulation IFC-67 [1]. The basic equations, backward equations, and region-boundary equations were programmed using series of additions and multiplications as given in the Horner algorithm in order to perform the computation as quickly as possible.

The Newton method was used for performing the iterations. The derivatives of the basic equations needed for the Newton method were formed analytically. As starting points for these iterations, single fixed values were used. These values are located in the centres of the respective region, subregion, or region boundary. Starting values defined in this way are called single fixed values in the following.

2.3.7.1 Computing-Time Ratios for Calculations with Basic Equations via Iterations in Comparison with the Use of Backward and Region-Boundary Equations

In order to express how many times the calculations with the backward equations are faster than the iterative calculations with the basic equations, the quantity Computing-Time Ratio (*CTR*) was defined by the following relation:

$$CTR = \frac{\text{Computing time of the iterative calculation with the basic equations}}{\text{Computing time of the calculation with the backward or region-boundary equations}} \qquad (2.70)$$

These *CTR* values were determined as ratios when the missing value(s) for the independent variable(s) of the IAPWS-IF97 basic equations are calculated one time from the respective basic equation via iteration and the other time directly from the corresponding backward equation(s) and (if necessary) backward function(s). Single fixed values, see above, were selected as starting values for the iterations, and the permissible values for the numerical consistency given in Sec. 2.3.2 were used as iteration accuracies in the iterations with the basic equations.

Table 2.135 summarizes the *CTR* values obtained for the given input variables (p,h), (p,s), (h,s), and (p,T). The calculations with the backward equations are between 10 and 46 times faster than the iterative calculations with the basic equations alone.

Table 2.135 Computing-time ratios (*CTR*) obtained from calculating the missing independent variable(s) of the IAPWS-IF97 basic equations for the given input variables (p,h), (p,s), (h,s), and (p,T), one time from iteration with the basic equations and the other time directly from the backward equations and backward functions; the definition of the *CTR* value is given in Eq. (2.70)

Input variables	Region	Used backward equations and backward functions	*CTR*
(p,h)	1	$T_1(p,h)$	25
	2	$T_2(p,h)$	11
	3	$T_3(p,h)$ and $v_3(p,h)$	14
(p,s)	1	$T_1(p,s)$	38
	2	$T_2(p,s)$	14
	3	$T_3(p,s)$ and $v_3(p,s)$	14
(h,s)	1	$p_1(h,s)$ and $T_1(h,s)^{\mathrm{a}}$	35
	2	$p_2(h,s)$ and $T_2(h,s)^{\mathrm{a}}$	46
	3	$p_3(h,s)$ and $T_3(h,s)^{\mathrm{a}}$ and $v_3(h,s)^{\mathrm{a}}$	10
	4	$T_{\mathrm{s}}(h,s)$ and $p_{\mathrm{s}}(h,s)^{\mathrm{a}}$ and $x(h,s)^{\mathrm{a}}$	14[b]
(p,T)	3	$v_3(p,T)$	17

[a] Backward function.

[b] This *CTR* value differs from that given in [19], because it also includes the computing time for the calculation of $x(h,s)$.

When using only the basic equations in connection with the input variables (p,h), (p,s), or (h,s), the region boundaries can only be calculated by iterating the corresponding basic equation. These boundaries are listed in Table 2.136. In order to avoid such time-consuming iterations, there are corresponding region-boundary equations that are also listed in Table 2.136 and numerically described in Secs. 2.3.3.1d, 2.3.4.1d, and 2.3.5.2. Table 2.136 summarizes the *CTR* values for the calculations with the basic equations (via iteration) and directly with the region-boundary equations. The calculations using the respective region-boundary equation are between 7 and 128 times faster than the iterations.

In conclusion, the comparisons show that calculations with backward equations, backward functions, and region-boundary equations are between 12 and 50 times faster than calculations with the basic equations via iterations. These factors result from the *CTR* values for the backward equations and backward functions of Table 2.135 and contain the fast determination of the respective region with the region-boundary equations shown in Table 2.136.

Table 2.136 Computing-time ratios when calculating the region boundaries one time from the basic equations via iteration and the other time directly from the region-boundary equations; the definition of the *CTR* value is given in Eq. (2.70)

Input variables	Boundary	Boundary between regions	Region-boundary equation	*CTR*
(p,h)	$x=0$ $x=1$	3 and 4	$p_{s,3}(h)$	31
(p,s)	$x=0$ $x=1$	3 and 4	$p_{s,3}(s)$	50
(h,s)	$x=0$	1 and 4	$h'_1(s)$	39
		3 and 4	$h'_{3a}(s)$	128[a]
	$x=1$	2 and 4	$h''_{2ab}(s)$, $h''_{2c3b}(s)$	22
		3 and 4	$h''_{2c3b}(s)$	118[a]
	623.15 K	1 and 3	$h_{B13}(s)$	19
	$p_{B23}(T)$	2 and 3	$T_{B23}(h,s)$ and $p_{2c}(h,s)$	7

[a] These *CTR* values differ from that given in [19], because the iterative calculation of $h'(s)$ and $h''(s)$ for region 3 was performed in a different manner.

Taking into account the frequency of use for the various combination of variables in process modelling, the calculations of heat-cycles, boilers, and particularly of steam turbines can be expected to be 2 to 3 times faster when using the backward equations and region-boundary equations.

2.3.7.2 Computing-Time Ratios for Iterations with Basic Equations Using Single Fixed Values or Values from Backward Equations as Starting Points

For applications where the demands on numerical consistency are extremely high, iterations with the basic equations might be necessary. These iterations can be carried out with two different starting values, namely single fixed values (as described at the beginning of Sec. 2.3.7) and values calculated from the backward equations. In order to compare the computing times of the two ways of calculating the starting values for the iterations, computing-time ratios are determined by the following relation:

$$CTR = \frac{\text{Computing time for the iteration with the single fixed values as starting values}}{\text{Computing time for the iteration with starting values from the backward equations}} \tag{2.71}$$

Table 2.137 shows how much faster the iterations with the basic equations are when values from backward equations are used to provide starting values for the iterations instead of using single fixed values. In this comparison, the relative iteration accuracy was set to 10^{-6} as it is usually used for such iterations. The achieved *CTR* factors between 1.5 and 4.4 show that the time to reach convergence of the iteration is clearly reduced when backward equations are used for the calculation of starting values. On average, the iterative calculations will be two times faster when using values from backward equations as starting points in comparison when using single fixed values in the centre of the respective region or of the subregion boundary.

Table 2.137 Computing-time ratios for calculations with the basic equations using single fixed values as starting values for the iterations in comparison with starting values from backward equations; the definition of the *CTR* values is given in Eq. (2.71)

Input variables	Region	Used backward equations and backward functions	*CTR* [b]
(p,h)	1	$T_1(p,h)$	2.0
	2	$T_2(p,h)$	2.0
	3	$T_3(p,h)$ and $v_3(p,h)$	1.8
(p,s)	1	$T_1(p,s)$	2.1
	2	$T_2(p,s)$	2.0
	3	$T_3(p,s)$ and $v_3(p,s)$	1.7
(h,s)	1	$p_1(h,s)$ and $T_1(h,s)$[a]	2.1
	2	$p_2(h,s)$ and $T_2(h,s)$[a]	4.4
	3	$p_3(h,s)$ and $T_3(h,s)$[a] and $v_3(h,s)$ [a]	1.5
	4	$T_s(h,s)$ and $p_s(h,s)$[a] and $x(h,s)$ [a]	1.9
(p,T)	3	$v_3(p,T)$	3.1

[a] Backward function.
[b] These *CTR* values were determined by K. Miyagawa for IAPWS (personal communication, 2006).

2.4 Partial Derivatives of Thermodynamic Properties Using IAPWS-IF97

Partial derivatives of thermodynamic properties of water and steam are required for solving equation systems in heat cycle, boiler, and turbine calculations and particularly for modelling non-stationary processes. When using the basic equations of IAPWS-IF97, all of the first and second partial derivatives of various properties can be calculated with high accuracy. The formulas for the determination of the general partial derivatives

$$\left(\frac{\partial z}{\partial x}\right)_y (p,T) \quad \text{based on the basic equations for regions 1, 2, and 5, and}$$

$$\left(\frac{\partial z}{\partial x}\right)_y (v,T) \quad \text{based on the basic equation for region 3}$$

are given in Sec. 2.4.1 and Sec. 2.4.2, respectively. The variables x, y, and z can represent any thermodynamic property. In this section, formulas are given for the properties pressure p, temperature T, and the specific properties volume v, internal energy u, enthalpy h, entropy s, Gibbs free energy g, and Helmholtz free energy f.

The algorithms are also given in the IAPWS Advisory Note No. 3 “Calculation of Thermodynamic Derivatives for Water and Steam from the IAPWS Formulations” [26]. The basic method and additional details for determining any thermodynamic derivative can be found in [27].

The application of the method will be described in Sec. 2.4.3 by means of two examples. The calculation of any derivative by using the tables in Part B or the interactive program "IAPWS-IF97 Electronic Steam Tables" in Part D of this book will be described in Sec. 2.4.4.

2.4.1 Partial Derivatives Based on the Basic Equations for Regions 1, 2, and 5

The general expression for the determination of any partial derivative $(\partial z/\partial x)_y$ from an equation of state as a function of pressure p and temperature T has the form

$$\left(\frac{\partial z}{\partial x}\right)_y = \frac{\left(\frac{\partial z}{\partial p}\right)_T \left(\frac{\partial y}{\partial T}\right)_p - \left(\frac{\partial z}{\partial T}\right)_p \left(\frac{\partial y}{\partial p}\right)_T}{\left(\frac{\partial x}{\partial p}\right)_T \left(\frac{\partial y}{\partial T}\right)_p - \left(\frac{\partial x}{\partial T}\right)_p \left(\frac{\partial y}{\partial p}\right)_T} \; . \tag{2.72}$$

The variables x, y, and z can represent any thermodynamic property. Table 2.138 summarizes the formulas for calculating the partial derivatives of the properties p, T, v, u, h, s, g, and f with respect to p and T that are needed in Eq. (2.72). For example, for the variable $z = v$, the expression $(\partial z/\partial p)_T$ means $(\partial v/\partial p)_T$ which is equal to $-v\,\kappa_T$ according to Table 2.138. In addition to the values of the parameters p and T, values of the five quantities specific volume v, specific entropy s, specific isobaric heat capacity c_p, isobaric cubic expansion coefficient α_v, and isothermal compressibility κ_T are required. These quantities contain the first and second derivatives of the Gibbs free energy g with respect to p at constant T and vice versa. Depending on the region in which the given values of p and T are located, these five quantities can be calculated from the IAPWS-IF97 basic equations for regions 1, 2, 2 (metastable), or 5, namely $g_1(p,T)$, $g_2(p,T)$, $g_{2,\mathrm{meta}}(p,T)$, or $g_5(p,T)$ corresponding to Eqs. (2.3), (2.6), (2.9), or (2.15).

Table 2.138 Derivatives of x, y, and z with respect to p at constant T and vice versa, where x, y, and z can be any of the quantities p, T, v, u, h, s, g, or f

x, y, z	$\left(\frac{\partial x}{\partial T}\right)_p, \left(\frac{\partial y}{\partial T}\right)_p, \left(\frac{\partial z}{\partial T}\right)_p$	$\left(\frac{\partial x}{\partial p}\right)_T, \left(\frac{\partial y}{\partial p}\right)_T, \left(\frac{\partial z}{\partial p}\right)_T$
p	0	1
T	1	0
v	$v\alpha_v$	$-v\kappa_T$
u	$c_p - p v \alpha_v$	$v(p\kappa_T - T\alpha_v)$
h	c_p	$v(1 - T\alpha_v)$
s	c_p/T	$-v\alpha_v$
g	$-s$	v
f	$-p v \alpha_v - s$	$p v \kappa_T$

2.4.2 Partial Derivatives Based on the Basic Equation for Region 3

The general expression for the determination of any partial derivative $(\partial z/\partial x)_y$ from an equation of state as a function of the specific volume v and temperature T reads:

$$\left(\frac{\partial z}{\partial x}\right)_y = \frac{\left(\frac{\partial z}{\partial v}\right)_T \left(\frac{\partial y}{\partial T}\right)_v - \left(\frac{\partial z}{\partial T}\right)_v \left(\frac{\partial y}{\partial v}\right)_T}{\left(\frac{\partial x}{\partial v}\right)_T \left(\frac{\partial y}{\partial T}\right)_v - \left(\frac{\partial x}{\partial T}\right)_v \left(\frac{\partial y}{\partial v}\right)_T} \tag{2.73}$$

The variables x, y, and z can represent any thermodynamic property. Table 2.139 contains formulas to calculate the partial derivatives of the properties p, T, v, u, h, s, g, and f with respect to v and T that are needed in Eq. (2.73). In addition to the values of the variables v and T, the values of the five quantities pressure p, specific entropy s, specific isochoric heat capacity c_v, relative pressure coefficient α_p, and isothermal stress coefficient β_p are required. These quantities contain the first and second derivatives of the Helmholtz free energy f with respect to v at constant T and vice versa. For the values given for v and T, the five quantities p, s, c_v, α_p, and β_p are calculated from the IAPWS-IF97 basic equation for region 3, $f_3(\rho,T)$, Eq. (2.11), with $\rho = 1/v$.

Table 2.139 Derivatives of x, y, and z with respect to v at constant T and vice versa, where x, y, and z can be any of the quantities p, T, v, u, h, s, g, or f

x, y, z	$\left(\frac{\partial x}{\partial v}\right)_T, \left(\frac{\partial y}{\partial v}\right)_T, \left(\frac{\partial z}{\partial v}\right)_T$	$\left(\frac{\partial x}{\partial T}\right)_v, \left(\frac{\partial y}{\partial T}\right)_v, \left(\frac{\partial z}{\partial T}\right)_v$
p	$-p\beta_p$	$p\alpha_p$
T	0	1
v	1	0
u	$p(T\alpha_p - 1)$	c_v
h	$p(T\alpha_p - v\beta_p)$	$c_v + pv\alpha_p$
s	$p\alpha_p$	c_v/T
g	$-pv\beta_p$	$pv\alpha_p - s$
f	$-p$	$-s$

2.4.3 Examples for Deriving Any Partial Derivative from the Basic Equations

As examples, the partial derivative $(\partial u/\partial p)_v$ is to be derived from a basic equation $g(p,T)$ for regions 1, 2, 2 (metastable), and 5 and from the basic equation $f_3(\rho,T)$ of region 3.

2.4.3.1 Example for Deriving the Partial Derivative $(\partial u/\partial p)_v$ for Regions 1, 2, and 5

Since the basic equations for regions 1, 2, 2 (metastable), and 5 are fundamental equations of the Gibbs free energy $g(p,T)$, Eq. (2.72) and Table 2.138 have to be used for forming the corresponding partial derivative. The comparison of the required partial derivative $(\partial u/\partial p)_v$

with the general expression for the partial derivative according to Eq. (2.72) results in $z = u$, $x = p$, and $y = v$. With these assignments, Eq. (2.72) reads formally:

$$\left(\frac{\partial u}{\partial p}\right)_v = \frac{\left(\frac{\partial u}{\partial p}\right)_T \left(\frac{\partial v}{\partial T}\right)_p - \left(\frac{\partial u}{\partial T}\right)_p \left(\frac{\partial v}{\partial p}\right)_T}{\left(\frac{\partial p}{\partial p}\right)_T \left(\frac{\partial v}{\partial T}\right)_p - \left(\frac{\partial p}{\partial T}\right)_p \left(\frac{\partial v}{\partial p}\right)_T} \tag{2.74}$$

According to Table 2.138, the partial derivatives are:

$$\left(\frac{\partial u}{\partial p}\right)_T = v(p\,\kappa_T - T\,\alpha_v) \qquad \left(\frac{\partial v}{\partial T}\right)_p = v\,\alpha_v$$

$$\left(\frac{\partial u}{\partial T}\right)_p = c_p - p\,v\,\alpha_v \qquad \left(\frac{\partial v}{\partial p}\right)_T = -v\,\kappa_T \tag{2.75}$$

$$\left(\frac{\partial p}{\partial p}\right)_T = 1 \qquad \left(\frac{\partial p}{\partial T}\right)_p = 0$$

The insertion of these results into Eq. (2.74) yields

$$\left(\frac{\partial u}{\partial p}\right)_v = -v\,T\,\alpha_v + \frac{c_p\,\kappa_T}{\alpha_v} \; . \tag{2.76}$$

Depending on the given values for p and T, the properties v, c_p, α_v, and κ_T can be calculated from one of the basic equations $g(p,T)$ for regions 1, 2, 2 (metastable), or 5 corresponding to Eqs. (2.3), (2.6), (2.9), or (2.15), respectively. Other partial derivatives can be determined in an analogous way.

2.4.3.2 Example for the Derivation of the Partial Derivative $(\partial u/\partial p)_v$ for Region 3

Since the basic equation for region 3 is a fundamental equation of the Helmholtz free energy, $f_3(\rho,T)$, Eq. (2.73) and Table 2.139 have to be used for forming the corresponding partial derivative. The comparison of the needed partial derivative $(\partial u/\partial p)_v$ with the general expression for the partial derivative according to Eq. (2.73) results in $z = u$, $x = p$, and $y = v$. With these assignments, Eq. (2.73) reads formally:

$$\left(\frac{\partial u}{\partial p}\right)_v = \frac{\left(\frac{\partial u}{\partial v}\right)_T \left(\frac{\partial v}{\partial T}\right)_v - \left(\frac{\partial u}{\partial T}\right)_v \left(\frac{\partial v}{\partial v}\right)_T}{\left(\frac{\partial p}{\partial v}\right)_T \left(\frac{\partial v}{\partial T}\right)_v - \left(\frac{\partial p}{\partial T}\right)_v \left(\frac{\partial v}{\partial v}\right)_T} \tag{2.77}$$

According to Table 2.139, the partial derivatives are:

$$\left(\frac{\partial u}{\partial v}\right)_T = p\left(T\alpha_p - 1\right) \qquad \left(\frac{\partial v}{\partial T}\right)_v = 0$$
$$\left(\frac{\partial u}{\partial T}\right)_v = c_v \qquad \left(\frac{\partial v}{\partial v}\right)_T = 1 \tag{2.78}$$
$$\left(\frac{\partial p}{\partial v}\right)_T = -p\beta_p \qquad \left(\frac{\partial p}{\partial T}\right)_v = p\alpha_p$$

The insertion of these results into Eq. (2.77) yields

$$\left(\frac{\partial u}{\partial p}\right)_v = \frac{c_v}{p\alpha_p} \ . \tag{2.79}$$

For the given values for v and T, the properties p, c_v, and α_p are calculated from the basic equation $f_3(\rho, T)$, Eq. (2.11), for region 3. Other partial derivatives can be determined in an analogous way.

2.4.4 The Calculation of Any Partial Derivative Using the Tables in Part B or the Program "IAPWS-IF97 Electronic Steam Tables" in Part D

The tables in Part B of this book contain values for the thermodynamic properties specific volume v, specific entropy s, specific isobaric heat capacity c_p, isobaric cubic expansion coefficient α_v, and isothermal compressibility κ_T in pressure-temperature grids over the range of validity of IAPWS-IF97 except for the high-temperature region. These properties can also be calculated over the entire range of validity of IAPWS-IF97 including the high temperature region using the interactive program "IAPWS-IF97 Electronic Steam Tables" in Part D.

Since the properties v, s, c_p, α_v, and κ_T are tabulated and calculable, the following equation can be used for determining any partial derivative:

$$\left(\frac{\partial z}{\partial x}\right)_y = \frac{\left(\frac{\partial z}{\partial p}\right)_T \left(\frac{\partial y}{\partial T}\right)_p - \left(\frac{\partial z}{\partial T}\right)_p \left(\frac{\partial y}{\partial p}\right)_T}{\left(\frac{\partial x}{\partial p}\right)_T \left(\frac{\partial y}{\partial T}\right)_p - \left(\frac{\partial x}{\partial T}\right)_p \left(\frac{\partial y}{\partial p}\right)_T} \ . \tag{2.80}$$

In all of the partial derivatives, the variables x, y, z can represent any thermodynamic property. Table 2.140 comprises the formulas to calculate the partial derivatives of the properties pressure p, temperature T, specific volume v, specific internal energy u, specific enthalpy h, specific entropy s, specific Gibbs free energy g, and specific Helmholtz free energy f with respect to pressure p and temperature T that are needed in Eq. (2.80). For example, for the variable $z = v$, the expression $(\partial z/\partial p)_T$ means $(\partial v/\partial p)_T$, which is equal to $-v\,\kappa_T$ according to Table 2.140.

Table 2.140 Derivatives of x, y, and z with respect to p at constant T and vice versa, where x, y, and z can be any of the quantities p, T, v, u, h, s, g, or f

x, y, z	$\left(\frac{\partial x}{\partial T}\right)_p, \left(\frac{\partial y}{\partial T}\right)_p, \left(\frac{\partial z}{\partial T}\right)_p$	$\left(\frac{\partial x}{\partial p}\right)_T, \left(\frac{\partial y}{\partial p}\right)_T, \left(\frac{\partial z}{\partial p}\right)_T$
p	0	1
T	1	0
v	$v\alpha_v$	$-v\kappa_T$
u	$c_p - pv\alpha_v$	$v(p\kappa_T - T\alpha_v)$
h	c_p	$v(1 - T\alpha_v)$
s	c_p/T	$-v\alpha_v$
g	$-s$	v
f	$-pv\alpha_v - s$	$pv\kappa_T$

2.4.4.1 The Calculation of Any Partial Derivative Using the Tables in Part B

As described at the beginning of Sec. 2.4.4, Eq. (2.80) and Table 2.140 should be used for calculating any partial derivative from tabulated properties. For the single-phase region, values for v, s, and c_p needed in Table 2.140 are given in Table 3 in Part B, while values for α_v and κ_T can be taken from Tables 9 and 10 in Part B. For the saturated liquid or saturated vapour, Table 1 in Part B contains values for v, s, and c_p, while values for α_v and κ_T are given in Table 6 in Part B.

Example

The partial derivative $(\partial h/\partial s)_v$ is calculated for p = 300 bar and t = 400 °C.

The comparison of the needed derivative $(\partial h/\partial s)_v$ with Eq. (2.80) leads to the assignments $z = h$, $x = s$, and $y = v$. Based on these assignments, Eq. (2.80) results in

$$\left(\frac{\partial h}{\partial s}\right)_v = \frac{\left(\frac{\partial h}{\partial p}\right)_T \left(\frac{\partial v}{\partial T}\right)_p - \left(\frac{\partial h}{\partial T}\right)_p \left(\frac{\partial v}{\partial p}\right)_T}{\left(\frac{\partial s}{\partial p}\right)_T \left(\frac{\partial v}{\partial T}\right)_p - \left(\frac{\partial s}{\partial T}\right)_p \left(\frac{\partial v}{\partial p}\right)_T}. \tag{2.81}$$

The expressions for the partial derivatives in Eq. (2.81) are formed with the help of Table 2.140 and one obtains:

$$\begin{aligned} \left(\frac{\partial h}{\partial p}\right)_T &= v\left(1 - T\alpha_v\right) & \left(\frac{\partial v}{\partial T}\right)_p &= v\alpha_v \\ \left(\frac{\partial h}{\partial T}\right)_p &= c_p & \left(\frac{\partial v}{\partial p}\right)_T &= -v\kappa_T \\ \left(\frac{\partial s}{\partial p}\right)_T &= -v\alpha_v & \left(\frac{\partial s}{\partial T}\right)_p &= T^{-1}c_p \end{aligned} \tag{2.82}$$

Inserting these results into Eq. (2.81) yields the final equation for the calculation of the needed partial derivative

$$\left(\frac{\partial h}{\partial s}\right)_v = \frac{c_p\,\kappa_T + v\,\alpha_v\left(1 - T\,\alpha_v\right)}{T^{-1}\,c_p\,\kappa_T - v\,\alpha_v^2} \quad . \tag{2.83}$$

Now, the values for the quantities v, c_p, α_v, and κ_T for the given values for p and T are taken from Tables 3, 9, and 10 in Part B, namely:

Table 3: $v = 0.002\,796\,41\ \mathrm{m^3\,kg^{-1}}$, $c_p = 25.797\ \mathrm{kJ\,kg^{-1}\,K^{-1}}$

Table 9: $\alpha_v = 37\,835 \times 10^{-6}\ \mathrm{K^{-1}}$

Table 10: $\kappa_T = 120.34 \times 10^{-6}\ \mathrm{kPa^{-1}}$

Thus, the result for the partial derivative amounts to

$$\left(\frac{\partial h}{\partial s}\right)_v = 846.95\ \mathrm{K}.$$

Any other partial derivative can be determined using the printed tables in Part B in an analogous way.

2.4.4.2 The Calculation of Any Partial Derivative Using the Program "IAPWS-IF97 Electronic Steam Tables" in Part D

All quantities that are required for the calculation of any partial derivative can be precisely determined with the program on the CD "IAPWS-IF97 Electronic Steam Tables" accompanying the book as Part D. As described at the beginning of Sec. 2.4.4, Eq. (2.80) and Table 2.140 can be used to determine any partial derivative. For the single-phase region, the CD allows the calculation of the needed properties v, s, c_p, α_v, and κ_T as a function of p and T over the entire range of IAPWS-IF97 (including the high-temperature region 5). For the saturated liquid and saturated vapour, these properties can be calculated as a function of p or T.

Example

The partial derivative $(\partial h/\partial s)_v$ is calculated for $p = 200$ bar and $t = 600$ °C.

The comparison of the required derivative $(\partial h/\partial s)_v$ with Eq. (2.80) leads to the assignments $z = h$, $x = s$, and $y = v$. With these assignments, Eq. (2.80) results in Eq. (2.81). The partial derivatives in Eq. (2.81) can be obtained with the help of Table 2.140. Equation (2.82) yields the results for these partial derivatives. The insertion of these results into Eq. (2.81) leads to the final equation, Eq. (2.83), for the needed partial derivative, namely

$$\left(\frac{\partial h}{\partial s}\right)_v = \frac{c_p\,\kappa_T + v\,\alpha_v\left(1 - T\,\alpha_v\right)}{T^{-1}\,c_p\,\kappa_T - v\,\alpha_v^2} \, .$$

Now, the values for the quantities v, c_p, α_v, and κ_T for the given values of p and T can be calculated with the Electronic Steam Tables:

$$v = 0.018\,184\,403\ \mathrm{m^3\,kg^{-1}}$$
$$c_p = 2.781\,218\,2\ \mathrm{kJ\,kg^{-1}\,K^{-1}}$$
$$\alpha_v = 1.709\,976\,8 \times 10^{-3}\ \mathrm{K^{-1}}$$
$$\kappa_T = 55.595\,449 \times 10^{-6}\ \mathrm{kPa^{-1}}$$

Thus, the value for the partial derivative is

$$\left(\frac{\partial h}{\partial s}\right)_v = 1\,124.0875\ \mathrm{K}.$$

Other thermodynamic derivatives can be determined using the program "IAPWS-IF97 Electronic Steam Tables" in an analogous way.

2.5 Uncertainties of IAPWS-IF97

This section summarizes the uncertainties of the basic equations of the industrial formulation IAPWS-IF97 given in Sec. 2.2.

The uncertainties in specific volume, specific isobaric heat capacity, speed of sound, and saturation pressure are given in Sec. 2.5.1, while the uncertainties in specific enthalpy and in enthalpy differences are summarized in Sec. 2.5.2. Section 2.5.3 illustrates the high numerical consistency of the basic equations of IAPWS-IF97 along the region boundaries between regions 1 and 3, regions 2 and 3, and regions 2 and 5. The estimated uncertainties in these properties result from two contributions:

- Uncertainties of the scientific standard for the thermodynamic properties of water and steam, the IAPWS-95 formulation [8, 9] that computed the input values for the development of the basic equations of the industrial formulation IAPWS-IF97. The uncertainties of IAPWS-95 are mainly based on the estimated uncertainties of the selected experimental data for each of the properties [8, 9] that were used for the development of IAPWS-95.
- Deviations of IAPWS-IF97 from IAPWS-95 regarding the properties taken into consideration.

The uncertainties of IAPWS-IF97 for the various properties are given as tolerance values. As used here, "tolerance" means the range of possible values as judged by IAPWS, and no statistical significance can be attached to it.

2.5.1 Uncertainties in the Properties Specific Volume, Specific Isobaric Heat Capacity, Speed of Sound, and Saturation Pressure

In this section the uncertainties of IAPWS-IF97 in specific volume v, specific isobaric heat capacity c_p, speed of sound w, and saturation pressure p_s are presented. Based on our assessment, the uncertainty values given for these properties can be considered as estimates of a combined expanded uncertainty with a coverage factor of two corresponding to a confidence level of 95%.

The uncertainties in v, c_p, and w calculated from IAPWS-IF97 in the single-phase region are indicated in Figs. 2.27, 2.28, and 2.29. The uncertainty values for c_p and w, given in Figs. 2.28 and 2.29, increase drastically when approaching the critical point. The statement "no definitive uncertainty estimates possible" for temperatures above 1273 K is based on the fact that this range is beyond the range of validity of IAPWS-95 and the corresponding input values for IAPWS-IF97 were obtained by extrapolating IAPWS-95. Various tests of IAPWS-95 [8, 9] showed that these extrapolations yielded reasonable values.

The estimated uncertainties in the saturation pressure p_s calculated from the IAPWS-IF97 are given in Fig. 2.30.

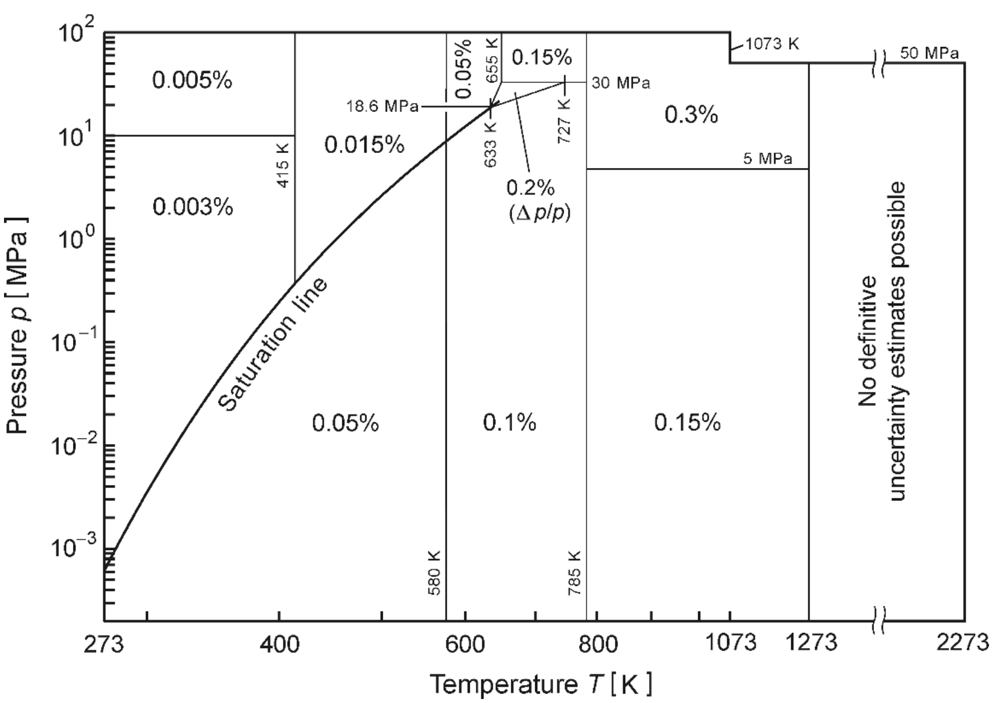

Fig. 2.27 Percentage uncertainties in specific volume estimated for the basic equations for regions 1 to 3 and 5 of IAPWS-IF97. In the enlarged critical region (triangle), the uncertainty is given as a percentage uncertainty in pressure, $\Delta p/p$. This region is bordered by the two isochores $0.0019\ \mathrm{m^3\,kg^{-1}}$ and $0.0069\ \mathrm{m^3\,kg^{-1}}$ and the given values of pressure and temperature. The positions of the lines separating the uncertainty regions are approximate.

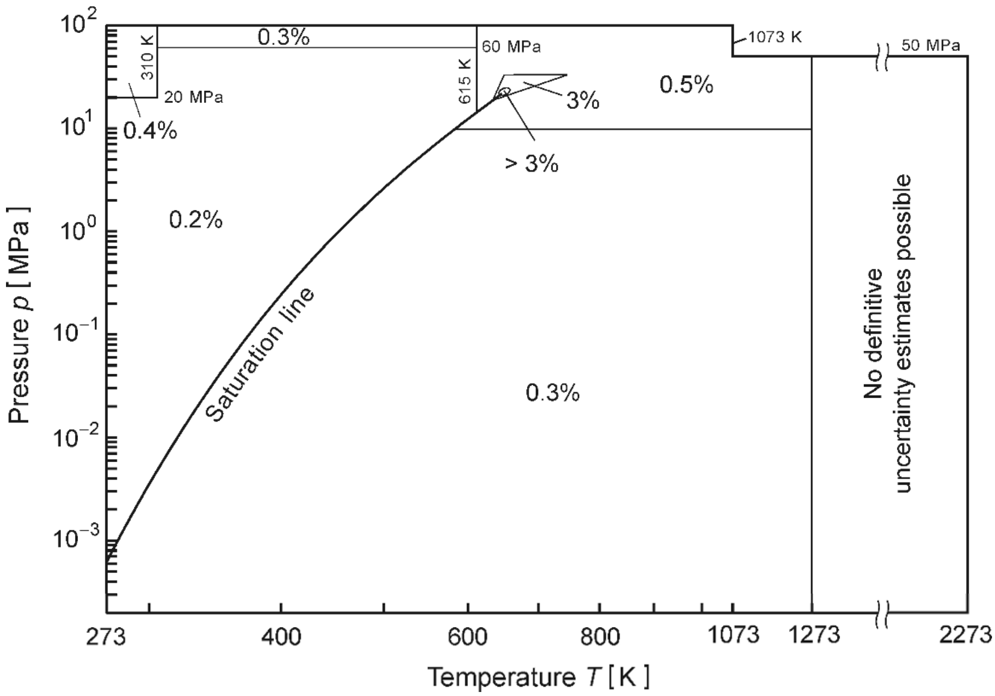

Fig. 2.28 Percentage uncertainties in specific isobaric heat capacity estimated for the basic equations for regions 1 to 3 and 5 of IAPWS-IF97. The definition of the triangle showing the enlarged critical region is given in Fig. 2.27. The positions of the lines separating the uncertainty regions are approximate.

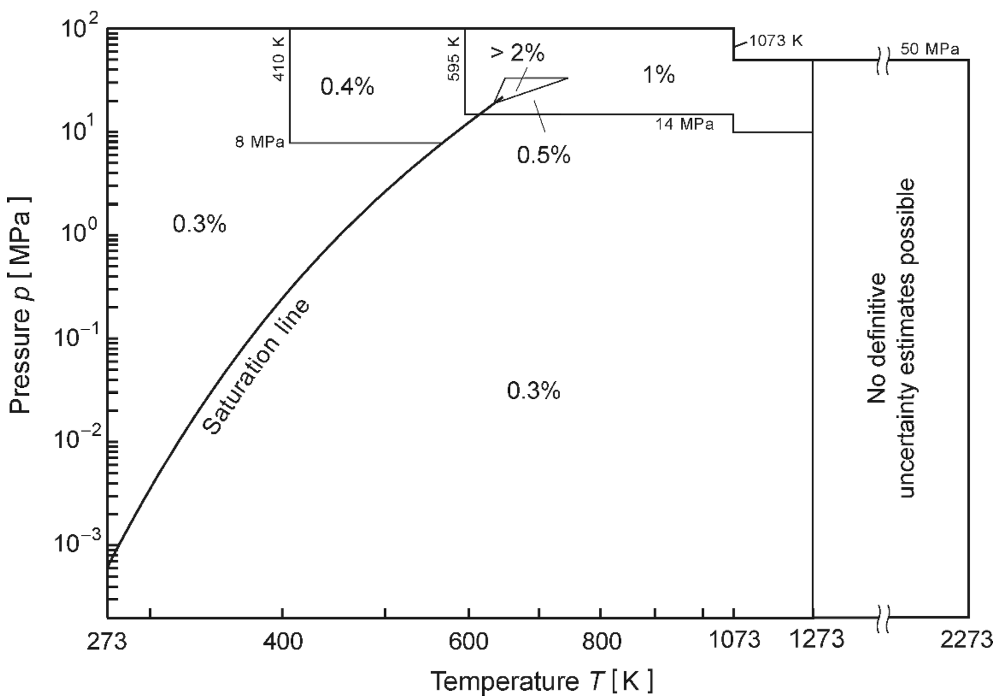

Fig. 2.29 Percentage uncertainties in speed of sound estimated for the basic equations for regions 1 to 3 and 5 of IAPWS-IF97. The definition of the triangle showing the enlarged critical region is given in Fig. 2.27. The positions of the lines separating the uncertainty regions are approximate.

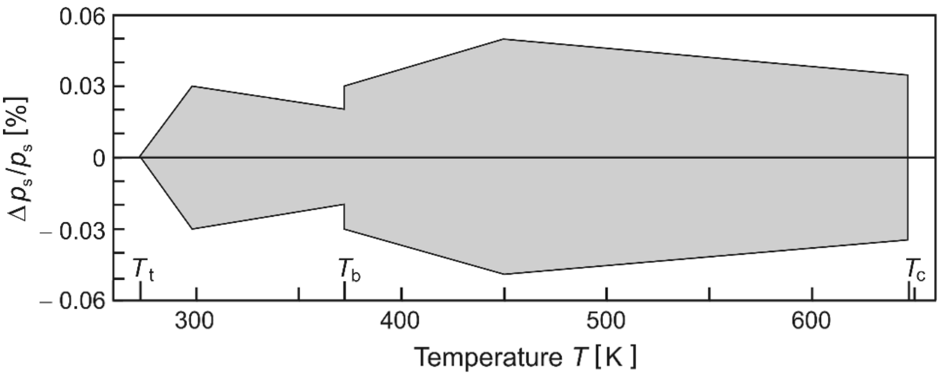

Fig. 2.30 Percentage uncertainties in saturation pressure estimated for the saturation-pressure equation, Eq. (2.13).

2.5.2 Uncertainties in the Properties Specific Enthalpy, Enthalpy Differences, and Enthalpy of Vaporization

When IAPWS-IF97 was adopted in 1997, estimates for the uncertainty in specific enthalpy calculated from IAPWS-IF97 were not given [9, 15]. However, modern procedures of acceptance tests on energy-conversion and power plants (e.g. VDI Guideline 2048 [28]) require values for the uncertainty in specific enthalpy of H_2O. Thus, corresponding uncertainty values were derived [29] and adopted by IAPWS as Advisory Note No. 1 [30]. This note presents the assumptions and further details for determining these uncertainty values.

Figure 2.31 shows the uncertainties in specific enthalpy calculated from the basic equations of the industrial formulation IAPWS-IF97. The procedure of estimating these uncertainties is described in [30]. The enthalpy values calculated from IAPWS-IF97 and from IAPWS-95 relate to the same enthalpy reference point given in Eq. (2.5).

For numerous technical applications, the uncertainty in enthalpy *differences* is needed. However, when calculating such uncertainties from the uncertainties of the enthalpies given in Fig. 2.31 (i.e. related to the enthalpy reference point of IAPWS-IF97), one obtains unrealistically large percentage uncertainties, particularly for relatively small enthalpy differences. Therefore, uncertainties in enthalpy differences were determined as described in [30]. Different sizes of enthalpy differences were calculated in different directions, namely along isobars, Δh_p, and differences in initial and final states corresponding to adiabatic reversible (isentropic) and adiabatic irreversible paths, Δh_{ad}, representing state paths in steam turbines, boiler feed pumps, and hydroturbines. Enthalpy differences between 10 kJ kg^{-1} and 1000 kJ kg^{-1} have been taken in consideration for the gas region, and between 1 kJ kg^{-1} and 10 kJ kg^{-1} for the liquid region. Apart from the uncertainties of isobaric enthalpy differences $\Delta(\Delta h_p)/\Delta h_p$ in the gas region for pressures up to 1 MPa, all of the other uncertainty values given do not significantly depend on the size of the enthalpy differences considered. As a result of all these comparisons, the estimated percentage uncertainties of enthalpy differences calculated from the basic equations of the industrial formulation IAPWS-IF97 are summarized in Figs. 2.32 and 2.33.

The uncertainty in the enthalpy of vaporization, Δh_{v}, given as the difference between the enthalpies of the saturated vapour and saturated liquid, $h'' - h'$, was also estimated as described in [30]. The results of estimating the uncertainties in enthalpy of vaporization in this way are shown in Fig. 2.34.

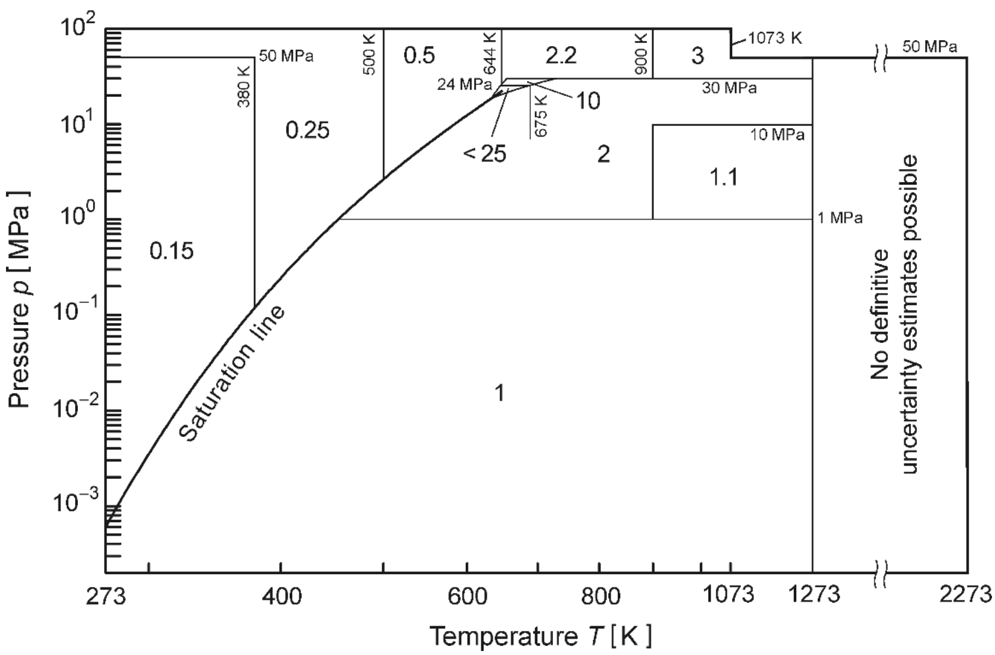

Fig. 2.31 Absolute uncertainties Δh in kJ kg^{-1} in specific enthalpy h estimated for the basic equations for regions 1 to 3 and 5 of IAPWS-IF97. The definition of the triangle showing the enlarged critical region is given in Fig. 2.27. The positions of the lines separating the uncertainty regions are approximate.

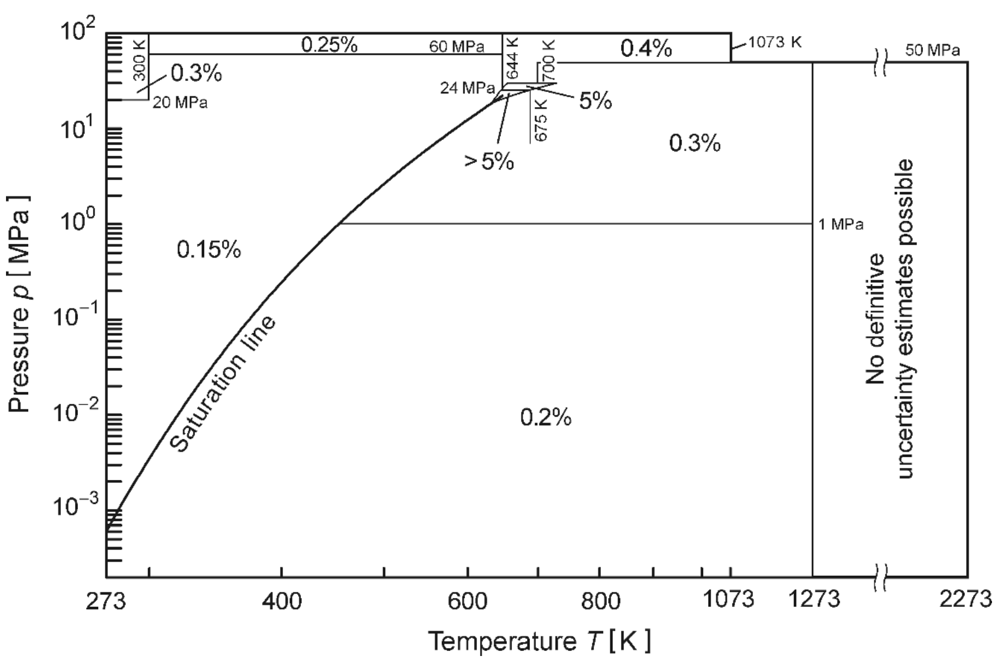

Fig. 2.32 Percentage uncertainties $\Delta(\Delta h_p)/\Delta h_p$ in *isobaric* enthalpy differences Δh_p estimated for the basic equations for regions 1 to 3 and 5 of IAPWS-IF97. In the gas region, the uncertainty values correspond to enthalpy differences of $10 \leq \Delta h_p/(\text{kJ kg}^{-1}) \leq 1000$. For isobaric enthalpy differences $\Delta h_p \geq 100$ kJ kg^{-1} and $p \leq 1$ MPa, the uncertainties are smaller than the values given, e.g. 0.15% for $\Delta h_p = 500$ kJ kg^{-1} and 0.1% for $\Delta h_p = 1000$ kJ kg^{-1}. In the liquid region, the uncertainty values correspond to enthalpy differences of $1 \leq \Delta h_p/(\text{kJ kg}^{-1}) \leq 10$. The definition of the triangle showing the enlarged critical region is given in Fig. 2.27. The positions of the lines separating the uncertainty regions are approximate.

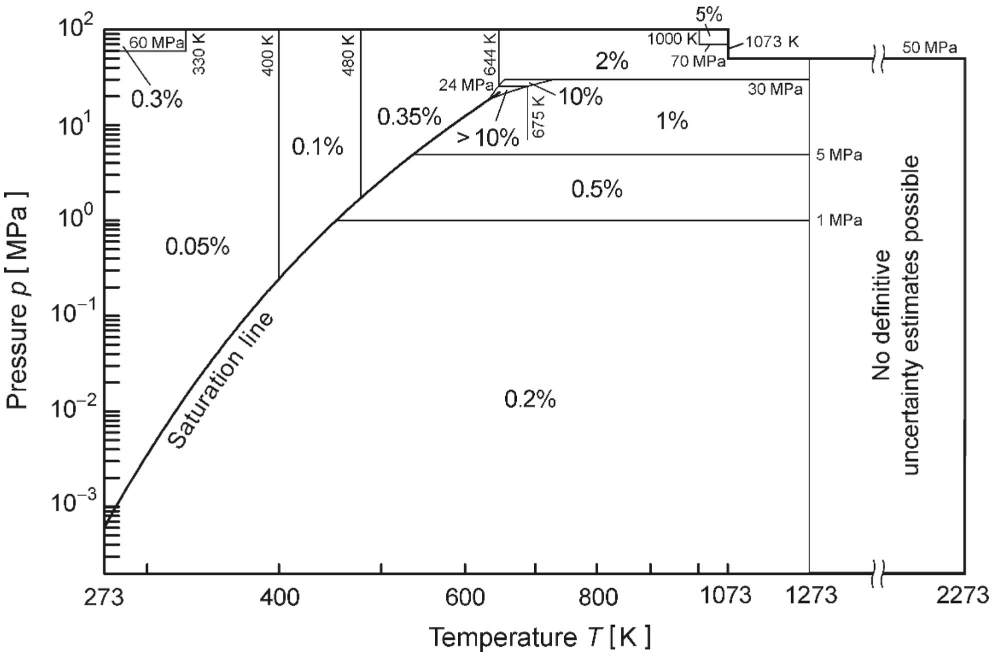

Fig. 2.33 Percentage uncertainties $\Delta(\Delta h_{ad})/\Delta h_{ad}$ in *adiabatic* enthalpy differences Δh_{ad} estimated for the basic equation for regions 1 to 3 and 5 of IAPWS-IF97. The uncertainty values given relate to enthalpy differences along adiabatic reversible (isentropic) and adiabatic irreversible paths (state paths in steam turbines, boiler feed pumps, and hydroturbines). In the gas region, the uncertainty values correspond to enthalpy differences of $10 \le \Delta h_{ad}/(\text{kJ kg}^{-1}) \le 1000$, whereas in the liquid region, the uncertainty values correspond to enthalpy differences of $1 \le \Delta h_{ad}/(\text{kJ kg}^{-1}) \le 10$. The definition of the triangle showing the enlarged critical region is given in Fig. 2.27. The positions of the lines separating the uncertainty regions are approximate.

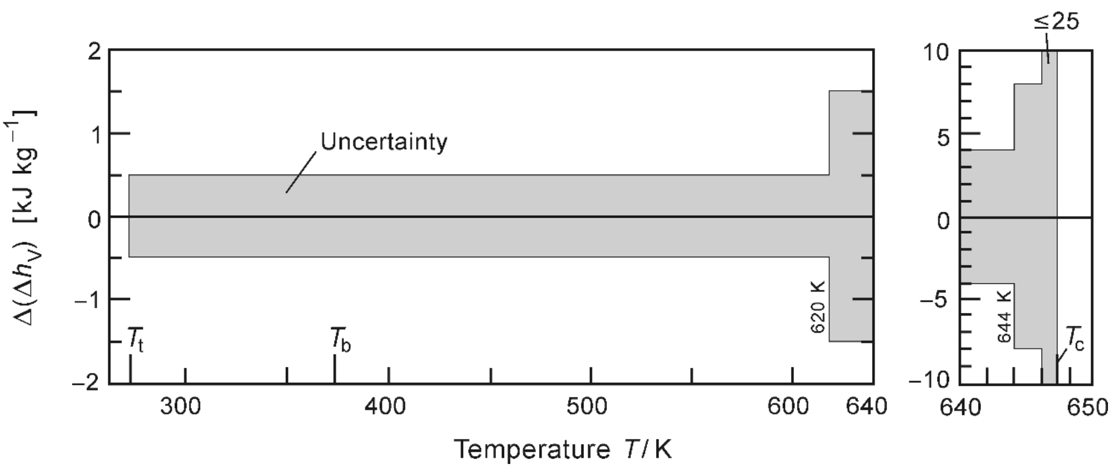

Fig. 2.34 Absolute uncertainties $\Delta(\Delta h_v)$ in enthalpy of vaporization Δh_v estimated for the basic equations for regions 1 to 3 and 5 of IAPWS-IF97. These uncertainty values only correspond to temperatures $273.15\text{ K} \le T \le 647\text{ K}$ ($T_c = 647.096$ K according to Eq. (1.4)).

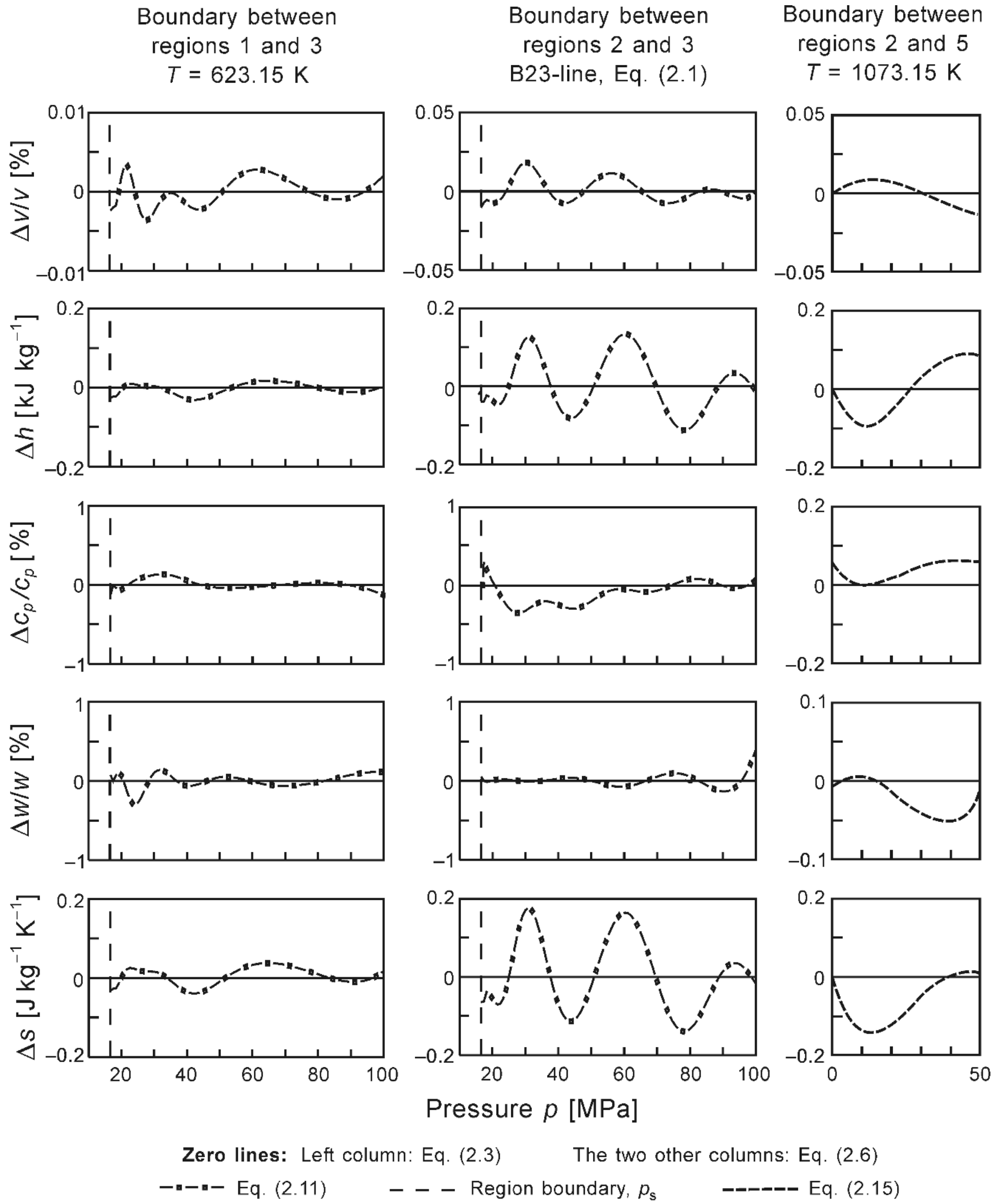

Fig. 2.35 Inconsistencies $\Delta v/v$ in specific volume, Δh in specific enthalpy, Δs in specific entropy, $\Delta c_p/c_p$ in specific isobaric heat capacity, and $\Delta w/w$ in speed of sound, along the boundary between regions 1 and 3 (left column), the boundary between regions 2 and 3 (middle column), and the boundary between regions 2 and 5 (right column).

2.5.3 Consistencies at Boundaries between Single-Phase Regions

Consistency investigations along the boundaries between the single-phase regions of IAPWS-IF97 were performed for the following basic equations and region boundaries as given in Fig. 2.2:

- Equations (2.3) and (2.11) along the 623.15 K isotherm for pressures of 16.53 MPa (corresponding to the saturation pressure p_s(623.15 K)) to 100 MPa. This part of the isotherm forms the boundary between regions 1 and 3.
- Equations (2.6) and (2.11) along the boundary between regions 2 and 3 defined by the equation $p_{B23}(T)$, Eq. (2.1), for temperatures between 623.15 K and 863.15 K.
- Equations (2.6) and (2.15) along the 1073.15 K isotherm for $p \leq 50$ MPa corresponding to the boundary between regions 2 and 5.

Figure 2.35, see the previous page, presents the results of these consistency investigations as percentage deviation diagrams for the properties v, c_p, and w and as absolute deviation diagrams for the properties h and s. The inconsistencies between the basic equations along the corresponding region boundaries are small enough to suffice for common technical applications.

3 Equations for Transport Properties and Other Properties

Aside from the development of international standard equations for the thermodynamic properties of water and steam, IAPWS has also initiated and coordinated the development of equations for transport properties and for other properties. The current IAPWS equations for the dynamic viscosity and thermal conductivity for industrial applications are presented in Secs. 3.1 and 3.2. The current IAPWS equations for the surface tension, dielectric constant, and refractive index are described in Secs. 3.3 to 3.5. The correlation equations for these properties (except for surface tension) contain density as one of the input variables. In order to calculate these properties for given values of pressure and temperature, the density must first be determined. For these density calculations, the equations for the dielectric constant and refractive index are based on the scientific formulation IAPWS-95 [8, 9] rather than the industrial formulation IAPWS-IF97. However, except for the near-critical region, differences in density calculations from IAPWS-95 and IAPWS-IF97 are negligibly small. Thus, for industrial applications, the input density for these equations for given values of pressure and temperature can be calculated from the corresponding basic equations of the industrial formulation IAPWS-IF97 described in Sec. 2.2. This procedure was applied to calculate the values for the transport properties and other properties listed in the tables in Part B of this book and for the calculation of these properties from the interactive program "IAPWS-IF97 Electronic Steam Tables" in Part D as well.

3.1 Equation for the Viscosity for Industrial Applications

The "Release on the IAPWS Formulation 2008 for the Viscosity of Ordinary Water Substances", which the presented correlation equation for the dynamic viscosity is based on, will be adopted at the IAPWS Meeting in 2008 [31]. This release replaces the release on the viscosity issued in 2003 [32]. A discussion of the background, development, and validation of this viscosity equation is presented in the background paper [33].

According to the IAPWS Release [31], the correlation equation for viscosity consists of three functions, which are multiplicatively connected. For industrial applications, the third function (called $\bar{\mu}_2$ in the release) may be set to unity. This function, the so-called critical enhancement, is only significant over a very small range around the critical point (for more details see below). Since the industrial use is the main focus of this book, only the first two functions are considered here.

The correlation equation for the dynamic viscosity η for industrial applications is given in dimensionless form, $\Psi = \eta/\eta^*$, and consists of the two functions Ψ_0 and Ψ_1 that are multiplied with each other. The equation reads

$$\frac{\eta(\rho,T)}{\eta^*} = \Psi(\delta,\theta) = \Psi_0(\theta)\cdot\Psi_1(\delta,\theta) \ , \tag{3.1}$$

where $\delta = \rho/\rho^*$ and $\theta = T/T^*$, with $\eta^* = 1\times10^{-6}$ Pa s, and Ψ_0 and Ψ_1 according to Eqs. (3.2) and (3.3). The first function of Eq. (3.1), $\Psi_0(\theta)$, represents the viscosity in the ideal-gas limit and has the form

$$\Psi_0(\theta) = \theta^{0.5}\left[\sum_{i=1}^{4} n_i^{\mathrm{o}}\,\theta^{1-i}\right]^{-1} \ , \tag{3.2}$$

where $\theta = T/T^*$ with $T^* = T_\mathrm{c} = 647.096$ K according to Eq. (1.4). The coefficients n_i^{o} are listed in Table 3.1. The equation for the second function of Eq. (3.1), $\Psi_1(\delta,\theta)$, reads

$$\Psi_1(\delta,\theta) = \exp\left[\delta\sum_{i=1}^{21} n_i\,(\delta-1)^{I_i}\left(\theta^{-1}-1\right)^{J_i}\right] , \tag{3.3}$$

where $\delta = \rho/\rho^*$ and $\theta = T^*/T$ with $\rho^* = \rho_\mathrm{c}$ and $T^* = T_\mathrm{c}$, where the critical density $\rho_\mathrm{c} = 322\ \mathrm{kg\,m^{-3}}$ and the critical temperature $T_\mathrm{c} = 647.096$ K according to Eqs. (1.6) and (1.4). Table 3.2 contains the coefficients n_i and exponents I_i and J_i of Eq. (3.3).

Table 3.1 Coefficients of Eq. (3.2)

i	n_i^{o}	i	n_i^{o}
1	$0.167\,752\times10^{-1}$	3	$0.636\,656\,4\times10^{-2}$
2	$0.220\,462\times10^{-1}$	4	$-0.241\,605\times10^{-2}$

Table 3.2 Coefficients and exponents of Eq. (3.3)

i	I_i	J_i	n_i	i	I_i	J_i	n_i
1	0	0	$0.520\,094$	12	2	2	$-0.772\,479$
2	0	1	$0.850\,895\times10^{-1}$	13	2	3	$-0.489\,837$
3	0	2	$-0.108\,374\times10^{1}$	14	2	4	$-0.257\,040$
4	0	3	$-0.289\,555$	15	3	0	$0.161\,913$
5	1	0	$0.222\,531$	16	3	1	$0.257\,399$
6	1	1	$0.999\,115$	17	4	0	$-0.325\,372\times10^{-1}$
7	1	2	$0.188\,797\times10^{1}$	18	4	3	$0.698\,452\times10^{-1}$
8	1	3	$0.126\,613\times10^{1}$	19	5	4	$0.872\,102\times10^{-2}$
9	1	5	$0.120\,573$	20	6	3	$-0.435\,673\times10^{-2}$
10	2	0	$-0.281\,378$	21	6	5	$-0.593\,264\times10^{-3}$
11	2	1	$-0.906\,851$				

If the dynamic viscosity is calculated from Eq. (3.1) for given values of *pressure* and temperature, then the input quantity reduced density δ has to be calculated first. According to the release [31], this density does not have to be calculated from the IAPWS-95 formulation [8, 9], but can also be determined from the IAPWS-IF97 basic equations, Eq. (2.3), (2.6), (2.11),

or (2.15), as described in Sec. 2.2. With this approach, the error is much smaller than the uncertainty of Eq. (3.1), as long as the state point given by the values for the input pressure and temperature is outside the near-critical region defined in the subpoint "Estimated Uncertainty" given below. Accordingly, the viscosity values listed in the corresponding tables in Part B and calculable with the Electronic Steam Tables in Part D are based on the density calculation from IAPWS-IF97.

Range of Validity. Figure 3.1 illustrates the range of validity of the viscosity equation for industrial applications, Eq. (3.1), in a p-T diagram.

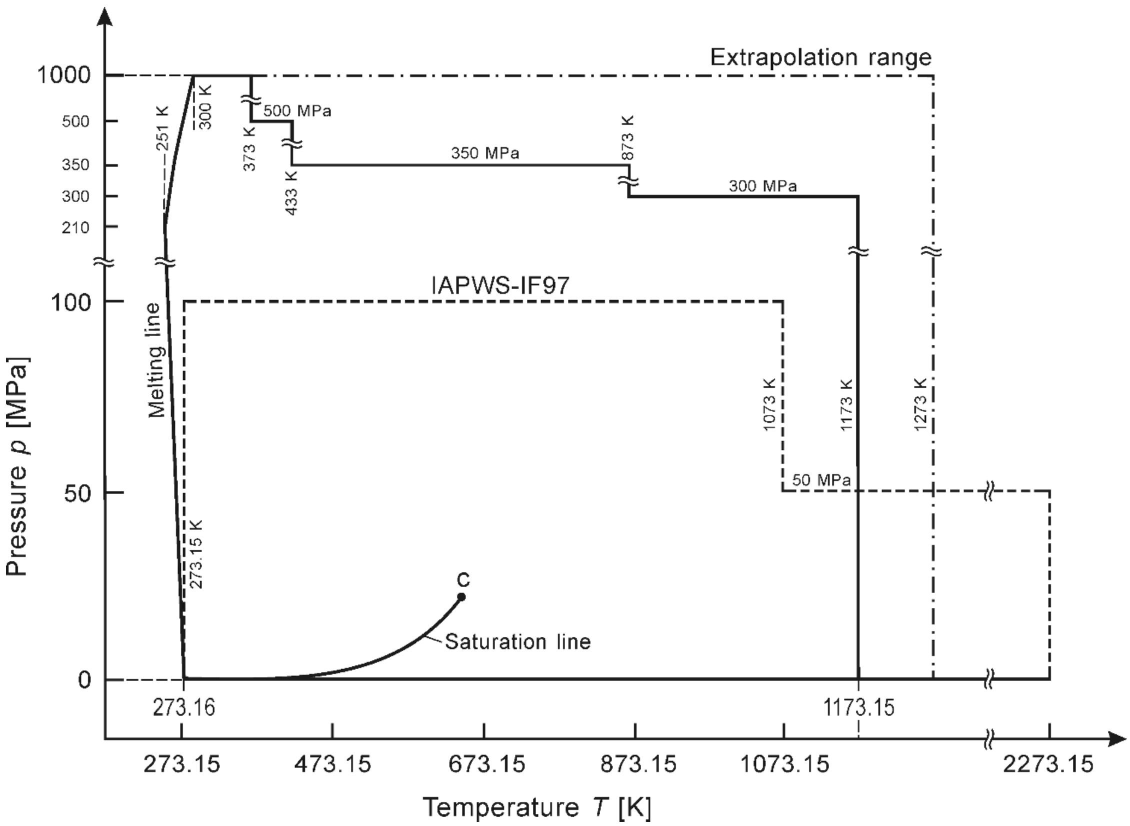

Fig. 3.1 Range of validity of the viscosity equation for industrial applications, Eq. (3.1); its extrapolation range is given by dashed-dotted lines. The validity range of IAPWS-IF97 shown by dashed lines is plotted for comparison.

The numerical definition of the range of validity of Eq. (3.1) is given by the following relations:

$$
\begin{array}{rclcrcl}
0 < & p & < p_t & \qquad & 273.16\ \mathrm{K} \le & T & \le 1173.15\ \mathrm{K} \\
p_t \le & p & \le 300\ \mathrm{MPa} & & T_m(p) \le & T & \le 1173.15\ \mathrm{K} \\
300\ \mathrm{MPa} < & p & \le 350\ \mathrm{MPa} & & T_m(p) \le & T & \le 873.15\ \mathrm{K} \\
350\ \mathrm{MPa} < & p & \le 500\ \mathrm{MPa} & & T_m(p) \le & T & \le 433.15\ \mathrm{K} \\
500\ \mathrm{MPa} < & p & \le 1000\ \mathrm{MPa} & & T_m(p) \le & T & \le 373.15\ \mathrm{K},
\end{array}
$$

where $p_t = 0.000\,611\,657$ MPa is the triple-point pressure according to Eq. (1.8), and T_m is the pressure dependent melting temperature [17]. Statements on the extrapolation capability of Eq. (3.1) are given in the release [31]. According to these statements, Eq. (3.1) behaves

reasonably when extrapolated to pressures up to 1000 MPa and temperatures up to 1273.15 K. On the low-temperature side, Eq. (3.1) can be used for pressures up to 0.101 325 MPa beginning with 273.15 K, because this temperature is only 0.01 K or less below the melting temperature $T_m(p)$. (For higher pressures up to 390 MPa, the melting temperature $T_m(p)$ is less than 273.15 K.) When the density is calculated for given values of pressure and temperature from IAPWS-IF97, Eq. (3.1) may only be used in the range of validity of IAPWS-IF97. Thus, for pressures up to 50 MPa, Eq. (3.1) can be also used for temperatures above 1073.15 K up to 1273.15 K, see also Fig. 3.1. Outside the IAPWS-IF97 range of validity, the scientific formulation IAPWS-95 [8, 9] should be used for the density calculation.

Computer-Program Verification. To assist the user in computer-program verification of Eq. (3.1), Table 3.3 contains corresponding test values.

Table 3.3 Dynamic viscosity values calculated from Eq. (3.1) for selected temperatures and pressures [a]

Property	T = 298.15 K p = 0.1 MPa	T = 873.15 K p = 20 MPa	T = 673.15 K p = 60 MPa
ρ [kg m^{-3}] (IAPWS-IF97)	$0.997\,047\,435 \times 10^{3}$	$0.549\,921\,814 \times 10^{2}$	$0.612\,391\,201 \times 10^{3}$ [b]
η [Pa s]	$0.890\,022\,551 \times 10^{-3}$	$0.339\,743\,835 \times 10^{-4}$	$0.726\,093\,560 \times 10^{-4}$

[a] Programmed functions should be verified using 8 byte real values for all variables.

[b] The density value of this test point, which is located in region 3 of IAPWS-IF97, was calculated from Eq. (2.11) via iteration.

Estimated Uncertainty. The uncertainties in viscosity calculated from Eq. (3.1) are summarized in Fig. 3.2; they can be considered as estimates of a combined expanded uncertainty with a coverage factor of two corresponding to a confidence level of 95%. The viscosity equation reproduces the ISO recommended value of the viscosity at 20 °C (293.15 K) and standard atmospheric pressure within the number of digits given in [34]; it also agrees with all values from 288.15 K to 313.15 K at atmospheric pressure in [34] within the stated uncertainty of 0.17% at 293.15 K.

The uncertainty value of 2%, also given in Fig. 3.2 for the near-critical region, only refers to the viscosity equation for scientific use that includes the critical-enhancement function according to Eqs. (14) to (21) in the release [31]. Due to the absence of the function for the critical enhancement in Eq. (3.1), in the near-critical region the uncertainty of the viscosity equation for industrial applications is greater than 2%. This near-critical region is defined by the following range of temperature and density:

$$645.91\ \mathrm{K} \le T \le 650.77\ \mathrm{K} \qquad 245.8\ \mathrm{kg\,m^{-3}} \le \rho \le 405.3\ \mathrm{kg\,m^{-3}},$$

see also Fig. 3.2.

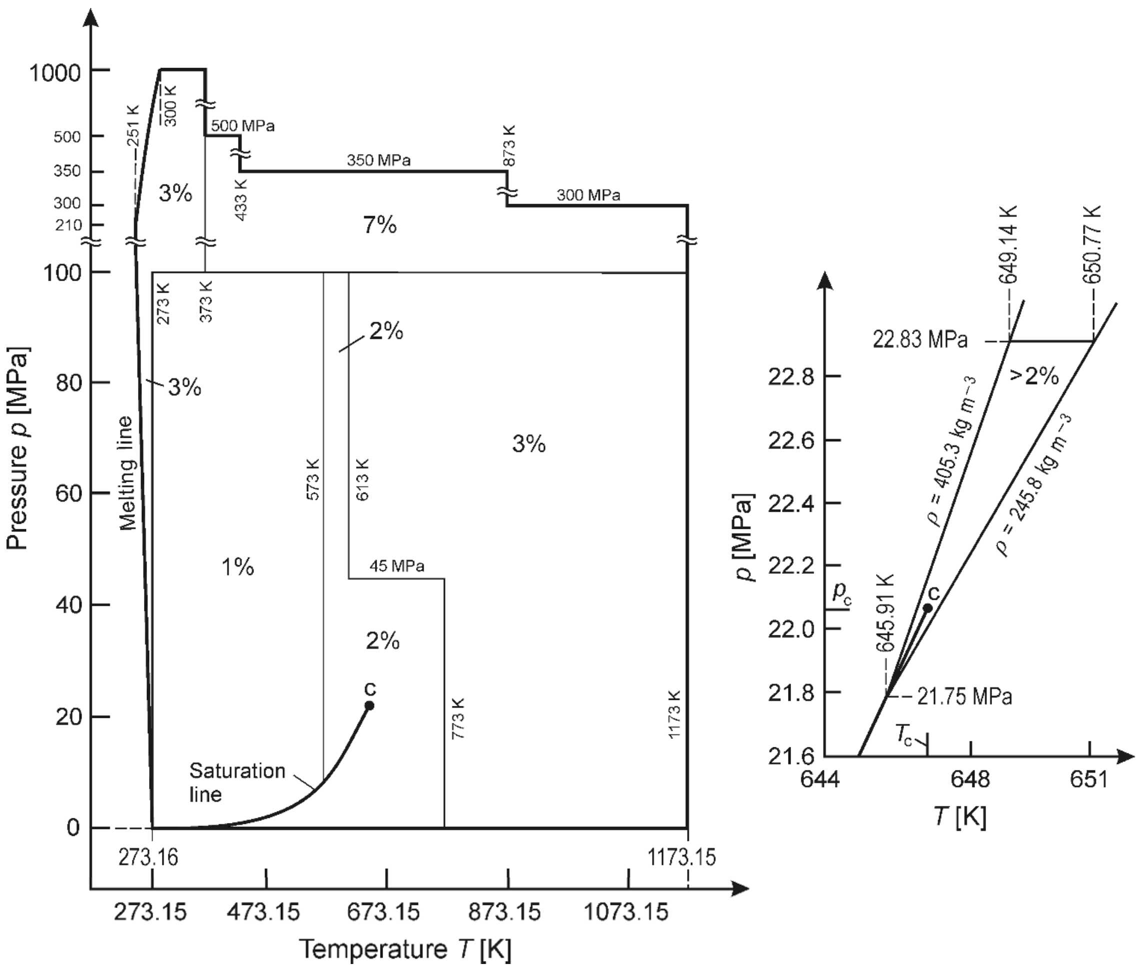

Fig. 3.2 Percentage uncertainties in viscosity estimated for the viscosity equation, Eq. (3.1). In the near-critical region, shown in the enlarged diagram on the right, the uncertainty of Eq. (3.1) is greater than 2%. The positions of the lines separating the uncertainty regions are approximate.

3.2 Equation for the Thermal Conductivity for Industrial Use

The correlation equation for the thermal conductivity for industrial use is based on the IAPWS "Revised Release on the IAPS Formulation 1985 for the Thermal Conductivity of Ordinary Water Substance," issued in 1998 [35].

According to this IAPWS Release [35], the correlation equation for the thermal conductivity λ for industrial use is given in dimensionless form, $\Lambda = \lambda/\lambda^*$, and consists of the sum of three functions. The equation reads

$$\frac{\lambda(\rho,T)}{\lambda^*} = \Lambda(\delta,\theta) = \Lambda_0(\theta) + \Lambda_1(\delta) + \Lambda_2(\delta,\theta) \ , \tag{3.4}$$

where $\delta = \rho/\rho^*$ and $\theta = T/T^*$, with $\lambda^* = 1\ \mathrm{W\ m^{-1}\ K^{-1}}$, and Λ_0, Λ_1, and Λ_2 according to Eqs. (3.5) to (3.7). The function $\Lambda_0(\theta)$ represents the thermal conductivity in the ideal-gas limit and has the form

$$\Lambda_0(\theta) = \theta^{0.5} \sum_{i=1}^{4} n_i^{\mathrm{o}} \, \theta^{i-1} \quad , \tag{3.5}$$

where $\theta = T/T^*$ with $T^* = 647.26$ K; the coefficients n_i^{o} are listed in Table 3.4. The correlation equation for the second function of Eq. (3.4), $\Lambda_1(\delta)$, reads

$$\Lambda_1(\delta) = n_1 + n_2\,\delta + n_3 \exp\left[n_4 \left(\delta + n_5\right)^2 \right] , \tag{3.6}$$

where $\delta = \rho/\rho^*$ and $\theta = T/T^*$ with $\rho^* = 317.7\ \mathrm{kg\,m^{-3}}$ and $T^* = 647.26$ K. The coefficients n_i are given in Table 3.5. The function $\Lambda_2(\delta,\theta)$ is defined by

$$\begin{aligned} \Lambda_2(\delta,\theta) = {} & \left(n_1 \theta^{-10} + n_2\right) \delta^{1.8} \exp\left[n_3 \left(1 - \delta^{2.8}\right)\right] \\ & + n_4\, A\, \delta^B \exp\left[\left(\frac{B}{1+B}\right)\left(1 - \delta^{1+B}\right)\right] \\ & + n_5 \exp\left[n_6\, \theta^{1.5} + n_7\, \delta^{-5}\right] , \end{aligned} \tag{3.7}$$

where $\delta = \rho/\rho^*$ and $\theta = T/T^*$ with $\rho^* = 317.7\ \mathrm{kg\,m^{-3}}$ and $T^* = 647.26$ K, and A and B according to Eqs. (3.7a) and (3.7b). The functions A and B have the form

$$A(\theta) = 2 + n_8 (\Delta\theta)^{-0.6} , \tag{3.7a}$$

$$B(\theta) = \begin{cases} (\Delta\theta)^{-1} & \text{for } \theta \ge 1 \\ n_9 (\Delta\theta)^{-0.6} & \text{for } \theta < 1 \end{cases} \tag{3.7b}$$

$$\text{with} \qquad \Delta\theta = \left|\theta - 1\right| + n_{10} . \tag{3.7c}$$

The coefficients n_i of Eqs. (3.7) and (3.7a) to (3.7c) are listed in Table 3.6.

Table 3.4 Coefficients of Eq. (3.5)

i	n_i^{o}	i	n_i^{o}
1	$0.102\,811 \times 10^{-1}$	3	$0.156\,146 \times 10^{-1}$
2	$0.299\,621 \times 10^{-1}$	4	$-0.422\,464 \times 10^{-2}$

Table 3.5 Coefficients of Eq. (3.6)

i	n_i	i	n_i
1	$-0.397\,070$	4	$-0.171\,587$
2	$0.400\,302$	5	$0.239\,219 \times 10^{1}$
3	$0.106\,000 \times 10^{1}$		

Table 3.6 Coefficients of Eqs. (3.7) and (3.7a) to (3.7c)

i	n_i	i	n_i
1	$0.701\,309 \times 10^{-1}$	6	$-0.411\,717 \times 10^{1}$
2	$0.118\,520 \times 10^{-1}$	7	$-0.617\,937 \times 10^{1}$
3	$0.642\,857$	8	$0.822\,994 \times 10^{-1}$
4	$0.169\,937 \times 10^{-2}$	9	$0.100\,932 \times 10^{2}$
5	$-0.102\,000 \times 10^{1}$	10	$0.308\,976 \times 10^{-2}$

If the thermal conductivity is calculated from Eq. (3.4) for given values of *pressure* and temperature, then the input quantity reduced density δ has to be calculated first. According to the release [35], this density is calculated from the IAPWS-IF97 basic equations, Eqs. (2.3), (2.6), or (2.11) as described in Sec. 2.2.

Range of Validity. IAPWS endorses the validity of Eq. (3.4) for the thermal conductivity for industrial use in the following range of pressures and temperatures:

$$0 < p \le 40\ \text{MPa} \qquad 273.15\ \text{K} \le T \le 1073.15\ \text{K}$$
$$40\ \text{MPa} < p \le 70\ \text{MPa} \qquad 273.15\ \text{K} \le T \le 923.15\ \text{K}$$
$$70\ \text{MPa} < p \le 100\ \text{MPa} \qquad 273.15\ \text{K} \le T \le 773.15\ \text{K}$$

The range of validity of Eq. (3.4), defined above, is illustrated in Fig. 3.3. For comparison, the range of validity of IAPWS-IF97 and the extrapolation range of Eq. (3.4), see below, are also shown.

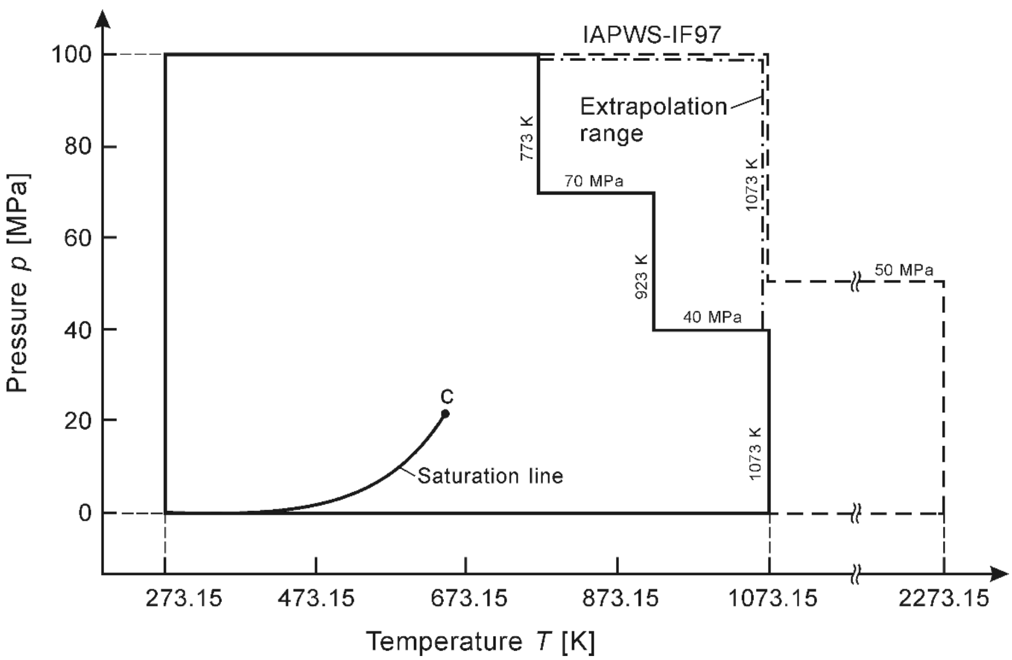

Fig. 3.3 Range of validity of the thermal-conductivity equation for industrial use, Eq. (3.4). The greater validity range of IAPWS-IF97 shown by the dashed lines is plotted for comparison. The extrapolation range of Eq. 3.4 is illustrated by the dashed-dotted line, see next page.

Figure 3.3 shows that the thermal-conductivity equation for industrial use, Eq. (3.4), covers the temperature range of the main part of IAPWS-IF97 (regions 1 to 4, temperatures up to 1073.15 K) only for pressures up to 40 MPa. For higher pressures, the temperature range of

Eq. (3.4) is limited to 923.15 K for pressures between 40 MPa and 70 MPa, and to 773.15 K for pressures between 70 MPa and 100 MPa.

However, if somewhat greater margins of error are tolerable, Eq. (3.4) can be extrapolated up to 1073.15 K for pressures up to 100 MPa. In order to give an impression of the error caused by such an extrapolation, Fig. 3.4 shows the differences between the thermal-conductivity equation for industrial use, Eq. (3.4), and the λ equation for scientific use [35][22] which covers the entire pressure and temperature range of IAPWS-IF97. It can be seen that for $T = 1073.15$ K, the thermal conductivity calculated with Eq. (3.4) deviates from the values obtained with the scientific equation by up to about 9% (e.g. at 70 MPa). However, this difference should be viewed with the perspective that even within the range of validity of Eq. (3.4) the differences in the λ values from the equation for scientific use reach up to about 5% (e.g. at 50 MPa).

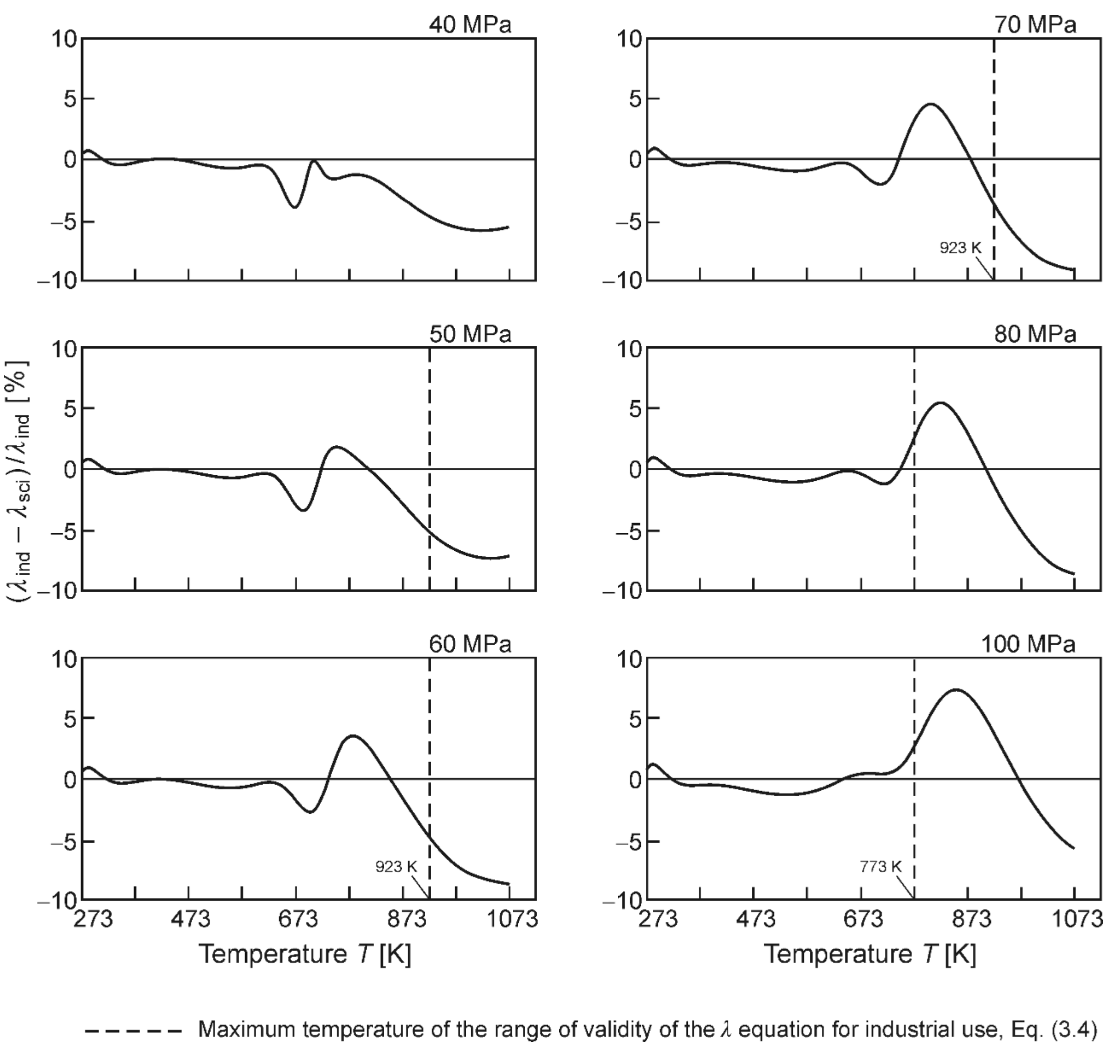

Fig. 3.4 Percentage differences between values for the thermal conductivity λ calculated from the equation for industrial use, Eq. (3.4), and values determined from the equation for scientific use [35].

[22] The thermal-conductivity equations for industrial use and for scientific use are described in the same release [35].

Users interested in the pressure range $p > 40$ MPa must decide whether the extrapolation error of Eq. (3.4) described above is acceptable. If not, the thermal conductivity has to be calculated from the significantly more complex equation for scientific use.

The thermal conductivity listed in the tables in Part B was calculated from the equation for industrial use, Eq. (3.4), even for pressures up to 100 MPa, where the equation had to be extrapolated. The program "IAPWS-IF97 Electronic Steam Tables" presented in Part D calculates the thermal conductivity from Eq. (3.4), even if extrapolation is required.

Computer-Program Verification. To assist the user in computer-program verification of Eq. (3.4), Table 3.7 contains corresponding test values.

Table 3.7 Thermal conductivity values calculated from Eq. (3.4) for selected temperatures and pressures [a]

Property	$T = 298.15$ K $p = 0.1$ MPa	$T = 873.15$ K $p = 10$ MPa	$T = 673.15$ K $p = 40$ MPa
ρ [kg m^{-3}] (IAPWS-IF97)	$0.997\,047\,435 \times 10^{3}$	$0.260\,569\,558 \times 10^{2}$	$0.523\,371\,289 \times 10^{3}$ [b]
λ [W m^{-1} K^{-1}]	0.607 509 806	$0.867\,570\,353 \times 10^{-1}$	0.398 506 911

[a] Programmed functions should be verified using 8 byte real values for all variables.

[b] The density value of this test point, which is located in region 3 of IAPWS-IF97, was calculated from Eq. (2.11) via iteration.

Estimated Uncertainty. The estimated uncertainty in thermal conductivity calculated from Eq. (3.4) is based on the uncertainties of the input data used for the development of Eq. (3.4). These uncertainty values are given in Tables A.I and A.II in Appendix A of the release [35].

In the critical region, however, one can expect greater uncertainties in Eq. (3.4) than those derived from the uncertainty of the experimental data, because the λ equation for industrial use, Eq. (3.4), is not able to correctly follow the steep increase of the experimental data for λ in this region. In order to give an impression of the greater uncertainties of Eq. (3.4) in the critical region, Fig. 3.5 shows the differences in thermal conductivity calculated from Eq. (3.4) and from the λ equation for scientific use [35]. Relevant differences occur for temperatures between the critical temperature $T_c = 647.096$ K, Eq. (1.4), and about 2 K above T_c in a small pressure range only.

The huge difference extremely close to the critical temperature and critical pressure p_c is based on the fact that the λ equation for scientific use [35] yields an infinite value for λ_c at the critical point, whereas the corresponding λ value from the industrial equation, Eq. (3.4), remains finite. However, this great difference extremely close to T_c only occurs in a very small pressure range, see Fig. 3.5.

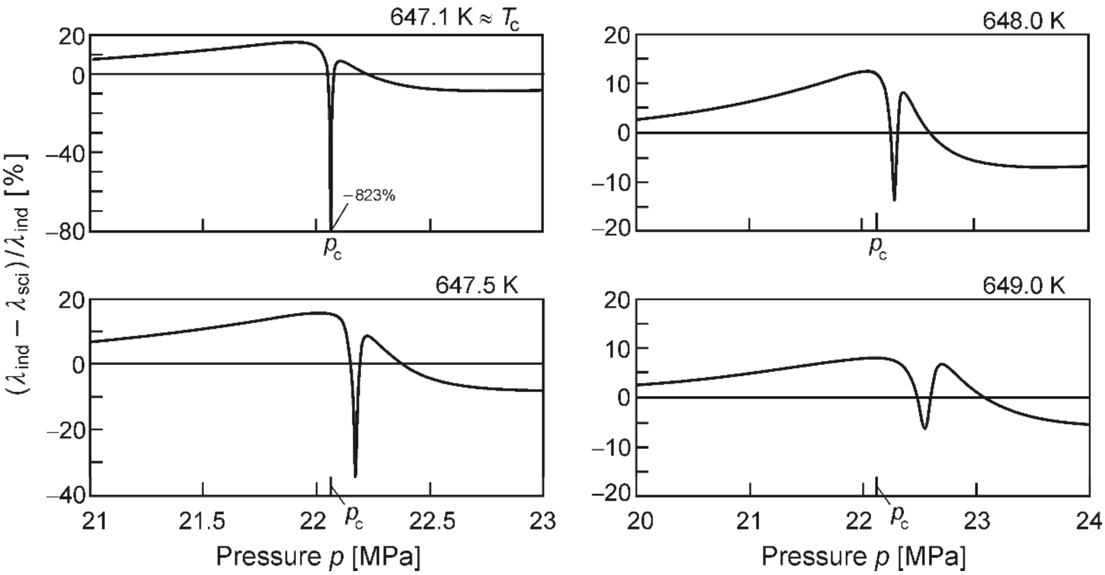

Fig. 3.5 Percentage differences between values for the thermal conductivity λ in the critical region calculated from the equation for industrial use, Eq. (3.4), and values determined from the equation for scientific use [35].

3.3 Equation for the Surface Tension

In 1975, the experimental results of the surface tension σ of the interface between the liquid and vapour phases of water were critically examined by IAPWS. As a result, IAPWS recommended table values of surface tension, which were adjusted to ITS-90 [6] in 1994 [36]. An equation for the surface tension as a function of temperature was fitted to these table values and is given in the "IAPWS Release on Surface Tension of Ordinary Water Substance" [36].

The equation for the surface tension has the following form:

$$\frac{\sigma}{\sigma^*} = 235.8\,(1-\theta)^{1.256}\left[1-0.625\,(1-\theta)\right], \tag{3.8}$$

where $\sigma^* = 1 \times 10^{-3}\ \mathrm{N\,m^{-1}}$ and $\theta = T/T^*$ with $T^* = T_c$, where the critical temperature $T_c = 647.096$ K according to Eq. (1.4).

Range of Validity. Equation (3.8) is valid along the entire vapour-liquid saturation line from the triple-point temperature T_t, Eq. (1.7), to the critical temperature T_c, Eq. (1.4), and can be extrapolated to $T = 273.15$ K so that it covers the temperature range

$$273.15\ \mathrm{K} \le T \le 647.096\ \mathrm{K}.$$

Computer-Program Verification. To assist the user in computer-program verification of Eq (3.8), Table 3.8 contains corresponding test values.

Table 3.8 Surface tension values calculated from Eq. (3.8) for selected temperatures [a]

T [K]	σ [N m^{-1}]
300	$0.716\,859\,625 \times 10^{-1}$
450	$0.428\,914\,992 \times 10^{-1}$
600	$0.837\,561\,087 \times 10^{-2}$

[a] Programmed functions should be verified using 8 byte real values for all variables.

Estimated Uncertainty. The estimated uncertainty in surface tension calculated from Eq. (3.8) is based on the uncertainties of the input data used for the development of Eq. (3.8). These uncertainty values are given in Table 1 of the release [36].

3.4 Equation for the Dielectric Constant

A collection of experimental data available for the dielectric constant ε (relative static dielectric constant or relative static permittivity) was published in 1995 [37]. Based on a selected set of these data, an equation for the dielectric constant was developed [38]. This equation, which has its physical basis in the so-called $\bar{g}$-factor proposed by Harris and Alder [39], was approved by IAPWS in 1997 and is given in the "Release on the Static Dielectric Constant of Ordinary Water Substance for Temperatures from 238 K to 873 K and Pressures up to 1000 MPa" [40].

The equation for the dielectric constant reads

$$\varepsilon(\rho,T) = \frac{1 + A + 5B + \left(9 + 2A + 18B + A^2 + 10AB + 9B^2\right)^{0.5}}{4(1-B)} , \tag{3.9}$$

where the functions A and B are given by

$$A(\rho,T) = \frac{N_\mathrm{A}\,\mu^2 \rho \bar{g}}{M \varepsilon_0 k T} , \tag{3.9a}$$

and

$$B(\rho) = \frac{N_\mathrm{A}\,\alpha \rho}{3 M \varepsilon_0} . \tag{3.9b}$$

The values of the quantities k, N_A, α, ε_0, μ, and M used in Eqs. (3.9a) and (3.9b) are given in Table 3.9. The correlation equation for the Harris-Alder $\bar{g}$-factor in Eq. (3.9a) reads

$$\bar{g}(\delta,\tau) = 1 + \sum_{i=1}^{11} n_i\, \delta^{I_i}\, \tau^{J_i} + n_{12}\,\delta \left(\frac{T_\mathrm{c}}{228\,\mathrm{K}} \tau^{-1} - 1 \right)^{-1.2} , \tag{3.9c}$$

where $\delta = \rho/\rho^*$ and $\tau = T^*/T$ with $\rho^* = \rho_\mathrm{c}$ and $T^* = T_\mathrm{c}$, where the critical density $\rho_\mathrm{c} = 322\ \mathrm{kg\,m^{-3}}$ and the critical temperature $T_\mathrm{c} = 647.096\ \mathrm{K}$ according to Eqs. (1.6) and (1.4). Table 3.10 contains the coefficients n_i and exponents I_i and J_i of Eq. (3.9c).

Table 3.9 Quantities used in Eqs. (3.9a) and (3.9b)

Quantity	Value
Boltzmann's constant k	$1.380\,658 \times 10^{-23}$ J K^{-1}
Avogadro's number N_A	$6.022\,136\,7 \times 10^{23}$ mol^{-1}
Mean molecular polarizability α	1.636×10^{-40} C^2 J^{-1} m^2
Permittivity of vacuum ε_0	$8.854\,187\,817 \times 10^{-12}$ C^2 J^{-1} m^{-1}
Molecular dipole moment μ	6.138×10^{-30} C m
Molar mass M [a]	0.018 015 268 kg mol^{-1}

[a] This value for M is in accordance with the release [40] and must be used in Eqs. (3.9a) and (3.9b), although it differs slightly from the current value for the molar mass given as Eq. (1.3).

Table 3.10 Coefficients and exponents of Eq. (3.9c)

i	I_i	J_i	n_i	i	I_i	J_i	n_i
1	1	0.25	0.978 224 486 826	7	4	2	$0.949\,327\,488\,264 \times 10^{-1}$
2	1	1	−0.957 771 379 375	8	5	2	$-0.980\,469\,816\,509 \times 10^{-2}$
3	1	2.5	0.237 511 794 148	9	6	5	$0.165\,167\,634\,970 \times 10^{-4}$
4	2	1.5	0.714 692 244 396	10	7	0.5	$0.937\,359\,795\,772 \times 10^{-4}$
5	3	1.5	−0.298 217 036 956	11	10	10	$-0.123\,179\,218\,720 \times 10^{-9}$
6	3	2.5	−0.108 863 472 196	12	–	–	$0.196\,096\,504\,426 \times 10^{-2}$

If the dielectric constant is calculated from Eq. (3.9) for given values of *pressure* and temperature, then the input quantity density ρ has to be calculated first. For this density calculation, the use of the IAPWS-95 formulation [8, 9] is recommended in the release [40]. However, as mentioned at the beginning of Chap. 3, for industrial use it is recommended that the IAPWS-IF97 basic equations, Eqs (2.3), (2.6), or (2.11), be used for calculating the input density for Eq. (3.9). For this application, the difference between IAPWS-IF97 and IAPWS-95 is negligible compared with the estimated uncertainty of Eq. (3.9). Accordingly, the values of the dielectric constant listed in the corresponding tables in Part B were calculated in this manner.

Range of Validity. Equation (3.9) covers the following range of temperatures and pressures:

$$273.15\text{ K} \le T \le 323.15\text{ K} \qquad 0 < p \le p_{\max}$$
$$323.15\text{ K} < T \le 873.15\text{ K} \qquad 0 < p \le 600\text{ MPa}$$

The value of $p_{\max}$ corresponds to the ice VI melting pressure [17] at the corresponding temperature or 1000 MPa, whichever is smaller. Equation (3.9) is also valid for the metastable subcooled liquid at atmospheric pressure (0.101325 MPa) for temperatures from 273.15 K down to 238.15 K. Furthermore, Eq. (3.9) extrapolates smoothly up to at least 1200 K and 1200 MPa [40]. The dielectric constant can also be calculated within this extrapolation range with the program "IAPWS-IF97 Electronic Steam Tables" in Part D, assuming that it is within the range of validity of IAPWS-IF97. For the tables in Part B, ε was calculated up to 1073.15 K.

Computer-Program Verification. To assist the user in computer-program verification of Eq. (3.9), Table 3.11 contains corresponding test values.

Table 3.11 Dielectric constant values calculated from Eq. (3.9) for selected temperatures and pressures [a]

Property	$T = 298.15$ K $p = 5$ MPa	$T = 873.15$ K $p = 10$ MPa	$T = 673.15$ K $p = 40$ MPa
ρ [kg m^{-3}] (IAPWS-IF97)	$0.999\,242\,866 \times 10^{3}$	$0.260\,569\,558 \times 10^{2}$	$0.523\,371\,289 \times 10^{3}$ [b]
ε [–]	$0.785\,907\,250 \times 10^{2}$	$0.112\,620\,970 \times 10^{1}$	$0.103\,126\,058 \times 10^{2}$

[a] Programmed functions should be verified using 8 byte real values for all variables.

[b] The density value of this test point, which is located in region 3 of IAPWS-IF97, was calculated from Eq. (2.11) via iteration.

Estimated Uncertainty. The estimated uncertainty in dielectric constant ε calculated from Eq. (3.9) is based on the uncertainties of the input data used for the development of Eq. (3.9). These uncertainty values are given in Table 3 of the release [40].

3.5 Equation for the Refractive Index

Based on a comprehensive collection of experimental data of the refractive index n of water and steam [41], an equation for the Lorentz-Lorenz function dependent on density, temperature, and wavelength was developed in 1990 [42, 43]. This equation was refitted to the experimental data after converting the temperatures to the ITS-90 temperature scale [6] and calculating densities from IAPWS-95 [8, 9] (the current scientific standard of IAPWS for the thermodynamic properties). The refitted equation was approved by IAPWS in 1997 and is given in the "Release on the Refractive Index of Ordinary Water Substance as a Function of Wavelength, Temperature and Pressure" [44].

The equation for the refractive index n from the release was rearranged into a form explicit in n and has then the following form:

$$n\left(\rho, T, \bar{\lambda}\right) = \left(\frac{2A+1}{1-A}\right)^{0.5}, \tag{3.10}$$

where the function A is given by

$$A\left(\delta, \theta, \bar{\Lambda}\right) = \delta\left(a_0 + a_1\delta + a_2\theta + a_3\bar{\Lambda}^2\theta + a_4\bar{\Lambda}^{-2} + \frac{a_5}{\bar{\Lambda}^2 - \bar{\Lambda}_{\mathrm{UV}}^2} + \frac{a_6}{\bar{\Lambda}^2 - \bar{\Lambda}_{\mathrm{IR}}^2} + a_7\delta^2\right) \tag{3.10a}$$

with $\delta = \rho/\rho^*$, $\theta = T/T^*$, and $\bar{\Lambda} = \bar{\lambda}/\bar{\lambda}^*$, where $\rho^* = 1000\ \mathrm{kg\,m^{-3}}$, $T^* = 273.15$ K, and $\bar{\lambda}^* = 0.589\ \mu\mathrm{m}$. The values of the reduced effective infrared resonance $\bar{\Lambda}_{\mathrm{IR}}$ and the reduced effective ultraviolet resonance $\bar{\Lambda}_{\mathrm{UV}}$ are given by $\bar{\Lambda}_{\mathrm{IR}} = 5.432\,937$ and $\bar{\Lambda}_{\mathrm{UV}} = 0.229\,202$. The coefficients a_i of Eq. (3.10a) are listed in Table 3.12.

Table 3.12 Coefficients of Eq. (3.10a)

i	a_i	i	a_i
0	$0.244\,257\,733$	4	$0.158\,920\,570 \times 10^{-2}$
1	$0.974\,634\,476 \times 10^{-2}$	5	$0.245\,934\,259 \times 10^{-2}$
2	$-0.373\,234\,996 \times 10^{-2}$	6	$0.900\,704\,920$
3	$0.268\,678\,472 \times 10^{-3}$	7	$-0.166\,626\,219 \times 10^{-1}$

If the refractive index is calculated from Eq. (3.10) for given values of *pressure* and temperature, then the input quantity reduced density δ has to be calculated first. For this density calculation, the use of IAPWS-95 formulation [8, 9] is recommended in the release [44]. However, as mentioned at the beginning of Chap. 3, for industrial use it is recommended that the IAPWS-IF97 basic equations, Eqs. (2.3), (2.6), or (2.11), be used for calculating the input density for Eq. (3.10). For this application, the difference between IAPWS-IF97 and IAPWS-95 is negligible compared with the estimated uncertainty of Eq. (3.10). Accordingly, values of the refractive index listed in the corresponding tables in Part B were calculated in this manner. The Electronic Steam Tables in Part D also calculate the refractive index with input densities from IAPWS-IF97.

Range of Validity. IAPWS endorses Eq. (3.10) in the following validity range regarding temperature, density, and wavelength:

$$\begin{aligned} 261.15\ \mathrm{K} &\le T \le 773.15\ \mathrm{K} \\ 0 &< \rho \le 1060\ \mathrm{kg\ m^{-3}} \\ 0.2\ \mu\mathrm{m} &\le \lambda \le 1.1\ \mu\mathrm{m} \end{aligned}$$

The extrapolation of the equation to longer wavelengths seems to be reasonable in liquid water at wavelengths up to 1.9 μm [44].

Computer-Program Verification. To assist the user in computer-program verification of Eq. (3.10), Table 3.13 contains corresponding test values.

Table 3.13 Refractive-index values calculated from Eq. (3.10) for selected temperatures, pressures, and wavelengths [a]

Property	$T = 298.15$ K $p = 0.1$ MPa	$T = 773.15$ K $p = 10$ MPa	$T = 673.15$ K $p = 40$ MPa
ρ [kg m^{-3}] (IAPWS-IF97)	$0.997\,047\,435 \times 10^3$	$0.304\,758\,534 \times 10^2$	$0.523\,371\,289 \times 10^3$ [b]
n [–] for $\bar{\lambda} = 0.2265$ μm	$0.139\,277\,824 \times 10^1$	$0.101\,098\,988 \times 10^1$	$0.119\,757\,252 \times 10^1$
n [–] for $\bar{\lambda} = 0.5893$ μm	$0.133\,285\,819 \times 10^1$	$0.100\,949\,307 \times 10^1$	$0.116\,968\,699 \times 10^1$

[a] Programmed functions should be verified using 8 byte real values for all variables.
[b] The density value of this test point, which is located in region 3 of IAPWS-IF97, was calculated from Eq. (2.11) via iteration.

Estimated Uncertainty. The estimated uncertainty in refractive index calculated from Eq. (3.10) is based on the uncertainties of the input data used for the development of Eq. (3.10). These uncertainty values are given in Table 2 of the release [44].

Part B

Tables of the Properties of Water and Steam

Table 1 Saturation state
(Temperature table)

The temperature table contains values on the saturated liquid ($'$) and saturated vapour ($''$) lines for the following thermodynamic and transport properties in the temperature range from 0 °C up to the critical temperature t_c = 373.946 °C:

- Saturation pressure p_s
- Specific volume v
- Specific enthalpy h
- Specific enthalpy of vaporization Δh_v
- Specific entropy s
- Specific entropy of vaporization Δs_v
- Specific isobaric heat capacity c_p
- Speed of sound w
- Isentropic exponent κ
- Dynamic viscosity η
- Thermal conductivity λ

For given temperatures, the saturation pressures p_s were calculated from the IAPWS-IF97 saturation-pressure equation, Eq. (2.13).

For temperatures $t \leq 350$ °C and input values for t and p_s, all of the *thermodynamic* properties on the saturated-liquid and saturated-vapour lines were determined from the basic equations for regions 1 and 2, Eqs. (2.3) and (2.6).

For $t > 350$ °C and input values of t and p_s, the densities ρ' and ρ'' (and thus also the specific volumes v' and v'') were calculated by iterating the basic equation for region 3, Eq. (2.11). With the values for (ρ', t) and (ρ'', t), the other thermodynamic properties were determined from the basic equation, Eq. (2.11). The values of the properties calculated in this manner differ in the last digits from the values of the first edition of the book. This difference is based on the fact that in the first edition all three properties p_s, ρ', and ρ'' were calculated from Eq. (2.11) via the so-called Maxwell criterion, i.e. without using the saturation-pressure equation, Eq. (2.13).

The *transport* properties dynamic viscosity η and thermal conductivity λ were calculated from the equations for industrial applications, Eq. (3.1), and industrial use, Eq. (3.4). The densities ρ' and ρ'' needed in these equations were determined from the IAPWS-IF97 basic equations as described above.

Further saturation properties are listed in Tables 6, 11, and 15.

Table 1 Saturation state
(Temperature table)

t [°C]	T [K]	p_s [bar]	v' [$m^3\ kg^{-1}$]	v''	h'	h'' [$kJ\ kg^{-1}$]	Δh_v	s' [$kJ\ kg^{-1}\ K^{-1}$]	s''
0	273.15	0.006112127	0.00100021	206.140	−0.04159	2500.89	2500.93	−0.0001545	9.1558
0.01[a]	273.16	0.006116570	0.00100021	205.997	0.0006118	2500.91	2500.91	0	9.1555
1	274.15	0.00657088	0.00100015	192.445	4.17665	2502.73	2498.55	0.015260	9.1291
2	275.15	0.00705988	0.00100011	179.764	8.39160	2504.57	2496.17	0.030606	9.1027
3	276.15	0.00758082	0.00100008	168.014	12.6035	2506.40	2493.80	0.045886	9.0765
4	277.15	0.00813549	0.00100007	157.121	16.8127	2508.24	2491.42	0.061101	9.0506
5	278.15	0.00872575	0.00100008	147.017	21.0194	2510.07	2489.05	0.076252	9.0249
6	279.15	0.00935353	0.00100011	137.638	25.2237	2511.91	2486.68	0.091340	8.9994
7	280.15	0.0100209	0.00100014	128.928	29.4258	2513.74	2484.31	0.10637	8.9742
8	281.15	0.0107299	0.00100020	120.834	33.6260	2515.57	2481.94	0.12133	8.9492
9	282.15	0.0114828	0.00100027	113.309	37.8244	2517.40	2479.58	0.13624	8.9244
10	283.15	0.0122818	0.00100035	106.309	42.0211	2519.23	2477.21	0.15109	8.8998
11	284.15	0.0131295	0.00100044	99.7927	46.2162	2521.06	2474.84	0.16587	8.8755
12	285.15	0.0140282	0.00100055	93.7243	50.4100	2522.89	2472.48	0.18061	8.8514
13	286.15	0.0149806	0.00100067	88.0698	54.6024	2524.71	2470.11	0.19528	8.8275
14	287.15	0.0159894	0.00100080	82.7981	58.7936	2526.54	2467.75	0.20990	8.8038
15	288.15	0.0170574	0.00100095	77.8807	62.9837	2528.36	2465.38	0.22447	8.7804
16	289.15	0.0181876	0.00100110	73.2915	67.1727	2530.19	2463.01	0.23898	8.7571
17	290.15	0.0193829	0.00100127	69.0063	71.3608	2532.01	2460.65	0.25344	8.7341
18	291.15	0.0206466	0.00100145	65.0029	75.5479	2533.83	2458.28	0.26785	8.7112
19	292.15	0.0219818	0.00100164	61.2609	79.7343	2535.65	2455.92	0.28220	8.6886
20	293.15	0.0233921	0.00100184	57.7615	83.9199	2537.47	2453.55	0.29650	8.6661
21	294.15	0.0248810	0.00100205	54.4873	88.1048	2539.29	2451.18	0.31075	8.6439
22	295.15	0.0264521	0.00100228	51.4225	92.2890	2541.10	2448.81	0.32495	8.6218
23	296.15	0.0281092	0.00100251	48.5521	96.4727	2542.92	2446.45	0.33910	8.6000
24	297.15	0.0298563	0.00100275	45.8626	100.656	2544.73	2444.08	0.35320	8.5783
25	298.15	0.0316975	0.00100301	43.3414	104.838	2546.54	2441.71	0.36726	8.5568
26	299.15	0.0336369	0.00100327	40.9768	109.021	2548.35	2439.33	0.38126	8.5355
27	300.15	0.0356789	0.00100354	38.7582	113.202	2550.16	2436.96	0.39521	8.5144
28	301.15	0.0378281	0.00100382	36.6754	117.384	2551.97	2434.59	0.40912	8.4934
29	302.15	0.0400892	0.00100411	34.7194	121.565	2553.78	2432.21	0.42298	8.4727
30	303.15	0.0424669	0.00100441	32.8816	125.745	2555.58	2429.84	0.43679	8.4521
31	304.15	0.0449663	0.00100472	31.1540	129.926	2557.39	2427.46	0.45056	8.4317
32	305.15	0.0475925	0.00100504	29.5295	134.106	2559.19	2425.08	0.46428	8.4115
33	306.15	0.0503508	0.00100536	28.0010	138.286	2560.99	2422.70	0.47795	8.3914
34	307.15	0.0532469	0.00100570	26.5624	142.465	2562.79	2420.32	0.49158	8.3715
35	308.15	0.0562862	0.00100604	25.2078	146.645	2564.58	2417.94	0.50517	8.3518
36	309.15	0.0594747	0.00100639	23.9318	150.824	2566.38	2415.56	0.51871	8.3323
37	310.15	0.0628185	0.00100675	22.7292	155.004	2568.17	2413.17	0.53220	8.3129
38	311.15	0.0663237	0.00100712	21.5954	159.183	2569.96	2410.78	0.54566	8.2936
39	312.15	0.0699968	0.00100749	20.5261	163.362	2571.75	2408.39	0.55906	8.2746
40	313.15	0.0738443	0.00100788	19.5170	167.541	2573.54	2406.00	0.57243	8.2557
41	314.15	0.0778731	0.00100827	18.5646	171.720	2575.33	2403.61	0.58575	8.2369
42	315.15	0.0820901	0.00100867	17.6652	175.899	2577.11	2401.21	0.59903	8.2183
43	316.15	0.0865026	0.00100908	16.8155	180.079	2578.89	2398.82	0.61227	8.1999
44	317.15	0.0911180	0.00100949	16.0126	184.258	2580.67	2396.42	0.62547	8.1816

[a] Triple-point temperature.

Table 1 Saturation state – Continued (Temperature table)

t	c'_p	c''_p	w'	w''	κ'	κ''	η'	η''	λ'	λ''
[°C]	[kJ kg^{-1} K^{-1}]		[m s^{-1}]		[–]		[10^{-6} Pa s]		[10^{-3} W m^{-1} K^{-1}]	
0	4.2199	1.8882	1402.3	408.88	3216538	1.3269	1792.0	8.945	562.0	16.49
0.01[a]	4.2199	1.8882	1402.3	408.89	3214432	1.3269	1791.4	8.946	562.0	16.49
1	4.2165	1.8889	1407.2	409.61	3013281	1.3268	1731.2	8.974	564.1	16.56
2	4.2134	1.8895	1412.1	410.34	2824038	1.3268	1673.7	9.003	566.2	16.64
3	4.2105	1.8902	1416.8	411.07	2647765	1.3267	1619.2	9.032	568.2	16.71
4	4.2078	1.8909	1421.5	411.80	2483500	1.3266	1567.4	9.061	570.3	16.78
5	4.2054	1.8917	1426.0	412.53	2330358	1.3266	1518.3	9.090	572.3	16.85
6	4.2031	1.8924	1430.5	413.25	2187526	1.3265	1471.6	9.120	574.3	16.92
7	4.2011	1.8932	1434.9	413.97	2054253	1.3264	1427.2	9.149	576.2	17.00
8	4.1992	1.8940	1439.1	414.69	1929849	1.3264	1384.8	9.179	578.1	17.07
9	4.1974	1.8949	1443.3	415.41	1813676	1.3263	1344.5	9.209	580.0	17.14
10	4.1958	1.8957	1447.4	416.13	1705145	1.3262	1306.0	9.238	581.9	17.21
11	4.1943	1.8966	1451.4	416.84	1603714	1.3262	1269.2	9.268	583.8	17.29
12	4.1930	1.8975	1455.3	417.55	1508881	1.3261	1234.1	9.299	585.6	17.36
13	4.1917	1.8985	1459.1	418.26	1420182	1.3260	1200.5	9.329	587.4	17.43
14	4.1905	1.8994	1462.8	418.97	1337189	1.3259	1168.4	9.359	589.2	17.51
15	4.1894	1.9004	1466.4	419.68	1259505	1.3258	1137.6	9.390	591.0	17.58
16	4.1884	1.9014	1470.0	420.38	1186764	1.3257	1108.1	9.420	592.7	17.65
17	4.1875	1.9025	1473.4	421.08	1118624	1.3257	1079.9	9.451	594.4	17.73
18	4.1866	1.9035	1476.8	421.79	1054772	1.3256	1052.7	9.482	596.1	17.80
19	4.1858	1.9046	1480.1	422.48	994916	1.3255	1026.7	9.513	597.8	17.88
20	4.1851	1.9057	1483.3	423.18	938786	1.3254	1001.6	9.544	599.5	17.95
21	4.1844	1.9069	1486.4	423.88	886129	1.3253	977.6	9.575	601.1	18.03
22	4.1838	1.9080	1489.4	424.57	836715	1.3252	954.4	9.607	602.7	18.10
23	4.1832	1.9092	1492.4	425.26	790326	1.3251	932.1	9.638	604.3	18.18
24	4.1827	1.9104	1495.2	425.95	746762	1.3250	910.7	9.669	605.9	18.25
25	4.1822	1.9116	1498.0	426.63	705837	1.3249	890.0	9.701	607.5	18.33
26	4.1817	1.9129	1500.7	427.32	667378	1.3248	870.1	9.733	609.0	18.40
27	4.1813	1.9141	1503.4	428.00	631223	1.3247	850.9	9.764	610.5	18.48
28	4.1809	1.9154	1505.9	428.68	597224	1.3246	832.4	9.796	612.0	18.55
29	4.1806	1.9167	1508.4	429.36	565239	1.3245	814.5	9.828	613.5	18.63
30	4.1803	1.9180	1510.8	430.04	535141	1.3244	797.2	9.860	615.0	18.71
31	4.1800	1.9194	1513.2	430.72	506808	1.3243	780.5	9.892	616.4	18.78
32	4.1798	1.9207	1515.4	431.39	480128	1.3242	764.4	9.924	617.8	18.86
33	4.1795	1.9221	1517.6	432.06	454996	1.3241	748.8	9.957	619.2	18.94
34	4.1794	1.9235	1519.8	432.73	431314	1.3240	733.7	9.989	620.6	19.01
35	4.1792	1.9249	1521.8	433.40	408993	1.3239	719.1	10.02	622.0	19.09
36	4.1791	1.9263	1523.8	434.07	387946	1.3238	705.0	10.05	623.3	19.17
37	4.1790	1.9278	1525.8	434.73	368094	1.3237	691.3	10.09	624.7	19.25
38	4.1789	1.9292	1527.6	435.40	349365	1.3235	678.0	10.12	626.0	19.32
39	4.1788	1.9307	1529.4	436.06	331688	1.3234	665.2	10.15	627.3	19.40
40	4.1788	1.9322	1531.1	436.72	314999	1.3233	652.7	10.18	628.6	19.48
41	4.1788	1.9337	1532.8	437.37	299239	1.3232	640.6	10.22	629.8	19.56
42	4.1788	1.9353	1534.4	438.03	284351	1.3231	628.9	10.25	631.1	19.64
43	4.1788	1.9368	1536.0	438.68	270282	1.3230	617.5	10.28	632.3	19.72
44	4.1789	1.9384	1537.5	439.33	256983	1.3229	606.5	10.32	633.5	19.80

[a] Triple-point temperature.

Table 1 Saturation state – Continued (Temperature table)

t	T	p_s	v'	v''	h'	h''	Δh_v	s'	s''
[°C]	[K]	[bar]	[$m^3 kg^{-1}$]			[$kJ kg^{-1}$]		[$kJ kg^{-1} K^{-1}$]	
45	318.15	0.0959439	0.00100991	15.2534	188.437	2582.45	2394.02	0.63862	8.1634
46	319.15	0.100988	0.00101034	14.5355	192.617	2584.23	2391.61	0.65174	8.1454
47	320.15	0.106259	0.00101078	13.8562	196.796	2586.00	2389.21	0.66481	8.1276
48	321.15	0.111764	0.00101123	13.2132	200.976	2587.77	2386.80	0.67785	8.1099
49	322.15	0.117512	0.00101168	12.6045	205.156	2589.54	2384.39	0.69084	8.0923
50	323.15	0.123513	0.00101214	12.0279	209.336	2591.31	2381.97	0.70379	8.0749
51	324.15	0.129774	0.00101260	11.4815	213.517	2593.08	2379.56	0.71671	8.0576
52	325.15	0.136305	0.00101308	10.9637	217.697	2594.84	2377.14	0.72958	8.0405
53	326.15	0.143116	0.00101356	10.4726	221.878	2596.60	2374.72	0.74242	8.0235
54	327.15	0.150215	0.00101404	10.0069	226.059	2598.35	2372.30	0.75522	8.0066
55	328.15	0.157614	0.00101454	9.56492	230.241	2600.11	2369.87	0.76798	7.9899
56	329.15	0.165322	0.00101504	9.14543	234.423	2601.86	2367.44	0.78070	7.9733
57	330.15	0.173350	0.00101555	8.74712	238.605	2603.61	2365.01	0.79339	7.9568
58	331.15	0.181708	0.00101606	8.36879	242.788	2605.36	2362.57	0.80603	7.9405
59	332.15	0.190407	0.00101658	8.00932	246.971	2607.10	2360.13	0.81864	7.9243
60	333.15	0.199458	0.00101711	7.66766	251.154	2608.85	2357.69	0.83122	7.9082
61	334.15	0.208873	0.00101765	7.34281	255.338	2610.58	2355.25	0.84375	7.8922
62	335.15	0.218664	0.00101819	7.03384	259.523	2612.32	2352.80	0.85625	7.8764
63	336.15	0.228842	0.00101874	6.73990	263.708	2614.05	2350.35	0.86872	7.8607
64	337.15	0.239421	0.00101929	6.46015	267.893	2615.78	2347.89	0.88115	7.8451
65	338.15	0.250411	0.00101985	6.19383	272.079	2617.51	2345.43	0.89354	7.8296
66	339.15	0.261827	0.00102042	5.94021	276.266	2619.23	2342.97	0.90590	7.8142
67	340.15	0.273680	0.00102100	5.69861	280.453	2620.96	2340.50	0.91823	7.7990
68	341.15	0.285986	0.00102158	5.46840	284.641	2622.67	2338.03	0.93052	7.7839
69	342.15	0.298756	0.00102216	5.24896	288.829	2624.39	2335.56	0.94277	7.7689
70	343.15	0.312006	0.00102276	5.03973	293.018	2626.10	2333.08	0.95499	7.7540
71	344.15	0.325750	0.00102336	4.84018	297.208	2627.81	2330.60	0.96718	7.7392
72	345.15	0.340001	0.00102396	4.64980	301.398	2629.51	2328.11	0.97933	7.7245
73	346.15	0.354775	0.00102458	4.46812	305.589	2631.21	2325.62	0.99146	7.7100
74	347.15	0.370088	0.00102520	4.29469	309.781	2632.91	2323.13	1.0035	7.6955
75	348.15	0.385954	0.00102582	4.12908	313.974	2634.60	2320.63	1.0156	7.6812
76	349.15	0.402389	0.00102645	3.97090	318.167	2636.29	2318.13	1.0276	7.6669
77	350.15	0.419409	0.00102709	3.81978	322.361	2637.98	2315.62	1.0396	7.6528
78	351.15	0.437031	0.00102773	3.67535	326.556	2639.66	2313.11	1.0516	7.6388
79	352.15	0.455271	0.00102838	3.53729	330.752	2641.34	2310.59	1.0635	7.6248
80	353.15	0.474147	0.00102904	3.40527	334.949	2643.01	2308.07	1.0754	7.6110
81	354.15	0.493676	0.00102970	3.27899	339.146	2644.68	2305.54	1.0873	7.5973
82	355.15	0.513875	0.00103037	3.15818	343.345	2646.35	2303.01	1.0991	7.5837
83	356.15	0.534762	0.00103105	3.04257	347.544	2648.01	2300.47	1.1109	7.5701
84	357.15	0.556355	0.00103173	2.93190	351.745	2649.67	2297.93	1.1227	7.5567
85	358.15	0.578675	0.00103242	2.82593	355.946	2651.33	2295.38	1.1344	7.5434
86	359.15	0.601738	0.00103311	2.72445	360.148	2652.98	2292.83	1.1461	7.5301
87	360.15	0.625565	0.00103381	2.62722	364.352	2654.62	2290.27	1.1578	7.5170
88	361.15	0.650174	0.00103451	2.53406	368.556	2656.26	2287.70	1.1694	7.5039
89	362.15	0.675587	0.00103522	2.44476	372.762	2657.90	2285.14	1.1811	7.4909

Table 1 Saturation state – Continued (Temperature table)

t [°C]	c'_p [kJ kg^{-1} K^{-1}]	c''_p	w' [m s^{-1}]	w''	κ' [–]	κ''	η' [10^{-6} Pa s]	η''	λ' [10^{-3} W m^{-1} K^{-1}]	λ''
45	4.1790	1.9400	1538.9	439.98	244408	1.3228	595.8	10.35	634.7	19.88
46	4.1791	1.9416	1540.3	440.63	232515	1.3227	585.3	10.38	635.9	19.96
47	4.1792	1.9432	1541.6	441.28	221263	1.3226	575.2	10.42	637.1	20.04
48	4.1794	1.9449	1542.8	441.92	210614	1.3224	565.4	10.45	638.2	20.12
49	4.1796	1.9466	1544.0	442.56	200533	1.3223	555.8	10.48	639.3	20.20
50	4.1798	1.9482	1545.2	443.20	190987	1.3222	546.5	10.52	640.5	20.28
51	4.1800	1.9500	1546.3	443.84	181945	1.3221	537.5	10.55	641.6	20.36
52	4.1802	1.9517	1547.3	444.48	173378	1.3220	528.6	10.58	642.6	20.44
53	4.1805	1.9534	1548.3	445.11	165259	1.3219	520.1	10.62	643.7	20.52
54	4.1808	1.9552	1549.2	445.74	157561	1.3218	511.7	10.65	644.8	20.61
55	4.1811	1.9570	1550.1	446.37	150262	1.3217	503.6	10.68	645.8	20.69
56	4.1814	1.9588	1550.9	447.00	143338	1.3216	495.7	10.72	646.8	20.77
57	4.1818	1.9607	1551.7	447.63	136769	1.3214	488.0	10.75	647.8	20.85
58	4.1821	1.9625	1552.4	448.25	130534	1.3213	480.5	10.79	648.8	20.94
59	4.1825	1.9644	1553.1	448.88	124615	1.3212	473.2	10.82	649.8	21.02
60	4.1829	1.9664	1553.7	449.50	118994	1.3211	466.0	10.85	650.8	21.10
61	4.1834	1.9683	1554.3	450.11	113655	1.3210	459.1	10.89	651.7	21.19
62	4.1838	1.9703	1554.8	450.73	108583	1.3209	452.3	10.92	652.6	21.27
63	4.1843	1.9723	1555.3	451.34	103762	1.3208	445.7	10.96	653.6	21.36
64	4.1848	1.9743	1555.8	451.95	99180	1.3206	439.2	10.99	654.5	21.44
65	4.1853	1.9764	1556.2	452.56	94823	1.3205	432.9	11.02	655.3	21.53
66	4.1859	1.9785	1556.5	453.17	90679	1.3204	426.7	11.06	656.2	21.61
67	4.1864	1.9806	1556.8	453.77	86736	1.3203	420.7	11.09	657.1	21.70
68	4.1870	1.9828	1557.1	454.38	82985	1.3202	414.9	11.13	657.9	21.79
69	4.1876	1.9850	1557.3	454.98	79414	1.3200	409.1	11.16	658.8	21.87
70	4.1882	1.9873	1557.5	455.57	76015	1.3199	403.5	11.19	659.6	21.96
71	4.1889	1.9895	1557.6	456.17	72777	1.3198	398.1	11.23	660.4	22.05
72	4.1896	1.9919	1557.7	456.76	69694	1.3197	392.7	11.26	661.2	22.14
73	4.1902	1.9942	1557.7	457.35	66756	1.3195	387.5	11.30	661.9	22.23
74	4.1910	1.9966	1557.7	457.94	63956	1.3194	382.4	11.33	662.7	22.32
75	4.1917	1.9990	1557.7	458.52	61287	1.3193	377.4	11.37	663.4	22.41
76	4.1924	2.0015	1557.6	459.11	58742	1.3191	372.5	11.40	664.2	22.50
77	4.1932	2.0041	1557.5	459.69	56315	1.3190	367.8	11.44	664.9	22.59
78	4.1940	2.0066	1557.4	460.26	54000	1.3189	363.1	11.47	665.6	22.68
79	4.1948	2.0092	1557.2	460.84	51791	1.3187	358.5	11.50	666.3	22.77
80	4.1956	2.0119	1557.0	461.41	49684	1.3186	354.0	11.54	667.0	22.86
81	4.1965	2.0146	1556.7	461.98	47671	1.3185	349.7	11.57	667.6	22.95
82	4.1974	2.0174	1556.4	462.55	45750	1.3183	345.4	11.61	668.3	23.04
83	4.1983	2.0202	1556.1	463.11	43915	1.3182	341.2	11.64	668.9	23.14
84	4.1992	2.0231	1555.7	463.67	42163	1.3180	337.1	11.68	669.5	23.23
85	4.2001	2.0260	1555.3	464.23	40488	1.3179	333.1	11.71	670.1	23.32
86	4.2011	2.0290	1554.8	464.79	38888	1.3177	329.1	11.75	670.7	23.42
87	4.2020	2.0321	1554.4	465.34	37359	1.3176	325.3	11.78	671.3	23.51
88	4.2030	2.0352	1553.8	465.89	35896	1.3174	321.5	11.82	671.9	23.61
89	4.2041	2.0383	1553.3	466.44	34498	1.3173	317.8	11.85	672.5	23.70

Table 1 Saturation state – Continued (Temperature table)

t [°C]	T [K]	p_s [bar]	v' [m³ kg⁻¹]	v'' [m³ kg⁻¹]	h' [kJ kg⁻¹]	h'' [kJ kg⁻¹]	Δh_v [kJ kg⁻¹]	s' [kJ kg⁻¹ K⁻¹]	s'' [kJ kg⁻¹ K⁻¹]
90	363.15	0.701824	0.00103594	2.35915	376.968	2659.53	2282.56	1.1927	7.4781
91	364.15	0.728904	0.00103667	2.27705	381.176	2661.16	2279.98	1.2042	7.4653
92	365.15	0.756849	0.00103740	2.19830	385.385	2662.78	2277.39	1.2158	7.4526
93	366.15	0.785681	0.00103813	2.12275	389.595	2664.39	2274.80	1.2273	7.4400
94	367.15	0.815420	0.00103887	2.05025	393.806	2666.01	2272.20	1.2387	7.4275
95	368.15	0.846089	0.00103962	1.98065	398.019	2667.61	2269.60	1.2502	7.4150
96	369.15	0.877711	0.00104038	1.91383	402.232	2669.22	2266.98	1.2616	7.4027
97	370.15	0.910308	0.00104114	1.84965	406.447	2670.81	2264.37	1.2730	7.3904
98	371.15	0.943902	0.00104190	1.78801	410.663	2672.40	2261.74	1.2844	7.3782
99	372.15	0.978518	0.00104268	1.72878	414.880	2673.99	2259.11	1.2957	7.3661
100	373.15	1.01418	0.00104346	1.67186	419.099	2675.57	2256.47	1.3070	7.3541
102	375.15	1.08873	0.00104503	1.56454	427.541	2678.72	2251.18	1.3296	7.3303
104	377.15	1.16776	0.00104663	1.46529	435.988	2681.84	2245.85	1.3520	7.3068
106	379.15	1.25147	0.00104826	1.37342	444.440	2684.94	2240.50	1.3743	7.2836
108	381.15	1.34007	0.00104991	1.28831	452.899	2688.02	2235.12	1.3965	7.2607
110	383.15	1.43376	0.00105158	1.20939	461.363	2691.07	2229.70	1.4187	7.2380
112	385.15	1.53277	0.00105328	1.13615	469.834	2694.09	2224.26	1.4407	7.2157
114	387.15	1.63734	0.00105500	1.06813	478.312	2697.09	2218.78	1.4626	7.1937
116	389.15	1.74768	0.00105675	1.00489	486.796	2700.07	2213.27	1.4844	7.1719
118	391.15	1.86404	0.00105853	0.946070	495.287	2703.02	2207.73	1.5062	7.1504
120	393.15	1.98665	0.00106033	0.891304	503.785	2705.93	2202.15	1.5278	7.1291
122	395.15	2.11578	0.00106215	0.840276	512.290	2708.82	2196.53	1.5494	7.1081
124	397.15	2.25168	0.00106400	0.792695	520.803	2711.69	2190.88	1.5708	7.0873
126	399.15	2.39460	0.00106588	0.748294	529.323	2714.52	2185.19	1.5922	7.0668
128	401.15	2.54481	0.00106778	0.706832	537.851	2717.32	2179.47	1.6134	7.0465
130	403.15	2.70260	0.00106971	0.668084	546.388	2720.09	2173.70	1.6346	7.0264
132	405.15	2.86823	0.00107167	0.631849	554.933	2722.83	2167.89	1.6557	7.0066
134	407.15	3.04199	0.00107365	0.597939	563.486	2725.53	2162.04	1.6767	6.9869
136	409.15	3.22417	0.00107566	0.566183	572.048	2728.20	2156.15	1.6977	6.9675
138	411.15	3.41508	0.00107770	0.536425	580.620	2730.84	2150.22	1.7185	6.9483
140	413.15	3.61501	0.00107976	0.508519	589.200	2733.44	2144.24	1.7393	6.9293
142	415.15	3.82427	0.00108185	0.482334	597.790	2736.01	2138.22	1.7600	6.9105
144	417.15	4.04318	0.00108397	0.457748	606.390	2738.54	2132.15	1.7806	6.8918
146	419.15	4.27205	0.00108612	0.434648	615.000	2741.04	2126.04	1.8011	6.8734
148	421.15	4.51122	0.00108830	0.412931	623.621	2743.50	2119.88	1.8216	6.8551
150	423.15	4.76101	0.00109050	0.392502	632.252	2745.92	2113.67	1.8420	6.8370
152	425.15	5.02177	0.00109274	0.373273	640.893	2748.30	2107.41	1.8623	6.8191
154	427.15	5.29383	0.00109501	0.355162	649.546	2750.64	2101.10	1.8825	6.8014
156	429.15	5.57755	0.00109730	0.338095	658.211	2752.95	2094.74	1.9027	6.7838
158	431.15	5.87329	0.00109963	0.322002	666.887	2755.21	2088.32	1.9228	6.7664
160	433.15	6.18139	0.00110199	0.306818	675.575	2757.43	2081.86	1.9428	6.7491
162	435.15	6.50224	0.00110438	0.292486	684.275	2759.61	2075.33	1.9627	6.7320
164	437.15	6.83619	0.00110680	0.278948	692.988	2761.75	2068.76	1.9826	6.7150
166	439.15	7.18364	0.00110925	0.266155	701.714	2763.84	2062.13	2.0025	6.6982
168	441.15	7.54495	0.00111174	0.254059	710.453	2765.89	2055.44	2.0222	6.6815

Table 1 Saturation state – Continued
(Temperature table)

t	c'_p	c''_p	w'	w''	κ'	κ''	η'	η''	λ'	λ''
[°C]	[kJ kg^{-1} K^{-1}]		[m s^{-1}]		[–]		[10^{-6} Pa s]		[10^{-3} W m^{-1} K^{-1}]	
90	4.2051	2.0415	1552.7	466.98	33160	1.3171	314.2	11.89	673.0	23.80
91	4.2062	2.0448	1552.1	467.52	31881	1.3169	310.6	11.92	673.5	23.90
92	4.2072	2.0482	1551.4	468.06	30656	1.3168	307.1	11.95	674.1	23.99
93	4.2083	2.0516	1550.8	468.60	29484	1.3166	303.7	11.99	674.6	24.09
94	4.2095	2.0551	1550.0	469.13	28363	1.3164	300.4	12.02	675.1	24.19
95	4.2106	2.0586	1549.3	469.66	27288	1.3163	297.1	12.06	675.5	24.29
96	4.2118	2.0623	1548.5	470.18	26260	1.3161	293.9	12.09	676.0	24.39
97	4.2130	2.0660	1547.7	470.71	25275	1.3159	290.7	12.13	676.5	24.49
98	4.2142	2.0697	1546.9	471.23	24331	1.3157	287.6	12.16	676.9	24.59
99	4.2154	2.0736	1546.0	471.74	23426	1.3155	284.6	12.20	677.3	24.69
100	4.2166	2.0775	1545.1	472.26	22559	1.3153	281.6	12.23	677.8	24.79
102	4.2192	2.0856	1543.2	473.27	20931	1.3150	275.8	12.30	678.6	25.00
104	4.2219	2.0940	1541.2	474.28	19434	1.3146	270.2	12.37	679.3	25.21
106	4.2246	2.1027	1539.0	475.26	18056	1.3142	264.8	12.44	680.0	25.42
108	4.2274	2.1118	1536.8	476.24	16786	1.3137	259.6	12.51	680.7	25.63
110	4.2304	2.1212	1534.4	477.20	15616	1.3133	254.6	12.58	681.3	25.85
112	4.2334	2.1310	1532.0	478.15	14537	1.3128	249.8	12.65	681.8	26.06
114	4.2365	2.1411	1529.4	479.08	13541	1.3124	245.1	12.72	682.4	26.28
116	4.2397	2.1517	1526.7	480.00	12620	1.3119	240.6	12.79	682.8	26.51
118	4.2430	2.1626	1523.9	480.90	11769	1.3114	236.2	12.86	683.2	26.73
120	4.2464	2.1740	1521.0	481.79	10982	1.3109	232.0	12.93	683.6	26.96
122	4.2499	2.1858	1518.0	482.66	10254	1.3104	228.0	13.00	683.9	27.19
124	4.2535	2.1979	1514.9	483.52	9579.0	1.3098	224.0	13.07	684.2	27.43
126	4.2571	2.2105	1511.7	484.36	8953.5	1.3093	220.2	13.13	684.5	27.67
128	4.2609	2.2236	1508.4	485.19	8373.3	1.3087	216.5	13.20	684.6	27.91
130	4.2648	2.2370	1505.0	486.00	7834.9	1.3082	212.9	13.27	684.8	28.15
132	4.2689	2.2509	1501.5	486.79	7334.8	1.3076	209.5	13.34	684.9	28.40
134	4.2730	2.2653	1497.9	487.57	6870.2	1.3070	206.1	13.41	685.0	28.65
136	4.2772	2.2800	1494.3	488.34	6438.1	1.3064	202.9	13.48	685.0	28.90
138	4.2816	2.2953	1490.5	489.08	6036.2	1.3057	199.7	13.55	684.9	29.16
140	4.2860	2.3109	1486.6	489.81	5662.0	1.3051	196.6	13.62	684.9	29.42
142	4.2906	2.3270	1482.7	490.53	5313.5	1.3044	193.7	13.69	684.8	29.68
144	4.2953	2.3436	1478.6	491.22	4988.6	1.3038	190.8	13.76	684.6	29.95
146	4.3002	2.3606	1474.5	491.90	4685.7	1.3031	188.0	13.82	684.4	30.22
148	4.3052	2.3780	1470.3	492.57	4403.1	1.3024	185.3	13.89	684.1	30.50
150	4.3103	2.3959	1466.0	493.22	4139.3	1.3018	182.6	13.96	683.9	30.77
152	4.3155	2.4142	1461.6	493.85	3892.9	1.3011	180.0	14.03	683.5	31.06
154	4.3209	2.4329	1457.1	494.46	3662.7	1.3004	177.5	14.10	683.2	31.34
156	4.3264	2.4521	1452.5	495.06	3447.4	1.2997	175.1	14.17	682.8	31.63
158	4.3321	2.4717	1447.9	495.64	3246.0	1.2990	172.7	14.24	682.3	31.92
160	4.3379	2.4918	1443.2	496.21	3057.5	1.2982	170.4	14.30	681.8	32.22
162	4.3439	2.5123	1438.4	496.75	2881.0	1.2975	168.2	14.37	681.3	32.52
164	4.3501	2.5332	1433.5	497.28	2715.7	1.2968	166.0	14.44	680.7	32.83
166	4.3564	2.5545	1428.5	497.80	2560.8	1.2961	163.9	14.51	680.1	33.14
168	4.3628	2.5763	1423.4	498.30	2415.5	1.2953	161.8	14.58	679.4	33.45

Table 1 Saturation state – Continued (Temperature table)

t [°C]	T [K]	p_s [bar]	v' [$m^3\ kg^{-1}$]	v''	h'	h'' [$kJ\ kg^{-1}$]	Δh_v	s' [$kJ\ kg^{-1}\ K^{-1}$]	s''
170	443.15	7.92053	0.00111426	0.242616	719.206	2767.89	2048.69	2.0419	6.6649
172	445.15	8.31077	0.00111682	0.231785	727.973	2769.85	2041.88	2.0616	6.6485
174	447.15	8.71606	0.00111941	0.221528	736.755	2771.77	2035.01	2.0811	6.6322
176	449.15	9.13681	0.00112203	0.211810	745.551	2773.63	2028.08	2.1007	6.6161
178	451.15	9.57343	0.00112469	0.202598	754.362	2775.45	2021.09	2.1201	6.6000
180	453.15	10.0263	0.00112739	0.193862	763.188	2777.22	2014.03	2.1395	6.5841
182	455.15	10.4960	0.00113012	0.185572	772.030	2778.94	2006.91	2.1589	6.5682
184	457.15	10.9827	0.00113289	0.177703	780.889	2780.61	1999.72	2.1782	6.5525
186	459.15	11.4871	0.00113570	0.170229	789.764	2782.23	1992.47	2.1974	6.5369
188	461.15	12.0094	0.00113855	0.163127	798.656	2783.80	1985.14	2.2166	6.5214
190	463.15	12.5502	0.00114144	0.156377	807.566	2785.31	1977.74	2.2358	6.5060
192	465.15	13.1099	0.00114437	0.149957	816.494	2786.77	1970.28	2.2549	6.4907
194	467.15	13.6889	0.00114734	0.143848	825.440	2788.18	1962.74	2.2739	6.4755
196	469.15	14.2877	0.00115036	0.138034	834.405	2789.53	1955.12	2.2929	6.4603
198	471.15	14.9069	0.00115341	0.132497	843.389	2790.82	1947.44	2.3119	6.4453
200	473.15	15.5467	0.00115651	0.127222	852.393	2792.06	1939.67	2.3308	6.4303
202	475.15	16.2078	0.00115966	0.122195	861.417	2793.24	1931.82	2.3497	6.4154
204	477.15	16.8906	0.00116285	0.117402	870.463	2794.36	1923.90	2.3685	6.4006
206	479.15	17.5955	0.00116609	0.112830	879.529	2795.42	1915.89	2.3873	6.3858
208	481.15	18.3231	0.00116937	0.108467	888.618	2796.42	1907.80	2.4060	6.3711
210	483.15	19.0739	0.00117271	0.104302	897.729	2797.35	1899.62	2.4248	6.3565
212	485.15	19.8483	0.00117609	0.100325	906.863	2798.22	1891.36	2.4434	6.3420
214	487.15	20.6470	0.00117953	0.0965249	916.021	2799.03	1883.01	2.4621	6.3275
216	489.15	21.4702	0.00118302	0.0928934	925.203	2799.77	1874.57	2.4807	6.3130
218	491.15	22.3187	0.00118656	0.0894214	934.409	2800.45	1866.04	2.4993	6.2986
220	493.15	23.1929	0.00119016	0.0861007	943.642	2801.05	1857.41	2.5178	6.2842
222	495.15	24.0933	0.00119381	0.0829236	952.900	2801.59	1848.69	2.5363	6.2699
224	497.15	25.0205	0.00119752	0.0798826	962.185	2802.05	1839.87	2.5548	6.2557
226	499.15	25.9749	0.00120129	0.0769710	971.498	2802.45	1830.95	2.5733	6.2414
228	501.15	26.9572	0.00120512	0.0741823	980.839	2802.76	1821.93	2.5917	6.2272
230	503.15	27.9679	0.00120901	0.0715102	990.210	2803.01	1812.80	2.6102	6.2131
232	505.15	29.0075	0.00121297	0.0689492	999.609	2803.18	1803.57	2.6285	6.1989
234	507.15	30.0767	0.00121699	0.0664936	1009.04	2803.27	1794.23	2.6469	6.1848
236	509.15	31.1758	0.00122108	0.0641385	1018.50	2803.28	1784.78	2.6653	6.1707
238	511.15	32.3056	0.00122523	0.0618788	1028.00	2803.21	1775.22	2.6836	6.1566
240	513.15	33.4665	0.00122946	0.0597101	1037.52	2803.06	1765.54	2.7019	6.1425
242	515.15	34.6592	0.00123376	0.0576280	1047.08	2802.82	1755.74	2.7203	6.1285
244	517.15	35.8843	0.00123814	0.0556284	1056.68	2802.50	1745.82	2.7385	6.1144
246	519.15	37.1423	0.00124259	0.0537073	1066.31	2802.10	1735.78	2.7568	6.1003
248	521.15	38.4338	0.00124712	0.0518612	1075.98	2801.60	1725.62	2.7751	6.0863
250	523.15	39.7594	0.00125174	0.0500866	1085.69	2801.01	1715.33	2.7934	6.0722
252	525.15	41.1197	0.00125644	0.0483801	1095.43	2800.33	1704.90	2.8117	6.0582
254	527.15	42.5154	0.00126122	0.0467386	1105.22	2799.56	1694.34	2.8299	6.0441
256	529.15	43.9471	0.00126610	0.0451592	1115.04	2798.69	1683.64	2.8482	6.0300
258	531.15	45.4153	0.00127107	0.0436390	1124.91	2797.71	1672.80	2.8664	6.0158

Table 1 Saturation state – Continued (Temperature table)

t	c'_p	c''_p	w'	w''	κ'	κ''	η'	η''	λ'	λ''
[°C]	[kJ kg^{-1} K^{-1}]		[m s^{-1}]		[–]		[10^{-6} Pa s]		[10^{-3} W m^{-1} K^{-1}]	
170	4.3695	2.5985	1418.3	498.78	2279.1	1.2946	159.8	14.64	678.7	33.77
172	4.3763	2.6212	1413.0	499.24	2151.2	1.2939	157.8	14.71	678.0	34.09
174	4.3833	2.6443	1407.7	499.68	2031.1	1.2931	155.9	14.78	677.2	34.42
176	4.3906	2.6679	1402.3	500.11	1918.3	1.2924	154.0	14.85	676.4	34.75
178	4.3980	2.6919	1396.9	500.52	1812.2	1.2916	152.2	14.92	675.5	35.08
180	4.4056	2.7164	1391.3	500.92	1712.5	1.2909	150.4	14.99	674.6	35.42
182	4.4134	2.7414	1385.7	501.29	1618.8	1.2902	148.6	15.05	673.7	35.77
184	4.4214	2.7669	1380.0	501.65	1530.5	1.2894	146.9	15.12	672.7	36.12
186	4.4296	2.7928	1374.2	501.99	1447.5	1.2887	145.3	15.19	671.7	36.47
188	4.4381	2.8193	1368.3	502.31	1369.3	1.2879	143.6	15.26	670.6	36.83
190	4.4468	2.8464	1362.4	502.61	1295.7	1.2872	142.0	15.33	669.5	37.19
192	4.4557	2.8739	1356.4	502.90	1226.3	1.2864	140.5	15.39	668.3	37.56
194	4.4649	2.9021	1350.3	503.16	1160.8	1.2857	139.0	15.46	667.2	37.94
196	4.4743	2.9308	1344.1	503.41	1099.1	1.2850	137.5	15.53	665.9	38.32
198	4.4840	2.9601	1337.8	503.63	1040.9	1.2842	136.0	15.60	664.7	38.70
200	4.4940	2.9900	1331.5	503.84	986.01	1.2835	134.6	15.67	663.4	39.10
202	4.5043	3.0206	1325.1	504.03	934.17	1.2827	133.2	15.73	662.0	39.49
204	4.5148	3.0518	1318.6	504.19	885.21	1.2820	131.8	15.80	660.7	39.89
206	4.5256	3.0837	1312.0	504.34	838.97	1.2812	130.5	15.87	659.2	40.30
208	4.5368	3.1163	1305.4	504.46	795.28	1.2804	129.2	15.94	657.8	40.72
210	4.5482	3.1496	1298.7	504.57	753.98	1.2797	127.9	16.01	656.3	41.14
212	4.5600	3.1837	1291.9	504.65	714.94	1.2789	126.6	16.08	654.7	41.57
214	4.5722	3.2186	1285.0	504.71	678.02	1.2782	125.4	16.15	653.2	42.00
216	4.5846	3.2542	1278.1	504.75	643.09	1.2774	124.1	16.22	651.5	42.44
218	4.5975	3.2907	1271.0	504.76	610.04	1.2766	122.9	16.29	649.9	42.89
220	4.6107	3.3280	1263.9	504.76	578.76	1.2759	121.8	16.35	648.2	43.34
222	4.6243	3.3662	1256.8	504.73	549.14	1.2751	120.6	16.42	646.4	43.80
224	4.6383	3.4053	1249.5	504.68	521.09	1.2743	119.5	16.49	644.7	44.27
226	4.6528	3.4453	1242.2	504.60	494.52	1.2735	118.4	16.56	642.8	44.75
228	4.6676	3.4863	1234.8	504.50	469.35	1.2728	117.3	16.63	641.0	45.23
230	4.6829	3.5283	1227.3	504.38	445.49	1.2720	116.2	16.70	639.1	45.72
232	4.6987	3.5713	1219.8	504.23	422.87	1.2712	115.1	16.78	637.1	46.23
234	4.7150	3.6154	1212.2	504.05	401.43	1.2704	114.1	16.85	635.2	46.73
236	4.7317	3.6606	1204.5	503.85	381.09	1.2696	113.1	16.92	633.1	47.25
238	4.7490	3.7070	1196.7	503.63	361.80	1.2688	112.1	16.99	631.1	47.78
240	4.7668	3.7545	1188.8	503.38	343.49	1.2680	111.1	17.06	629.0	48.32
242	4.7852	3.8033	1180.9	503.10	326.12	1.2672	110.1	17.13	626.8	48.87
244	4.8042	3.8534	1172.9	502.79	309.63	1.2664	109.1	17.21	624.6	49.42
246	4.8238	3.9048	1164.8	502.46	293.97	1.2656	108.2	17.28	622.4	49.99
248	4.8441	3.9576	1156.6	502.10	279.10	1.2648	107.2	17.35	620.1	50.57
250	4.8650	4.0119	1148.4	501.71	264.98	1.2640	106.3	17.43	617.8	51.16
252	4.8866	4.0677	1140.0	501.30	251.56	1.2632	105.4	17.50	615.5	51.76
254	4.9089	4.1251	1131.6	500.85	238.81	1.2624	104.5	17.58	613.0	52.38
256	4.9320	4.1843	1123.1	500.38	226.70	1.2616	103.6	17.66	610.6	53.01
258	4.9560	4.2452	1114.5	499.87	215.179	1.2608	102.7	17.73	608.1	53.65

Table 1 Saturation state – Continued (Temperature table)

t [°C]	T [K]	p_s [bar]	v' [$m^3\ kg^{-1}$]	v''	h'	h'' [$kJ\ kg^{-1}$]	Δh_v	s' [$kJ\ kg^{-1}\ K^{-1}$]	s''
260	533.15	46.9207	0.00127613	0.0421755	1134.83	2796.64	1661.82	2.8847	6.0017
262	535.15	48.4640	0.00128129	0.0407660	1144.78	2795.47	1650.68	2.9030	5.9875
264	537.15	50.0457	0.00128656	0.0394082	1154.79	2794.19	1639.40	2.9213	5.9733
266	539.15	51.6666	0.00129193	0.0380997	1164.84	2792.80	1627.96	2.9396	5.9590
268	541.15	53.3273	0.00129741	0.0368385	1174.94	2791.30	1616.36	2.9579	5.9448
270	543.15	55.0284	0.00130301	0.0356224	1185.09	2789.69	1604.60	2.9762	5.9304
272	545.15	56.7706	0.00130872	0.0344496	1195.30	2787.96	1592.66	2.9945	5.9160
274	547.15	58.5547	0.00131455	0.0333180	1205.55	2786.11	1580.56	3.0129	5.9016
276	549.15	60.3812	0.00132052	0.0322260	1215.87	2784.14	1568.28	3.0312	5.8871
278	551.15	62.2510	0.00132661	0.0311719	1226.24	2782.05	1555.81	3.0496	5.8725
280	553.15	64.1646	0.00133285	0.0301540	1236.67	2779.82	1543.15	3.0681	5.8578
282	555.15	66.1228	0.00133922	0.0291708	1247.16	2777.47	1530.30	3.0865	5.8431
284	557.15	68.1264	0.00134575	0.0282208	1257.72	2774.97	1517.25	3.1050	5.8283
286	559.15	70.1760	0.00135243	0.0273027	1268.34	2772.34	1504.00	3.1236	5.8134
288	561.15	72.2724	0.00135928	0.0264152	1279.03	2769.56	1490.53	3.1421	5.7984
290	563.15	74.4164	0.00136629	0.0255568	1289.80	2766.63	1476.84	3.1608	5.7832
292	565.15	76.6087	0.00137349	0.0247265	1300.63	2763.55	1462.92	3.1794	5.7680
294	567.15	78.8502	0.00138087	0.0239231	1311.54	2760.31	1448.76	3.1982	5.7526
296	569.15	81.1415	0.00138844	0.0231454	1322.54	2756.90	1434.37	3.2170	5.7372
298	571.15	83.4835	0.00139622	0.0223924	1333.61	2753.33	1419.72	3.2358	5.7215
300	573.15	85.8771	0.00140422	0.0216631	1344.77	2749.57	1404.80	3.2547	5.7058
305	578.15	92.0919	0.00142524	0.0199370	1373.07	2739.38	1366.30	3.3024	5.6656
310	583.15	98.6475	0.00144788	0.0183389	1402.00	2727.92	1325.92	3.3506	5.6243
315	588.15	105.558	0.00147239	0.0168557	1431.63	2715.08	1283.45	3.3994	5.5816
320	593.15	112.839	0.00149906	0.0154759	1462.05	2700.67	1238.62	3.4491	5.5373
325	598.15	120.505	0.00152830	0.0141887	1493.37	2684.48	1191.11	3.4997	5.4911
330	603.15	128.575	0.00156060	0.0129840	1525.74	2666.25	1140.51	3.5516	5.4425
335	608.15	137.067	0.00159667	0.0118522	1559.34	2645.60	1086.26	3.6048	5.3910
340	613.15	146.002	0.00163751	0.0107838	1594.45	2622.07	1027.62	3.6599	5.3359
345	618.15	155.401	0.00168460	0.0097698	1631.44	2595.01	963.57	3.7175	5.2763
350	623.15	165.292	0.00174007	0.0088009	1670.86	2563.59	892.73	3.7783	5.2109
355	628.15	175.701	0.00180780	0.0078660	1713.71	2526.45	812.74	3.8438	5.1377
360	633.15	186.664	0.00189451	0.0069449	1761.49	2480.99	719.50	3.9164	5.0527
365	638.15	198.222	0.00201561	0.0060044	1817.59	2422.00	604.41	4.0011	4.9482
370	643.15	210.434	0.00222209	0.0049462	1892.64	2333.50	440.86	4.1142	4.7996
371	644.15	212.964	0.00229020	0.0046914	1913.25	2307.45	394.20	4.1453	4.7573
372	645.15	215.528	0.00238170	0.0043985	1938.54	2274.69	336.15	4.1836	4.7046
373	646.15	218.132	0.00252643	0.0040212	1974.14	2227.55	253.42	4.2377	4.6299
373.946[a]	647.096	220.640	0.00310559		2087.55		0	4.4120	

[a] Critical temperature.

Table 1 Saturation state – Continued
(Temperature table)

t [°C]	c'_p [kJ kg^{-1} K^{-1}]	c''_p	w' [m s^{-1}]	w''	κ' [–]	κ''	η' [10^{-6} Pa s]	η''	λ' [10^{-3} W m^{-1} K^{-1}]	λ''
260	4.981	4.3080	1105.8	499.33	204.228	1.2600	101.8	17.81	605.6	54.30
262	5.006	4.3728	1097.0	498.77	193.814	1.2592	100.9	17.89	603.0	54.97
264	5.033	4.4398	1088.2	498.17	183.910	1.2583	100.1	17.97	600.4	55.66
266	5.061	4.5090	1079.2	497.53	174.488	1.2575	99.25	18.05	597.7	56.36
268	5.089	4.5806	1070.1	496.87	165.523	1.2567	98.41	18.13	595.0	57.08
270	5.119	4.6547	1061.0	496.16	156.993	1.2559	97.58	18.21	592.2	57.81
272	5.150	4.7316	1051.7	495.43	148.874	1.2550	96.76	18.29	589.4	58.57
274	5.182	4.8114	1042.3	494.65	141.145	1.2542	95.95	18.37	586.6	59.34
276	5.215	4.8942	1032.8	493.84	133.788	1.2533	95.14	18.46	583.7	60.14
278	5.250	4.9804	1023.2	493.00	126.782	1.2525	94.34	18.54	580.7	60.95
280	5.286	5.0701	1013.5	492.11	120.111	1.2516	93.55	18.63	577.7	61.79
282	5.324	5.1636	1003.7	491.18	113.759	1.2508	92.76	18.72	574.7	62.65
284	5.363	5.2611	993.72	490.21	107.709	1.2499	91.98	18.81	571.6	63.54
286	5.404	5.3629	983.64	489.20	101.947	1.2490	91.20	18.90	568.5	64.45
288	5.447	5.4693	973.44	488.14	96.459	1.2481	90.43	18.99	565.3	65.40
290	5.492	5.5806	963.12	487.04	91.232	1.2472	89.66	19.08	562.0	66.37
292	5.539	5.6971	952.67	485.89	86.255	1.2463	88.89	19.18	558.7	67.37
294	5.588	5.8192	942.10	484.69	81.516	1.2454	88.13	19.28	555.4	68.41
296	5.640	5.9473	931.42	483.45	77.005	1.2445	87.37	19.38	551.9	69.48
298	5.694	6.0818	920.61	482.16	72.710	1.2436	86.61	19.48	548.5	70.60
300	5.752	6.2231	909.69	480.81	68.623	1.2427	85.86	19.58	545.0	71.75
305	5.908	6.6096	881.91	477.21	59.257	1.2404	83.97	19.85	535.9	74.83
310	6.088	7.0513	853.50	473.27	51.002	1.2381	82.09	20.13	526.5	78.24
315	6.297	7.5610	824.43	468.96	43.732	1.2360	80.21	20.44	516.7	82.05
320	6.541	8.1575	794.58	464.25	37.325	1.2342	78.31	20.77	506.5	86.35
325	6.833	8.8689	763.55	459.12	31.656	1.2328	76.39	21.13	495.8	91.27
330	7.189	9.7381	730.70	453.52	26.609	1.2320	74.43	21.53	484.8	96.96
335	7.635	10.830	695.31	447.37	22.090	1.2320	72.42	21.97	473.3	103.7
340	8.217	12.241	657.03	440.59	18.056	1.2329	70.33	22.48	461.4	111.7
345	9.002	14.112	616.71	433.05	14.528	1.2352	68.14	23.06	449.1	121.7
350	10.102	16.641	576.91	424.63	11.572	1.2395	65.80	23.74	436.5	134.5
355	11.858	20.714	531.75	414.79	8.902	1.2449	63.23	24.57	423.8	151.7
360	14.874	27.570	483.70	402.76	6.616	1.2513	60.32	25.64	411.9	176.6
365	21.476	42.013	430.66	387.25	4.642	1.2600	56.81	27.12	404.0	217.7
370	47.096	93.401	370.01	364.77	2.928	1.2784	51.90	29.60	418.1	309.5
371	64.099	125.065	356.40	358.38	2.604	1.2855	50.51	30.40	432.6	347.0
372	101.160	190.326	342.02	350.51	2.279	1.2959	48.80	31.46	462.0	403.7
373	231.907	401.126	326.59	339.58	1.935	1.3146	46.38	33.11	535.0	507.0
373.946[a]	∞[b]		–[b]		–[b]		39.33[c]		810.6[c]	

[a] Critical temperature.

[b] At the critical point, IAPWS-IF97 does not yield accurate values for c_p, w, and κ.

[c] The industrial equations for η and λ, Eqs. (3.1) and (3.4), do not represent the enhancement in the near-critical region. If more accurate values are needed in this region, the scientific equations for η [31] and λ [35] should be used.

Table 2 Saturation state
(Pressure table)

The pressure table contains values on the saturated liquid ($'$) and saturated vapour ($''$) lines for the following thermodynamic properties in the pressure range from $p = 0.006\,112\,127$ bar up to the critical pressure $p_c = 220.64$ bar:

- Saturation temperature t_s
- Specific volume v
- Specific enthalpy h
- Specific enthalpy of vaporization Δh_v
- Specific entropy s
- Specific entropy of vaporization Δs_v

For given pressures p, the saturation temperatures t_s were calculated from the IAPWS-IF97 saturation-temperature equation, Eq. (2.14).

For pressures $p \leq 165.292$ bar and input values for p and t_s, the properties on the saturated-liquid and saturated-vapour lines were determined from the basic equations for regions 1 and 2, Eqs. (2.3) and (2.6).

For $p > 165.292$ bar and input values for p and t_s, the densities ρ' and ρ'' (and thus also the specific volumes v' and v'') were calculated by iterating the basic equation for region 3, Eq. (2.11). Then, with the values for (ρ', t_s) and (ρ'', t_s), the other thermodynamic properties were determined from the basic equation, Eq. (2.11). The values of the properties calculated in this manner differ in the last digits from the values of the first edition of the book. This difference is based on the fact that in the first edition all three properties t_s, ρ', and ρ'' were calculated from Eq. (2.11) via the so-called Maxwell criterion, i.e. without using the saturation-temperature equation, Eq. (2.14).

Further saturation properties are listed in Tables 1, 6, 11, and 15.

Table 2 Saturation state
(Pressure table)

p	t_s	v'	v''	h'	h''	Δh_v	s'	s''	Δs_v
[bar]	[°C]	[$m^3 kg^{-1}$]		[$kJ kg^{-1}$]			[$kJ kg^{-1} K^{-1}$]		
0.006112127	0	0.00100021	206.140	−0.04159	2500.89	2500.93	−0.0001545	9.1558	9.1559
0.006116570[a]	0.01	0.00100021	205.997	0.0006118	2500.91	2500.91	0	9.1555	9.1555
0.007	1.88090	0.00100011	181.223	7.88979	2504.35	2496.46	0.028782	9.1058	9.0770
0.008	3.76142	0.00100007	159.646	15.8087	2507.80	2491.99	0.057477	9.0567	8.9992
0.009	5.44443	0.00100009	142.763	22.8881	2510.89	2488.00	0.082965	9.0135	8.9305
0.01	6.96963	0.00100014	129.183	29.2982	2513.68	2484.38	0.10591	8.9749	8.8690
0.02	17.4953	0.00100136	66.9896	73.4346	2532.91	2459.48	0.26058	8.7227	8.4621
0.03	24.0799	0.00100277	45.6550	100.990	2544.88	2443.89	0.35433	8.5766	8.2222
0.04	28.9615	0.00100410	34.7925	121.404	2553.71	2432.31	0.42245	8.4735	8.0510
0.05	32.8755	0.00100532	28.1863	137.765	2560.77	2423.00	0.47625	8.3939	7.9177
0.06	36.1603	0.00100645	23.7342	151.494	2566.67	2415.17	0.52087	8.3291	7.8083
0.07	39.0009	0.00100749	20.5252	163.366	2571.76	2408.39	0.55908	8.2746	7.7155
0.08	41.5101	0.00100847	18.0994	173.852	2576.24	2402.39	0.59253	8.2274	7.6349
0.09	43.7618	0.00100939	16.1997	183.262	2580.25	2396.99	0.62233	8.1859	7.5636
0.1	45.8075	0.00101026	14.6706	191.812	2583.89	2392.07	0.64922	8.1489	7.4997
0.2	60.0586	0.00101714	7.64815	251.400	2608.95	2357.55	0.83195	7.9072	7.0753
0.3	69.0954	0.00102222	5.22856	289.229	2624.55	2335.32	0.94394	7.7675	6.8235
0.4	75.8568	0.00102636	3.99311	317.566	2636.05	2318.48	1.0259	7.6690	6.6431
0.5	81.3167	0.00102991	3.24015	340.476	2645.21	2304.74	1.0910	7.5930	6.5020
0.6	85.9258	0.00103306	2.73183	359.837	2652.85	2293.02	1.1452	7.5311	6.3859
0.7	89.9315	0.00103589	2.36490	376.680	2659.42	2282.74	1.1919	7.4790	6.2871
0.8	93.4854	0.00103849	2.08719	391.639	2665.18	2273.54	1.2328	7.4339	6.2011
0.9	96.6870	0.00104090	1.86946	405.128	2670.31	2265.19	1.2694	7.3942	6.1248
1.0	99.6059	0.00104315	1.69402	417.436	2674.95	2257.51	1.3026	7.3588	6.0562
1.01325[b]	99.9743	0.00104344	1.67330	418.991	2675.53	2256.54	1.3067	7.3544	6.0477
1.1	102.292	0.00104526	1.54955	428.775	2679.18	2250.40	1.3328	7.3268	5.9940
1.2	104.784	0.00104727	1.42845	439.299	2683.06	2243.76	1.3608	7.2976	5.9369
1.3	107.109	0.00104917	1.32541	449.132	2686.65	2237.52	1.3867	7.2708	5.8842
1.4	109.292	0.00105098	1.23665	458.367	2689.99	2231.62	1.4109	7.2460	5.8352
1.5	111.350	0.00105272	1.15936	467.081	2693.11	2226.03	1.4335	7.2229	5.7894
1.6	113.298	0.00105440	1.09143	475.336	2696.04	2220.71	1.4549	7.2014	5.7464
1.7	115.149	0.00105601	1.03124	483.184	2698.81	2215.62	1.4752	7.1811	5.7059
1.8	116.912	0.00105756	0.977534	490.668	2701.42	2210.75	1.4944	7.1620	5.6677
1.9	118.597	0.00105906	0.929299	497.825	2703.89	2206.07	1.5127	7.1440	5.6313
2.0	120.212	0.00106052	0.885735	504.684	2706.24	2201.56	1.5301	7.1269	5.5968
2.1	121.761	0.00106193	0.846187	511.273	2708.48	2197.21	1.5468	7.1106	5.5638
2.2	123.251	0.00106331	0.810119	517.615	2710.62	2193.00	1.5628	7.0951	5.5323
2.3	124.688	0.00106464	0.777086	523.731	2712.66	2188.93	1.5782	7.0802	5.5021
2.4	126.074	0.00106595	0.746716	529.637	2714.62	2184.98	1.5930	7.0660	5.4731
2.5	127.414	0.00106722	0.718697	535.350	2716.50	2181.15	1.6072	7.0524	5.4452
2.6	128.711	0.00106846	0.692763	540.884	2718.31	2177.42	1.6210	7.0393	5.4183
2.7	129.968	0.00106968	0.668687	546.251	2720.04	2173.79	1.6343	7.0267	5.3924
2.8	131.188	0.00107087	0.646274	551.462	2721.72	2170.26	1.6472	7.0146	5.3674
2.9	132.373	0.00107203	0.625355	556.527	2723.33	2166.81	1.6597	7.0029	5.3432
3.0	133.525	0.00107318	0.605785	561.455	2724.89	2163.44	1.6718	6.9916	5.3198
3.1	134.647	0.00107430	0.587436	566.255	2726.40	2160.14	1.6835	6.9806	5.2971
3.2	135.740	0.00107540	0.570196	570.935	2727.86	2156.92	1.6950	6.9700	5.2751
3.3	136.806	0.00107648	0.553966	575.500	2729.27	2153.77	1.7061	6.9597	5.2537
3.4	137.845	0.00107754	0.538658	579.957	2730.64	2150.68	1.7169	6.9498	5.2329

[a] Pressure at the triple point.

[b] This pressure corresponds to 1 atm.

Table 2 Saturation state – Continued
(Pressure table)

p	t_s	v'	v''	h'	h''	Δh_v	s'	s''	Δs_v
[bar]	[°C]	[$m^3\,kg^{-1}$]		[$kJ\,kg^{-1}$]			[$kJ\,kg^{-1}\,K^{-1}$]		
3.5	138.861	0.00107858	0.524196	584.311	2731.97	2147.65	1.7275	6.9401	5.2126
3.6	139.853	0.00107961	0.510510	588.569	2733.25	2144.68	1.7378	6.9307	5.1929
3.7	140.823	0.00108062	0.497539	592.735	2734.51	2141.77	1.7478	6.9215	5.1737
3.8	141.773	0.00108161	0.485228	596.813	2735.72	2138.91	1.7576	6.9126	5.1550
3.9	142.702	0.00108259	0.473527	600.808	2736.91	2136.10	1.7672	6.9039	5.1367
4.0	143.613	0.00108356	0.462392	604.723	2738.06	2133.33	1.7766	6.8954	5.1188
4.1	144.505	0.00108451	0.451781	608.563	2739.18	2130.62	1.7858	6.8872	5.1014
4.2	145.380	0.00108545	0.441658	612.330	2740.27	2127.94	1.7948	6.8791	5.0843
4.3	146.238	0.00108638	0.431990	616.027	2741.33	2125.31	1.8036	6.8712	5.0676
4.4	147.081	0.00108729	0.422747	619.657	2742.37	2122.72	1.8122	6.8635	5.0513
4.5	147.908	0.00108820	0.413900	623.224	2743.39	2120.16	1.8206	6.8560	5.0353
4.6	148.721	0.00108909	0.405425	626.730	2744.38	2117.65	1.8289	6.8486	5.0197
4.7	149.519	0.00108997	0.397299	630.177	2745.34	2115.16	1.8371	6.8414	5.0043
4.8	150.305	0.00109084	0.389499	633.567	2746.28	2112.72	1.8450	6.8343	4.9892
4.9	151.077	0.00109170	0.382007	636.902	2747.21	2110.30	1.8529	6.8274	4.9745
5.0	151.836	0.00109256	0.374804	640.185	2748.11	2107.92	1.8606	6.8206	4.9600
5.5	155.462	0.00109668	0.342592	655.877	2752.33	2096.45	1.8972	6.7885	4.8913
6.0	158.832	0.00110061	0.315575	670.501	2756.14	2085.64	1.9311	6.7592	4.8281
6.5	161.986	0.00110436	0.292581	684.216	2759.60	2075.38	1.9626	6.7321	4.7695
7.0	164.953	0.00110797	0.272764	697.143	2762.75	2065.61	1.9921	6.7070	4.7149
7.5	167.755	0.00111144	0.255503	709.384	2765.64	2056.26	2.0198	6.6835	4.6637
8.0	170.414	0.00111479	0.240328	721.018	2768.30	2047.28	2.0460	6.6615	4.6156
8.5	172.943	0.00111803	0.226878	732.113	2770.76	2038.65	2.0708	6.6408	4.5700
9.0	175.358	0.00112118	0.214874	742.725	2773.04	2030.31	2.0944	6.6212	4.5268
9.5	177.669	0.00112425	0.204090	752.901	2775.15	2022.25	2.1169	6.6027	4.4857
10.0	179.886	0.00112723	0.194349	762.683	2777.12	2014.44	2.1384	6.5850	4.4465
10.5	182.017	0.00113015	0.185504	772.105	2778.95	2006.85	2.1591	6.5681	4.4091
11.0	184.070	0.00113299	0.177436	781.198	2780.67	1999.47	2.1789	6.5520	4.3731
11.5	186.050	0.00113578	0.170045	789.988	2782.27	1992.28	2.1979	6.5365	4.3386
12.0	187.965	0.00113850	0.163250	798.499	2783.77	1985.27	2.2163	6.5217	4.3054
12.5	189.817	0.00114118	0.156979	806.751	2785.17	1978.42	2.2340	6.5074	4.2734
13.0	191.613	0.00114380	0.151175	814.764	2786.49	1971.73	2.2512	6.4936	4.2425
13.5	193.355	0.00114638	0.145786	822.552	2787.73	1965.18	2.2678	6.4804	4.2126
14.0	195.047	0.00114892	0.140768	830.132	2788.89	1958.76	2.2839	6.4675	4.1836
14.5	196.693	0.00115141	0.136084	837.516	2789.98	1952.47	2.2995	6.4551	4.1556
15.0	198.295	0.00115387	0.131702	844.717	2791.01	1946.29	2.3147	6.4431	4.1284
15.5	199.856	0.00115629	0.127593	851.745	2791.97	1940.23	2.3294	6.4314	4.1019
16.0	201.378	0.00115868	0.123732	858.610	2792.88	1934.27	2.3438	6.4200	4.0762
16.5	202.864	0.00116103	0.120097	865.322	2793.73	1928.41	2.3578	6.4090	4.0512
17.0	204.315	0.00116336	0.116668	871.888	2794.53	1922.64	2.3715	6.3983	4.0268
17.5	205.733	0.00116565	0.113428	878.316	2795.28	1916.96	2.3848	6.3878	4.0030
18.0	207.120	0.00116792	0.110362	884.614	2795.99	1911.37	2.3978	6.3776	3.9798
18.5	208.477	0.00117016	0.107456	890.788	2796.65	1905.86	2.4105	6.3676	3.9571
19.0	209.806	0.00117238	0.104698	896.844	2797.26	1900.42	2.4229	6.3579	3.9350
19.5	211.108	0.00117458	0.102076	902.786	2797.84	1895.06	2.4351	6.3484	3.9133

Table 2 Saturation state – Continued (Pressure table)

p [bar]	t_s [°C]	v' [$m^3\,kg^{-1}$]	v'' [$m^3\,kg^{-1}$]	h' [$kJ\,kg^{-1}$]	h'' [$kJ\,kg^{-1}$]	Δh_v [$kJ\,kg^{-1}$]	s' [$kJ\,kg^{-1}\,K^{-1}$]	s'' [$kJ\,kg^{-1}\,K^{-1}$]	Δs_v [$kJ\,kg^{-1}\,K^{-1}$]
20.0	212.385	0.00117675	0.0995805	908.622	2798.38	1889.76	2.4470	6.3392	3.8921
20.5	213.637	0.00117890	0.0972026	914.355	2798.89	1884.53	2.4587	6.3301	3.8714
21.0	214.865	0.00118103	0.0949339	919.989	2799.36	1879.37	2.4701	6.3212	3.8511
21.5	216.071	0.00118314	0.0927671	925.530	2799.80	1874.27	2.4814	6.3125	3.8311
22.0	217.256	0.00118524	0.0906953	930.981	2800.20	1869.22	2.4924	6.3040	3.8116
22.5	218.420	0.00118731	0.0887123	936.345	2800.58	1864.23	2.5032	6.2956	3.7924
23.0	219.564	0.00118937	0.0868125	941.626	2800.92	1859.30	2.5138	6.2874	3.7736
23.5	220.689	0.00119141	0.0849906	946.827	2801.24	1854.42	2.5242	6.2793	3.7551
24.0	221.795	0.00119343	0.0832421	951.952	2801.54	1849.58	2.5344	6.2714	3.7370
24.5	222.885	0.00119544	0.0815623	957.003	2801.80	1844.80	2.5445	6.2636	3.7191
25.0	223.956	0.00119744	0.0799474	961.983	2802.04	1840.06	2.5544	6.2560	3.7015
25.5	225.012	0.00119942	0.0783935	966.895	2802.26	1835.37	2.5642	6.2485	3.6843
26.0	226.052	0.00120139	0.0768973	971.740	2802.45	1830.71	2.5738	6.2411	3.6673
26.5	227.076	0.00120334	0.0754556	976.521	2802.63	1826.11	2.5832	6.2338	3.6506
27.0	228.086	0.00120528	0.0740653	981.241	2802.78	1821.54	2.5925	6.2266	3.6341
27.5	229.081	0.00120721	0.0727238	985.901	2802.91	1817.01	2.6017	6.2196	3.6179
28.0	230.063	0.00120913	0.0714285	990.503	2803.02	1812.51	2.6107	6.2126	3.6019
28.5	231.031	0.00121104	0.0701770	995.050	2803.11	1808.06	2.6196	6.2058	3.5861
29.0	231.986	0.00121294	0.0689671	999.542	2803.18	1803.63	2.6284	6.1990	3.5706
29.5	232.928	0.00121482	0.0677968	1003.98	2803.23	1799.25	2.6371	6.1924	3.5553
30.0	233.858	0.00121670	0.0666641	1008.37	2803.26	1794.89	2.6456	6.1858	3.5402
30.5	234.777	0.00121857	0.0655672	1012.71	2803.28	1790.57	2.6541	6.1793	3.5253
31.0	235.684	0.00122042	0.0645044	1017.00	2803.28	1786.28	2.6624	6.1729	3.5105
31.5	236.580	0.00122227	0.0634741	1021.25	2803.27	1782.02	2.6706	6.1666	3.4960
32.0	237.464	0.00122411	0.0624748	1025.45	2803.24	1777.79	2.6787	6.1604	3.4817
32.5	238.339	0.00122594	0.0615052	1029.61	2803.19	1773.58	2.6867	6.1542	3.4675
33.0	239.203	0.00122777	0.0605639	1033.72	2803.13	1769.41	2.6946	6.1481	3.4535
33.5	240.057	0.00122958	0.0596497	1037.79	2803.05	1765.26	2.7025	6.1421	3.4397
34.0	240.901	0.00123139	0.0587614	1041.83	2802.96	1761.14	2.7102	6.1362	3.4260
34.5	241.736	0.00123319	0.0578979	1045.82	2802.86	1757.04	2.7178	6.1303	3.4125
35.0	242.562	0.00123498	0.0570582	1049.78	2802.74	1752.97	2.7254	6.1245	3.3991
35.5	243.378	0.00123677	0.0562413	1053.69	2802.61	1748.92	2.7329	6.1188	3.3859
36.0	244.186	0.00123855	0.0554463	1057.57	2802.47	1744.90	2.7403	6.1131	3.3728
36.5	244.986	0.00124032	0.0546722	1061.42	2802.31	1740.89	2.7476	6.1075	3.3599
37.0	245.776	0.00124209	0.0539183	1065.23	2802.15	1736.91	2.7548	6.1019	3.3471
37.5	246.559	0.00124385	0.0531837	1069.01	2801.97	1732.96	2.7619	6.0964	3.3345
38.0	247.334	0.00124560	0.0524678	1072.76	2801.78	1729.02	2.7690	6.0910	3.3219
38.5	248.101	0.00124735	0.0517698	1076.47	2801.57	1725.10	2.7760	6.0856	3.3095
39.0	248.861	0.00124910	0.0510890	1080.15	2801.36	1721.21	2.7830	6.0802	3.2973
39.5	249.613	0.00125084	0.0504248	1083.80	2801.13	1717.33	2.7898	6.0749	3.2851
40.0	250.358	0.00125257	0.0497766	1087.43	2800.90	1713.47	2.7967	6.0697	3.2731
40.5	251.095	0.00125430	0.0491438	1091.02	2800.65	1709.63	2.8034	6.0645	3.2611
41.0	251.826	0.00125602	0.0485259	1094.58	2800.39	1705.81	2.8101	6.0594	3.2493
41.5	252.550	0.00125774	0.0479223	1098.12	2800.13	1702.01	2.8167	6.0543	3.2376
42.0	253.267	0.00125946	0.0473326	1101.63	2799.85	1698.22	2.8232	6.0492	3.2260

Table 2 **Saturation state** – Continued
(Pressure table)

p [bar]	t_s [°C]	v' [$m^3\,kg^{-1}$]	v'' [$m^3\,kg^{-1}$]	h' [$kJ\,kg^{-1}$]	h'' [$kJ\,kg^{-1}$]	Δh_v [$kJ\,kg^{-1}$]	s' [$kJ\,kg^{-1}\,K^{-1}$]	s'' [$kJ\,kg^{-1}\,K^{-1}$]	Δs_v [$kJ\,kg^{-1}\,K^{-1}$]
42.5	253.978	0.00126117	0.0467562	1105.11	2799.57	1694.46	2.8297	6.0442	3.2145
43.0	254.683	0.00126288	0.0461927	1108.57	2799.27	1690.70	2.8362	6.0393	3.2031
43.5	255.381	0.00126458	0.0456417	1112.00	2798.97	1686.97	2.8425	6.0343	3.1918
44.0	256.073	0.00126628	0.0451027	1115.40	2798.65	1683.25	2.8488	6.0294	3.1806
44.5	256.759	0.00126797	0.0445754	1118.79	2798.33	1679.54	2.8551	6.0246	3.1695
45.0	257.439	0.00126966	0.0440593	1122.14	2798.00	1675.85	2.8613	6.0198	3.1585
45.5	258.114	0.00127135	0.0435542	1125.48	2797.66	1672.18	2.8675	6.0150	3.1475
46.0	258.783	0.00127304	0.0430596	1128.79	2797.31	1668.52	2.8736	6.0103	3.1367
46.5	259.446	0.00127472	0.0425753	1132.08	2796.95	1664.87	2.8797	6.0056	3.1260
47.0	260.104	0.00127639	0.0421009	1135.34	2796.59	1661.24	2.8857	6.0010	3.1153
47.5	260.757	0.00127807	0.0416361	1138.59	2796.21	1657.62	2.8916	5.9963	3.1047
48.0	261.404	0.00127974	0.0411806	1141.81	2795.83	1654.02	2.8975	5.9917	3.0942
48.5	262.046	0.00128141	0.0407341	1145.01	2795.44	1650.43	2.9034	5.9872	3.0838
49.0	262.683	0.00128308	0.0402964	1148.20	2795.04	1646.85	2.9092	5.9827	3.0734
49.5	263.316	0.00128474	0.0398672	1151.36	2794.64	1643.28	2.9150	5.9782	3.0632
50	263.943	0.00128641	0.0394463	1154.50	2794.23	1639.73	2.9207	5.9737	3.0530
51	265.183	0.00128972	0.0386282	1160.73	2793.38	1632.65	2.9321	5.9649	3.0328
52	266.405	0.00129303	0.0378403	1166.88	2792.51	1625.62	2.9433	5.9562	3.0129
53	267.610	0.00129633	0.0370811	1172.97	2791.60	1618.64	2.9543	5.9475	2.9933
54	268.797	0.00129962	0.0363488	1178.98	2790.67	1611.69	2.9652	5.9390	2.9739
55	269.967	0.00130291	0.0356422	1184.92	2789.72	1604.79	2.9759	5.9307	2.9548
56	271.121	0.00130619	0.0349597	1190.81	2788.74	1597.93	2.9865	5.9224	2.9359
57	272.260	0.00130947	0.0343003	1196.63	2787.73	1591.10	2.9969	5.9141	2.9173
58	273.383	0.00131274	0.0336627	1202.39	2786.70	1584.31	3.0072	5.9060	2.8988
59	274.492	0.00131601	0.0330458	1208.09	2785.64	1577.55	3.0174	5.8980	2.8806
60	275.586	0.00131927	0.0324487	1213.73	2784.56	1570.83	3.0274	5.8901	2.8626
61	276.667	0.00132253	0.0318703	1219.32	2783.46	1564.14	3.0374	5.8822	2.8448
62	277.734	0.00132579	0.0313098	1224.86	2782.33	1557.48	3.0472	5.8744	2.8272
63	278.788	0.00132905	0.0307664	1230.34	2781.19	1550.84	3.0569	5.8667	2.8098
64	279.830	0.00133231	0.0302392	1235.78	2780.02	1544.24	3.0665	5.8591	2.7926
65	280.859	0.00133557	0.0297276	1241.17	2778.83	1537.66	3.0760	5.8515	2.7755
66	281.876	0.00133882	0.0292308	1246.51	2777.62	1531.11	3.0854	5.8440	2.7586
67	282.881	0.00134208	0.0287482	1251.81	2776.39	1524.58	3.0947	5.8366	2.7419
68	283.875	0.00134534	0.0282792	1257.06	2775.13	1518.07	3.1039	5.8292	2.7253
69	284.858	0.00134860	0.0278231	1262.27	2773.86	1511.59	3.1130	5.8219	2.7089
70	285.830	0.00135186	0.0273796	1267.44	2772.57	1505.13	3.1220	5.8146	2.6926
71	286.791	0.00135512	0.0269479	1272.57	2771.26	1498.69	3.1309	5.8074	2.6765
72	287.743	0.00135839	0.0265277	1277.65	2769.93	1492.27	3.1398	5.8003	2.6605
73	288.684	0.00136165	0.0261185	1282.70	2768.58	1485.87	3.1485	5.7932	2.6447
74	289.615	0.00136493	0.0257198	1287.72	2767.21	1479.49	3.1572	5.7862	2.6290
75	290.537	0.00136820	0.0253313	1292.70	2765.82	1473.12	3.1658	5.7792	2.6134
76	291.449	0.00137149	0.0249525	1297.64	2764.41	1466.78	3.1743	5.7722	2.5979
77	292.352	0.00137477	0.0245831	1302.55	2762.99	1460.44	3.1827	5.7653	2.5826
78	293.247	0.00137806	0.0242227	1307.42	2761.55	1454.12	3.1911	5.7584	2.5673
79	294.132	0.00138136	0.0238709	1312.27	2760.09	1447.82	3.1994	5.7516	2.5522

Table 2 Saturation state – Continued (Pressure table)

p [bar]	t_s [°C]	v' [m^3 kg^{-1}]	v''	h'	h'' [kJ kg^{-1}]	Δh_v	s'	s'' [kJ kg^{-1} K^{-1}]	Δs_v
80	295.009	0.00138466	0.0235275	1317.08	2758.61	1441.53	3.2077	5.7448	2.5372
81	295.878	0.00138797	0.0231922	1321.86	2757.12	1435.25	3.2158	5.7381	2.5223
82	296.738	0.00139129	0.0228646	1326.61	2755.60	1428.99	3.2239	5.7314	2.5075
83	297.591	0.00139461	0.0225446	1331.34	2754.07	1422.74	3.2320	5.7247	2.4928
84	298.435	0.00139795	0.0222317	1336.03	2752.52	1416.49	3.2399	5.7181	2.4782
85	299.272	0.00140129	0.0219258	1340.70	2750.96	1410.26	3.2478	5.7115	2.4637
86	300.102	0.00140464	0.0216266	1345.34	2749.38	1404.04	3.2557	5.7050	2.4493
87	300.924	0.00140799	0.0213340	1349.96	2747.78	1397.82	3.2635	5.6984	2.4349
88	301.738	0.00141136	0.0210476	1354.54	2746.16	1391.62	3.2712	5.6919	2.4207
89	302.546	0.00141474	0.0207673	1359.11	2744.53	1385.42	3.2789	5.6855	2.4065
90	303.347	0.00141812	0.0204929	1363.65	2742.88	1379.23	3.2866	5.6790	2.3924
91	304.141	0.00142152	0.0202242	1368.17	2741.22	1373.05	3.2942	5.6726	2.3784
92	304.928	0.00142493	0.0199610	1372.66	2739.53	1366.87	3.3017	5.6662	2.3645
93	305.709	0.00142834	0.0197031	1377.14	2737.83	1360.70	3.3092	5.6598	2.3507
94	306.483	0.00143177	0.0194503	1381.59	2736.12	1354.53	3.3166	5.6535	2.3369
95	307.251	0.00143522	0.0192026	1386.02	2734.38	1348.37	3.3240	5.6472	2.3232
96	308.013	0.00143867	0.0189597	1390.43	2732.64	1342.21	3.3313	5.6409	2.3095
97	308.768	0.00144214	0.0187214	1394.81	2730.87	1336.06	3.3386	5.6346	2.2960
98	309.518	0.00144562	0.0184878	1399.18	2729.09	1329.90	3.3459	5.6283	2.2824
99	310.262	0.00144911	0.0182585	1403.54	2727.29	1323.75	3.3531	5.6221	2.2690
100	310.999	0.00145262	0.0180336	1407.87	2725.47	1317.61	3.3603	5.6159	2.2556
105	314.606	0.00147038	0.0169687	1429.27	2716.14	1286.88	3.3956	5.5850	2.1895
110	318.081	0.00148855	0.0159939	1450.28	2706.39	1256.12	3.4300	5.5545	2.1246
115	321.436	0.00150718	0.0150972	1470.95	2696.21	1225.26	3.4636	5.5243	2.0607
120	324.678	0.00152633	0.0142689	1491.33	2685.58	1194.26	3.4965	5.4941	1.9977
125	327.816	0.00154607	0.0135006	1511.46	2674.49	1163.02	3.5288	5.4640	1.9353
130	330.857	0.00156649	0.0127851	1531.40	2662.89	1131.49	3.5606	5.4339	1.8733
135	333.806	0.00158766	0.0121163	1551.19	2650.77	1099.58	3.5920	5.4036	1.8116
140	336.669	0.00160971	0.0114889	1570.88	2638.09	1067.21	3.6230	5.3730	1.7500
145	339.452	0.00163276	0.0108981	1590.51	2624.81	1034.29	3.6538	5.3422	1.6884
150	342.158	0.00165696	0.0103401	1610.15	2610.86	1000.71	3.6844	5.3108	1.6264
155	344.792	0.00168249	0.00981114	1629.85	2596.22	966.37	3.7150	5.2789	1.5638
160	347.357	0.00170954	0.00930813	1649.67	2580.80	931.13	3.7457	5.2463	1.5006
165	349.856	0.00173833	0.00882826	1669.68	2564.57	894.88	3.7765	5.2129	1.4364
170	352.293	0.00176934	0.00836934	1690.04	2547.41	857.38	3.8077	5.1785	1.3708
175	354.671	0.00180286	0.00792681	1710.76	2529.11	818.35	3.8393	5.1428	1.3035
180	356.992	0.00183949	0.00749867	1732.02	2509.53	777.51	3.8717	5.1055	1.2339
185	359.258	0.00188000	0.00708178	1753.99	2488.41	734.42	3.9050	5.0663	1.1613
190	361.471	0.00192545	0.00667261	1776.89	2465.41	688.52	3.9396	5.0246	1.0849
195	363.633	0.00197747	0.00626677	1801.08	2440.00	638.92	3.9762	4.9795	1.0034
200	365.746	0.00203865	0.00585828	1827.10	2411.39	584.29	4.0154	4.9299	0.91452
205	367.811	0.00211358	0.00543778	1855.90	2378.16	522.26	4.0588	4.8736	0.81481
210	369.827	0.00221186	0.00498768	1889.40	2337.54	448.15	4.1093	4.8062	0.69699
215	371.795	0.00236016	0.00446300	1932.81	2282.18	349.38	4.1749	4.7166	0.54171
220	373.707	0.00275039	0.00357662	2021.92	2164.18	142.27	4.3109	4.5308	0.21993
220.640[a]	373.946	0.00310559		2087.55		0	4.4120		0

[a] Pressure at the critical point.

Table 3 Single-phase region
(0 °C to 800 °C)

This table contains values for the following thermodynamic and transport properties in the single-phase region for temperatures from 0 °C to 800 °C and for pressures from 0.006 112 127 bar to 1000 bar (regions 1 to 3 of IAPWS-IF97):

- Specific volume v
- Specific enthalpy h
- Specific entropy s
- Specific isobaric heat capacity c_p
- Speed of sound w
- Isentropic exponent κ
- Dynamic viscosity η
- Thermal conductivity λ

The *thermodynamic* properties v, h, s, c_p, w, and κ were calculated from the IAPWS-IF97 basic equations, Eqs. (2.3), (2.6), and (2.11). The calculation of the saturation properties is described in the introduction to Table 1. Values for the properties v, h, s, c_p, and w for temperatures above 800 °C up to 2000 °C and up to 500 bar (high temperature region 5) are listed in Table 4.

The *transport* properties dynamic viscosity η and thermal conductivity λ were calculated from the equations for industrial applications, Eq. (3.1), and industrial use, Eq. (3.4). The values for the density ρ needed for these equations were determined from the IAPWS-IF97 basic equations, see above.

The values for the thermal conductivity beyond the range of validity of the λ equation for industrial use were obtained by extrapolating Eq. (3.4) as described in Sec. 3.2 under the subpoint “Range of Validity.”

Table 3 Single-phase region
(0 °C to 800 °C)

$p =$ **0.006112127 bar**

t [°C]	v [$m^3\,kg^{-1}$]	h [$kJ\,kg^{-1}$]	s [$kJ\,kg^{-1}\,K^{-1}$]	c_p [$kJ\,kg^{-1}\,K^{-1}$]	w [$m\,s^{-1}$]	κ [–]	η [10^{-6} Pa s]	λ [$10^{-3}\,W\,m^{-1}\,K^{-1}$]
$t_s = 0$ °C				**Saturation**				
Liquid	0.00100021	– 0.041586	– 0.000154542	4.2199	1402.3	3216538	1792.0	562.0
Vapour	206.140	2500.89	9.1558	1.8882	408.88	1.3269	8.945	16.49
2	207.657	2504.66	9.1695	1.8822	410.50	1.3277	9.003	16.64
4	209.173	2508.42	9.1831	1.8780	412.08	1.3282	9.062	16.78
6	210.688	2512.18	9.1966	1.8750	413.63	1.3286	9.121	16.92
8	212.203	2515.92	9.2100	1.8730	415.15	1.3288	9.180	17.07
10	213.717	2519.67	9.2233	1.8716	416.65	1.3289	9.240	17.21
12	215.231	2523.41	9.2364	1.8706	418.13	1.3290	9.301	17.36
14	216.744	2527.15	9.2495	1.8700	419.60	1.3290	9.362	17.50
16	218.258	2530.89	9.2625	1.8696	421.06	1.3290	9.424	17.65
18	219.771	2534.63	9.2754	1.8694	422.51	1.3290	9.486	17.79
20	221.284	2538.37	9.2882	1.8693	423.95	1.3289	9.549	17.94
25	225.065	2547.71	9.3198	1.8695	427.53	1.3287	9.707	18.31
30	228.846	2557.06	9.3509	1.8701	431.07	1.3285	9.869	18.69
35	232.626	2566.42	9.3815	1.8708	434.57	1.3282	10.03	19.06
40	236.406	2575.77	9.4116	1.8718	438.03	1.3279	10.20	19.44
45	240.185	2585.13	9.4413	1.8728	441.47	1.3276	10.37	19.82
50	243.964	2594.50	9.4705	1.8740	444.87	1.3272	10.54	20.21
55	247.743	2603.87	9.4993	1.8753	448.25	1.3269	10.71	20.60
60	251.521	2613.25	9.5276	1.8767	451.59	1.3265	10.89	20.99
65	255.299	2622.64	9.5556	1.8781	454.90	1.3262	11.06	21.39
70	259.077	2632.03	9.5832	1.8797	458.19	1.3258	11.24	21.79
75	262.855	2641.44	9.6104	1.8813	461.44	1.3254	11.42	22.19
80	266.632	2650.85	9.6372	1.8831	464.67	1.3249	11.60	22.59
85	270.409	2660.27	9.6637	1.8849	467.88	1.3245	11.78	23.00
90	274.186	2669.70	9.6898	1.8867	471.05	1.3240	11.97	23.41
95	277.963	2679.14	9.7157	1.8887	474.20	1.3236	12.15	23.83
100	281.740	2688.58	9.7411	1.8907	477.33	1.3231	12.34	24.25
110	289.294	2707.51	9.7912	1.8949	483.51	1.3221	12.71	25.09
120	296.847	2726.48	9.8401	1.8993	489.59	1.3211	13.09	25.95
130	304.399	2745.50	9.8878	1.9039	495.58	1.3201	13.48	26.82
140	311.952	2764.56	9.9346	1.9087	501.49	1.3190	13.86	27.70
150	319.504	2783.67	9.9803	1.9137	507.31	1.3179	14.25	28.59
160	327.056	2802.84	10.025	1.9188	513.05	1.3168	14.65	29.50
170	334.608	2822.05	10.069	1.9240	518.72	1.3156	15.04	30.41
180	342.160	2841.32	10.112	1.9294	524.31	1.3145	15.44	31.34
190	349.712	2860.64	10.154	1.9348	529.83	1.3133	15.84	32.28
200	357.264	2880.01	10.195	1.9404	535.28	1.3121	16.24	33.24
210	364.816	2899.45	10.236	1.9460	540.66	1.3109	16.64	34.20
220	372.367	2918.93	10.276	1.9517	545.98	1.3097	17.05	35.18
230	379.919	2938.48	10.315	1.9575	551.23	1.3085	17.45	36.17
240	387.470	2958.08	10.354	1.9633	556.43	1.3073	17.86	37.17

Table 3 Single-phase region – Continued (0 °C to 800 °C)

p = 0.006112127 bar								
t	*v*	*h*	*s*	c_p	*w*	*κ*	*η*	*λ*
[°C]	[$m^3\ kg^{-1}$]	[$kJ\ kg^{-1}$]	[$kJ\ kg^{-1}\ K^{-1}$]	[$kJ\ kg^{-1}\ K^{-1}$]	[$m\ s^{-1}$]	[–]	[10^{-6} Pa s]	[$10^{-3}\ W\ m^{-1}\ K^{-1}$]
250	395.022	2977.75	10.392	1.9692	561.56	1.3061	18.27	38.18
260	402.573	2997.47	10.429	1.9752	566.64	1.3049	18.68	39.20
270	410.125	3017.25	10.466	1.9812	571.67	1.3037	19.09	40.23
280	417.676	3037.09	10.502	1.9873	576.64	1.3025	19.50	41.28
290	425.227	3057.00	10.538	1.9934	581.56	1.3013	19.91	42.33
300	432.779	3076.96	10.573	1.9996	586.43	1.3001	20.32	43.40
310	440.330	3096.99	10.608	2.0058	591.25	1.2989	20.74	44.48
320	447.881	3117.08	10.642	2.0120	596.02	1.2977	21.15	45.56
330	455.432	3137.23	10.675	2.0183	600.74	1.2965	21.56	46.66
340	462.984	3157.44	10.709	2.0247	605.42	1.2953	21.98	47.77
350	470.535	3177.72	10.741	2.0310	610.06	1.2941	22.39	48.89
360	478.086	3198.07	10.774	2.0374	614.65	1.2929	22.80	50.02
370	485.637	3218.47	10.806	2.0439	619.20	1.2917	23.22	51.16
380	493.188	3238.94	10.837	2.0504	623.70	1.2905	23.63	52.31
390	500.740	3259.48	10.869	2.0569	628.17	1.2893	24.04	53.47
400	508.291	3280.08	10.899	2.0635	632.60	1.2881	24.46	54.64
410	515.842	3300.75	10.930	2.0701	636.99	1.2869	24.87	55.82
420	523.393	3321.48	10.960	2.0767	641.34	1.2858	25.28	57.00
430	530.944	3342.28	10.990	2.0834	645.65	1.2846	25.69	58.20
440	538.495	3363.15	11.019	2.0901	649.93	1.2834	26.10	59.41
450	546.046	3384.08	11.048	2.0968	654.18	1.2822	26.51	60.62
460	553.598	3405.09	11.077	2.1036	658.39	1.2811	26.93	61.85
470	561.149	3426.16	11.106	2.1103	662.56	1.2799	27.34	63.08
480	568.700	3447.29	11.134	2.1172	666.70	1.2788	27.74	64.32
490	576.251	3468.50	11.162	2.1240	670.81	1.2776	28.15	65.57
500	583.802	3489.77	11.190	2.1309	674.89	1.2765	28.56	66.83
510	591.353	3511.12	11.217	2.1378	678.94	1.2753	28.97	68.10
520	598.904	3532.53	11.244	2.1447	682.96	1.2742	29.38	69.37
530	606.455	3554.01	11.271	2.1517	686.95	1.2731	29.78	70.65
540	614.006	3575.56	11.298	2.1586	690.90	1.2720	30.19	71.94
550	621.557	3597.18	11.324	2.1656	694.83	1.2708	30.59	73.24
560	629.108	3618.88	11.351	2.1726	698.74	1.2697	31.00	74.55
570	636.660	3640.64	11.376	2.1796	702.61	1.2686	31.40	75.86
580	644.211	3662.47	11.402	2.1867	706.46	1.2675	31.80	77.18
590	651.762	3684.37	11.428	2.1937	710.29	1.2664	32.20	78.51
600	659.313	3706.34	11.453	2.2008	714.08	1.2654	32.60	79.84
650	697.068	3817.27	11.577	2.2362	732.71	1.2601	34.60	86.61
700	734.823	3929.96	11.695	2.2716	750.77	1.2550	36.56	93.51
750	772.578	4044.43	11.810	2.3070	768.31	1.2501	38.51	100.5
800	810.333	4160.66	11.921	2.3423	785.38	1.2454	40.43	107.7

Table 3 Single-phase region – Continued (0 °C to 800 °C)

$p = 0.01$ bar

t [°C]	v [m^3 kg^{-1}]	h [kJ kg^{-1}]	s [kJ kg^{-1} K^{-1}]	c_p [kJ kg^{-1} K^{-1}]	w [m s^{-1}]	κ [–]	η [10^{-6} Pa s]	λ [10^{-3} W m^{-1} K^{-1}]
0	0.00100021	–0.04119	–0.0001545	4.2199	1402.3	1965991	1792.0	562.0
2	0.00100011	8.39190	0.030607	4.2133	1412.1	1993738	1673.7	566.2
4	0.00100007	16.8129	0.061101	4.2078	1421.5	2020451	1567.4	570.3
6	0.00100011	25.2237	0.091340	4.2031	1430.5	2046110	1471.6	574.3
$t_s = 6.96963$ °C				**Saturation**				
Liquid	0.00100014	29.2982	0.10591	4.2011	1434.7	2058167	1428.5	576.1
Vapour	129.183	2513.68	8.9749	1.8932	413.95	1.3265	9.148	16.99
8	129.662	2515.63	8.9819	1.8898	414.78	1.3269	9.179	17.07
10	130.590	2519.41	8.9953	1.8846	416.36	1.3275	9.239	17.21
12	131.517	2523.17	9.0085	1.8810	417.91	1.3279	9.300	17.36
14	132.444	2526.93	9.0216	1.8784	419.42	1.3282	9.361	17.50
16	133.370	2530.68	9.0347	1.8765	420.91	1.3284	9.423	17.65
18	134.296	2534.44	9.0476	1.8752	422.39	1.3285	9.485	17.80
20	135.222	2538.19	9.0604	1.8743	423.85	1.3285	9.548	17.94
25	137.536	2547.55	9.0921	1.8732	427.45	1.3285	9.706	18.31
30	139.849	2556.92	9.1233	1.8730	431.00	1.3283	9.868	18.69
35	142.162	2566.28	9.1539	1.8733	434.51	1.3281	10.03	19.06
40	144.474	2575.65	9.1841	1.8739	437.99	1.3278	10.20	19.44
45	146.785	2585.02	9.2138	1.8747	441.43	1.3275	10.37	19.83
50	149.096	2594.40	9.2430	1.8757	444.83	1.3272	10.54	20.21
55	151.407	2603.78	9.2718	1.8768	448.21	1.3268	10.71	20.60
60	153.717	2613.17	9.3002	1.8780	451.56	1.3265	10.88	20.99
65	156.027	2622.56	9.3282	1.8793	454.87	1.3261	11.06	21.39
70	158.337	2631.96	9.3558	1.8808	458.16	1.3257	11.24	21.79
75	160.647	2641.37	9.3830	1.8823	461.42	1.3253	11.42	22.19
80	162.957	2650.79	9.4099	1.8840	464.65	1.3249	11.60	22.59
85	165.266	2660.21	9.4364	1.8857	467.85	1.3245	11.78	23.00
90	167.575	2669.64	9.4625	1.8875	471.03	1.3240	11.96	23.41
95	169.884	2679.08	9.4883	1.8894	474.19	1.3236	12.15	23.83
100	172.193	2688.54	9.5138	1.8913	477.31	1.3231	12.34	24.25
110	176.811	2707.47	9.5639	1.8954	483.49	1.3221	12.71	25.09
120	181.428	2726.44	9.6128	1.8997	489.58	1.3211	13.09	25.95
130	186.045	2745.46	9.6606	1.9043	495.57	1.3201	13.47	26.82
140	190.662	2764.53	9.7073	1.9090	501.48	1.3190	13.86	27.70
150	195.279	2783.65	9.7530	1.9140	507.30	1.3179	14.25	28.59
160	199.895	2802.81	9.7978	1.9190	513.04	1.3168	14.64	29.50
170	204.512	2822.03	9.8416	1.9242	518.71	1.3156	15.04	30.41
180	209.128	2841.30	9.8846	1.9295	524.30	1.3145	15.44	31.34
190	213.744	2860.62	9.9268	1.9350	529.82	1.3133	15.84	32.28
200	218.360	2880.00	9.9682	1.9405	535.27	1.3121	16.24	33.24
210	222.976	2899.43	10.009	1.9461	540.65	1.3109	16.64	34.20
220	227.592	2918.92	10.049	1.9518	545.97	1.3097	17.05	35.18
230	232.208	2938.47	10.088	1.9576	551.23	1.3085	17.45	36.17
240	236.823	2958.07	10.127	1.9634	556.42	1.3073	17.86	37.17

Table 3 Single-phase region – Continued (0 °C to 800 °C)

$p = 0.01$ bar

t [°C]	v [m^3 kg^{-1}]	h [kJ kg^{-1}]	s [kJ kg^{-1} K^{-1}]	c_p [kJ kg^{-1} K^{-1}]	w [m s^{-1}]	κ [–]	η [10^{-6} Pa s]	λ [10^{-3} W m^{-1} K^{-1}]
250	241.439	2977.73	10.165	1.9693	561.56	1.3061	18.27	38.18
260	246.055	2997.46	10.202	1.9753	566.64	1.3049	18.68	39.20
270	250.670	3017.24	10.239	1.9813	571.67	1.3037	19.09	40.23
280	255.286	3037.08	10.275	1.9874	576.64	1.3025	19.50	41.28
290	259.902	3056.99	10.310	1.9935	581.56	1.3013	19.91	42.33
300	264.517	3076.95	10.346	1.9996	586.43	1.3001	20.32	43.40
310	269.133	3096.98	10.380	2.0058	591.24	1.2989	20.74	44.48
320	273.748	3117.07	10.414	2.0121	596.02	1.2977	21.15	45.56
330	278.364	3137.22	10.448	2.0184	600.74	1.2965	21.56	46.66
340	282.979	3157.44	10.481	2.0247	605.42	1.2953	21.98	47.77
350	287.595	3177.72	10.514	2.0311	610.05	1.2941	22.39	48.89
360	292.210	3198.06	10.547	2.0375	614.65	1.2929	22.80	50.02
370	296.826	3218.47	10.579	2.0439	619.20	1.2917	23.22	51.16
380	301.441	3238.94	10.610	2.0504	623.70	1.2905	23.63	52.31
390	306.057	3259.47	10.641	2.0569	628.17	1.2893	24.04	53.47
400	310.672	3280.08	10.672	2.0635	632.60	1.2881	24.46	54.64
410	315.288	3300.74	10.703	2.0701	636.99	1.2869	24.87	55.82
420	319.903	3321.48	10.733	2.0767	641.34	1.2858	25.28	57.00
430	324.518	3342.28	10.763	2.0834	645.65	1.2846	25.69	58.20
440	329.134	3363.15	10.792	2.0901	649.93	1.2834	26.10	59.41
450	333.749	3384.08	10.821	2.0968	654.18	1.2822	26.51	60.62
460	338.365	3405.08	10.850	2.1036	658.38	1.2811	26.93	61.85
470	342.980	3426.15	10.879	2.1104	662.56	1.2799	27.34	63.08
480	347.595	3447.29	10.907	2.1172	666.70	1.2788	27.74	64.32
490	352.211	3468.50	10.935	2.1240	670.81	1.2776	28.15	65.57
500	356.826	3489.77	10.962	2.1309	674.89	1.2765	28.56	66.83
510	361.441	3511.11	10.990	2.1378	678.94	1.2753	28.97	68.10
520	366.057	3532.53	11.017	2.1447	682.96	1.2742	29.38	69.37
530	370.672	3554.01	11.044	2.1517	686.94	1.2731	29.78	70.65
540	375.288	3575.56	11.071	2.1586	690.90	1.2720	30.19	71.94
550	379.903	3597.18	11.097	2.1656	694.83	1.2708	30.59	73.24
560	384.518	3618.87	11.123	2.1726	698.74	1.2697	31.00	74.55
570	389.134	3640.63	11.149	2.1797	702.61	1.2686	31.40	75.86
580	393.749	3662.47	11.175	2.1867	706.46	1.2675	31.80	77.18
590	398.364	3684.37	11.201	2.1937	710.29	1.2664	32.20	78.51
600	402.980	3706.34	11.226	2.2008	714.08	1.2654	32.60	79.84
650	426.056	3817.26	11.349	2.2362	732.71	1.2601	34.60	86.61
700	449.133	3929.96	11.468	2.2716	750.77	1.2550	36.56	93.51
750	472.209	4044.43	11.583	2.3070	768.31	1.2501	38.51	100.5
800	495.286	4160.66	11.694	2.3423	785.38	1.2454	40.43	107.7

Table 3 Single-phase region – Continued (0 °C to 800 °C)

$p =$ 0.05 bar

t [°C]	v [m³ kg⁻¹]	h [kJ kg⁻¹]	s [kJ kg⁻¹ K⁻¹]	c_p [kJ kg⁻¹ K⁻¹]	w [m s⁻¹]	κ [–]	η [10⁻⁶ Pa s]	λ [10⁻³ W m⁻¹ K⁻¹]
0	0.00100020	−0.03712	−0.0001543	4.2199	1402.3	393202	1792.0	562.0
2	0.00100010	8.39594	0.030607	4.2133	1412.1	398752	1673.7	566.2
4	0.00100007	16.8169	0.061101	4.2078	1421.5	404095	1567.4	570.3
6	0.00100010	25.2277	0.091339	4.2031	1430.5	409226	1471.6	574.3
8	0.00100020	33.6299	0.12133	4.1992	1439.1	414145	1384.8	578.1
10	0.00100034	42.0248	0.15108	4.1958	1447.4	418850	1306.0	581.9
12	0.00100055	50.4135	0.18061	4.1930	1455.3	423342	1234.1	585.6
14	0.00100080	58.7968	0.20990	4.1905	1462.8	427622	1168.4	589.2
16	0.00100110	67.1757	0.23898	4.1884	1470.0	431691	1108.1	592.7
18	0.00100145	75.5507	0.26785	4.1866	1476.8	435552	1052.7	596.1
20	0.00100184	83.9224	0.29650	4.1851	1483.3	439207	1001.6	599.5
25	0.00100300	104.840	0.36726	4.1822	1498.0	447467	890.0	607.5
30	0.00100441	125.746	0.43679	4.1803	1510.8	454516	797.2	615.0
t_s = 32.8755 °C				**Saturation**				
Liquid	0.00100532	137.765	0.47625	4.1796	1517.4	458044	750.7	619.0
Vapour	28.1863	2560.77	8.3939	1.9219	431.98	1.3241	9.953	18.93
35	28.3849	2564.84	8.4072	1.9143	433.63	1.3249	10.02	19.09
40	28.8514	2574.38	8.4379	1.9032	437.34	1.3259	10.19	19.46
45	29.3170	2583.88	8.4680	1.8976	440.91	1.3262	10.36	19.84
50	29.7822	2593.36	8.4976	1.8947	444.40	1.3262	10.53	20.23
55	30.2469	2602.83	8.5266	1.8931	447.83	1.3261	10.70	20.61
60	30.7112	2612.29	8.5553	1.8924	451.21	1.3258	10.88	21.01
65	31.1753	2621.75	8.5834	1.8921	454.56	1.3256	11.05	21.40
70	31.6392	2631.21	8.6112	1.8922	457.87	1.3252	11.23	21.80
75	32.1028	2640.68	8.6386	1.8926	461.15	1.3249	11.41	22.20
80	32.5663	2650.14	8.6656	1.8933	464.40	1.3245	11.59	22.60
85	33.0296	2659.61	8.6922	1.8941	467.62	1.3241	11.78	23.01
90	33.4927	2669.08	8.7185	1.8951	470.82	1.3237	11.96	23.42
95	33.9557	2678.56	8.7444	1.8963	473.98	1.3233	12.15	23.84
100	34.4186	2688.05	8.7700	1.8977	477.12	1.3228	12.33	24.25
110	35.3441	2707.04	8.8202	1.9007	483.33	1.3219	12.71	25.10
120	36.2692	2726.06	8.8692	1.9042	489.43	1.3209	13.09	25.95
130	37.1941	2745.12	8.9171	1.9081	495.44	1.3199	13.47	26.82
140	38.1187	2764.22	8.9639	1.9122	501.36	1.3189	13.86	27.70
150	39.0431	2783.37	9.0097	1.9167	507.20	1.3178	14.25	28.60
160	39.9673	2802.56	9.0545	1.9214	512.95	1.3167	14.64	29.50
170	40.8914	2821.80	9.0984	1.9263	518.63	1.3155	15.04	30.42
180	41.8154	2841.08	9.1415	1.9313	524.22	1.3144	15.44	31.35
190	42.7393	2860.42	9.1837	1.9365	529.75	1.3132	15.84	32.29
200	43.6631	2879.82	9.2251	1.9419	535.21	1.3121	16.24	33.24
210	44.5868	2899.26	9.2658	1.9473	540.59	1.3109	16.64	34.21
220	45.5105	2918.76	9.3057	1.9529	545.92	1.3097	17.05	35.18
230	46.4341	2938.32	9.3450	1.9586	551.18	1.3085	17.45	36.17
240	47.3577	2957.93	9.3836	1.9643	556.38	1.3073	17.86	37.17

Table 3 Single-phase region – Continued (0 °C to 800 °C)

p = 0.05 bar								
t	v	h	s	c_p	w	κ	η	λ
[°C]	[$m^3\,kg^{-1}$]	[$kJ\,kg^{-1}$]	[$kJ\,kg^{-1}\,K^{-1}$]	[$kJ\,kg^{-1}\,K^{-1}$]	[$m\,s^{-1}$]	[–]	[10^{-6} Pa s]	[$10^{-3}\,W\,m^{-1}\,K^{-1}$]
250	48.2812	2977.61	9.4216	1.9701	561.52	1.3061	18.27	38.18
260	49.2047	2997.34	9.4589	1.9760	566.60	1.3049	18.68	39.20
270	50.1282	3017.13	9.4957	1.9819	571.63	1.3037	19.09	40.24
280	51.0516	3036.98	9.5319	1.9879	576.60	1.3025	19.50	41.28
290	51.9750	3056.89	9.5676	1.9940	581.52	1.3013	19.91	42.34
300	52.8984	3076.86	9.6027	2.0001	586.39	1.3001	20.32	43.40
310	53.8217	3096.89	9.6374	2.0063	591.22	1.2989	20.74	44.48
320	54.7451	3116.98	9.6715	2.0125	595.99	1.2977	21.15	45.57
330	55.6684	3137.14	9.7052	2.0188	600.72	1.2965	21.56	46.67
340	56.5917	3157.36	9.7385	2.0251	605.40	1.2953	21.98	47.78
350	57.5150	3177.64	9.7713	2.0314	610.03	1.2941	22.39	48.89
360	58.4382	3197.99	9.8037	2.0378	614.63	1.2929	22.80	50.02
370	59.3615	3218.40	9.8357	2.0442	619.18	1.2917	23.22	51.16
380	60.2847	3238.87	9.8673	2.0507	623.68	1.2905	23.63	52.31
390	61.2080	3259.41	9.8985	2.0572	628.15	1.2893	24.04	53.47
400	62.1312	3280.01	9.9293	2.0637	632.58	1.2881	24.46	54.64
410	63.0544	3300.68	9.9598	2.0703	636.97	1.2869	24.87	55.82
420	63.9776	3321.42	9.9899	2.0769	641.32	1.2857	25.28	57.01
430	64.9008	3342.22	10.020	2.0836	645.64	1.2846	25.69	58.20
440	65.8240	3363.09	10.049	2.0903	649.92	1.2834	26.10	59.41
450	66.7472	3384.03	10.078	2.0970	654.16	1.2822	26.51	60.63
460	67.6704	3405.03	10.107	2.1038	658.37	1.2811	26.93	61.85
470	68.5936	3426.10	10.136	2.1105	662.55	1.2799	27.34	63.08
480	69.5167	3447.24	10.164	2.1173	666.69	1.2788	27.74	64.32
490	70.4399	3468.45	10.192	2.1242	670.80	1.2776	28.15	65.57
500	71.3631	3489.73	10.220	2.1311	674.88	1.2765	28.56	66.83
510	72.2862	3511.07	10.247	2.1380	678.93	1.2753	28.97	68.10
520	73.2094	3532.49	10.274	2.1449	682.95	1.2742	29.38	69.37
530	74.1325	3553.97	10.301	2.1518	686.94	1.2731	29.78	70.66
540	75.0556	3575.52	10.328	2.1588	690.90	1.2720	30.19	71.95
550	75.9788	3597.14	10.354	2.1658	694.83	1.2708	30.59	73.25
560	76.9019	3618.84	10.380	2.1728	698.73	1.2697	31.00	74.55
570	77.8250	3640.60	10.406	2.1798	702.61	1.2686	31.40	75.86
580	78.7482	3662.43	10.432	2.1868	706.46	1.2675	31.80	77.18
590	79.6713	3684.34	10.458	2.1938	710.28	1.2664	32.20	78.51
600	80.5944	3706.31	10.483	2.2009	714.08	1.2654	32.60	79.84
650	85.2100	3817.24	10.607	2.2363	732.70	1.2601	34.60	86.61
700	89.8255	3929.94	10.725	2.2717	750.76	1.2550	36.56	93.52
750	94.4410	4044.41	10.840	2.3071	768.31	1.2501	38.51	100.5
800	99.0564	4160.64	10.951	2.3423	785.38	1.2454	40.43	107.7

Table 3 Single-phase region – Continued (0 °C to 800 °C)

$p =$ **0.1 bar**

t [°C]	v [m^3 kg^{-1}]	h [kJ kg^{-1}]	s [kJ kg^{-1} K^{-1}]	c_p [kJ kg^{-1} K^{-1}]	w [m s^{-1}]	κ [–]	η [10^{-6} Pa s]	λ [10^{-3} W m^{-1} K^{-1}]
0	0.00100020	–0.03202	–0.0001539	4.2199	1402.3	196604	1792.0	562.0
2	0.00100010	8.40098	0.030607	4.2133	1412.1	199379	1673.7	566.2
4	0.00100007	16.8219	0.061101	4.2078	1421.5	202050	1567.4	570.3
6	0.00100010	25.2326	0.091339	4.2031	1430.5	204616	1471.6	574.3
8	0.00100019	33.6348	0.12133	4.1991	1439.2	207075	1384.8	578.1
10	0.00100034	42.0296	0.15108	4.1958	1447.4	209428	1306.0	581.9
12	0.00100054	50.4183	0.18061	4.1929	1455.3	211674	1234.1	585.6
14	0.00100080	58.8017	0.20990	4.1905	1462.8	213814	1168.4	589.2
16	0.00100110	67.1805	0.23898	4.1884	1470.0	215848	1108.1	592.7
18	0.00100145	75.5555	0.26785	4.1866	1476.8	217779	1052.7	596.1
20	0.00100184	83.9271	0.29650	4.1851	1483.3	219606	1001.6	599.5
25	0.00100300	104.845	0.36725	4.1822	1498.0	223737	890.0	607.5
30	0.00100441	125.750	0.43679	4.1803	1510.8	227261	797.2	615.0
35	0.00100604	146.649	0.50517	4.1792	1521.8	230209	719.1	622.0
40	0.00100788	167.543	0.57243	4.1788	1531.2	232610	652.7	628.6
45	0.00100991	188.438	0.63862	4.1790	1538.9	234495	595.8	634.7
t_s = 45.8075 °C				**Saturation**				
Liquid	0.00101026	191.812	0.64922	4.1791	1540.0	234753	587.3	635.7
Vapour	14.6706	2583.89	8.1489	1.9413	440.51	1.3227	10.38	19.94
50	14.8674	2591.99	8.1741	1.9272	443.67	1.3240	10.52	20.26
55	15.1015	2601.60	8.2037	1.9178	447.26	1.3246	10.69	20.64
60	15.3353	2611.18	8.2326	1.9124	450.74	1.3248	10.87	21.03
65	15.5687	2620.73	8.2611	1.9091	454.14	1.3247	11.05	21.42
70	15.8018	2630.27	8.2891	1.9071	457.50	1.3246	11.23	21.82
75	16.0347	2639.80	8.3167	1.9058	460.81	1.3243	11.41	22.22
80	16.2674	2649.33	8.3438	1.9051	464.09	1.3240	11.59	22.62
85	16.4999	2658.86	8.3706	1.9048	467.33	1.3236	11.77	23.03
90	16.7323	2668.38	8.3970	1.9048	470.55	1.3233	11.95	23.43
95	16.9646	2677.90	8.4231	1.9051	473.73	1.3229	12.14	23.85
100	17.1967	2687.43	8.4488	1.9057	476.89	1.3225	12.33	24.26
110	17.6607	2706.50	8.4992	1.9074	483.12	1.3216	12.70	25.11
120	18.1243	2725.58	8.5484	1.9098	489.25	1.3207	13.08	25.96
130	18.5876	2744.69	8.5964	1.9128	495.28	1.3197	13.47	26.83
140	19.0507	2763.84	8.6433	1.9163	501.22	1.3187	13.86	27.71
150	19.5136	2783.02	8.6892	1.9201	507.07	1.3176	14.25	28.60
160	19.9763	2802.24	8.7340	1.9243	512.83	1.3166	14.64	29.51
170	20.4389	2821.51	8.7780	1.9288	518.52	1.3154	15.04	30.42
180	20.9013	2840.82	8.8211	1.9336	524.13	1.3143	15.43	31.35
190	21.3637	2860.18	8.8634	1.9385	529.66	1.3132	15.83	32.29
200	21.8260	2879.59	8.9048	1.9436	535.13	1.3120	16.24	33.25
210	22.2882	2899.05	8.9455	1.9489	540.52	1.3108	16.64	34.21
220	22.7504	2918.57	8.9855	1.9543	545.85	1.3097	17.05	35.19
230	23.2124	2938.14	9.0248	1.9598	551.12	1.3085	17.45	36.18
240	23.6745	2957.76	9.0634	1.9654	556.32	1.3073	17.86	37.18

Table 3 Single-phase region – Continued (0 °C to 800 °C)

$p = 0.1$ bar

t [°C]	v [m^3 kg^{-1}]	h [kJ kg^{-1}]	s [kJ kg^{-1} K^{-1}]	c_p [kJ kg^{-1} K^{-1}]	w [m s^{-1}]	κ [–]	η [10^{-6} Pa s]	λ [10^{-3} W m^{-1} K^{-1}]
250	24.1365	2977.45	9.1014	1.9711	561.46	1.3061	18.27	38.19
260	24.5985	2997.19	9.1388	1.9769	566.55	1.3049	18.68	39.21
270	25.0604	3016.98	9.1756	1.9827	571.58	1.3037	19.09	40.24
280	25.5223	3036.84	9.2118	1.9887	576.56	1.3025	19.50	41.29
290	25.9842	3056.76	9.2475	1.9947	581.48	1.3013	19.91	42.34
300	26.4460	3076.73	9.2827	2.0007	586.36	1.3001	20.32	43.41
310	26.9078	3096.77	9.3173	2.0069	591.18	1.2989	20.74	44.49
320	27.3696	3116.87	9.3515	2.0130	595.96	1.2977	21.15	45.57
330	27.8314	3137.03	9.3852	2.0192	600.68	1.2965	21.56	46.67
340	28.2932	3157.26	9.4185	2.0255	605.37	1.2953	21.98	47.78
350	28.7550	3177.54	9.4513	2.0318	610.00	1.2941	22.39	48.90
360	29.2167	3197.89	9.4837	2.0382	614.60	1.2929	22.80	50.03
370	29.6785	3218.31	9.5157	2.0446	619.15	1.2917	23.22	51.17
380	30.1402	3238.79	9.5473	2.0510	623.66	1.2905	23.63	52.32
390	30.6019	3259.33	9.5785	2.0575	628.13	1.2893	24.04	53.48
400	31.0636	3279.94	9.6093	2.0641	632.56	1.2881	24.46	54.64
410	31.5253	3300.61	9.6398	2.0706	636.95	1.2869	24.87	55.82
420	31.9870	3321.35	9.6699	2.0772	641.30	1.2857	25.28	57.01
430	32.4486	3342.15	9.6997	2.0839	645.62	1.2846	25.69	58.21
440	32.9103	3363.03	9.7292	2.0905	649.90	1.2834	26.10	59.41
450	33.3720	3383.96	9.7584	2.0972	654.15	1.2822	26.51	60.63
460	33.8336	3404.97	9.7872	2.1040	658.36	1.2811	26.93	61.85
470	34.2953	3426.04	9.8158	2.1107	662.53	1.2799	27.34	63.09
480	34.7569	3447.19	9.8440	2.1175	666.68	1.2788	27.74	64.33
490	35.2185	3468.40	9.8720	2.1244	670.79	1.2776	28.15	65.58
500	35.6802	3489.67	9.8997	2.1312	674.87	1.2765	28.56	66.84
510	36.1418	3511.02	9.9271	2.1381	678.92	1.2753	28.97	68.10
520	36.6034	3532.44	9.9543	2.1450	682.94	1.2742	29.38	69.38
530	37.0650	3553.92	9.9812	2.1520	686.92	1.2731	29.78	70.66
540	37.5267	3575.48	10.008	2.1589	690.88	1.2720	30.19	71.95
550	37.9883	3597.10	10.034	2.1659	694.82	1.2708	30.59	73.25
560	38.4499	3618.79	10.061	2.1729	698.72	1.2697	31.00	74.55
570	38.9115	3640.56	10.086	2.1799	702.60	1.2686	31.40	75.87
580	39.3731	3662.39	10.112	2.1869	706.45	1.2675	31.80	77.19
590	39.8347	3684.30	10.138	2.1940	710.27	1.2664	32.20	78.51
600	40.2963	3706.27	10.163	2.2010	714.07	1.2654	32.61	79.85
650	42.6042	3817.20	10.287	2.2364	732.70	1.2601	34.60	86.61
700	44.9121	3929.91	10.405	2.2718	750.76	1.2550	36.56	93.52
750	47.2199	4044.38	10.520	2.3071	768.31	1.2501	38.51	100.6
800	49.5278	4160.62	10.631	2.3424	785.38	1.2454	40.43	107.7

Table 3 Single-phase region – Continued (0 °C to 800 °C)

p = 0.5 bar

t [°C]	v [$m^3\ kg^{-1}$]	h [$kJ\ kg^{-1}$]	s [$kJ\ kg^{-1}\ K^{-1}$]	c_p [$kJ\ kg^{-1}\ K^{-1}$]	w [$m\ s^{-1}$]	κ [–]	η [10^{-6} Pa s]	λ [$10^{-3}\ W\ m^{-1}\ K^{-1}$]
0	0.00100018	0.008728	–0.0001512	4.2197	1402.4	39325	1791.9	562.0
2	0.00100008	8.44134	0.030608	4.2131	1412.1	39880	1673.6	566.2
4	0.00100005	16.8619	0.061101	4.2076	1421.6	40414	1567.4	570.3
6	0.00100008	25.2723	0.091338	4.2029	1430.6	40928	1471.5	574.3
8	0.00100017	33.6741	0.12133	4.1990	1439.2	41420	1384.8	578.2
10	0.00100032	42.0687	0.15108	4.1956	1447.5	41890	1305.9	581.9
12	0.00100053	50.4570	0.18060	4.1928	1455.4	42339	1234.1	585.6
14	0.00100078	58.8401	0.20990	4.1904	1462.9	42767	1168.4	589.2
16	0.00100108	67.2187	0.23898	4.1883	1470.0	43174	1108.1	592.7
18	0.00100143	75.5934	0.26784	4.1865	1476.9	43560	1052.7	596.2
20	0.00100182	83.9648	0.29649	4.1850	1483.3	43926	1001.6	599.5
25	0.00100298	104.882	0.36724	4.1820	1498.1	44752	890.0	607.5
30	0.00100439	125.787	0.43678	4.1802	1510.9	45457	797.2	615.0
35	0.00100602	146.685	0.50515	4.1791	1521.9	46047	719.1	622.0
40	0.00100786	167.579	0.57241	4.1787	1531.2	46527	652.7	628.6
45	0.00100990	188.472	0.63861	4.1789	1539.0	46904	595.8	634.7
50	0.00101212	209.369	0.70378	4.1797	1545.2	47183	546.5	640.5
55	0.00101452	230.270	0.76796	4.1810	1550.1	47371	503.6	645.8
60	0.00101710	251.180	0.83120	4.1829	1553.8	47472	466.0	650.8
65	0.00101984	272.100	0.89353	4.1853	1556.2	47493	432.9	655.4
70	0.00102275	293.033	0.95498	4.1882	1557.5	47437	403.5	659.6
75	0.00102582	313.983	1.0156	4.1917	1557.7	47309	377.4	663.4
80	0.00102904	334.951	1.0754	4.1956	1557.0	47115	354.0	667.0
t_s = 81.3167 °C				**Saturation**				
Liquid	0.00102991	340.476	1.0910	4.1968	1556.6	47053	348.3	667.8
Vapour	3.24015	2645.21	7.5930	2.0155	462.16	1.3184	11.58	22.98
85	3.27556	2652.61	7.6137	2.0024	464.81	1.3191	11.72	23.26
90	3.32345	2662.59	7.6414	1.9896	468.28	1.3196	11.91	23.64
95	3.37119	2672.51	7.6685	1.9804	471.66	1.3198	12.10	24.03
100	3.41878	2682.40	7.6952	1.9732	474.97	1.3197	12.29	24.43
110	3.51362	2702.07	7.7472	1.9630	481.45	1.3194	12.67	25.24
120	3.60809	2721.67	7.7977	1.9562	487.78	1.3189	13.05	26.07
130	3.70224	2741.21	7.8468	1.9519	493.98	1.3182	13.44	26.92
140	3.79615	2760.71	7.8946	1.9494	500.06	1.3174	13.83	27.79
150	3.88985	2780.20	7.9412	1.9484	506.03	1.3166	14.22	28.67
160	3.98338	2799.68	7.9867	1.9486	511.90	1.3157	14.62	29.57
170	4.07677	2819.18	8.0312	1.9498	517.67	1.3147	15.02	30.48
180	4.17003	2838.68	8.0747	1.9518	523.36	1.3137	15.42	31.41
190	4.26319	2858.21	8.1174	1.9544	528.96	1.3126	15.82	32.35
200	4.35627	2877.77	8.1591	1.9576	534.48	1.3115	16.22	33.30
210	4.44926	2897.37	8.2001	1.9612	539.93	1.3104	16.63	34.26
220	4.54220	2917.00	8.2403	1.9652	545.31	1.3093	17.03	35.23
230	4.63507	2936.67	8.2798	1.9696	550.61	1.3082	17.44	36.22
240	4.72790	2956.39	8.3186	1.9742	555.86	1.3070	17.85	37.22

Table 3 Single-phase region – Continued (0 °C to 800 °C)

$p = 0.5$ bar

t [°C]	v [m^3 kg^{-1}]	h [kJ kg^{-1}]	s [kJ kg^{-1} K^{-1}]	c_p [kJ kg^{-1} K^{-1}]	w [m s^{-1}]	κ [–]	η [10^{-6} Pa s]	λ [10^{-3} W m^{-1} K^{-1}]
250	4.82069	2976.16	8.3568	1.9790	561.03	1.3059	18.26	38.23
260	4.91343	2995.97	8.3943	1.9840	566.15	1.3047	18.67	39.25
270	5.00615	3015.84	8.4312	1.9893	571.21	1.3035	19.08	40.28
280	5.09883	3035.76	8.4676	1.9946	576.21	1.3023	19.49	41.32
290	5.19148	3055.73	8.5034	2.0001	581.16	1.3011	19.91	42.38
300	5.28411	3075.76	8.5386	2.0057	586.05	1.3000	20.32	43.44
310	5.37672	3095.85	8.5733	2.0115	590.89	1.2988	20.73	44.52
320	5.46931	3115.99	8.6076	2.0173	595.69	1.2976	21.15	45.61
330	5.56188	3136.19	8.6414	2.0232	600.43	1.2964	21.56	46.70
340	5.65444	3156.46	8.6747	2.0292	605.13	1.2952	21.97	47.81
350	5.74698	3176.78	8.7076	2.0353	609.78	1.2940	22.39	48.93
360	5.83950	3197.16	8.7400	2.0414	614.39	1.2928	22.80	50.06
370	5.93201	3217.61	8.7721	2.0476	618.95	1.2916	23.21	51.20
380	6.02452	3238.11	8.8037	2.0539	623.47	1.2904	23.63	52.35
390	6.11701	3258.68	8.8349	2.0602	627.95	1.2893	24.04	53.51
400	6.20949	3279.32	8.8658	2.0665	632.39	1.2881	24.45	54.67
410	6.30196	3300.01	8.8964	2.0730	636.79	1.2869	24.87	55.85
420	6.39442	3320.78	8.9265	2.0794	641.15	1.2857	25.28	57.04
430	6.48687	3341.60	8.9564	2.0860	645.48	1.2846	25.69	58.24
440	6.57932	3362.49	8.9859	2.0925	649.76	1.2834	26.10	59.44
450	6.67176	3383.45	9.0150	2.0991	654.02	1.2822	26.51	60.66
460	6.76420	3404.48	9.0439	2.1058	658.23	1.2811	26.93	61.88
470	6.85662	3425.57	9.0725	2.1124	662.42	1.2799	27.34	63.11
480	6.94904	3446.73	9.1008	2.1192	666.57	1.2788	27.75	64.35
490	7.04146	3467.95	9.1288	2.1259	670.68	1.2776	28.15	65.60
500	7.13387	3489.24	9.1565	2.1327	674.77	1.2765	28.56	66.86
510	7.22628	3510.61	9.1839	2.1395	678.82	1.2753	28.97	68.13
520	7.31868	3532.04	9.2111	2.1464	682.84	1.2742	29.38	69.40
530	7.41108	3553.53	9.2381	2.1532	686.84	1.2731	29.78	70.69
540	7.50347	3575.10	9.2648	2.1601	690.80	1.2720	30.19	71.98
550	7.59586	3596.74	9.2912	2.1671	694.74	1.2708	30.59	73.27
560	7.68825	3618.44	9.3174	2.1740	698.64	1.2697	31.00	74.58
570	7.78063	3640.22	9.3434	2.1810	702.52	1.2686	31.40	75.89
580	7.87301	3662.06	9.3691	2.1879	706.38	1.2675	31.80	77.21
590	7.96539	3683.98	9.3947	2.1949	710.21	1.2665	32.21	78.54
600	8.05776	3705.96	9.4200	2.2019	714.01	1.2654	32.61	79.87
650	8.51960	3816.94	9.5436	2.2371	732.65	1.2601	34.60	86.63
700	8.98138	3929.67	9.6625	2.2724	750.72	1.2550	36.57	93.54
750	9.44312	4044.18	9.7772	2.3076	768.28	1.2501	38.51	100.6
800	9.90483	4160.44	9.8882	2.3428	785.36	1.2454	40.43	107.7

Table 3 Single-phase region – Continued (0 °C to 800 °C)

p = 1 bar								
t [°C]	v [$m^3\,kg^{-1}$]	h [$kJ\,kg^{-1}$]	s [$kJ\,kg^{-1}\,K^{-1}$]	c_p [$kJ\,kg^{-1}\,K^{-1}$]	w [$m\,s^{-1}$]	κ [–]	η [10^{-6} Pa s]	λ [$10^{-3}\,W\,m^{-1}\,K^{-1}$]
0	0.00100016	0.05966	–0.0001478	4.2194	1402.4	19665	1791.8	562.0
2	0.00100006	8.49179	0.030610	4.2129	1412.2	19943	1673.5	566.2
4	0.00100003	16.9119	0.061101	4.2074	1421.6	20210	1567.3	570.3
6	0.00100006	25.3219	0.091336	4.2027	1430.7	20467	1471.5	574.3
8	0.00100015	33.7233	0.12133	4.1988	1439.3	20713	1384.7	578.2
10	0.00100030	42.1174	0.15108	4.1955	1447.6	20948	1305.9	582.0
12	0.00100050	50.5054	0.18060	4.1926	1455.4	21172	1234.0	585.7
14	0.00100076	58.8881	0.20989	4.1902	1463.0	21386	1168.3	589.3
16	0.00100106	67.2664	0.23897	4.1881	1470.1	21590	1108.1	592.8
18	0.00100141	75.6407	0.26783	4.1863	1476.9	21783	1052.7	596.2
20	0.00100180	84.0118	0.29648	4.1848	1483.4	21966	1001.6	599.5
25	0.00100296	104.928	0.36723	4.1819	1498.2	22379	890.0	607.5
30	0.00100437	125.833	0.43676	4.1800	1511.0	22731	797.2	615.0
35	0.00100600	146.730	0.50513	4.1790	1522.0	23026	719.1	622.0
40	0.00100784	167.623	0.57239	4.1786	1531.3	23266	652.7	628.6
45	0.00100987	188.516	0.63859	4.1788	1539.0	23455	595.8	634.8
50	0.00101210	209.412	0.70375	4.1796	1545.3	23595	546.5	640.5
55	0.00101450	230.313	0.76794	4.1809	1550.2	23689	503.6	645.8
60	0.00101708	251.222	0.83117	4.1828	1553.9	23739	466.0	650.8
65	0.00101982	272.141	0.89350	4.1852	1556.3	23749	432.9	655.4
70	0.00102273	293.074	0.95495	4.1881	1557.6	23722	403.6	659.6
75	0.00102579	314.023	1.0156	4.1915	1557.8	23658	377.4	663.5
80	0.00102902	334.991	1.0754	4.1955	1557.1	23561	354.1	667.0
85	0.00103239	355.979	1.1344	4.2000	1555.4	23432	333.1	670.2
90	0.00103593	376.992	1.1926	4.2050	1552.8	23275	314.2	673.0
95	0.00103962	398.030	1.2502	4.2106	1549.3	23090	297.1	675.5
t_s = 99.6059 °C				**Saturation**				
Liquid	0.00104315	417.436	1.3026	4.2161	1545.5	22896	282.8	677.6
Vapour	1.69402	2674.95	7.3588	2.0759	472.05	1.3154	12.22	24.75
100	1.69596	2675.77	7.3610	2.0741	472.34	1.3155	12.23	24.78
110	1.74482	2696.32	7.4154	2.0399	479.27	1.3165	12.62	25.51
120	1.79324	2716.61	7.4676	2.0187	485.89	1.3166	13.01	26.29
130	1.84132	2736.72	7.5181	2.0039	492.31	1.3163	13.40	27.10
140	1.88913	2756.70	7.5671	1.9933	498.57	1.3158	13.80	27.94
150	1.93673	2776.59	7.6147	1.9857	504.70	1.3152	14.19	28.80
160	1.98414	2796.42	7.6610	1.9805	510.70	1.3145	14.59	29.68
170	2.03140	2816.21	7.7062	1.9772	516.59	1.3137	14.99	30.58
180	2.07853	2835.97	7.7503	1.9755	522.38	1.3129	15.39	31.49
190	2.12556	2855.72	7.7934	1.9751	528.07	1.3119	15.80	32.42
200	2.17249	2875.48	7.8356	1.9757	533.67	1.3110	16.20	33.37
210	2.21935	2895.24	7.8769	1.9772	539.19	1.3099	16.61	34.33
220	2.26614	2915.02	7.9174	1.9793	544.62	1.3089	17.02	35.30
230	2.31287	2934.83	7.9572	1.9821	549.98	1.3078	17.43	36.28
240	2.35955	2954.66	7.9962	1.9854	555.27	1.3067	17.84	37.27

Table 3 Single-phase region – Continued (0 °C to 800 °C)

				p = 1 bar				
t	v	h	s	c_p	w	κ	η	λ
[°C]	[$m^3\,kg^{-1}$]	[$kJ\,kg^{-1}$]	[$kJ\,kg^{-1}\,K^{-1}$]	[$kJ\,kg^{-1}\,K^{-1}$]	[$m\,s^{-1}$]	[–]	[10^{-6} Pa s]	[$10^{-3}\,W\,m^{-1}\,K^{-1}$]
250	2.40619	2974.54	8.0346	1.9891	560.49	1.3056	18.25	38.28
260	2.45279	2994.45	8.0723	1.9932	565.65	1.3045	18.66	39.30
270	2.49935	3014.40	8.1094	1.9975	570.74	1.3033	19.07	40.33
280	2.54588	3034.40	8.1458	2.0022	575.77	1.3022	19.49	41.37
290	2.59239	3054.45	8.1818	2.0070	580.75	1.3010	19.90	42.43
300	2.63887	3074.54	8.2171	2.0121	585.67	1.2998	20.31	43.49
310	2.68533	3094.69	8.2520	2.0173	590.54	1.2987	20.73	44.57
320	2.73176	3114.89	8.2863	2.0227	595.35	1.2975	21.14	45.65
330	2.77818	3135.14	8.3202	2.0282	600.11	1.2963	21.56	46.75
340	2.82458	3155.45	8.3536	2.0338	604.83	1.2951	21.97	47.86
350	2.87097	3175.82	8.3865	2.0396	609.50	1.2939	22.38	48.97
360	2.91735	3196.24	8.4190	2.0454	614.12	1.2928	22.80	50.10
370	2.96371	3216.73	8.4511	2.0514	618.70	1.2916	23.21	51.24
380	3.01006	3237.27	8.4828	2.0574	623.23	1.2904	23.63	52.39
390	3.05639	3257.87	8.5141	2.0635	627.73	1.2892	24.04	53.54
400	3.10272	3278.54	8.5451	2.0697	632.18	1.2881	24.45	54.71
410	3.14904	3299.27	8.5756	2.0759	636.59	1.2869	24.87	55.89
420	3.19535	3320.06	8.6059	2.0822	640.96	1.2857	25.28	57.08
430	3.24165	3340.91	8.6357	2.0886	645.30	1.2845	25.69	58.27
440	3.28795	3361.83	8.6653	2.0950	649.59	1.2834	26.10	59.48
450	3.33424	3382.81	8.6945	2.1015	653.85	1.2822	26.51	60.69
460	3.38052	3403.86	8.7234	2.1080	658.08	1.2811	26.93	61.92
470	3.42679	3424.97	8.7520	2.1146	662.27	1.2799	27.34	63.15
480	3.47306	3446.15	8.7803	2.1212	666.43	1.2788	27.75	64.39
490	3.51932	3467.40	8.8083	2.1279	670.55	1.2776	28.16	65.64
500	3.56558	3488.71	8.8361	2.1345	674.64	1.2765	28.56	66.90
510	3.61184	3510.09	8.8635	2.1413	678.70	1.2753	28.97	68.16
520	3.65809	3531.53	8.8907	2.1480	682.73	1.2742	29.38	69.44
530	3.70433	3553.05	8.9177	2.1548	686.73	1.2731	29.78	70.72
540	3.75057	3574.63	8.9444	2.1617	690.70	1.2720	30.19	72.01
550	3.79681	3596.28	8.9709	2.1685	694.64	1.2709	30.60	73.30
560	3.84304	3618.00	8.9971	2.1754	698.55	1.2698	31.00	74.61
570	3.88928	3639.79	9.0231	2.1823	702.44	1.2687	31.40	75.92
580	3.93550	3661.65	9.0489	2.1892	706.29	1.2676	31.81	77.24
590	3.98173	3683.58	9.0744	2.1962	710.12	1.2665	32.21	78.57
600	4.02795	3705.57	9.0998	2.2031	713.93	1.2654	32.61	79.90
650	4.25902	3816.60	9.2234	2.2381	732.59	1.2601	34.60	86.66
700	4.49004	3929.38	9.3424	2.2732	750.68	1.2550	36.57	93.57
750	4.72101	4043.92	9.4571	2.3083	768.24	1.2502	38.51	100.6
800	4.95196	4160.21	9.5681	2.3434	785.34	1.2455	40.43	107.7

Table 3 Single-phase region – Continued (0 °C to 800 °C)

p = 2 bar

t [°C]	v [$m^3\ kg^{-1}$]	h [$kJ\ kg^{-1}$]	s [$kJ\ kg^{-1}\ K^{-1}$]	c_p [$kJ\ kg^{-1}\ K^{-1}$]	w [$m\ s^{-1}$]	κ [–]	η [10^{-6} Pa s]	λ [$10^{-3}\ W\ m^{-1}\ K^{-1}$]
0	0.00100011	0.16152	–0.0001411	4.2189	1402.6	9835.3	1791.5	562.1
2	0.00100001	8.59268	0.030613	4.2124	1412.4	9974.1	1673.3	566.3
4	0.00099998	17.0119	0.061101	4.2069	1421.8	10108	1567.1	570.4
6	0.00100001	25.4210	0.091333	4.2023	1430.8	10236	1471.3	574.4
8	0.00100010	33.8216	0.12132	4.1984	1439.5	10359	1384.6	578.2
10	0.00100025	42.2150	0.15107	4.1951	1447.7	10477	1305.8	582.0
12	0.00100045	50.6022	0.18058	4.1922	1455.6	10589	1234.0	585.7
14	0.00100071	58.9842	0.20988	4.1898	1463.1	10696	1168.3	589.3
16	0.00100101	67.3618	0.23895	4.1878	1470.3	10798	1108.0	592.8
18	0.00100136	75.7355	0.26781	4.1860	1477.1	10894	1052.6	596.2
20	0.00100175	84.1059	0.29646	4.1845	1483.6	10986	1001.6	599.6
25	0.00100292	105.021	0.36721	4.1816	1498.3	11192	890.0	607.6
30	0.00100432	125.924	0.43673	4.1798	1511.1	11369	797.2	615.1
35	0.00100595	146.820	0.50510	4.1787	1522.1	11516	719.1	622.1
40	0.00100779	167.712	0.57235	4.1783	1531.5	11636	652.7	628.7
45	0.00100983	188.604	0.63854	4.1785	1539.2	11730	595.8	634.8
50	0.00101205	209.498	0.70371	4.1793	1545.5	11800	546.5	640.6
55	0.00101446	230.398	0.76789	4.1807	1550.4	11847	503.7	645.9
60	0.00101703	251.306	0.83112	4.1825	1554.0	11873	466.1	650.9
65	0.00101977	272.224	0.89344	4.1849	1556.5	11878	432.9	655.4
70	0.00102268	293.156	0.95489	4.1879	1557.8	11864	403.6	659.7
75	0.00102575	314.104	1.0155	4.1913	1558.0	11832	377.5	663.5
80	0.00102897	335.070	1.0753	4.1953	1557.2	11784	354.1	667.0
85	0.00103235	356.058	1.1343	4.1998	1555.6	11720	333.1	670.2
90	0.00103588	377.069	1.1926	4.2048	1553.0	11641	314.2	673.1
95	0.00103957	398.107	1.2501	4.2103	1549.5	11548	297.1	675.6
100	0.00104341	419.173	1.3069	4.2164	1545.3	11443	281.6	677.8
110	0.00105155	461.405	1.4186	4.2302	1534.6	11197	254.6	681.3
120	0.00106033	503.786	1.5278	4.2464	1521.0	10909	232.0	683.6
t_s = 120.212 °C				**Saturation**				
Liquid	0.00106052	504.684	1.5301	4.2467	1520.7	10903	231.6	683.6
Vapour	0.885735	2706.24	7.1269	2.1752	481.88	1.3108	12.93	26.99
130	0.910412	2727.25	7.1796	2.1232	488.81	1.3122	13.33	27.64
140	0.935281	2748.31	7.2312	2.0902	495.51	1.3126	13.73	28.37
150	0.959894	2769.09	7.2809	2.0667	501.97	1.3125	14.13	29.15
160	0.984303	2789.66	7.3290	2.0492	508.26	1.3122	14.54	29.97
170	1.00854	2810.09	7.3756	2.0359	514.39	1.3118	14.94	30.83
180	1.03265	2830.39	7.4209	2.0261	520.39	1.3112	15.35	31.71
190	1.05663	2850.62	7.4650	2.0189	526.26	1.3105	15.76	32.61
200	1.08052	2870.78	7.5081	2.0139	532.02	1.3098	16.17	33.54
210	1.10432	2890.90	7.5502	2.0106	537.68	1.3089	16.58	34.48
220	1.12805	2911.00	7.5914	2.0089	543.23	1.3080	16.99	35.44
230	1.15172	2931.08	7.6317	2.0083	548.70	1.3071	17.40	36.41
240	1.17534	2951.17	7.6712	2.0087	554.09	1.3061	17.81	37.40

Table 3 Single-phase region – Continued (0 °C to 800 °C)

p = 2 bar								
t [°C]	v [m³ kg⁻¹]	h [kJ kg⁻¹]	s [kJ kg⁻¹ K⁻¹]	c_p [kJ kg⁻¹ K⁻¹]	w [m s⁻¹]	κ [–]	η [10⁻⁶ Pa s]	λ [10⁻³ W m⁻¹ K⁻¹]
250	1.19891	2971.26	7.7100	2.0100	559.40	1.3050	18.23	38.40
260	1.22244	2991.37	7.7481	2.0120	564.63	1.3040	18.64	39.41
270	1.24593	3011.50	7.7855	2.0145	569.80	1.3029	19.06	40.44
280	1.26939	3031.66	7.8223	2.0176	574.89	1.3018	19.47	41.48
290	1.29282	3051.85	7.8584	2.0211	579.93	1.3007	19.89	42.53
300	1.31623	3072.08	7.8940	2.0250	584.90	1.2996	20.30	43.59
310	1.33962	3092.35	7.9291	2.0291	589.81	1.2984	20.72	44.66
320	1.36298	3112.67	7.9636	2.0336	594.67	1.2973	21.13	45.74
330	1.38632	3133.03	7.9977	2.0383	599.48	1.2961	21.55	46.84
340	1.40965	3153.43	8.0312	2.0432	604.23	1.2950	21.96	47.94
350	1.43296	3173.89	8.0643	2.0483	608.93	1.2938	22.38	49.06
360	1.45626	3194.40	8.0970	2.0535	613.59	1.2927	22.79	50.18
370	1.47955	3214.96	8.1292	2.0590	618.20	1.2915	23.21	51.32
380	1.50282	3235.58	8.1610	2.0645	622.76	1.2903	23.62	52.47
390	1.52608	3256.25	8.1924	2.0702	627.28	1.2892	24.04	53.62
400	1.54934	3276.98	8.2235	2.0760	631.75	1.2880	24.45	54.79
410	1.57258	3297.77	8.2541	2.0818	636.19	1.2868	24.86	55.97
420	1.59581	3318.62	8.2844	2.0878	640.58	1.2857	25.28	57.15
430	1.61904	3339.53	8.3144	2.0939	644.93	1.2845	25.69	58.35
440	1.64226	3360.50	8.3440	2.1000	649.25	1.2834	26.10	59.55
450	1.66547	3381.53	8.3733	2.1062	653.53	1.2822	26.51	60.76
460	1.68868	3402.62	8.4022	2.1125	657.77	1.2811	26.93	61.99
470	1.71187	3423.78	8.4309	2.1189	661.97	1.2799	27.34	63.22
480	1.73507	3445.00	8.4593	2.1253	666.14	1.2788	27.75	64.46
490	1.75825	3466.29	8.4873	2.1317	670.28	1.2776	28.16	65.70
500	1.78144	3487.64	8.5151	2.1382	674.39	1.2765	28.57	66.96
510	1.80462	3509.05	8.5426	2.1448	678.46	1.2754	28.97	68.23
520	1.82779	3530.53	8.5699	2.1514	682.50	1.2742	29.38	69.50
530	1.85096	3552.08	8.5969	2.1580	686.51	1.2731	29.79	70.78
540	1.87412	3573.69	8.6236	2.1647	690.49	1.2720	30.19	72.07
550	1.89728	3595.37	8.6501	2.1715	694.44	1.2709	30.60	73.37
560	1.92044	3617.12	8.6764	2.1782	698.36	1.2698	31.00	74.67
570	1.94360	3638.94	8.7024	2.1850	702.26	1.2687	31.41	75.98
580	1.96675	3660.82	8.7282	2.1918	706.12	1.2676	31.81	77.30
590	1.98990	3682.77	8.7538	2.1986	709.96	1.2665	32.21	78.63
600	2.01304	3704.79	8.7792	2.2055	713.78	1.2654	32.61	79.96
650	2.12873	3815.93	8.9029	2.2400	732.47	1.2602	34.60	86.72
700	2.24437	3928.80	9.0220	2.2748	750.59	1.2551	36.57	93.62
750	2.35996	4043.41	9.1368	2.3096	768.18	1.2502	38.52	100.6
800	2.47553	4159.76	9.2479	2.3445	785.29	1.2455	40.44	107.8

Table 3 Single-phase region – Continued (0 °C to 800 °C)

t	*v*	*h*	*s*	c_p	*w*	*κ*	*η*	*λ*
[°C]	[$m^3 kg^{-1}$]	[$kJ kg^{-1}$]	[$kJ kg^{-1} K^{-1}$]	[$kJ kg^{-1} K^{-1}$]	[$m s^{-1}$]	[–]	[10^{-6} Pa s]	[$10^{-3} W m^{-1} K^{-1}$]
p = 3 bar								
0	0.00100005	0.26336	−0.0001343	4.2184	1402.8	6558.7	1791.3	562.1
2	0.000999956	8.69356	0.030616	4.2119	1412.5	6651.2	1673.1	566.3
4	0.000999926	17.1118	0.061101	4.2065	1421.9	6740.3	1567.0	570.4
6	0.000999960	25.5201	0.091330	4.2019	1431.0	6825.9	1471.2	574.4
8	0.00100005	33.9199	0.12131	4.1980	1439.6	6907.9	1384.5	578.3
10	0.00100020	42.3125	0.15106	4.1947	1447.9	6986.3	1305.7	582.1
12	0.00100041	50.6990	0.18057	4.1919	1455.8	7061.2	1233.9	585.8
14	0.00100066	59.0803	0.20986	4.1895	1463.3	7132.6	1168.2	589.4
16	0.00100096	67.4571	0.23893	4.1874	1470.4	7200.4	1108.0	592.9
18	0.00100131	75.8302	0.26779	4.1857	1477.3	7264.8	1052.6	596.3
20	0.00100171	84.2000	0.29644	4.1842	1483.7	7325.7	1001.5	599.6
25	0.00100287	105.113	0.36718	4.1813	1498.5	7463.4	890.0	607.6
30	0.00100428	126.015	0.43670	4.1795	1511.3	7581.0	797.2	615.1
35	0.00100591	146.909	0.50507	4.1784	1522.3	7679.3	719.1	622.1
40	0.00100775	167.800	0.57232	4.1781	1531.6	7759.4	652.8	628.7
45	0.00100978	188.691	0.63850	4.1783	1539.4	7822.3	595.8	634.9
50	0.00101201	209.584	0.70366	4.1791	1545.7	7869.0	546.6	640.6
55	0.00101441	230.483	0.76784	4.1804	1550.6	7900.3	503.7	646.0
60	0.00101699	251.390	0.83107	4.1823	1554.2	7917.3	466.1	650.9
65	0.00101973	272.307	0.89339	4.1847	1556.6	7920.8	433.0	655.5
70	0.00102263	293.238	0.95483	4.1877	1557.9	7911.5	403.6	659.7
75	0.00102570	314.184	1.0154	4.1911	1558.2	7890.4	377.5	663.6
80	0.00102892	335.150	1.0752	4.1951	1557.4	7858.1	354.1	667.1
85	0.00103230	356.136	1.1342	4.1996	1555.7	7815.4	333.1	670.3
90	0.00103583	377.146	1.1925	4.2046	1553.2	7762.9	314.2	673.1
95	0.00103952	398.183	1.2500	4.2101	1549.7	7701.2	297.1	675.7
100	0.00104335	419.248	1.3069	4.2162	1545.5	7631.1	281.6	677.9
110	0.00105150	461.477	1.4185	4.2300	1534.8	7467.2	254.7	681.4
120	0.00106027	503.856	1.5277	4.2461	1521.2	7275.4	232.1	683.7
130	0.00106969	546.408	1.6346	4.2648	1505.1	7059.0	212.9	684.8
t_s = 133.525 °C				**Saturation**				
Liquid	0.00107318	561.455	1.6718	4.2720	1498.8	6977.4	206.9	684.9
Vapour	0.605785	2724.89	6.9916	2.2618	487.39	1.3071	13.39	28.59
140	0.616994	2739.36	7.0269	2.2099	492.17	1.3087	13.66	28.97
150	0.634032	2761.18	7.0791	2.1593	499.11	1.3097	14.07	29.63
160	0.650828	2782.60	7.1291	2.1254	505.73	1.3099	14.48	30.36
170	0.667436	2803.72	7.1773	2.1002	512.12	1.3098	14.89	31.15
180	0.683892	2824.62	7.2239	2.0809	518.34	1.3096	15.31	31.98
190	0.700221	2845.35	7.2692	2.0661	524.41	1.3091	15.72	32.85
200	0.716445	2865.95	7.3132	2.0548	530.33	1.3086	16.13	33.74
210	0.732579	2886.46	7.3561	2.0463	536.13	1.3079	16.55	34.66
220	0.748636	2906.89	7.3979	2.0401	541.82	1.3071	16.96	35.60
230	0.764629	2927.26	7.4388	2.0359	547.40	1.3063	17.38	36.56
240	0.780565	2947.61	7.4789	2.0332	552.89	1.3054	17.79	37.53

Table 3 Single-phase region – Continued (0 °C to 800 °C)

p = 3 bar								
t [°C]	v [$m^3\ kg^{-1}$]	h [$kJ\ kg^{-1}$]	s [$kJ\ kg^{-1}\ K^{-1}$]	c_p [$kJ\ kg^{-1}\ K^{-1}$]	w [$m\ s^{-1}$]	κ [–]	η [10^{-6} Pa s]	λ [$10^{-3}\ W\ m^{-1}\ K^{-1}$]
250	0.796452	2967.93	7.5181	2.0318	558.29	1.3045	18.21	38.53
260	0.812296	2988.25	7.5566	2.0315	563.60	1.3035	18.62	39.53
270	0.828103	3008.57	7.5943	2.0322	568.84	1.3025	19.04	40.55
280	0.843877	3028.89	7.6314	2.0336	574.00	1.3015	19.46	41.58
290	0.859621	3049.24	7.6679	2.0356	579.10	1.3004	19.87	42.63
300	0.875339	3069.61	7.7037	2.0382	584.12	1.2993	20.29	43.69
310	0.891034	3090.01	7.7390	2.0413	589.09	1.2982	20.71	44.76
320	0.906708	3110.43	7.7737	2.0447	593.99	1.2971	21.12	45.84
330	0.922363	3130.90	7.8079	2.0486	598.84	1.2960	21.54	46.93
340	0.938000	3151.41	7.8417	2.0527	603.63	1.2948	21.95	48.03
350	0.953622	3171.96	7.8749	2.0571	608.37	1.2937	22.37	49.14
360	0.969230	3192.55	7.9077	2.0618	613.05	1.2926	22.79	50.27
370	0.984824	3213.19	7.9400	2.0667	617.69	1.2914	23.20	51.40
380	1.00041	3233.89	7.9720	2.0717	622.28	1.2903	23.62	52.55
390	1.01598	3254.63	8.0035	2.0769	626.83	1.2891	24.03	53.70
400	1.03154	3275.42	8.0346	2.0823	631.33	1.2880	24.45	54.87
410	1.04709	3296.27	8.0654	2.0878	635.78	1.2868	24.86	56.04
420	1.06263	3317.18	8.0957	2.0934	640.20	1.2856	25.28	57.23
430	1.07817	3338.14	8.1258	2.0992	644.57	1.2845	25.69	58.42
440	1.09369	3359.17	8.1554	2.1050	648.90	1.2833	26.10	59.62
450	1.10921	3380.25	8.1848	2.1110	653.20	1.2822	26.52	60.83
460	1.12473	3401.39	8.2138	2.1170	657.46	1.2810	26.93	62.06
470	1.14023	3422.59	8.2426	2.1231	661.68	1.2799	27.34	63.29
480	1.15573	3443.85	8.2710	2.1293	665.86	1.2788	27.75	64.52
490	1.17123	3465.17	8.2991	2.1356	670.02	1.2776	28.16	65.77
500	1.18672	3486.56	8.3269	2.1419	674.13	1.2765	28.57	67.03
510	1.20221	3508.01	8.3545	2.1483	678.22	1.2754	28.98	68.29
520	1.21769	3529.53	8.3818	2.1548	682.27	1.2743	29.38	69.56
530	1.23317	3551.11	8.4089	2.1613	686.29	1.2731	29.79	70.84
540	1.24864	3572.75	8.4356	2.1678	690.28	1.2720	30.20	72.13
550	1.26411	3594.46	8.4622	2.1744	694.24	1.2709	30.60	73.43
560	1.27957	3616.24	8.4885	2.1810	698.17	1.2698	31.01	74.73
570	1.29504	3638.08	8.5145	2.1877	702.08	1.2687	31.41	76.04
580	1.31050	3659.99	8.5404	2.1944	705.95	1.2676	31.81	77.36
590	1.32595	3681.97	8.5660	2.2011	709.80	1.2666	32.21	78.68
600	1.34141	3704.02	8.5914	2.2078	713.62	1.2655	32.62	80.02
650	1.41863	3815.26	8.7152	2.2419	732.35	1.2602	34.61	86.77
700	1.49581	3928.21	8.8344	2.2764	750.49	1.2552	36.58	93.67
750	1.57295	4042.90	8.9493	2.3109	768.11	1.2503	38.52	100.7
800	1.65005	4159.31	9.0604	2.3456	785.24	1.2456	40.44	107.8

Table 3 Single-phase region – Continued (0 °C to 800 °C)

				p = 4 bar				
t	v	h	s	c_p	w	κ	η	λ
[°C]	[$m^3\,kg^{-1}$]	[$kJ\,kg^{-1}$]	[$kJ\,kg^{-1}\,K^{-1}$]	[$kJ\,kg^{-1}\,K^{-1}$]	[$m\,s^{-1}$]	[–]	[10^{-6} Pa s]	[$10^{-3}\,W\,m^{-1}\,K^{-1}$]
0	0.00100000	0.36519	−0.0001277	4.2179	1402.9	4920.4	1791.1	562.2
2	0.000999906	8.79442	0.030619	4.2115	1412.7	4989.8	1673.0	566.4
4	0.000999877	17.2118	0.061101	4.2061	1422.1	5056.6	1566.8	570.5
6	0.000999911	25.6192	0.091327	4.2015	1431.1	5120.8	1471.1	574.5
8	0.00100001	34.0182	0.12131	4.1976	1439.8	5182.3	1384.4	578.4
10	0.00100016	42.4100	0.15105	4.1943	1448.0	5241.1	1305.6	582.1
12	0.00100036	50.7957	0.18056	4.1915	1455.9	5297.3	1233.8	585.8
14	0.00100061	59.1763	0.20985	4.1891	1463.4	5350.8	1168.2	589.4
16	0.00100092	67.5525	0.23892	4.1871	1470.6	5401.7	1107.9	592.9
18	0.00100127	75.9249	0.26777	4.1854	1477.4	5450.0	1052.6	596.4
20	0.00100166	84.2941	0.29642	4.1839	1483.9	5495.7	1001.5	599.7
25	0.00100283	105.206	0.36715	4.1810	1498.6	5599.0	890.0	607.7
30	0.00100423	126.106	0.43667	4.1792	1511.5	5687.2	797.2	615.2
35	0.00100586	146.999	0.50503	4.1782	1522.5	5761.0	719.1	622.2
40	0.00100770	167.889	0.57228	4.1778	1531.8	5821.1	652.8	628.8
45	0.00100974	188.778	0.63846	4.1781	1539.5	5868.3	595.8	634.9
50	0.00101196	209.671	0.70361	4.1789	1545.8	5903.3	546.6	640.7
55	0.00101437	230.568	0.76779	4.1802	1550.7	5926.8	503.7	646.0
60	0.00101694	251.474	0.83101	4.1821	1554.4	5939.6	466.1	651.0
65	0.00101968	272.390	0.89333	4.1845	1556.8	5942.2	433.0	655.5
70	0.00102259	293.320	0.95477	4.1874	1558.1	5935.3	403.6	659.8
75	0.00102565	314.265	1.0154	4.1909	1558.4	5919.4	377.5	663.6
80	0.00102887	335.229	1.0752	4.1949	1557.6	5895.2	354.1	667.1
85	0.00103225	356.215	1.1342	4.1993	1555.9	5863.2	333.2	670.3
90	0.00103578	377.224	1.1924	4.2044	1553.4	5823.9	314.3	673.2
95	0.00103947	398.259	1.2499	4.2099	1549.9	5777.7	297.2	675.7
100	0.00104330	419.323	1.3068	4.2160	1545.7	5725.1	281.7	677.9
110	0.00105144	461.550	1.4185	4.2297	1535.0	5602.3	254.7	681.4
120	0.00106021	503.926	1.5276	4.2459	1521.5	5458.4	232.1	683.7
130	0.00106963	546.476	1.6345	4.2645	1505.3	5296.2	213.0	684.9
140	0.00107974	589.225	1.7392	4.2859	1486.7	5117.8	196.7	684.9
t_s = 143.613 °C				**Saturation**				
Liquid	0.00108356	604.723	1.7766	4.2944	1479.4	5049.8	191.3	684.6
Vapour	0.462392	2738.06	6.8954	2.3403	491.09	1.3039	13.74	29.90
150	0.470887	2752.78	6.9305	2.2749	495.98	1.3060	14.01	30.23
160	0.483935	2775.19	6.9828	2.2121	503.07	1.3074	14.43	30.84
170	0.496761	2797.09	7.0328	2.1708	509.78	1.3078	14.84	31.54
180	0.509418	2818.64	7.0809	2.1403	516.24	1.3079	15.26	32.31
190	0.521938	2839.92	7.1274	2.1167	522.51	1.3077	15.68	33.12
200	0.534345	2860.99	7.1724	2.0984	528.61	1.3073	16.10	33.98
210	0.546656	2881.90	7.2161	2.0841	534.56	1.3068	16.51	34.87
220	0.558886	2902.69	7.2587	2.0732	540.38	1.3062	16.93	35.78
230	0.571047	2923.37	7.3002	2.0649	546.08	1.3055	17.35	36.72
240	0.583149	2943.99	7.3408	2.0588	551.68	1.3048	17.77	37.68

Table 3 Single-phase region – Continued
(0 °C to 800 °C)

$p = 4$ bar								
t [°C]	v [m^3 kg^{-1}]	h [kJ kg^{-1}]	s [kJ kg^{-1} K^{-1}]	c_p [kJ kg^{-1} K^{-1}]	w [m s^{-1}]	κ [–]	η [10^{-6} Pa s]	λ [10^{-3} W m^{-1} K^{-1}]
250	0.595199	2964.56	7.3805	2.0546	557.17	1.3039	18.19	38.66
260	0.607205	2985.09	7.4194	2.0519	562.57	1.3030	18.60	39.66
270	0.619173	3005.60	7.4575	2.0504	567.88	1.3021	19.02	40.67
280	0.631106	3026.10	7.4949	2.0500	573.11	1.3011	19.44	41.70
290	0.643008	3046.60	7.5316	2.0505	578.26	1.3001	19.86	42.74
300	0.654884	3067.11	7.5677	2.0518	583.34	1.2990	20.28	43.79
310	0.666736	3087.64	7.6032	2.0537	588.36	1.2980	20.69	44.86
320	0.678566	3108.19	7.6381	2.0561	593.31	1.2969	21.11	45.93
330	0.690376	3128.76	7.6725	2.0591	598.19	1.2958	21.53	47.02
340	0.702170	3149.37	7.7064	2.0624	603.02	1.2947	21.95	48.12
350	0.713947	3170.01	7.7398	2.0661	607.80	1.2936	22.37	49.23
360	0.725709	3190.69	7.7728	2.0702	612.52	1.2924	22.78	50.35
370	0.737458	3211.42	7.8052	2.0745	617.18	1.2913	23.20	51.49
380	0.749196	3232.18	7.8373	2.0790	621.80	1.2902	23.61	52.63
390	0.760921	3253.00	7.8689	2.0838	626.37	1.2890	24.03	53.78
400	0.772637	3273.86	7.9001	2.0887	630.90	1.2879	24.45	54.95
410	0.784343	3294.77	7.9310	2.0938	635.38	1.2868	24.86	56.12
420	0.796040	3315.74	7.9614	2.0991	639.81	1.2856	25.28	57.30
430	0.807729	3336.76	7.9915	2.1046	644.20	1.2845	25.69	58.49
440	0.819410	3357.83	8.0213	2.1101	648.56	1.2833	26.10	59.70
450	0.831084	3378.96	8.0507	2.1158	652.87	1.2822	26.52	60.91
460	0.842751	3400.15	8.0798	2.1216	657.14	1.2810	26.93	62.13
470	0.854413	3421.39	8.1086	2.1275	661.38	1.2799	27.34	63.36
480	0.866068	3442.69	8.1371	2.1334	665.58	1.2788	27.75	64.59
490	0.877718	3464.06	8.1652	2.1395	669.75	1.2776	28.16	65.84
500	0.889363	3485.49	8.1931	2.1456	673.88	1.2765	28.57	67.10
510	0.901003	3506.97	8.2207	2.1519	677.98	1.2754	28.98	68.36
520	0.912638	3528.52	8.2481	2.1581	682.04	1.2743	29.39	69.63
530	0.924269	3550.14	8.2752	2.1645	686.07	1.2732	29.79	70.91
540	0.935896	3571.81	8.3020	2.1709	690.07	1.2720	30.20	72.20
550	0.947520	3593.55	8.3286	2.1773	694.04	1.2709	30.60	73.49
560	0.959139	3615.36	8.3549	2.1838	697.99	1.2698	31.01	74.79
570	0.970756	3637.23	8.3810	2.1904	701.90	1.2688	31.41	76.10
580	0.982369	3659.17	8.4069	2.1969	705.78	1.2677	31.82	77.42
590	0.993979	3681.17	8.4325	2.2036	709.64	1.2666	32.22	78.74
600	1.00559	3703.24	8.4579	2.2102	713.47	1.2655	32.62	80.07
650	1.06359	3814.59	8.5819	2.2439	732.23	1.2603	34.61	86.83
700	1.12153	3927.63	8.7012	2.2779	750.40	1.2552	36.58	93.72
750	1.17944	4042.38	8.8161	2.3122	768.04	1.2504	38.53	100.7
800	1.23731	4158.85	8.9273	2.3466	785.19	1.2457	40.45	107.9

Table 3 Single-phase region – Continued (0 °C to 800 °C)

$p =$ **5 bar**

t [°C]	v [m^3 kg^{-1}]	h [kJ kg^{-1}]	s [kJ kg^{-1} K^{-1}]	c_p [kJ kg^{-1} K^{-1}]	w [m s^{-1}]	κ [–]	η [10^{-6} Pa s]	λ [10^{-3} W m^{-1} K^{-1}]
0	0.000999953	0.46700	−0.0001210	4.2174	1403.1	3937.4	1790.9	562.3
2	0.000999856	8.89527	0.030622	4.2110	1412.9	3992.9	1672.8	566.5
4	0.000999827	17.3117	0.061100	4.2056	1422.3	4046.4	1566.7	570.6
6	0.000999862	25.7183	0.091324	4.2011	1431.3	4097.7	1471.0	574.5
8	0.000999957	34.1164	0.12130	4.1972	1439.9	4146.9	1384.3	578.4
10	0.00100011	42.5075	0.15104	4.1939	1448.2	4194.0	1305.5	582.2
12	0.00100031	50.8925	0.18055	4.1912	1456.1	4239.0	1233.7	585.9
14	0.00100057	59.2724	0.20984	4.1888	1463.6	4281.8	1168.1	589.5
16	0.00100087	67.6479	0.23890	4.1868	1470.8	4322.5	1107.9	593.0
18	0.00100122	76.0196	0.26776	4.1850	1477.6	4361.1	1052.5	596.4
20	0.00100161	84.3882	0.29640	4.1836	1484.0	4397.7	1001.5	599.7
25	0.00100278	105.298	0.36713	4.1807	1498.8	4480.4	890.0	607.7
30	0.00100419	126.197	0.43664	4.1789	1511.6	4550.9	797.2	615.2
35	0.00100582	147.089	0.50500	4.1779	1522.6	4609.9	719.2	622.2
40	0.00100766	167.978	0.57224	4.1776	1531.9	4658.0	652.8	628.8
45	0.00100970	188.866	0.63842	4.1778	1539.7	4695.8	595.8	635.0
50	0.00101192	209.757	0.70357	4.1786	1546.0	4723.8	546.6	640.7
55	0.00101432	230.653	0.76774	4.1800	1550.9	4742.7	503.7	646.1
60	0.00101690	251.558	0.83096	4.1819	1554.5	4752.9	466.1	651.0
65	0.00101964	272.473	0.89327	4.1843	1557.0	4755.0	433.0	655.6
70	0.00102254	293.401	0.95471	4.1872	1558.3	4749.5	403.7	659.8
75	0.00102561	314.346	1.0153	4.1907	1558.6	4736.9	377.5	663.7
80	0.00102883	335.309	1.0751	4.1946	1557.8	4717.5	354.2	667.2
85	0.00103220	356.293	1.1341	4.1991	1556.1	4692.0	333.2	670.4
90	0.00103573	377.301	1.1923	4.2041	1553.5	4660.5	314.3	673.2
95	0.00103942	398.335	1.2499	4.2097	1550.1	4623.6	297.2	675.8
100	0.00104325	419.399	1.3067	4.2157	1545.9	4581.5	281.7	678.0
110	0.00105139	461.623	1.4184	4.2295	1535.2	4483.3	254.7	681.5
120	0.00106016	503.996	1.5275	4.2456	1521.7	4368.3	232.1	683.8
130	0.00106957	546.543	1.6344	4.2642	1505.6	4238.6	213.0	684.9
140	0.00107967	589.290	1.7391	4.2856	1487.0	4095.9	196.7	685.0
150	0.00109049	632.266	1.8419	4.3102	1466.0	3941.9	182.6	683.9
t_s = 151.836 °C				**Saturation**				
Liquid	0.00109256	640.185	1.8606	4.3151	1462.0	3912.5	180.2	683.6
Vapour	0.374804	2748.11	6.8206	2.4127	493.80	1.3011	14.02	31.03
160	0.383660	2767.38	6.8655	2.3176	500.18	1.3042	14.37	31.42
170	0.394255	2790.19	6.9176	2.2500	507.32	1.3056	14.79	32.00
180	0.404655	2812.45	6.9672	2.2048	514.07	1.3061	15.22	32.68
190	0.414905	2834.32	7.0150	2.1711	520.56	1.3062	15.64	33.44
200	0.425034	2855.90	7.0611	2.1448	526.84	1.3061	16.06	34.24
210	0.435060	2877.24	7.1057	2.1242	532.96	1.3058	16.48	35.10
220	0.445001	2898.40	7.1491	2.1080	538.92	1.3053	16.90	35.98
230	0.454870	2919.41	7.1912	2.0954	544.74	1.3047	17.32	36.90
240	0.464676	2940.31	7.2324	2.0856	550.44	1.3041	17.74	37.85

Table 3 Single-phase region – Continued
(0 °C to 800 °C)

p = 5 bar								
t	v	h	s	c_p	w	κ	η	λ
[°C]	[$m^3\ kg^{-1}$]	[$kJ\ kg^{-1}$]	[$kJ\ kg^{-1}\ K^{-1}$]	[$kJ\ kg^{-1}\ K^{-1}$]	[$m\ s^{-1}$]	[–]	[10^{-6} Pa s]	[$10^{-3}\ W\ m^{-1}\ K^{-1}$]
250	0.474429	2961.13	7.2726	2.0783	556.03	1.3033	18.16	38.81
260	0.484135	2981.88	7.3119	2.0730	561.51	1.3025	18.58	39.80
270	0.493801	3002.59	7.3503	2.0693	566.90	1.3016	19.00	40.80
280	0.503432	3023.28	7.3881	2.0670	572.20	1.3007	19.42	41.82
290	0.513031	3043.94	7.4251	2.0659	577.42	1.2998	19.84	42.85
300	0.522603	3064.60	7.4614	2.0657	582.55	1.2988	20.26	43.90
310	0.532150	3085.26	7.4972	2.0664	587.62	1.2977	20.68	44.96
320	0.541675	3105.93	7.5323	2.0678	592.61	1.2967	21.10	46.03
330	0.551180	3126.61	7.5669	2.0698	597.55	1.2956	21.52	47.12
340	0.560667	3147.32	7.6010	2.0723	602.41	1.2945	21.94	48.21
350	0.570138	3168.06	7.6345	2.0753	607.22	1.2934	22.36	49.32
360	0.579594	3188.83	7.6676	2.0786	611.98	1.2923	22.78	50.44
370	0.589037	3209.63	7.7002	2.0823	616.68	1.2912	23.19	51.57
380	0.598467	3230.48	7.7323	2.0864	621.32	1.2901	23.61	52.71
390	0.607886	3251.36	7.7641	2.0906	625.92	1.2890	24.03	53.86
400	0.617294	3272.29	7.7954	2.0952	630.47	1.2878	24.44	55.03
410	0.626693	3293.27	7.8263	2.0999	634.97	1.2867	24.86	56.20
420	0.636083	3314.29	7.8569	2.1048	639.43	1.2856	25.27	57.38
430	0.645465	3335.36	7.8871	2.1099	643.84	1.2844	25.69	58.57
440	0.654838	3356.49	7.9169	2.1152	648.21	1.2833	26.10	59.77
450	0.664205	3377.67	7.9464	2.1206	652.54	1.2822	26.52	60.98
460	0.673565	3398.90	7.9756	2.1261	656.83	1.2810	26.93	62.20
470	0.682919	3420.19	8.0044	2.1318	661.09	1.2799	27.34	63.43
480	0.692267	3441.54	8.0329	2.1376	665.30	1.2788	27.75	64.66
490	0.701609	3462.94	8.0612	2.1434	669.48	1.2776	28.16	65.91
500	0.710947	3484.41	8.0891	2.1494	673.62	1.2765	28.57	67.16
510	0.720279	3505.93	8.1168	2.1554	677.73	1.2754	28.98	68.42
520	0.729607	3527.52	8.1442	2.1615	681.81	1.2743	29.39	69.70
530	0.738931	3549.16	8.1713	2.1677	685.85	1.2732	29.80	70.97
540	0.748250	3570.87	8.1981	2.1740	689.86	1.2721	30.20	72.26
550	0.757566	3592.64	8.2247	2.1803	693.85	1.2710	30.61	73.55
560	0.766878	3614.48	8.2511	2.1866	697.80	1.2699	31.01	74.86
570	0.776187	3636.38	8.2772	2.1931	701.72	1.2688	31.42	76.16
580	0.785493	3658.34	8.3031	2.1995	705.61	1.2677	31.82	77.48
590	0.794796	3680.37	8.3288	2.2060	709.48	1.2666	32.22	78.80
600	0.804095	3702.46	8.3543	2.2126	713.31	1.2656	32.62	80.13
650	0.850556	3813.91	8.4784	2.2458	732.11	1.2603	34.62	86.88
700	0.896964	3927.05	8.5977	2.2795	750.31	1.2553	36.59	93.78
750	0.943332	4041.87	8.7128	2.3135	767.98	1.2504	38.53	100.8
800	0.989667	4158.40	8.8240	2.3477	785.14	1.2458	40.45	107.9

Table 3 Single-phase region – Continued (0 °C to 800 °C)

$p =$ **10 bar**

t [°C]	v [m^3 kg^{-1}]	h [kJ kg^{-1}]	s [kJ kg^{-1} K^{-1}]	c_p [kJ kg^{-1} K^{-1}]	w [m s^{-1}]	κ [–]	η [10^{-6} Pa s]	λ [10^{-3} W m^{-1} K^{-1}]
0	0.000999699	0.97582	−0.00008842	4.2150	1403.8	1971.4	1789.7	562.6
2	0.000999606	9.39927	0.030637	4.2087	1413.6	1999.2	1671.8	566.8
4	0.000999581	17.8112	0.061099	4.2034	1423.1	2025.9	1565.9	570.8
6	0.000999618	26.2135	0.091307	4.1990	1432.1	2051.6	1470.3	574.8
8	0.000999716	34.6076	0.12127	4.1952	1440.7	2076.2	1383.7	578.7
10	0.000999870	42.9948	0.15100	4.1921	1449.0	2099.8	1305.1	582.5
12	0.00100008	51.3761	0.18049	4.1894	1456.9	2122.3	1233.4	586.2
14	0.00100033	59.7525	0.20977	4.1871	1464.4	2143.7	1167.8	589.8
16	0.00100064	68.1246	0.23882	4.1851	1471.5	2164.1	1107.6	593.3
18	0.00100099	76.4931	0.26766	4.1834	1478.4	2183.4	1052.3	596.7
20	0.00100139	84.8585	0.29630	4.1820	1484.8	2201.7	1001.3	600.0
25	0.00100255	105.761	0.36700	4.1793	1499.6	2243.1	889.9	608.0
30	0.00100396	126.653	0.43649	4.1776	1512.4	2278.4	797.2	615.5
35	0.00100560	147.538	0.50482	4.1766	1523.4	2307.9	719.2	622.5
40	0.00100744	168.421	0.57204	4.1763	1532.8	2332.0	652.8	629.1
45	0.00100947	189.303	0.63820	4.1766	1540.5	2350.9	595.9	635.2
50	0.00101170	210.188	0.70334	4.1775	1546.8	2365.0	546.7	641.0
55	0.00101410	231.079	0.76749	4.1789	1551.7	2374.4	503.8	646.3
60	0.00101667	251.977	0.83070	4.1808	1555.4	2379.6	466.3	651.3
65	0.00101941	272.887	0.89299	4.1832	1557.9	2380.7	433.1	655.9
70	0.00102231	293.810	0.95441	4.1861	1559.2	2378.0	403.8	660.1
75	0.00102537	314.749	1.0150	4.1896	1559.5	2371.7	377.7	663.9
80	0.00102859	335.707	1.0748	4.1935	1558.7	2362.1	354.3	667.5
85	0.00103196	356.686	1.1338	4.1980	1557.1	2349.4	333.3	670.7
90	0.00103549	377.688	1.1920	4.2030	1554.5	2333.7	314.4	673.5
95	0.00103917	398.717	1.2495	4.2085	1551.1	2315.3	297.3	676.0
100	0.00104300	419.774	1.3063	4.2146	1546.9	2294.3	281.8	678.3
110	0.00105112	461.987	1.4179	4.2283	1536.3	2245.4	254.8	681.8
120	0.00105988	504.348	1.5271	4.2443	1522.8	2188.0	232.2	684.1
130	0.00106928	546.882	1.6339	4.2629	1506.8	2123.3	213.1	685.2
140	0.00107936	589.614	1.7386	4.2841	1488.3	2052.1	196.8	685.3
150	0.00109015	632.575	1.8414	4.3086	1467.4	1975.2	182.7	684.2
160	0.00110171	675.797	1.9423	4.3366	1444.3	1893.4	170.5	682.1
170	0.00111410	719.320	2.0417	4.3687	1418.9	1807.1	159.8	678.9
t_s = 179.886 °C				**Saturation**				
Liquid	0.00112723	762.683	2.1384	4.4051	1391.6	1718.1	150.5	674.7
Vapour	0.194349	2777.12	6.5850	2.7150	500.89	1.2910	14.98	35.40
180	0.194418	2777.43	6.5857	2.7119	501.00	1.2911	14.99	35.40
190	0.200319	2803.52	6.6426	2.5285	509.69	1.2969	15.43	35.64
200	0.206004	2828.27	6.6955	2.4288	517.32	1.2991	15.88	36.06
210	0.211542	2852.20	6.7455	2.3614	524.41	1.3000	16.32	36.62
220	0.216966	2875.55	6.7934	2.3105	531.18	1.3005	16.75	37.28
230	0.222297	2898.45	6.8393	2.2702	537.69	1.3006	17.19	38.03
240	0.227551	2920.98	6.8837	2.2378	543.99	1.3005	17.63	38.84

Table 3 Single-phase region – Continued (0 °C to 800 °C)

t	v	h	s	c_p	w	κ	η	λ
				p = 10 bar				
[°C]	[$m^3\ kg^{-1}$]	[$kJ\ kg^{-1}$]	[$kJ\ kg^{-1}\ K^{-1}$]	[$kJ\ kg^{-1}\ K^{-1}$]	[$m\ s^{-1}$]	[–]	[10^{-6} Pa s]	[$10^{-3}\ W\ m^{-1}\ K^{-1}$]
250	0.232739	2943.22	6.9266	2.2116	550.11	1.3002	18.06	39.70
260	0.237871	2965.23	6.9683	2.1905	556.06	1.2999	18.49	40.60
270	0.242955	2987.05	7.0088	2.1735	561.86	1.2994	18.92	41.53
280	0.247998	3008.71	7.0484	2.1600	567.53	1.2988	19.35	42.49
290	0.253004	3030.25	7.0870	2.1492	573.08	1.2981	19.78	43.48
300	0.257979	3051.70	7.1247	2.1408	578.51	1.2973	20.21	44.49
310	0.262926	3073.08	7.1617	2.1344	583.85	1.2965	20.63	45.52
320	0.267848	3094.40	7.1979	2.1297	589.09	1.2956	21.06	46.57
330	0.272749	3115.68	7.2335	2.1263	594.25	1.2947	21.48	47.63
340	0.277629	3136.93	7.2685	2.1242	599.32	1.2938	21.91	48.70
350	0.282492	3158.16	7.3028	2.1231	604.32	1.2928	22.33	49.80
360	0.287339	3179.39	7.3366	2.1228	609.24	1.2918	22.75	50.90
370	0.292172	3200.62	7.3699	2.1233	614.10	1.2907	23.17	52.01
380	0.296991	3221.86	7.4026	2.1245	618.89	1.2897	23.59	53.14
390	0.301799	3243.11	7.4349	2.1262	623.62	1.2886	24.01	54.28
400	0.306595	3264.39	7.4668	2.1284	628.30	1.2876	24.43	55.44
410	0.311381	3285.68	7.4982	2.1311	632.92	1.2865	24.85	56.60
420	0.316158	3307.01	7.5292	2.1341	637.48	1.2854	25.27	57.77
430	0.320927	3328.37	7.5598	2.1375	642.00	1.2843	25.69	58.96
440	0.325687	3349.76	7.5900	2.1412	646.47	1.2832	26.10	60.15
450	0.330440	3371.19	7.6198	2.1451	650.89	1.2821	26.52	61.35
460	0.335186	3392.66	7.6493	2.1494	655.26	1.2810	26.93	62.56
470	0.339926	3414.18	7.6785	2.1538	659.59	1.2799	27.35	63.79
480	0.344659	3435.74	7.7073	2.1584	663.88	1.2788	27.76	65.02
490	0.349387	3457.35	7.7358	2.1632	668.13	1.2777	28.17	66.26
500	0.354110	3479.00	7.7640	2.1682	672.34	1.2766	28.58	67.51
510	0.358828	3500.71	7.7919	2.1733	676.52	1.2755	28.99	68.76
520	0.363541	3522.47	7.8195	2.1786	680.65	1.2744	29.40	70.03
530	0.368250	3544.28	7.8468	2.1840	684.75	1.2733	29.81	71.30
540	0.372955	3566.15	7.8739	2.1895	688.82	1.2722	30.22	72.58
550	0.377656	3588.07	7.9007	2.1951	692.85	1.2711	30.62	73.87
560	0.382354	3610.05	7.9272	2.2008	696.85	1.2700	31.03	75.17
570	0.387048	3632.09	7.9535	2.2066	700.82	1.2690	31.43	76.48
580	0.391738	3654.19	7.9795	2.2125	704.76	1.2679	31.84	77.79
590	0.396426	3676.34	8.0054	2.2185	708.66	1.2668	32.24	79.11
600	0.401111	3698.56	8.0309	2.2245	712.54	1.2658	32.64	80.43
650	0.424497	3810.55	8.1557	2.2555	731.51	1.2606	34.64	87.16
700	0.447829	3924.12	8.2755	2.2875	749.86	1.2556	36.61	94.04
750	0.471121	4039.31	8.3909	2.3201	767.64	1.2508	38.55	101.0
800	0.494380	4156.14	8.5024	2.3532	784.91	1.2462	40.47	108.2

Table 3 Single-phase region – Continued (0 °C to 800 °C)

p = 20 bar

t [°C]	v [m^3 kg^{-1}]	h [kJ kg^{-1}]	s [kJ kg^{-1} K^{-1}]	c_p [kJ kg^{-1} K^{-1}]	w [m s^{-1}]	κ [–]	η [10^{-6} Pa s]	λ [10^{-3} W m^{-1} K^{-1}]
0	0.000999193	1.99229	−0.00002608	4.2100	1405.4	988.40	1787.5	563.2
2	0.000999107	10.4062	0.030665	4.2041	1415.2	1002.3	1670.0	567.3
4	0.000999088	18.8091	0.061094	4.1990	1424.6	1015.7	1564.3	571.4
6	0.000999132	27.2029	0.091271	4.1948	1433.7	1028.6	1469.0	575.4
8	0.000999235	35.5890	0.12121	4.1913	1442.3	1040.9	1382.7	579.3
10	0.000999394	43.9685	0.15090	4.1883	1450.6	1052.7	1304.2	583.0
12	0.000999605	52.3425	0.18038	4.1858	1458.4	1063.9	1232.6	586.7
14	0.000999866	60.7118	0.20962	4.1836	1466.0	1074.7	1167.2	590.3
16	0.00100018	69.0772	0.23865	4.1818	1473.1	1084.9	1107.2	593.8
18	0.00100053	77.4392	0.26747	4.1802	1479.9	1094.5	1051.9	597.2
20	0.00100093	85.7984	0.29609	4.1789	1486.4	1103.7	1001.0	600.6
25	0.00100210	106.686	0.36674	4.1764	1501.2	1124.4	889.8	608.5
30	0.00100352	127.564	0.43618	4.1749	1514.0	1142.1	797.2	616.0
35	0.00100515	148.437	0.50447	4.1741	1525.0	1156.9	719.3	623.0
40	0.00100700	169.306	0.57166	4.1739	1534.4	1169.0	653.0	629.6
45	0.00100903	190.177	0.63778	4.1743	1542.2	1178.5	596.1	635.7
50	0.00101125	211.050	0.70287	4.1752	1548.5	1185.6	546.9	641.5
55	0.00101365	231.929	0.76699	4.1766	1553.4	1190.3	504.1	646.8
60	0.00101622	252.817	0.83016	4.1786	1557.1	1193.0	466.5	651.8
65	0.00101896	273.716	0.89243	4.1810	1559.6	1193.6	433.4	656.4
70	0.00102185	294.628	0.95382	4.1840	1561.0	1192.3	404.0	660.6
75	0.00102491	315.556	1.0144	4.1874	1561.3	1189.2	377.9	664.5
80	0.00102812	336.503	1.0741	4.1914	1560.6	1184.4	354.6	668.0
85	0.00103148	357.471	1.1331	4.1958	1559.0	1178.1	333.6	671.2
90	0.00103500	378.462	1.1913	4.2008	1556.5	1170.3	314.7	674.1
95	0.00103867	399.479	1.2487	4.2063	1553.1	1161.2	297.6	676.6
100	0.00104249	420.526	1.3055	4.2123	1549.0	1150.8	282.1	678.8
110	0.00105059	462.715	1.4171	4.2259	1538.4	1126.4	255.1	682.3
120	0.00105932	505.051	1.5262	4.2418	1525.1	1097.8	232.5	684.7
130	0.00106869	547.559	1.6329	4.2601	1509.2	1065.6	213.4	685.9
140	0.00107873	590.263	1.7376	4.2812	1490.8	1030.1	197.1	685.9
150	0.00108948	633.193	1.8403	4.3053	1470.1	991.86	183.0	684.9
160	0.00110099	676.382	1.9411	4.3330	1447.2	951.08	170.8	682.8
170	0.00111332	719.867	2.0404	4.3647	1422.0	908.11	160.1	679.6
180	0.00112654	763.691	2.1382	4.4011	1394.6	863.22	150.6	675.4
190	0.00114075	807.906	2.2347	4.4430	1365.0	816.67	142.2	670.1
200	0.00115606	852.572	2.3301	4.4914	1333.2	768.70	134.7	663.8
210	0.00117260	897.760	2.4246	4.5476	1299.0	719.55	127.9	656.4
t_s = 212.385 °C				**Saturation**				
Liquid	0.00117675	908.622	2.4470	4.5623	1290.6	707.68	126.4	654.4
Vapour	0.0995805	2798.38	6.3392	3.1904	504.66	1.2788	16.09	41.65
220	0.102167	2821.67	6.3868	2.9487	512.58	1.2858	16.45	41.46
230	0.105394	2850.17	6.4440	2.7665	521.47	1.2901	16.92	41.50
240	0.108488	2877.21	6.4972	2.6481	529.47	1.2920	17.39	41.78

Table 3 Single-phase region – Continued (0 °C to 800 °C)

$p = 20$ bar

t [°C]	v [m^3 kg^{-1}]	h [kJ kg^{-1}]	s [kJ kg^{-1} K^{-1}]	c_p [kJ kg^{-1} K^{-1}]	w [m s^{-1}]	κ [–]	η [10^{-6} Pa s]	λ [10^{-3} W m^{-1} K^{-1}]
250	0.111484	2903.23	6.5474	2.5602	536.96	1.2931	17.85	42.22
260	0.114400	2928.47	6.5952	2.4909	544.07	1.2938	18.30	42.80
270	0.117251	2953.09	6.6410	2.4349	550.89	1.2941	18.75	43.48
280	0.120046	2977.21	6.6850	2.3890	557.44	1.2943	19.20	44.25
290	0.122794	3000.90	6.7274	2.3512	563.78	1.2942	19.65	45.07
300	0.125501	3024.25	6.7685	2.3201	569.91	1.2940	20.09	45.95
310	0.128174	3047.32	6.8084	2.2944	575.87	1.2937	20.53	46.87
320	0.130816	3070.16	6.8472	2.2733	581.67	1.2932	20.97	47.83
330	0.133431	3092.80	6.8851	2.2559	587.33	1.2926	21.41	48.82
340	0.136023	3115.28	6.9221	2.2417	592.86	1.2920	21.84	49.83
350	0.138594	3137.64	6.9582	2.2301	598.27	1.2913	22.28	50.87
360	0.141147	3159.89	6.9937	2.2207	603.57	1.2905	22.71	51.92
370	0.143683	3182.06	7.0284	2.2133	608.77	1.2897	23.14	52.99
380	0.146205	3204.16	7.0625	2.2074	613.88	1.2888	23.56	54.09
390	0.148712	3226.21	7.0960	2.2030	618.91	1.2879	23.99	55.20
400	0.151208	3248.23	7.1290	2.1997	623.85	1.2869	24.42	56.32
410	0.153693	3270.21	7.1614	2.1974	628.72	1.2860	24.84	57.46
420	0.156167	3292.18	7.1933	2.1961	633.52	1.2850	25.26	58.61
430	0.158632	3314.14	7.2248	2.1955	638.25	1.2840	25.69	59.77
440	0.161088	3336.09	7.2558	2.1957	642.92	1.2830	26.11	60.95
450	0.163537	3358.05	7.2863	2.1964	647.52	1.2819	26.53	62.13
460	0.165978	3380.02	7.3165	2.1976	652.08	1.2809	26.94	63.33
470	0.168413	3402.01	7.3463	2.1994	656.57	1.2799	27.36	64.54
480	0.170841	3424.01	7.3757	2.2015	661.02	1.2788	27.78	65.75
490	0.173263	3446.04	7.4048	2.2041	665.41	1.2777	28.19	66.98
500	0.175680	3468.09	7.4335	2.2069	669.76	1.2767	28.60	68.22
510	0.178092	3490.18	7.4619	2.2101	674.06	1.2756	29.02	69.46
520	0.180499	3512.30	7.4899	2.2136	678.32	1.2746	29.43	70.72
530	0.182902	3534.45	7.5177	2.2173	682.54	1.2735	29.84	71.98
540	0.185300	3556.64	7.5451	2.2212	686.71	1.2725	30.25	73.25
550	0.187694	3578.88	7.5723	2.2254	690.85	1.2714	30.66	74.53
560	0.190085	3601.15	7.5992	2.2297	694.95	1.2704	31.06	75.82
570	0.192472	3623.47	7.6258	2.2342	699.01	1.2693	31.47	77.11
580	0.194856	3645.84	7.6522	2.2389	703.04	1.2683	31.88	78.42
590	0.197237	3668.25	7.6783	2.2437	707.03	1.2672	32.28	79.73
600	0.199614	3690.71	7.7042	2.2486	710.99	1.2662	32.68	81.05
650	0.211464	3803.79	7.8301	2.2750	730.32	1.2611	34.68	87.74
700	0.223260	3918.24	7.9509	2.3035	748.96	1.2562	36.65	94.59
750	0.235015	4034.16	8.0670	2.3333	766.98	1.2515	38.60	101.6
800	0.246737	4151.59	8.1791	2.3642	784.44	1.2470	40.52	108.6

Table 3 Single-phase region – Continued
(0 °C to 800 °C)

p = 30 bar

t [°C]	v [m^3 kg^{-1}]	h [kJ kg^{-1}]	s [kJ kg^{-1} K^{-1}]	c_p [kJ kg^{-1} K^{-1}]	w [m s^{-1}]	κ [–]	η [10^{-6} Pa s]	λ [10^{-3} W m^{-1} K^{-1}]
0	0.000998688	3.00722	0.00003247	4.2052	1407.0	660.74	1785.3	563.7
2	0.000998609	11.4117	0.030689	4.1995	1416.8	670.04	1668.1	567.9
4	0.000998597	19.8057	0.061086	4.1947	1426.2	678.98	1562.8	572.0
6	0.000998647	28.1911	0.091233	4.1907	1435.2	687.57	1467.7	576.0
8	0.000998755	36.5691	0.12114	4.1874	1443.9	695.80	1381.6	579.8
10	0.000998919	44.9410	0.15081	4.1846	1452.1	703.67	1303.3	583.6
12	0.000999135	53.3078	0.18026	4.1822	1460.0	711.18	1231.9	587.3
14	0.000999400	61.6702	0.20948	4.1802	1467.6	718.33	1166.6	590.9
16	0.000999713	70.0289	0.23849	4.1785	1474.7	725.14	1106.7	594.4
18	0.00100007	78.3845	0.26729	4.1771	1481.5	731.60	1051.6	597.8
20	0.00100047	86.7374	0.29588	4.1759	1488.0	737.71	1000.7	601.1
25	0.00100165	107.611	0.36648	4.1736	1502.8	751.53	889.6	609.1
30	0.00100307	128.475	0.43588	4.1722	1515.6	763.34	797.2	616.5
35	0.00100471	149.334	0.50413	4.1716	1526.6	773.23	719.3	623.5
40	0.00100655	170.191	0.57127	4.1715	1536.0	781.31	653.1	630.1
45	0.00100859	191.050	0.63735	4.1719	1543.8	787.67	596.3	636.3
50	0.00101081	211.912	0.70241	4.1729	1550.1	792.41	547.1	642.0
55	0.00101321	232.780	0.76649	4.1744	1555.1	795.63	504.3	647.3
60	0.00101577	253.656	0.82963	4.1764	1558.8	797.41	466.7	652.3
65	0.00101851	274.544	0.89187	4.1788	1561.4	797.84	433.6	656.9
70	0.00102140	295.445	0.95322	4.1818	1562.7	797.01	404.3	661.1
75	0.00102445	316.363	1.0137	4.1853	1563.1	794.99	378.2	665.0
80	0.00102765	337.299	1.0734	4.1892	1562.5	791.86	354.8	668.5
85	0.00103101	358.256	1.1324	4.1937	1560.9	787.69	333.9	671.7
90	0.00103451	379.236	1.1905	4.1986	1558.4	782.54	315.0	674.6
95	0.00103817	400.242	1.2480	4.2041	1555.1	776.48	297.9	677.1
100	0.00104198	421.277	1.3048	4.2100	1551.0	769.57	282.4	679.4
110	0.00105006	463.443	1.4163	4.2235	1540.6	753.40	255.4	682.9
120	0.00105876	505.755	1.5253	4.2393	1527.4	734.45	232.8	685.3
130	0.00106810	548.237	1.6320	4.2574	1511.6	713.05	213.7	686.5
140	0.00107810	590.913	1.7365	4.2783	1493.3	689.50	197.3	686.6
150	0.00108881	633.813	1.8391	4.3022	1472.8	664.07	183.3	685.6
160	0.00110027	676.968	1.9399	4.3295	1450.0	636.98	171.0	683.5
170	0.00111254	720.415	2.0391	4.3608	1425.0	608.43	160.3	680.3
180	0.00112570	764.198	2.1368	4.3966	1397.9	578.61	150.9	676.2
190	0.00113983	808.366	2.2332	4.4379	1368.5	547.68	142.5	670.9
200	0.00115505	852.978	2.3285	4.4856	1336.9	515.81	135.0	664.7
210	0.00117148	898.104	2.4229	4.5409	1303.1	483.14	128.2	657.3
220	0.00118930	943.826	2.5165	4.6053	1266.9	449.85	121.9	648.9
230	0.00120872	990.247	2.6097	4.6810	1228.3	416.05	116.2	639.3
t_s = 233.858 °C				**Saturation**				
Liquid	0.00121670	1008.37	2.6456	4.7138	1212.7	402.91	114.2	635.3
Vapour	0.0666641	2803.26	6.1858	3.6123	504.07	1.2705	16.84	46.70
240	0.0682274	2824.56	6.2275	3.3435	511.35	1.2775	17.15	46.28

Table 3 Single-phase region – Continued (0 °C to 800 °C)

p = 30 bar								
t	v	h	s	c_p	w	κ	η	λ
[°C]	[$m^3\ kg^{-1}$]	[$kJ\ kg^{-1}$]	[$kJ\ kg^{-1}\ K^{-1}$]	[$kJ\ kg^{-1}\ K^{-1}$]	[$m\ s^{-1}$]	[–]	[10^{-6} Pa s]	[$10^{-3}\ W\ m^{-1}\ K^{-1}$]
250	0.0706225	2856.55	6.2893	3.0772	521.44	1.2834	17.64	45.95
260	0.0728884	2886.42	6.3458	2.9070	530.33	1.2862	18.12	45.94
270	0.0750596	2914.84	6.3987	2.7826	538.52	1.2879	18.59	46.18
280	0.0771560	2942.16	6.4485	2.6854	546.22	1.2890	19.06	46.60
290	0.0791913	2968.61	6.4959	2.6071	553.54	1.2897	19.53	47.15
300	0.0811753	2994.35	6.5412	2.5431	560.52	1.2902	19.98	47.81
310	0.0831160	3019.51	6.5847	2.4902	567.23	1.2904	20.44	48.56
320	0.0850197	3044.18	6.6267	2.4463	573.70	1.2904	20.89	49.38
330	0.0868914	3068.46	6.6673	2.4098	579.95	1.2903	21.34	50.25
340	0.0887354	3092.40	6.7066	2.3794	586.00	1.2900	21.79	51.16
350	0.0905550	3116.06	6.7449	2.3539	591.89	1.2896	22.23	52.11
360	0.0923533	3139.49	6.7822	2.3327	597.62	1.2891	22.67	53.09
370	0.0941327	3162.73	6.8186	2.3150	603.21	1.2885	23.11	54.09
380	0.0958952	3185.80	6.8542	2.3003	608.67	1.2878	23.54	55.13
390	0.0976427	3208.74	6.8891	2.2881	614.01	1.2870	23.97	56.21
400	0.0993766	3231.57	6.9233	2.2780	619.25	1.2863	24.41	57.30
410	0.101098	3254.31	6.9568	2.2698	624.39	1.2854	24.84	58.40
420	0.102809	3276.97	6.9897	2.2632	629.44	1.2846	25.26	59.52
430	0.104510	3299.58	7.0221	2.2579	634.40	1.2837	25.69	60.66
440	0.106201	3322.14	7.0540	2.2539	639.28	1.2827	26.12	61.81
450	0.107884	3344.66	7.0853	2.2508	644.09	1.2818	26.54	62.97
460	0.109559	3367.16	7.1162	2.2487	648.82	1.2808	26.96	64.15
470	0.111227	3389.64	7.1467	2.2474	653.49	1.2798	27.38	65.33
480	0.112888	3412.10	7.1767	2.2467	658.10	1.2788	27.80	66.53
490	0.114544	3434.57	7.2063	2.2467	662.65	1.2778	28.22	67.74
500	0.116193	3457.04	7.2356	2.2472	667.14	1.2768	28.63	68.97
510	0.117837	3479.52	7.2645	2.2483	671.58	1.2758	29.05	70.20
520	0.119476	3502.01	7.2930	2.2497	675.96	1.2748	29.46	71.44
530	0.121111	3524.51	7.3212	2.2516	680.30	1.2738	29.87	72.69
540	0.122741	3547.04	7.3491	2.2538	684.59	1.2728	30.28	73.95
550	0.124367	3569.59	7.3767	2.2564	688.83	1.2717	30.69	75.22
560	0.125990	3592.17	7.4039	2.2593	693.03	1.2707	31.10	76.49
570	0.127608	3614.78	7.4309	2.2624	697.19	1.2697	31.51	77.78
580	0.129224	3637.42	7.4576	2.2658	701.31	1.2687	31.92	79.07
590	0.130836	3660.09	7.4840	2.2694	705.39	1.2677	32.32	80.37
600	0.132445	3682.81	7.5102	2.2732	709.43	1.2667	32.73	81.68
650	0.140451	3796.99	7.6373	2.2948	729.13	1.2617	34.73	88.33
700	0.148403	3912.34	7.7590	2.3196	748.06	1.2569	36.70	95.15
750	0.156312	4028.99	7.8759	2.3467	766.32	1.2523	38.65	102.1
800	0.164189	4147.03	7.9885	2.3753	783.99	1.2478	40.57	109.1

Table 3 Single-phase region – Continued (0 °C to 800 °C)

$p =$ 40 bar								
t [°C]	v [$m^3 kg^{-1}$]	h [$kJ kg^{-1}$]	s [$kJ kg^{-1} K^{-1}$]	c_p [$kJ kg^{-1} K^{-1}$]	w [$m s^{-1}$]	κ [–]	η [10^{-6} Pa s]	λ [$10^{-3} W m^{-1} K^{-1}$]
0	0.000998184	4.02062	0.00008726	4.2003	1408.6	496.92	1783.2	564.3
2	0.000998113	12.4157	0.030710	4.1949	1418.4	503.90	1666.3	568.5
4	0.000998107	20.8009	0.061075	4.1904	1427.8	510.62	1561.3	572.6
6	0.000998163	29.1779	0.091192	4.1867	1436.8	517.07	1466.5	576.5
8	0.000998277	37.5481	0.12107	4.1835	1445.5	523.25	1380.6	580.4
10	0.000998446	45.9125	0.15071	4.1809	1453.7	529.16	1302.4	584.2
12	0.000998666	54.2720	0.18013	4.1787	1461.6	534.79	1231.2	587.8
14	0.000998936	62.6275	0.20933	4.1768	1469.1	540.17	1166.0	591.4
16	0.000999252	70.9796	0.23832	4.1753	1476.3	545.28	1106.2	594.9
18	0.000999613	79.3288	0.26709	4.1739	1483.1	550.13	1051.2	598.3
20	0.00100002	87.6755	0.29566	4.1728	1489.6	554.72	1000.4	601.6
25	0.00100120	108.534	0.36622	4.1708	1504.4	565.10	889.5	609.6
30	0.00100263	129.385	0.43557	4.1696	1517.2	573.97	797.2	617.1
35	0.00100427	150.231	0.50378	4.1690	1528.2	581.40	719.4	624.1
40	0.00100611	171.076	0.57088	4.1691	1537.6	587.48	653.2	630.6
45	0.00100815	191.923	0.63692	4.1696	1545.4	592.27	596.4	636.8
50	0.00101037	212.773	0.70195	4.1706	1551.8	595.84	547.3	642.5
55	0.00101276	233.630	0.76600	4.1722	1556.8	598.28	504.5	647.9
60	0.00101533	254.495	0.82910	4.1742	1560.5	599.64	467.0	652.8
65	0.00101806	275.372	0.89130	4.1767	1563.1	599.98	433.9	657.4
70	0.00102094	296.263	0.95263	4.1796	1564.5	599.38	404.6	661.6
75	0.00102398	317.169	1.0131	4.1831	1564.9	597.90	378.5	665.5
80	0.00102718	338.095	1.0728	4.1871	1564.3	595.57	355.1	669.1
85	0.00103053	359.041	1.1317	4.1915	1562.8	592.47	334.1	672.3
90	0.00103403	380.010	1.1898	4.1964	1560.3	588.64	315.2	675.1
95	0.00103768	401.006	1.2473	4.2018	1557.1	584.12	298.1	677.7
100	0.00104148	422.029	1.3040	4.2078	1553.0	578.97	282.6	679.9
110	0.00104953	464.172	1.4154	4.2212	1542.7	566.91	255.6	683.5
120	0.00105821	506.460	1.5244	4.2368	1529.6	552.75	233.0	685.9
130	0.00106751	548.916	1.6310	4.2548	1513.9	536.76	213.9	687.1
140	0.00107748	591.564	1.7355	4.2754	1495.9	519.17	197.6	687.2
150	0.00108814	634.433	1.8380	4.2990	1475.5	500.17	183.5	686.2
160	0.00109956	677.555	1.9388	4.3260	1452.9	479.92	171.3	684.2
170	0.00111177	720.966	2.0378	4.3569	1428.1	458.59	160.6	681.1
180	0.00112486	764.707	2.1354	4.3923	1401.1	436.30	151.1	676.9
190	0.00113892	808.829	2.2317	4.4330	1372.0	413.18	142.7	671.8
200	0.00115404	853.387	2.3269	4.4799	1340.6	389.35	135.2	665.5
210	0.00117037	898.451	2.4212	4.5342	1307.1	364.93	128.4	658.3
220	0.00118806	944.102	2.5147	4.5975	1271.2	340.03	122.2	649.9
230	0.00120732	990.438	2.6077	4.6717	1232.9	314.76	116.5	640.4
240	0.00122842	1037.58	2.7005	4.7595	1192.1	289.22	111.2	629.7

Table 3 Single-phase region – Continued (0 °C to 800 °C)

$p =$ 40 bar								
t [°C]	v [m^3 kg^{-1}]	h [kJ kg^{-1}]	s [kJ kg^{-1} K^{-1}]	c_p [kJ kg^{-1} K^{-1}]	w [m s^{-1}]	κ [–]	η [10^{-6} Pa s]	λ [10^{-3} W m^{-1} K^{-1}]
250	0.00125169	1085.69	2.7933	4.8646	1148.5	263.45	106.3	617.8
t_s = 250.358 °C				Saturation				
Liquid	0.00125257	1087.43	2.7967	4.8688	1146.9	262.53	106.1	617.4
Vapour	0.0497766	2800.90	6.0697	4.0217	501.64	1.2639	17.44	51.27
260	0.0517770	2837.19	6.1384	3.5536	513.78	1.2746	17.94	50.30
270	0.0536916	2871.20	6.2016	3.2702	524.26	1.2797	18.44	49.80
280	0.0554948	2902.88	6.2594	3.0774	533.58	1.2826	18.93	49.67
290	0.0572145	2932.91	6.3132	2.9332	542.18	1.2844	19.41	49.80
300	0.0588680	2961.65	6.3638	2.8199	550.23	1.2857	19.89	50.14
310	0.0604671	2989.38	6.4118	2.7285	557.85	1.2866	20.36	50.63
320	0.0620211	3016.28	6.4575	2.6536	565.10	1.2872	20.82	51.24
330	0.0635367	3042.49	6.5014	2.5915	572.04	1.2876	21.28	51.94
340	0.0650195	3068.14	6.5435	2.5399	578.71	1.2877	21.74	52.72
350	0.0664740	3093.32	6.5843	2.4967	585.14	1.2877	22.19	53.55
360	0.0679040	3118.10	6.6237	2.4604	591.35	1.2875	22.64	54.43
370	0.0693123	3142.55	6.6620	2.4299	597.38	1.2871	23.08	55.32
380	0.0707017	3166.71	6.6993	2.4042	603.23	1.2867	23.53	56.30
390	0.0720743	3190.64	6.7357	2.3825	608.93	1.2862	23.97	57.32
400	0.0734318	3214.37	6.7712	2.3642	614.49	1.2855	24.40	58.36
410	0.0747759	3237.94	6.8059	2.3488	619.92	1.2849	24.84	59.42
420	0.0761079	3261.36	6.8400	2.3359	625.24	1.2841	25.27	60.50
430	0.0774290	3284.66	6.8734	2.3251	630.45	1.2833	25.70	61.61
440	0.0787401	3307.87	6.9061	2.3162	635.56	1.2825	26.13	62.73
450	0.0800422	3330.99	6.9383	2.3088	640.58	1.2816	26.56	63.86
460	0.0813360	3354.05	6.9700	2.3027	645.51	1.2807	26.98	65.01
470	0.0826222	3377.05	7.0012	2.2979	650.36	1.2798	27.41	66.18
480	0.0839015	3400.01	7.0318	2.2941	655.14	1.2789	27.83	67.36
490	0.0851742	3422.94	7.0621	2.2913	659.84	1.2780	28.25	68.55
500	0.0864410	3445.84	7.0919	2.2892	664.48	1.2770	28.67	69.75
510	0.0877022	3468.72	7.1213	2.2879	669.06	1.2760	29.08	70.97
520	0.0889583	3491.60	7.1503	2.2872	673.58	1.2751	29.50	72.19
530	0.0902096	3514.47	7.1790	2.2871	678.04	1.2741	29.91	73.43
540	0.0914564	3537.34	7.2073	2.2875	682.44	1.2731	30.32	74.67
550	0.0926990	3560.22	7.2353	2.2883	686.80	1.2721	30.74	75.93
560	0.0939376	3583.11	7.2629	2.2896	691.10	1.2711	31.15	77.19
570	0.0951726	3606.01	7.2902	2.2913	695.36	1.2701	31.55	78.47
580	0.0964041	3628.93	7.3172	2.2933	699.58	1.2692	31.96	79.75
590	0.0976323	3651.88	7.3440	2.2956	703.75	1.2682	32.37	81.04
600	0.0988574	3674.85	7.3704	2.2982	707.87	1.2672	32.77	82.34
650	0.104943	3790.15	7.4989	2.3149	727.94	1.2624	34.78	88.95
700	0.110973	3906.41	7.6215	2.3360	747.17	1.2577	36.75	95.72
750	0.116961	4023.80	7.7391	2.3601	765.68	1.2531	38.70	102.6
800	0.122915	4142.46	7.8523	2.3865	783.55	1.2487	40.62	109.7

Table 3 Single-phase region – Continued (0 °C to 800 °C)

p = 50 bar

t [°C]	v [m^3 kg^{-1}]	h [kJ kg^{-1}]	s [kJ kg^{-1} K^{-1}]	c_p [kJ kg^{-1} K^{-1}]	w [m s^{-1}]	κ [–]	η [10^{-6} Pa s]	λ [10^{-3} W m^{-1} K^{-1}]
0	0.000997683	5.03250	0.0001383	4.1955	1410.2	398.63	1781.0	564.9
2	0.000997619	13.4183	0.030727	4.1904	1420.0	404.23	1664.5	569.1
4	0.000997620	21.7948	0.061060	4.1862	1429.4	409.61	1559.8	573.1
6	0.000997681	30.1635	0.091147	4.1827	1438.4	414.77	1465.2	577.1
8	0.000997801	38.5258	0.12100	4.1797	1447.1	419.72	1379.5	581.0
10	0.000997974	46.8827	0.15062	4.1773	1455.3	424.45	1301.6	584.7
12	0.000998199	55.2352	0.18001	4.1752	1463.2	428.97	1230.5	588.4
14	0.000998473	63.5838	0.20919	4.1735	1470.7	433.27	1165.4	592.0
16	0.000998793	71.9293	0.23815	4.1721	1477.9	437.36	1105.7	595.4
18	0.000999157	80.2722	0.26690	4.1708	1484.7	441.25	1050.8	598.8
20	0.000999564	88.6128	0.29545	4.1698	1491.2	444.92	1000.1	602.2
25	0.00100076	109.457	0.36596	4.1680	1506.0	453.24	889.4	610.1
30	0.00100219	130.294	0.43526	4.1670	1518.8	460.35	797.2	617.6
35	0.00100383	151.128	0.50343	4.1665	1529.9	466.31	719.5	624.6
40	0.00100567	171.960	0.57049	4.1667	1539.2	471.18	653.4	631.1
45	0.00100771	192.795	0.63650	4.1673	1547.1	475.03	596.6	637.3
50	0.00100993	213.634	0.70149	4.1684	1553.5	477.90	547.5	643.0
55	0.00101232	234.480	0.76550	4.1700	1558.5	479.87	504.7	648.4
60	0.00101488	255.334	0.82858	4.1720	1562.3	480.97	467.2	653.3
65	0.00101761	276.200	0.89074	4.1745	1564.8	481.27	434.1	657.9
70	0.00102049	297.080	0.95204	4.1775	1566.3	480.81	404.8	662.2
75	0.00102352	317.976	1.0125	4.1810	1566.7	479.64	378.7	666.0
80	0.00102671	338.891	1.0721	4.1849	1566.2	477.81	355.4	669.6
85	0.00103006	359.826	1.1310	4.1893	1564.7	475.35	334.4	672.8
90	0.00103355	380.785	1.1891	4.1942	1562.3	472.30	315.5	675.7
95	0.00103719	401.769	1.2465	4.1996	1559.1	468.71	298.4	678.2
100	0.00104098	422.782	1.3032	4.2055	1555.1	464.61	282.9	680.5
110	0.00104901	464.902	1.4146	4.2188	1544.8	455.01	255.9	684.1
120	0.00105765	507.165	1.5235	4.2343	1531.8	443.73	233.3	686.4
130	0.00106693	549.595	1.6301	4.2521	1516.3	430.99	214.2	687.7
140	0.00107686	592.216	1.7345	4.2725	1498.4	416.97	197.8	687.8
150	0.00108748	635.055	1.8369	4.2959	1478.1	401.82	183.8	686.9
160	0.00109885	678.144	1.9376	4.3225	1455.7	385.68	171.5	684.9
170	0.00111101	721.518	2.0366	4.3530	1431.1	368.67	160.8	681.8
180	0.00112403	765.219	2.1341	4.3879	1404.3	350.90	151.4	677.7
190	0.00113801	809.294	2.2303	4.4280	1375.4	332.47	143.0	672.6
200	0.00115304	853.800	2.3254	4.4743	1344.3	313.47	135.5	666.4
210	0.00116926	898.804	2.4195	4.5277	1311.0	293.99	128.7	659.2
220	0.00118683	944.384	2.5129	4.5899	1275.4	274.13	122.5	650.9
230	0.00120593	990.636	2.6057	4.6626	1237.5	253.98	116.8	641.5
240	0.00122684	1037.68	2.6983	4.7485	1197.1	233.60	111.5	630.9

Table 3 Single-phase region – Continued (0 °C to 800 °C)

p = 50 bar								
t [°C]	v [$m^3\ kg^{-1}$]	h [$kJ\ kg^{-1}$]	s [$kJ\ kg^{-1}\ K^{-1}$]	c_p [$kJ\ kg^{-1}\ K^{-1}$]	w [$m\ s^{-1}$]	κ [–]	η [10^{-6} Pa s]	λ [$10^{-3}\ W\ m^{-1}\ K^{-1}$]
250	0.00124987	1085.66	2.7909	4.8511	1153.9	213.06	106.6	619.1
260	0.00127548	1134.77	2.8839	4.9755	1107.7	192.38	101.9	606.0
t_s = 263.943 °C				**Saturation**				
Liquid	0.00128641	1154.50	2.9207	5.0322	1088.4	184.19	100.1	600.5
Vapour	0.0394463	2794.23	5.9737	4.4378	498.18	1.2584	17.96	55.64
270	0.0405675	2819.84	6.0211	4.0460	506.87	1.2666	18.28	54.69
280	0.0422746	2858.08	6.0909	3.6350	518.94	1.2740	18.80	53.68
290	0.0438562	2893.00	6.1535	3.3662	529.38	1.2780	19.30	53.18
300	0.0453466	2925.64	6.2109	3.1714	538.84	1.2806	19.79	53.03
310	0.0467667	2956.58	6.2645	3.0218	547.60	1.2824	20.28	53.15
320	0.0481304	2986.18	6.3148	2.9028	555.81	1.2837	20.76	53.48
330	0.0494477	3014.71	6.3625	2.8063	563.57	1.2846	21.23	53.95
340	0.0507261	3042.36	6.4080	2.7269	570.94	1.2852	21.70	54.54
350	0.0519714	3069.29	6.4515	2.6610	577.99	1.2856	22.16	55.22
360	0.0531884	3095.62	6.4934	2.6058	584.75	1.2858	22.61	55.95
370	0.0543809	3121.44	6.5339	2.5594	591.26	1.2857	23.07	56.70
380	0.0555520	3146.83	6.5731	2.5203	597.55	1.2855	23.52	57.59
390	0.0567042	3171.86	6.6111	2.4871	603.64	1.2852	23.96	58.55
400	0.0578398	3196.59	6.6481	2.4590	609.56	1.2848	24.41	59.53
410	0.0589607	3221.06	6.6842	2.4351	615.31	1.2843	24.85	60.53
420	0.0600683	3245.31	6.7194	2.4148	620.92	1.2837	25.28	61.57
430	0.0611641	3269.37	6.7539	2.3976	626.39	1.2830	25.72	62.62
440	0.0622491	3293.27	6.7877	2.3829	631.75	1.2823	26.15	63.71
450	0.0633245	3317.03	6.8208	2.3705	636.99	1.2815	26.58	64.81
460	0.0643910	3340.68	6.8532	2.3601	642.13	1.2807	27.01	65.93
470	0.0654495	3364.24	6.8851	2.3513	647.17	1.2799	27.44	67.07
480	0.0665006	3387.71	6.9165	2.3440	652.13	1.2790	27.86	68.22
490	0.0675449	3411.12	6.9474	2.3379	657.00	1.2781	28.28	69.39
500	0.0685829	3434.48	6.9778	2.3330	661.80	1.2772	28.70	70.58
510	0.0696152	3457.79	7.0078	2.3291	666.52	1.2763	29.12	71.77
520	0.0706420	3481.06	7.0373	2.3260	671.17	1.2754	29.54	72.98
530	0.0716639	3504.31	7.0664	2.3237	675.76	1.2744	29.95	74.20
540	0.0726812	3527.54	7.0952	2.3221	680.29	1.2735	30.37	75.43
550	0.0736941	3550.75	7.1235	2.3212	684.75	1.2725	30.78	76.67
560	0.0747029	3573.96	7.1516	2.3208	689.17	1.2716	31.19	77.92
570	0.0757080	3597.17	7.1793	2.3209	693.53	1.2706	31.60	79.18
580	0.0767095	3620.38	7.2066	2.3215	697.84	1.2697	32.01	80.45
590	0.0777077	3643.60	7.2337	2.3224	702.10	1.2687	32.42	81.73
600	0.0787027	3666.83	7.2604	2.3238	706.31	1.2678	32.82	83.02
650	0.0836367	3783.28	7.3901	2.3353	726.76	1.2630	34.83	89.58
700	0.0885146	3900.45	7.5137	2.3525	746.29	1.2584	36.80	96.31
750	0.0933495	4018.59	7.6321	2.3737	765.04	1.2540	38.75	103.2
800	0.0981510	4137.87	7.7459	2.3978	783.12	1.2496	40.67	110.2

Table 3 Single-phase region – Continued (0 °C to 800 °C)

p = 60 bar

t [°C]	v [$m^3\,kg^{-1}$]	h [$kJ\,kg^{-1}$]	s [$kJ\,kg^{-1}\,K^{-1}$]	c_p [$kJ\,kg^{-1}\,K^{-1}$]	w [$m\,s^{-1}$]	κ [–]	η [10^{-6} Pa s]	λ [$10^{-3}\,W\,m^{-1}\,K^{-1}$]
0	0.000997183	6.04286	0.0001856	4.1908	1411.8	333.11	1778.9	565.5
2	0.000997126	14.4195	0.030741	4.1860	1421.6	337.78	1662.8	569.7
4	0.000997133	22.7873	0.061042	4.1820	1431.0	342.27	1558.3	573.7
6	0.000997201	31.1478	0.091100	4.1787	1440.0	346.58	1464.0	577.7
8	0.000997326	39.5024	0.12092	4.1759	1448.7	350.71	1378.5	581.5
10	0.000997504	47.8519	0.15051	4.1737	1456.9	354.65	1300.7	585.3
12	0.000997733	56.1973	0.17988	4.1718	1464.8	358.42	1229.8	588.9
14	0.000998011	64.5391	0.20904	4.1702	1472.3	362.01	1164.9	592.5
16	0.000998335	72.8781	0.23798	4.1689	1479.5	365.42	1105.3	596.0
18	0.000998702	81.2147	0.26671	4.1678	1486.3	368.66	1050.4	599.4
20	0.000999112	89.5493	0.29524	4.1668	1492.8	371.73	999.9	602.7
25	0.00100031	110.379	0.36569	4.1652	1507.6	378.67	889.3	610.6
30	0.00100174	131.203	0.43496	4.1643	1520.4	384.60	797.1	618.1
35	0.00100339	152.024	0.50308	4.1641	1531.5	389.58	719.5	625.1
40	0.00100524	172.844	0.57010	4.1643	1540.9	393.65	653.5	631.7
45	0.00100727	193.667	0.63607	4.1650	1548.7	396.87	596.8	637.8
50	0.00100949	214.495	0.70103	4.1661	1555.1	399.28	547.7	643.5
55	0.00101188	235.329	0.76501	4.1678	1560.2	400.93	505.0	648.9
60	0.00101444	256.173	0.82805	4.1698	1564.0	401.87	467.5	653.9
65	0.00101716	277.028	0.89018	4.1724	1566.6	402.13	434.4	658.4
70	0.00102004	297.898	0.95145	4.1754	1568.1	401.76	405.1	662.7
75	0.00102307	318.783	1.0119	4.1788	1568.5	400.81	379.0	666.6
80	0.00102625	339.687	1.0715	4.1828	1568.0	399.29	355.6	670.1
85	0.00102958	360.612	1.1303	4.1872	1566.5	397.26	334.7	673.3
90	0.00103307	381.559	1.1884	4.1921	1564.2	394.74	315.8	676.2
95	0.00103670	402.533	1.2458	4.1974	1561.0	391.77	298.7	678.8
100	0.00104048	423.535	1.3024	4.2033	1557.1	388.37	283.2	681.0
110	0.00104849	465.632	1.4138	4.2165	1547.0	380.41	256.2	684.6
120	0.00105710	507.871	1.5226	4.2318	1534.1	371.05	233.6	687.0
130	0.00106635	550.276	1.6291	4.2495	1518.7	360.47	214.4	688.3
140	0.00107624	592.869	1.7335	4.2697	1500.9	348.83	198.1	688.5
150	0.00108682	635.679	1.8358	4.2927	1480.8	336.25	184.0	687.5
160	0.00109814	678.735	1.9364	4.3191	1458.5	322.85	171.8	685.6
170	0.00111024	722.073	2.0353	4.3492	1434.1	308.72	161.1	682.5
180	0.00112321	765.733	2.1327	4.3837	1407.5	293.96	151.6	678.5
190	0.00113711	809.763	2.2289	4.4232	1378.8	278.65	143.2	673.4
200	0.00115205	854.217	2.3238	4.4687	1348.0	262.87	135.7	667.3
210	0.00116817	899.160	2.4178	4.5213	1314.9	246.69	128.9	660.1
220	0.00118561	944.671	2.5110	4.5823	1279.7	230.19	122.7	651.9
230	0.00120456	990.841	2.6037	4.6537	1242.0	213.45	117.1	642.6
240	0.00122528	1037.79	2.6961	4.7378	1202.0	196.52	111.8	632.1

Table 3 Single-phase region – Continued (0 °C to 800 °C)

t [°C]	v [$m^3\,kg^{-1}$]	h [$kJ\,kg^{-1}$]	s [$kJ\,kg^{-1}\,K^{-1}$]	c_p [$kJ\,kg^{-1}\,K^{-1}$]	w [$m\,s^{-1}$]	κ [–]	η [10^{-6} Pa s]	λ [$10^{-3}\,W\,m^{-1}\,K^{-1}$]
p = 60 bar								
250	0.00124808	1085.65	2.7885	4.8379	1159.3	179.46	106.9	620.4
260	0.00127338	1134.61	2.8812	4.9589	1113.5	162.29	102.2	607.4
270	0.00130177	1184.92	2.9747	5.1082	1064.2	145.00	97.74	593.0
t_s = 275.586 °C				**Saturation**				
Liquid	0.00131927	1213.73	3.0274	5.2080	1034.8	135.28	95.31	584.3
Vapour	0.0324487	2784.56	5.8901	4.8768	494.01	1.2535	18.44	59.97
280	0.0331998	2805.25	5.9276	4.5160	501.07	1.2604	18.68	59.02
290	0.0347631	2847.50	6.0033	3.9812	514.56	1.2694	19.20	57.51
300	0.0361911	2885.49	6.0702	3.6378	526.04	1.2743	19.71	56.65
310	0.0375230	2920.58	6.1309	3.3929	536.29	1.2775	20.21	56.24
320	0.0387819	2953.55	6.1870	3.2078	545.69	1.2797	20.70	56.16
330	0.0399833	2984.87	6.2393	3.0626	554.43	1.2813	21.19	56.32
340	0.0411378	3014.89	6.2887	2.9459	562.64	1.2825	21.66	56.66
350	0.0422535	3043.86	6.3356	2.8504	570.41	1.2834	22.14	57.14
360	0.0433364	3071.96	6.3803	2.7714	577.79	1.2839	22.60	57.69
370	0.0443912	3099.33	6.4232	2.7054	584.85	1.2842	23.06	58.26
380	0.0454220	3126.10	6.4645	2.6499	591.62	1.2843	23.52	59.03
390	0.0464317	3152.36	6.5044	2.6030	598.14	1.2842	23.97	59.90
400	0.0474230	3178.18	6.5431	2.5632	604.44	1.2840	24.42	60.80
410	0.0483980	3203.64	6.5806	2.5293	610.54	1.2837	24.86	61.74
420	0.0493586	3228.79	6.6171	2.5004	616.47	1.2832	25.30	62.71
430	0.0503063	3253.66	6.6528	2.4757	622.23	1.2827	25.74	63.72
440	0.0512425	3278.31	6.6876	2.4545	627.84	1.2821	26.18	64.76
450	0.0521683	3302.76	6.7216	2.4364	633.32	1.2814	26.61	65.82
460	0.0530847	3327.05	6.7550	2.4209	638.68	1.2807	27.04	66.91
470	0.0539925	3351.19	6.7877	2.4077	643.93	1.2799	27.47	68.01
480	0.0548925	3375.21	6.8198	2.3964	649.07	1.2791	27.90	69.14
490	0.0557854	3399.12	6.8513	2.3868	654.12	1.2783	28.32	70.28
500	0.0566717	3422.95	6.8824	2.3787	659.07	1.2775	28.75	71.44
510	0.0575519	3446.70	6.9129	2.3719	663.95	1.2766	29.17	72.61
520	0.0584266	3470.39	6.9429	2.3663	668.74	1.2757	29.58	73.80
530	0.0592960	3494.03	6.9726	2.3616	673.46	1.2748	30.00	75.00
540	0.0601607	3517.63	7.0018	2.3579	678.11	1.2739	30.42	76.21
550	0.0610209	3541.19	7.0306	2.3550	682.70	1.2730	30.83	77.44
560	0.0618769	3564.73	7.0590	2.3528	687.22	1.2721	31.24	78.68
570	0.0627290	3588.25	7.0870	2.3512	691.69	1.2712	31.65	79.92
580	0.0635775	3611.76	7.1148	2.3503	696.09	1.2702	32.06	81.18
590	0.0644225	3635.26	7.1421	2.3498	700.45	1.2693	32.47	82.44
600	0.0652644	3658.76	7.1692	2.3499	704.75	1.2684	32.87	83.72
650	0.0694316	3776.36	7.3002	2.3559	725.58	1.2638	34.88	90.22
700	0.0735419	3894.47	7.4248	2.3692	745.42	1.2593	36.86	96.91
750	0.0776087	4013.37	7.5439	2.3874	764.42	1.2549	38.80	103.8
800	0.0816416	4133.27	7.6583	2.4092	782.69	1.2506	40.72	110.7

Table 3 Single-phase region – Continued (0 °C to 800 °C)

p = 70 bar

t [°C]	v [m^3 kg^{-1}]	h [kJ kg^{-1}]	s [kJ kg^{-1} K^{-1}]	c_p [kJ kg^{-1} K^{-1}]	w [m s^{-1}]	κ [–]	η [10^{-6} Pa s]	λ [10^{-3} W m^{-1} K^{-1}]
0	0.000996685	7.05172	0.0002293	4.1861	1413.3	286.31	1776.8	566.1
2	0.000996635	15.4192	0.030751	4.1816	1423.2	290.32	1661.0	570.2
4	0.000996648	23.7785	0.061022	4.1778	1432.6	294.17	1556.8	574.3
6	0.000996722	32.1309	0.091051	4.1747	1441.6	297.87	1462.8	578.2
8	0.000996852	40.4777	0.12084	4.1722	1450.3	301.41	1377.5	582.1
10	0.000997035	48.8199	0.15041	4.1701	1458.5	304.80	1299.9	585.8
12	0.000997269	57.1583	0.17976	4.1683	1466.4	308.03	1229.1	589.5
14	0.000997551	65.4934	0.20889	4.1669	1473.9	311.11	1164.3	593.1
16	0.000997878	73.8259	0.23780	4.1657	1481.1	314.04	1104.8	596.5
18	0.000998249	82.1563	0.26651	4.1647	1487.9	316.82	1050.1	599.9
20	0.000998662	90.4848	0.29502	4.1639	1494.4	319.45	999.6	603.2
25	0.000999867	111.300	0.36543	4.1625	1509.2	325.41	889.1	611.2
30	0.00100130	132.111	0.43465	4.1618	1522.0	330.50	797.1	618.6
35	0.00100295	152.919	0.50273	4.1616	1533.1	334.77	719.6	625.6
40	0.00100480	173.727	0.56971	4.1619	1542.5	338.27	653.6	632.2
45	0.00100684	194.539	0.63565	4.1627	1550.4	341.04	597.0	638.3
50	0.00100905	215.355	0.70057	4.1639	1556.8	343.12	547.9	644.1
55	0.00101144	236.179	0.76451	4.1656	1561.9	344.55	505.2	649.4
60	0.00101400	257.012	0.82752	4.1677	1565.7	345.36	467.7	654.4
65	0.00101671	277.856	0.88962	4.1702	1568.3	345.60	434.6	659.0
70	0.00101958	298.715	0.95086	4.1733	1569.9	345.30	405.3	663.2
75	0.00102261	319.590	1.0112	4.1767	1570.3	344.49	379.2	667.1
80	0.00102579	340.483	1.0708	4.1807	1569.9	343.21	355.9	670.6
85	0.00102911	361.397	1.1296	4.1851	1568.4	341.49	334.9	673.9
90	0.00103259	382.334	1.1877	4.1899	1566.1	339.34	316.0	676.7
95	0.00103621	403.297	1.2450	4.1952	1563.0	336.81	299.0	679.3
100	0.00103998	424.288	1.3017	4.2011	1559.1	333.91	283.4	681.6
110	0.00104797	466.362	1.4129	4.2142	1549.1	327.12	256.4	685.2
120	0.00105656	508.578	1.5217	4.2294	1536.3	319.13	233.8	687.6
130	0.00106577	550.957	1.6281	4.2468	1521.0	310.10	214.7	688.9
140	0.00107563	593.523	1.7324	4.2668	1503.3	300.16	198.3	689.1
150	0.00108617	636.303	1.8347	4.2897	1483.4	289.42	184.3	688.2
160	0.00109744	679.327	1.9352	4.3157	1461.3	277.97	172.0	686.2
170	0.00110949	722.629	2.0341	4.3454	1437.0	265.90	161.3	683.3
180	0.00112239	766.250	2.1314	4.3794	1410.7	253.29	151.9	679.2
190	0.00113621	810.234	2.2274	4.4184	1382.2	240.21	143.5	674.2
200	0.00115107	854.637	2.3223	4.4632	1351.6	226.72	136.0	668.1
210	0.00116708	899.522	2.4161	4.5149	1318.8	212.90	129.2	661.0
220	0.00118440	944.964	2.5092	4.5749	1283.8	198.80	123.0	652.9
230	0.00120320	991.054	2.6018	4.6449	1246.5	184.49	117.3	643.6
240	0.00122374	1037.90	2.6939	4.7272	1206.8	170.02	112.1	633.3

Table 3 Single-phase region – Continued
(0 °C to 800 °C)

				$p =$ 70 bar				
t	v	h	s	c_p	w	κ	η	λ
[°C]	[$m^3\ kg^{-1}$]	[$kJ\ kg^{-1}$]	[$kJ\ kg^{-1}\ K^{-1}$]	[$kJ\ kg^{-1}\ K^{-1}$]	[$m\ s^{-1}$]	[–]	[10^{-6} Pa s]	[$10^{-3}\ W\ m^{-1}\ K^{-1}$]
250	0.00124631	1085.65	2.7861	4.8250	1164.5	155.45	107.1	621.7
260	0.00127132	1134.47	2.8785	4.9428	1119.3	140.78	102.5	608.9
270	0.00129933	1184.60	2.9717	5.0874	1070.7	126.04	98.06	594.6
280	0.00133113	1236.34	3.0661	5.2698	1017.8	111.17	93.75	578.8
t_s = 285.830 °C				**Saturation**				
Liquid	0.00135186	1267.44	3.1220	5.4004	984.51	102.43	91.27	568.7
Vapour	0.0273796	2772.57	5.8146	5.3540	489.28	1.2491	18.89	64.37
290	0.0280439	2793.98	5.8528	4.9360	496.60	1.2563	19.12	63.22
300	0.0294938	2839.83	5.9335	4.2919	511.27	1.2661	19.65	61.24
310	0.0308034	2880.57	6.0040	3.8817	523.61	1.2715	20.16	60.06
320	0.0320146	2917.86	6.0674	3.5913	534.56	1.2751	20.66	59.41
330	0.0331520	2952.63	6.1255	3.3740	544.52	1.2777	21.16	59.14
340	0.0342317	2985.50	6.1796	3.2052	553.73	1.2796	21.65	59.15
350	0.0352650	3016.85	6.2303	3.0704	562.33	1.2810	22.12	59.36
360	0.0362600	3046.99	6.2783	2.9608	570.43	1.2820	22.60	59.69
370	0.0372229	3076.13	6.3240	2.8703	578.11	1.2827	23.06	60.01
380	0.0381585	3104.44	6.3677	2.7949	585.42	1.2831	23.53	60.63
390	0.0390705	3132.07	6.4096	2.7314	592.42	1.2833	23.98	61.40
400	0.0399621	3159.10	6.4501	2.6778	599.14	1.2833	24.44	62.20
410	0.0408358	3185.65	6.4892	2.6321	605.62	1.2831	24.89	63.05
420	0.0416938	3211.77	6.5272	2.5932	611.88	1.2828	25.33	63.95
430	0.0425378	3237.53	6.5641	2.5599	617.95	1.2824	25.77	64.90
440	0.0433694	3262.98	6.6000	2.5313	623.84	1.2819	26.21	65.88
450	0.0441898	3288.17	6.6351	2.5067	629.58	1.2814	26.65	66.90
460	0.0450001	3313.13	6.6694	2.4855	635.17	1.2808	27.08	67.94
470	0.0458014	3337.89	6.7029	2.4673	640.63	1.2801	27.51	69.01
480	0.0465944	3362.48	6.7358	2.4516	645.97	1.2793	27.94	70.10
490	0.0473799	3386.93	6.7681	2.4381	651.19	1.2786	28.37	71.21
500	0.0481585	3411.25	6.7997	2.4265	656.32	1.2778	28.79	72.35
510	0.0489308	3435.46	6.8308	2.4166	661.35	1.2770	29.21	73.50
520	0.0496972	3459.59	6.8614	2.4081	666.29	1.2761	29.63	74.66
530	0.0504583	3483.63	6.8916	2.4009	671.15	1.2753	30.05	75.84
540	0.0512144	3507.61	6.9212	2.3949	675.93	1.2744	30.47	77.03
550	0.0519658	3531.53	6.9505	2.3899	680.63	1.2735	30.88	78.24
560	0.0527130	3555.41	6.9793	2.3857	685.27	1.2726	31.30	79.46
570	0.0534561	3579.25	7.0078	2.3824	689.84	1.2717	31.71	80.69
580	0.0541955	3603.06	7.0358	2.3798	694.35	1.2708	32.12	81.93
590	0.0549314	3626.85	7.0635	2.3779	698.80	1.2699	32.52	83.18
600	0.0556641	3650.62	7.0909	2.3765	703.19	1.2690	32.93	84.44
650	0.0592843	3769.41	7.2232	2.3769	724.41	1.2645	34.94	90.89
700	0.0628467	3888.46	7.3488	2.3861	744.55	1.2601	36.92	97.53
750	0.0663652	4008.12	7.4687	2.4012	763.80	1.2558	38.86	104.3
800	0.0698494	4128.65	7.5837	2.4206	782.28	1.2516	40.78	111.3

Table 3 Single-phase region – Continued (0 °C to 800 °C)

p = 80 bar								
t [ºC]	v [m^3 kg^{-1}]	h [kJ kg^{-1}]	s [kJ kg^{-1} K^{-1}]	c_p [kJ kg^{-1} K^{-1}]	w [m s^{-1}]	κ [–]	η [10^{-6} Pa s]	λ [10^{-3} W m^{-1} K^{-1}]
0	0.000996188	8.05907	0.0002693	4.1814	1414.9	251.22	1774.7	566.7
2	0.000996145	16.4176	0.030758	4.1772	1424.8	254.73	1659.3	570.8
4	0.000996165	24.7683	0.060998	4.1737	1434.2	258.10	1555.4	574.9
6	0.000996245	33.1127	0.090998	4.1708	1443.2	261.34	1461.5	578.8
8	0.000996380	41.4519	0.12076	4.1685	1451.9	264.44	1376.5	582.6
10	0.000996568	49.7868	0.15031	4.1665	1460.1	267.41	1299.1	586.4
12	0.000996806	58.1182	0.17963	4.1649	1468.0	270.24	1228.4	590.0
14	0.000997092	66.4467	0.20873	4.1636	1475.5	272.94	1163.7	593.6
16	0.000997423	74.7728	0.23763	4.1625	1482.7	275.50	1104.4	597.1
18	0.000997797	83.0970	0.26632	4.1617	1489.5	277.94	1049.7	600.5
20	0.000998213	91.4196	0.29480	4.1609	1496.0	280.24	999.3	603.8
25	0.000999424	112.221	0.36516	4.1597	1510.7	285.46	889.0	611.7
30	0.00100086	133.018	0.43434	4.1592	1523.6	289.92	797.1	619.1
35	0.00100252	153.814	0.50238	4.1591	1534.7	293.67	719.7	626.1
40	0.00100437	174.610	0.56932	4.1596	1544.1	296.74	653.8	632.7
45	0.00100640	195.410	0.63522	4.1604	1552.0	299.17	597.1	638.8
50	0.00100862	216.215	0.70011	4.1617	1558.5	301.00	548.1	644.6
55	0.00101101	237.028	0.76402	4.1634	1563.6	302.26	505.4	649.9
60	0.00101356	257.850	0.82699	4.1656	1567.4	302.99	467.9	654.9
65	0.00101627	278.684	0.88906	4.1681	1570.1	303.21	434.9	659.5
70	0.00101913	299.532	0.95027	4.1712	1571.6	302.96	405.6	663.7
75	0.00102215	320.396	1.0106	4.1746	1572.2	302.26	379.5	667.6
80	0.00102532	341.279	1.0702	4.1786	1571.7	301.15	356.2	671.2
85	0.00102864	362.183	1.1290	4.1829	1570.3	299.66	335.2	674.4
90	0.00103211	383.109	1.1870	4.1878	1568.1	297.79	316.3	677.3
95	0.00103572	404.061	1.2443	4.1931	1565.0	295.59	299.2	679.9
100	0.00103948	425.041	1.3009	4.1989	1561.1	293.07	283.7	682.1
110	0.00104745	467.093	1.4121	4.2119	1551.2	287.15	256.7	685.7
120	0.00105601	509.285	1.5208	4.2269	1538.5	280.19	234.1	688.2
130	0.00106519	551.639	1.6272	4.2442	1523.4	272.32	214.9	689.5
140	0.00107502	594.178	1.7314	4.2640	1505.8	263.65	198.6	689.7
150	0.00108552	636.929	1.8337	4.2866	1486.0	254.29	184.5	688.8
160	0.00109674	679.921	1.9341	4.3123	1464.1	244.30	172.3	686.9
170	0.00110874	723.187	2.0328	4.3417	1440.0	233.78	161.6	684.0
180	0.00112157	766.768	2.1301	4.3752	1413.8	222.78	152.1	680.0
190	0.00113533	810.708	2.2260	4.4137	1385.6	211.37	143.7	675.0
200	0.00115010	855.061	2.3207	4.4578	1355.2	199.61	136.2	669.0
210	0.00116601	899.887	2.4145	4.5087	1322.7	187.55	129.4	661.9
220	0.00118320	945.262	2.5074	4.5677	1288.0	175.25	123.2	653.9
230	0.00120186	991.273	2.5998	4.6363	1251.0	162.77	117.6	644.7
240	0.00122222	1038.03	2.6918	4.7169	1211.6	150.15	112.3	634.4

Table 3 Single-phase region – Continued
(0 °C to 800 °C)

p = 80 bar

t [°C]	v [m³ kg⁻¹]	h [kJ kg⁻¹]	s [kJ kg⁻¹ K⁻¹]	c_p [kJ kg⁻¹ K⁻¹]	w [m s⁻¹]	κ [–]	η [10^{-6} Pa s]	λ [10^{-3} W m⁻¹ K⁻¹]
250	0.00124457	1085.66	2.7837	4.8125	1169.8	137.43	107.4	623.0
260	0.00126930	1134.34	2.8759	4.9272	1125.0	124.65	102.8	610.2
270	0.00129694	1184.29	2.9687	5.0674	1077.0	111.80	98.38	596.2
280	0.00132823	1235.81	3.0627	5.2431	1024.9	98.865	94.09	580.5
290	0.00136429	1289.33	3.1586	5.4713	967.72	85.803	89.87	563.1
t_s = 295.009 °C				**Saturation**				
Liquid	0.00138466	1317.08	3.2077	5.6140	936.73	79.212	87.74	553.6
Vapour	0.0235275	2758.61	5.7448	5.8831	484.07	1.2450	19.33	68.95
300	0.0242802	2786.38	5.7935	5.2870	493.56	1.2541	19.60	67.24
310	0.0256318	2835.27	5.8781	4.5559	509.11	1.2640	20.12	64.85
320	0.0268425	2878.35	5.9514	4.0905	522.16	1.2697	20.64	63.38
330	0.0279551	2917.53	6.0169	3.7620	533.69	1.2736	21.14	62.52
340	0.0289946	2953.87	6.0766	3.5176	544.12	1.2764	21.64	62.09
350	0.0299776	2988.06	6.1319	3.3288	553.71	1.2785	22.13	61.95
360	0.0309152	3020.57	6.1837	3.1789	562.64	1.2800	22.61	61.98
370	0.0318155	3051.73	6.2325	3.0573	571.02	1.2811	23.08	61.99
380	0.0326848	3081.79	6.2789	2.9572	578.94	1.2818	23.55	62.41
390	0.0335276	3110.93	6.3232	2.8738	586.46	1.2823	24.01	63.05
400	0.0343477	3139.31	6.3657	2.8037	593.65	1.2825	24.46	63.72
410	0.0351482	3167.04	6.4066	2.7444	600.54	1.2826	24.92	64.47
420	0.0359315	3194.23	6.4461	2.6939	607.17	1.2825	25.37	65.29
430	0.0366996	3220.95	6.4843	2.6507	613.56	1.2822	25.81	66.16
440	0.0374543	3247.26	6.5215	2.6136	619.75	1.2819	26.25	67.08
450	0.0381970	3273.23	6.5577	2.5817	625.75	1.2814	26.69	68.04
460	0.0389290	3298.91	6.5929	2.5541	631.59	1.2809	27.13	69.04
470	0.0396513	3324.33	6.6274	2.5303	637.27	1.2803	27.56	70.06
480	0.0403649	3349.53	6.6611	2.5097	642.82	1.2796	27.99	71.12
490	0.0410706	3374.53	6.6940	2.4919	648.24	1.2789	28.42	72.20
500	0.0417691	3399.37	6.7264	2.4765	653.54	1.2782	28.84	73.30
510	0.0424609	3424.07	6.7581	2.4631	658.73	1.2774	29.27	74.42
520	0.0431467	3448.64	6.7893	2.4516	663.82	1.2766	29.69	75.56
530	0.0438269	3473.11	6.8199	2.4416	668.82	1.2758	30.11	76.71
540	0.0445019	3497.48	6.8501	2.4331	673.73	1.2750	30.52	77.88
550	0.0451721	3521.77	6.8798	2.4258	678.56	1.2741	30.94	79.07
560	0.0458379	3546.00	6.9091	2.4196	683.31	1.2733	31.35	80.27
570	0.0464996	3570.17	6.9379	2.4144	687.99	1.2724	31.76	81.48
580	0.0471574	3594.29	6.9663	2.4101	692.60	1.2715	32.17	82.71
590	0.0478117	3618.37	6.9944	2.4066	697.15	1.2707	32.58	83.94
600	0.0484625	3642.42	7.0221	2.4038	701.64	1.2698	32.99	85.19
650	0.0516732	3762.42	7.1557	2.3983	723.25	1.2654	35.00	91.57
700	0.0548251	3882.42	7.2823	2.4032	743.70	1.2610	36.97	98.16
750	0.0579325	4002.86	7.4030	2.4152	763.20	1.2568	38.92	104.9
800	0.0610054	4124.02	7.5186	2.4322	781.88	1.2526	40.83	111.8

Table 3 Single-phase region – Continued (0 °C to 800 °C)

$p = 90$ bar

t [°C]	v [m^3 kg^{-1}]	h [kJ kg^{-1}]	s [kJ kg^{-1} K^{-1}]	c_p [kJ kg^{-1} K^{-1}]	w [m s^{-1}]	κ [–]	η [10^{-6} Pa s]	λ [10^{-3} W m^{-1} K^{-1}]
0	0.000995693	9.06495	0.0003056	4.1768	1416.6	223.92	1772.6	567.3
2	0.000995657	17.4145	0.030762	4.1728	1426.4	227.05	1657.5	571.4
4	0.000995683	25.7568	0.060971	4.1696	1435.8	230.05	1553.9	575.4
6	0.000995769	34.0933	0.090943	4.1669	1444.8	232.93	1460.3	579.4
8	0.000995909	42.4249	0.12068	4.1648	1453.5	235.69	1375.5	583.2
10	0.000996102	50.7526	0.15020	4.1630	1461.7	238.33	1298.2	586.9
12	0.000996345	59.0771	0.17949	4.1616	1469.6	240.85	1227.7	590.6
14	0.000996634	67.3990	0.20858	4.1604	1477.1	243.25	1163.2	594.1
16	0.000996969	75.7188	0.23745	4.1594	1484.3	245.53	1103.9	597.6
18	0.000997346	84.0368	0.26612	4.1586	1491.1	247.70	1049.4	601.0
20	0.000997765	92.3534	0.29459	4.1580	1497.6	249.75	999.0	604.3
25	0.000998982	113.141	0.36490	4.1570	1512.3	254.39	888.9	612.2
30	0.00100043	133.925	0.43403	4.1566	1525.2	258.37	797.1	619.7
35	0.00100208	154.708	0.50203	4.1567	1536.3	261.70	719.8	626.7
40	0.00100393	175.492	0.56894	4.1572	1545.7	264.44	653.9	633.2
45	0.00100597	196.281	0.63480	4.1582	1553.6	266.61	597.3	639.3
50	0.00100818	217.075	0.69965	4.1595	1560.1	268.24	548.3	645.1
55	0.00101057	237.876	0.76352	4.1613	1565.2	269.37	505.6	650.4
60	0.00101312	258.688	0.82647	4.1634	1569.1	270.03	468.2	655.4
65	0.00101582	279.511	0.88851	4.1660	1571.8	270.23	435.2	660.0
70	0.00101869	300.349	0.94968	4.1691	1573.4	270.02	405.9	664.2
75	0.00102170	321.203	1.0100	4.1726	1574.0	269.42	379.8	668.1
80	0.00102486	342.075	1.0695	4.1765	1573.5	268.44	356.4	671.7
85	0.00102818	362.968	1.1283	4.1808	1572.2	267.12	335.5	674.9
90	0.00103163	383.884	1.1863	4.1856	1570.0	265.48	316.6	677.8
95	0.00103524	404.825	1.2436	4.1909	1567.0	263.53	299.5	680.4
100	0.00103899	425.794	1.3001	4.1967	1563.1	261.30	284.0	682.7
110	0.00104693	467.824	1.4113	4.2096	1553.3	256.07	257.0	686.3
120	0.00105547	509.992	1.5199	4.2245	1540.8	249.91	234.3	688.8
130	0.00106462	552.321	1.6262	4.2417	1525.7	242.94	215.2	690.1
140	0.00107441	594.834	1.7304	4.2612	1508.3	235.26	198.9	690.3
150	0.00108487	637.556	1.8326	4.2836	1488.6	226.96	184.8	689.5
160	0.00109604	680.516	1.9329	4.3090	1466.8	218.11	172.5	687.6
170	0.00110799	723.747	2.0316	4.3380	1442.9	208.79	161.8	684.7
180	0.00112076	767.289	2.1288	4.3711	1417.0	199.05	152.4	680.8
190	0.00113445	811.185	2.2246	4.4090	1388.9	188.94	144.0	675.8
200	0.00114913	855.488	2.3192	4.4525	1358.8	178.51	136.5	669.8
210	0.00116494	900.257	2.4128	4.5026	1326.5	167.83	129.7	662.9
220	0.00118202	945.565	2.5057	4.5605	1292.1	156.93	123.5	654.8
230	0.00120054	991.499	2.5979	4.6279	1255.4	145.87	117.8	645.8
240	0.00122072	1038.16	2.6897	4.7069	1216.4	134.68	112.6	635.6

Table 3 Single-phase region – Continued
(0 °C to 800 °C)

p = 90 bar								
t [°C]	v [$m^3\,kg^{-1}$]	h [$kJ\,kg^{-1}$]	s [$kJ\,kg^{-1}\,K^{-1}$]	c_p [$kJ\,kg^{-1}\,K^{-1}$]	w [$m\,s^{-1}$]	κ [–]	η [10^{-6} Pa s]	λ [$10^{-3}\,W\,m^{-1}\,K^{-1}$]
250	0.00124285	1085.68	2.7814	4.8002	1174.9	123.41	107.7	624.2
260	0.00126731	1134.23	2.8733	4.9120	1130.7	112.09	103.1	611.6
270	0.00129459	1184.00	2.9658	5.0480	1083.3	100.71	98.69	597.7
280	0.00132540	1235.30	3.0594	5.2176	1032.0	89.283	94.42	582.3
290	0.00136079	1288.52	3.1547	5.4359	975.83	77.753	90.23	565.1
300	0.00140239	1344.27	3.2529	5.7305	913.54	66.121	86.03	545.9
t_s = 303.347 °C				**Saturation**				
Liquid	0.00141812	1363.65	3.2866	5.8542	891.17	62.225	84.59	538.9
Vapour	0.0204929	2742.88	5.6790	6.4762	478.44	1.2411	19.76	73.78
310	0.0214493	2782.61	5.7475	5.5578	491.95	1.2537	20.11	71.06
320	0.0227102	2833.89	5.8348	4.7670	508.10	1.2631	20.64	68.33
330	0.0238335	2878.87	5.9100	4.2599	521.69	1.2688	21.15	66.61
340	0.0248613	2919.58	5.9769	3.9023	533.66	1.2728	21.65	65.57
350	0.0258184	2957.22	6.0378	3.6370	544.46	1.2757	22.14	64.97
360	0.0267208	2992.53	6.0940	3.4328	554.36	1.2779	22.63	64.63
370	0.0275795	3026.01	6.1465	3.2710	563.55	1.2795	23.11	64.25
380	0.0284025	3058.05	6.1959	3.1400	572.15	1.2806	23.58	64.41
390	0.0291956	3088.89	6.2428	3.0323	580.26	1.2814	24.04	64.88
400	0.0299635	3118.75	6.2875	2.9425	587.95	1.2819	24.50	65.40
410	0.0307096	3147.79	6.3303	2.8671	595.29	1.2821	24.96	66.02
420	0.0314369	3176.13	6.3715	2.8031	602.31	1.2822	25.41	66.74
430	0.0321478	3203.88	6.4113	2.7486	609.06	1.2821	25.86	67.52
440	0.0328442	3231.13	6.4497	2.7018	615.56	1.2819	26.30	68.36
450	0.0335278	3257.94	6.4871	2.6617	621.85	1.2815	26.74	69.26
460	0.0341999	3284.38	6.5234	2.6270	627.95	1.2811	27.18	70.20
470	0.0348618	3310.50	6.5588	2.5970	633.87	1.2806	27.62	71.18
480	0.0355145	3336.33	6.5933	2.5710	639.63	1.2800	28.05	72.19
490	0.0361587	3361.93	6.6271	2.5484	645.24	1.2793	28.48	73.23
500	0.0367955	3387.31	6.6601	2.5287	650.72	1.2787	28.90	74.29
510	0.0374252	3412.51	6.6925	2.5116	656.08	1.2779	29.33	75.38
520	0.0380487	3437.55	6.7243	2.4967	661.33	1.2772	29.75	76.49
530	0.0386664	3462.45	6.7555	2.4838	666.48	1.2764	30.17	77.62
540	0.0392787	3487.23	6.7861	2.4726	671.52	1.2756	30.59	78.77
550	0.0398860	3511.91	6.8163	2.4629	676.48	1.2748	31.00	79.93
560	0.0404888	3536.49	6.8460	2.4545	681.35	1.2740	31.41	81.11
570	0.0410873	3561.00	6.8752	2.4473	686.14	1.2731	31.83	82.30
580	0.0416819	3585.44	6.9040	2.4411	690.86	1.2723	32.24	83.51
590	0.0422728	3609.83	6.9324	2.4359	695.50	1.2714	32.64	84.73
600	0.0428602	3634.16	6.9605	2.4316	700.08	1.2706	33.05	85.96
650	0.0457529	3755.39	7.0955	2.4199	722.10	1.2663	35.06	92.27
700	0.0485859	3876.36	7.2231	2.4205	742.86	1.2620	37.04	98.81
750	0.0513738	3997.58	7.3446	2.4293	762.61	1.2578	38.98	105.5
800	0.0541269	4119.38	7.4608	2.4438	781.49	1.2537	40.89	112.4

Table 3 Single-phase region – Continued (0 °C to 800 °C)

$p = 100$ bar

t [°C]	v [m^3 kg^{-1}]	h [kJ kg^{-1}]	s [kJ kg^{-1} K^{-1}]	c_p [kJ kg^{-1} K^{-1}]	w [m s^{-1}]	κ [–]	η [10^{-6} Pa s]	λ [10^{-3} W m^{-1} K^{-1}]
0	0.000995200	10.0693	0.0003384	4.1723	1418.2	202.09	1770.6	567.8
2	0.000995171	18.4100	0.030762	4.1686	1428.0	204.90	1655.8	572.0
4	0.000995203	26.7440	0.060942	4.1655	1437.4	207.61	1552.5	576.0
6	0.000995294	35.0726	0.090884	4.1631	1446.4	210.21	1459.1	579.9
8	0.000995440	43.3967	0.12060	4.1611	1455.1	212.69	1374.5	583.8
10	0.000995638	51.7173	0.15009	4.1595	1463.3	215.07	1297.4	587.5
12	0.000995884	60.0349	0.17936	4.1582	1471.2	217.34	1227.1	591.1
14	0.000996178	68.3503	0.20842	4.1572	1478.7	219.50	1162.6	594.7
16	0.000996516	76.6637	0.23727	4.1563	1485.9	221.56	1103.5	598.2
18	0.000996897	84.9757	0.26592	4.1557	1492.7	223.51	1049.0	601.5
20	0.000997318	93.2865	0.29437	4.1551	1499.2	225.36	998.8	604.8
25	0.000998541	114.060	0.36463	4.1543	1514.0	229.54	888.8	612.7
30	0.000999989	134.831	0.43372	4.1541	1526.8	233.12	797.1	620.2
35	0.00100165	155.601	0.50168	4.1543	1537.9	236.13	719.8	627.2
40	0.00100350	176.374	0.56855	4.1549	1547.4	238.60	654.0	633.7
45	0.00100554	197.151	0.63437	4.1559	1555.3	240.56	597.5	639.9
50	0.00100775	217.934	0.69919	4.1573	1561.8	242.04	548.5	645.6
55	0.00101013	238.725	0.76303	4.1591	1566.9	243.06	505.9	650.9
60	0.00101268	259.526	0.82594	4.1613	1570.8	243.66	468.4	655.9
65	0.00101538	280.339	0.88795	4.1639	1573.6	243.86	435.4	660.5
70	0.00101824	301.166	0.94909	4.1670	1575.2	243.67	406.1	664.8
75	0.00102125	322.009	1.0094	4.1705	1575.8	243.14	380.0	668.6
80	0.00102441	342.871	1.0689	4.1744	1575.4	242.27	356.7	672.2
85	0.00102771	363.754	1.1276	4.1787	1574.1	241.09	335.7	675.4
90	0.00103116	384.659	1.1856	4.1835	1571.9	239.62	316.9	678.3
95	0.00103475	405.590	1.2428	4.1888	1568.9	237.88	299.8	680.9
100	0.00103850	426.548	1.2994	4.1945	1565.1	235.89	284.2	683.2
110	0.00104641	468.555	1.4105	4.2073	1555.4	231.20	257.2	686.9
120	0.00105493	510.701	1.5190	4.2221	1543.0	225.68	234.6	689.4
130	0.00106405	553.005	1.6253	4.2391	1528.0	219.43	215.5	690.7
140	0.00107380	595.491	1.7294	4.2585	1510.7	212.54	199.1	691.0
150	0.00108422	638.184	1.8315	4.2806	1491.2	205.10	185.0	690.2
160	0.00109535	681.112	1.9318	4.3057	1469.6	197.16	172.8	688.3
170	0.00110724	724.309	2.0304	4.3343	1445.8	188.80	162.1	685.4
180	0.00111996	767.812	2.1274	4.3670	1420.1	180.06	152.6	681.5
190	0.00113357	811.665	2.2232	4.4044	1392.2	170.99	144.2	676.6
200	0.00114818	855.918	2.3177	4.4472	1362.3	161.64	136.7	670.7
210	0.00116389	900.631	2.4112	4.4965	1330.3	152.05	129.9	663.8
220	0.00118085	945.874	2.5039	4.5535	1296.1	142.27	123.8	655.8
230	0.00119922	991.731	2.5959	4.6196	1259.8	132.34	118.1	646.8
240	0.00121923	1038.30	2.6876	4.6970	1221.1	122.30	112.9	636.7

Table 3 Single-phase region – Continued (0 °C to 800 °C)

p = 100 bar								
t [°C]	v [$m^3\ kg^{-1}$]	h [$kJ\ kg^{-1}$]	s [$kJ\ kg^{-1}\ K^{-1}$]	c_p [$kJ\ kg^{-1}\ K^{-1}$]	w [$m\ s^{-1}$]	κ [–]	η [10^{-6} Pa s]	λ [$10^{-3}\ W\ m^{-1}\ K^{-1}$]
250	0.00124116	1085.72	2.7791	4.7883	1180.0	112.19	108.0	625.5
260	0.00126534	1134.13	2.8708	4.8972	1136.3	102.03	103.4	613.0
270	0.00129228	1183.74	2.9629	5.0293	1089.4	91.840	98.99	599.2
280	0.00132264	1234.82	3.0561	5.1931	1038.9	81.605	94.76	584.0
290	0.00135739	1287.75	3.1510	5.4023	983.78	71.300	90.60	567.0
300	0.00139804	1343.10	3.2484	5.6816	922.76	60.905	86.43	548.1
310	0.00144710	1401.77	3.3498	6.0782	854.92	50.507	82.16	526.8
t_s = 310.999 °C				**Saturation**				
Liquid	0.00145262	1407.87	3.3603	6.1275	847.74	49.474	81.72	524.5
Vapour	0.0180336	2725.47	5.6159	7.1472	472.44	1.2377	20.19	78.97
320	0.0192716	2782.66	5.7131	5.7468	491.71	1.2546	20.66	74.68
330	0.0204462	2835.67	5.8017	4.9228	508.20	1.2632	21.18	71.67
340	0.0214897	2882.06	5.8780	4.3885	522.16	1.2688	21.68	69.76
350	0.0224422	2923.96	5.9458	4.0118	534.45	1.2728	22.18	68.55
360	0.0233274	2962.61	6.0073	3.7324	545.52	1.2757	22.67	67.72
370	0.0241605	2998.82	6.0641	3.5174	555.64	1.2779	23.15	66.85
380	0.0249522	3033.11	6.1170	3.3471	565.02	1.2794	23.62	66.67
390	0.0257099	3065.87	6.1668	3.2092	573.79	1.2806	24.09	66.91
400	0.0264393	3097.38	6.2139	3.0958	582.04	1.2813	24.55	67.25
410	0.0271447	3127.85	6.2589	3.0013	589.86	1.2818	25.01	67.72
420	0.0278294	3157.45	6.3019	2.9217	597.31	1.2820	25.46	68.30
430	0.0284963	3186.32	6.3432	2.8542	604.44	1.2821	25.91	68.98
440	0.0291475	3214.57	6.3831	2.7965	611.28	1.2820	26.36	69.74
450	0.0297850	3242.28	6.4217	2.7470	617.87	1.2817	26.80	70.56
460	0.0304102	3269.53	6.4591	2.7043	624.24	1.2814	27.24	71.43
470	0.0310246	3296.38	6.4955	2.6674	630.41	1.2810	27.68	72.36
480	0.0316292	3322.89	6.5310	2.6354	636.39	1.2804	28.11	73.32
490	0.0322250	3349.11	6.5655	2.6076	642.21	1.2799	28.54	74.31
500	0.0328129	3375.06	6.5993	2.5833	647.89	1.2792	28.97	75.34
510	0.0333935	3400.78	6.6324	2.5622	653.42	1.2786	29.39	76.39
520	0.0339675	3426.31	6.6648	2.5437	658.83	1.2779	29.81	77.47
530	0.0345355	3451.67	6.6965	2.5275	664.12	1.2771	30.23	78.57
540	0.0350979	3476.87	6.7277	2.5134	669.31	1.2764	30.65	79.69
550	0.0356552	3501.94	6.7584	2.5011	674.39	1.2756	31.07	80.83
560	0.0362078	3526.90	6.7885	2.4904	679.39	1.2748	31.48	81.98
570	0.0367561	3551.75	6.8182	2.4811	684.29	1.2740	31.89	83.16
580	0.0373002	3576.52	6.8474	2.4730	689.11	1.2731	32.30	84.34
590	0.0378406	3601.22	6.8761	2.4660	693.86	1.2723	32.71	85.54
600	0.0383775	3625.84	6.9045	2.4600	698.54	1.2715	33.12	86.76
650	0.0410163	3748.32	7.0409	2.4420	720.95	1.2672	35.13	93.00
700	0.0435944	3870.27	7.1696	2.4380	742.03	1.2630	37.10	99.47
750	0.0461269	3992.28	7.2918	2.4435	762.03	1.2589	39.04	106.1
800	0.0486242	4114.73	7.4087	2.4555	781.12	1.2548	40.95	113.0

Table 3 Single-phase region – Continued (0 °C to 800 °C)

$p = 110$ bar

t [°C]	v [$m^3\,kg^{-1}$]	h [$kJ\,kg^{-1}$]	s [$kJ\,kg^{-1}\,K^{-1}$]	c_p [$kJ\,kg^{-1}\,K^{-1}$]	w [$m\,s^{-1}$]	κ [–]	η [10^{-6} Pa s]	λ [$10^{-3}\,W\,m^{-1}\,K^{-1}$]
0	0.000994708	11.0723	0.0003675	4.1678	1419.8	184.23	1768.6	568.4
2	0.000994686	19.4042	0.030760	4.1643	1429.6	186.79	1654.1	572.6
4	0.000994725	27.7299	0.060909	4.1615	1439.0	189.25	1551.1	576.6
6	0.000994821	36.0507	0.090824	4.1593	1448.1	191.62	1458.0	580.5
8	0.000994972	44.3674	0.12051	4.1575	1456.7	193.88	1373.5	584.3
10	0.000995175	52.6808	0.14998	4.1560	1464.9	196.04	1296.6	588.0
12	0.000995426	60.9917	0.17922	4.1549	1472.8	198.11	1226.4	591.7
14	0.000995723	69.3006	0.20826	4.1540	1480.3	200.07	1162.1	595.2
16	0.000996064	77.6078	0.23709	4.1533	1487.5	201.94	1103.1	598.7
18	0.000996448	85.9137	0.26572	4.1527	1494.3	203.72	1048.7	602.1
20	0.000996873	94.2187	0.29414	4.1523	1500.8	205.40	998.5	605.4
25	0.000998101	114.978	0.36436	4.1517	1515.6	209.21	888.7	613.3
30	0.000999554	135.736	0.43341	4.1516	1528.4	212.47	797.1	620.7
35	0.00100121	156.495	0.50132	4.1519	1539.5	215.21	719.9	627.7
40	0.00100307	177.256	0.56816	4.1526	1549.0	217.46	654.2	634.2
45	0.00100511	198.021	0.63394	4.1537	1556.9	219.25	597.7	640.4
50	0.00100732	218.793	0.69873	4.1551	1563.4	220.60	548.7	646.1
55	0.00100970	239.573	0.76254	4.1570	1568.6	221.54	506.1	651.4
60	0.00101224	260.363	0.82542	4.1592	1572.5	222.09	468.7	656.4
65	0.00101494	281.166	0.88739	4.1619	1575.3	222.27	435.7	661.0
70	0.00101779	301.983	0.94851	4.1649	1576.9	222.12	406.4	665.3
75	0.00102080	322.816	1.0088	4.1684	1577.6	221.64	380.3	669.2
80	0.00102395	343.668	1.0682	4.1723	1577.2	220.86	357.0	672.7
85	0.00102724	364.540	1.1269	4.1767	1576.0	219.80	336.0	676.0
90	0.00103069	385.435	1.1849	4.1814	1573.8	218.47	317.1	678.9
95	0.00103427	406.355	1.2421	4.1866	1570.9	216.90	300.0	681.5
100	0.00103800	427.302	1.2986	4.1923	1567.1	215.09	284.5	683.8
110	0.00104590	469.287	1.4096	4.2050	1557.5	210.85	257.5	687.4
120	0.00105439	511.409	1.5182	4.2197	1545.2	205.85	234.9	689.9
130	0.00106348	553.689	1.6244	4.2366	1530.3	200.19	215.7	691.3
140	0.00107320	596.148	1.7284	4.2557	1513.2	193.95	199.4	691.6
150	0.00108358	638.813	1.8304	4.2776	1493.8	187.21	185.3	690.8
160	0.00109467	681.710	1.9306	4.3024	1472.3	180.02	173.0	689.0
170	0.00110651	724.873	2.0291	4.3307	1448.7	172.44	162.3	686.1
180	0.00111916	768.337	2.1261	4.3630	1423.1	164.52	152.9	682.3
190	0.00113270	812.147	2.2217	4.3998	1395.5	156.30	144.5	677.4
200	0.00114723	856.351	2.3162	4.4420	1365.8	147.82	137.0	671.5
210	0.00116284	901.009	2.4096	4.4906	1334.0	139.13	130.2	664.7
220	0.00117969	946.187	2.5021	4.5466	1300.2	130.27	124.0	656.8
230	0.00119792	991.970	2.5940	4.6115	1264.1	121.27	118.4	647.8
240	0.00121777	1038.45	2.6855	4.6873	1225.8	112.17	113.1	637.8

Table 3 Single-phase region – Continued (0 °C to 800 °C)

p = 110 bar

t [°C]	v [m^3 kg^{-1}]	h [kJ kg^{-1}]	s [kJ kg^{-1} K^{-1}]	c_p [kJ kg^{-1} K^{-1}]	w [m s^{-1}]	κ [–]	η [10^{-6} Pa s]	λ [10^{-3} W m^{-1} K^{-1}]
250	0.00123948	1085.76	2.7768	4.7766	1185.1	103.01	108.3	626.7
260	0.00126341	1134.04	2.8682	4.8828	1141.8	93.802	103.7	614.3
270	0.00129002	1183.49	2.9601	5.0112	1095.5	84.572	99.30	600.7
280	0.00131993	1234.36	3.0529	5.1695	1045.7	75.314	95.08	585.6
290	0.00135407	1287.02	3.1473	5.3703	991.56	66.008	90.95	568.9
300	0.00139383	1341.98	3.2440	5.6357	931.80	56.629	86.83	550.4
310	0.00144151	1400.08	3.3445	6.0070	865.35	47.225	82.62	529.4
t_s = 318.081 °C				**Saturation**				
Liquid	0.00148855	1450.28	3.4300	6.4427	806.15	39.689	79.04	510.4
Vapour	0.0159939	2706.39	5.5545	7.9168	466.11	1.2349	20.64	84.64
320	0.0162775	2721.07	5.5793	7.4062	471.35	1.2408	20.74	83.28
330	0.0175664	2786.37	5.6885	5.8578	492.74	1.2565	21.24	78.10
340	0.0186580	2840.45	5.7775	5.0240	509.38	1.2642	21.74	74.90
350	0.0196272	2887.79	5.8541	4.4777	523.55	1.2696	22.23	72.82
360	0.0205114	2930.53	5.9221	4.0917	536.03	1.2735	22.72	71.36
370	0.0213326	2969.95	5.9839	3.8048	547.26	1.2763	23.20	69.85
380	0.0221050	3006.84	6.0408	3.5836	557.53	1.2784	23.68	69.22
390	0.0228384	3041.77	6.0939	3.4080	567.03	1.2798	24.15	69.18
400	0.0235398	3075.12	6.1438	3.2658	575.91	1.2809	24.61	69.28
410	0.0242145	3107.17	6.1911	3.1485	584.26	1.2816	25.07	69.57
420	0.0248665	3138.15	6.2361	3.0507	592.17	1.2820	25.53	70.00
430	0.0254991	3168.23	6.2792	2.9682	599.70	1.2822	25.98	70.56
440	0.0261148	3197.55	6.3206	2.8980	606.91	1.2822	26.43	71.21
450	0.0267157	3226.23	6.3605	2.8381	613.82	1.2821	26.87	71.95
460	0.0273036	3254.34	6.3991	2.7865	620.47	1.2818	27.31	72.75
470	0.0278799	3281.98	6.4366	2.7419	626.90	1.2815	27.74	73.60
480	0.0284459	3309.20	6.4730	2.7033	633.12	1.2810	28.18	74.51
490	0.0290026	3336.06	6.5084	2.6697	639.15	1.2805	28.61	75.45
500	0.0295510	3362.61	6.5430	2.6405	645.02	1.2799	29.04	76.43
510	0.0300918	3388.89	6.5767	2.6149	650.74	1.2793	29.46	77.45
520	0.0306258	3414.92	6.6098	2.5925	656.31	1.2786	29.88	78.49
530	0.0311535	3440.74	6.6421	2.5729	661.76	1.2779	30.30	79.56
540	0.0316754	3466.39	6.6738	2.5557	667.09	1.2772	30.72	80.65
550	0.0321920	3491.87	6.7050	2.5406	672.31	1.2764	31.14	81.76
560	0.0327038	3517.20	6.7356	2.5273	677.42	1.2756	31.55	82.89
570	0.0332110	3542.42	6.7657	2.5158	682.44	1.2748	31.96	84.04
580	0.0337141	3567.52	6.7953	2.5056	687.38	1.2740	32.37	85.20
590	0.0342133	3592.53	6.8244	2.4968	692.22	1.2732	32.78	86.38
600	0.0347089	3617.46	6.8531	2.4891	697.00	1.2724	33.19	87.58
650	0.0371405	3741.21	6.9910	2.4643	719.82	1.2682	35.19	93.74
700	0.0395103	3864.16	7.1207	2.4558	741.21	1.2641	37.16	100.2
750	0.0418340	3986.97	7.2437	2.4578	761.46	1.2600	39.10	106.8
800	0.0441222	4110.07	7.3612	2.4674	780.75	1.2560	41.01	113.5

Table 3 Single-phase region – Continued (0 °C to 800 °C)

p = 120 bar

t [°C]	v [m^3 kg^{-1}]	h [kJ kg^{-1}]	s [kJ kg^{-1} K^{-1}]	c_p [kJ kg^{-1} K^{-1}]	w [m s^{-1}]	κ [–]	η [10^{-6} Pa s]	λ [10^{-3} W m^{-1} K^{-1}]
0	0.000994218	12.0737	0.0003931	4.1633	1421.4	169.34	1766.6	569.0
2	0.000994202	20.3970	0.030754	4.1601	1431.2	171.70	1652.5	573.1
4	0.000994247	28.7145	0.060873	4.1575	1440.6	173.96	1549.7	577.1
6	0.000994350	37.0275	0.090760	4.1555	1449.7	176.12	1456.8	581.1
8	0.000994506	45.3369	0.12042	4.1539	1458.3	178.20	1372.5	584.9
10	0.000994713	53.6433	0.14986	4.1526	1466.6	180.19	1295.8	588.6
12	0.000994968	61.9475	0.17909	4.1516	1474.4	182.08	1225.8	592.2
14	0.000995269	70.2499	0.20810	4.1508	1481.9	183.88	1161.6	595.8
16	0.000995614	78.5509	0.23691	4.1502	1489.1	185.60	1102.6	599.2
18	0.000996001	86.8509	0.26551	4.1498	1495.9	187.23	1048.4	602.6
20	0.000996429	95.1500	0.29392	4.1494	1502.4	188.77	998.3	605.9
25	0.000997663	115.896	0.36409	4.1490	1517.2	192.26	888.6	613.8
30	0.000999120	136.641	0.43309	4.1491	1530.0	195.26	797.2	621.2
35	0.00100078	157.387	0.50097	4.1495	1541.2	197.78	720.0	628.2
40	0.00100264	178.136	0.56777	4.1503	1550.6	199.84	654.3	634.7
45	0.00100468	198.891	0.63352	4.1515	1558.6	201.49	597.8	640.9
50	0.00100689	219.652	0.69827	4.1530	1565.1	202.73	549.0	646.6
55	0.00100927	240.421	0.76205	4.1549	1570.3	203.60	506.3	651.9
60	0.00101181	261.201	0.82489	4.1571	1574.2	204.11	468.9	656.9
65	0.00101450	281.993	0.88684	4.1598	1577.0	204.29	435.9	661.5
70	0.00101735	302.800	0.94792	4.1629	1578.7	204.15	406.6	665.8
75	0.00102035	323.622	1.0082	4.1664	1579.4	203.72	380.6	669.7
80	0.00102349	344.464	1.0676	4.1703	1579.1	203.02	357.2	673.3
85	0.00102678	365.326	1.1263	4.1746	1577.8	202.05	336.3	676.5
90	0.00103022	386.210	1.1842	4.1793	1575.7	200.85	317.4	679.4
95	0.00103379	407.120	1.2414	4.1845	1572.8	199.41	300.3	682.0
100	0.00103751	428.056	1.2978	4.1902	1569.1	197.77	284.8	684.3
110	0.00104539	470.020	1.4088	4.2028	1559.6	193.89	257.8	688.0
120	0.00105385	512.119	1.5173	4.2174	1547.4	189.33	235.1	690.5
130	0.00106291	554.374	1.6234	4.2340	1532.6	184.16	216.0	691.9
140	0.00107260	596.807	1.7274	4.2530	1515.6	178.46	199.6	692.2
150	0.00108294	639.443	1.8294	4.2746	1496.4	172.30	185.5	691.4
160	0.00109398	682.309	1.9295	4.2992	1475.0	165.73	173.3	689.6
170	0.00110577	725.438	2.0279	4.3271	1451.6	158.80	162.6	686.8
180	0.00111836	768.865	2.1248	4.3590	1426.2	151.56	153.1	683.0
190	0.00113184	812.632	2.2204	4.3953	1398.8	144.05	144.7	678.2
200	0.00114628	856.788	2.3147	4.4369	1369.3	136.31	137.2	672.4
210	0.00116180	901.391	2.4080	4.4847	1337.8	128.36	130.4	665.6
220	0.00117853	946.506	2.5004	4.5397	1304.1	120.26	124.3	657.7
230	0.00119664	992.215	2.5921	4.6035	1268.4	112.04	118.6	648.9
240	0.00121632	1038.61	2.6834	4.6779	1230.4	103.72	113.4	638.9

Table 3 Single-phase region – Continued (0 °C to 800 °C)

p = 120 bar

t [°C]	v [$m^3\,kg^{-1}$]	h [$kJ\,kg^{-1}$]	s [$kJ\,kg^{-1}\,K^{-1}$]	c_p [$kJ\,kg^{-1}\,K^{-1}$]	w [$m\,s^{-1}$]	κ [–]	η [10^{-6} Pa s]	λ [$10^{-3}\,W\,m^{-1}\,K^{-1}$]
250	0.00123783	1085.81	2.7745	4.7652	1190.1	95.346	108.5	627.9
260	0.00126151	1133.97	2.8657	4.8688	1147.2	86.937	104.0	615.7
270	0.00128779	1183.26	2.9573	4.9936	1101.5	78.508	99.60	602.2
280	0.00131728	1233.94	3.0498	5.1467	1052.4	70.063	95.40	587.3
290	0.00135084	1286.33	3.1436	5.3398	999.16	61.587	91.30	570.8
300	0.00138976	1340.93	3.2397	5.5924	940.65	53.056	87.22	552.5
310	0.00143614	1398.49	3.3393	5.9411	875.62	44.489	83.07	532.0
320	0.00149369	1460.31	3.4444	6.4621	803.26	35.998	78.70	508.7
t_s = 324.678 °C				**Saturation**				
Liquid	0.00152633	1491.33	3.4965	6.8126	765.59	32.001	76.51	496.5
Vapour	0.0142689	2685.58	5.4941	8.8189	459.46	1.2329	21.11	90.93
330	0.0150236	2728.14	5.5650	7.3313	474.22	1.2474	21.36	86.66
340	0.0162112	2793.47	5.6725	5.8968	494.92	1.2591	21.84	81.36
350	0.0172227	2848.01	5.7607	5.0746	511.54	1.2661	22.32	78.01
360	0.0181226	2895.87	5.8369	4.5309	525.77	1.2711	22.80	75.68
370	0.0189442	2939.15	5.9047	4.1447	538.33	1.2748	23.28	73.37
380	0.0197077	2979.09	5.9664	3.8563	549.63	1.2774	23.76	72.13
390	0.0204258	3016.49	6.0232	3.6329	559.97	1.2793	24.23	71.73
400	0.0211077	3051.90	6.0762	3.4551	569.54	1.2806	24.69	71.53
410	0.0217597	3085.70	6.1261	3.3106	578.47	1.2815	25.15	71.59
420	0.0223867	3118.19	6.1733	3.1912	586.89	1.2821	25.60	71.85
430	0.0229924	3149.59	6.2182	3.0914	594.85	1.2825	26.05	72.26
440	0.0235799	3180.07	6.2613	3.0071	602.43	1.2826	26.50	72.79
450	0.0241515	3209.77	6.3027	2.9353	609.68	1.2826	26.94	73.43
460	0.0247091	3238.81	6.3425	2.8737	616.64	1.2824	27.38	74.14
470	0.0252545	3267.28	6.3811	2.8207	623.34	1.2821	27.82	74.92
480	0.0257890	3295.25	6.4185	2.7748	629.81	1.2817	28.25	75.76
490	0.0263138	3322.79	6.4548	2.7349	636.07	1.2813	28.68	76.65
500	0.0268298	3349.97	6.4902	2.7002	642.14	1.2807	29.11	77.58
510	0.0273378	3376.81	6.5247	2.6698	648.04	1.2801	29.54	78.55
520	0.0278387	3403.37	6.5584	2.6432	653.79	1.2795	29.96	79.55
530	0.0283331	3429.69	6.5914	2.6199	659.39	1.2788	30.38	80.59
540	0.0288215	3455.78	6.6237	2.5993	664.86	1.2781	30.80	81.64
550	0.0293045	3481.68	6.6553	2.5813	670.22	1.2774	31.21	82.72
560	0.0297824	3507.41	6.6864	2.5654	675.46	1.2766	31.62	83.83
570	0.0302557	3533.00	6.7169	2.5514	680.60	1.2758	32.04	84.95
580	0.0307247	3558.45	6.7469	2.5391	685.64	1.2751	32.45	86.09
590	0.0311897	3583.78	6.7764	2.5283	690.60	1.2743	32.85	87.25
600	0.0316511	3609.02	6.8055	2.5188	695.46	1.2734	33.26	88.42
650	0.0339104	3734.07	6.9448	2.4871	718.70	1.2693	35.26	94.50
700	0.0361069	3858.03	7.0756	2.4737	740.40	1.2652	37.23	100.8
750	0.0382567	3981.64	7.1994	2.4723	760.90	1.2612	39.16	107.4
800	0.0403706	4105.40	7.3175	2.4793	780.40	1.2571	41.07	114.1

Table 3 Single-phase region – Continued
(0 °C to 800 °C)

p = 130 bar								
t [ºC]	v [$m^3\ kg^{-1}$]	h [$kJ\ kg^{-1}$]	s [$kJ\ kg^{-1}\ K^{-1}$]	c_p [$kJ\ kg^{-1}\ K^{-1}$]	w [$m\ s^{-1}$]	κ [–]	η [10^{-6} Pa s]	λ [$10^{-3}\ W\ m^{-1}\ K^{-1}$]
0	0.000993730	13.0737	0.0004152	4.1589	1423.0	156.75	1764.6	569.6
2	0.000993721	21.3884	0.030744	4.1559	1432.8	158.93	1650.8	573.7
4	0.000993772	29.6978	0.060835	4.1536	1442.3	161.01	1548.3	577.7
6	0.000993880	38.0031	0.090694	4.1518	1451.3	163.02	1455.7	581.6
8	0.000994041	46.3052	0.12033	4.1503	1459.9	164.94	1371.6	585.4
10	0.000994253	54.6047	0.14974	4.1492	1468.2	166.77	1295.0	589.1
12	0.000994512	62.9022	0.17895	4.1484	1476.1	168.52	1225.1	592.8
14	0.000994817	71.1982	0.20794	4.1477	1483.6	170.19	1161.1	596.3
16	0.000995166	79.4931	0.23672	4.1472	1490.7	171.77	1102.2	599.8
18	0.000995556	87.7871	0.26531	4.1468	1497.5	173.28	1048.0	603.1
20	0.000995986	96.0805	0.29370	4.1466	1504.0	174.70	998.0	606.4
25	0.000997226	116.813	0.36382	4.1464	1518.8	177.93	888.5	614.3
30	0.000998687	137.545	0.43278	4.1466	1531.7	180.70	797.2	621.7
35	0.00100035	158.279	0.50062	4.1471	1542.8	183.02	720.1	628.7
40	0.00100221	179.017	0.56738	4.1480	1552.3	184.94	654.4	635.2
45	0.00100425	199.760	0.63309	4.1493	1560.2	186.46	598.0	641.4
50	0.00100646	220.510	0.69781	4.1508	1566.8	187.62	549.2	647.1
55	0.00100883	241.269	0.76155	4.1528	1572.0	188.42	506.5	652.5
60	0.00101137	262.038	0.82437	4.1551	1576.0	188.90	469.2	657.4
65	0.00101406	282.820	0.88629	4.1577	1578.8	189.07	436.2	662.0
70	0.00101691	303.616	0.94734	4.1608	1580.5	188.95	406.9	666.3
75	0.00101990	324.429	1.0075	4.1643	1581.2	188.56	380.8	670.2
80	0.00102304	345.260	1.0670	4.1682	1580.9	187.92	357.5	673.8
85	0.00102632	366.112	1.1256	4.1725	1579.7	187.04	336.6	677.0
90	0.00102975	386.986	1.1835	4.1773	1577.7	185.93	317.7	679.9
95	0.00103332	407.885	1.2406	4.1824	1574.8	184.62	300.6	682.5
100	0.00103703	428.811	1.2971	4.1880	1571.1	183.10	285.0	684.8
110	0.00104488	470.752	1.4080	4.2006	1561.7	179.55	258.0	688.5
120	0.00105332	512.828	1.5164	4.2150	1549.5	175.35	235.4	691.1
130	0.00106235	555.059	1.6225	4.2315	1534.9	170.59	216.2	692.5
140	0.00107200	597.467	1.7264	4.2503	1518.0	165.35	199.9	692.8
150	0.00108231	640.074	1.8283	4.2717	1498.9	159.68	185.8	692.1
160	0.00109331	682.910	1.9283	4.2960	1477.7	153.64	173.5	690.3
170	0.00110504	726.005	2.0267	4.3236	1454.5	147.26	162.8	687.5
180	0.00111758	769.394	2.1235	4.3550	1429.2	140.60	153.4	683.7
190	0.00113098	813.119	2.2190	4.3908	1402.0	133.69	145.0	679.0
200	0.00114535	857.228	2.3132	4.4318	1372.7	126.56	137.4	673.2
210	0.00116077	901.776	2.4064	4.4789	1341.5	119.25	130.7	666.4
220	0.00117740	946.830	2.4986	4.5330	1308.1	111.79	124.5	658.7
230	0.00119537	992.466	2.5903	4.5957	1272.6	104.22	118.9	649.9
240	0.00121489	1038.78	2.6814	4.6686	1235.0	96.568	113.7	640.0

Table 3 Single-phase region – Continued (0 °C to 800 °C)

$p =$ **130 bar**

t [°C]	v [m^3 kg^{-1}]	h [kJ kg^{-1}]	s [kJ kg^{-1} K^{-1}]	c_p [kJ kg^{-1} K^{-1}]	w [m s^{-1}]	κ [–]	η [10^{-6} Pa s]	λ [10^{-3} W m^{-1} K^{-1}]
250	0.00123620	1085.88	2.7723	4.7540	1195.0	88.861	108.8	629.1
260	0.00125964	1133.91	2.8632	4.8552	1152.6	81.123	104.2	617.0
270	0.00128561	1183.05	2.9546	4.9766	1107.4	73.372	99.90	603.6
280	0.00131469	1233.53	3.0466	5.1248	1058.9	65.611	95.72	588.9
290	0.00134768	1285.67	3.1401	5.3106	1006.6	57.835	91.65	572.6
300	0.00138581	1339.92	3.2355	5.5515	949.29	50.021	87.60	554.6
310	0.00143098	1396.99	3.3342	5.8798	885.71	42.170	83.50	534.5
320	0.00148654	1458.02	3.4380	6.3606	815.02	34.373	79.22	511.7
330	0.00155907	1525.23	3.5503	7.1610	733.04	26.512	74.52	485.3
t_s = 330.857 °C				**Saturation**				
Liquid	0.00156649	1531.40	3.5606	7.2579	724.84	25.799	74.09	482.9
Vapour	0.0127851	2662.89	5.4339	9.9072	452.50	1.2320	21.60	98.03
340	0.0140296	2738.92	5.5589	7.1954	478.10	1.2533	21.99	89.81
350	0.0151195	2803.61	5.6635	5.8727	498.14	1.2625	22.45	84.47
360	0.0160546	2858.09	5.7503	5.0817	514.59	1.2688	22.92	80.91
370	0.0168896	2906.10	5.8255	4.5530	528.76	1.2734	23.39	77.55
380	0.0176538	2949.64	5.8927	4.1742	541.28	1.2766	23.85	75.48
390	0.0183647	2989.90	5.9539	3.8893	552.57	1.2789	24.32	74.59
400	0.0190341	3027.64	6.0104	3.6672	562.91	1.2806	24.78	74.03
410	0.0196699	3063.39	6.0631	3.4896	572.49	1.2817	25.24	73.82
420	0.0202779	3097.54	6.1127	3.3448	581.45	1.2825	25.69	73.86
430	0.0208627	3130.37	6.1598	3.2248	589.88	1.2830	26.14	74.10
440	0.0214277	3162.10	6.2046	3.1242	597.87	1.2832	26.59	74.49
450	0.0219756	3192.90	6.2475	3.0391	605.48	1.2833	27.03	75.01
460	0.0225087	3222.92	6.2887	2.9664	612.75	1.2832	27.47	75.62
470	0.0230287	3252.27	6.3285	2.9040	619.74	1.2829	27.90	76.32
480	0.0235371	3281.03	6.3669	2.8501	626.46	1.2826	28.34	77.09
490	0.0240353	3309.29	6.4042	2.8033	632.95	1.2822	28.77	77.91
500	0.0245243	3337.12	6.4404	2.7626	639.23	1.2817	29.19	78.79
510	0.0250051	3364.56	6.4757	2.7270	645.33	1.2811	29.62	79.71
520	0.0254784	3391.67	6.5101	2.6959	651.25	1.2805	30.04	80.67
530	0.0259448	3418.49	6.5437	2.6685	657.02	1.2798	30.46	81.66
540	0.0264052	3445.05	6.5765	2.6445	662.64	1.2792	30.88	82.68
550	0.0268598	3471.39	6.6087	2.6233	668.13	1.2784	31.29	83.73
560	0.0273093	3497.53	6.6403	2.6046	673.50	1.2777	31.70	84.80
570	0.0277541	3523.49	6.6713	2.5880	678.76	1.2769	32.11	85.90
580	0.0281944	3549.29	6.7017	2.5734	683.92	1.2762	32.52	87.01
590	0.0286306	3574.96	6.7316	2.5606	688.98	1.2754	32.93	88.15
600	0.0290630	3600.51	6.7610	2.5492	693.94	1.2746	33.34	89.30
650	0.0311769	3726.89	6.9018	2.5102	717.59	1.2705	35.34	95.28
700	0.0332270	3851.87	7.0336	2.4919	739.61	1.2664	37.30	101.6
750	0.0352298	3976.29	7.1583	2.4869	760.36	1.2624	39.23	108.1
800	0.0371964	4100.72	7.2771	2.4913	780.05	1.2584	41.13	114.8

Table 3 Single-phase region – Continued (0 °C to 800 °C)

$p =$ **140 bar**

t [°C]	v [$m^3 kg^{-1}$]	h [$kJ kg^{-1}$]	s [$kJ kg^{-1} K^{-1}$]	c_p [$kJ kg^{-1} K^{-1}$]	w [$m s^{-1}$]	κ [–]	η [10^{-6} Pa s]	λ [$10^{-3} W m^{-1} K^{-1}$]
0	0.000993243	14.0723	0.0004338	4.1545	1424.7	145.96	1762.6	570.2
2	0.000993240	22.3784	0.030732	4.1518	1434.5	147.98	1649.2	574.3
4	0.000993298	30.6799	0.060793	4.1497	1443.9	149.92	1546.9	578.3
6	0.000993411	38.9776	0.090625	4.1481	1452.9	151.78	1454.5	582.2
8	0.000993577	47.2724	0.12023	4.1468	1461.6	153.57	1370.6	586.0
10	0.000993794	55.5650	0.14962	4.1458	1469.8	155.27	1294.2	589.7
12	0.000994058	63.8559	0.17880	4.1451	1477.7	156.90	1224.5	593.3
14	0.000994366	72.1456	0.20777	4.1446	1485.2	158.45	1160.5	596.9
16	0.000994718	80.4344	0.23654	4.1442	1492.3	159.92	1101.8	600.3
18	0.000995112	88.7225	0.26510	4.1439	1499.1	161.32	1047.7	603.7
20	0.000995544	97.0102	0.29347	4.1438	1505.6	162.64	997.8	607.0
25	0.000996790	117.729	0.36355	4.1438	1520.4	165.64	888.4	614.8
30	0.000998255	138.448	0.43247	4.1441	1533.3	168.22	797.2	622.3
35	0.000999923	159.170	0.50027	4.1448	1544.4	170.38	720.2	629.2
40	0.00100178	179.897	0.56699	4.1458	1553.9	172.16	654.6	635.8
45	0.00100382	200.629	0.63267	4.1471	1561.9	173.58	598.2	641.9
50	0.00100603	221.368	0.69735	4.1487	1568.4	174.66	549.4	647.6
55	0.00100840	242.116	0.76106	4.1507	1573.7	175.41	506.8	653.0
60	0.00101094	262.875	0.82385	4.1530	1577.7	175.87	469.4	657.9
65	0.00101363	283.647	0.88573	4.1557	1580.5	176.03	436.4	662.5
70	0.00101647	304.433	0.94675	4.1588	1582.3	175.93	407.2	666.8
75	0.00101945	325.235	1.0069	4.1623	1583.0	175.57	381.1	670.7
80	0.00102258	346.056	1.0663	4.1662	1582.7	174.98	357.8	674.3
85	0.00102586	366.898	1.1249	4.1705	1581.6	174.17	336.8	677.5
90	0.00102928	387.762	1.1828	4.1752	1579.6	173.15	317.9	680.5
95	0.00103284	408.650	1.2399	4.1803	1576.7	171.93	300.8	683.1
100	0.00103654	429.566	1.2963	4.1859	1573.1	170.54	285.3	685.4
110	0.00104437	471.485	1.4072	4.1983	1563.8	167.25	258.3	689.1
120	0.00105278	513.539	1.5155	4.2127	1551.7	163.37	235.7	691.7
130	0.00106179	555.745	1.6215	4.2290	1537.2	158.97	216.5	693.1
140	0.00107141	598.127	1.7254	4.2476	1520.4	154.11	200.1	693.4
150	0.00108168	640.707	1.8272	4.2688	1501.4	148.87	186.0	692.7
160	0.00109263	683.512	1.9272	4.2928	1480.4	143.27	173.8	691.0
170	0.00110432	726.573	2.0255	4.3200	1457.3	137.37	163.1	688.2
180	0.00111679	769.925	2.1222	4.3511	1432.2	131.20	153.6	684.5
190	0.00113013	813.609	2.2176	4.3864	1405.2	124.80	145.2	679.7
200	0.00114442	857.671	2.3117	4.4269	1376.2	118.20	137.7	674.0
210	0.00115975	902.166	2.4048	4.4732	1345.1	111.44	130.9	667.3
220	0.00117627	947.158	2.4969	4.5265	1312.0	104.53	124.8	659.6
230	0.00119411	992.722	2.5884	4.5880	1276.8	97.521	119.1	650.9
240	0.00121347	1038.95	2.6794	4.6595	1239.5	90.434	113.9	641.1

Table 3 Single-phase region – Continued
(0 °C to 800 °C)

p = 140 bar

t [°C]	v [$m^3\,kg^{-1}$]	h [$kJ\,kg^{-1}$]	s [$kJ\,kg^{-1}\,K^{-1}$]	c_p [$kJ\,kg^{-1}\,K^{-1}$]	w [$m\,s^{-1}$]	κ [–]	η [10^{-6} Pa s]	λ [$10^{-3}\,W\,m^{-1}\,K^{-1}$]
250	0.00123460	1085.95	2.7701	4.7431	1199.9	83.298	109.1	630.3
260	0.00125779	1133.86	2.8608	4.8419	1157.9	76.136	104.5	618.3
270	0.00128346	1182.85	2.9518	4.9600	1113.2	68.964	100.2	605.1
280	0.00131214	1233.15	3.0436	5.1037	1065.4	61.789	96.04	590.5
290	0.00134461	1285.05	3.1366	5.2826	1013.9	54.609	91.99	574.4
300	0.00138198	1338.97	3.2315	5.5128	957.73	47.409	87.98	556.7
310	0.00142603	1395.56	3.3293	5.8226	895.59	40.176	83.93	536.9
320	0.00147974	1455.87	3.4319	6.2683	826.50	32.974	79.72	514.6
330	0.00154886	1521.80	3.5421	6.9830	748.38	25.829	75.16	489.0
t_s = 336.669 °C				**Saturation**				
Liquid	0.00160971	1570.88	3.6230	7.8117	682.84	20.690	71.73	469.4
Vapour	0.0114889	2638.09	5.3730	11.260	445.18	1.2322	22.13	106.2
340	0.0119989	2672.38	5.4291	9.4878	457.16	1.2442	22.24	101.63
350	0.0132316	2752.92	5.5595	7.0059	482.90	1.2588	22.63	92.79
360	0.0142288	2816.39	5.6605	5.7978	502.28	1.2665	23.07	87.36
370	0.0150919	2870.38	5.7452	5.0539	518.43	1.2721	23.52	82.58
380	0.0158666	2918.26	5.8190	4.5496	532.40	1.2761	23.98	79.37
390	0.0165779	2961.83	5.8853	4.1840	544.80	1.2789	24.43	77.84
400	0.0172410	3002.23	5.9457	3.9064	556.02	1.2808	24.89	76.82
410	0.0178661	3040.16	6.0017	3.6884	566.31	1.2822	25.34	76.26
420	0.0184603	3076.14	6.0539	3.5132	575.85	1.2831	25.79	76.05
430	0.0190290	3110.53	6.1032	3.3697	584.79	1.2837	26.24	76.09
440	0.0195762	3143.61	6.1499	3.2504	593.21	1.2840	26.68	76.31
450	0.0201049	3175.60	6.1945	3.1500	601.20	1.2841	27.12	76.70
460	0.0206177	3206.66	6.2371	3.0648	608.81	1.2841	27.56	77.20
470	0.0211167	3236.94	6.2782	2.9920	616.09	1.2839	28.00	77.80
480	0.0216034	3266.54	6.3177	2.9293	623.08	1.2836	28.43	78.49
490	0.0220794	3295.55	6.3560	2.8750	629.81	1.2832	28.86	79.24
500	0.0225457	3324.06	6.3931	2.8278	636.31	1.2828	29.28	80.05
510	0.0230034	3352.13	6.4292	2.7867	642.60	1.2822	29.70	80.92
520	0.0234533	3379.81	6.4643	2.7506	648.71	1.2816	30.13	81.83
530	0.0238961	3407.15	6.4986	2.7190	654.64	1.2810	30.54	82.77
540	0.0243326	3434.20	6.5320	2.6911	660.42	1.2803	30.96	83.76
550	0.0247632	3460.99	6.5648	2.6666	666.05	1.2796	31.37	84.77
560	0.0251885	3487.54	6.5968	2.6449	671.55	1.2789	31.79	85.81
570	0.0256089	3513.89	6.6283	2.6256	676.93	1.2781	32.20	86.87
580	0.0260247	3540.06	6.6591	2.6086	682.20	1.2774	32.60	87.96
590	0.0264364	3566.07	6.6894	2.5936	687.37	1.2766	33.01	89.07
600	0.0268442	3591.94	6.7192	2.5803	692.43	1.2758	33.42	90.20
650	0.0288338	3719.67	6.8615	2.5336	716.49	1.2717	35.41	96.08
700	0.0307586	3845.69	6.9944	2.5103	738.83	1.2676	37.37	102.3
750	0.0326354	3970.94	7.1200	2.5017	759.83	1.2636	39.30	108.7
800	0.0344758	4096.02	7.2393	2.5033	779.72	1.2596	41.19	115.4

Table 3 Single-phase region – Continued (0 °C to 800 °C)

p = 150 bar

t [°C]	v [m^3 kg^{-1}]	h [kJ kg^{-1}]	s [kJ kg^{-1} K^{-1}]	c_p [kJ kg^{-1} K^{-1}]	w [m s^{-1}]	κ [–]	η [10^{-6} Pa s]	λ [10^{-3} W m^{-1} K^{-1}]
0	0.000992757	15.0694	0.0004489	4.1501	1426.3	136.61	1760.7	570.8
2	0.000992762	23.3671	0.030716	4.1477	1436.1	138.50	1647.5	574.8
4	0.000992825	31.6606	0.060749	4.1458	1445.5	140.31	1545.6	578.8
6	0.000992944	39.9508	0.090554	4.1444	1454.6	142.05	1453.4	582.7
8	0.000993115	48.2384	0.12014	4.1433	1463.2	143.72	1369.7	586.5
10	0.000993336	56.5242	0.14950	4.1425	1471.4	145.31	1293.5	590.2
12	0.000993604	64.8086	0.17866	4.1419	1479.3	146.83	1223.8	593.9
14	0.000993917	73.0920	0.20761	4.1415	1486.8	148.27	1160.0	597.4
16	0.000994272	81.3747	0.23635	4.1412	1493.9	149.65	1101.4	600.8
18	0.000994669	89.6570	0.26490	4.1411	1500.8	150.95	1047.4	604.2
20	0.000995104	97.9391	0.29324	4.1410	1507.2	152.19	997.5	607.5
25	0.000996356	118.644	0.36328	4.1412	1522.0	155.00	888.3	615.4
30	0.000997825	139.351	0.43215	4.1417	1534.9	157.40	797.2	622.8
35	0.000999495	160.061	0.49991	4.1424	1546.0	159.43	720.3	629.7
40	0.00100135	180.776	0.56660	4.1435	1555.5	161.09	654.7	636.3
45	0.00100339	201.497	0.63224	4.1449	1563.5	162.42	598.4	642.4
50	0.00100560	222.226	0.69689	4.1466	1570.1	163.43	549.6	648.1
55	0.00100798	242.963	0.76057	4.1486	1575.4	164.14	507.0	653.5
60	0.00101051	263.712	0.82332	4.1509	1579.4	164.57	469.6	658.4
65	0.00101319	284.473	0.88518	4.1537	1582.2	164.73	436.7	663.0
70	0.00101603	305.249	0.94617	4.1568	1584.0	164.64	407.4	667.3
75	0.00101901	326.042	1.0063	4.1603	1584.8	164.31	381.4	671.2
80	0.00102213	346.853	1.0657	4.1642	1584.6	163.77	358.0	674.8
85	0.00102540	367.684	1.1242	4.1684	1583.4	163.01	337.1	678.1
90	0.00102881	388.538	1.1821	4.1731	1581.5	162.07	318.2	681.0
95	0.00103236	409.416	1.2392	4.1782	1578.7	160.94	301.1	683.6
100	0.00103606	430.321	1.2956	4.1838	1575.1	159.65	285.6	685.9
110	0.00104387	472.219	1.4064	4.1961	1565.8	156.59	258.6	689.7
120	0.00105225	514.250	1.5147	4.2103	1553.9	152.98	235.9	692.2
130	0.00106123	556.432	1.6206	4.2266	1539.5	148.89	216.7	693.7
140	0.00107082	598.788	1.7244	4.2450	1522.8	144.37	200.4	694.0
150	0.00108105	641.340	1.8262	4.2659	1504.0	139.49	186.3	693.4
160	0.00109196	684.115	1.9261	4.2896	1483.1	134.28	174.0	691.7
170	0.00110359	727.143	2.0243	4.3166	1460.1	128.79	163.3	688.9
180	0.00111601	770.459	2.1209	4.3472	1435.2	123.05	153.8	685.2
190	0.00112929	814.101	2.2162	4.3821	1408.4	117.10	145.4	680.5
200	0.00114350	858.117	2.3102	4.4219	1379.6	110.96	137.9	674.9
210	0.00115874	902.559	2.4032	4.4675	1348.7	104.66	131.2	668.2
220	0.00117515	947.491	2.4952	4.5200	1315.9	98.234	125.0	660.6
230	0.00119286	992.985	2.5865	4.5804	1281.0	91.710	119.4	651.9
240	0.00121207	1039.13	2.6774	4.6506	1244.0	85.114	114.2	642.2

Table 3 Single-phase region – Continued (0 °C to 800 °C)

p = 150 bar								
t [°C]	v [$m^3\,kg^{-1}$]	h [$kJ\,kg^{-1}$]	s [$kJ\,kg^{-1}\,K^{-1}$]	c_p [$kJ\,kg^{-1}\,K^{-1}$]	w [$m\,s^{-1}$]	κ [–]	η [10^{-6} Pa s]	λ [$10^{-3}\,W\,m^{-1}\,K^{-1}$]
250	0.00123301	1086.04	2.7679	4.7325	1204.7	78.474	109.3	631.5
260	0.00125597	1133.83	2.8584	4.8289	1163.1	71.810	104.8	619.6
270	0.00128134	1182.68	2.9491	4.9440	1118.9	65.139	100.5	606.5
280	0.00130964	1232.79	3.0406	5.0833	1071.7	58.470	96.35	592.1
290	0.00134160	1284.45	3.1331	5.2558	1021.0	51.805	92.32	576.2
300	0.00137826	1338.06	3.2275	5.4760	965.96	45.133	88.35	558.7
310	0.00142125	1394.21	3.3246	5.7692	905.25	38.440	84.35	539.3
320	0.00147328	1453.85	3.4260	6.1839	837.75	31.758	80.21	517.4
330	0.00153936	1518.64	3.5343	6.8289	762.35	25.170	75.77	492.5
340	0.00163107	1592.27	3.6553	8.0647	666.58	18.161	70.67	463.3
t_s = 342.158 °C				**Saturation**				
Liquid	0.00165696	1610.15	3.6844	8.5252	639.77	16.468	69.40	456.2
Vapour	0.0103401	2610.86	5.3108	12.982	437.44	1.2337	22.72	115.8
350	0.0114807	2693.00	5.4435	8.7885	464.90	1.2551	22.91	104.1
360	0.0125823	2769.56	5.5654	6.7740	488.52	1.2645	23.28	95.55
370	0.0134930	2831.40	5.6624	5.6868	507.20	1.2710	23.69	88.78
380	0.0142893	2884.61	5.7445	5.0003	522.93	1.2758	24.13	83.95
390	0.0150084	2932.11	5.8166	4.5264	536.62	1.2791	24.57	81.54
400	0.0156711	2975.55	5.8817	4.1778	548.83	1.2814	25.02	79.94
410	0.0162904	3015.93	5.9412	3.9102	559.91	1.2829	25.46	78.97
420	0.0168752	3053.94	5.9965	3.6985	570.10	1.2840	25.91	78.45
430	0.0174318	3090.04	6.0482	3.5273	579.58	1.2847	26.35	78.24
440	0.0179649	3124.58	6.0970	3.3864	588.46	1.2851	26.79	78.28
450	0.0184781	3157.84	6.1433	3.2687	596.85	1.2852	27.23	78.50
460	0.0189743	3190.02	6.1875	3.1695	604.81	1.2852	27.66	78.88
470	0.0194557	3221.28	6.2298	3.0851	612.40	1.2851	28.10	79.37
480	0.0199243	3251.76	6.2706	3.0126	619.67	1.2848	28.53	79.96
490	0.0203814	3281.57	6.3099	2.9501	626.65	1.2845	28.95	80.64
500	0.0208285	3310.79	6.3479	2.8960	633.37	1.2840	29.38	81.38
510	0.0212665	3339.51	6.3848	2.8487	639.87	1.2835	29.80	82.18
520	0.0216964	3367.79	6.4207	2.8074	646.16	1.2829	30.22	83.04
530	0.0221191	3395.68	6.4556	2.7712	652.26	1.2823	30.64	83.94
540	0.0225351	3423.22	6.4897	2.7393	658.20	1.2816	31.05	84.88
550	0.0229451	3450.47	6.5230	2.7112	663.97	1.2809	31.46	85.85
560	0.0233495	3477.46	6.5556	2.6863	669.61	1.2802	31.87	86.85
570	0.0237489	3504.21	6.5875	2.6643	675.11	1.2794	32.28	87.89
580	0.0241437	3530.75	6.6188	2.6447	680.50	1.2787	32.69	88.94
590	0.0245342	3557.11	6.6496	2.6274	685.77	1.2779	33.10	90.03
600	0.0249207	3583.31	6.6797	2.6120	690.93	1.2771	33.50	91.13
650	0.0268030	3712.41	6.8235	2.5575	715.41	1.2730	35.49	96.91
700	0.0286193	3839.48	6.9576	2.5288	738.07	1.2689	37.45	103.0
750	0.0303871	3965.56	7.0839	2.5166	759.31	1.2649	39.37	109.4
800	0.0321182	4091.33	7.2039	2.5155	779.40	1.2609	41.26	116.0

Table 3 Single-phase region – Continued (0 °C to 800 °C)

p = 160 bar								
t	v	h	s	c_p	w	κ	η	λ
[°C]	[$m^3\ kg^{-1}$]	[$kJ\ kg^{-1}$]	[$kJ\ kg^{-1}\ K^{-1}$]	[$kJ\ kg^{-1}\ K^{-1}$]	[$m\ s^{-1}$]	[–]	[10^{-6} Pa s]	[$10^{-3}\ W\ m^{-1}\ K^{-1}$]
0	0.000992274	16.0651	0.0004606	4.1458	1427.9	128.43	1758.7	571.3
2	0.000992285	24.3545	0.030697	4.1437	1437.7	130.20	1645.9	575.4
4	0.000992354	32.6401	0.060701	4.1420	1447.2	131.90	1544.3	579.4
6	0.000992478	40.9228	0.090479	4.1408	1456.2	133.53	1452.3	583.3
8	0.000992655	49.2033	0.12004	4.1399	1464.8	135.10	1368.8	587.1
10	0.000992880	57.4824	0.14938	4.1392	1473.1	136.59	1292.7	590.8
12	0.000993152	65.7603	0.17851	4.1387	1480.9	138.01	1223.2	594.4
14	0.000993469	74.0374	0.20744	4.1385	1488.4	139.37	1159.5	597.9
16	0.000993828	82.3141	0.23616	4.1383	1495.6	140.66	1101.0	601.4
18	0.000994227	90.5906	0.26469	4.1382	1502.4	141.89	1047.1	604.7
20	0.000994665	98.8671	0.29302	4.1382	1508.8	143.05	997.3	608.0
25	0.000995923	119.559	0.36301	4.1386	1523.6	145.68	888.2	615.9
30	0.000997395	140.253	0.43184	4.1392	1536.5	147.94	797.2	623.3
35	0.000999068	160.952	0.49956	4.1401	1547.6	149.84	720.4	630.2
40	0.00100093	181.655	0.56621	4.1413	1557.2	151.41	654.9	636.8
45	0.00100297	202.365	0.63182	4.1427	1565.2	152.66	598.6	642.9
50	0.00100518	223.083	0.69643	4.1445	1571.8	153.61	549.8	648.6
55	0.00100755	243.810	0.76008	4.1465	1577.0	154.28	507.2	654.0
60	0.00101008	264.549	0.82280	4.1489	1581.1	154.68	469.9	658.9
65	0.00101276	285.300	0.88463	4.1516	1584.0	154.84	436.9	663.6
70	0.00101559	306.066	0.94559	4.1548	1585.8	154.76	407.7	667.8
75	0.00101856	326.848	1.0057	4.1583	1586.6	154.46	381.6	671.7
80	0.00102168	347.649	1.0650	4.1621	1586.4	153.95	358.3	675.3
85	0.00102494	368.470	1.1236	4.1664	1585.3	153.25	337.4	678.6
90	0.00102835	389.314	1.1814	4.1711	1583.4	152.37	318.5	681.5
95	0.00103189	410.182	1.2384	4.1762	1580.6	151.32	301.4	684.1
100	0.00103558	431.076	1.2948	4.1817	1577.1	150.11	285.8	686.5
110	0.00104337	472.953	1.4056	4.1939	1567.9	147.26	258.8	690.2
120	0.00105173	514.961	1.5138	4.2080	1556.1	143.89	236.2	692.8
130	0.00106067	557.120	1.6197	4.2241	1541.8	140.07	217.0	694.3
140	0.00107023	599.450	1.7234	4.2423	1525.2	135.85	200.6	694.7
150	0.00108042	641.975	1.8251	4.2630	1506.5	131.29	186.5	694.0
160	0.00109129	684.720	1.9250	4.2865	1485.7	126.42	174.3	692.3
170	0.00110288	727.715	2.0231	4.3131	1463.0	121.29	163.5	689.6
180	0.00111524	770.994	2.1197	4.3434	1438.2	115.92	154.1	686.0
190	0.00112845	814.596	2.2148	4.3778	1411.6	110.36	145.7	681.3
200	0.00114258	858.566	2.3088	4.4171	1382.9	104.62	138.2	675.7
210	0.00115774	902.956	2.4016	4.4620	1352.3	98.728	131.4	669.1
220	0.00117404	947.828	2.4935	4.5136	1319.8	92.722	125.3	661.5
230	0.00119163	993.254	2.5847	4.5730	1285.1	86.622	119.6	652.9
240	0.00121069	1039.32	2.6754	4.6418	1248.4	80.456	114.4	643.3

Table 3 Single-phase region – Continued (0 °C to 800 °C)

p = 160 bar

t [°C]	v [$m^3\,kg^{-1}$]	h [$kJ\,kg^{-1}$]	s [$kJ\,kg^{-1}\,K^{-1}$]	c_p [$kJ\,kg^{-1}\,K^{-1}$]	w [$m\,s^{-1}$]	κ [–]	η [10^{-6} Pa s]	λ [$10^{-3}\,W\,m^{-1}\,K^{-1}$]
250	0.00123144	1086.13	2.7657	4.7220	1209.5	74.248	109.6	632.6
260	0.00125418	1133.81	2.8560	4.8163	1168.3	68.020	105.1	620.9
270	0.00127926	1182.51	2.9465	4.9284	1124.6	61.787	100.8	607.9
280	0.00130720	1232.45	3.0376	5.0636	1078.0	55.561	96.65	593.6
290	0.00133866	1283.89	3.1297	5.2301	1028.0	49.344	92.65	578.0
300	0.00137464	1337.20	3.2236	5.4411	973.99	43.132	88.71	560.7
310	0.00141664	1392.93	3.3200	5.7190	914.67	36.910	84.75	541.6
320	0.00146711	1451.94	3.4203	6.1063	848.79	30.692	80.68	520.2
330	0.00153049	1515.71	3.5269	6.6932	775.52	24.560	76.35	495.9
340	0.00161627	1587.27	3.6445	7.7439	687.82	18.295	71.47	467.7
t_s = 347.357 °C				**Saturation**				
Liquid	0.00170954	1649.67	3.7457	9.4729	597.67	13.059	67.06	443.2
Vapour	0.00930813	2580.80	5.2463	15.207	429.20	1.2369	23.36	127.4
350	0.00976565	2616.99	5.3045	12.413	441.49	1.2475	23.36	120.9
360	0.0110599	2715.63	5.4616	8.1928	472.82	1.2634	23.57	106.4
370	0.0120464	2788.30	5.5755	6.5172	494.85	1.2705	23.92	96.61
380	0.0128781	2848.27	5.6680	5.5538	512.76	1.2760	24.32	89.41
390	0.0136131	2900.49	5.7474	4.9289	527.98	1.2798	24.74	85.80
400	0.0142810	2947.46	5.8177	4.4882	541.32	1.2824	25.17	83.45
410	0.0148991	2990.62	5.8814	4.1588	553.28	1.2841	25.61	81.97
420	0.0154783	3030.88	5.9399	3.9032	564.18	1.2853	26.04	81.07
430	0.0160263	3068.85	5.9943	3.6993	574.24	1.2860	26.48	80.59
440	0.0165486	3104.99	6.0453	3.5333	583.62	1.2864	26.91	80.40
450	0.0170494	3139.61	6.0935	3.3960	592.43	1.2866	27.35	80.44
460	0.0175320	3172.98	6.1393	3.2809	600.76	1.2866	27.78	80.67
470	0.0179988	3205.29	6.1831	3.1835	608.68	1.2865	28.21	81.04
480	0.0184520	3236.70	6.2251	3.1004	616.23	1.2862	28.63	81.53
490	0.0188931	3267.34	6.2655	3.0289	623.47	1.2859	29.06	82.11
500	0.0193237	3297.31	6.3045	2.9671	630.42	1.2854	29.48	82.78
510	0.0197449	3326.71	6.3423	2.9134	637.13	1.2849	29.90	83.51
520	0.0201577	3355.60	6.3790	2.8664	643.61	1.2844	30.32	84.31
530	0.0205628	3384.05	6.4146	2.8253	649.89	1.2837	30.73	85.15
540	0.0209611	3412.12	6.4494	2.7891	655.98	1.2831	31.15	86.04
550	0.0213532	3439.85	6.4832	2.7572	661.91	1.2824	31.56	86.97
560	0.0217396	3467.28	6.5164	2.7290	667.68	1.2816	31.97	87.94
570	0.0221208	3494.44	6.5488	2.7039	673.31	1.2809	32.37	88.93
580	0.0224972	3521.37	6.5805	2.6817	678.81	1.2801	32.78	89.96
590	0.0228693	3548.08	6.6117	2.6620	684.18	1.2793	33.18	91.01
600	0.0232373	3574.61	6.6422	2.6444	689.45	1.2785	33.59	92.09
650	0.0250259	3705.11	6.7876	2.5817	714.35	1.2744	35.57	97.75
700	0.0267475	3833.26	6.9228	2.5477	737.32	1.2703	37.52	103.8
750	0.0284200	3960.18	7.0499	2.5316	758.80	1.2662	39.44	110.1
800	0.0300554	4086.62	7.1706	2.5277	779.09	1.2622	41.33	116.6

Table 3 Single-phase region – Continued (0 °C to 800 °C)

p = 170 bar								
t	v	h	s	c_p	w	κ	η	λ
[°C]	[$m^3\,kg^{-1}$]	[$kJ\,kg^{-1}$]	[$kJ\,kg^{-1}\,K^{-1}$]	[$kJ\,kg^{-1}\,K^{-1}$]	[$m\,s^{-1}$]	[–]	[10^{-6} Pa s]	[$10^{-3}\,W\,m^{-1}\,K^{-1}$]
0	0.000991792	17.0594	0.0004688	4.1416	1429.6	121.21	1756.8	571.9
2	0.000991809	25.3405	0.030675	4.1396	1439.4	122.88	1644.3	576.0
4	0.000991884	33.6183	0.060651	4.1382	1448.8	124.48	1542.9	580.0
6	0.000992014	41.8936	0.090403	4.1372	1457.8	126.02	1451.2	583.8
8	0.000992196	50.1671	0.11994	4.1364	1466.4	127.49	1367.9	587.6
10	0.000992426	58.4394	0.14925	4.1359	1474.7	128.90	1292.0	591.3
12	0.000992702	66.7109	0.17836	4.1356	1482.5	130.24	1222.6	594.9
14	0.000993022	74.9819	0.20727	4.1354	1490.0	131.52	1159.0	598.5
16	0.000993384	83.2527	0.23597	4.1354	1497.2	132.74	1100.6	601.9
18	0.000993787	91.5234	0.26448	4.1354	1504.0	133.89	1046.8	605.3
20	0.000994228	99.7943	0.29279	4.1355	1510.5	134.98	997.1	608.5
25	0.000995491	120.473	0.36273	4.1360	1525.2	137.46	888.1	616.4
30	0.000996967	141.155	0.43152	4.1368	1538.1	139.59	797.2	623.8
35	0.000998643	161.841	0.49921	4.1378	1549.3	141.38	720.5	630.7
40	0.00100051	182.534	0.56582	4.1391	1558.8	142.86	655.0	637.3
45	0.00100254	203.233	0.63139	4.1406	1566.8	144.04	598.8	643.4
50	0.00100475	223.940	0.69597	4.1424	1573.4	144.94	550.0	649.1
55	0.00100712	244.657	0.75959	4.1445	1578.7	145.58	507.5	654.5
60	0.00100965	265.385	0.82228	4.1469	1582.8	145.96	470.1	659.4
65	0.00101232	286.126	0.88408	4.1496	1585.7	146.11	437.2	664.1
70	0.00101515	306.882	0.94501	4.1528	1587.6	146.04	407.9	668.3
75	0.00101812	327.654	1.0051	4.1563	1588.4	145.77	381.9	672.2
80	0.00102123	348.445	1.0644	4.1601	1588.2	145.30	358.6	675.8
85	0.00102449	369.256	1.1229	4.1644	1587.2	144.64	337.6	679.1
90	0.00102788	390.090	1.1807	4.1691	1585.3	143.82	318.7	682.0
95	0.00103142	410.948	1.2377	4.1741	1582.6	142.84	301.6	684.7
100	0.00103509	431.832	1.2941	4.1796	1579.1	141.71	286.1	687.0
110	0.00104286	473.687	1.4048	4.1918	1570.0	139.03	259.1	690.8
120	0.00105120	515.673	1.5129	4.2057	1558.2	135.87	236.4	693.4
130	0.00106012	557.808	1.6188	4.2217	1544.1	132.29	217.3	694.9
140	0.00106964	600.113	1.7224	4.2397	1527.6	128.33	200.9	695.3
150	0.00107980	642.611	1.8241	4.2602	1509.0	124.05	186.8	694.6
160	0.00109062	685.326	1.9238	4.2834	1488.4	119.48	174.5	693.0
170	0.00110216	728.289	2.0219	4.3097	1465.7	114.66	163.8	690.3
180	0.00111447	771.532	2.1184	4.3396	1441.2	109.63	154.3	686.7
190	0.00112761	815.093	2.2135	4.3735	1414.7	104.40	145.9	682.1
200	0.00114167	859.018	2.3073	4.4123	1386.3	99.017	138.4	676.5
210	0.00115674	903.357	2.4000	4.4565	1355.9	93.492	131.6	669.9
220	0.00117294	948.170	2.4918	4.5073	1323.6	87.855	125.5	662.4
230	0.00119041	993.528	2.5829	4.5657	1289.2	82.130	119.9	653.9
240	0.00120932	1039.51	2.6734	4.6332	1252.8	76.343	114.7	644.4

Table 3 Single-phase region – Continued (0 °C to 800 °C)

				p = 170 bar				
t	v	h	s	c_p	w	κ	η	λ
[ºC]	[m^3 kg^{-1}]	[kJ kg^{-1}]	[kJ kg^{-1} K^{-1}]	[kJ kg^{-1} K^{-1}]	[m s^{-1}]	[–]	[10^{-6} Pa s]	[10^{-3} W m^{-1} K^{-1}]
250	0.00122989	1086.23	2.7635	4.7118	1214.2	70.517	109.9	633.8
260	0.00125241	1133.80	2.8536	4.8040	1173.4	64.673	105.3	622.1
270	0.00127722	1182.36	2.9439	4.9132	1130.2	58.826	101.1	609.3
280	0.00130479	1232.13	3.0346	5.0445	1084.1	52.989	96.96	595.2
290	0.00133579	1283.35	3.1264	5.2054	1034.9	47.166	92.98	579.7
300	0.00137112	1336.38	3.2197	5.4078	981.82	41.356	89.07	562.7
310	0.00141219	1391.71	3.3154	5.6719	923.83	35.550	85.15	543.8
320	0.00146122	1450.14	3.4148	6.0346	859.60	29.746	81.14	522.8
330	0.00152215	1512.98	3.5198	6.5721	788.20	24.009	76.91	499.1
340	0.00160297	1582.79	3.6346	7.4849	706.04	18.293	72.21	471.8
350	0.00172701	1666.59	3.7701	9.6869	591.09	11.900	66.37	439.2
t_s = 352.293 °C				**Saturation**				
Liquid	0.00176934	1690.04	3.8077	10.818	556.15	10.283	64.65	430.6
Vapour	0.00836934	2547.41	5.1785	18.309	420.26	1.2414	24.10	141.7
360	0.00960222	2650.94	5.3431	10.547	454.04	1.2629	24.00	121.7
370	0.0107120	2739.76	5.4823	7.6571	481.09	1.2710	24.23	106.9
380	0.0115978	2808.65	5.5887	6.2541	501.74	1.2768	24.56	96.06
390	0.0123584	2866.66	5.6768	5.4104	518.80	1.2811	24.95	90.76
400	0.0130376	2917.78	5.7533	4.8463	533.46	1.2840	25.35	87.44
410	0.0136588	2964.10	5.8217	4.4391	546.41	1.2858	25.77	85.32
420	0.0142360	3006.88	5.8838	4.1301	558.09	1.2870	26.20	83.97
430	0.0147785	3046.93	5.9412	3.8874	568.78	1.2877	26.62	83.14
440	0.0152928	3084.79	5.9947	3.6923	578.69	1.2881	27.05	82.69
450	0.0157838	3120.89	6.0449	3.5325	587.95	1.2883	27.48	82.52
460	0.0162552	3155.53	6.0925	3.3996	596.66	1.2883	27.90	82.58
470	0.0167099	3188.95	6.1378	3.2878	604.92	1.2882	28.33	82.81
480	0.0171500	3221.34	6.1811	3.1928	612.77	1.2879	28.75	83.18
490	0.0175776	3252.85	6.2227	3.1115	620.27	1.2875	29.17	83.66
500	0.0179940	3283.61	6.2627	3.0414	627.47	1.2871	29.59	84.24
510	0.0184006	3313.71	6.3014	2.9806	634.39	1.2866	30.01	84.90
520	0.0187985	3343.25	6.3389	2.9276	641.06	1.2860	30.42	85.63
530	0.0191884	3372.29	6.3752	2.8812	647.52	1.2853	30.84	86.42
540	0.0195713	3400.89	6.4106	2.8405	653.77	1.2847	31.25	87.25
550	0.0199477	3429.11	6.4451	2.8046	659.85	1.2839	31.66	88.14
560	0.0203183	3457.00	6.4788	2.7728	665.76	1.2832	32.06	89.06
570	0.0206836	3484.58	6.5117	2.7446	671.51	1.2824	32.47	90.02
580	0.0210440	3511.90	6.5439	2.7196	677.13	1.2816	32.87	91.01
590	0.0213998	3538.98	6.5755	2.6974	682.61	1.2808	33.28	92.03
600	0.0217515	3565.86	6.6064	2.6776	687.98	1.2800	33.68	93.07
650	0.0234577	3697.79	6.7534	2.6063	713.30	1.2759	35.66	98.62
700	0.0250959	3827.01	6.8897	2.5667	736.58	1.2717	37.60	104.6
750	0.0266844	3954.78	7.0178	2.5467	758.31	1.2676	39.51	110.8
800	0.0282354	4081.90	7.1391	2.5401	778.80	1.2636	41.40	117.3

Table 3 Single-phase region – Continued (0 °C to 800 °C)

p = 180 bar								
t	v	h	s	c_p	w	κ	η	λ
[°C]	[$m^3\,kg^{-1}$]	[$kJ\,kg^{-1}$]	[$kJ\,kg^{-1}\,K^{-1}$]	[$kJ\,kg^{-1}\,K^{-1}$]	[$m\,s^{-1}$]	[–]	[10^{-6} Pa s]	[$10^{-3}\,W\,m^{-1}\,K^{-1}$]
0	0.000991311	18.0523	0.0004737	4.1373	1431.2	114.80	1755.0	572.5
2	0.000991335	26.3252	0.030650	4.1357	1441.0	116.37	1642.8	576.6
4	0.000991416	34.5952	0.060598	4.1344	1450.5	117.89	1541.6	580.5
6	0.000991551	42.8632	0.090323	4.1336	1459.5	119.34	1450.1	584.4
8	0.000991738	51.1298	0.11983	4.1330	1468.1	120.73	1367.0	588.2
10	0.000991972	59.3954	0.14913	4.1327	1476.3	122.06	1291.2	591.9
12	0.000992253	67.6605	0.17821	4.1325	1484.2	123.33	1222.0	595.5
14	0.000992576	75.9254	0.20710	4.1324	1491.7	124.54	1158.5	599.0
16	0.000992942	84.1903	0.23578	4.1325	1498.8	125.69	1100.2	602.4
18	0.000993347	92.4553	0.26426	4.1326	1505.6	126.78	1046.5	605.8
20	0.000993791	100.721	0.29256	4.1328	1512.1	127.81	996.8	609.1
25	0.000995060	121.386	0.36246	4.1335	1526.8	130.16	888.1	616.9
30	0.000996541	142.056	0.43121	4.1344	1539.7	132.17	797.2	624.3
35	0.000998219	162.731	0.49885	4.1355	1550.9	133.86	720.6	631.3
40	0.00100008	183.412	0.56543	4.1369	1560.4	135.26	655.2	637.8
45	0.00100212	204.100	0.63097	4.1384	1568.5	136.38	598.9	643.9
50	0.00100433	224.796	0.69552	4.1403	1575.1	137.24	550.2	649.6
55	0.00100670	245.503	0.75910	4.1424	1580.4	137.84	507.7	655.0
60	0.00100922	266.221	0.82176	4.1449	1584.5	138.21	470.4	659.9
65	0.00101189	286.952	0.88353	4.1476	1587.5	138.36	437.4	664.6
70	0.00101471	307.698	0.94443	4.1508	1589.3	138.30	408.2	668.8
75	0.00101768	328.461	1.0045	4.1543	1590.2	138.04	382.2	672.8
80	0.00102079	349.241	1.0638	4.1582	1590.1	137.60	358.8	676.3
85	0.00102404	370.043	1.1223	4.1624	1589.0	136.99	337.9	679.6
90	0.00102742	390.866	1.1800	4.1670	1587.2	136.22	319.0	682.6
95	0.00103095	411.714	1.2370	4.1721	1584.5	135.29	301.9	685.2
100	0.00103462	432.587	1.2933	4.1775	1581.1	134.23	286.4	687.5
110	0.00104236	474.421	1.4040	4.1896	1572.1	131.72	259.3	691.3
120	0.00105068	516.385	1.5121	4.2035	1560.4	128.74	236.7	693.9
130	0.00105957	558.497	1.6178	4.2192	1546.3	125.37	217.5	695.4
140	0.00106906	600.777	1.7214	4.2371	1530.0	121.64	201.1	695.9
150	0.00107918	643.247	1.8230	4.2574	1511.5	117.61	187.0	695.3
160	0.00108996	685.933	1.9227	4.2803	1491.0	113.31	174.8	693.6
170	0.00110145	728.864	2.0207	4.3063	1468.5	108.77	164.0	691.0
180	0.00111371	772.071	2.1171	4.3358	1444.1	104.03	154.6	687.4
190	0.00112679	815.593	2.2121	4.3693	1417.8	99.113	146.2	682.8
200	0.00114077	859.473	2.3058	4.4075	1389.6	94.039	138.7	677.3
210	0.00115575	903.761	2.3985	4.4511	1359.4	88.836	131.9	670.8
220	0.00117185	948.516	2.4902	4.5011	1327.3	83.527	125.7	663.3
230	0.00118920	993.807	2.5811	4.5585	1293.3	78.135	120.1	654.9
240	0.00120796	1039.72	2.6714	4.6248	1257.1	72.685	114.9	645.4

Table 3 Single-phase region – Continued (0 °C to 800 °C)

p = 180 bar								
t [°C]	v [m^3 kg^{-1}]	h [kJ kg^{-1}]	s [kJ kg^{-1} K^{-1}]	c_p [kJ kg^{-1} K^{-1}]	w [m s^{-1}]	κ [–]	η [10^{-6} Pa s]	λ [10^{-3} W m^{-1} K^{-1}]
250	0.00122836	1086.34	2.7614	4.7018	1218.9	67.198	110.1	634.9
260	0.00125066	1133.80	2.8513	4.7919	1178.5	61.694	105.6	623.4
270	0.00127520	1182.23	2.9413	4.8984	1135.7	56.191	101.3	610.7
280	0.00130243	1231.83	3.0317	5.0260	1090.2	50.698	97.26	596.7
290	0.00133297	1282.84	3.1231	5.1816	1041.7	45.223	93.30	581.4
300	0.00136769	1335.60	3.2160	5.3761	989.47	39.769	89.41	564.6
310	0.00140788	1390.56	3.3110	5.6275	932.73	34.330	85.54	546.0
320	0.00145557	1448.44	3.4095	5.9683	870.13	28.898	81.59	525.4
330	0.00151428	1510.43	3.5131	6.4631	800.55	23.512	77.44	502.2
340	0.00159084	1578.71	3.6253	7.2691	722.19	18.214	72.89	475.7
350	0.00170295	1658.65	3.7546	8.9989	619.19	12.508	67.45	444.5
t_s = 356.992 °C				**Saturation**				
Liquid	0.00183949	1732.02	3.8717	12.840	513.11	7.9515	62.12	418.9
Vapour	0.00749867	2509.53	5.1055	22.966	410.33	1.2474	24.96	160.4
360	0.00810999	2566.03	5.1950	15.820	428.85	1.2599	24.72	146.2
370	0.00945130	2683.67	5.3795	9.3270	465.42	1.2733	24.64	121.1
380	0.0104189	2764.89	5.5048	7.1712	489.69	1.2786	24.87	104.3
390	0.0112174	2830.24	5.6041	5.9991	509.01	1.2832	25.20	96.60
400	0.0119147	2886.31	5.6881	5.2645	525.21	1.2862	25.57	91.99
410	0.0125434	2936.27	5.7618	4.7572	539.29	1.2881	25.96	89.07
420	0.0131220	2981.89	5.8281	4.3826	551.82	1.2892	26.37	87.16
430	0.0136617	3024.21	5.8887	4.0939	563.20	1.2899	26.78	85.92
440	0.0141706	3063.96	5.9448	3.8649	573.67	1.2902	27.20	85.17
450	0.0146541	3101.65	5.9973	3.6792	583.40	1.2903	27.62	84.76
460	0.0151165	3137.66	6.0468	3.5262	592.52	1.2903	28.04	84.62
470	0.0155610	3172.26	6.0936	3.3983	601.13	1.2901	28.46	84.69
480	0.0159901	3205.69	6.1383	3.2902	609.29	1.2898	28.88	84.92
490	0.0164060	3238.12	6.1811	3.1981	617.07	1.2894	29.29	85.30
500	0.0168102	3269.69	6.2222	3.1190	624.51	1.2889	29.71	85.78
510	0.0172042	3300.53	6.2618	3.0506	631.65	1.2884	30.12	86.36
520	0.0175890	3330.73	6.3002	2.9911	638.52	1.2878	30.53	87.01
530	0.0179656	3360.38	6.3373	2.9391	645.16	1.2871	30.95	87.73
540	0.0183350	3389.54	6.3734	2.8935	651.58	1.2864	31.35	88.52
550	0.0186977	3418.27	6.4085	2.8533	657.80	1.2857	31.76	89.35
560	0.0190544	3446.62	6.4427	2.8179	663.85	1.2849	32.17	90.22
570	0.0194055	3474.64	6.4762	2.7864	669.73	1.2841	32.57	91.14
580	0.0197517	3502.36	6.5089	2.7585	675.47	1.2833	32.97	92.09
590	0.0200933	3529.82	6.5408	2.7336	681.06	1.2825	33.37	93.08
600	0.0204306	3557.04	6.5722	2.7114	686.53	1.2816	33.77	94.09
650	0.0220638	3690.42	6.7208	2.6313	712.27	1.2774	35.75	99.51
700	0.0236279	3820.74	6.8583	2.5859	735.86	1.2732	37.68	105.4
750	0.0251418	3949.37	6.9872	2.5620	757.84	1.2691	39.59	111.6
800	0.0266179	4077.18	7.1091	2.5525	778.51	1.2650	41.47	118.0

Table 3 Single-phase region – Continued (0 °C to 800 °C)

p = 190 bar								
t	v	h	s	c_p	w	κ	η	λ
[°C]	[$m^3\,kg^{-1}$]	[$kJ\,kg^{-1}$]	[$kJ\,kg^{-1}\,K^{-1}$]	[$kJ\,kg^{-1}\,K^{-1}$]	[$m\,s^{-1}$]	[–]	[10^{-6} Pa s]	[$10^{-3}\,W\,m^{-1}\,K^{-1}$]
0	0.000990832	19.0438	0.0004752	4.1332	1432.9	109.06	1753.1	573.1
2	0.000990862	27.3086	0.030622	4.1317	1442.7	110.55	1641.2	577.1
4	0.000990950	35.5710	0.060542	4.1307	1452.1	111.99	1540.3	581.1
6	0.000991090	43.8317	0.090241	4.1301	1461.1	113.37	1449.0	585.0
8	0.000991281	52.0913	0.11972	4.1296	1469.7	114.69	1366.1	588.7
10	0.000991520	60.3504	0.14900	4.1294	1478.0	115.95	1290.5	592.4
12	0.000991805	68.6092	0.17806	4.1294	1485.8	117.15	1221.4	596.0
14	0.000992132	76.8680	0.20692	4.1294	1493.3	118.30	1158.1	599.5
16	0.000992501	85.1270	0.23559	4.1296	1500.4	119.39	1099.8	603.0
18	0.000992910	93.3864	0.26405	4.1298	1507.2	120.42	1046.2	606.3
20	0.000993356	101.646	0.29232	4.1301	1513.7	121.40	996.6	609.6
25	0.000994630	122.299	0.36218	4.1310	1528.5	123.62	888.0	617.4
30	0.000996115	142.956	0.43089	4.1320	1541.4	125.53	797.3	624.8
35	0.000997796	163.619	0.49850	4.1333	1552.5	127.14	720.7	631.8
40	0.000999661	184.289	0.56504	4.1347	1562.1	128.47	655.3	638.3
45	0.00100170	204.967	0.63054	4.1363	1570.1	129.53	599.1	644.4
50	0.00100391	225.653	0.69506	4.1382	1576.8	130.34	550.4	650.1
55	0.00100627	246.349	0.75861	4.1404	1582.1	130.92	507.9	655.5
60	0.00100879	267.057	0.82124	4.1429	1586.2	131.27	470.6	660.5
65	0.00101146	287.778	0.88298	4.1457	1589.2	131.42	437.7	665.1
70	0.00101428	308.514	0.94385	4.1488	1591.1	131.36	408.5	669.3
75	0.00101724	329.267	1.0039	4.1523	1592.0	131.13	382.4	673.3
80	0.00102034	350.038	1.0631	4.1562	1591.9	130.72	359.1	676.9
85	0.00102358	370.829	1.1216	4.1604	1590.9	130.14	338.2	680.1
90	0.00102696	391.642	1.1793	4.1650	1589.1	129.41	319.3	683.1
95	0.00103048	412.480	1.2363	4.1700	1586.4	128.55	302.2	685.7
100	0.00103414	433.343	1.2926	4.1754	1583.1	127.54	286.6	688.1
110	0.00104187	475.156	1.4032	4.1874	1574.1	125.17	259.6	691.9
120	0.00105016	517.098	1.5112	4.2012	1562.6	122.37	236.9	694.5
130	0.00105902	559.186	1.6169	4.2168	1548.6	119.18	217.8	696.0
140	0.00106848	601.441	1.7205	4.2345	1532.3	115.66	201.4	696.5
150	0.00107856	643.885	1.8220	4.2546	1514.0	111.85	187.3	695.9
160	0.00108930	686.542	1.9216	4.2773	1493.6	107.79	175.0	694.3
170	0.00110075	729.440	2.0195	4.3029	1471.3	103.50	164.3	691.7
180	0.00111295	772.612	2.1159	4.3321	1447.1	99.025	154.8	688.1
190	0.00112596	816.095	2.2108	4.3652	1420.9	94.376	146.4	683.6
200	0.00113987	859.931	2.3044	4.4028	1392.9	89.583	138.9	678.1
210	0.00115477	904.169	2.3969	4.4458	1363.0	84.667	132.1	671.7
220	0.00117077	948.867	2.4885	4.4950	1331.1	79.652	126.0	664.2
230	0.00118800	994.092	2.5793	4.5514	1297.3	74.558	120.4	655.9
240	0.00120662	1039.92	2.6695	4.6165	1261.4	69.408	115.2	646.5

Table 3 Single-phase region – Continued (0 °C to 800 °C)

p = 190 bar

t [°C]	v [m^3 kg^{-1}]	h [kJ kg^{-1}]	s [kJ kg^{-1} K^{-1}]	c_p [kJ kg^{-1} K^{-1}]	w [m s^{-1}]	κ [–]	η [10^{-6} Pa s]	λ [10^{-3} W m^{-1} K^{-1}]
250	0.00122685	1086.46	2.7593	4.6920	1223.6	64.225	110.4	636.1
260	0.00124894	1133.81	2.8489	4.7802	1183.5	59.026	105.9	624.6
270	0.00127322	1182.11	2.9387	4.8841	1141.1	53.829	101.6	612.0
280	0.00130012	1231.55	3.0289	5.0081	1096.2	48.644	97.55	598.2
290	0.00133022	1282.36	3.1199	5.1587	1048.3	43.480	93.62	583.1
300	0.00136435	1334.85	3.2123	5.3458	996.96	38.342	89.76	566.5
310	0.00140370	1389.45	3.3067	5.5856	941.38	33.228	85.92	548.2
320	0.00145015	1446.83	3.4043	5.9066	880.37	28.130	82.02	527.9
330	0.00150684	1508.03	3.5066	6.3642	812.62	23.065	77.95	505.3
340	0.00157967	1574.97	3.6167	7.0846	737.04	18.099	73.54	479.5
350	0.00168259	1651.88	3.7410	8.4936	643.78	12.964	68.41	449.5
360	0.00187327	1755.11	3.9053	13.638	501.01	7.0523	61.04	413.9
t_s = 361.471 °C				**Saturation**				
Liquid	0.00192545	1776.89	3.9396	16.241	468.69	6.0046	59.37	408.9
Vapour	0.00667261	2465.41	5.0246	30.621	398.64	1.2535	26.02	186.4
370	0.00821777	2616.04	5.2606	12.169	446.59	1.2773	25.26	142.3
380	0.00931447	2715.73	5.4145	8.4188	476.36	1.2822	25.28	115.0
390	0.0101678	2790.66	5.5283	6.7384	498.48	1.2862	25.51	103.6
400	0.0108911	2852.77	5.6213	5.7605	516.53	1.2893	25.83	97.24
410	0.0115321	2906.98	5.7013	5.1209	531.88	1.2911	26.19	93.29
420	0.0121153	2955.79	5.7722	4.6649	545.37	1.2921	26.57	90.70
430	0.0126550	3000.65	5.8365	4.3211	557.49	1.2926	26.97	88.98
440	0.0131606	3042.47	5.8955	4.0525	568.56	1.2928	27.37	87.85
450	0.0136386	3081.88	5.9504	3.8372	578.79	1.2928	27.78	87.16
460	0.0140938	3119.34	6.0019	3.6613	588.34	1.2926	28.19	86.80
470	0.0145300	3155.20	6.0504	3.5153	597.31	1.2924	28.60	86.69
480	0.0149498	3189.72	6.0966	3.3928	605.79	1.2920	29.01	86.77
490	0.0153557	3223.12	6.1406	3.2889	613.85	1.2915	29.42	87.02
500	0.0157493	3255.55	6.1829	3.2000	621.54	1.2910	29.84	87.40
510	0.0161322	3287.16	6.2235	3.1233	628.91	1.2904	30.24	87.88
520	0.0165056	3318.05	6.2627	3.0569	635.99	1.2898	30.65	88.46
530	0.0168706	3348.32	6.3006	2.9989	642.81	1.2891	31.06	89.11
540	0.0172280	3378.06	6.3374	2.9482	649.39	1.2883	31.47	89.83
550	0.0175785	3407.31	6.3732	2.9035	655.77	1.2876	31.87	90.60
560	0.0179229	3436.14	6.4080	2.8641	661.96	1.2868	32.27	91.43
570	0.0182616	3464.61	6.4419	2.8292	667.97	1.2859	32.68	92.30
580	0.0185951	3492.74	6.4751	2.7982	673.82	1.2851	33.08	93.21
590	0.0189240	3520.58	6.5076	2.7706	679.53	1.2843	33.47	94.16
600	0.0192485	3548.16	6.5393	2.7460	685.10	1.2834	33.87	95.14
650	0.0208166	3683.03	6.6895	2.6567	711.26	1.2790	35.84	100.4
700	0.0223146	3814.46	6.8282	2.6054	735.16	1.2748	37.77	106.2
750	0.0237617	3943.95	6.9580	2.5774	757.38	1.2706	39.67	112.3
800	0.0251707	4072.46	7.0806	2.5650	778.24	1.2664	41.54	118.7

Table 3 Single-phase region – Continued (0 °C to 800 °C)

p = 200 bar								
t	v	h	s	c_p	w	κ	η	λ
[°C]	[$m^3\ kg^{-1}$]	[$kJ\ kg^{-1}$]	[$kJ\ kg^{-1}\ K^{-1}$]	[$kJ\ kg^{-1}\ K^{-1}$]	[$m\ s^{-1}$]	[–]	[10^{-6} Pa s]	[$10^{-3}\ W\ m^{-1}\ K^{-1}$]
0	0.000990355	20.0338	0.0004733	4.1290	1434.5	103.89	1751.2	573.6
2	0.000990391	28.2906	0.030591	4.1278	1444.3	105.32	1639.7	577.7
4	0.000990484	36.5454	0.060484	4.1270	1453.7	106.68	1539.0	581.6
6	0.000990630	44.7990	0.090157	4.1265	1462.8	107.99	1448.0	585.5
8	0.000990826	53.0518	0.11962	4.1263	1471.4	109.25	1365.2	589.3
10	0.000991070	61.3043	0.14886	4.1262	1479.6	110.45	1289.8	593.0
12	0.000991358	69.5568	0.17791	4.1263	1487.4	111.59	1220.8	596.6
14	0.000991689	77.8096	0.20675	4.1265	1494.9	112.68	1157.6	600.1
16	0.000992062	86.0628	0.23539	4.1267	1502.1	113.71	1099.5	603.5
18	0.000992473	94.3166	0.26384	4.1271	1508.9	114.70	1045.9	606.8
20	0.000992922	102.571	0.29209	4.1274	1515.3	115.63	996.4	610.1
25	0.000994202	123.211	0.36190	4.1285	1530.1	117.74	887.9	617.9
30	0.000995690	143.856	0.43057	4.1297	1543.0	119.55	797.3	625.3
35	0.000997374	164.508	0.49814	4.1310	1554.1	121.09	720.8	632.3
40	0.000999240	185.166	0.56464	4.1325	1563.7	122.35	655.5	638.8
45	0.00100128	205.833	0.63012	4.1342	1571.8	123.36	599.3	644.9
50	0.00100348	226.509	0.69460	4.1361	1578.4	124.14	550.6	650.6
55	0.00100585	247.195	0.75813	4.1384	1583.8	124.69	508.2	656.0
60	0.00100837	267.893	0.82072	4.1409	1587.9	125.03	470.9	661.0
65	0.00101103	288.604	0.88243	4.1437	1590.9	125.17	437.9	665.6
70	0.00101385	309.330	0.94327	4.1468	1592.9	125.13	408.7	669.8
75	0.00101680	330.073	1.0033	4.1503	1593.8	124.91	382.7	673.8
80	0.00101990	350.834	1.0625	4.1542	1593.7	124.52	359.4	677.4
85	0.00102313	371.615	1.1209	4.1584	1592.8	123.98	338.4	680.6
90	0.00102651	392.419	1.1786	4.1630	1591.0	123.29	319.5	683.6
95	0.00103002	413.246	1.2356	4.1680	1588.4	122.47	302.4	686.3
100	0.00103366	434.100	1.2918	4.1734	1585.0	121.52	286.9	688.6
110	0.00104137	475.892	1.4024	4.1853	1576.2	119.28	259.9	692.4
120	0.00104964	517.811	1.5104	4.1989	1564.7	116.63	237.2	695.1
130	0.00105847	559.877	1.6160	4.2144	1550.8	113.61	218.0	696.6
140	0.00106790	602.107	1.7195	4.2320	1534.7	110.28	201.6	697.1
150	0.00107795	644.524	1.8209	4.2518	1516.5	106.67	187.5	696.5
160	0.00108865	687.152	1.9205	4.2742	1496.2	102.82	175.2	695.0
170	0.00110005	730.018	2.0183	4.2996	1474.0	98.760	164.5	692.4
180	0.00111219	773.155	2.1146	4.3284	1450.0	94.516	155.0	688.9
190	0.00112515	816.599	2.2094	4.3610	1424.0	90.112	146.6	684.4
200	0.00113899	860.391	2.3030	4.3982	1396.2	85.571	139.1	678.9
210	0.00115380	904.580	2.3954	4.4405	1366.4	80.914	132.4	672.5
220	0.00116970	949.222	2.4868	4.4889	1334.8	76.162	126.2	665.2
230	0.00118681	994.382	2.5775	4.5444	1301.2	71.336	120.6	656.8
240	0.00120530	1040.14	2.6675	4.6084	1265.7	66.457	115.5	647.5

Table 3 Single-phase region – Continued (0 °C to 800 °C)

t [°C]	v [m^3 kg^{-1}]	h [kJ kg^{-1}]	s [kJ kg^{-1} K^{-1}]	c_p [kJ kg^{-1} K^{-1}]	w [m s^{-1}]	κ [–]	η [10^{-6} Pa s]	λ [10^{-3} W m^{-1} K^{-1}]
				p = 200 bar				
250	0.00122536	1086.58	2.7572	4.6824	1228.1	61.546	110.7	637.2
260	0.00124724	1133.83	2.8466	4.7687	1188.5	56.622	106.2	625.8
270	0.00127126	1182.01	2.9362	4.8701	1146.5	51.700	101.9	613.4
280	0.00129784	1231.29	3.0261	4.9908	1102.1	46.792	97.85	599.7
290	0.00132752	1281.91	3.1167	5.1366	1054.8	41.907	93.93	584.7
300	0.00136109	1334.14	3.2087	5.3168	1004.3	37.050	90.10	568.3
310	0.00139965	1388.40	3.3025	5.5459	949.79	32.226	86.29	550.3
320	0.00144494	1445.30	3.3993	5.8491	890.30	27.428	82.44	530.4
330	0.00149977	1505.79	3.5004	6.2740	824.41	22.659	78.45	508.2
340	0.00156931	1571.52	3.6085	6.9239	751.10	17.975	74.16	483.1
350	0.00166487	1645.95	3.7288	8.1062	664.96	13.280	69.27	454.1
360	0.00182472	1740.13	3.8787	11.460	542.74	8.0716	62.79	419.8
t_s = 365.746 °C				**Saturation**				
Liquid	0.00203865	1827.10	4.0154	23.200	422.20	4.3719	56.20	403.7
Vapour	0.00585828	2411.39	4.9299	45.677	384.50	1.2618	27.40	226.5
370	0.00692374	2526.48	5.1095	18.660	421.11	1.2806	26.29	179.3
380	0.00825779	2659.19	5.3144	10.221	461.33	1.2886	25.82	129.4
390	0.00918976	2747.17	5.4482	7.6925	487.08	1.2908	25.90	112.1
400	0.00994958	2816.84	5.5525	6.3601	507.34	1.2935	26.14	103.4
410	0.0106082	2876.05	5.6398	5.5410	524.18	1.2951	26.45	98.08
420	0.0111994	2928.51	5.7160	4.9820	538.73	1.2957	26.80	94.64
430	0.0117416	2976.18	5.7843	4.5718	551.66	1.2960	27.17	92.33
440	0.0122459	3020.26	5.8466	4.2568	563.37	1.2959	27.56	90.77
450	0.0127202	3061.53	5.9041	4.0074	574.13	1.2957	27.95	89.76
460	0.0131699	3100.57	5.9577	3.8056	584.12	1.2954	28.35	89.14
470	0.0135992	3137.77	6.0081	3.6395	593.47	1.2950	28.76	88.82
480	0.0140113	3173.45	6.0558	3.5010	602.28	1.2945	29.16	88.73
490	0.0144085	3207.86	6.1012	3.3841	610.63	1.2939	29.57	88.84
500	0.0147929	3241.19	6.1445	3.2845	618.58	1.2933	29.97	89.10
510	0.0151662	3273.59	6.1862	3.1990	626.18	1.2927	30.38	89.48
520	0.0155296	3305.21	6.2263	3.1251	633.46	1.2920	30.78	89.97
530	0.0158842	3336.13	6.2650	3.0608	640.47	1.2912	31.18	90.54
540	0.0162309	3366.45	6.3026	3.0046	647.23	1.2904	31.59	91.19
550	0.0165707	3396.24	6.3390	2.9552	653.76	1.2896	31.99	91.91
560	0.0169040	3425.57	6.3744	2.9116	660.09	1.2888	32.39	92.68
570	0.0172316	3454.49	6.4089	2.8731	666.23	1.2879	32.79	93.51
580	0.0175539	3483.05	6.4426	2.8389	672.20	1.2870	33.18	94.37
590	0.0178714	3511.28	6.4755	2.8084	678.02	1.2862	33.58	95.28
600	0.0181844	3539.23	6.5077	2.7812	683.69	1.2853	33.97	96.22
650	0.0196942	3675.59	6.6596	2.6824	710.26	1.2808	35.93	101.4
700	0.0211327	3808.15	6.7994	2.6251	734.48	1.2764	37.85	107.0
750	0.0225198	3938.52	6.9301	2.5930	756.93	1.2721	39.74	113.0
800	0.0238685	4067.73	7.0534	2.5775	777.99	1.2679	41.61	119.3

Table 3 Single-phase region – Continued (0 °C to 800 °C)

p = 210 bar

t [°C]	v [m^3 kg^{-1}]	h [kJ kg^{-1}]	s [kJ kg^{-1} K^{-1}]	c_p [kJ kg^{-1} K^{-1}]	w [m s^{-1}]	κ [–]	η [10^{-6} Pa s]	λ [10^{-3} W m^{-1} K^{-1}]
0	0.000989879	21.0225	0.0004681	4.1249	1436.2	99.223	1749.4	574.2
2	0.000989922	29.2714	0.030557	4.1240	1446.0	100.58	1638.2	578.3
4	0.000990021	37.5187	0.060422	4.1234	1455.4	101.88	1537.8	582.2
6	0.000990172	45.7651	0.090070	4.1231	1464.4	103.13	1446.9	586.1
8	0.000990373	54.0111	0.11950	4.1230	1473.0	104.33	1364.3	589.8
10	0.000990621	62.2571	0.14873	4.1231	1481.2	105.47	1289.1	593.5
12	0.000990913	70.5035	0.17775	4.1233	1489.1	106.56	1220.2	597.1
14	0.000991248	78.7503	0.20657	4.1236	1496.6	107.59	1157.1	600.6
16	0.000991623	86.9977	0.23519	4.1239	1503.7	108.58	1099.1	604.0
18	0.000992038	95.2460	0.26362	4.1243	1510.5	109.52	1045.6	607.4
20	0.000992490	103.495	0.29186	4.1248	1516.9	110.41	996.2	610.6
25	0.000993775	124.122	0.36163	4.1260	1531.7	112.42	887.8	618.5
30	0.000995267	144.755	0.43026	4.1273	1544.6	114.15	797.3	625.8
35	0.000996953	165.395	0.49779	4.1288	1555.8	115.61	720.9	632.8
40	0.000998821	186.043	0.56425	4.1303	1565.3	116.82	655.6	639.3
45	0.00100086	206.699	0.62969	4.1321	1573.4	117.79	599.5	645.4
50	0.00100306	227.364	0.69414	4.1341	1580.1	118.53	550.9	651.1
55	0.00100543	248.040	0.75764	4.1363	1585.5	119.06	508.4	656.5
60	0.00100794	268.728	0.82021	4.1389	1589.7	119.38	471.1	661.5
65	0.00101061	289.430	0.88188	4.1417	1592.7	119.52	438.2	666.1
70	0.00101341	310.146	0.94270	4.1449	1594.6	119.48	409.0	670.3
75	0.00101636	330.879	1.0027	4.1484	1595.6	119.28	383.0	674.3
80	0.00101945	351.630	1.0619	4.1522	1595.5	118.91	359.6	677.9
85	0.00102268	372.402	1.1203	4.1565	1594.6	118.40	338.7	681.2
90	0.00102605	393.196	1.1779	4.1610	1592.9	117.75	319.8	684.1
95	0.00102955	414.013	1.2349	4.1660	1590.3	116.98	302.7	686.8
100	0.00103319	434.856	1.2911	4.1713	1587.0	116.08	287.2	689.1
110	0.00104088	476.627	1.4016	4.1832	1578.2	113.95	260.1	692.9
120	0.00104912	518.525	1.5095	4.1967	1566.8	111.43	237.5	695.6
130	0.00105793	560.567	1.6151	4.2121	1553.1	108.57	218.3	697.2
140	0.00106733	602.773	1.7185	4.2294	1537.0	105.40	201.9	697.7
150	0.00107734	645.164	1.8199	4.2491	1518.9	101.98	187.8	697.1
160	0.00108800	687.763	1.9194	4.2712	1498.8	98.322	175.5	695.6
170	0.00109935	730.598	2.0172	4.2963	1476.8	94.466	164.7	693.1
180	0.00111144	773.700	2.1133	4.3247	1452.9	90.435	155.3	689.6
190	0.00112433	817.105	2.2081	4.3570	1427.1	86.253	146.9	685.1
200	0.00113810	860.854	2.3015	4.3936	1399.4	81.940	139.4	679.7
210	0.00115284	904.995	2.3939	4.4353	1369.9	77.516	132.6	673.4
220	0.00116864	949.581	2.4852	4.4830	1338.5	73.003	126.5	666.1
230	0.00118563	994.678	2.5757	4.5376	1305.2	68.419	120.9	657.8
240	0.00120399	1040.36	2.6656	4.6004	1269.9	63.785	115.7	648.6

Table 3 Single-phase region – Continued (0 °C to 800 °C)

$p = $ **210 bar**								
t	v	h	s	c_p	w	κ	η	λ
[°C]	[$m^3\ kg^{-1}$]	[$kJ\ kg^{-1}$]	[$kJ\ kg^{-1}\ K^{-1}$]	[$kJ\ kg^{-1}\ K^{-1}$]	[$m\ s^{-1}$]	[–]	[10^{-6} Pa s]	[$10^{-3}\ W\ m^{-1}\ K^{-1}$]
250	0.00122388	1086.72	2.7551	4.6730	1232.7	59.120	110.9	638.3
260	0.00124557	1133.86	2.8444	4.7574	1193.3	54.444	106.4	627.1
270	0.00126934	1181.92	2.9337	4.8565	1151.8	49.770	102.2	614.7
280	0.00129560	1231.05	3.0233	4.9739	1107.9	45.113	98.14	601.2
290	0.00132488	1281.47	3.1136	5.1153	1061.2	40.479	94.24	586.4
300	0.00135790	1333.46	3.2051	5.2890	1011.5	35.876	90.43	570.2
310	0.00139572	1387.40	3.2984	5.5082	957.98	31.311	86.66	552.4
320	0.00143992	1443.85	3.3944	5.7953	899.91	26.782	82.86	532.8
330	0.00149304	1503.67	3.4944	6.1914	835.88	22.284	78.93	511.0
340	0.00155965	1568.32	3.6007	6.7821	764.68	17.853	74.75	486.6
350	0.00164910	1640.67	3.7177	7.7974	683.51	13.490	70.06	458.5
360	0.00178888	1728.76	3.8579	10.254	575.48	8.8159	64.17	425.5
$t_s = 369.827$ °C				**Saturation**				
Liquid	0.00221186	1889.40	4.1093	45.064	372.29	2.9839	52.12	416.4
Vapour	0.00498768	2337.54	4.8062	89.516	365.77	1.2773	29.48	304.2
370	0.00509894	2351.56	4.8280	74.153	370.03	1.2787	29.21	293.7
380	0.00721582	2591.72	5.1993	13.178	443.49	1.2980	26.61	150.1
390	0.00826552	2698.69	5.3619	8.9597	474.64	1.2979	26.40	122.7
400	0.00907522	2778.04	5.4807	7.1006	497.56	1.2990	26.51	110.6
410	0.00975791	2843.27	5.5769	6.0327	516.15	1.3001	26.76	103.5
420	0.0103607	2899.92	5.6593	5.3404	531.89	1.3003	27.06	99.04
430	0.0109077	2950.74	5.7321	4.8492	545.70	1.3001	27.40	96.02
440	0.0114127	2997.30	5.7978	4.4796	558.10	1.2996	27.77	93.95
450	0.0118849	3040.60	5.8581	4.1910	569.42	1.2991	28.15	92.56
460	0.0123306	3081.31	5.9140	3.9600	579.87	1.2985	28.53	91.64
470	0.0127544	3119.94	5.9664	3.7714	589.61	1.2979	28.92	91.09
480	0.0131599	3156.85	6.0157	3.6151	598.77	1.2973	29.32	90.81
490	0.0135498	3192.33	6.0625	3.4839	607.42	1.2966	29.72	90.76
500	0.0139262	3226.59	6.1071	3.3728	615.63	1.2959	30.12	90.88
510	0.0142910	3259.83	6.1498	3.2777	623.46	1.2952	30.51	91.15
520	0.0146455	3292.19	6.1909	3.1957	630.95	1.2944	30.91	91.54
530	0.0149909	3323.79	6.2305	3.1247	638.15	1.2936	31.31	92.04
540	0.0153282	3354.71	6.2687	3.0627	645.08	1.2927	31.71	92.61
550	0.0156583	3385.06	6.3058	3.0083	651.76	1.2919	32.11	93.26
560	0.0159818	3414.90	6.3419	2.9604	658.23	1.2910	32.51	93.98
570	0.0162994	3444.29	6.3769	2.9180	664.51	1.2901	32.90	94.75
580	0.0166115	3473.28	6.4111	2.8805	670.60	1.2891	33.30	95.57
590	0.0169188	3501.91	6.4445	2.8470	676.53	1.2882	33.69	96.43
600	0.0172215	3530.23	6.4771	2.8172	682.30	1.2873	34.08	97.34
650	0.0186787	3668.13	6.6307	2.7086	709.29	1.2826	36.02	102.3
700	0.0200635	3801.83	6.7718	2.6450	733.82	1.2781	37.94	107.9
750	0.0213964	3933.08	6.9033	2.6086	756.50	1.2737	39.82	113.8
800	0.0226905	4062.99	7.0273	2.5902	777.74	1.2694	41.68	120.0

Table 3 Single-phase region – Continued (0 °C to 800 °C)

p = 220 bar								
t	v	h	s	c_p	w	κ	η	λ
[ºC]	[m^3 kg^{-1}]	[kJ kg^{-1}]	[kJ kg^{-1} K^{-1}]	[kJ kg^{-1} K^{-1}]	[m s^{-1}]	[–]	[10^{-6} Pa s]	[10^{-3} W m^{-1} K^{-1}]
0	0.000989405	22.0098	0.0004596	4.1209	1437.8	94.978	1747.6	574.8
2	0.000989454	30.2508	0.030520	4.1201	1447.7	96.275	1636.6	578.8
4	0.000989558	38.4907	0.060358	4.1198	1457.1	97.520	1536.5	582.8
6	0.000989715	46.7300	0.089980	4.1196	1466.1	98.712	1445.9	586.6
8	0.000989921	54.9693	0.11939	4.1197	1474.7	99.853	1363.5	590.4
10	0.000990173	63.2089	0.14859	4.1199	1482.9	100.94	1288.4	594.1
12	0.000990469	71.4491	0.17759	4.1203	1490.7	101.98	1219.7	597.6
14	0.000990808	79.6900	0.20639	4.1207	1498.2	102.97	1156.7	601.1
16	0.000991186	87.9318	0.23500	4.1211	1505.3	103.92	1098.7	604.6
18	0.000991604	96.1745	0.26340	4.1216	1512.1	104.81	1045.3	607.9
20	0.000992058	104.418	0.29162	4.1221	1518.6	105.66	996.0	611.2
25	0.000993349	125.032	0.36135	4.1235	1533.3	107.58	887.8	619.0
30	0.000994845	145.654	0.42994	4.1250	1546.2	109.24	797.4	626.3
35	0.000996534	166.282	0.49743	4.1265	1557.4	110.63	721.0	633.3
40	0.000998403	186.919	0.56386	4.1282	1567.0	111.79	655.8	639.8
45	0.00100044	207.564	0.62927	4.1300	1575.1	112.72	599.7	645.9
50	0.00100265	228.220	0.69369	4.1321	1581.8	113.43	551.1	651.6
55	0.00100501	248.885	0.75715	4.1343	1587.2	113.94	508.6	657.0
60	0.00100752	269.563	0.81969	4.1369	1591.4	114.25	471.4	661.9
65	0.00101018	290.255	0.88134	4.1398	1594.4	114.39	438.5	666.6
70	0.00101298	310.962	0.94212	4.1429	1596.4	114.35	409.3	670.8
75	0.00101593	331.685	1.0021	4.1464	1597.3	114.16	383.2	674.8
80	0.00101901	352.427	1.0612	4.1503	1597.4	113.82	359.9	678.4
85	0.00102223	373.188	1.1196	4.1545	1596.5	113.33	339.0	681.7
90	0.00102559	393.972	1.1772	4.1591	1594.8	112.72	320.1	684.6
95	0.00102909	414.780	1.2341	4.1640	1592.2	111.98	303.0	687.3
100	0.00103272	435.613	1.2904	4.1693	1589.0	111.13	287.4	689.7
110	0.00104038	477.363	1.4008	4.1811	1580.3	109.11	260.4	693.5
120	0.00104860	519.239	1.5087	4.1945	1569.0	106.71	237.7	696.2
130	0.00105739	561.259	1.6142	4.2097	1555.3	103.99	218.5	697.8
140	0.00106675	603.440	1.7175	4.2269	1539.4	100.97	202.1	698.3
150	0.00107673	645.804	1.8189	4.2463	1521.4	97.713	188.0	697.8
160	0.00108735	688.375	1.9183	4.2683	1501.4	94.233	175.7	696.3
170	0.00109866	731.179	2.0160	4.2931	1479.5	90.562	165.0	693.7
180	0.00111069	774.247	2.1121	4.3211	1455.7	86.725	155.5	690.3
190	0.00112353	817.614	2.2068	4.3529	1430.1	82.743	147.1	685.9
200	0.00113723	861.320	2.3001	4.3891	1402.6	78.637	139.6	680.5
210	0.00115188	905.412	2.3923	4.4302	1373.3	74.426	132.8	674.2
220	0.00116758	949.944	2.4836	4.4771	1342.2	70.129	126.7	667.0
230	0.00118447	994.978	2.5740	4.5309	1309.1	65.765	121.1	658.8
240	0.00120269	1040.59	2.6637	4.5926	1274.1	61.353	116.0	649.6

Table 3 Single-phase region – Continued
(0 °C to 800 °C)

t	v	h	s	c_p	w	κ	η	λ
				$p =$ 220 bar				
[°C]	[$m^3 kg^{-1}$]	[$kJ kg^{-1}$]	[$kJ kg^{-1} K^{-1}$]	[$kJ kg^{-1} K^{-1}$]	[$m s^{-1}$]	[–]	[10^{-6} Pa s]	[$10^{-3} W m^{-1} K^{-1}$]
250	0.00122242	1086.86	2.7530	4.6638	1237.2	56.913	111.2	639.5
260	0.00124391	1133.90	2.8421	4.7464	1198.2	52.461	106.7	628.3
270	0.00126744	1181.84	2.9312	4.8432	1157.1	48.014	102.5	616.0
280	0.00129340	1230.82	3.0205	4.9576	1113.6	43.583	98.43	602.6
290	0.00132229	1281.06	3.1105	5.0947	1067.5	39.176	94.55	588.0
300	0.00135480	1332.82	3.2016	5.2623	1018.5	34.803	90.76	572.0
310	0.00139190	1386.45	3.2944	5.4724	965.96	30.471	87.02	554.4
320	0.00143507	1442.47	3.3896	5.7448	909.21	26.184	83.26	535.2
330	0.00148663	1501.67	3.4886	6.1153	846.98	21.934	79.39	513.8
340	0.00155059	1565.33	3.5933	6.6555	777.89	17.738	75.31	489.9
350	0.00163487	1635.90	3.7074	7.5429	700.27	13.634	70.79	462.7
360	0.00176017	1719.47	3.8404	9.4598	602.89	9.3863	65.33	430.9
370	0.00202856	1842.65	4.0333	18.352	452.83	4.5948	56.68	394.8
t_s = 373.707 °C				Saturation				
Liquid	0.00275039	2021.92	4.3109	1163.9	315.24	1.6423	43.22	688.2
Vapour	0.00357662	2164.18	4.5308	1707.2	326.11	1.3516	35.62	677.4
380	0.00612498	2504.56	5.0556	19.419	420.44	1.3118	27.89	183.9
390	0.00737736	2643.66	5.2671	10.722	460.90	1.3088	27.06	136.5
400	0.00825503	2735.76	5.4050	8.0332	487.13	1.3066	26.98	119.2
410	0.00896956	2808.37	5.5121	6.6169	507.74	1.3064	27.12	109.8
420	0.00958798	2869.89	5.6015	5.7489	524.85	1.3059	27.37	104.0
430	0.0101423	2924.25	5.6794	5.1572	539.62	1.3050	27.67	100.1
440	0.0106498	2973.55	5.7491	4.7230	552.76	1.3041	28.00	97.43
450	0.0111214	3019.05	5.8124	4.3894	564.66	1.3031	28.36	95.58
460	0.0115644	3061.57	5.8708	4.1251	575.59	1.3022	28.73	94.33
470	0.0119839	3101.72	5.9252	3.9113	585.74	1.3014	29.11	93.51
480	0.0123840	3139.92	5.9763	3.7354	595.25	1.3005	29.49	93.02
490	0.0127675	3176.52	6.0246	3.5887	604.20	1.2997	29.88	92.79
500	0.0131370	3211.77	6.0704	3.4649	612.68	1.2988	30.27	92.76
510	0.0134943	3245.88	6.1143	3.3595	620.75	1.2980	30.66	92.91
520	0.0138410	3279.01	6.1563	3.2689	628.46	1.2971	31.06	93.19
530	0.0141782	3311.30	6.1968	3.1906	635.85	1.2962	31.45	93.59
540	0.0145070	3342.86	6.2358	3.1225	642.95	1.2952	31.84	94.09
550	0.0148284	3373.78	6.2736	3.0628	649.79	1.2943	32.24	94.67
560	0.0151431	3404.14	6.3103	3.0104	656.41	1.2933	32.63	95.32
570	0.0154516	3434.01	6.3459	2.9640	662.81	1.2924	33.02	96.04
580	0.0157547	3463.44	6.3806	2.9230	669.02	1.2914	33.41	96.81
590	0.0160527	3492.48	6.4145	2.8864	675.06	1.2904	33.80	97.62
600	0.0163461	3521.18	6.4475	2.8538	680.94	1.2894	34.19	98.49
650	0.0177555	3660.64	6.6029	2.7351	708.34	1.2845	36.12	103.3
700	0.0190916	3795.49	6.7451	2.6651	733.17	1.2798	38.03	108.7
750	0.0203752	3927.63	6.8776	2.6244	756.09	1.2753	39.91	114.6
800	0.0216197	4058.25	7.0022	2.6029	777.51	1.2710	41.76	120.8

Table 3 Single-phase region – Continued (0 °C to 800 °C)

p = 230 bar								
t	v	h	s	c_p	w	κ	η	λ
[°C]	[$m^3\,kg^{-1}$]	[$kJ\,kg^{-1}$]	[$kJ\,kg^{-1}\,K^{-1}$]	[$kJ\,kg^{-1}\,K^{-1}$]	[$m\,s^{-1}$]	[–]	[10^{-6} Pa s]	[$10^{-3}\,W\,m^{-1}\,K^{-1}$]
0	0.000988932	22.9958	0.0004478	4.1169	1439.5	91.103	1745.8	575.3
2	0.000988987	31.2290	0.030480	4.1164	1449.3	92.345	1635.2	579.4
4	0.000989098	39.4615	0.060291	4.1162	1458.7	93.536	1535.3	583.3
6	0.000989259	47.6938	0.089888	4.1162	1467.7	94.678	1444.8	587.2
8	0.000989470	55.9265	0.11928	4.1165	1476.3	95.770	1362.6	590.9
10	0.000989726	64.1597	0.14846	4.1168	1484.5	96.813	1287.7	594.6
12	0.000990027	72.3938	0.17743	4.1173	1492.4	97.809	1219.1	598.2
14	0.000990369	80.6288	0.20621	4.1178	1499.8	98.757	1156.2	601.7
16	0.000990751	88.8649	0.23480	4.1183	1507.0	99.659	1098.4	605.1
18	0.000991171	97.1022	0.26318	4.1189	1513.7	100.52	1045.0	608.4
20	0.000991628	105.341	0.29138	4.1195	1520.2	101.33	995.8	611.7
25	0.000992924	125.942	0.36107	4.1211	1535.0	103.17	887.7	619.5
30	0.000994424	146.551	0.42962	4.1227	1547.9	104.75	797.4	626.9
35	0.000996115	167.169	0.49707	4.1243	1559.0	106.09	721.1	633.8
40	0.000997986	187.795	0.56347	4.1261	1568.6	107.20	655.9	640.3
45	0.00100003	208.430	0.62885	4.1279	1576.7	108.09	599.9	646.4
50	0.00100223	229.074	0.69323	4.1300	1583.4	108.77	551.3	652.1
55	0.00100459	249.730	0.75666	4.1324	1588.9	109.26	508.9	657.5
60	0.00100710	270.398	0.81917	4.1349	1593.1	109.57	471.6	662.4
65	0.00100975	291.080	0.88079	4.1378	1596.1	109.70	438.7	667.1
70	0.00101255	311.777	0.94155	4.1410	1598.1	109.67	409.5	671.3
75	0.00101549	332.491	1.0015	4.1445	1599.1	109.49	383.5	675.3
80	0.00101857	353.223	1.0606	4.1484	1599.2	109.16	360.2	678.9
85	0.00102179	373.975	1.1190	4.1526	1598.3	108.71	339.2	682.2
90	0.00102514	394.749	1.1766	4.1571	1596.7	108.12	320.3	685.2
95	0.00102863	415.547	1.2334	4.1620	1594.2	107.42	303.2	687.8
100	0.00103225	436.370	1.2896	4.1673	1590.9	106.61	287.7	690.2
110	0.00103989	478.099	1.4000	4.1790	1582.3	104.68	260.7	694.0
120	0.00104809	519.954	1.5078	4.1923	1571.1	102.40	238.0	696.7
130	0.00105685	561.951	1.6133	4.2074	1557.5	99.801	218.8	698.3
140	0.00106618	604.108	1.7166	4.2244	1541.7	96.929	202.4	698.9
150	0.00107613	646.446	1.8178	4.2436	1523.8	93.818	188.2	698.4
160	0.00108671	688.988	1.9172	4.2653	1504.0	90.498	176.0	696.9
170	0.00109797	731.762	2.0148	4.2898	1482.2	86.997	165.2	694.4
180	0.00110995	774.796	2.1109	4.3175	1458.6	83.336	155.8	691.0
190	0.00112273	818.125	2.2054	4.3490	1433.1	79.537	147.4	686.6
200	0.00113636	861.789	2.2987	4.3846	1405.8	75.620	139.8	681.3
210	0.00115093	905.833	2.3908	4.4252	1376.7	71.602	133.1	675.0
220	0.00116654	950.311	2.4819	4.4714	1345.8	67.503	127.0	667.8
230	0.00118331	995.283	2.5722	4.5242	1313.0	63.340	121.4	659.7
240	0.00120140	1040.82	2.6618	4.5849	1278.2	59.131	116.2	650.6

Table 3 Single-phase region – Continued
(0 °C to 800 °C)

$p =$ 230 bar								
t	v	h	s	c_p	w	κ	η	λ
[°C]	[$m^3\ kg^{-1}$]	[$kJ\ kg^{-1}$]	[$kJ\ kg^{-1}\ K^{-1}$]	[$kJ\ kg^{-1}\ K^{-1}$]	[$m\ s^{-1}$]	[–]	[10^{-6} Pa s]	[$10^{-3}\ W\ m^{-1}\ K^{-1}$]
250	0.00122098	1087.01	2.7510	4.6547	1241.6	54.895	111.4	640.6
260	0.00124228	1133.95	2.8399	4.7357	1203.0	50.648	106.9	629.5
270	0.00126557	1181.77	2.9287	4.8302	1162.2	46.407	102.7	617.3
280	0.00129124	1230.61	3.0178	4.9417	1119.3	42.182	98.72	604.0
290	0.00131975	1280.68	3.1075	5.0748	1073.8	37.984	94.85	589.5
300	0.00135176	1332.20	3.1982	5.2367	1025.4	33.819	91.09	573.7
310	0.00138818	1385.54	3.2905	5.4382	973.75	29.698	87.37	556.4
320	0.00143039	1441.16	3.3850	5.6972	918.21	25.627	83.65	537.5
330	0.00148049	1499.78	3.4830	6.0449	857.71	21.605	79.85	516.5
340	0.00154206	1562.55	3.5862	6.5417	790.73	17.629	75.85	493.1
350	0.00162186	1631.55	3.6978	7.3278	715.91	13.740	71.48	466.7
360	0.00173609	1711.59	3.8252	8.8860	626.70	9.8359	66.34	436.0
370	0.00194534	1818.84	3.9932	13.808	501.72	5.6260	59.12	397.9
380	0.00478243	2364.90	4.8334	43.289	384.28	1.3425	30.71	258.7
390	0.00650424	2579.46	5.1599	13.418	445.15	1.3246	27.98	155.2
400	0.00747730	2689.22	5.3242	9.2285	475.96	1.3172	27.56	129.8
410	0.00823325	2771.01	5.4449	7.3217	498.93	1.3146	27.55	117.2
420	0.00887190	2838.27	5.5426	6.2188	517.58	1.3129	27.72	109.6
430	0.00943607	2896.64	5.6262	5.5007	533.42	1.3111	27.97	104.6
440	0.00994790	2948.96	5.7001	4.9894	547.34	1.3094	28.26	101.2
450	0.0104203	2996.84	5.7668	4.6037	559.86	1.3078	28.59	98.86
460	0.0108617	3041.31	5.8279	4.3020	571.30	1.3065	28.94	97.21
470	0.0112780	3083.08	5.8845	4.0600	581.87	1.3052	29.30	96.09
480	0.0116736	3122.66	5.9374	3.8624	591.73	1.3041	29.68	95.36
490	0.0120518	3160.44	5.9872	3.6985	601.00	1.3031	30.05	94.93
500	0.0124153	3196.72	6.0345	3.5610	609.75	1.3020	30.44	94.74
510	0.0127660	3231.73	6.0795	3.4445	618.07	1.3010	30.82	94.75
520	0.0131056	3265.67	6.1225	3.3447	625.99	1.3000	31.21	94.92
530	0.0134355	3298.67	6.1639	3.2587	633.57	1.2990	31.59	95.22
540	0.0137567	3330.88	6.2037	3.1841	640.85	1.2980	31.98	95.63
550	0.0140703	3362.39	6.2422	3.1189	647.85	1.2969	32.37	96.13
560	0.0143770	3393.28	6.2795	3.0616	654.60	1.2959	32.76	96.71
570	0.0146774	3423.64	6.3158	3.0111	661.14	1.2948	33.15	97.37
580	0.0149721	3453.52	6.3510	2.9664	667.47	1.2938	33.53	98.08
590	0.0152618	3482.98	6.3853	2.9266	673.62	1.2927	33.92	98.85
600	0.0155467	3512.07	6.4188	2.8912	679.60	1.2916	34.31	99.67
650	0.0169127	3653.11	6.5759	2.7619	707.42	1.2865	36.23	104.3
700	0.0182044	3789.13	6.7195	2.6854	732.54	1.2816	38.12	109.6
750	0.0194430	3922.17	6.8528	2.6403	755.69	1.2770	39.99	115.4
800	0.0206422	4053.50	6.9781	2.6157	777.29	1.2726	41.84	121.5

Table 3 Single-phase region – Continued (0 °C to 800 °C)

p = 240 bar

t	v	h	s	c_p	w	κ	η	λ
[ºC]	[$m^3\ kg^{-1}$]	[$kJ\ kg^{-1}$]	[$kJ\ kg^{-1}\ K^{-1}$]	[$kJ\ kg^{-1}\ K^{-1}$]	[$m\ s^{-1}$]	[–]	[10^{-6} Pa s]	[$10^{-3}\ W\ m^{-1}\ K^{-1}$]
0	0.000988461	23.9804	0.0004328	4.1129	1441.2	87.552	1744.1	575.9
2	0.000988522	32.2058	0.030436	4.1126	1451.0	88.743	1633.7	579.9
4	0.000988638	40.4310	0.060222	4.1126	1460.4	89.885	1534.1	583.9
6	0.000988805	48.6565	0.089794	4.1128	1469.4	90.980	1443.8	587.7
8	0.000989020	56.8825	0.11916	4.1132	1478.0	92.027	1361.8	591.5
10	0.000989281	65.1095	0.14832	4.1137	1486.2	93.028	1287.0	595.1
12	0.000989585	73.3375	0.17727	4.1143	1494.0	93.982	1218.5	598.7
14	0.000989931	81.5667	0.20603	4.1149	1501.5	94.891	1155.8	602.2
16	0.000990316	89.7972	0.23459	4.1156	1508.6	95.756	1098.0	605.6
18	0.000990739	98.0290	0.26296	4.1162	1515.4	96.577	1044.8	608.9
20	0.000991199	106.262	0.29115	4.1169	1521.8	97.356	995.6	612.2
25	0.000992500	126.851	0.36079	4.1186	1536.6	99.122	887.7	620.0
30	0.000994005	147.449	0.42930	4.1204	1549.5	100.64	797.4	627.4
35	0.000995698	168.055	0.49672	4.1221	1560.7	101.93	721.2	634.3
40	0.000997570	188.670	0.56308	4.1239	1570.3	102.99	656.1	640.8
45	0.000999610	209.294	0.62842	4.1259	1578.4	103.84	600.1	646.9
50	0.00100181	229.929	0.69278	4.1280	1585.1	104.50	551.5	652.6
55	0.00100417	250.575	0.75618	4.1304	1590.6	104.97	509.1	658.0
60	0.00100668	271.233	0.81865	4.1330	1594.8	105.27	471.9	662.9
65	0.00100933	291.905	0.88024	4.1359	1597.9	105.40	439.0	667.6
70	0.00101213	312.593	0.94097	4.1391	1599.9	105.38	409.8	671.8
75	0.00101506	333.297	1.0009	4.1426	1600.9	105.21	383.7	675.8
80	0.00101813	354.019	1.0600	4.1464	1601.0	104.90	360.4	679.4
85	0.00102134	374.762	1.1183	4.1506	1600.2	104.46	339.5	682.7
90	0.00102469	395.526	1.1759	4.1551	1598.5	103.91	320.6	685.7
95	0.00102817	416.314	1.2327	4.1600	1596.1	103.24	303.5	688.3
100	0.00103178	437.127	1.2889	4.1653	1592.9	102.47	288.0	690.7
110	0.00103941	478.836	1.3992	4.1769	1584.4	100.63	260.9	694.6
120	0.00104758	520.669	1.5070	4.1901	1573.3	98.447	238.2	697.3
130	0.00105631	562.643	1.6124	4.2050	1559.8	95.965	219.0	698.9
140	0.00106562	604.776	1.7156	4.2219	1544.0	93.220	202.6	699.5
150	0.00107552	647.089	1.8168	4.2409	1526.3	90.247	188.5	699.0
160	0.00108606	689.603	1.9161	4.2624	1506.5	87.075	176.2	697.5
170	0.00109728	732.346	2.0137	4.2866	1484.9	83.728	165.5	695.1
180	0.00110922	775.346	2.1096	4.3140	1461.4	80.228	156.0	691.7
190	0.00112193	818.638	2.2041	4.3450	1436.1	76.597	147.6	687.4
200	0.00113549	862.260	2.2973	4.3802	1409.0	72.853	140.1	682.1
210	0.00114998	906.258	2.3893	4.4202	1380.1	69.013	133.3	675.9
220	0.00116550	950.682	2.4803	4.4657	1349.4	65.094	127.2	668.7
230	0.00118217	995.593	2.5705	4.5177	1316.8	61.115	121.6	660.7
240	0.00120013	1041.06	2.6600	4.5773	1282.4	57.092	116.4	651.6

Table 3 Single-phase region – Continued
(0 °C to 800 °C)

p = 240 bar								
t [°C]	v [m^3 kg^{-1}]	h [kJ kg^{-1}]	s [kJ kg^{-1} K^{-1}]	c_p [kJ kg^{-1} K^{-1}]	w [m s^{-1}]	κ [–]	η [10^{-6} Pa s]	λ [10^{-3} W m^{-1} K^{-1}]
250	0.00121955	1087.17	2.7490	4.6458	1246.0	53.043	111.7	641.6
260	0.00124066	1134.01	2.8376	4.7252	1207.7	48.984	107.2	630.7
270	0.00126373	1181.72	2.9263	4.8176	1167.4	44.931	103.0	618.6
280	0.00128911	1230.42	3.0151	4.9262	1124.8	40.896	99.00	605.5
290	0.00131725	1280.31	3.1045	5.0555	1079.9	36.887	95.15	591.1
300	0.00134878	1331.62	3.1948	5.2120	1032.2	32.913	91.41	575.5
310	0.00138457	1384.67	3.2866	5.4056	981.37	28.983	87.72	558.4
320	0.00142586	1439.91	3.3805	5.6524	926.94	25.108	84.04	539.7
330	0.00147461	1497.99	3.4776	5.9796	868.05	21.291	80.28	519.1
340	0.00153400	1559.93	3.5794	6.4387	803.19	17.523	76.36	496.2
350	0.00160989	1627.56	3.6888	7.1423	730.87	13.825	72.12	470.5
360	0.00171529	1704.72	3.8116	8.4459	647.89	10.197	67.25	440.8
370	0.00189103	1802.54	3.9649	11.773	538.24	6.3833	60.87	403.9
380	0.00261206	2025.16	4.3076	67.846	355.44	2.0153	45.49	422.8
390	0.00561344	2500.75	5.0320	18.200	426.49	1.3501	29.36	182.3
400	0.00673124	2637.37	5.2366	10.804	463.97	1.3325	28.30	143.0
410	0.00754038	2730.75	5.3744	8.1820	489.68	1.3250	28.07	125.8
420	0.00820459	2804.86	5.4821	6.7651	510.09	1.3214	28.12	116.0
430	0.00878146	2867.81	5.5723	5.8859	527.11	1.3183	28.30	109.7
440	0.00929927	2923.48	5.6509	5.2815	541.87	1.3156	28.56	105.4
450	0.00977372	2973.96	5.7212	4.8354	555.03	1.3133	28.85	102.4
460	0.0102146	3020.53	5.7852	4.4912	566.99	1.3113	29.18	100.3
470	0.0106287	3064.02	5.8441	4.2179	577.99	1.3097	29.52	98.84
480	0.0110207	3105.06	5.8990	3.9963	588.23	1.3082	29.88	97.84
490	0.0113944	3144.08	5.9504	3.8138	597.81	1.3068	30.24	97.19
500	0.0117526	3181.43	5.9991	3.6614	606.84	1.3056	30.61	96.83
510	0.0120975	3217.39	6.0453	3.5328	615.40	1.3044	30.99	96.68
520	0.0124309	3252.15	6.0894	3.4232	623.54	1.3032	31.36	96.72
530	0.0127542	3285.90	6.1317	3.3290	631.32	1.3021	31.75	96.91
540	0.0130686	3318.78	6.1723	3.2474	638.77	1.3009	32.13	97.23
550	0.0133751	3350.89	6.2116	3.1764	645.93	1.2998	32.51	97.65
560	0.0136745	3382.33	6.2496	3.1141	652.83	1.2986	32.89	98.16
570	0.0139675	3413.19	6.2864	3.0593	659.50	1.2975	33.28	98.75
580	0.0142547	3443.54	6.3222	3.0107	665.95	1.2963	33.66	99.40
590	0.0145367	3473.43	6.3570	2.9676	672.21	1.2952	34.04	100.1
600	0.0148139	3502.91	6.3910	2.9292	678.29	1.2940	34.43	100.9
650	0.0161403	3645.56	6.5499	2.7892	706.51	1.2886	36.33	105.3
700	0.0173913	3782.76	6.6946	2.7060	731.93	1.2835	38.22	110.5
750	0.0185887	3916.71	6.8289	2.6564	755.31	1.2788	40.08	116.2
800	0.0197464	4048.76	6.9549	2.6286	777.08	1.2742	41.91	122.2

Table 3 Single-phase region – Continued (0 °C to 800 °C)

p = 250 bar

t [°C]	v [$m^3\,kg^{-1}$]	h [$kJ\,kg^{-1}$]	s [$kJ\,kg^{-1}\,K^{-1}$]	c_p [$kJ\,kg^{-1}\,K^{-1}$]	w [$m\,s^{-1}$]	κ [–]	η [10^{-6} Pa s]	λ [$10^{-3}\,W\,m^{-1}\,K^{-1}$]
0	0.000987991	24.9636	0.0004146	4.1090	1442.9	84.286	1742.3	576.5
2	0.000988059	33.1814	0.030390	4.1089	1452.7	85.430	1632.2	580.5
4	0.000988180	41.3994	0.060149	4.1091	1462.1	86.527	1532.9	584.4
6	0.000988352	49.6180	0.089697	4.1095	1471.0	87.579	1442.8	588.3
8	0.000988572	57.8375	0.11904	4.1100	1479.6	88.585	1361.0	592.0
10	0.000988837	66.0582	0.14817	4.1107	1487.8	89.546	1286.3	595.7
12	0.000989145	74.2802	0.17711	4.1114	1495.7	90.462	1218.0	599.2
14	0.000989495	82.5037	0.20585	4.1121	1503.1	91.336	1155.3	602.7
16	0.000989883	90.7286	0.23439	4.1128	1510.2	92.166	1097.7	606.1
18	0.000990309	98.9550	0.26274	4.1136	1517.0	92.955	1044.5	609.5
20	0.000990772	107.183	0.29091	4.1144	1523.5	93.703	995.4	612.7
25	0.000992078	127.759	0.36051	4.1162	1538.2	95.399	887.6	620.5
30	0.000993586	148.345	0.42898	4.1181	1551.1	96.859	797.5	627.9
35	0.000995282	168.940	0.49636	4.1199	1562.3	98.094	721.3	634.8
40	0.000997155	189.545	0.56269	4.1218	1571.9	99.118	656.2	641.3
45	0.000999196	210.159	0.62800	4.1238	1580.0	99.941	600.3	647.4
50	0.00100140	230.783	0.69232	4.1260	1586.8	100.57	551.7	653.1
55	0.00100375	251.419	0.75569	4.1284	1592.2	101.03	509.3	658.5
60	0.00100626	272.068	0.81814	4.1311	1596.5	101.32	472.1	663.4
65	0.00100891	292.730	0.87970	4.1340	1599.6	101.45	439.2	668.1
70	0.00101170	313.408	0.94040	4.1372	1601.7	101.43	410.0	672.3
75	0.00101463	334.103	1.0003	4.1407	1602.7	101.27	384.0	676.3
80	0.00101770	354.815	1.0593	4.1445	1602.8	100.98	360.7	679.9
85	0.00102090	375.548	1.1176	4.1487	1602.1	100.56	339.8	683.2
90	0.00102424	396.303	1.1752	4.1532	1600.4	100.03	320.9	686.2
95	0.00102771	417.081	1.2320	4.1580	1598.0	99.393	303.8	688.9
100	0.00103131	437.884	1.2881	4.1633	1594.9	98.654	288.2	691.2
110	0.00103892	479.573	1.3984	4.1748	1586.4	96.897	261.2	695.1
120	0.00104707	521.385	1.5061	4.1879	1575.4	94.811	238.5	697.8
130	0.00105577	563.337	1.6115	4.2027	1562.0	92.435	219.3	699.5
140	0.00106505	605.446	1.7147	4.2194	1546.4	89.808	202.9	700.1
150	0.00107492	647.732	1.8158	4.2383	1528.7	86.962	188.7	699.6
160	0.00108543	690.219	1.9150	4.2595	1509.1	83.924	176.5	698.2
170	0.00109660	732.931	2.0125	4.2834	1487.6	80.719	165.7	695.8
180	0.00110848	775.898	2.1084	4.3105	1464.3	77.369	156.2	692.4
190	0.00112114	819.153	2.2028	4.3411	1439.1	73.892	147.8	688.1
200	0.00113463	862.734	2.2959	4.3758	1412.2	70.306	140.3	682.9
210	0.00114905	906.685	2.3878	4.4152	1383.5	66.629	133.6	676.7
220	0.00116448	951.057	2.4787	4.4601	1352.9	62.877	127.4	669.6
230	0.00118104	995.908	2.5688	4.5113	1320.6	59.066	121.8	661.6
240	0.00119887	1041.31	2.6581	4.5698	1286.4	55.214	116.7	652.6

Table 3 Single-phase region – Continued (0 °C to 800 °C)

p = 250 bar								
t	v	h	s	c_p	w	κ	η	λ
[°C]	[m^3 kg^{-1}]	[kJ kg^{-1}]	[kJ kg^{-1} K^{-1}]	[kJ kg^{-1} K^{-1}]	[m s^{-1}]	[–]	[10^{-6} Pa s]	[10^{-3} W m^{-1} K^{-1}]
250	0.00121814	1087.33	2.7469	4.6371	1250.4	51.337	111.9	642.7
260	0.00123907	1134.08	2.8355	4.7149	1212.4	47.451	107.5	631.8
270	0.00126191	1181.67	2.9239	4.8052	1172.4	43.571	103.3	619.9
280	0.00128701	1230.24	3.0125	4.9112	1130.3	39.710	99.28	606.9
290	0.00131480	1279.96	3.1016	5.0369	1085.9	35.875	95.45	592.7
300	0.00134587	1331.06	3.1915	5.1883	1038.9	32.075	91.72	577.2
310	0.00138104	1383.84	3.2828	5.3745	988.82	28.320	88.07	560.4
320	0.00142148	1438.72	3.3761	5.6099	935.42	24.623	84.42	541.9
330	0.00146897	1496.28	3.4723	5.9188	878.00	20.991	80.71	521.7
340	0.00152637	1557.48	3.5729	6.3448	815.21	17.416	76.86	499.2
350	0.00159879	1623.86	3.6803	6.9800	745.33	13.898	72.74	474.1
360	0.00169695	1698.64	3.7993	8.0944	667.09	10.490	68.09	445.4
370	0.00185029	1789.93	3.9424	10.565	568.12	6.9776	62.27	410.1
380	0.00221835	1935.67	4.1670	23.184	426.79	3.2844	52.50	389.2
390	0.00464707	2395.53	4.8656	28.461	403.34	1.4003	31.76	226.2
400	0.00600480	2578.59	5.1399	13.003	450.94	1.3546	29.29	160.0
410	0.00688351	2687.10	5.2999	9.2401	480.01	1.3389	28.71	136.1
420	0.00757934	2769.45	5.4196	7.4062	502.36	1.3319	28.60	123.3
430	0.00817194	2837.67	5.5174	6.3206	520.68	1.3270	28.69	115.3
440	0.00869748	2897.06	5.6013	5.6026	536.34	1.3230	28.88	110.0
450	0.00917520	2950.38	5.6755	5.0860	550.18	1.3196	29.14	106.3
460	0.00961657	2999.20	5.7426	4.6938	562.68	1.3169	29.43	103.7
470	0.0100292	3044.53	5.8040	4.3856	574.13	1.3147	29.75	101.8
480	0.0104184	3087.11	5.8609	4.1377	584.74	1.3127	30.09	100.5
490	0.0107884	3127.44	5.9141	3.9347	594.64	1.3110	30.44	99.59
500	0.0111420	3165.92	5.9642	3.7661	603.96	1.3095	30.80	99.02
510	0.0114818	3202.85	6.0117	3.6245	612.76	1.3081	31.16	98.71
520	0.0118096	3238.48	6.0569	3.5044	621.13	1.3067	31.53	98.61
530	0.0121270	3272.99	6.1001	3.4014	629.10	1.3054	31.90	98.68
540	0.0124352	3306.55	6.1416	3.3126	636.72	1.3041	32.28	98.89
550	0.0127352	3339.28	6.1816	3.2354	644.04	1.3028	32.66	99.22
560	0.0130280	3371.29	6.2203	3.1679	651.09	1.3015	33.03	99.65
570	0.0133143	3402.67	6.2577	3.1085	657.88	1.3003	33.41	100.2
580	0.0135946	3433.49	6.2941	3.0560	664.45	1.2990	33.79	100.8
590	0.0138696	3463.81	6.3294	3.0094	670.82	1.2978	34.17	101.4
600	0.0141397	3493.69	6.3638	2.9679	677.01	1.2966	34.55	102.1
650	0.0154297	3637.97	6.5246	2.8168	705.63	1.2908	36.44	106.4
700	0.0166433	3776.37	6.6706	2.7267	731.35	1.2855	38.31	111.5
750	0.0178029	3911.23	6.8057	2.6725	754.94	1.2806	40.16	117.0
800	0.0189224	4044.00	6.9324	2.6415	776.89	1.2759	41.99	123.0

Table 3 Single-phase region – Continued (0 °C to 800 °C)

p = 260 bar

t [°C]	v [m^3 kg^{-1}]	h [kJ kg^{-1}]	s [kJ kg^{-1} K^{-1}]	c_p [kJ kg^{-1} K^{-1}]	w [m s^{-1}]	κ [–]	η [10^{-6} Pa s]	λ [10^{-3} W m^{-1} K^{-1}]
0	0.000987523	25.9455	0.0003931	4.1051	1444.5	81.271	1740.6	577.0
2	0.000987597	34.1558	0.030341	4.1052	1454.3	82.372	1630.8	581.1
4	0.000987724	42.3666	0.060074	4.1056	1463.7	83.428	1531.7	585.0
6	0.000987901	50.5784	0.089597	4.1062	1472.7	84.440	1441.8	588.8
8	0.000988125	58.7914	0.11891	4.1069	1481.3	85.408	1360.1	592.6
10	0.000988395	67.0059	0.14803	4.1076	1489.5	86.332	1285.6	596.2
12	0.000988707	75.2220	0.17694	4.1084	1497.3	87.214	1217.4	599.8
14	0.000989059	83.4397	0.20566	4.1093	1504.8	88.054	1154.9	603.3
16	0.000989451	91.6591	0.23419	4.1101	1511.9	88.853	1097.3	606.7
18	0.000989880	99.8802	0.26252	4.1110	1518.7	89.612	1044.3	610.0
20	0.000990345	108.103	0.29067	4.1118	1525.1	90.332	995.2	613.2
25	0.000991657	128.667	0.36022	4.1138	1539.8	91.964	887.5	621.0
30	0.000993169	149.241	0.42866	4.1158	1552.7	93.369	797.5	628.4
35	0.000994867	169.825	0.49600	4.1178	1563.9	94.558	721.4	635.3
40	0.000996742	190.419	0.56230	4.1197	1573.6	95.544	656.4	641.8
45	0.000998783	211.023	0.62757	4.1218	1581.7	96.338	600.5	647.9
50	0.00100098	231.637	0.69186	4.1240	1588.5	96.950	551.9	653.6
55	0.00100334	252.263	0.75520	4.1265	1593.9	97.391	509.6	659.0
60	0.00100584	272.902	0.81762	4.1291	1598.2	97.671	472.4	663.9
65	0.00100849	293.555	0.87916	4.1321	1601.4	97.798	439.5	668.6
70	0.00101127	314.223	0.93983	4.1353	1603.4	97.782	410.3	672.8
75	0.00101420	334.908	0.99967	4.1388	1604.5	97.632	384.3	676.8
80	0.00101726	355.612	1.0587	4.1426	1604.7	97.355	361.0	680.4
85	0.00102046	376.335	1.1170	4.1468	1603.9	96.960	340.0	683.7
90	0.00102379	397.080	1.1745	4.1513	1602.3	96.453	321.1	686.7
95	0.00102725	417.848	1.2313	4.1561	1599.9	95.843	304.0	689.4
100	0.00103084	438.641	1.2874	4.1613	1596.8	95.136	288.5	691.8
110	0.00103843	480.310	1.3976	4.1727	1588.5	93.454	261.4	695.6
120	0.00104656	522.101	1.5053	4.1857	1577.5	91.454	238.7	698.4
130	0.00105524	564.030	1.6106	4.2004	1564.2	89.177	219.5	700.1
140	0.00106449	606.116	1.7137	4.2170	1548.7	86.659	203.1	700.7
150	0.00107433	648.377	1.8148	4.2356	1531.1	83.929	189.0	700.2
160	0.00108479	690.836	1.9140	4.2566	1511.6	81.016	176.7	698.8
170	0.00109592	733.518	2.0114	4.2803	1490.3	77.942	165.9	696.4
180	0.00110775	776.452	2.1072	4.3070	1467.1	74.728	156.5	693.1
190	0.00112035	819.670	2.2015	4.3373	1442.1	71.393	148.1	688.8
200	0.00113378	863.210	2.2945	4.3715	1415.3	67.954	140.6	683.6
210	0.00114812	907.116	2.3863	4.4104	1386.8	64.427	133.8	677.5
220	0.00116346	951.435	2.4771	4.4546	1356.5	60.829	127.7	670.5
230	0.00117991	996.227	2.5671	4.5049	1324.4	57.174	122.1	662.5
240	0.00119762	1041.56	2.6563	4.5625	1290.4	53.479	116.9	653.7

Table 3 Single-phase region – Continued (0 °C to 800 °C)

p = 260 bar								
t	v	h	s	c_p	w	κ	η	λ
[°C]	[$m^3\ kg^{-1}$]	[$kJ\ kg^{-1}$]	[$kJ\ kg^{-1}\ K^{-1}$]	[$kJ\ kg^{-1}\ K^{-1}$]	[$m\ s^{-1}$]	[–]	[10^{-6} Pa s]	[$10^{-3}\ W\ m^{-1}\ K^{-1}$]
250	0.00121675	1087.51	2.7449	4.6286	1254.7	49.761	112.2	643.8
260	0.00123750	1134.16	2.8333	4.7048	1217.0	46.034	107.7	633.0
270	0.00126012	1181.64	2.9215	4.7932	1177.4	42.314	103.5	621.2
280	0.00128495	1230.08	3.0099	4.8966	1135.8	38.612	99.56	608.2
290	0.00131240	1279.64	3.0987	5.0188	1091.9	34.938	95.74	594.2
300	0.00134302	1330.53	3.1882	5.1654	1045.4	31.298	92.04	578.9
310	0.00137760	1383.05	3.2791	5.3447	996.13	27.704	88.40	562.3
320	0.00141722	1437.58	3.3718	5.5697	943.68	24.168	84.79	544.1
330	0.00146353	1494.67	3.4672	5.8618	887.58	20.703	81.13	524.2
340	0.00151912	1555.16	3.5667	6.2589	826.76	17.306	77.35	502.2
350	0.00158845	1620.44	3.6723	6.8365	759.34	13.961	73.33	477.7
360	0.00168051	1693.16	3.7880	7.8050	684.72	10.730	68.85	449.8
370	0.00181755	1779.58	3.9234	9.7460	593.74	7.4598	63.46	416.1
380	0.00208694	1901.05	4.1107	16.212	474.65	4.1520	55.60	385.9
390	0.00355176	2242.70	4.6290	47.316	379.01	1.5556	36.84	301.2
400	0.00528668	2510.55	5.0304	16.237	436.89	1.3886	30.65	182.5
410	0.00625640	2639.46	5.2206	10.554	469.97	1.3578	29.50	148.5
420	0.00699044	2731.76	5.3548	8.1627	494.42	1.3450	29.16	131.7
430	0.00760205	2806.08	5.4612	6.8141	514.15	1.3374	29.13	121.6
440	0.00813711	2869.65	5.5510	5.9567	530.78	1.3316	29.25	115.0
450	0.00861924	2926.06	5.6296	5.3574	545.33	1.3270	29.45	110.5
460	0.00906196	2977.30	5.7000	4.9105	558.38	1.3233	29.71	107.3
470	0.00947390	3024.60	5.7640	4.5635	570.28	1.3203	30.00	104.9
480	0.00986106	3068.80	5.8231	4.2866	581.27	1.3178	30.32	103.3
490	0.0102278	3110.51	5.8781	4.0614	591.50	1.3157	30.65	102.1
500	0.0105776	3150.16	5.9298	3.8754	601.10	1.3138	31.00	101.3
510	0.0109128	3188.11	5.9785	3.7198	610.16	1.3121	31.35	100.8
520	0.0112356	3224.64	6.0249	3.5883	618.74	1.3105	31.71	100.6
530	0.0115477	3259.95	6.0691	3.4761	626.91	1.3090	32.07	100.5
540	0.0118502	3294.21	6.1115	3.3796	634.71	1.3075	32.44	100.6
550	0.0121444	3327.58	6.1523	3.2959	642.19	1.3061	32.81	100.9
560	0.0124312	3360.17	6.1917	3.2229	649.38	1.3047	33.18	101.2
570	0.0127112	3392.07	6.2297	3.1587	656.30	1.3033	33.56	101.6
580	0.0129853	3423.37	6.2666	3.1021	662.99	1.3019	33.93	102.2
590	0.0132538	3454.13	6.3025	3.0520	669.47	1.3006	34.30	102.8
600	0.0135174	3484.42	6.3374	3.0073	675.75	1.2993	34.68	103.4
650	0.0147740	3630.36	6.5000	2.8447	704.78	1.2931	36.55	107.5
700	0.0159531	3769.97	6.6473	2.7476	730.78	1.2875	38.41	112.4
750	0.0170777	3905.75	6.7833	2.6888	754.59	1.2824	40.25	117.9
800	0.0181620	4039.25	6.9107	2.6545	776.71	1.2776	42.08	123.7

Table 3 Single-phase region – Continued (0 °C to 800 °C)

$p = 270$ bar

t [°C]	v [$m^3\,kg^{-1}$]	h [$kJ\,kg^{-1}$]	s [$kJ\,kg^{-1}\,K^{-1}$]	c_p [$kJ\,kg^{-1}\,K^{-1}$]	w [$m\,s^{-1}$]	κ [–]	η [10^{-6} Pa s]	λ [$10^{-3}\,W\,m^{-1}\,K^{-1}$]
0	0.000987056	26.9261	0.0003685	4.1012	1446.2	78.481	1738.9	577.6
2	0.000987136	35.1288	0.030289	4.1016	1456.0	79.542	1629.4	581.6
4	0.000987269	43.3326	0.059997	4.1022	1465.4	80.560	1530.5	585.5
6	0.000987451	51.5376	0.089496	4.1029	1474.4	81.534	1440.9	589.4
8	0.000987680	59.7442	0.11879	4.1037	1483.0	82.467	1359.3	593.1
10	0.000987954	67.9526	0.14788	4.1046	1491.2	83.357	1285.0	596.7
12	0.000988270	76.1628	0.17678	4.1056	1499.0	84.207	1216.9	600.3
14	0.000988626	84.3748	0.20547	4.1065	1506.4	85.016	1154.5	603.8
16	0.000989021	92.5888	0.23398	4.1074	1513.5	85.786	1097.0	607.2
18	0.000989452	100.805	0.26230	4.1084	1520.3	86.517	1044.0	610.5
20	0.000989920	109.022	0.29042	4.1093	1526.7	87.210	995.0	613.8
25	0.000991237	129.574	0.35994	4.1115	1541.5	88.784	887.5	621.5
30	0.000992753	150.137	0.42834	4.1136	1554.4	90.138	797.5	628.9
35	0.000994454	170.710	0.49565	4.1156	1565.6	91.285	721.5	635.8
40	0.000996329	191.293	0.56191	4.1177	1575.2	92.236	656.6	642.3
45	0.000998371	211.886	0.62715	4.1198	1583.3	93.003	600.7	648.4
50	0.00100057	232.491	0.69141	4.1221	1590.1	93.595	552.2	654.1
55	0.00100292	253.107	0.75472	4.1245	1595.6	94.022	509.8	659.4
60	0.00100542	273.736	0.81711	4.1272	1599.9	94.294	472.6	664.4
65	0.00100807	294.380	0.87861	4.1302	1603.1	94.420	439.7	669.1
70	0.00101085	315.038	0.93926	4.1334	1605.2	94.407	410.6	673.3
75	0.00101377	335.714	0.99908	4.1369	1606.3	94.266	384.5	677.3
80	0.00101683	356.408	1.0581	4.1407	1606.5	94.002	361.2	680.9
85	0.00102002	377.122	1.1163	4.1449	1605.8	93.625	340.3	684.2
90	0.00102334	397.857	1.1738	4.1493	1604.2	93.140	321.4	687.2
95	0.00102679	418.616	1.2306	4.1541	1601.9	92.556	304.3	689.9
100	0.00103038	439.399	1.2867	4.1593	1598.8	91.878	288.8	692.3
110	0.00103795	481.048	1.3968	4.1707	1590.5	90.265	261.7	696.2
120	0.00104606	522.818	1.5044	4.1836	1579.6	88.346	239.0	698.9
130	0.00105471	564.725	1.6097	4.1981	1566.4	86.160	219.8	700.6
140	0.00106393	606.786	1.7128	4.2145	1551.0	83.742	203.4	701.3
150	0.00107373	649.022	1.8138	4.2330	1533.5	81.121	189.2	700.9
160	0.00108416	691.454	1.9129	4.2538	1514.2	78.322	176.9	699.5
170	0.00109524	734.106	2.0102	4.2772	1492.9	75.370	166.2	697.1
180	0.00110703	777.007	2.1060	4.3036	1469.9	72.282	156.7	693.8
190	0.00111957	820.189	2.2002	4.3334	1445.0	69.079	148.3	689.6
200	0.00113293	863.689	2.2931	4.3672	1418.5	65.775	140.8	684.4
210	0.00114719	907.549	2.3849	4.4056	1390.1	62.387	134.0	678.3
220	0.00116245	951.818	2.4756	4.4491	1360.0	58.931	127.9	671.4
230	0.00117880	996.551	2.5654	4.4987	1328.1	55.420	122.3	663.5
240	0.00119639	1041.81	2.6544	4.5553	1294.4	51.871	117.2	654.6

Table 3 Single-phase region – Continued
(0 °C to 800 °C)

$p =$ 270 bar

t [°C]	v [m^3 kg^{-1}]	h [kJ kg^{-1}]	s [kJ kg^{-1} K^{-1}]	c_p [kJ kg^{-1} K^{-1}]	w [m s^{-1}]	κ [–]	η [10^{-6} Pa s]	λ [10^{-3} W m^{-1} K^{-1}]
250	0.00121537	1087.68	2.7430	4.6202	1258.9	48.299	112.4	644.9
260	0.00123594	1134.25	2.8311	4.6949	1221.6	44.720	108.0	634.1
270	0.00125835	1181.62	2.9192	4.7814	1182.4	41.147	103.8	622.4
280	0.00128292	1229.93	3.0073	4.8823	1141.1	37.593	99.83	609.6
290	0.00131003	1279.33	3.0958	5.0012	1097.7	34.067	96.03	595.7
300	0.00134023	1330.03	3.1850	5.1433	1051.9	30.576	92.35	580.6
310	0.00137424	1382.30	3.2754	5.3161	1003.3	27.129	88.74	564.1
320	0.00141309	1436.49	3.3676	5.5315	951.73	23.740	85.15	546.2
330	0.00145829	1493.13	3.4622	5.8084	896.83	20.427	81.54	526.6
340	0.00151220	1552.97	3.5606	6.1798	837.81	17.192	77.81	505.0
350	0.00157876	1617.24	3.6646	6.7084	772.86	14.013	73.89	481.0
360	0.00166561	1688.19	3.7775	7.5614	701.06	10.929	69.57	454.0
370	0.00179010	1770.78	3.9069	9.1448	616.33	7.8594	64.51	421.7
380	0.00200824	1878.90	4.0737	13.310	511.31	4.8216	57.71	389.2
390	0.00273436	2096.01	4.4031	37.553	389.20	2.0517	44.40	357.2
400	0.00456638	2429.83	4.9032	21.142	422.18	1.4456	32.65	213.2
410	0.00565255	2586.98	5.1351	12.234	459.66	1.3844	30.49	163.7
420	0.00643319	2691.52	5.2870	9.0550	486.30	1.3615	29.83	141.5
430	0.00706716	2772.93	5.4037	7.3768	507.54	1.3500	29.63	128.8
440	0.00761356	2841.18	5.5001	6.3483	525.20	1.3418	29.66	120.6
450	0.00810120	2900.98	5.5833	5.6513	540.48	1.3355	29.80	115.1
460	0.00854606	2954.83	5.6573	5.1423	554.10	1.3306	30.02	111.1
470	0.00895799	3004.22	5.7242	4.7521	566.46	1.3267	30.28	108.3
480	0.00934365	3050.14	5.7856	4.4435	577.84	1.3235	30.57	106.3
490	0.00970785	3093.29	5.8425	4.1941	588.40	1.3209	30.88	104.8
500	0.0100542	3134.17	5.8958	3.9893	598.28	1.3186	31.21	103.8
510	0.0103854	3173.18	5.9459	3.8187	607.59	1.3165	31.55	103.1
520	0.0107038	3210.63	5.9934	3.6752	616.39	1.3147	31.90	102.6
530	0.0110110	3246.76	6.0387	3.5531	624.76	1.3129	32.25	102.4
540	0.0113084	3281.75	6.0820	3.4484	632.74	1.3112	32.61	102.4
550	0.0115973	3315.78	6.1236	3.3579	640.37	1.3096	32.97	102.6
560	0.0118785	3348.95	6.1636	3.2791	647.70	1.3081	33.34	102.8
570	0.0121529	3381.39	6.2023	3.2100	654.76	1.3065	33.70	103.2
580	0.0124211	3413.18	6.2398	3.1492	661.57	1.3050	34.07	103.6
590	0.0126838	3444.40	6.2762	3.0953	668.15	1.3036	34.44	104.2
600	0.0129413	3475.11	6.3116	3.0473	674.53	1.3021	34.81	104.8
650	0.0141670	3622.73	6.4760	2.8730	703.95	1.2955	36.67	108.6
700	0.0153142	3763.55	6.6246	2.7687	730.23	1.2896	38.51	113.4
750	0.0164064	3900.27	6.7616	2.7051	754.26	1.2843	40.34	118.7
800	0.0174580	4034.50	6.8897	2.6676	776.55	1.2793	42.16	124.5

Table 3 Single-phase region – Continued (0 °C to 800 °C)

t [°C]	v [m^3 kg^{-1}]	h [kJ kg^{-1}]	s [kJ kg^{-1} K^{-1}]	c_p [kJ kg^{-1} K^{-1}]	w [m s^{-1}]	κ [–]	η [10^{-6} Pa s]	λ [10^{-3} W m^{-1} K^{-1}]
				p = 280 bar				
0	0.000986591	27.9053	0.0003407	4.0974	1447.9	75.891	1737.2	578.2
2	0.000986677	36.1007	0.030234	4.0980	1457.7	76.915	1628.0	582.2
4	0.000986815	44.2973	0.059917	4.0987	1467.1	77.896	1529.3	586.1
6	0.000987002	52.4957	0.089391	4.0996	1476.1	78.837	1439.9	589.9
8	0.000987236	60.6960	0.11866	4.1006	1484.6	79.736	1358.5	593.6
10	0.000987514	68.8983	0.14773	4.1017	1492.8	80.595	1284.3	597.3
12	0.000987834	77.1026	0.17661	4.1027	1500.6	81.415	1216.4	600.8
14	0.000988193	85.3091	0.20529	4.1037	1508.1	82.196	1154.0	604.3
16	0.000988591	93.5176	0.23377	4.1048	1515.2	82.938	1096.7	607.7
18	0.000989026	101.728	0.26207	4.1058	1521.9	83.644	1043.8	611.0
20	0.000989496	109.941	0.29018	4.1068	1528.4	84.313	994.8	614.3
25	0.000990818	130.480	0.35966	4.1091	1543.1	85.831	887.4	622.0
30	0.000992338	151.032	0.42801	4.1113	1556.0	87.138	797.6	629.4
35	0.000994041	171.594	0.49529	4.1135	1567.2	88.246	721.6	636.3
40	0.000995918	192.166	0.56151	4.1156	1576.8	89.165	656.7	642.8
45	0.000997960	212.749	0.62672	4.1178	1585.0	89.906	600.8	648.9
50	0.00100016	233.344	0.69095	4.1201	1591.8	90.479	552.4	654.6
55	0.00100251	253.951	0.75423	4.1226	1597.3	90.894	510.0	659.9
60	0.00100501	274.570	0.81659	4.1253	1601.6	91.159	472.8	664.9
65	0.00100765	295.204	0.87807	4.1283	1604.8	91.283	440.0	669.6
70	0.00101043	315.853	0.93869	4.1315	1607.0	91.274	410.8	673.8
75	0.00101334	336.520	0.99848	4.1350	1608.1	91.140	384.8	677.8
80	0.00101639	357.204	1.0575	4.1388	1608.3	90.889	361.5	681.4
85	0.00101958	377.909	1.1157	4.1430	1607.6	90.528	340.6	684.7
90	0.00102289	398.634	1.1732	4.1474	1606.1	90.064	321.7	687.7
95	0.00102634	419.383	1.2299	4.1522	1603.8	89.504	304.6	690.4
100	0.00102992	440.157	1.2859	4.1573	1600.7	88.853	289.0	692.8
110	0.00103747	481.785	1.3960	4.1686	1592.5	87.304	262.0	696.7
120	0.00104555	523.534	1.5036	4.1814	1581.7	85.460	239.3	699.5
130	0.00105418	565.420	1.6088	4.1959	1568.6	83.359	220.0	701.2
140	0.00106337	607.458	1.7118	4.2121	1553.3	81.034	203.6	701.8
150	0.00107314	649.668	1.8128	4.2304	1536.0	78.513	189.5	701.5
160	0.00108353	692.073	1.9118	4.2509	1516.7	75.821	177.2	700.1
170	0.00109457	734.696	2.0091	4.2741	1495.6	72.981	166.4	697.8
180	0.00110631	777.564	2.1047	4.3002	1472.6	70.011	156.9	694.5
190	0.00111879	820.710	2.1989	4.3297	1448.0	66.929	148.5	690.3
200	0.00113209	864.170	2.2918	4.3630	1421.6	63.751	141.0	685.2
210	0.00114628	907.986	2.3834	4.4008	1393.4	60.492	134.3	679.2
220	0.00116144	952.204	2.4740	4.4437	1363.5	57.167	128.1	672.2
230	0.00117770	996.880	2.5637	4.4925	1331.8	53.790	122.6	664.4
240	0.00119516	1042.08	2.6526	4.5482	1298.4	50.376	117.4	655.6

Table 3 Single-phase region – Continued (0 °C to 800 °C)

p = 280 bar								
t	v	h	s	c_p	w	κ	η	λ
[°C]	[$m^3\ kg^{-1}$]	[$kJ\ kg^{-1}$]	[$kJ\ kg^{-1}\ K^{-1}$]	[$kJ\ kg^{-1}\ K^{-1}$]	[$m\ s^{-1}$]	[–]	[10^{-6} Pa s]	[$10^{-3}\ W\ m^{-1}\ K^{-1}$]
250	0.00121400	1087.87	2.7410	4.6120	1263.2	46.941	112.7	645.9
260	0.00123440	1134.35	2.8290	4.6852	1226.1	43.498	108.2	635.3
270	0.00125661	1181.61	2.9168	4.7699	1187.3	40.061	104.1	623.6
280	0.00128092	1229.79	3.0047	4.8684	1146.4	36.644	100.1	611.0
290	0.00130771	1279.04	3.0929	4.9842	1103.5	33.255	96.32	597.2
300	0.00133750	1329.55	3.1818	5.1219	1058.2	29.902	92.65	582.2
310	0.00137097	1381.57	3.2718	5.2887	1010.3	26.592	89.06	566.0
320	0.00140908	1435.45	3.3634	5.4951	959.59	23.339	85.51	548.3
330	0.00145324	1491.66	3.4574	5.7582	905.78	20.163	81.93	529.0
340	0.00150559	1550.90	3.5548	6.1067	848.38	17.073	78.27	507.8
350	0.00156965	1614.25	3.6573	6.5932	785.84	14.051	74.42	484.3
360	0.00165196	1683.64	3.7677	7.3526	716.33	11.093	70.25	458.0
370	0.00176645	1763.10	3.8922	8.6798	636.68	8.1956	65.45	427.0
380	0.00195213	1862.42	4.0454	11.672	541.56	5.3658	59.35	394.2
390	0.00239786	2022.34	4.2882	23.482	428.02	2.7287	49.49	367.9
400	0.00385452	2334.42	4.7552	27.310	409.44	1.5533	35.67	254.0
410	0.00507063	2529.06	5.0424	14.334	449.43	1.4227	31.77	182.4
420	0.00590405	2648.46	5.2160	10.103	478.15	1.3830	30.62	152.9
430	0.00656344	2738.07	5.3444	8.0188	500.89	1.3652	30.22	136.8
440	0.00712296	2811.60	5.4483	6.7824	519.63	1.3538	30.12	126.8
450	0.00761715	2875.11	5.5367	5.9700	535.67	1.3454	30.19	120.1
460	0.00806487	2931.77	5.6145	5.3900	549.86	1.3389	30.35	115.3
470	0.00847736	2983.38	5.6845	4.9518	562.68	1.3339	30.57	111.9
480	0.00886205	3031.12	5.7483	4.6086	574.44	1.3298	30.83	109.4
490	0.00922415	3075.78	5.8072	4.3330	585.34	1.3266	31.12	107.6
500	0.00956757	3117.94	5.8621	4.1079	595.51	1.3238	31.43	106.3
510	0.00989528	3158.06	5.9136	3.9213	605.06	1.3213	31.76	105.4
520	0.0102096	3196.47	5.9624	3.7649	614.09	1.3191	32.09	104.8
530	0.0105124	3233.44	6.0087	3.6324	622.65	1.3171	32.43	104.4
540	0.0108052	3269.18	6.0529	3.5191	630.80	1.3152	32.78	104.3
550	0.0110891	3303.87	6.0953	3.4214	638.60	1.3134	33.14	104.3
560	0.0113653	3337.65	6.1361	3.3366	646.07	1.3116	33.50	104.5
570	0.0116344	3370.64	6.1755	3.2624	653.25	1.3100	33.86	104.7
580	0.0118973	3402.93	6.2136	3.1971	660.17	1.3083	34.22	105.1
590	0.0121545	3434.61	6.2505	3.1393	666.86	1.3067	34.58	105.6
600	0.0124065	3465.74	6.2863	3.0880	673.34	1.3052	34.95	106.1
650	0.0136035	3615.07	6.4527	2.9016	703.15	1.2980	36.78	109.7
700	0.0147212	3757.13	6.6026	2.7900	729.71	1.2918	38.62	114.4
750	0.0157832	3894.78	6.7405	2.7216	753.95	1.2863	40.44	119.6
800	0.0168046	4029.74	6.8693	2.6808	776.40	1.2811	42.24	125.3

Table 3 Single-phase region – Continued (0 °C to 800 °C)

$p = 290$ bar								
t	v	h	s	c_p	w	κ	η	λ
[°C]	[$m^3\ kg^{-1}$]	[$kJ\ kg^{-1}$]	[$kJ\ kg^{-1}\ K^{-1}$]	[$kJ\ kg^{-1}\ K^{-1}$]	[$m\ s^{-1}$]	[–]	[10^{-6} Pa s]	[$10^{-3}\ W\ m^{-1}\ K^{-1}$]
0	0.000986128	28.8833	0.0003098	4.0936	1449.6	73.480	1735.5	578.7
2	0.000986219	37.0712	0.030177	4.0944	1459.4	74.469	1626.6	582.7
4	0.000986363	45.2610	0.059834	4.0954	1468.8	75.418	1528.2	586.6
6	0.000986555	53.4527	0.089285	4.0964	1477.7	76.326	1438.9	590.5
8	0.000986793	61.6467	0.11853	4.0975	1486.3	77.195	1357.8	594.2
10	0.000987075	69.8429	0.14758	4.0987	1494.5	78.025	1283.7	597.8
12	0.000987399	78.0415	0.17644	4.0999	1502.3	78.816	1215.9	601.4
14	0.000987762	86.2424	0.20510	4.1010	1509.7	79.570	1153.6	604.8
16	0.000988163	94.4455	0.23356	4.1021	1516.8	80.288	1096.3	608.2
18	0.000988601	102.651	0.26184	4.1032	1523.6	80.969	1043.5	611.5
20	0.000989073	110.858	0.28994	4.1043	1530.0	81.615	994.6	614.8
25	0.000990401	131.386	0.35937	4.1068	1544.7	83.082	887.4	622.6
30	0.000991924	151.926	0.42769	4.1091	1557.6	84.345	797.6	629.9
35	0.000993630	172.477	0.49493	4.1113	1568.9	85.416	721.7	636.8
40	0.000995508	193.039	0.56112	4.1135	1578.5	86.306	656.9	643.3
45	0.000997550	213.612	0.62630	4.1158	1586.7	87.023	601.0	649.4
50	0.000999748	234.197	0.69050	4.1181	1593.5	87.579	552.6	655.1
55	0.00100210	254.794	0.75375	4.1207	1599.0	87.982	510.3	660.4
60	0.00100459	275.404	0.81608	4.1234	1603.3	88.240	473.1	665.4
65	0.00100723	296.028	0.87753	4.1264	1606.6	88.362	440.2	670.0
70	0.00101000	316.668	0.93812	4.1296	1608.7	88.356	411.1	674.3
75	0.00101292	337.325	0.99788	4.1331	1609.9	88.230	385.1	678.3
80	0.00101596	358.000	1.0568	4.1370	1610.1	87.991	361.8	681.9
85	0.00101914	378.695	1.1150	4.1411	1609.5	87.645	340.8	685.2
90	0.00102245	399.412	1.1725	4.1455	1608.0	87.200	321.9	688.2
95	0.00102589	420.151	1.2292	4.1503	1605.7	86.662	304.8	690.9
100	0.00102946	440.915	1.2852	4.1554	1602.7	86.037	289.3	693.3
110	0.00103699	482.524	1.3953	4.1666	1594.5	84.548	262.2	697.2
120	0.00104505	524.252	1.5028	4.1793	1583.8	82.773	239.5	700.0
130	0.00105365	566.115	1.6079	4.1936	1570.8	80.751	220.3	701.8
140	0.00106281	608.130	1.7109	4.2097	1555.6	78.512	203.9	702.4
150	0.00107255	650.316	1.8118	4.2278	1538.3	76.084	189.7	702.1
160	0.00108291	692.693	1.9107	4.2481	1519.2	73.491	177.4	700.7
170	0.00109390	735.287	2.0079	4.2710	1498.2	70.756	166.7	698.4
180	0.00110559	778.123	2.1035	4.2968	1475.4	67.895	157.2	695.2
190	0.00111802	821.234	2.1976	4.3259	1450.9	64.927	148.8	691.0
200	0.00113126	864.654	2.2904	4.3588	1424.6	61.866	141.3	686.0
210	0.00114537	908.425	2.3819	4.3961	1396.7	58.727	134.5	680.0
220	0.00116045	952.593	2.4724	4.4384	1366.9	55.524	128.4	673.1
230	0.00117660	997.212	2.5620	4.4865	1335.5	52.271	122.8	665.3
240	0.00119395	1042.35	2.6508	4.5413	1302.3	48.983	117.7	656.6

Table 3 Single-phase region – Continued (0 °C to 800 °C)

$p =$ **290 bar**

t [°C]	v [m^3 kg^{-1}]	h [kJ kg^{-1}]	s [kJ kg^{-1} K^{-1}]	c_p [kJ kg^{-1} K^{-1}]	w [m s^{-1}]	κ [–]	η [10^{-6} Pa s]	λ [10^{-3} W m^{-1} K^{-1}]
250	0.00121265	1088.06	2.7390	4.6039	1267.4	45.674	112.9	647.0
260	0.00123289	1134.45	2.8269	4.6757	1230.6	42.358	108.5	636.4
270	0.00125489	1181.62	2.9145	4.7586	1192.1	39.049	104.3	624.9
280	0.00127895	1229.67	3.0022	4.8549	1151.6	35.759	100.4	612.3
290	0.00130543	1278.77	3.0901	4.9677	1109.2	32.497	96.60	598.7
300	0.00133482	1329.09	3.1787	5.1013	1064.5	29.272	92.95	583.9
310	0.00136777	1380.89	3.2683	5.2623	1017.3	26.089	89.39	567.8
320	0.00140518	1434.46	3.3594	5.4604	967.29	22.961	85.86	550.3
330	0.00144835	1490.27	3.4527	5.7108	914.46	19.910	82.32	531.3
340	0.00149926	1548.93	3.5491	6.0387	858.50	16.951	78.71	510.5
350	0.00156105	1611.44	3.6503	6.4887	798.21	14.074	74.94	487.5
360	0.00163937	1679.45	3.7585	7.1709	730.70	11.231	70.89	461.8
370	0.00174564	1756.30	3.8789	8.3066	655.26	8.4815	66.31	432.0
380	0.00190856	1849.25	4.0223	10.600	567.61	5.8210	60.72	399.7
390	0.00223436	1982.05	4.2239	17.412	465.23	3.3403	52.66	372.4
400	0.00323055	2234.27	4.6012	29.847	406.40	1.7630	39.84	297.7
410	0.00451117	2465.14	4.9418	16.932	439.90	1.4792	33.45	205.4
420	0.00539945	2602.20	5.1411	11.360	470.18	1.4118	31.59	166.3
430	0.00608785	2701.40	5.2833	8.7469	494.26	1.3837	30.89	146.0
440	0.00666203	2780.85	5.3955	7.2640	514.09	1.3680	30.64	133.7
450	0.00716374	2848.43	5.4896	6.3158	530.90	1.3567	30.62	125.6
460	0.00761495	2908.10	5.5716	5.6546	545.67	1.3483	30.72	119.9
470	0.00802851	2962.08	5.6447	5.1630	558.96	1.3419	30.89	115.8
480	0.00841266	3011.73	5.7111	4.7820	571.10	1.3369	31.12	112.8
490	0.00877310	3057.98	5.7721	4.4782	582.32	1.3328	31.38	110.6
500	0.00911401	3101.48	5.8287	4.2313	592.78	1.3295	31.67	109.0
510	0.00943859	3142.75	5.8817	4.0277	602.58	1.3266	31.98	107.9
520	0.00974931	3182.15	5.9317	3.8576	611.83	1.3240	32.30	107.1
530	0.0100481	3219.99	5.9791	3.7140	620.58	1.3217	32.63	106.5
540	0.0103366	3256.50	6.0243	3.5916	628.91	1.3195	32.97	106.2
550	0.0106160	3291.88	6.0676	3.4864	636.86	1.3174	33.31	106.1
560	0.0108875	3326.28	6.1091	3.3953	644.47	1.3155	33.66	106.2
570	0.0111518	3359.82	6.1491	3.3157	651.78	1.3136	34.02	106.4
580	0.0114097	3392.62	6.1878	3.2458	658.82	1.3118	34.37	106.7
590	0.0116618	3424.77	6.2253	3.1841	665.61	1.3100	34.73	107.1
600	0.0119087	3456.33	6.2616	3.1293	672.19	1.3083	35.09	107.5
650	0.0130790	3607.38	6.4299	2.9305	702.37	1.3007	36.90	110.9
700	0.0141692	3750.69	6.5811	2.8114	729.21	1.2941	38.72	115.4
750	0.0152033	3889.28	6.7200	2.7382	753.66	1.2883	40.53	120.5
800	0.0161963	4024.99	6.8495	2.6940	776.26	1.2829	42.33	126.1

Table 3 Single-phase region – Continued
(0 °C to 800 °C)

p = 300 bar								
t	v	h	s	c_p	w	κ	η	λ
[°C]	[$m^3\,kg^{-1}$]	[$kJ\,kg^{-1}$]	[$kJ\,kg^{-1}\,K^{-1}$]	[$kJ\,kg^{-1}\,K^{-1}$]	[$m\,s^{-1}$]	[–]	[10^{-6} Pa s]	[$10^{-3}\,W\,m^{-1}\,K^{-1}$]
0	0.000985665	29.8599	0.0002758	4.0899	1451.3	71.230	1733.9	579.3
2	0.000985763	38.0406	0.030116	4.0909	1461.1	72.187	1625.2	583.3
4	0.000985912	46.2234	0.059748	4.0920	1470.5	73.104	1527.0	587.2
6	0.000986109	54.4086	0.089176	4.0932	1479.4	73.983	1438.0	591.0
8	0.000986352	62.5964	0.11840	4.0945	1488.0	74.823	1357.0	594.7
10	0.000986638	70.7866	0.14743	4.0958	1496.1	75.626	1283.0	598.3
12	0.000986965	78.9794	0.17626	4.0970	1503.9	76.391	1215.4	601.9
14	0.000987332	87.1748	0.20490	4.0983	1511.4	77.120	1153.2	605.4
16	0.000987736	95.3726	0.23335	4.0995	1518.5	77.814	1096.0	608.8
18	0.000988176	103.573	0.26161	4.1007	1525.2	78.473	1043.3	612.1
20	0.000988652	111.775	0.28969	4.1018	1531.7	79.098	994.5	615.3
25	0.000989984	132.291	0.35908	4.1044	1546.4	80.517	887.4	623.1
30	0.000991511	152.819	0.42737	4.1069	1559.3	81.739	797.7	630.4
35	0.000993220	173.360	0.49457	4.1092	1570.5	82.776	721.8	637.3
40	0.000995099	193.911	0.56073	4.1115	1580.1	83.637	657.0	643.8
45	0.000997141	214.475	0.62588	4.1138	1588.3	84.333	601.2	649.9
50	0.000999339	235.050	0.69004	4.1162	1595.1	84.873	552.8	655.6
55	0.00100169	255.637	0.75326	4.1188	1600.7	85.264	510.5	660.9
60	0.00100418	276.238	0.81557	4.1215	1605.1	85.516	473.3	665.9
65	0.00100681	296.853	0.87699	4.1245	1608.3	85.637	440.5	670.5
70	0.00100958	317.483	0.93755	4.1278	1610.5	85.634	411.3	674.8
75	0.00101249	338.131	0.99729	4.1313	1611.7	85.515	385.3	678.8
80	0.00101553	358.797	1.0562	4.1351	1611.9	85.286	362.0	682.4
85	0.00101870	379.482	1.1144	4.1392	1611.3	84.955	341.1	685.7
90	0.00102200	400.189	1.1718	4.1436	1609.9	84.528	322.2	688.7
95	0.00102544	420.919	1.2285	4.1484	1607.6	84.010	305.1	691.4
100	0.00102900	441.673	1.2845	4.1534	1604.6	83.409	289.6	693.8
110	0.00103651	483.262	1.3945	4.1646	1596.6	81.975	262.5	697.8
120	0.00104455	524.970	1.5019	4.1772	1586.0	80.266	239.8	700.6
130	0.00105313	566.811	1.6070	4.1914	1573.0	78.316	220.5	702.3
140	0.00106226	608.803	1.7099	4.2073	1557.9	76.158	204.1	703.0
150	0.00107197	650.964	1.8107	4.2252	1540.7	73.817	189.9	702.7
160	0.00108228	693.315	1.9097	4.2453	1521.7	71.317	177.6	701.4
170	0.00109324	735.879	2.0068	4.2680	1500.8	68.679	166.9	699.1
180	0.00110488	778.683	2.1023	4.2935	1478.2	65.920	157.4	695.9
190	0.00111725	821.759	2.1964	4.3222	1453.8	63.057	149.0	691.8
200	0.00113043	865.140	2.2890	4.3547	1427.7	60.105	141.5	686.7
210	0.00114447	908.867	2.3805	4.3915	1399.9	57.078	134.7	680.8
220	0.00115946	952.986	2.4709	4.4332	1370.4	53.989	128.6	673.9
230	0.00117552	997.550	2.5603	4.4805	1339.2	50.852	123.0	666.2
240	0.00119275	1042.62	2.6490	4.5344	1306.2	47.682	117.9	657.6

Table 3 Single-phase region – Continued (0 °C to 800 °C)

p = 300 bar								
t [°C]	v [$m^3\,kg^{-1}$]	h [$kJ\,kg^{-1}$]	s [$kJ\,kg^{-1}\,K^{-1}$]	c_p [$kJ\,kg^{-1}\,K^{-1}$]	w [$m\,s^{-1}$]	κ [–]	η [10^{-6} Pa s]	λ [$10^{-3}\,W\,m^{-1}\,K^{-1}$]
250	0.00121131	1088.26	2.7371	4.5959	1271.5	44.490	113.2	648.0
260	0.00123138	1134.57	2.8248	4.6664	1235.1	41.293	108.7	637.6
270	0.00125319	1181.63	2.9122	4.7476	1196.9	38.102	104.6	626.1
280	0.00127700	1229.56	2.9997	4.8417	1156.8	34.930	100.6	613.6
290	0.00130318	1278.51	3.0874	4.9516	1114.8	31.788	96.88	600.1
300	0.00133219	1328.66	3.1756	5.0814	1070.6	28.681	93.25	585.5
310	0.00136464	1380.23	3.2648	5.2370	1024.1	25.616	89.71	569.6
320	0.00140138	1433.51	3.3554	5.4272	974.84	22.604	86.21	552.3
330	0.00144362	1488.93	3.4481	5.6659	922.91	19.667	82.71	533.6
340	0.00149319	1547.07	3.5437	5.9753	868.21	16.827	79.14	513.1
350	0.00155290	1608.80	3.6435	6.3935	809.96	14.082	75.44	490.6
360	0.00162769	1675.57	3.7498	7.0110	744.31	11.345	71.49	465.5
370	0.00172705	1750.19	3.8667	7.9986	672.42	8.7269	67.11	436.8
380	0.00187297	1838.26	4.0026	9.8342	590.65	6.2087	61.90	405.2
390	0.00213310	1955.23	4.1802	14.344	497.30	3.8646	54.94	377.1
400	0.00279641	2152.37	4.4750	25.797	419.63	2.0990	44.20	328.1
410	0.00398397	2395.84	4.8342	19.685	432.54	1.5654	35.62	232.8
420	0.00492092	2552.87	5.0625	12.730	462.80	1.4509	32.76	182.0
430	0.00563824	2662.82	5.2201	9.5627	487.80	1.4067	31.67	156.4
440	0.00622812	2748.86	5.3416	7.7964	508.64	1.3847	31.23	141.3
450	0.00673815	2820.91	5.4419	6.6908	526.23	1.3699	31.09	131.5
460	0.00719339	2883.84	5.5284	5.9370	541.56	1.3591	31.11	124.8
470	0.00760843	2940.32	5.6049	5.3861	555.31	1.3510	31.24	120.0
480	0.00799240	2991.99	5.6740	4.9638	567.83	1.3447	31.43	116.4
490	0.00835153	3039.89	5.7372	4.6297	579.37	1.3398	31.66	113.8
500	0.00869030	3084.79	5.7956	4.3597	590.11	1.3357	31.92	111.9
510	0.00901209	3127.24	5.8502	4.1378	600.16	1.3322	32.21	110.4
520	0.00931954	3167.67	5.9015	3.9532	609.62	1.3292	32.52	109.4
530	0.00961471	3206.41	5.9500	3.7979	618.57	1.3265	32.83	108.7
540	0.00989926	3243.71	5.9962	3.6660	627.07	1.3241	33.16	108.3
550	0.0101745	3279.79	6.0403	3.5529	635.17	1.3217	33.49	108.0
560	0.0104416	3314.82	6.0826	3.4552	642.92	1.3196	33.84	108.0
570	0.0107014	3348.94	6.1233	3.3701	650.36	1.3175	34.18	108.1
580	0.0109547	3382.25	6.1626	3.2955	657.51	1.3155	34.53	108.3
590	0.0112021	3414.87	6.2006	3.2296	664.40	1.3135	34.88	108.6
600	0.0114442	3446.87	6.2374	3.1713	671.07	1.3117	35.24	109.0
650	0.0125897	3599.68	6.4077	2.9598	701.63	1.3034	37.03	112.1
700	0.0136542	3744.24	6.5602	2.8331	728.73	1.2964	38.83	116.4
750	0.0146621	3883.78	6.7000	2.7549	753.38	1.2904	40.63	121.4
800	0.0156288	4020.23	6.8303	2.7072	776.14	1.2848	42.41	126.9

Table 3 Single-phase region – Continued (0 °C to 800 °C)

p = 350 bar								
t	v	h	s	c_p	w	κ	η	λ
[°C]	[$m^3\ kg^{-1}$]	[$kJ\ kg^{-1}$]	[$kJ\ kg^{-1}\ K^{-1}$]	[$kJ\ kg^{-1}\ K^{-1}$]	[$m\ s^{-1}$]	[–]	[10^{-6} Pa s]	[$10^{-3}\ W\ m^{-1}\ K^{-1}$]
0	0.000983377	34.7235	0.00006009	4.0717	1459.8	61.918	1725.9	582.1
2	0.000983504	42.8689	0.029772	4.0737	1469.6	62.741	1618.6	586.1
4	0.000983679	51.0183	0.059282	4.0757	1478.9	63.529	1521.5	589.9
6	0.000983901	59.1717	0.088596	4.0777	1487.9	64.284	1433.5	593.7
8	0.000984166	67.3291	0.11771	4.0796	1496.4	65.005	1353.3	597.4
10	0.000984472	75.4903	0.14664	4.0815	1504.5	65.694	1280.0	601.0
12	0.000984818	83.6551	0.17537	4.0833	1512.3	66.351	1212.9	604.5
14	0.000985201	91.8235	0.20392	4.0851	1519.7	66.977	1151.3	608.0
16	0.000985620	99.9953	0.23228	4.0867	1526.8	67.573	1094.5	611.3
18	0.000986074	108.170	0.26045	4.0882	1533.5	68.139	1042.1	614.6
20	0.000986562	116.348	0.28845	4.0897	1539.9	68.676	993.7	617.9
25	0.000987920	136.805	0.35764	4.0931	1554.6	69.896	887.2	625.6
30	0.000989465	157.279	0.42574	4.0961	1567.5	70.948	798.0	632.9
35	0.000991186	177.766	0.49277	4.0989	1578.7	71.843	722.4	639.8
40	0.000993072	198.267	0.55876	4.1015	1588.4	72.588	657.9	646.2
45	0.000995115	218.781	0.62376	4.1041	1596.6	73.192	602.2	652.3
50	0.000997310	239.307	0.68777	4.1067	1603.5	73.664	553.9	658.0
55	0.000999649	259.847	0.75085	4.1094	1609.2	74.009	511.7	663.4
60	0.00100213	280.402	0.81301	4.1123	1613.6	74.235	474.6	668.3
65	0.00100475	300.970	0.87429	4.1153	1617.0	74.349	441.8	673.0
70	0.00100750	321.555	0.93472	4.1186	1619.3	74.358	412.7	677.3
75	0.00101038	342.157	0.99433	4.1221	1620.6	74.267	386.7	681.3
80	0.00101340	362.777	1.0531	4.1259	1621.0	74.083	363.4	684.9
85	0.00101654	383.417	1.1112	4.1300	1620.5	73.811	342.4	688.2
90	0.00101981	404.077	1.1685	4.1343	1619.2	73.457	323.5	691.3
95	0.00102320	424.760	1.2250	4.1389	1617.2	73.026	306.4	694.0
100	0.00102672	445.467	1.2809	4.1439	1614.3	72.522	290.9	696.4
110	0.00103415	486.959	1.3906	4.1547	1606.7	71.317	263.8	700.4
120	0.00104208	528.565	1.4978	4.1668	1596.4	69.876	241.0	703.3
130	0.00105054	570.299	1.6026	4.1804	1583.9	68.230	221.8	705.1
140	0.00105953	612.178	1.7052	4.1956	1569.2	66.404	205.3	705.9
150	0.00106908	654.217	1.8058	4.2126	1552.6	64.422	191.1	705.7
160	0.00107921	696.437	1.9044	4.2317	1534.1	62.305	178.8	704.5
170	0.00108997	738.860	2.0012	4.2531	1513.8	60.069	168.1	702.4
180	0.00110137	781.509	2.0964	4.2772	1491.8	57.730	158.6	699.3
190	0.00111348	824.413	2.1900	4.3042	1468.1	55.304	150.2	695.3
200	0.00112635	867.605	2.2823	4.3347	1442.8	52.801	142.6	690.5
210	0.00114005	911.121	2.3733	4.3691	1415.8	50.235	135.9	684.8
220	0.00115464	955.002	2.4632	4.4080	1387.2	47.617	129.8	678.2
230	0.00117022	999.297	2.5521	4.4519	1357.0	44.959	124.2	670.7
240	0.00118691	1044.06	2.6402	4.5017	1325.2	42.272	119.1	662.4

Table 3 Single-phase region – Continued
(0 °C to 800 °C)

p = 350 bar								
t	v	h	s	c_p	w	κ	η	λ
[°C]	[$m^3\,kg^{-1}$]	[$kJ\,kg^{-1}$]	[$kJ\,kg^{-1}\,K^{-1}$]	[$kJ\,kg^{-1}\,K^{-1}$]	[$m\,s^{-1}$]	[–]	[10^{-6} Pa s]	[$10^{-3}\,W\,m^{-1}\,K^{-1}$]
250	0.00120482	1089.35	2.7276	4.5582	1291.7	39.568	114.4	653.2
260	0.00122412	1135.25	2.8145	4.6225	1256.7	36.859	110.0	643.1
270	0.00124500	1181.83	2.9011	4.6960	1220.0	34.156	105.9	632.0
280	0.00126769	1229.20	2.9875	4.7803	1181.7	31.472	102.0	620.1
290	0.00129248	1277.48	3.0740	4.8775	1141.7	28.816	98.26	607.2
300	0.00131974	1326.81	3.1608	4.9906	1100.0	26.197	94.70	593.2
310	0.00134995	1377.36	3.2483	5.1233	1056.4	23.619	91.25	578.1
320	0.00138375	1429.36	3.3367	5.2814	1010.6	21.088	87.86	561.9
330	0.00142201	1483.10	3.4265	5.4731	962.51	18.614	84.51	544.4
340	0.00146597	1538.97	3.5184	5.7111	912.29	16.221	81.15	525.4
350	0.00151746	1597.54	3.6131	6.0154	860.58	13.944	77.72	504.7
360	0.00157912	1659.61	3.7119	6.4251	803.72	11.688	74.17	482.2
370	0.00165556	1726.57	3.8169	7.0001	743.90	9.5504	70.41	457.3
380	0.00175487	1800.51	3.9309	7.8489	679.71	7.5220	66.31	430.0
390	0.00189300	1885.27	4.0597	9.2219	611.08	5.6361	61.65	402.4
400	0.00210562	1988.43	4.2140	11.651	540.68	3.9668	56.08	373.0
410	0.00247437	2123.59	4.4133	15.533	481.15	2.6732	49.24	336.7
420	0.00308182	2291.32	4.6570	17.030	458.49	1.9489	42.31	282.4
430	0.00378209	2447.74	4.8811	13.962	468.42	1.6576	37.83	228.9
440	0.00441306	2571.64	5.0561	11.005	486.97	1.5353	35.54	193.3
450	0.00495893	2670.97	5.1945	8.9762	506.01	1.4752	34.35	170.8
460	0.00543557	2753.55	5.3079	7.6253	523.37	1.4398	33.74	155.9
470	0.00586057	2824.83	5.4045	6.6833	538.90	1.4158	33.44	145.6
480	0.00624648	2888.06	5.4890	5.9984	552.99	1.3987	33.33	138.1
490	0.00660208	2945.34	5.5646	5.4791	565.94	1.3861	33.34	132.6
500	0.00693344	2998.02	5.6331	5.0715	577.93	1.3764	33.43	128.5
510	0.00724490	3047.03	5.6961	4.7434	589.10	1.3686	33.58	125.3
520	0.00753975	3093.08	5.7546	4.4747	599.56	1.3622	33.78	122.9
530	0.00782054	3136.68	5.8092	4.2519	609.41	1.3568	34.00	121.0
540	0.00808932	3178.24	5.8606	4.0652	618.71	1.3521	34.25	119.6
550	0.00834772	3218.08	5.9093	3.9073	627.54	1.3478	34.52	118.6
560	0.00859707	3256.46	5.9557	3.7724	635.93	1.3440	34.81	117.9
570	0.00883845	3293.59	6.0000	3.6563	643.95	1.3405	35.10	117.3
580	0.00907277	3329.64	6.0425	3.5554	651.62	1.3372	35.41	117.0
590	0.00930076	3364.74	6.0834	3.4671	659.00	1.3341	35.72	116.9
600	0.00952307	3399.02	6.1229	3.3894	666.10	1.3312	36.04	116.9
650	0.0105658	3560.87	6.3032	3.1103	698.37	1.3189	37.69	118.5
700	0.0115237	3711.88	6.4625	2.9435	726.71	1.3094	39.40	121.8
750	0.0124231	3856.26	6.6072	2.8396	752.31	1.3016	41.13	126.2
800	0.0132803	3996.48	6.7411	2.7744	775.78	1.2948	42.86	131.2

Table 3 Single-phase region – Continued (0 °C to 800 °C)

$p =$ 400 bar								
t [°C]	v [$m^3\,kg^{-1}$]	h [$kJ\,kg^{-1}$]	s [$kJ\,kg^{-1}\,K^{-1}$]	c_p [$kJ\,kg^{-1}\,K^{-1}$]	w [$m\,s^{-1}$]	κ [–]	η [10^{-6} Pa s]	λ [$10^{-3}\,W\,m^{-1}\,K^{-1}$]
0	0.000981126	39.5556	−0.0002298	4.0544	1468.5	54.946	1718.4	584.9
2	0.000981280	47.6674	0.029359	4.0573	1478.2	55.668	1612.3	588.8
4	0.000981481	55.7849	0.058755	4.0602	1487.5	56.359	1516.4	592.6
6	0.000981726	63.9080	0.087959	4.0629	1496.4	57.020	1429.2	596.4
8	0.000982012	72.0363	0.11697	4.0655	1504.9	57.652	1349.8	600.1
10	0.000982338	80.1697	0.14580	4.0679	1513.0	58.256	1277.2	603.6
12	0.000982701	88.3079	0.17444	4.0702	1520.7	58.831	1210.7	607.1
14	0.000983101	96.4505	0.20290	4.0724	1528.1	59.379	1149.5	610.6
16	0.000983535	104.597	0.23117	4.0744	1535.1	59.901	1093.2	613.9
18	0.000984002	112.748	0.25926	4.0763	1541.8	60.397	1041.2	617.2
20	0.000984502	120.902	0.28717	4.0781	1548.2	60.868	993.0	620.4
25	0.000985884	141.303	0.35618	4.0821	1562.9	61.938	887.1	628.1
30	0.000987447	161.723	0.42410	4.0857	1575.7	62.862	798.3	635.4
35	0.000989180	182.159	0.49096	4.0888	1587.0	63.650	723.1	642.2
40	0.000991072	202.611	0.55680	4.0918	1596.7	64.308	658.7	648.7
45	0.000993117	223.077	0.62164	4.0946	1605.0	64.843	603.3	654.7
50	0.000995309	243.557	0.68551	4.0974	1611.9	65.263	555.1	660.4
55	0.000997641	264.051	0.74844	4.1003	1617.6	65.573	512.9	665.8
60	0.00100011	284.560	0.81047	4.1033	1622.2	65.780	475.9	670.8
65	0.00100271	305.084	0.87162	4.1064	1625.6	65.889	443.1	675.4
70	0.00100545	325.624	0.93191	4.1097	1628.1	65.906	414.0	679.7
75	0.00100831	346.181	0.99139	4.1132	1629.5	65.836	388.0	683.7
80	0.00101130	366.757	1.0501	4.1170	1630.1	65.685	364.7	687.4
85	0.00101441	387.351	1.1080	4.1210	1629.7	65.457	343.8	690.7
90	0.00101765	407.967	1.1651	4.1252	1628.6	65.157	324.9	693.8
95	0.00102101	428.604	1.2216	4.1298	1626.7	64.790	307.7	696.5
100	0.00102449	449.265	1.2773	4.1346	1624.0	64.359	292.2	699.0
110	0.00103183	490.662	1.3868	4.1450	1616.7	63.325	265.1	703.0
120	0.00103966	532.169	1.4937	4.1567	1606.8	62.085	242.3	706.0
130	0.00104800	573.800	1.5983	4.1697	1594.7	60.664	223.0	707.9
140	0.00105685	615.569	1.7006	4.1843	1580.5	59.087	206.5	708.8
150	0.00106625	657.491	1.8009	4.2005	1564.3	57.373	192.3	708.6
160	0.00107622	699.585	1.8992	4.2186	1546.3	55.540	180.0	707.6
170	0.00108677	741.871	1.9957	4.2389	1526.5	53.605	169.2	705.6
180	0.00109796	784.371	2.0906	4.2616	1505.1	51.580	159.7	702.6
190	0.00110982	827.113	2.1839	4.2871	1482.1	49.478	151.3	698.8
200	0.00112241	870.124	2.2758	4.3158	1457.4	47.311	143.8	694.2
210	0.00113577	913.440	2.3663	4.3480	1431.2	45.088	137.0	688.6
220	0.00114999	957.098	2.4558	4.3843	1403.5	42.821	130.9	682.3
230	0.00116514	1001.14	2.5442	4.4252	1374.2	40.519	125.3	675.0
240	0.00118132	1045.62	2.6317	4.4713	1343.4	38.193	120.2	667.0

Table 3 Single-phase region – Continued
(0 °C to 800 °C)

p = 400 bar								
t	v	h	s	c_p	w	κ	η	λ
[°C]	[$m^3\ kg^{-1}$]	[$kJ\ kg^{-1}$]	[$kJ\ kg^{-1}\ K^{-1}$]	[$kJ\ kg^{-1}\ K^{-1}$]	[$m\ s^{-1}$]	[–]	[10^{-6} Pa s]	[$10^{-3}\ W\ m^{-1}\ K^{-1}$]
250	0.00119864	1090.59	2.7185	4.5234	1311.1	35.852	115.5	658.1
260	0.00121724	1136.11	2.8047	4.5824	1277.3	33.506	111.2	648.4
270	0.00123729	1182.26	2.8905	4.6493	1242.0	31.167	107.1	637.7
280	0.00125898	1229.13	2.9760	4.7254	1205.2	28.845	103.2	626.3
290	0.00128255	1276.80	3.0614	4.8123	1167.0	26.548	99.58	613.8
300	0.00130831	1325.41	3.1469	4.9120	1127.4	24.287	96.08	600.5
310	0.00133664	1375.10	3.2329	5.0272	1086.2	22.068	92.70	586.2
320	0.00136803	1426.02	3.3195	5.1615	1043.4	19.895	89.41	570.8
330	0.00140314	1478.41	3.4070	5.3198	998.69	17.771	86.17	554.2
340	0.00144284	1532.52	3.4960	5.5097	951.99	15.703	82.96	536.5
350	0.00148840	1588.74	3.5870	5.7424	903.62	13.715	79.73	517.3
360	0.00154152	1647.62	3.6807	6.0440	853.45	11.813	76.44	496.7
370	0.00160475	1709.93	3.7783	6.4342	800.77	9.9896	73.05	474.3
380	0.00168216	1776.72	3.8814	6.9509	745.75	8.2653	69.49	450.1
390	0.00178035	1849.61	3.9921	7.6679	688.52	6.6568	65.68	424.9
400	0.00191069	1931.13	4.1141	8.7012	630.14	5.1954	61.50	398.5
410	0.00209341	2025.18	4.2527	10.192	573.76	3.9314	56.83	370.5
420	0.00236117	2136.30	4.4142	12.045	526.61	2.9362	51.66	339.1
430	0.00274238	2263.84	4.5969	13.205	499.08	2.2707	46.48	301.2
440	0.00320965	2394.03	4.7807	12.554	493.66	1.8982	42.27	260.0
450	0.00369271	2511.77	4.9447	10.950	501.50	1.7027	39.44	225.0
460	0.00414901	2613.32	5.0842	9.3909	514.66	1.5960	37.69	199.1
470	0.00456732	2700.69	5.2026	8.1475	528.95	1.5315	36.62	180.5
480	0.00494969	2777.18	5.3048	7.1892	542.92	1.4888	35.97	167.1
490	0.00530040	2845.20	5.3946	6.4475	556.25	1.4594	35.60	157.1
500	0.00562490	2906.69	5.4746	5.8745	568.83	1.4381	35.41	149.7
510	0.00592790	2963.09	5.5471	5.4221	580.67	1.4220	35.34	144.0
520	0.00621295	3015.42	5.6135	5.0563	591.81	1.4093	35.37	139.5
530	0.00648280	3064.43	5.6749	4.7551	602.30	1.3990	35.45	136.1
540	0.00673966	3110.69	5.7322	4.5044	612.21	1.3903	35.59	133.3
550	0.00698531	3154.65	5.7859	4.2938	621.60	1.3828	35.76	131.2
560	0.00722123	3196.67	5.8366	4.1156	630.51	1.3763	35.96	129.5
570	0.00744864	3237.05	5.8848	3.9634	638.99	1.3704	36.19	128.2
580	0.00766855	3276.01	5.9308	3.8324	647.09	1.3651	36.43	127.2
590	0.00788179	3313.75	5.9747	3.7188	654.85	1.3602	36.69	126.5
600	0.00808906	3350.43	6.0170	3.6194	662.31	1.3557	36.96	125.9
650	0.00905378	3521.76	6.2079	3.2666	695.98	1.3375	38.44	125.7
700	0.00993098	3679.42	6.3743	3.0570	725.36	1.3245	40.03	127.8
750	0.0107484	3828.75	6.5239	2.9259	751.76	1.3145	41.68	131.4
800	0.0115229	3972.81	6.6614	2.8428	775.83	1.3059	43.34	135.8

Table 3 Single-phase region – Continued (0 °C to 800 °C)

p = 450 bar								
t [°C]	v [$m^3\,kg^{-1}$]	h [$kJ\,kg^{-1}$]	s [$kJ\,kg^{-1}\,K^{-1}$]	c_p [$kJ\,kg^{-1}\,K^{-1}$]	w [$m\,s^{-1}$]	κ [–]	η [10^{-6} Pa s]	λ [$10^{-3}\,W\,m^{-1}\,K^{-1}$]
0	0.000978910	44.3570	−0.0005911	4.0380	1477.2	49.534	1711.3	587.6
2	0.000979092	52.4368	0.028881	4.0418	1486.8	50.176	1606.5	591.5
4	0.000979317	60.5240	0.058167	4.0454	1496.1	50.791	1511.5	595.3
6	0.000979584	68.6182	0.087267	4.0487	1505.0	51.380	1425.2	599.0
8	0.000979891	76.7189	0.11618	4.0519	1513.4	51.942	1346.6	602.7
10	0.000980235	84.8257	0.14492	4.0549	1521.5	52.478	1274.6	606.2
12	0.000980616	92.9382	0.17347	4.0576	1529.2	52.990	1208.6	609.7
14	0.000981031	101.056	0.20183	4.0602	1536.5	53.478	1147.9	613.1
16	0.000981479	109.179	0.23002	4.0626	1543.5	53.942	1092.0	616.5
18	0.000981959	117.306	0.25804	4.0648	1550.2	54.383	1040.3	619.7
20	0.000982470	125.438	0.28587	4.0669	1556.6	54.802	992.4	622.9
25	0.000983877	145.785	0.35469	4.0716	1571.2	55.755	887.1	630.6
30	0.000985457	166.153	0.42244	4.0756	1584.0	56.580	798.7	637.8
35	0.000987201	186.540	0.48914	4.0791	1595.2	57.284	723.8	644.6
40	0.000989100	206.944	0.55482	4.0824	1605.0	57.873	659.6	651.1
45	0.000991146	227.363	0.61952	4.0854	1613.3	58.355	604.3	657.1
50	0.000993335	247.798	0.68325	4.0884	1620.3	58.734	556.2	662.8
55	0.000995661	268.248	0.74604	4.0914	1626.1	59.017	514.1	668.2
60	0.000998120	288.712	0.80794	4.0945	1630.8	59.208	477.1	673.2
65	0.00100071	309.193	0.86896	4.0977	1634.3	59.313	444.4	677.8
70	0.00100342	329.689	0.92913	4.1010	1636.8	59.336	415.3	682.1
75	0.00100627	350.203	0.98848	4.1046	1638.4	59.282	389.3	686.1
80	0.00100923	370.735	1.0470	4.1083	1639.1	59.156	366.0	689.8
85	0.00101231	391.286	1.1048	4.1122	1638.9	58.962	345.1	693.2
90	0.00101552	411.858	1.1619	4.1164	1637.9	58.704	326.2	696.2
95	0.00101885	432.451	1.2182	4.1208	1636.1	58.386	309.1	699.0
100	0.00102229	453.067	1.2738	4.1255	1633.6	58.013	293.5	701.5
110	0.00102954	494.371	1.3830	4.1356	1626.6	57.111	266.3	705.6
120	0.00103728	535.783	1.4897	4.1469	1617.1	56.025	243.6	708.6
130	0.00104550	577.314	1.5940	4.1594	1605.4	54.779	224.3	710.6
140	0.00105423	618.976	1.6961	4.1733	1591.6	53.394	207.8	711.6
150	0.00106349	660.785	1.7961	4.1888	1575.8	51.888	193.5	711.6
160	0.00107329	702.757	1.8941	4.2060	1558.3	50.276	181.2	710.6
170	0.00108366	744.911	1.9904	4.2252	1539.0	48.573	170.4	708.7
180	0.00109464	787.269	2.0849	4.2467	1518.2	46.791	160.9	705.9
190	0.00110626	829.854	2.1778	4.2708	1495.7	44.940	152.4	702.3
200	0.00111858	872.694	2.2693	4.2977	1471.7	43.031	144.9	697.8
210	0.00113163	915.820	2.3595	4.3280	1446.3	41.074	138.1	692.4
220	0.00114550	959.266	2.4485	4.3620	1419.3	39.078	132.0	686.3
230	0.00116024	1003.07	2.5365	4.4001	1390.9	37.051	126.5	679.3
240	0.00117596	1047.28	2.6235	4.4430	1361.0	35.003	121.4	671.5

Table 3 Single-phase region – Continued
(0 °C to 800 °C)

				p = 450 bar				
t	v	h	s	c_p	w	κ	η	λ[a]
[°C]	[$m^3\,kg^{-1}$]	[$kJ\,kg^{-1}$]	[$kJ\,kg^{-1}\,K^{-1}$]	[$kJ\,kg^{-1}\,K^{-1}$]	[$m\,s^{-1}$]	[–]	[10^{-6} Pa s]	[$10^{-3}\,W\,m^{-1}\,K^{-1}$]
250	0.00119273	1091.95	2.7097	4.4912	1329.7	32.942	116.7	662.9
260	0.00121070	1137.13	2.7952	4.5455	1297.0	30.878	112.3	653.5
270	0.00122999	1182.88	2.8803	4.6068	1263.0	28.819	108.3	643.2
280	0.00125078	1229.29	2.9649	4.6759	1227.6	26.775	104.5	632.2
290	0.00127328	1276.43	3.0494	4.7542	1191.0	24.755	100.8	620.2
300	0.00129774	1324.41	3.1338	4.8431	1153.1	22.767	97.40	607.4
310	0.00132446	1373.34	3.2185	4.9444	1113.9	20.819	94.08	593.7
320	0.00135384	1423.35	3.3035	5.0604	1073.5	18.917	90.87	579.0
330	0.00138638	1474.60	3.3892	5.1943	1031.8	17.064	87.73	563.4
340	0.00142273	1527.31	3.4758	5.3502	988.47	15.261	84.63	546.6
350	0.00146378	1581.70	3.5638	5.5342	943.48	13.514	81.55	528.7
360	0.00151077	1638.21	3.6538	5.7706	896.96	11.834	78.45	509.5
370	0.00156525	1697.31	3.7464	6.0587	849.12	10.236	75.30	489.0
380	0.00162960	1759.62	3.8425	6.4163	799.96	8.7265	72.07	467.0
390	0.00170730	1825.97	3.9433	6.8740	749.57	7.3132	68.72	443.9
400	0.00180356	1897.57	4.0505	7.4719	698.58	6.0130	65.18	419.9
410	0.00192638	1976.02	4.1661	8.2532	648.37	4.8494	61.42	394.8
420	0.00208760	2063.30	4.2930	9.2300	601.62	3.8529	57.41	368.6
430	0.00230226	2160.87	4.4327	10.269	562.72	3.0565	53.22	340.7
440	0.00258092	2267.51	4.5833	10.954	536.65	2.4796	49.12	310.2
450	0.00291525	2377.29	4.7362	10.865	525.21	2.1027	45.54	277.9
460	0.00327789	2482.58	4.8808	10.120	525.29	1.8707	42.77	247.6
470	0.00364221	2578.97	5.0114	9.1498	532.14	1.7277	40.79	222.4
480	0.00399223	2665.37	5.1269	8.1730	542.26	1.6368	39.44	202.7
490	0.00432350	2743.09	5.2294	7.3838	553.37	1.5739	38.52	187.4
500	0.00463436	2813.35	5.3209	6.6881	564.91	1.5303	37.92	175.7
510	0.00492546	2877.28	5.4030	6.1183	576.39	1.4989	37.54	166.7
520	0.00519926	2936.08	5.4776	5.6582	587.51	1.4753	37.32	159.6
530	0.00545811	2990.72	5.5461	5.2804	598.14	1.4566	37.21	154.0
540	0.00570395	3041.90	5.6094	4.9655	608.27	1.4415	37.19	149.5
550	0.00593841	3090.19	5.6685	4.7004	617.92	1.4288	37.23	145.9
560	0.00616289	3136.04	5.7238	4.4759	627.11	1.4180	37.32	143.1
570	0.00637862	3179.82	5.7761	4.2848	635.87	1.4086	37.45	140.7
580	0.00658662	3221.83	5.8256	4.1212	644.23	1.4003	37.61	138.9
590	0.00678777	3262.32	5.8728	3.9799	652.24	1.3928	37.80	137.4
600	0.00698279	3301.49	5.9179	3.8571	659.93	1.3860	38.01	136.2
650	0.00788480	3482.55	6.1197	3.4264	694.56	1.3596	39.26	133.6
700	0.00869794	3647.00	6.2932	3.1723	724.75	1.3420	40.72	134.3
750	0.00945071	3801.34	6.4479	3.0133	751.81	1.3291	42.26	136.9
800	0.0101602	3949.28	6.5891	2.9118	776.34	1.3182	43.85	140.7

[a] The λ values below the dashed line are beyond the range of validity of the λ equation for industrial use, Eq. (3.4); for details of this extrapolation, see Sec. 3.2. If more accurate λ values are needed in this range, the λ equation for scientific use [35] should be used.

Table 3 Single-phase region – Continued (0 °C to 800 °C)

p = 500 bar

t [°C]	v [m^3 kg^{-1}]	h [kJ kg^{-1}]	s [kJ kg^{-1} K^{-1}]	c_p [kJ kg^{-1} K^{-1}]	w [m s^{-1}]	κ [–]	η [10^{-6} Pa s]	λ [10^{-3} W m^{-1} K^{-1}]
0	0.000976730	49.1286	−0.001021	4.0225	1485.9	45.212	1704.7	590.3
2	0.000976937	57.1781	0.028341	4.0270	1495.6	45.791	1601.0	594.2
4	0.000977186	65.2365	0.057522	4.0313	1504.8	46.345	1507.0	598.0
6	0.000977475	73.3031	0.086523	4.0353	1513.6	46.875	1421.6	601.7
8	0.000977801	81.3773	0.11534	4.0390	1522.0	47.381	1343.6	605.3
10	0.000978164	89.4588	0.14399	4.0424	1530.0	47.864	1272.2	608.8
12	0.000978561	97.5468	0.17245	4.0456	1537.7	48.324	1206.7	612.3
14	0.000978991	105.641	0.20074	4.0486	1545.0	48.763	1146.5	615.7
16	0.000979453	113.741	0.22885	4.0513	1551.9	49.181	1090.9	619.0
18	0.000979945	121.846	0.25678	4.0538	1558.6	49.578	1039.6	622.2
20	0.000980468	129.956	0.28454	4.0562	1564.9	49.956	992.0	625.4
25	0.000981897	150.250	0.35319	4.0614	1579.5	50.815	887.2	633.0
30	0.000983494	170.569	0.42077	4.0659	1592.3	51.559	799.2	640.2
35	0.000985249	190.908	0.48732	4.0698	1603.5	52.196	724.5	647.0
40	0.000987154	211.266	0.55285	4.0733	1613.3	52.731	660.6	653.5
45	0.000989203	231.640	0.61740	4.0765	1621.6	53.169	605.4	659.5
50	0.000991389	252.031	0.68099	4.0797	1628.7	53.516	557.4	665.2
55	0.000993708	272.437	0.74366	4.0828	1634.6	53.776	515.4	670.5
60	0.000996157	292.859	0.80542	4.0860	1639.3	53.955	478.4	675.5
65	0.000998732	313.297	0.86631	4.0892	1643.0	54.056	445.7	680.2
70	0.00100143	333.751	0.92636	4.0926	1645.6	54.084	416.6	684.5
75	0.00100425	354.223	0.98558	4.0961	1647.3	54.043	390.7	688.5
80	0.00100719	374.713	1.0440	4.0998	1648.1	53.936	367.4	692.2
85	0.00101025	395.221	1.1017	4.1037	1648.0	53.769	346.4	695.6
90	0.00101343	415.750	1.1586	4.1078	1647.2	53.544	327.5	698.7
95	0.00101672	436.300	1.2148	4.1121	1645.5	53.266	310.4	701.5
100	0.00102013	456.872	1.2703	4.1167	1643.2	52.937	294.8	704.0
110	0.00102730	498.087	1.3793	4.1265	1636.5	52.140	267.6	708.2
120	0.00103494	539.405	1.4858	4.1374	1627.4	51.178	244.8	711.3
130	0.00104306	580.838	1.5898	4.1494	1616.0	50.071	225.5	713.3
140	0.00105167	622.397	1.6917	4.1627	1602.5	48.840	209.0	714.3
150	0.00106078	664.096	1.7914	4.1774	1587.2	47.498	194.7	714.4
160	0.00107043	705.951	1.8891	4.1938	1570.1	46.063	182.3	713.6
170	0.00108062	747.979	1.9851	4.2121	1551.4	44.544	171.5	711.8
180	0.00109140	790.199	2.0793	4.2324	1531.0	42.955	162.0	709.1
190	0.00110280	832.635	2.1719	4.2551	1509.1	41.304	153.5	705.6
200	0.00111486	875.311	2.2631	4.2806	1485.8	39.602	146.0	701.3
210	0.00112763	918.256	2.3529	4.3090	1460.9	37.856	139.2	696.1
220	0.00114116	961.503	2.4415	4.3409	1434.7	36.074	133.1	690.2
230	0.00115553	1005.09	2.5290	4.3766	1407.0	34.266	127.6	683.4
240	0.00117080	1049.05	2.6155	4.4165	1378.0	32.439	122.5	675.8

Table 3 Single-phase region – Continued (0 °C to 800 °C)

p = 500 bar

t [°C]	v [m^3 kg^{-1}]	h [kJ kg^{-1}]	s [kJ kg^{-1} K^{-1}]	c_p [kJ kg^{-1} K^{-1}]	w [m s^{-1}]	κ [–]	η [10^{-6} Pa s]	λ[a] [10^{-3} W m^{-1} K^{-1}]
250	0.00118708	1093.43	2.7012	4.4613	1347.7	30.601	117.8	667.5
260	0.00120446	1138.29	2.7861	4.5115	1316.0	28.759	113.5	658.4
270	0.00122307	1183.68	2.8704	4.5678	1283.1	26.923	109.4	648.5
280	0.00124305	1229.67	2.9543	4.6310	1249.0	25.100	105.7	637.8
290	0.00126459	1276.33	3.0379	4.7020	1213.7	23.298	102.1	626.3
300	0.00128789	1323.74	3.1214	4.7819	1177.3	21.526	98.67	614.0
310	0.00131322	1372.00	3.2049	4.8719	1139.9	19.790	95.41	600.8
320	0.00134088	1421.22	3.2885	4.9736	1101.5	18.097	92.25	586.8
330	0.00137128	1471.52	3.3726	5.0889	1062.1	16.453	89.19	571.9
340	0.00140492	1523.05	3.4574	5.2200	1021.7	14.859	86.19	556.0
350	0.00144244	1575.98	3.5430	5.3700	980.05	13.318	83.22	539.1
360	0.00148475	1630.63	3.6300	5.5620	936.04	11.802	80.26	521.1
370	0.00153293	1687.35	3.7189	5.7866	891.79	10.376	77.30	502.0
380	0.00158849	1746.51	3.8101	6.0531	846.77	9.0278	74.29	481.7
390	0.00165351	1808.60	3.9045	6.3776	801.09	7.7623	71.22	460.4
400	0.00173089	1874.31	4.0028	6.7781	755.14	6.5889	68.07	438.3
410	0.00182467	1944.47	4.1063	7.2713	709.70	5.5207	64.80	415.3
420	0.00194037	2020.07	4.2161	7.8636	666.13	4.5737	61.41	391.5
430	0.00208504	2101.99	4.3334	8.5275	626.51	3.7651	57.90	367.2
440	0.00226604	2190.53	4.4585	9.1599	593.57	3.1096	54.37	342.0
450	0.00248744	2284.44	4.5892	9.5672	569.96	2.6120	50.97	315.7
460	0.00274521	2380.52	4.7212	9.5776	556.72	2.2580	47.93	289.0
470	0.00302709	2474.69	4.8488	9.2032	552.52	2.0170	45.41	263.2
480	0.00331861	2563.86	4.9680	8.6087	554.76	1.8547	43.45	240.3
490	0.00360858	2646.56	5.0770	7.8969	560.89	1.7436	41.98	221.1
500	0.00388941	2722.52	5.1759	7.3090	568.92	1.6644	40.92	205.5
510	0.00415994	2792.70	5.2661	6.7313	578.20	1.6073	40.16	192.9
520	0.00441748	2857.36	5.3482	6.2131	588.07	1.5657	39.63	182.8
530	0.00466236	2917.25	5.4232	5.7787	598.00	1.5340	39.28	174.7
540	0.00489567	2973.16	5.4924	5.4136	607.73	1.5088	39.05	168.2
550	0.00511848	3025.70	5.5566	5.1031	617.16	1.4883	38.92	162.9
560	0.00533183	3075.37	5.6166	4.8372	626.25	1.4711	38.88	158.5
570	0.00553667	3122.57	5.6729	4.6091	634.99	1.4565	38.89	155.0
580	0.00573390	3167.66	5.7261	4.4131	643.38	1.4438	38.95	152.0
590	0.00592433	3210.92	5.7765	4.2440	651.44	1.4327	39.05	149.6
600	0.00610867	3252.61	5.8245	4.0973	659.20	1.4227	39.18	147.7
650	0.00695746	3443.48	6.0372	3.5873	694.26	1.3856	40.17	142.3
700	0.00771757	3614.76	6.2180	3.2881	724.96	1.3620	41.45	141.4
750	0.00841745	3774.13	6.3777	3.1008	752.51	1.3455	42.88	143.0
800	0.00907413	3925.96	6.5226	2.9813	777.37	1.3319	44.39	145.9

[a] The λ values below the dashed line are beyond the range of validity of the λ equation for industrial use, Eq. (3.4); for details of this extrapolation, see Sec. 3.2. If more accurate λ values are needed in this range, the λ equation for scientific use [35] should be used.

Table 3 Single-phase region – Continued (0 °C to 800 °C)

p = 600 bar								
t	v	h	s	c_p	w	κ	η	λ
[°C]	[m^3 kg^{-1}]	[kJ kg^{-1}]	[kJ kg^{-1} K^{-1}]	[kJ kg^{-1} K^{-1}]	[m s^{-1}]	[–]	[10^{-6} Pa s]	[10^{-3} W m^{-1} K^{-1}]
0	0.000972471	58.5861	– 0.002077	3.9937	1503.7	38.750	1692.8	595.7
2	0.000972727	66.5794	0.027080	3.9996	1513.2	39.233	1591.2	599.5
4	0.000973021	74.5842	0.056067	4.0051	1522.3	39.695	1499.0	603.2
6	0.000973350	82.5995	0.084884	4.0102	1531.0	40.136	1415.0	606.9
8	0.000973714	90.6246	0.11353	4.0148	1539.3	40.557	1338.3	610.4
10	0.000974111	98.6586	0.14200	4.0191	1547.2	40.959	1268.1	613.9
12	0.000974539	106.701	0.17031	4.0230	1554.8	41.343	1203.5	617.3
14	0.000974998	114.751	0.19844	4.0267	1562.0	41.708	1144.1	620.7
16	0.000975486	122.807	0.22640	4.0300	1568.9	42.056	1089.2	624.0
18	0.000976002	130.870	0.25419	4.0331	1575.5	42.387	1038.4	627.2
20	0.000976545	138.939	0.28181	4.0359	1581.8	42.702	991.4	630.3
25	0.000978019	159.135	0.35012	4.0422	1596.2	43.419	887.6	637.9
30	0.000979648	179.359	0.41739	4.0474	1609.0	44.043	800.3	645.0
35	0.000981425	199.608	0.48364	4.0519	1620.2	44.578	726.2	651.8
40	0.000983342	219.877	0.54889	4.0559	1630.0	45.029	662.6	658.2
45	0.000985394	240.166	0.61316	4.0595	1638.4	45.402	607.6	664.2
50	0.000987575	260.472	0.67649	4.0630	1645.6	45.699	559.8	669.9
55	0.000989883	280.795	0.73890	4.0663	1651.6	45.925	517.9	675.2
60	0.000992312	301.135	0.80042	4.0696	1656.4	46.084	481.0	680.2
65	0.000994862	321.491	0.86107	4.0729	1660.3	46.179	448.3	684.9
70	0.000997528	341.864	0.92087	4.0763	1663.1	46.213	419.3	689.2
75	0.00100031	362.255	0.97987	4.0798	1665.0	46.190	393.3	693.2
80	0.00100321	382.663	1.0381	4.0835	1666.0	46.113	370.0	697.0
85	0.00100621	403.090	1.0955	4.0873	1666.2	45.985	349.1	700.4
90	0.00100933	423.536	1.1522	4.0913	1665.6	45.809	330.2	703.5
95	0.00101256	444.003	1.2082	4.0954	1664.2	45.589	313.0	706.3
100	0.00101591	464.490	1.2634	4.0997	1662.2	45.326	297.4	708.9
110	0.00102292	505.533	1.3720	4.1090	1656.1	44.686	270.2	713.2
120	0.00103039	546.672	1.4780	4.1191	1647.6	43.907	247.3	716.4
130	0.00103830	587.918	1.5816	4.1302	1636.9	43.008	227.9	718.6
140	0.00104668	629.280	1.6829	4.1424	1624.2	42.005	211.3	719.8
150	0.00105553	670.770	1.7822	4.1558	1609.6	40.910	197.0	720.0
160	0.00106488	712.401	1.8794	4.1707	1593.4	39.737	184.6	719.4
170	0.00107475	754.189	1.9748	4.1872	1575.5	38.494	173.8	717.8
180	0.00108516	796.150	2.0684	4.2055	1556.2	37.193	164.2	715.4
190	0.00109614	838.305	2.1604	4.2258	1535.3	35.840	155.7	712.2
200	0.00110773	880.675	2.2509	4.2485	1513.1	34.445	148.2	708.1
210	0.00111996	923.284	2.3400	4.2738	1489.4	33.013	141.4	703.3
220	0.00113289	966.161	2.4279	4.3020	1464.5	31.552	135.3	697.7
230	0.00114657	1009.33	2.5145	4.3334	1438.2	30.068	129.7	691.3
240	0.00116107	1052.84	2.6002	4.3684	1410.8	28.569	124.7	684.2

Table 3 Single-phase region – Continued (0 °C to 800 °C)

p = 600 bar

t [°C]	v [m^3 kg^{-1}]	h [kJ kg^{-1}]	s [kJ kg^{-1} K^{-1}]	c_p [kJ kg^{-1} K^{-1}]	w [m s^{-1}]	κ [–]	η [10^{-6} Pa s]	λ[a] [10^{-3} W m^{-1} K^{-1}]
250	0.00117644	1096.72	2.6848	4.4073	1382.1	27.061	120.0	676.4
260	0.00119279	1141.00	2.7687	4.4507	1352.2	25.550	115.7	667.8
270	0.00121019	1185.75	2.8518	4.4988	1321.3	24.043	111.7	658.5
280	0.00122878	1231.00	2.9344	4.5523	1289.3	22.548	108.0	648.5
290	0.00124867	1276.81	3.0165	4.6117	1256.4	21.070	104.4	637.8
300	0.00127003	1323.25	3.0982	4.6775	1222.6	19.616	101.1	626.3
310	0.00129303	1370.38	3.1797	4.7504	1188.0	18.192	97.91	614.1
320	0.00131791	1418.28	3.2612	4.8309	1152.7	16.804	94.85	601.2
330	0.00134492	1467.03	3.3427	4.9198	1116.8	15.456	91.90	587.5
340	0.00137438	1516.71	3.4244	5.0175	1080.4	14.154	89.04	573.0
350	0.00140668	1567.41	3.5064	5.1244	1043.5	12.901	86.24	557.7
360	0.00144230	1619.30	3.5890	5.2592	1004.8	11.666	83.49	541.6
370	0.00148191	1672.64	3.6726	5.4109	965.62	10.487	80.76	524.6
380	0.00152621	1727.58	3.7573	5.5800	926.26	9.3691	78.05	506.8
390	0.00157615	1784.32	3.8435	5.7733	886.78	8.3153	75.33	488.1
400	0.00163294	1843.15	3.9316	5.9975	847.38	7.3289	72.61	468.8
410	0.00169811	1904.39	4.0219	6.2571	808.45	6.4149	69.86	448.8
420	0.00177352	1968.41	4.1149	6.5524	770.53	5.5794	67.10	428.3
430	0.00186141	2035.54	4.2111	6.8777	734.35	4.8286	64.30	407.4
440	0.00196432	2106.01	4.3106	7.2170	700.87	4.1678	61.51	386.3
450	0.00208469	2179.82	4.4134	7.5398	671.18	3.6015	58.74	365.2
460	0.00222434	2256.60	4.5188	7.7999	646.41	3.1309	56.06	344.1
470	0.00238359	2335.44	4.6256	7.9454	627.42	2.7526	53.53	323.2
480	0.00256059	2415.00	4.7319	7.9414	614.48	2.4577	51.23	302.7
490	0.00275152	2493.77	4.8358	7.7888	607.17	2.2330	49.21	283.0
500	0.00295158	2570.40	4.9356	7.5220	604.53	2.0636	47.51	264.6
510	0.00315612	2643.99	5.0302	7.1881	605.44	1.9357	46.12	248.1
520	0.00336069	2713.90	5.1189	6.7994	608.68	1.8374	45.00	233.7
530	0.00356327	2780.22	5.2020	6.4533	613.85	1.7625	44.11	221.3
540	0.00376176	2842.90	5.2796	6.0859	620.17	1.7040	43.43	210.7
550	0.00395482	2902.06	5.3519	5.7534	627.13	1.6574	42.91	201.8
560	0.00414208	2958.09	5.4195	5.4575	634.37	1.6192	42.52	194.2
570	0.00432345	3011.32	5.4830	5.1919	641.73	1.5875	42.24	187.9
580	0.00449897	3062.02	5.5428	4.9539	649.10	1.5609	42.05	182.5
590	0.00466889	3110.48	5.5993	4.7424	656.43	1.5382	41.93	177.9
600	0.00483355	3156.95	5.6528	4.5557	663.64	1.5186	41.88	174.1
650	0.00559084	3366.76	5.8867	3.9007	697.48	1.4502	42.19	162.1
700	0.00626511	3551.39	6.0815	3.5151	728.16	1.4105	43.07	157.2
750	0.00688181	3720.64	6.2512	3.2730	756.11	1.3846	44.23	156.2
800	0.00745681	3880.15	6.4034	3.1193	781.16	1.3639	45.54	157.4

[a] The λ values below the dashed line are beyond the range of validity of the λ equation for industrial use, Eq. (3.4); for details of this extrapolation, see Sec. 3.2. If more accurate λ values are needed in this range, the λ equation for scientific use [35] should be used.

Table 3 Single-phase region – Continued (0 °C to 800 °C)

$p = 700$ bar

t [°C]	v [m^3 kg^{-1}]	h [kJ kg^{-1}]	s [kJ kg^{-1} K^{-1}]	c_p [kJ kg^{-1} K^{-1}]	w [m s^{-1}]	κ [–]	η [10^{-6} Pa s]	λ [10^{-3} W m^{-1} K^{-1}]
0	0.000968343	67.9346	−0.003378	3.9678	1521.6	34.155	1682.5	600.9
2	0.000968644	75.8774	0.025594	3.9749	1531.0	34.569	1582.8	604.7
4	0.000968980	83.8338	0.054406	3.9814	1540.0	34.964	1492.2	608.3
6	0.000969347	91.8027	0.083056	3.9874	1548.6	35.341	1409.6	611.9
8	0.000969746	99.7830	0.11154	3.9928	1556.8	35.702	1334.0	615.5
10	0.000970175	107.774	0.13986	3.9978	1564.6	36.045	1264.7	618.9
12	0.000970632	115.774	0.16802	4.0024	1572.1	36.373	1201.0	622.3
14	0.000971117	123.783	0.19601	4.0066	1579.2	36.686	1142.3	625.6
16	0.000971629	131.800	0.22383	4.0104	1586.0	36.983	1088.0	628.9
18	0.000972167	139.824	0.25149	4.0139	1592.5	37.267	1037.8	632.0
20	0.000972730	147.856	0.27898	4.0172	1598.7	37.536	991.2	635.1
25	0.000974245	167.960	0.34698	4.0242	1613.0	38.151	888.4	642.6
30	0.000975905	188.096	0.41395	4.0301	1625.7	38.688	801.7	649.7
35	0.000977702	208.259	0.47992	4.0351	1636.9	39.149	728.0	656.5
40	0.000979630	228.446	0.54491	4.0395	1646.7	39.541	664.7	662.8
45	0.000981686	248.654	0.60893	4.0435	1655.1	39.865	609.9	668.8
50	0.000983863	268.881	0.67201	4.0472	1662.4	40.126	562.2	674.5
55	0.000986160	289.125	0.73418	4.0507	1668.5	40.327	520.4	679.8
60	0.000988572	309.387	0.79546	4.0541	1673.5	40.471	483.6	684.8
65	0.000991097	329.666	0.85588	4.0575	1677.5	40.560	451.0	689.5
70	0.000993734	349.962	0.91546	4.0609	1680.5	40.598	422.0	693.8
75	0.000996480	370.275	0.97423	4.0644	1682.6	40.586	396.0	697.9
80	0.000999335	390.606	1.0322	4.0680	1683.8	40.529	372.7	701.6
85	0.00100230	410.955	1.0894	4.0717	1684.2	40.429	351.7	705.1
90	0.00100536	431.323	1.1459	4.0755	1683.8	40.287	332.8	708.2
95	0.00100854	451.711	1.2017	4.0795	1682.7	40.107	315.6	711.1
100	0.00101181	472.118	1.2567	4.0836	1680.9	39.892	300.0	713.7
110	0.00101869	512.997	1.3648	4.0923	1675.3	39.361	272.7	718.1
120	0.00102598	553.967	1.4704	4.1018	1667.4	38.712	249.8	721.4
130	0.00103371	595.035	1.5735	4.1120	1657.3	37.959	230.3	723.7
140	0.00104188	636.211	1.6744	4.1233	1645.3	37.117	213.7	725.1
150	0.00105049	677.504	1.7732	4.1355	1631.5	36.197	199.4	725.5
160	0.00105957	718.926	1.8699	4.1491	1616.0	35.210	186.9	725.0
170	0.00106913	760.490	1.9648	4.1640	1599.0	34.163	176.0	723.7
180	0.00107920	802.211	2.0579	4.1805	1580.5	33.066	166.4	721.5
190	0.00108981	844.106	2.1493	4.1988	1560.6	31.926	157.9	718.5
200	0.00110097	886.194	2.2392	4.2191	1539.4	30.748	150.3	714.7
210	0.00111273	928.496	2.3277	4.2417	1516.9	29.539	143.5	710.2
220	0.00112512	971.037	2.4149	4.2668	1493.1	28.305	137.4	704.9
230	0.00113819	1013.84	2.5008	4.2947	1468.1	27.052	131.8	698.9
240	0.00115199	1056.94	2.5856	4.3256	1442.0	25.785	126.8	692.2

Table 3 Single-phase region – Continued (0 °C to 800 °C)

p = 700 bar								
t	v	h	s	c_p	w	κ	η	λ[a]
[°C]	[$m^3\,kg^{-1}$]	[$kJ\,kg^{-1}$]	[$kJ\,kg^{-1}\,K^{-1}$]	[$kJ\,kg^{-1}\,K^{-1}$]	[$m\,s^{-1}$]	[–]	[10^{-6} Pa s]	[$10^{-3}\,W\,m^{-1}\,K^{-1}$]
250	0.00116659	1100.36	2.6694	4.3598	1414.7	24.509	122.1	684.8
260	0.00118204	1144.15	2.7523	4.3976	1386.4	23.231	117.8	676.7
270	0.00119842	1188.33	2.8344	4.4393	1357.2	21.957	113.9	667.9
280	0.00121583	1232.95	2.9158	4.4853	1327.0	20.692	110.1	658.5
290	0.00123436	1278.05	2.9966	4.5358	1296.1	19.442	106.7	648.4
300	0.00125413	1323.68	3.0769	4.5912	1264.4	18.212	103.4	637.7
310	0.00127529	1369.89	3.1569	4.6516	1232.2	17.007	100.2	626.3
320	0.00129798	1416.73	3.2365	4.7174	1199.4	15.832	97.26	614.2
330	0.00132241	1464.26	3.3160	4.7885	1166.2	14.691	94.40	601.5
340	0.00134877	1512.52	3.3953	4.8648	1132.6	13.587	91.63	588.1
350	0.00137734	1561.57	3.4747	4.9456	1098.8	12.523	88.95	574.0
360	0.00140839	1611.49	3.5541	5.0456	1064.4	11.492	86.33	559.3
370	0.00144236	1662.50	3.6341	5.1581	1028.9	10.485	83.76	543.9
380	0.00147965	1714.68	3.7146	5.2776	993.30	9.5259	81.23	527.8
390	0.00152079	1768.09	3.7957	5.4083	957.83	8.6180	78.72	511.0
400	0.00156639	1822.89	3.8778	5.5547	922.59	7.7629	76.24	493.7
410	0.00161722	1879.25	3.9609	5.7192	887.84	6.9631	73.78	475.9
420	0.00167415	1937.34	4.0453	5.9017	853.87	6.2214	71.32	457.6
430	0.00173821	1997.33	4.1312	6.0990	821.07	5.5407	68.88	439.0
440	0.00181047	2059.35	4.2188	6.3049	789.90	4.9233	66.46	420.2
450	0.00189208	2123.43	4.3080	6.5096	760.87	4.3710	64.07	401.3
460	0.00198407	2189.49	4.3987	6.6990	734.52	3.8846	61.73	382.6
470	0.00208719	2257.30	4.4906	6.8558	711.40	3.4639	59.47	364.2
480	0.00220176	2326.43	4.5830	6.9619	691.97	3.1068	57.32	346.1
490	0.00232737	2396.31	4.6752	7.0021	676.51	2.8092	55.32	328.6
500	0.00246294	2466.23	4.7662	6.9693	665.04	2.5653	53.48	311.7
510	0.00260674	2535.47	4.8552	6.8670	657.31	2.3678	51.85	295.6
520	0.00275670	2603.38	4.9413	6.7073	652.87	2.2088	50.42	280.5
530	0.00291072	2669.48	5.0242	6.5070	651.17	2.0811	49.19	266.6
540	0.00306666	2733.39	5.1032	6.2797	652.00	1.9803	48.15	253.9
550	0.00322318	2795.01	5.1786	6.0369	654.19	1.8968	47.29	242.7
560	0.00337846	2854.09	5.2499	5.7814	657.60	1.8286	46.58	232.7
570	0.00353176	2910.72	5.3175	5.5472	661.76	1.7714	46.01	223.9
580	0.00368255	2965.08	5.3816	5.3277	666.47	1.7231	45.55	216.3
590	0.00383038	3017.31	5.4424	5.1190	671.62	1.6823	45.19	209.6
600	0.00397492	3067.51	5.5003	4.9233	677.13	1.6478	44.92	203.8
650	0.00464832	3293.57	5.7522	4.1825	706.51	1.5341	44.45	184.4
700	0.00525194	3490.45	5.9600	3.7267	735.57	1.4717	44.85	175.0
750	0.00580362	3668.96	6.1390	3.4357	762.99	1.4330	45.69	171.0
800	0.00631671	3835.81	6.2982	3.2526	787.58	1.4028	46.77	170.0

[a] The λ values below the dashed line are beyond the range of validity of the λ equation for industrial use, Eq. (3.4); for details of this extrapolation, see Sec. 3.2. If more accurate λ values are needed in this range, the λ equation for scientific use [35] should be used.

Table 3 Single-phase region – Continued (0 °C to 800 °C)

$p =$ **800 bar**

t [°C]	v [m^3 kg^{-1}]	h [kJ kg^{-1}]	s [kJ kg^{-1} K^{-1}]	c_p [kJ kg^{-1} K^{-1}]	w [m s^{-1}]	κ [–]	η [10^{-6} Pa s]	λ [10^{-3} W m^{-1} K^{-1}]
0	0.000964341	77.1804	−0.004907	3.9446	1539.6	30.724	1673.7	606.1
2	0.000964684	85.0779	0.023900	3.9527	1548.9	31.086	1575.7	609.8
4	0.000965058	92.9907	0.052555	3.9600	1557.8	31.431	1486.5	613.4
6	0.000965460	100.918	0.081053	3.9667	1566.2	31.760	1405.1	616.9
8	0.000965892	108.857	0.10939	3.9728	1574.3	32.074	1330.6	620.4
10	0.000966350	116.809	0.13758	3.9784	1582.0	32.374	1262.2	623.8
12	0.000966834	124.770	0.16560	3.9835	1589.4	32.659	1199.2	627.2
14	0.000967344	132.742	0.19345	3.9881	1596.4	32.932	1141.1	630.4
16	0.000967879	140.723	0.22115	3.9923	1603.1	33.192	1087.4	633.7
18	0.000968437	148.711	0.24868	3.9962	1609.6	33.439	1037.7	636.8
20	0.000969019	156.707	0.27605	3.9998	1615.7	33.674	991.4	639.9
25	0.000970572	176.726	0.34377	4.0076	1629.9	34.212	889.4	647.3
30	0.000972260	196.781	0.41047	4.0140	1642.4	34.682	803.3	654.4
35	0.000974076	216.865	0.47618	4.0194	1653.6	35.088	729.9	661.1
40	0.000976016	236.974	0.54092	4.0242	1663.3	35.434	666.9	667.4
45	0.000978074	257.106	0.60469	4.0284	1671.8	35.721	612.3	673.4
50	0.000980249	277.257	0.66754	4.0322	1679.1	35.954	564.8	679.0
55	0.000982535	297.427	0.72948	4.0359	1685.3	36.135	523.1	684.3
60	0.000984931	317.616	0.79054	4.0394	1690.4	36.266	486.3	689.3
65	0.000987434	337.821	0.85074	4.0428	1694.5	36.350	453.7	694.0
70	0.000990043	358.044	0.91010	4.0463	1697.7	36.389	424.7	698.4
75	0.000992756	378.284	0.96866	4.0497	1699.9	36.386	398.7	702.4
80	0.000995572	398.542	1.0264	4.0533	1701.3	36.343	375.4	706.2
85	0.000998489	418.817	1.0834	4.0569	1701.9	36.262	354.4	709.7
90	0.00100151	439.110	1.1397	4.0605	1701.7	36.145	335.4	712.8
95	0.00100463	459.422	1.1953	4.0643	1700.8	35.994	318.2	715.7
100	0.00100785	479.754	1.2501	4.0683	1699.3	35.812	302.6	718.4
110	0.00101459	520.477	1.3578	4.0765	1694.2	35.362	275.2	722.8
120	0.00102173	561.286	1.4630	4.0853	1686.7	34.808	252.2	726.3
130	0.00102928	602.186	1.5657	4.0948	1677.2	34.164	232.7	728.7
140	0.00103724	643.185	1.6661	4.1052	1665.8	33.441	216.0	730.2
150	0.00104564	684.292	1.7645	4.1164	1652.7	32.651	201.6	730.8
160	0.00105447	725.517	1.8607	4.1287	1637.9	31.802	189.1	730.5
170	0.00106375	766.871	1.9551	4.1423	1621.6	30.901	178.2	729.3
180	0.00107351	808.368	2.0477	4.1572	1604.0	29.957	168.6	727.4
190	0.00108377	850.022	2.1387	4.1738	1585.0	28.975	160.0	724.6
200	0.00109454	891.849	2.2280	4.1921	1564.7	27.960	152.4	721.1
210	0.00110587	933.870	2.3159	4.2124	1543.2	26.918	145.6	716.8
220	0.00111778	976.104	2.4024	4.2348	1520.5	25.854	139.5	711.8
230	0.00113031	1018.57	2.4877	4.2597	1496.7	24.773	133.9	706.1
240	0.00114350	1061.31	2.5718	4.2872	1471.8	23.679	128.8	699.8

Table 3 Single-phase region – Continued (0 °C to 800 °C)

p = 800 bar

t [°C]	v [m^3 kg^{-1}]	h [kJ kg^{-1}]	s [kJ kg^{-1} K^{-1}]	c_p [kJ kg^{-1} K^{-1}]	w [m s^{-1}]	κ [–]	η [10^{-6} Pa s]	λ[a] [10^{-3} W m^{-1} K^{-1}]
250	0.00115740	1104.33	2.6548	4.3174	1445.8	22.577	124.2	692.8
260	0.00117207	1147.67	2.7368	4.3508	1419.0	21.473	119.9	685.1
270	0.00118757	1191.35	2.8180	4.3873	1391.2	20.371	115.9	676.8
280	0.00120397	1235.42	2.8984	4.4273	1362.6	19.277	112.2	667.9
290	0.00122135	1279.91	2.9781	4.4708	1333.4	18.195	108.8	658.4
300	0.00123981	1324.85	3.0572	4.5181	1303.5	17.131	105.5	648.2
310	0.00125944	1370.29	3.1358	4.5692	1273.2	16.088	102.5	637.5
320	0.00128038	1416.25	3.2140	4.6241	1242.5	15.071	99.53	626.2
330	0.00130275	1462.78	3.2918	4.6825	1211.5	14.083	96.73	614.3
340	0.00132672	1509.91	3.3693	4.7440	1180.3	13.126	94.03	601.7
350	0.00135245	1557.67	3.4465	4.8076	1149.0	12.203	91.43	588.7
360	0.00138016	1606.10	3.5236	4.8842	1117.3	11.305	88.91	575.0
370	0.00141010	1655.38	3.6008	4.9727	1084.6	10.428	86.44	560.8
380	0.00144256	1705.56	3.6783	5.0634	1051.8	9.5864	84.04	546.0
390	0.00147784	1756.67	3.7559	5.1586	1019.2	8.7860	81.67	530.7
400	0.00151632	1808.76	3.8339	5.2623	986.85	8.0282	79.35	514.9
410	0.00155843	1861.95	3.9123	5.3768	954.96	7.3147	77.06	498.7
420	0.00160468	1916.33	3.9913	5.5024	923.76	6.6472	74.80	482.1
430	0.00165561	1972.03	4.0711	5.6371	893.49	6.0274	72.57	465.2
440	0.00171181	2029.10	4.1517	5.7774	864.44	5.4566	70.36	448.1
450	0.00177388	2087.58	4.2331	5.9181	836.91	4.9356	68.20	430.9
460	0.00184240	2147.44	4.3153	6.0528	811.19	4.4645	66.08	413.7
470	0.00191784	2208.59	4.3982	6.1737	787.59	4.0430	64.02	396.7
480	0.00200054	2270.84	4.4814	6.2727	766.40	3.6701	62.03	380.1
490	0.00209065	2333.94	4.5646	6.3420	747.86	3.3440	60.14	363.9
500	0.00218803	2397.56	4.6474	6.3749	732.12	3.0622	58.36	348.2
510	0.00229222	2461.31	4.7294	6.3679	719.27	2.8212	56.71	333.1
520	0.00240251	2524.78	4.8099	6.3205	709.24	2.6172	55.20	318.7
530	0.00251797	2587.59	4.8886	6.2361	701.86	2.4454	53.84	305.0
540	0.00263750	2649.40	4.9651	6.1206	696.86	2.3015	52.62	292.2
550	0.00276004	2709.93	5.0391	5.9817	693.95	2.1810	51.56	280.2
560	0.00288461	2768.96	5.1103	5.8423	692.89	2.0804	50.63	269.2
570	0.00301014	2826.43	5.1789	5.6505	693.29	1.9960	49.83	259.1
580	0.00313543	2882.02	5.2445	5.4708	694.79	1.9245	49.16	250.0
590	0.00326009	2935.89	5.3072	5.3034	696.96	1.8625	48.59	241.9
600	0.00338369	2988.09	5.3674	5.1372	699.81	1.8092	48.12	234.6
650	0.00397500	3225.67	5.6321	4.4081	721.80	1.6384	46.86	208.5
700	0.00451614	3432.92	5.8509	3.9135	747.63	1.5471	46.75	194.3
750	0.00501331	3619.74	6.0382	3.5834	773.31	1.4911	47.24	187.0
800	0.00547622	3793.32	6.2039	3.3765	796.77	1.4491	48.07	183.7

[a] The λ values below the dashed line are beyond the range of validity of the λ equation for industrial use, Eq. (3.4); for details of this extrapolation, see Sec. 3.2. If more accurate λ values are needed in this range, the λ equation for scientific use [35] should be used.

Table 3 Single-phase region – Continued (0 °C to 800 °C)

p = 900 bar								
t [°C]	v [m^3 kg^{-1}]	h [kJ kg^{-1}]	s [kJ kg^{-1} K^{-1}]	c_p [kJ kg^{-1} K^{-1}]	w [m s^{-1}]	κ [–]	η [10^{-6} Pa s]	λ [10^{-3} W m^{-1} K^{-1}]
0	0.000960457	86.3292	−0.006646	3.9240	1557.6	28.066	1666.4	611.1
2	0.000960839	94.1861	0.022013	3.9328	1566.8	28.387	1569.9	614.7
4	0.000961249	102.060	0.050526	3.9408	1575.5	28.693	1482.0	618.3
6	0.000961685	109.949	0.078888	3.9480	1583.9	28.984	1401.6	621.8
8	0.000962146	117.852	0.10710	3.9547	1591.8	29.262	1328.0	625.3
10	0.000962632	125.767	0.13515	3.9607	1599.4	29.528	1260.3	628.6
12	0.000963141	133.694	0.16305	3.9662	1606.7	29.781	1198.0	631.9
14	0.000963674	141.631	0.19079	3.9712	1613.6	30.022	1140.5	635.2
16	0.000964229	149.578	0.21837	3.9757	1620.3	30.252	1087.3	638.4
18	0.000964807	157.534	0.24579	3.9799	1626.6	30.471	1037.9	641.5
20	0.000965406	165.498	0.27304	3.9838	1632.7	30.680	992.1	644.5
25	0.000966995	185.438	0.34049	3.9921	1646.7	31.157	890.7	651.9
30	0.000968709	205.416	0.40694	3.9989	1659.2	31.575	805.1	658.9
35	0.000970544	225.426	0.47241	4.0047	1670.2	31.936	732.1	665.6
40	0.000972494	245.462	0.53691	4.0097	1680.0	32.245	669.3	671.9
45	0.000974556	265.522	0.60046	4.0141	1688.5	32.503	614.8	677.8
50	0.000976727	285.602	0.66309	4.0181	1695.8	32.714	567.4	683.5
55	0.000979004	305.702	0.72481	4.0219	1702.0	32.878	525.7	688.8
60	0.000981385	325.821	0.78566	4.0255	1707.2	32.998	489.0	693.8
65	0.000983867	345.957	0.84565	4.0289	1711.4	33.077	456.4	698.4
70	0.000986450	366.110	0.90481	4.0324	1714.7	33.116	427.4	702.8
75	0.000989132	386.280	0.96317	4.0358	1717.0	33.118	401.4	706.9
80	0.000991911	406.468	1.0207	4.0392	1718.6	33.084	378.1	710.7
85	0.000994788	426.673	1.0776	4.0427	1719.3	33.017	357.1	714.2
90	0.000997760	446.895	1.1336	4.0463	1719.3	32.918	338.1	717.4
95	0.00100083	467.136	1.1890	4.0499	1718.6	32.789	320.8	720.3
100	0.00100399	487.395	1.2436	4.0537	1717.1	32.632	305.1	723.0
110	0.00101061	527.970	1.3509	4.0614	1712.5	32.241	277.7	727.5
120	0.00101760	568.625	1.4557	4.0697	1705.5	31.759	254.7	731.1
130	0.00102499	609.366	1.5580	4.0785	1696.4	31.197	235.1	733.6
140	0.00103277	650.198	1.6581	4.0881	1685.5	30.565	218.4	735.2
150	0.00104096	691.129	1.7560	4.0984	1673.0	29.874	203.9	736.0
160	0.00104955	732.168	1.8518	4.1096	1658.8	29.131	191.3	735.8
170	0.00105858	773.325	1.9458	4.1220	1643.3	28.343	180.4	734.8
180	0.00106806	814.612	2.0379	4.1355	1626.3	27.516	170.7	733.1
190	0.00107799	856.041	2.1283	4.1505	1608.1	26.656	162.1	730.5
200	0.00108842	897.627	2.2171	4.1670	1588.7	25.767	154.5	727.2
210	0.00109935	939.387	2.3045	4.1853	1568.2	24.855	147.6	723.2
220	0.00111082	981.340	2.3904	4.2055	1546.5	23.923	141.5	718.5
230	0.00112286	1023.51	2.4751	4.2278	1523.8	22.975	135.9	713.1
240	0.00113551	1065.90	2.5585	4.2524	1500.0	22.016	130.8	707.1

Table 3 Single-phase region – Continued (0 °C to 800 °C)

$p =$ **900 bar**

t [°C]	v [m^3 kg^{-1}]	h [kJ kg^{-1}]	s [kJ kg^{-1} K^{-1}]	c_p [kJ kg^{-1} K^{-1}]	w [m s^{-1}]	κ [–]	η [10^{-6} Pa s]	λ[a] [10^{-3} W m^{-1} K^{-1}]
250	0.00114880	1108.56	2.6408	4.2794	1475.3	21.050	126.2	700.4
260	0.00116279	1151.50	2.7221	4.3090	1449.6	20.081	121.9	693.1
270	0.00117752	1194.75	2.8025	4.3412	1423.2	19.113	117.9	685.2
280	0.00119304	1238.34	2.8820	4.3763	1396.0	18.151	114.3	676.8
290	0.00120944	1282.29	2.9608	4.4143	1368.3	17.199	110.8	667.7
300	0.00122677	1326.63	3.0388	4.4553	1340.0	16.262	107.6	658.1
310	0.00124513	1371.40	3.1163	4.4990	1311.3	15.343	104.6	648.0
320	0.00126461	1416.62	3.1931	4.5456	1282.3	14.447	101.7	637.3
330	0.00128530	1462.32	3.2695	4.5944	1253.1	13.575	98.92	626.0
340	0.00130734	1508.52	3.3455	4.6451	1223.9	12.731	96.28	614.3
350	0.00133085	1555.23	3.4211	4.6966	1194.6	11.915	93.74	602.0
360	0.00135598	1602.48	3.4963	4.7569	1164.6	11.115	91.29	589.2
370	0.00138288	1650.41	3.5714	4.8293	1134.4	10.339	88.90	576.0
380	0.00141177	1699.07	3.6465	4.9015	1103.9	9.5900	86.59	562.2
390	0.00144285	1748.44	3.7215	4.9744	1073.4	8.8727	84.32	548.1
400	0.00147635	1798.57	3.7965	5.0518	1043.2	8.1899	82.11	533.5
410	0.00151255	1849.50	3.8716	5.1360	1013.3	7.5433	79.94	518.5
420	0.00155177	1901.32	3.9469	5.2278	984.10	6.9344	77.81	503.2
430	0.00159435	1954.08	4.0225	5.3261	955.66	6.3647	75.71	487.7
440	0.00164064	2007.85	4.0984	5.4287	928.21	5.8350	73.66	471.9
450	0.00169102	2062.66	4.1747	5.5323	901.99	5.3458	71.64	456.0
460	0.00174581	2118.49	4.2514	5.6329	877.19	4.8972	69.66	440.1
470	0.00180534	2175.29	4.3284	5.7260	854.00	4.4886	67.74	424.3
480	0.00186984	2232.97	4.4055	5.8072	832.59	4.1192	65.88	408.6
490	0.00193946	2291.38	4.4825	5.8719	813.12	3.7878	64.09	393.4
500	0.00201426	2350.34	4.5593	5.9164	795.71	3.4927	62.39	378.5
510	0.00209412	2409.63	4.6355	5.9376	780.46	3.2319	60.78	364.1
520	0.00217882	2469.01	4.7108	5.9338	767.39	3.0031	59.28	350.3
530	0.00226798	2528.22	4.7850	5.9049	756.51	2.8038	57.88	337.1
540	0.00236112	2587.02	4.8578	5.8520	747.72	2.6310	56.60	324.6
550	0.00245764	2645.19	4.9288	5.7777	740.90	2.4818	55.44	312.7
560	0.00255695	2702.52	4.9981	5.6856	735.90	2.3533	54.40	301.6
570	0.00265839	2758.85	5.0653	5.5795	732.51	2.2427	53.47	291.1
580	0.00276137	2814.10	5.1304	5.4615	729.90	2.1437	52.65	281.4
590	0.00286529	2868.06	5.1933	5.3323	729.49	2.0636	51.93	272.4
600	0.00296954	2920.76	5.2540	5.2063	729.74	1.9925	51.30	264.2
650	0.00348226	3164.41	5.5255	4.5583	742.76	1.7603	49.35	233.1
700	0.00396634	3379.54	5.7526	4.0692	764.23	1.6361	48.71	214.5
750	0.00441586	3573.51	5.9470	3.7127	786.67	1.5571	48.84	203.9
800	0.00483599	3753.02	6.1184	3.4861	808.37	1.5014	49.41	198.2

[a] The λ values below the dashed line are beyond the range of validity of the λ equation for industrial use, Eq. (3.4); for details of this extrapolation, see Sec. 3.2. If more accurate λ values are needed in this range, the λ equation for scientific use [35] should be used.

Table 3 Single-phase region – Continued (0 °C to 800 °C)

p = 1000 bar

t [°C]	v [$m^3\,kg^{-1}$]	h [$kJ\,kg^{-1}$]	s [$kJ\,kg^{-1}\,K^{-1}$]	c_p [$kJ\,kg^{-1}\,K^{-1}$]	w [$m\,s^{-1}$]	κ [–]	η [10^{-6} Pa s]	λ [$10^{-3}\,W\,m^{-1}\,K^{-1}$]
0	0.000956687	95.3860	–0.008582	3.9057	1575.5	25.947	1660.6	616.0
2	0.000957105	103.207	0.019946	3.9150	1584.6	26.235	1565.3	619.6
4	0.000957548	111.046	0.048331	3.9235	1593.2	26.509	1478.5	623.2
6	0.000958014	118.900	0.076571	3.9312	1601.4	26.770	1399.1	626.6
8	0.000958503	126.770	0.10466	3.9382	1609.3	27.020	1326.2	630.0
10	0.000959015	134.653	0.13260	3.9446	1616.8	27.257	1259.3	633.4
12	0.000959548	142.548	0.16038	3.9503	1624.0	27.484	1197.5	636.6
14	0.000960102	150.454	0.18801	3.9556	1630.8	27.700	1140.5	639.8
16	0.000960677	158.370	0.21549	3.9604	1637.3	27.906	1087.7	643.0
18	0.000961273	166.295	0.24280	3.9649	1643.6	28.103	1038.7	646.1
20	0.000961888	174.229	0.26996	3.9689	1649.6	28.290	993.1	649.1
25	0.000963510	194.096	0.33716	3.9777	1663.4	28.718	892.4	656.4
30	0.000965249	214.003	0.40337	3.9849	1675.8	29.094	807.1	663.4
35	0.000967101	233.943	0.46861	3.9909	1686.8	29.419	734.4	670.0
40	0.000969061	253.911	0.53289	3.9961	1696.4	29.698	671.8	676.3
45	0.000971126	273.903	0.59623	4.0007	1704.9	29.932	617.5	682.2
50	0.000973294	293.917	0.65864	4.0048	1712.2	30.122	570.1	687.8
55	0.000975562	313.950	0.72016	4.0086	1718.5	30.272	528.5	693.1
60	0.000977929	334.003	0.78081	4.0122	1723.7	30.383	491.7	698.1
65	0.000980392	354.072	0.84061	4.0157	1728.0	30.456	459.2	702.8
70	0.000982950	374.160	0.89957	4.0191	1731.3	30.494	430.1	707.2
75	0.000985603	394.264	0.95774	4.0225	1733.8	30.498	404.1	711.3
80	0.000988348	414.385	1.0151	4.0259	1735.4	30.471	380.8	715.1
85	0.000991185	434.523	1.0717	4.0293	1736.2	30.413	359.7	718.6
90	0.000994115	454.678	1.1276	4.0327	1736.3	30.327	340.7	721.8
95	0.000997135	474.850	1.1828	4.0362	1735.7	30.214	323.4	724.8
100	0.00100025	495.040	1.2373	4.0397	1734.4	30.075	307.7	727.5
110	0.00100674	535.473	1.3442	4.0471	1730.0	29.730	280.2	732.1
120	0.00101361	575.982	1.4486	4.0548	1723.4	29.302	257.1	735.7
130	0.00102084	616.571	1.5505	4.0630	1714.7	28.803	237.5	738.4
140	0.00102844	657.245	1.6502	4.0718	1704.3	28.242	220.7	740.2
150	0.00103643	698.010	1.7477	4.0813	1692.1	27.627	206.2	741.0
160	0.00104482	738.873	1.8431	4.0916	1678.5	26.966	193.5	741.0
170	0.00105361	779.845	1.9366	4.1028	1663.6	26.266	182.5	740.2
180	0.00106282	820.934	2.0283	4.1152	1647.3	25.532	172.8	738.6
190	0.00107246	862.152	2.1183	4.1288	1629.8	24.768	164.2	736.2
200	0.00108256	903.513	2.2066	4.1437	1611.2	23.979	156.5	733.2
210	0.00109313	945.032	2.2935	4.1603	1591.5	23.169	149.6	729.4
220	0.00110421	986.725	2.3789	4.1785	1570.7	22.342	143.5	724.9
230	0.00111581	1028.61	2.4630	4.1987	1548.9	21.501	137.9	719.8
240	0.00112796	1070.70	2.5458	4.2207	1526.2	20.649	132.8	714.0

Table 3 Single-phase region – Continued
(0 °C to 800 °C)

p = 1000 bar								
t	v	h	s	c_p	w	κ	η	λ[a]
[°C]	[$m^3\,kg^{-1}$]	[$kJ\,kg^{-1}$]	[$kJ\,kg^{-1}\,K^{-1}$]	[$kJ\,kg^{-1}\,K^{-1}$]	[$m\,s^{-1}$]	[–]	[10^{-6} Pa s]	[$10^{-3}\,W\,m^{-1}\,K^{-1}$]
250	0.00114071	1113.03	2.6275	4.2449	1502.5	19.791	128.1	707.7
260	0.00115408	1155.61	2.7081	4.2714	1478.1	18.930	123.8	700.8
270	0.00116813	1198.47	2.7878	4.3001	1452.8	18.069	119.9	693.2
280	0.00118289	1241.62	2.8665	4.3311	1426.9	17.212	116.2	685.2
290	0.00119843	1285.10	2.9444	4.3646	1400.4	16.364	112.8	676.6
300	0.00121480	1328.92	3.0215	4.4003	1373.4	15.527	109.6	667.4
310	0.00123207	1373.11	3.0980	4.4382	1346.1	14.707	106.6	657.8
320	0.00125031	1417.69	3.1738	4.4781	1318.5	13.904	103.7	647.6
330	0.00126961	1462.68	3.2490	4.5197	1290.8	13.124	101.0	637.0
340	0.00129006	1508.09	3.3236	4.5622	1263.0	12.366	98.41	625.9
350	0.00131176	1553.92	3.3978	4.6048	1235.2	11.632	95.92	614.3
360	0.00133481	1600.21	3.4715	4.6541	1207.4	10.922	93.51	602.3
370	0.00135934	1647.05	3.5449	4.7144	1179.3	10.232	91.19	589.8
380	0.00138548	1694.50	3.6181	4.7739	1150.7	9.5566	88.94	576.9
390	0.00141337	1742.53	3.6910	4.8320	1121.9	8.9058	86.75	563.7
400	0.00144317	1791.14	3.7638	4.8917	1093.3	8.2826	84.62	550.0
410	0.00147508	1840.37	3.8364	4.9557	1065.0	7.6892	82.54	536.1
420	0.00150929	1890.27	3.9089	5.0253	1037.2	7.1273	80.50	521.9
430	0.00154605	1940.90	3.9814	5.1001	1010.0	6.5981	78.51	507.4
440	0.00158559	1992.29	4.0540	5.1784	983.70	6.1028	76.55	492.7
450	0.00162815	2044.47	4.1267	5.2581	958.43	5.6419	74.64	477.9
460	0.00167397	2097.44	4.1994	5.3363	934.37	5.2154	72.77	463.1
470	0.00172324	2151.18	4.2722	5.4102	911.66	4.8230	70.94	448.2
480	0.00177614	2205.62	4.3450	5.4766	890.42	4.4639	69.18	433.5
490	0.00183278	2260.68	4.4176	5.5326	870.75	4.1369	67.47	419.0
500	0.00189324	2316.23	4.4899	5.5757	852.73	3.8407	65.83	404.8
510	0.00195750	2372.14	4.5618	5.6038	836.42	3.5740	64.27	391.1
520	0.00202548	2428.25	4.6330	5.6155	821.87	3.3348	62.79	377.7
530	0.00209703	2484.39	4.7033	5.6101	809.07	3.1215	61.40	364.9
540	0.00217192	2540.40	4.7726	5.5877	798.03	2.9322	60.11	352.7
550	0.00224984	2596.09	4.8407	5.5490	788.69	2.7647	58.91	341.0
560	0.00233047	2651.33	4.9074	5.4954	780.97	2.6172	57.81	329.9
570	0.00241341	2705.96	4.9726	5.4288	774.80	2.4874	56.80	319.5
580	0.00249829	2759.87	5.0361	5.3512	770.05	2.3735	55.89	309.6
590	0.00258472	2812.94	5.0980	5.2687	769.69	2.2920	55.07	300.3
600	0.00267226	2865.07	5.1580	5.1706	766.53	2.1988	54.34	291.7
650	0.00311448	3110.60	5.4316	4.6275	767.31	1.8904	51.83	257.3
700	0.00354616	3330.76	5.6640	4.1910	784.08	1.7336	50.71	235.0
750	0.00395319	3530.68	5.8644	3.8235	801.50	1.6250	50.48	221.3
800	0.00433551	3715.19	6.0405	3.5762	821.00	1.5547	50.78	213.2

[a] The λ values below the dashed line are beyond the range of validity of the λ equation for industrial use, Eq. (3.4); for details of this extrapolation, see Sec. 3.2. If more accurate λ values are needed in this range, the λ equation for scientific use [35] should be used.

Table 4 High-temperature region
(800 °C to 2000 °C)

This table contains values for the following thermodynamic properties in the high-temperature region (region 5 of IAPWS-IF97) for temperatures from 800 °C to 2000 °C and for pressures from 0.006 112 127 bar to 500 bar:

- Specific volume v
- Specific enthalpy h
- Specific entropy s
- Specific isobaric heat capacity c_p
- Speed of sound w

These thermodynamic properties were calculated from the IAPWS-IF97 basic equation for region 5, Eq. (2.15), except for the temperature t = 800 °C. At 800 °C, the properties were determined from the basic equation of region 2, Eq. (2.6), because the boundary t = 800 °C between regions 2 and 5 belongs to region 2; see the comment at the beginning of Sec. 2.2.

With the values for v and w given in this table, the isentropic exponent κ can easily be calculated from the relation $\kappa = w^2/(pv)$.

Table 4 High-temperature region
(800 °C to 2000 °C)

	p = 0.006112127 bar					p = 0.01 bar				
t [°C]	v [m^3 kg^{-1}]	h [kJ kg^{-1}]	s [kJ kg^{-1} K^{-1}]	c_p [kJ kg^{-1} K^{-1}]	w [m s^{-1}]	v [m^3 kg^{-1}]	h [kJ kg^{-1}]	s [kJ kg^{-1} K^{-1}]	c_p [kJ kg^{-1} K^{-1}]	w [m s^{-1}]
800	810.333	4160.66	11.921	2.3423	785.38	495.286	4160.66	11.694	2.3423	785.38
825	829.211	4219.48	11.975	2.3606	793.72	506.824	4219.48	11.748	2.3606	793.72
850	848.089	4278.71	12.029	2.3774	802.02	518.362	4278.71	11.801	2.3774	802.02
875	866.966	4338.35	12.081	2.3942	810.21	529.900	4338.35	11.854	2.3942	810.21
900	885.844	4398.42	12.133	2.4109	818.31	541.439	4398.42	11.906	2.4109	818.31
925	904.721	4458.90	12.184	2.4276	826.31	552.977	4458.90	11.957	2.4276	826.31
950	923.599	4519.80	12.234	2.4442	834.22	564.515	4519.79	12.007	2.4442	834.22
975	942.476	4581.11	12.284	2.4606	842.05	576.053	4581.10	12.057	2.4606	842.05
1000	961.354	4642.82	12.333	2.4769	849.80	587.591	4642.82	12.106	2.4769	849.80
1025	980.231	4704.95	12.381	2.4930	857.47	599.130	4704.95	12.154	2.4930	857.47
1050	999.109	4767.47	12.429	2.5089	865.06	610.668	4767.47	12.202	2.5089	865.06
1075	1017.99	4830.39	12.476	2.5245	872.58	622.206	4830.39	12.249	2.5245	872.58
1100	1036.86	4893.70	12.522	2.5400	880.04	633.744	4893.70	12.295	2.5400	880.04
1125	1055.74	4957.39	12.568	2.5551	887.43	645.282	4957.39	12.341	2.5551	887.43
1150	1074.62	5021.45	12.614	2.5701	894.76	656.821	5021.45	12.387	2.5701	894.76
1175	1093.50	5085.89	12.659	2.5847	902.02	668.359	5085.89	12.431	2.5847	902.02
1200	1112.37	5150.68	12.703	2.5991	909.23	679.897	5150.68	12.476	2.5991	909.23
1225	1131.25	5215.84	12.747	2.6132	916.38	691.435	5215.84	12.520	2.6132	916.38
1250	1150.13	5281.34	12.790	2.6270	923.47	702.973	5281.34	12.563	2.6270	923.47
1275	1169.01	5347.19	12.833	2.6406	930.51	714.512	5347.19	12.606	2.6406	930.51
1300	1187.88	5413.37	12.876	2.6538	937.50	726.050	5413.37	12.648	2.6538	937.50
1325	1206.76	5479.87	12.917	2.6668	944.43	737.588	5479.87	12.690	2.6668	944.43
1350	1225.64	5546.70	12.959	2.6795	951.32	749.126	5546.70	12.732	2.6795	951.32
1375	1244.52	5613.85	13.000	2.6919	958.16	760.664	5613.85	12.773	2.6919	958.16
1400	1263.39	5681.30	13.041	2.7041	964.95	772.202	5681.30	12.813	2.7041	964.95
1425	1282.27	5749.05	13.081	2.7160	971.69	783.741	5749.05	12.854	2.7160	971.69
1450	1301.15	5817.10	13.121	2.7276	978.39	795.279	5817.09	12.893	2.7276	978.39
1475	1320.03	5885.43	13.160	2.7389	985.05	806.817	5885.43	12.933	2.7389	985.05
1500	1338.90	5954.04	13.199	2.7501	991.66	818.355	5954.04	12.972	2.7501	991.66
1525	1357.78	6022.93	13.238	2.7609	998.23	829.893	6022.93	13.010	2.7609	998.23
1550	1376.66	6092.08	13.276	2.7715	1004.8	841.431	6092.08	13.048	2.7715	1004.8
1575	1395.54	6161.50	13.314	2.7819	1011.3	852.970	6161.50	13.086	2.7819	1011.3
1600	1414.41	6231.18	13.351	2.7921	1017.7	864.508	6231.18	13.124	2.7921	1017.7
1625	1433.29	6301.10	13.388	2.8020	1024.1	876.046	6301.10	13.161	2.8020	1024.1
1650	1452.17	6371.27	13.425	2.8117	1030.5	887.584	6371.27	13.198	2.8117	1030.5
1675	1471.05	6441.69	13.461	2.8212	1036.8	899.122	6441.69	13.234	2.8212	1036.8
1700	1489.92	6512.33	13.497	2.8305	1043.1	910.660	6512.33	13.270	2.8305	1043.1
1725	1508.80	6583.21	13.533	2.8397	1049.4	922.199	6583.21	13.306	2.8397	1049.4
1750	1527.68	6654.32	13.568	2.8486	1055.6	933.737	6654.32	13.341	2.8486	1055.6
1775	1546.56	6725.64	13.603	2.8574	1061.8	945.275	6725.64	13.376	2.8574	1061.8
1800	1565.43	6797.19	13.638	2.8661	1067.9	956.813	6797.19	13.411	2.8661	1067.9
1850	1603.19	6940.91	13.707	2.8829	1080.1	979.889	6940.91	13.479	2.8829	1080.1
1900	1640.94	7085.47	13.774	2.8992	1092.2	1002.97	7085.47	13.547	2.8992	1092.2
1950	1678.70	7230.83	13.840	2.9152	1104.1	1026.04	7230.83	13.613	2.9152	1104.1
2000	1716.45	7376.98	13.905	2.9307	1115.9	1049.12	7376.98	13.678	2.9307	1115.9

Table 4 High-temperature region – Continued (800 °C to 2000 °C)

	p = 0.1 bar					p = 1 bar				
t	v	h	s	c_p	w	v	h	s	c_p	w
[°C]	[$m^3\,kg^{-1}$]	[$kJ\,kg^{-1}$]	[$kJ\,kg^{-1}\,K^{-1}$]	[$kJ\,kg^{-1}\,K^{-1}$]	[$m\,s^{-1}$]	[$m^3\,kg^{-1}$]	[$kJ\,kg^{-1}$]	[$kJ\,kg^{-1}\,K^{-1}$]	[$kJ\,kg^{-1}\,K^{-1}$]	[$m\,s^{-1}$]
800	49.5278	4160.62	10.631	2.3424	785.38	4.95196	4160.21	9.5681	2.3434	785.34
825	50.6817	4219.44	10.685	2.3607	793.72	5.06743	4219.06	9.6223	2.3616	793.69
850	51.8356	4278.67	10.739	2.3775	802.02	5.18289	4278.31	9.6757	2.3783	801.99
875	52.9894	4338.32	10.791	2.3942	810.21	5.29834	4337.97	9.7282	2.3950	810.19
900	54.1433	4398.38	10.843	2.4110	818.31	5.41379	4398.06	9.7800	2.4117	818.29
925	55.2972	4458.87	10.894	2.4277	826.31	5.52923	4458.56	9.8310	2.4283	826.30
950	56.4511	4519.76	10.944	2.4442	834.22	5.64467	4519.47	9.8813	2.4449	834.22
975	57.6049	4581.08	10.994	2.4607	842.05	5.76011	4580.80	9.9309	2.4613	842.05
1000	58.7588	4642.80	11.043	2.4770	849.80	5.87554	4642.54	9.9799	2.4775	849.80
1025	59.9127	4704.92	11.091	2.4930	857.47	5.99097	4704.67	10.028	2.4936	857.47
1050	61.0665	4767.45	11.139	2.5089	865.06	6.10640	4767.21	10.076	2.5094	865.07
1075	62.2204	4830.37	11.186	2.5246	872.59	6.22182	4830.14	10.123	2.5251	872.60
1100	63.3742	4893.67	11.232	2.5400	880.04	6.33724	4893.46	10.170	2.5404	880.06
1125	64.5281	4957.36	11.278	2.5552	887.43	6.45266	4957.16	10.216	2.5556	887.45
1150	65.6819	5021.43	11.324	2.5701	894.76	6.56808	5021.24	10.261	2.5705	894.78
1175	66.8358	5085.87	11.369	2.5847	902.02	6.68350	5085.69	10.306	2.5851	902.05
1200	67.9896	5150.67	11.413	2.5991	909.23	6.79891	5150.49	10.350	2.5995	909.26
1225	69.1435	5215.82	11.457	2.6132	916.38	6.91432	5215.66	10.394	2.6136	916.41
1250	70.2973	5281.32	11.500	2.6270	923.47	7.02973	5281.17	10.438	2.6274	923.50
1275	71.4512	5347.17	11.543	2.6406	930.51	7.14514	5347.02	10.480	2.6409	930.55
1300	72.6050	5413.35	11.586	2.6538	937.50	7.26055	5413.21	10.523	2.6541	937.53
1325	73.7589	5479.86	11.628	2.6668	944.44	7.37596	5479.73	10.565	2.6671	944.47
1350	74.9127	5546.69	11.669	2.6795	951.32	7.49136	5546.56	10.606	2.6798	951.36
1375	76.0665	5613.84	11.710	2.6920	958.16	7.60677	5613.72	10.647	2.6922	958.20
1400	77.2204	5681.29	11.751	2.7041	964.95	7.72217	5681.17	10.688	2.7044	964.99
1425	78.3742	5749.04	11.791	2.7160	971.70	7.83757	5748.93	10.728	2.7162	971.74
1450	79.5280	5817.08	11.831	2.7276	978.40	7.95297	5816.98	10.768	2.7278	978.44
1475	80.6819	5885.42	11.870	2.7390	985.05	8.06837	5885.32	10.807	2.7392	985.10
1500	81.8357	5954.03	11.909	2.7501	991.67	8.18377	5953.94	10.846	2.7503	991.71
1525	82.9895	6022.92	11.948	2.7609	998.24	8.29917	6022.83	10.885	2.7611	998.28
1550	84.1434	6092.08	11.986	2.7715	1004.8	8.41457	6091.99	10.923	2.7717	1004.8
1575	85.2972	6161.49	12.024	2.7819	1011.3	8.52996	6161.42	10.961	2.7821	1011.3
1600	86.4510	6231.17	12.061	2.7921	1017.7	8.64536	6231.10	10.998	2.7922	1017.8
1625	87.6049	6301.10	12.098	2.8020	1024.1	8.76076	6301.03	11.035	2.8022	1024.2
1650	88.7587	6371.27	12.135	2.8117	1030.5	8.87615	6371.20	11.072	2.8119	1030.5
1675	89.9125	6441.68	12.171	2.8212	1036.8	8.99155	6441.62	11.108	2.8214	1036.9
1700	91.0663	6512.33	12.207	2.8306	1043.1	9.10694	6512.27	11.145	2.8307	1043.2
1725	92.2202	6583.21	12.243	2.8397	1049.4	9.22234	6583.15	11.180	2.8398	1049.4
1750	93.3740	6654.31	12.278	2.8487	1055.6	9.33773	6654.26	11.216	2.8488	1055.6
1775	94.5278	6725.64	12.313	2.8575	1061.8	9.45312	6725.59	11.251	2.8576	1061.8
1800	95.6816	6797.18	12.348	2.8661	1067.9	9.56851	6797.14	11.285	2.8662	1068.0
1850	97.9893	6940.91	12.417	2.8829	1080.1	9.79930	6940.87	11.354	2.8830	1080.2
1900	100.297	7085.47	12.484	2.8993	1092.2	10.0301	7085.43	11.421	2.8994	1092.2
1950	102.605	7230.83	12.550	2.9152	1104.1	10.2609	7230.80	11.487	2.9153	1104.2
2000	104.912	7376.98	12.615	2.9307	1115.9	10.4916	7376.95	11.552	2.9308	1116.0

Table 4 High-temperature region – Continued (800 °C to 2000 °C)

	p = 2 bar					p = 5 bar				
t [°C]	v [m^3 kg^{-1}]	h [kJ kg^{-1}]	s [kJ kg^{-1} K^{-1}]	c_p [kJ kg^{-1} K^{-1}]	w [m s^{-1}]	v [m^3 kg^{-1}]	h [kJ kg^{-1}]	s [kJ kg^{-1} K^{-1}]	c_p [kJ kg^{-1} K^{-1}]	w [m s^{-1}]
800	2.47553	4159.76	9.2479	2.3445	785.29	0.989667	4158.40	8.8240	2.3477	785.14
825	2.53331	4218.63	9.3021	2.3626	793.65	1.01283	4217.34	8.8782	2.3655	793.54
850	2.59107	4277.90	9.3555	2.3792	801.96	1.03598	4276.69	8.9317	2.3820	801.88
875	2.64883	4337.59	9.4080	2.3959	810.17	1.05913	4336.44	8.9843	2.3984	810.10
900	2.70659	4397.69	9.4598	2.4125	818.28	1.08227	4396.61	9.0361	2.4149	818.23
925	2.76434	4458.21	9.5108	2.4291	826.29	1.10541	4457.19	9.0872	2.4314	826.26
950	2.82209	4519.15	9.5612	2.4456	834.21	1.12855	4518.17	9.1376	2.4477	834.20
975	2.87984	4580.49	9.6108	2.4619	842.05	1.15168	4579.57	9.1873	2.4639	842.05
1000	2.93758	4642.24	9.6598	2.4781	849.81	1.17481	4641.37	9.2363	2.4800	849.82
1025	2.99532	4704.40	9.7082	2.4942	857.48	1.19793	4703.57	9.2847	2.4959	857.51
1050	3.05306	4766.95	9.7559	2.5100	865.09	1.22105	4766.16	9.3325	2.5116	865.12
1075	3.11079	4829.89	9.8030	2.5256	872.62	1.24417	4829.15	9.3796	2.5271	872.67
1100	3.16852	4893.23	9.8496	2.5409	880.08	1.26729	4892.52	9.4262	2.5424	880.14
1125	3.22625	4956.94	9.8955	2.5561	887.48	1.29040	4956.27	9.4722	2.5575	887.54
1150	3.28398	5021.03	9.9410	2.5709	894.81	1.31351	5020.39	9.5177	2.5723	894.88
1175	3.34170	5085.48	9.9859	2.5855	902.08	1.33663	5084.88	9.5626	2.5868	902.16
1200	3.39942	5150.30	10.030	2.5999	909.29	1.35973	5149.73	9.6070	2.6011	909.38
1225	3.45715	5215.48	10.074	2.6139	916.44	1.38284	5214.93	9.6509	2.6151	916.54
1250	3.51487	5281.00	10.117	2.6277	923.54	1.40595	5280.48	9.6943	2.6288	923.64
1275	3.57258	5346.86	10.160	2.6412	930.58	1.42905	5346.37	9.7372	2.6423	930.69
1300	3.63030	5413.06	10.203	2.6545	937.57	1.45215	5412.59	9.7796	2.6554	937.69
1325	3.68802	5479.58	10.245	2.6674	944.51	1.47525	5479.14	9.8216	2.6683	944.63
1350	3.74573	5546.42	10.286	2.6801	951.40	1.49835	5546.00	9.8631	2.6810	951.53
1375	3.80345	5613.58	10.327	2.6925	958.24	1.52145	5613.18	9.9042	2.6933	958.37
1400	3.86116	5681.05	10.368	2.7046	965.04	1.54455	5680.67	9.9448	2.7054	965.17
1425	3.91887	5748.81	10.408	2.7165	971.78	1.56765	5748.45	9.9850	2.7172	971.92
1450	3.97658	5816.87	10.448	2.7281	978.49	1.59074	5816.53	10.025	2.7288	978.63
1475	4.03429	5885.21	10.487	2.7394	985.14	1.61384	5884.89	10.064	2.7401	985.29
1500	4.09200	5953.84	10.526	2.7505	991.76	1.63693	5953.53	10.103	2.7512	991.91
1525	4.14971	6022.74	10.565	2.7613	998.33	1.66003	6022.45	10.142	2.7620	998.48
1550	4.20741	6091.90	10.603	2.7719	1004.9	1.68312	6091.63	10.180	2.7725	1005.0
1575	4.26512	6161.33	10.641	2.7823	1011.4	1.70621	6161.07	10.218	2.7829	1011.5
1600	4.32282	6231.01	10.678	2.7924	1017.8	1.72930	6230.77	10.255	2.7930	1018.0
1625	4.38053	6300.95	10.715	2.8023	1024.2	1.75239	6300.72	10.292	2.8029	1024.4
1650	4.43823	6371.13	10.752	2.8121	1030.6	1.77548	6370.91	10.329	2.8126	1030.7
1675	4.49594	6441.55	10.789	2.8216	1036.9	1.79857	6441.35	10.365	2.8221	1037.1
1700	4.55364	6512.21	10.825	2.8309	1043.2	1.82166	6512.01	10.402	2.8313	1043.4
1725	4.61134	6583.09	10.860	2.8400	1049.5	1.84475	6582.91	10.437	2.8405	1049.6
1750	4.66905	6654.20	10.896	2.8489	1055.7	1.86784	6654.04	10.473	2.8494	1055.9
1775	4.72675	6725.54	10.931	2.8577	1061.9	1.89093	6725.38	10.508	2.8581	1062.1
1800	4.78445	6797.09	10.965	2.8663	1068.0	1.91401	6796.94	10.542	2.8668	1068.2
1850	4.89985	6940.83	11.034	2.8832	1080.2	1.96019	6940.70	10.611	2.8836	1080.4
1900	5.01525	7085.40	11.101	2.8995	1092.3	2.00636	7085.29	10.678	2.8998	1092.5
1950	5.13065	7230.77	11.167	2.9154	1104.2	2.05253	7230.68	10.744	2.9157	1104.4
2000	5.24605	7376.93	11.232	2.9309	1116.0	2.09870	7376.85	10.809	2.9312	1116.2

Table 4 High-temperature region – Continued (800 °C to 2000 °C)

t	p = 10 bar					p = 20 bar				
t [°C]	v [$m^3 kg^{-1}$]	h [$kJ kg^{-1}$]	s [$kJ kg^{-1} K^{-1}$]	c_p [$kJ kg^{-1} K^{-1}$]	w [$m s^{-1}$]	v [$m^3 kg^{-1}$]	h [$kJ kg^{-1}$]	s [$kJ kg^{-1} K^{-1}$]	c_p [$kJ kg^{-1} K^{-1}$]	w [$m s^{-1}$]
800	0.494380	4156.14	8.5024	2.3532	784.91	0.246737	4151.59	8.1791	2.3642	784.44
825	0.506006	4215.19	8.5568	2.3705	793.36	0.252594	4210.89	8.2337	2.3805	793.01
850	0.517621	4274.66	8.6103	2.3866	801.73	0.258439	4270.59	8.2874	2.3959	801.45
875	0.529230	4334.52	8.6630	2.4027	810.00	0.264280	4330.68	8.3403	2.4114	809.78
900	0.540835	4394.79	8.7149	2.4189	818.15	0.270116	4391.17	8.3925	2.4270	818.01
925	0.552435	4455.47	8.7661	2.4351	826.21	0.275947	4452.04	8.4438	2.4427	826.12
950	0.564032	4516.55	8.8166	2.4512	834.18	0.281775	4513.30	8.4944	2.4583	834.14
975	0.575625	4578.03	8.8663	2.4673	842.05	0.287599	4574.95	8.5443	2.4739	842.06
1000	0.587214	4639.91	8.9154	2.4831	849.85	0.293419	4637.00	8.5935	2.4894	849.90
1025	0.598801	4702.19	8.9639	2.4989	857.56	0.299237	4699.42	8.6421	2.5048	857.65
1050	0.610384	4764.85	9.0117	2.5144	865.19	0.305051	4762.23	8.6900	2.5200	865.33
1075	0.621965	4827.91	9.0589	2.5298	872.75	0.310863	4825.42	8.7373	2.5350	872.92
1100	0.633544	4891.34	9.1055	2.5449	880.24	0.316673	4888.98	8.7840	2.5498	880.44
1125	0.645120	4955.15	9.1515	2.5598	887.66	0.322480	4952.91	8.8302	2.5645	887.89
1150	0.656695	5019.33	9.1970	2.5745	895.01	0.328285	5017.20	8.8757	2.5789	895.27
1175	0.668267	5083.87	9.2420	2.5889	902.30	0.334088	5081.85	8.9208	2.5931	902.59
1200	0.679837	5148.77	9.2864	2.6031	909.54	0.339890	5146.86	8.9653	2.6070	909.85
1225	0.691406	5214.02	9.3304	2.6170	916.71	0.345689	5212.20	9.0093	2.6207	917.04
1250	0.702973	5279.62	9.3738	2.6306	923.82	0.351488	5277.89	9.0527	2.6342	924.17
1275	0.714539	5345.55	9.4167	2.6440	930.88	0.357284	5343.91	9.0957	2.6474	931.25
1300	0.726104	5411.81	9.4592	2.6571	937.88	0.363080	5410.26	9.1382	2.6603	938.27
1325	0.737667	5478.40	9.5012	2.6699	944.84	0.368874	5476.92	9.1803	2.6730	945.24
1350	0.749229	5545.30	9.5427	2.6824	951.74	0.374666	5543.90	9.2219	2.6854	952.16
1375	0.760789	5612.52	9.5838	2.6947	958.59	0.380458	5611.19	9.2630	2.6975	959.03
1400	0.772349	5680.04	9.6245	2.7068	965.40	0.386249	5678.78	9.3037	2.7094	965.85
1425	0.783908	5747.85	9.6647	2.7185	972.15	0.392038	5746.66	9.3440	2.7211	972.62
1450	0.795466	5815.96	9.7045	2.7300	978.86	0.397827	5814.83	9.3838	2.7325	979.34
1475	0.807022	5884.35	9.7439	2.7413	985.53	0.403615	5883.28	9.4233	2.7436	986.02
1500	0.818578	5953.02	9.7829	2.7523	992.15	0.409402	5952.01	9.4623	2.7545	992.65
1525	0.830134	6021.97	9.8215	2.7630	998.73	0.415188	6021.00	9.5010	2.7652	999.24
1550	0.841688	6091.17	9.8597	2.7736	1005.3	0.420973	6090.27	9.5392	2.7756	1005.8
1575	0.853242	6160.64	9.8976	2.7839	1011.8	0.426758	6159.78	9.5771	2.7858	1012.3
1600	0.864795	6230.37	9.9351	2.7939	1018.2	0.432542	6229.55	9.6146	2.7958	1018.8
1625	0.876348	6300.34	9.9722	2.8038	1024.6	0.438325	6299.57	9.6517	2.8056	1025.2
1650	0.887900	6370.55	10.009	2.8134	1031.0	0.444108	6369.83	9.6885	2.8152	1031.6
1675	0.899451	6441.01	10.045	2.8229	1037.4	0.449891	6440.33	9.7249	2.8245	1037.9
1700	0.911002	6511.70	10.081	2.8321	1043.7	0.455672	6511.06	9.7610	2.8337	1044.2
1725	0.922552	6582.61	10.117	2.8412	1049.9	0.461454	6582.01	9.7967	2.8428	1050.5
1750	0.934102	6653.75	10.152	2.8501	1056.2	0.467234	6653.19	9.8321	2.8516	1056.7
1775	0.945651	6725.12	10.188	2.8589	1062.3	0.473015	6724.59	9.8672	2.8603	1062.9
1800	0.957200	6796.70	10.222	2.8674	1068.5	0.478794	6796.21	9.9019	2.8688	1069.1
1850	0.980297	6940.49	10.291	2.8842	1080.7	0.490353	6940.07	9.9705	2.8855	1081.3
1900	1.00339	7085.11	10.358	2.9004	1092.8	0.501910	7084.74	10.038	2.9016	1093.4
1950	1.02649	7230.53	10.424	2.9163	1104.7	0.513466	7230.22	10.104	2.9173	1105.3
2000	1.04958	7376.73	10.489	2.9317	1116.5	0.525020	7376.47	10.169	2.9328	1117.1

Table 4 High-temperature region – Continued (800 °C to 2000 °C)

	p = 50 bar					p = 100 bar				
t	v	h	s	c_p	w	v	h	s	c_p	w
[°C]	[$m^3\,kg^{-1}$]	[$kJ\,kg^{-1}$]	[$kJ\,kg^{-1}\,K^{-1}$]	[$kJ\,kg^{-1}\,K^{-1}$]	[$m\,s^{-1}$]	[$m^3\,kg^{-1}$]	[$kJ\,kg^{-1}$]	[$kJ\,kg^{-1}\,K^{-1}$]	[$kJ\,kg^{-1}\,K^{-1}$]	[$m\,s^{-1}$]
800	0.098151	4137.87	7.7459	2.3978	783.12	0.048624	4114.73	7.4087	2.4555	781.12
825	0.100547	4197.92	7.8012	2.4110	791.98	0.049866	4176.13	7.4652	2.4639	790.40
850	0.102931	4258.36	7.8556	2.4242	800.65	0.051098	4237.84	7.5207	2.4731	799.44
875	0.105311	4319.14	7.9091	2.4378	809.19	0.052324	4299.79	7.5753	2.4831	808.32
900	0.107686	4380.25	7.9618	2.4517	817.59	0.053546	4362.00	7.6289	2.4937	817.04
925	0.110056	4441.72	8.0136	2.4657	825.88	0.054762	4424.48	7.6816	2.5048	825.61
950	0.112422	4503.54	8.0647	2.4799	834.06	0.055975	4487.24	7.7334	2.5164	834.04
975	0.114785	4565.71	8.1150	2.4941	842.13	0.057184	4550.30	7.7845	2.5282	842.35
1000	0.117144	4628.25	8.1646	2.5083	850.10	0.058389	4613.66	7.8347	2.5403	850.53
1025	0.119500	4691.13	8.2136	2.5226	857.97	0.059592	4677.32	7.8843	2.5526	858.61
1050	0.121853	4754.37	8.2618	2.5367	865.76	0.060791	4741.29	7.9331	2.5649	866.58
1075	0.124204	4817.97	8.3094	2.5508	873.46	0.061988	4805.57	7.9812	2.5773	874.45
1100	0.126552	4881.91	8.3564	2.5648	881.07	0.063182	4870.16	8.0287	2.5898	882.22
1125	0.128898	4946.20	8.4028	2.5786	888.61	0.064374	4935.05	8.0755	2.6022	889.91
1150	0.131241	5010.84	8.4486	2.5922	896.08	0.065564	5000.26	8.1217	2.6145	897.51
1175	0.133583	5075.81	8.4939	2.6057	903.47	0.066752	5065.78	8.1674	2.6268	905.03
1200	0.135923	5141.12	8.5386	2.6190	910.80	0.067938	5131.60	8.2124	2.6390	912.47
1225	0.138261	5206.76	8.5828	2.6321	918.06	0.069122	5197.73	8.2569	2.6510	919.83
1250	0.140598	5272.72	8.6265	2.6449	925.26	0.070305	5264.15	8.3009	2.6629	927.13
1275	0.142933	5339.01	8.6696	2.6576	932.39	0.071486	5330.87	8.3444	2.6747	934.36
1300	0.145267	5405.60	8.7123	2.6700	939.47	0.072666	5397.88	8.3873	2.6863	941.52
1325	0.147599	5472.51	8.7545	2.6822	946.48	0.073845	5465.18	8.4297	2.6977	948.62
1350	0.149931	5539.71	8.7962	2.6942	953.45	0.075022	5532.77	8.4717	2.7089	955.65
1375	0.152261	5607.21	8.8375	2.7059	960.36	0.076198	5600.63	8.5132	2.7200	962.63
1400	0.154590	5675.01	8.8783	2.7175	967.22	0.077373	5668.76	8.5542	2.7308	969.55
1425	0.156918	5743.09	8.9187	2.7287	974.02	0.078548	5737.17	8.5948	2.7415	976.42
1450	0.159245	5811.44	8.9587	2.7398	980.78	0.079721	5805.83	8.6349	2.7520	983.23
1475	0.161572	5880.07	8.9982	2.7506	987.49	0.080893	5874.76	8.6746	2.7622	989.99
1500	0.163897	5948.97	9.0373	2.7612	994.15	0.082065	5943.94	8.7139	2.7723	996.70
1525	0.166222	6018.13	9.0761	2.7716	1000.8	0.083236	6013.38	8.7528	2.7822	1003.4
1550	0.168546	6087.55	9.1144	2.7817	1007.3	0.084406	6083.05	8.7913	2.7919	1010.0
1575	0.170869	6157.22	9.1524	2.7917	1013.9	0.085575	6152.97	8.8294	2.8015	1016.5
1600	0.173192	6227.13	9.1899	2.8014	1020.4	0.086744	6223.13	8.8671	2.8108	1023.1
1625	0.175513	6297.29	9.2271	2.8110	1026.8	0.087912	6293.51	8.9044	2.8200	1029.5
1650	0.177835	6367.68	9.2640	2.8204	1033.2	0.089079	6364.12	8.9414	2.8290	1036.0
1675	0.180156	6438.30	9.3005	2.8295	1039.6	0.090246	6434.96	8.9780	2.8378	1042.4
1700	0.182476	6509.15	9.3366	2.8385	1045.9	0.091412	6506.01	9.0142	2.8465	1048.7
1725	0.184796	6580.23	9.3724	2.8474	1052.2	0.092578	6577.28	9.0501	2.8550	1055.0
1750	0.187115	6651.52	9.4078	2.8560	1058.4	0.093744	6648.76	9.0857	2.8634	1061.3
1775	0.189434	6723.03	9.4430	2.8645	1064.6	0.094909	6720.45	9.1209	2.8716	1067.5
1800	0.191752	6794.75	9.4778	2.8729	1070.8	0.096073	6792.34	9.1558	2.8797	1073.7
1850	0.196388	6938.80	9.5464	2.8893	1083.0	0.098401	6936.72	9.2246	2.8956	1086.0
1900	0.201022	7083.66	9.6139	2.9051	1095.1	0.100727	7081.89	9.2922	2.9110	1098.1
1950	0.205654	7229.31	9.6801	2.9206	1107.1	0.103052	7227.82	9.3586	2.9261	1110.1
2000	0.210286	7375.72	9.7453	2.9358	1118.9	0.105376	7374.49	9.4238	2.9409	1121.9

Table 4 High-temperature region – Continued (800 °C to 2000 °C)

t	p = 200 bar					p = 300 bar				
	v	h	s	c_p	w	v	h	s	c_p	w
[°C]	[$m^3\,kg^{-1}$]	[$kJ\,kg^{-1}$]	[$kJ\,kg^{-1}\,K^{-1}$]	[$kJ\,kg^{-1}\,K^{-1}$]	[$m\,s^{-1}$]	[$m^3\,kg^{-1}$]	[$kJ\,kg^{-1}$]	[$kJ\,kg^{-1}\,K^{-1}$]	[$kJ\,kg^{-1}\,K^{-1}$]	[$m\,s^{-1}$]
800	0.023869	4067.73	7.0534	2.5775	777.99	0.015629	4020.23	6.8303	2.7072	776.14
825	0.024533	4132.09	7.1126	2.5757	787.91	0.016100	4087.79	6.8924	2.6937	786.59
850	0.025189	4196.48	7.1705	2.5755	797.67	0.016564	4154.99	6.9529	2.6829	796.99
875	0.025839	4260.88	7.2273	2.5774	807.19	0.017022	4221.96	7.0119	2.6754	807.08
900	0.026484	4325.36	7.2828	2.5808	816.50	0.017475	4288.78	7.0695	2.6707	816.91
925	0.027124	4389.93	7.3373	2.5855	825.60	0.017922	4355.51	7.1257	2.6683	826.49
950	0.027760	4454.64	7.3907	2.5913	834.53	0.018366	4422.21	7.1808	2.6679	835.85
975	0.028392	4519.51	7.4432	2.5980	843.28	0.018805	4488.92	7.2348	2.6690	845.00
1000	0.029021	4584.55	7.4948	2.6055	851.88	0.019241	4555.67	7.2878	2.6715	853.96
1025	0.029646	4649.79	7.5456	2.6135	860.33	0.019674	4622.50	7.3398	2.6751	862.75
1050	0.030268	4715.23	7.5955	2.6220	868.65	0.020103	4689.44	7.3908	2.6796	871.37
1075	0.030888	4780.89	7.6447	2.6310	876.84	0.020530	4756.49	7.4410	2.6849	879.84
1100	0.031505	4846.78	7.6931	2.6402	884.91	0.020955	4823.68	7.4904	2.6908	888.17
1125	0.032120	4912.90	7.7408	2.6497	892.86	0.021377	4891.03	7.5390	2.6972	896.37
1150	0.032733	4979.27	7.7879	2.6593	900.71	0.021797	4958.55	7.5869	2.7041	904.44
1175	0.033343	5045.87	7.8343	2.6691	908.46	0.022215	5026.24	7.6340	2.7114	912.39
1200	0.033952	5112.72	7.8800	2.6790	916.12	0.022631	5094.12	7.6805	2.7189	920.24
1225	0.034559	5179.82	7.9252	2.6889	923.69	0.023046	5162.19	7.7263	2.7267	927.98
1250	0.035165	5247.17	7.9698	2.6989	931.17	0.023458	5230.46	7.7715	2.7346	935.62
1275	0.035769	5314.77	8.0138	2.7088	938.56	0.023870	5298.92	7.8161	2.7427	943.17
1300	0.036372	5382.61	8.0573	2.7186	945.88	0.024280	5367.59	7.8601	2.7508	950.63
1325	0.036973	5450.70	8.1002	2.7285	953.13	0.024689	5436.46	7.9035	2.7590	958.00
1350	0.037574	5519.03	8.1426	2.7382	960.30	0.025097	5505.54	7.9464	2.7673	965.30
1375	0.038173	5587.61	8.1846	2.7479	967.41	0.025503	5574.83	7.9888	2.7755	972.52
1400	0.038771	5656.42	8.2260	2.7574	974.45	0.025909	5644.32	8.0306	2.7838	979.66
1425	0.039368	5725.48	8.2670	2.7669	981.42	0.026313	5714.02	8.0720	2.7920	986.73
1450	0.039964	5794.77	8.3075	2.7762	988.34	0.026717	5783.92	8.1129	2.8002	993.73
1475	0.040559	5864.29	8.3475	2.7854	995.19	0.027120	5854.02	8.1532	2.8083	1000.7
1500	0.041154	5934.03	8.3871	2.7945	1002.0	0.027522	5924.33	8.1932	2.8164	1007.5
1525	0.041748	6004.01	8.4263	2.8034	1008.7	0.027923	5994.84	8.2327	2.8244	1014.4
1550	0.042340	6074.20	8.4651	2.8122	1015.4	0.028323	6065.55	8.2717	2.8323	1021.1
1575	0.042933	6144.62	8.5035	2.8209	1022.1	0.028723	6136.45	8.3103	2.8401	1027.8
1600	0.043524	6215.25	8.5414	2.8294	1028.6	0.029122	6207.55	8.3486	2.8478	1034.5
1625	0.044115	6286.09	8.5790	2.8378	1035.2	0.029521	6278.85	8.3864	2.8555	1041.0
1650	0.044706	6357.14	8.6162	2.8461	1041.7	0.029919	6350.33	8.4238	2.8630	1047.6
1675	0.045296	6428.39	8.6530	2.8542	1048.1	0.030316	6422.00	8.4608	2.8705	1054.1
1700	0.045885	6499.85	8.6894	2.8623	1054.5	0.030713	6493.85	8.4975	2.8779	1060.5
1725	0.046474	6571.50	8.7255	2.8702	1060.9	0.031109	6565.89	8.5337	2.8852	1066.9
1750	0.047062	6643.35	8.7612	2.8780	1067.2	0.031505	6638.11	8.5697	2.8924	1073.2
1775	0.047650	6715.40	8.7966	2.8856	1073.4	0.031901	6710.51	8.6052	2.8995	1079.5
1800	0.048237	6787.63	8.8317	2.8932	1079.7	0.032296	6783.08	8.6404	2.9066	1085.8
1850	0.049411	6932.67	8.9008	2.9081	1092.0	0.033085	6928.76	8.7099	2.9205	1098.2
1900	0.050584	7078.44	8.9687	2.9226	1104.2	0.033872	7075.12	8.7780	2.9341	1110.4
1950	0.051755	7224.93	9.0353	2.9369	1116.2	0.034658	7222.17	8.8449	2.9476	1122.4
2000	0.052924	7372.13	9.1008	2.9510	1128.0	0.035443	7369.88	8.9106	2.9610	1134.3

Table 4 High-temperature region – Continued (800 °C to 2000 °C)

t	p = 400 bar					p = 500 bar				
t	v	h	s	c_p	w	v	h	s	c_p	w
[°C]	[$m^3\,kg^{-1}$]	[$kJ\,kg^{-1}$]	[$kJ\,kg^{-1}\,K^{-1}$]	[$kJ\,kg^{-1}\,K^{-1}$]	[$m\,s^{-1}$]	[$m^3\,kg^{-1}$]	[$kJ\,kg^{-1}$]	[$kJ\,kg^{-1}\,K^{-1}$]	[$kJ\,kg^{-1}\,K^{-1}$]	[$m\,s^{-1}$]
800	0.011523	3972.81	6.6614	2.8428	775.83	0.009074	3925.96	6.5226	2.9813	777.37
825	0.011897	4043.64	6.7266	2.8158	786.78	0.009389	4000.07	6.5908	2.9395	788.87
850	0.012264	4113.74	6.7897	2.7931	797.69	0.009697	4073.10	6.6566	2.9042	800.12
875	0.012625	4183.33	6.8510	2.7755	808.26	0.010000	4145.33	6.7202	2.8759	811.00
900	0.012981	4252.55	6.9106	2.7620	818.51	0.010297	4216.94	6.7819	2.8533	821.53
925	0.013332	4321.47	6.9687	2.7521	828.48	0.010589	4288.04	6.8419	2.8355	831.77
950	0.013679	4390.17	7.0255	2.7450	838.19	0.010876	4358.75	6.9003	2.8216	841.72
975	0.014021	4458.74	7.0810	2.7403	847.66	0.011160	4429.15	6.9573	2.8109	851.42
1000	0.014360	4527.21	7.1353	2.7376	856.92	0.011441	4499.31	7.0129	2.8029	860.89
1025	0.014696	4595.63	7.1885	2.7365	865.98	0.011718	4569.31	7.0674	2.7972	870.14
1050	0.015029	4664.04	7.2407	2.7369	874.85	0.011992	4639.19	7.1207	2.7934	879.20
1075	0.015359	4732.48	7.2920	2.7385	883.55	0.012264	4709.00	7.1730	2.7913	888.07
1100	0.015687	4800.98	7.3423	2.7410	892.10	0.012533	4778.77	7.2242	2.7904	896.78
1125	0.016012	4869.54	7.3918	2.7444	900.49	0.012800	4848.53	7.2746	2.7908	905.32
1150	0.016336	4938.20	7.4405	2.7485	908.75	0.013065	4918.31	7.3240	2.7921	913.71
1175	0.016657	5006.97	7.4884	2.7532	916.87	0.013328	4988.14	7.3727	2.7943	921.97
1200	0.016977	5075.87	7.5355	2.7584	924.88	0.013590	5058.03	7.4205	2.7971	930.09
1225	0.017295	5144.89	7.5820	2.7640	932.76	0.013849	5128.00	7.4676	2.8006	938.09
1250	0.017611	5214.07	7.6278	2.7699	940.54	0.014107	5198.07	7.5140	2.8046	945.97
1275	0.017926	5283.39	7.6729	2.7761	948.22	0.014364	5268.23	7.5597	2.8090	953.74
1300	0.018239	5352.88	7.7175	2.7826	955.79	0.014620	5338.52	7.6047	2.8137	961.41
1325	0.018552	5422.52	7.7614	2.7892	963.28	0.014874	5408.92	7.6492	2.8188	968.97
1350	0.018863	5492.34	7.8047	2.7960	970.67	0.015127	5479.46	7.6929	2.8241	976.44
1375	0.019173	5562.32	7.8475	2.8028	977.98	0.015379	5550.13	7.7362	2.8296	983.83
1400	0.019482	5632.48	7.8898	2.8098	985.21	0.015630	5620.94	7.7788	2.8353	991.12
1425	0.019790	5702.81	7.9315	2.8168	992.36	0.015880	5691.90	7.8209	2.8412	998.34
1450	0.020097	5773.32	7.9727	2.8239	999.44	0.016129	5763.00	7.8625	2.8471	1005.5
1475	0.020404	5844.01	8.0134	2.8309	1006.4	0.016378	5834.25	7.9035	2.8531	1012.5
1500	0.020709	5914.87	8.0537	2.8380	1013.4	0.016625	5905.66	7.9441	2.8592	1019.5
1525	0.021014	5985.90	8.0935	2.8450	1020.3	0.016872	5977.21	7.9841	2.8653	1026.4
1550	0.021318	6057.12	8.1328	2.8520	1027.1	0.017118	6048.92	8.0237	2.8715	1033.3
1575	0.021622	6128.51	8.1717	2.8590	1033.8	0.017364	6120.79	8.0629	2.8776	1040.1
1600	0.021924	6200.07	8.2101	2.8660	1040.5	0.017609	6192.80	8.1016	2.8838	1046.8
1625	0.022227	6271.80	8.2482	2.8729	1047.1	0.017853	6264.98	8.1399	2.8900	1053.5
1650	0.022528	6343.71	8.2858	2.8797	1053.7	0.018097	6337.30	8.1777	2.8961	1060.1
1675	0.022829	6415.79	8.3231	2.8865	1060.2	0.018340	6409.78	8.2152	2.9023	1066.6
1700	0.023130	6488.04	8.3599	2.8933	1066.7	0.018582	6482.42	8.2522	2.9084	1073.1
1725	0.023430	6560.45	8.3964	2.9000	1073.1	0.018825	6555.20	8.2889	2.9145	1079.5
1750	0.023729	6633.03	8.4325	2.9066	1079.5	0.019066	6628.14	8.3252	2.9206	1085.9
1775	0.024029	6705.78	8.4682	2.9132	1085.8	0.019308	6701.23	8.3611	2.9267	1092.3
1800	0.024327	6778.69	8.5036	2.9197	1092.1	0.019549	6774.47	8.3966	2.9327	1098.6
1850	0.024924	6925.00	8.5733	2.9327	1104.5	0.020029	6921.41	8.4666	2.9447	1111.0
1900	0.025519	7071.96	8.6417	2.9455	1116.7	0.020509	7068.94	8.5353	2.9567	1123.3
1950	0.026112	7219.55	8.7089	2.9582	1128.8	0.020987	7217.07	8.6027	2.9686	1135.3
2000	0.026705	7367.77	8.7748	2.9708	1140.7	0.021463	7365.80	8.6689	2.9805	1147.3

Table 5 Ideal-gas state

This table contains values for the following thermodynamic properties in the ideal-gas state for temperatures from 0 °C to 2000 °C:

- Specific isobaric heat capacity c_p^{o}
- Specific isochoric heat capacity c_v^{o}
- Specific enthalpy h^{o}
- Specific entropy s^{o} (p_0 = 0.006 112 127 bar)
- Speed of sound w^{o}
- Isentropic exponent κ^{o}
- Mean specific isobaric heat capacity $c_{p,\mathrm{m}}^{\mathrm{o}} = c_p^{\mathrm{o}}\Big|_{t_0}^{t} = \dfrac{1}{t-t_0}\displaystyle\int_{T_0}^{T} c_p^{\mathrm{o}}(T)\,\mathrm{d}T$ between the reference temperature t_0 = 0 °C and the tabulated temperature t

These thermodynamic properties were calculated from Eq. (2.7) for temperatures $t \leq 800$ °C and from Eq. (2.16) for temperatures $t > 800$ °C.

The listed values for the specific enthalpy h^{o}, the specific entropy s^{o}, and the mean specific isobaric heat capacity $c_{p,\mathrm{m}}^{\mathrm{o}}$ relate to the reference temperature t_0 = 0 °C, and for s^{o}, in addition, to the reference pressure p_0 = 0.006 112 127 bar. Due to this very low pressure, the difference (arising from the real-gas contribution) between the values for s given in Table 3 (for this pressure) and for s^{o} listed in this table is very small. The reference values for $h^{\mathrm{o}}(t_0)$ and $s^{\mathrm{o}}(p_0, t_0)$ are in accordance with the zero points of the specific internal energy and specific entropy given by Eq. (2.4).

Specific entropy values for pressures $p \neq p_0$ can be calculated from the equation

$$s^{\mathrm{o}}(p,t) = s^{\mathrm{o}}(p_0,t) - R\ln\left(\frac{p}{p_0}\right),$$

where the values $s^{\mathrm{o}}(p_0, t)$ are listed in the table, and R = 0.461 526 kJ kg^{-1} K^{-1} is the specific gas constant of water according to Eq. (1.1).

Table 5 Ideal-gas state

t	c_p^o	c_v^o	h^o	s^o	w^o	κ^o	$c_{p,m}^o$
				$p_0 = 0.006112127$ bar			
[°C]	[kJ kg^{-1} K^{-1}]	[kJ kg^{-1} K^{-1}]	[kJ kg^{-1}]	[kJ kg^{-1} K^{-1}]	[m s^{-1}]	[–]	[kJ kg^{-1} K^{-1}]
0	1.8589	1.3974	2501.42	9.1574	409.52	1.3303	1.8589
10	1.8611	1.3996	2520.02	9.2243	416.86	1.3298	1.8600
20	1.8634	1.4018	2538.64	9.2890	424.08	1.3292	1.8611
25	1.8646	1.4030	2547.96	9.3205	427.63	1.3289	1.8617
30	1.8658	1.4043	2557.29	9.3515	431.16	1.3287	1.8623
40	1.8685	1.4069	2575.96	9.4121	438.11	1.3280	1.8635
50	1.8714	1.4098	2594.66	9.4709	444.93	1.3274	1.8648
60	1.8745	1.4130	2613.39	9.5279	451.64	1.3266	1.8661
70	1.8780	1.4164	2632.15	9.5834	458.23	1.3258	1.8676
80	1.8816	1.4201	2650.95	9.6374	464.71	1.3250	1.8691
90	1.8856	1.4240	2669.78	9.6900	471.09	1.3241	1.8707
100	1.8897	1.4282	2688.66	9.7413	477.36	1.3232	1.8724
110	1.8941	1.4326	2707.58	9.7913	483.53	1.3222	1.8742
120	1.8986	1.4371	2726.54	9.8402	489.61	1.3211	1.8760
130	1.9034	1.4418	2745.55	9.8879	495.60	1.3201	1.8779
140	1.9082	1.4467	2764.61	9.9346	501.51	1.3190	1.8799
150	1.9133	1.4517	2783.72	9.9803	507.33	1.3179	1.8820
160	1.9184	1.4569	2802.87	10.025	513.07	1.3168	1.8841
170	1.9237	1.4622	2822.08	10.069	518.73	1.3156	1.8863
180	1.9291	1.4676	2841.35	10.112	524.32	1.3145	1.8885
190	1.9346	1.4731	2860.67	10.154	529.84	1.3133	1.8908
200	1.9402	1.4786	2880.04	10.195	535.29	1.3121	1.8931
210	1.9458	1.4843	2899.47	10.236	540.67	1.3109	1.8955
220	1.9516	1.4900	2918.96	10.276	545.99	1.3097	1.8979
230	1.9573	1.4958	2938.50	10.315	551.24	1.3085	1.9004
240	1.9632	1.5017	2958.10	10.354	556.43	1.3073	1.9029
250	1.9691	1.5076	2977.77	10.392	561.57	1.3061	1.9054
260	1.9751	1.5136	2997.49	10.429	566.65	1.3049	1.9080
270	1.9811	1.5196	3017.27	10.466	571.68	1.3037	1.9106
280	1.9872	1.5257	3037.11	10.502	576.65	1.3025	1.9132
290	1.9933	1.5318	3057.01	10.538	581.56	1.3013	1.9158
300	1.9995	1.5380	3076.98	10.573	586.43	1.3001	1.9185
310	2.0057	1.5442	3097.00	10.608	591.25	1.2989	1.9212
320	2.0120	1.5504	3117.09	10.642	596.02	1.2977	1.9240
330	2.0183	1.5567	3137.24	10.675	600.75	1.2965	1.9267
340	2.0246	1.5631	3157.46	10.709	605.43	1.2953	1.9295
350	2.0310	1.5695	3177.73	10.741	610.06	1.2941	1.9323
360	2.0374	1.5759	3198.08	10.774	614.65	1.2929	1.9352
370	2.0438	1.5823	3218.48	10.806	619.20	1.2917	1.9380
380	2.0503	1.5888	3238.95	10.837	623.71	1.2905	1.9409
390	2.0569	1.5953	3259.49	10.869	628.17	1.2893	1.9438
400	2.0634	1.6019	3280.09	10.899	632.60	1.2881	1.9467
410	2.0700	1.6085	3300.76	10.930	636.99	1.2869	1.9496
420	2.0767	1.6151	3321.49	10.960	641.34	1.2858	1.9526
430	2.0833	1.6218	3342.29	10.990	645.66	1.2846	1.9555
440	2.0900	1.6285	3363.16	11.019	649.94	1.2834	1.9585

Table 5 Ideal-gas state – Continued

$p_0 = 0.006112127$ bar

t [ºC]	c_p^o [kJ kg^{-1} K^{-1}]	c_v^o [kJ kg^{-1} K^{-1}]	h^o [kJ kg^{-1}]	s^o [kJ kg^{-1} K^{-1}]	w^o [m s^{-1}]	κ^o [–]	$c_{p,m}^o$ [kJ kg^{-1} K^{-1}]
450	2.0968	1.6352	3384.09	11.048	654.18	1.2822	1.9615
460	2.1035	1.6420	3405.09	11.077	658.39	1.2811	1.9645
470	2.1103	1.6488	3426.16	11.106	662.56	1.2799	1.9675
480	2.1171	1.6556	3447.30	11.134	666.71	1.2788	1.9706
490	2.1240	1.6625	3468.51	11.162	670.82	1.2776	1.9736
500	2.1309	1.6693	3489.78	11.190	674.89	1.2765	1.9767
510	2.1378	1.6763	3511.12	11.217	678.94	1.2753	1.9798
520	2.1447	1.6832	3532.54	11.244	682.96	1.2742	1.9829
530	2.1517	1.6901	3554.02	11.271	686.95	1.2731	1.9860
540	2.1586	1.6971	3575.57	11.298	690.91	1.2720	1.9892
550	2.1656	1.7041	3597.19	11.324	694.84	1.2708	1.9923
560	2.1726	1.7111	3618.88	11.351	698.74	1.2697	1.9955
570	2.1796	1.7181	3640.64	11.376	702.61	1.2686	1.9986
580	2.1867	1.7251	3662.47	11.402	706.46	1.2675	2.0018
590	2.1937	1.7322	3684.38	11.428	710.29	1.2664	2.0050
600	2.2008	1.7392	3706.35	11.453	714.08	1.2654	2.0082
610	2.2078	1.7463	3728.39	11.478	717.86	1.2643	2.0114
620	2.2149	1.7534	3750.51	11.503	721.61	1.2632	2.0147
630	2.2220	1.7605	3772.69	11.528	725.33	1.2622	2.0179
640	2.2291	1.7676	3794.95	11.552	729.03	1.2611	2.0211
650	2.2362	1.7746	3817.27	11.577	732.71	1.2601	2.0244
660	2.2433	1.7817	3839.67	11.601	736.36	1.2590	2.0277
670	2.2504	1.7888	3862.14	11.625	740.00	1.2580	2.0309
680	2.2574	1.7959	3884.68	11.648	743.61	1.2570	2.0342
690	2.2645	1.8030	3907.29	11.672	747.20	1.2560	2.0375
700	2.2716	1.8101	3929.97	11.695	750.77	1.2550	2.0408
710	2.2787	1.8172	3952.72	11.719	754.32	1.2540	2.0441
720	2.2858	1.8243	3975.54	11.742	757.84	1.2530	2.0474
730	2.2929	1.8313	3998.43	11.765	761.35	1.2520	2.0507
740	2.2999	1.8384	4021.40	11.788	764.84	1.2510	2.0540
750	2.3070	1.8455	4044.43	11.810	768.31	1.2501	2.0574
760	2.3141	1.8525	4067.54	11.833	771.76	1.2491	2.0607
770	2.3211	1.8596	4090.71	11.855	775.20	1.2482	2.0640
780	2.3282	1.8666	4113.96	11.877	778.61	1.2472	2.0674
790	2.3352	1.8737	4137.28	11.899	782.01	1.2463	2.0707
800	2.3423	1.8808	4160.66	11.921	785.38	1.2454	2.0741
820	2.3572	1.8957	4207.69	11.964	792.05	1.2435	2.0808
840	2.3707	1.9091	4254.97	12.007	798.71	1.2417	2.0876
860	2.3841	1.9226	4302.52	12.050	805.31	1.2401	2.0943
880	2.3975	1.9360	4350.33	12.091	811.84	1.2384	2.1010
900	2.4109	1.9494	4398.42	12.133	818.31	1.2368	2.1078
920	2.4243	1.9627	4446.77	12.174	824.72	1.2351	2.1145
940	2.4376	1.9760	4495.39	12.214	831.07	1.2336	2.1212
960	2.4508	1.9892	4544.27	12.254	837.36	1.2320	2.1280
980	2.4639	2.0024	4593.42	12.294	843.60	1.2305	2.1347

Table 5 Ideal-gas state – Continued

$p_0 = 0.006112127$ bar

t [°C]	c_p^o [kJ kg^{-1} K^{-1}]	c_v^o [kJ kg^{-1} K^{-1}]	h^o [kJ kg^{-1}]	s^o [kJ kg^{-1} K^{-1}]	w^o [m s^{-1}]	κ^o [–]	$c_{p,m}^o$ [kJ kg^{-1} K^{-1}]
1000	2.4769	2.0154	4642.83	12.333	849.80	1.2290	2.1414
1020	2.4898	2.0283	4692.49	12.371	855.94	1.2275	2.1481
1040	2.5025	2.0410	4742.42	12.410	862.03	1.2261	2.1548
1060	2.5152	2.0536	4792.59	12.448	868.08	1.2247	2.1615
1080	2.5276	2.0661	4843.02	12.485	874.08	1.2234	2.1682
1100	2.5400	2.0784	4893.70	12.522	880.04	1.2221	2.1748
1120	2.5521	2.0906	4944.62	12.559	885.96	1.2208	2.1814
1140	2.5641	2.1026	4995.78	12.596	891.83	1.2195	2.1880
1160	2.5759	2.1144	5047.18	12.632	897.67	1.2183	2.1946
1180	2.5876	2.1261	5098.82	12.668	903.47	1.2171	2.2012
1200	2.5991	2.1376	5150.69	12.703	909.23	1.2159	2.2077
1220	2.6104	2.1489	5202.78	12.738	914.95	1.2148	2.2142
1240	2.6215	2.1600	5255.10	12.773	920.64	1.2137	2.2207
1260	2.6325	2.1709	5307.64	12.807	926.29	1.2126	2.2272
1280	2.6432	2.1817	5360.40	12.842	931.91	1.2115	2.2336
1300	2.6538	2.1923	5413.37	12.876	937.50	1.2105	2.2400
1320	2.6642	2.2027	5466.55	12.909	943.05	1.2095	2.2463
1340	2.6745	2.2129	5519.94	12.942	948.57	1.2086	2.2526
1360	2.6845	2.2230	5573.53	12.975	954.06	1.2076	2.2589
1380	2.6944	2.2329	5627.31	13.008	959.52	1.2067	2.2651
1400	2.7041	2.2426	5681.30	13.041	964.95	1.2058	2.2713
1420	2.7136	2.2521	5735.48	13.073	970.35	1.2049	2.2775
1440	2.7230	2.2614	5789.84	13.105	975.72	1.2041	2.2836
1460	2.7322	2.2706	5844.39	13.136	981.06	1.2033	2.2897
1480	2.7412	2.2797	5899.13	13.168	986.37	1.2025	2.2957
1500	2.7501	2.2885	5954.04	13.199	991.66	1.2017	2.3017
1520	2.7588	2.2972	6009.13	13.230	996.92	1.2009	2.3077
1540	2.7673	2.3058	6064.39	13.260	1002.2	1.2002	2.3136
1560	2.7757	2.3142	6119.82	13.291	1007.4	1.1994	2.3195
1580	2.7839	2.3224	6175.42	13.321	1012.5	1.1987	2.3253
1600	2.7921	2.3305	6231.18	13.351	1017.7	1.1980	2.3311
1620	2.8000	2.3385	6287.10	13.381	1022.8	1.1974	2.3368
1640	2.8078	2.3463	6343.18	13.410	1027.9	1.1967	2.3425
1660	2.8155	2.3540	6399.41	13.439	1033.0	1.1961	2.3482
1680	2.8231	2.3616	6455.80	13.468	1038.1	1.1954	2.3538
1700	2.8305	2.3690	6512.33	13.497	1043.1	1.1948	2.3594
1720	2.8379	2.3763	6569.02	13.526	1048.1	1.1942	2.3649
1740	2.8451	2.3836	6625.85	13.554	1053.1	1.1936	2.3704
1760	2.8522	2.3907	6682.82	13.582	1058.1	1.1931	2.3758
1780	2.8592	2.3977	6739.94	13.610	1063.0	1.1925	2.3812
1800	2.8661	2.4045	6797.19	13.638	1067.9	1.1919	2.3865
1850	2.8829	2.4214	6940.91	13.707	1080.1	1.1906	2.3997
1900	2.8992	2.4377	7085.47	13.774	1092.2	1.1893	2.4127
1950	2.9152	2.4536	7230.83	13.840	1104.1	1.1881	2.4253
2000	2.9307	2.4692	7376.98	13.905	1115.9	1.1869	2.4378

Table 6 Saturation state: Compression factor z, Specific isochoric heat capacity c_v, Isobaric cubic expansion coefficient α_v, Isothermal compressibility κ_T

This table contains values on the saturated liquid (′) and saturated vapour (″) lines for the following thermodynamic properties for temperatures from $t = 0$ °C up to the critical temperature t_c = 373.946 °C:

- Compression factor (real-gas factor) $z = pv/(RT)$
- Specific isochoric heat capacity c_v
- Isobaric cubic expansion coefficient $\alpha_v = v^{-1}(\partial v/\partial T)_p$
- Isothermal compressibility $\kappa_T = -v^{-1}(\partial v/\partial p)_T$

For given temperatures, the saturation pressures p_s were calculated from the IAPWS-IF97 saturation-pressure equation, Eq. (2.13).

For temperatures $t \le 350$ °C and input values of t and p_s, the properties on the saturated-liquid and saturated-vapour lines were determined from the basic equations for regions 1 and 2, Eqs. (2.3) and (2.6).

For $t > 350$ °C and input values of t and p_s, the densities ρ' and ρ'' (and thus also the specific volumes v' and v'') were calculated by iterating the basic equation for region 3, Eq. (2.11). With the values of (ρ', t) and (ρ'', t), the other thermodynamic properties were determined from the basic equation, Eq. (2.11).

Table 6 Saturation state: Compression factor z, Specific isochoric heat capacity c_v, Isobaric cubic expansion coefficient α_v, Isothermal compressibility κ_T

t [°C]	z' [–]	z'' [–]	c'_v [kJ kg^{-1} K^{-1}]	c''_v [kJ kg^{-1} K^{-1}]	α'_v [10^{-6} K^{-1}]	α''_v [10^{-6} K^{-1}]	κ'_T [10^{-6} kPa^{-1}]	κ''_T [10^{-6} kPa^{-1}]
0	0.00000	0.99944	4.2174	1.4221	−68.073	3681.2	0.50895	1637128
0.01[a]	0.00000	0.99944	4.2174	1.4221	−67.890	3681.1	0.50891	1635939
1	0.00001	0.99941	4.2151	1.4226	−50.101	3668.4	0.50522	1522872
2	0.00001	0.99939	4.2128	1.4232	−32.744	3655.7	0.50164	1417432
3	0.00001	0.99936	4.2103	1.4237	−15.967	3643.2	0.49822	1320068
4	0.00001	0.99933	4.2078	1.4243	0.26721	3630.7	0.49494	1230105
5	0.00001	0.99930	4.2052	1.4248	15.989	3618.4	0.49180	1146932
6	0.00001	0.99927	4.2026	1.4254	31.229	3606.2	0.48880	1069989
7	0.00001	0.99923	4.1999	1.4261	46.014	3594.1	0.48592	998769
8	0.00001	0.99920	4.1971	1.4267	60.370	3582.1	0.48317	932806
9	0.00001	0.99916	4.1942	1.4274	74.321	3570.3	0.48054	871678
10	0.00001	0.99912	4.1912	1.4280	87.889	3558.5	0.47802	814997
11	0.00001	0.99909	4.1882	1.4287	101.09	3546.9	0.47562	762411
12	0.00001	0.99905	4.1851	1.4294	113.96	3535.3	0.47332	713596
13	0.00001	0.99900	4.1820	1.4302	126.50	3523.9	0.47112	668257
14	0.00001	0.99896	4.1787	1.4309	138.73	3512.6	0.46903	626124
15	0.00001	0.99892	4.1754	1.4317	150.67	3501.4	0.46703	586948
16	0.00001	0.99887	4.1720	1.4325	162.33	3490.3	0.46512	550502
17	0.00001	0.99882	4.1686	1.4333	173.72	3479.3	0.46330	516579
18	0.00002	0.99877	4.1650	1.4341	184.87	3468.4	0.46157	484987
19	0.00002	0.99872	4.1615	1.4350	195.78	3457.6	0.45993	455551
20	0.00002	0.99867	4.1578	1.4358	206.46	3446.9	0.45836	428109
22	0.00002	0.99856	4.1503	1.4376	227.18	3425.8	0.45547	378629
24	0.00002	0.99844	4.1425	1.4394	247.11	3405.2	0.45287	335498
25	0.00002	0.99838	4.1385	1.4403	256.80	3395.0	0.45168	316031
26	0.00002	0.99832	4.1345	1.4413	266.31	3384.9	0.45055	297829
28	0.00003	0.99818	4.1262	1.4432	284.86	3365.0	0.44850	264867
30	0.00003	0.99804	4.1178	1.4452	302.80	3345.5	0.44671	235969
32	0.00003	0.99789	4.1091	1.4472	320.18	3326.4	0.44515	210588
34	0.00004	0.99773	4.1003	1.4493	337.04	3307.7	0.44382	188256
36	0.00004	0.99757	4.0913	1.4515	353.43	3289.3	0.44271	168572
38	0.00005	0.99739	4.0821	1.4536	369.38	3271.4	0.44180	151192
40	0.00005	0.99720	4.0728	1.4558	384.92	3253.7	0.44110	135820
42	0.00006	0.99700	4.0633	1.4581	400.08	3236.5	0.44058	122202
44	0.00006	0.99679	4.0537	1.4604	414.88	3219.6	0.44025	110117
46	0.00007	0.99657	4.0440	1.4627	429.36	3203.0	0.44010	99378
48	0.00008	0.99634	4.0342	1.4651	443.53	3186.9	0.44011	89817
50	0.00008	0.99609	4.0243	1.4675	457.42	3171.1	0.44029	81294
52	0.00009	0.99584	4.0144	1.4699	471.04	3155.6	0.44063	73684
54	0.00010	0.99556	4.0043	1.4724	484.41	3140.6	0.44113	66879
56	0.00011	0.99528	3.9942	1.4750	497.54	3125.8	0.44177	60786
58	0.00012	0.99498	3.9840	1.4776	510.46	3111.5	0.44257	55321

[a] Triple-point temperature.

Table 6 Saturation state: Compression factor z, Specific isochoric heat capacity c_v, Isobaric cubic expansion coefficient α_v, Isothermal compressibility κ_T – Continued

t [°C]	z' [–]	z''	c_v' [kJ kg^{-1} K^{-1}]	c_v''	α_v' [10^{-6} K^{-1}]	α_v''	κ_T' [10^{-6} kPa^{-1}]	κ_T''
60	0.00013	0.99467	3.9738	1.4802	523.17	3097.5	0.44350	50414
62	0.00014	0.99434	3.9636	1.4829	535.70	3083.9	0.44458	46002
64	0.00016	0.99400	3.9533	1.4857	548.05	3070.7	0.44579	42029
66	0.00017	0.99364	3.9430	1.4885	560.23	3057.8	0.44714	38446
68	0.00019	0.99326	3.9326	1.4915	572.25	3045.3	0.44862	35212
70	0.00020	0.99287	3.9223	1.4945	584.13	3033.2	0.45023	32289
72	0.00022	0.99246	3.9119	1.4976	595.88	3021.5	0.45197	29643
74	0.00024	0.99203	3.9015	1.5008	607.51	3010.2	0.45383	27246
76	0.00026	0.99158	3.8912	1.5041	619.01	2999.3	0.45582	25070
78	0.00028	0.99111	3.8808	1.5074	630.42	2988.7	0.45793	23095
80	0.00030	0.99062	3.8704	1.5110	641.72	2978.6	0.46017	21298
82	0.00032	0.99012	3.8601	1.5146	652.93	2968.9	0.46252	19662
84	0.00035	0.98959	3.8497	1.5183	664.07	2959.6	0.46500	18171
86	0.00038	0.98904	3.8394	1.5222	675.12	2950.7	0.46760	16810
88	0.00040	0.98847	3.8291	1.5262	686.11	2942.3	0.47032	15568
90	0.00043	0.98787	3.8188	1.5304	697.04	2934.3	0.47316	14431
92	0.00047	0.98726	3.8085	1.5347	707.92	2926.7	0.47612	13391
94	0.00050	0.98662	3.7983	1.5392	718.75	2919.6	0.47920	12438
96	0.00054	0.98595	3.7880	1.5439	729.53	2912.9	0.48240	11564
98	0.00057	0.98526	3.7779	1.5487	740.29	2906.7	0.48572	10761
100	0.00061	0.98454	3.7677	1.5537	751.01	2901.0	0.48917	10023
105	0.00073	0.98264	3.7424	1.5671	777.74	2888.7	0.49832	8426.2
110	0.00085	0.98057	3.7174	1.5817	804.42	2879.6	0.50826	7122.2
115	0.00100	0.97831	3.6926	1.5977	831.13	2873.6	0.51901	6051.8
120	0.00116	0.97587	3.6680	1.6152	857.98	2870.9	0.53060	5168.3
125	0.00135	0.97324	3.6437	1.6342	885.03	2871.5	0.54306	4435.3
130	0.00155	0.97040	3.6197	1.6546	912.38	2875.6	0.55644	3824.1
135	0.00179	0.96735	3.5959	1.6766	940.10	2883.1	0.57078	3312.1
140	0.00205	0.96408	3.5725	1.7001	968.29	2894.2	0.58615	2881.1
145	0.00234	0.96059	3.5493	1.7250	997.03	2908.9	0.60260	2516.8
150	0.00266	0.95687	3.5264	1.7512	1026.4	2927.1	0.62021	2207.5
155	0.00301	0.95291	3.5039	1.7787	1056.5	2949.1	0.63905	1943.8
160	0.00341	0.94871	3.4817	1.8073	1087.5	2974.8	0.65923	1718.1
165	0.00384	0.94426	3.4598	1.8369	1119.3	3004.2	0.68084	1524.2
170	0.00432	0.93956	3.4383	1.8674	1152.2	3037.7	0.70399	1357.0
175	0.00484	0.93461	3.4171	1.8989	1186.3	3075.2	0.72882	1212.4
180	0.00540	0.92939	3.3963	1.9311	1221.7	3117.0	0.75547	1086.8
185	0.00603	0.92390	3.3759	1.9641	1258.4	3163.3	0.78410	977.46
190	0.00670	0.91813	3.3558	1.9978	1296.8	3214.4	0.81490	881.93
195	0.00744	0.91208	3.3362	2.0324	1336.8	3270.6	0.84806	798.24

Table 6 Saturation state: Compression factor z, Specific isochoric heat capacity c_v, Isobaric cubic expansion coefficient α_v, Isothermal compressibility κ_T – Continued

t [°C]	z' [–]	z'' [–]	c'_v [kJ kg^{-1} K^{-1}]	c''_v [kJ kg^{-1} K^{-1}]	α'_v [10^{-6} K^{-1}]	α''_v [10^{-6} K^{-1}]	κ'_T [10^{-6} kPa^{-1}]	κ''_T [10^{-6} kPa^{-1}]
200	0.00823	0.90575	3.3170	2.0677	1378.8	3332.3	0.88383	724.72
205	0.00910	0.89912	3.2982	2.1038	1422.8	3399.9	0.92245	659.96
210	0.01003	0.89218	3.2799	2.1407	1469.2	3473.9	0.96422	602.78
215	0.01104	0.88494	3.2621	2.1785	1518.0	3554.8	1.0095	552.17
220	0.01213	0.87738	3.2447	2.2171	1569.7	3643.1	1.0586	507.27
225	0.01330	0.86949	3.2278	2.2565	1624.4	3739.5	1.1121	467.37
230	0.01456	0.86126	3.2114	2.2967	1682.6	3844.7	1.1704	431.84
235	0.01592	0.85269	3.1956	2.3377	1744.6	3959.5	1.2341	400.14
240	0.01737	0.84376	3.1802	2.3795	1810.8	4084.9	1.3039	371.82
245	0.01894	0.83446	3.1655	2.4220	1881.8	4221.9	1.3807	346.49
250	0.02061	0.82478	3.1513	2.4653	1958.2	4371.9	1.4653	323.81
255	0.02241	0.81471	3.1378	2.5093	2040.7	4536.3	1.5591	303.49
260	0.02433	0.80423	3.1249	2.5543	2130.1	4717.0	1.6634	285.29
265	0.02640	0.79332	3.1127	2.6003	2227.4	4916.4	1.7798	268.98
270	0.02860	0.78198	3.1012	2.6476	2333.8	5137.2	1.9106	254.40
275	0.03097	0.77017	3.0906	2.6964	2450.8	5382.9	2.0583	241.39
280	0.03350	0.75788	3.0809	2.7470	2580.3	5657.6	2.2262	229.82
285	0.03621	0.74508	3.0722	2.7998	2724.3	5966.4	2.4182	219.58
290	0.03912	0.73174	3.0645	2.8549	2885.7	6315.5	2.6396	210.61
295	0.04224	0.71782	3.0579	2.9124	3067.7	6712.6	2.8966	202.82
300	0.04559	0.70329	3.0525	2.9724	3274.5	7166.8	3.1973	196.19
305	0.04919	0.68809	3.0481	3.0347	3511.4	7690.0	3.5520	190.67
310	0.05307	0.67217	3.0447	3.0990	3785.1	8297.5	3.9744	186.29
315	0.05726	0.65547	3.0425	3.1652	4104.6	9010.3	4.4833	183.09
320	0.06179	0.63790	3.0418	3.2332	4482.9	9858.2	5.1060	181.16
325	0.06671	0.61936	3.0437	3.3038	4939.2	10885	5.8851	180.70
330	0.07208	0.59971	3.0499	3.3780	5504.0	12157	6.8895	181.99
335	0.07797	0.57879	3.0629	3.4575	6226.5	13774	8.2330	185.49
340	0.08449	0.55638	3.0851	3.5435	7185.6	15888	10.103	191.91
345	0.09176	0.53217	3.1162	3.6349	8504.5	18732	12.796	202.25
350	0.10001	0.50581	3.1513	3.7257	10365	22660	16.759	218.02
355	0.10956	0.47672	3.2092	3.8564	13414	28945	23.624	245.57
360	0.12102	0.44364	3.2884	4.0060	18809	39736	36.627	294.64
365	0.13566	0.40411	3.4148	4.1910	30979	62943	68.346	401.37
370	0.15753	0.35065	3.6617	4.4328	79652	148007	208.76	783.27
371	0.16406	0.33607	3.7474	4.4926	112324	201421	308.40	1016.8
372	0.17240	0.31838	3.8625	4.5582	183758	312832	533.26	1494.9
373	0.18480	0.29414	4.0389	4.6282	435715	679124	1360.1	3022.4
373.946[a]	0.22944		–[b]		∞[b]		∞[b]	

[a] Critical temperature.

[b] At the critical point, IAPWS-IF97 does not yield accurate values for c_v, α_v, and κ_T.

Table 7 Compression factor z

For the single-phase region, this table contains values for the

- Compression factor (real-gas factor) $z = pv/(RT)$

for temperatures from 0 °C to 800 °C and pressures from 0.006 112 127 bar to 1000 bar (regions 1 to 3 of IAPWS-IF97). The values for the needed specific volume v were determined from the IAPWS-IF97 basic equations, Eqs. (2.3), (2.6), and (2.11).

The horizontal lines in the columns indicate the transition from the liquid phase to the vapour phase.

Values for the compression factor for temperatures above 800 °C up to 2000 °C and pressures up to 500 bar can be calculated with the program “IAPWS-IF97 Electronic Steam Tables” in Part D.

Table 7 Compression factor z [–] [a]

t [°C]	p [bar] 0.006112127	0.01	0.1	0.5	1	2	3	4	5	6	7
0	0.00000	0.00001	0.00008	0.00040	0.00079	0.00159	0.00238	0.00317	0.00397	0.00476	0.00555
5	0.99952	0.00001	0.00008	0.00039	0.00078	0.00156	0.00234	0.00312	0.00389	0.00467	0.00545
10	0.99958	0.99930	0.00008	0.00038	0.00077	0.00153	0.00230	0.00306	0.00383	0.00459	0.00536
15	0.99963	0.99938	0.00008	0.00038	0.00075	0.00151	0.00226	0.00301	0.00376	0.00451	0.00527
20	0.99967	0.99945	0.00007	0.00037	0.00074	0.00148	0.00222	0.00296	0.00370	0.00444	0.00518
25	0.99970	0.99951	0.00007	0.00036	0.00073	0.00146	0.00219	0.00292	0.00364	0.00437	0.00510
30	0.99973	0.99955	0.00007	0.00036	0.00072	0.00144	0.00215	0.00287	0.00359	0.00431	0.00502
35	0.99975	0.99960	0.00007	0.00035	0.00071	0.00141	0.00212	0.00283	0.00354	0.00424	0.00495
40	0.99977	0.99963	0.00007	0.00035	0.00070	0.00139	0.00209	0.00279	0.00349	0.00418	0.00488
45	0.99979	0.99966	0.00007	0.00034	0.00069	0.00138	0.00206	0.00275	0.00344	0.00413	0.00481
50	0.99981	0.99969	0.99686	0.00034	0.00068	0.00136	0.00204	0.00271	0.00339	0.00407	0.00475
60	0.99984	0.99974	0.99737	0.00033	0.00066	0.00132	0.00198	0.00265	0.00331	0.00397	0.00463
70	0.99986	0.99978	0.99776	0.00032	0.00065	0.00129	0.00194	0.00258	0.00323	0.00387	0.00452
80	0.99988	0.99981	0.99807	0.00032	0.00063	0.00126	0.00189	0.00253	0.00316	0.00379	0.00442
90	0.99990	0.99983	0.99833	0.99147	0.00062	0.00124	0.00185	0.00247	0.00309	0.00371	0.00433
100	0.99991	0.99985	0.99854	0.99257	0.98477	0.00121	0.00182	0.00242	0.00303	0.00363	0.00424
125	0.99993	0.99989	0.99893	0.99458	0.98898	0.97722	0.00174	0.00232	0.00290	0.00348	0.00406
150	0.99995	0.99992	0.99919	0.99589	0.99169	0.98302	0.97396	0.96447	0.00279	0.00335	0.00391
175	0.99996	0.99994	0.99936	0.99680	0.99355	0.98689	0.98004	0.97298	0.96570	0.95819	0.95043
200	0.99997	0.99995	0.99949	0.99745	0.99486	0.98962	0.98426	0.97878	0.97319	0.96748	0.96165
225	0.99997	0.99996	0.99959	0.99793	0.99583	0.99161	0.98731	0.98295	0.97853	0.97403	0.96947
250	0.99998	0.99997	0.99966	0.99829	0.99657	0.99310	0.98960	0.98605	0.98247	0.97884	0.97518
275	0.99998	0.99997	0.99972	0.99857	0.99714	0.99426	0.99135	0.98843	0.98547	0.98250	0.97949
300	0.99999	0.99998	0.99976	0.99880	0.99759	0.99517	0.99273	0.99028	0.98782	0.98534	0.98284
325	0.99999	0.99998	0.99980	0.99898	0.99796	0.99590	0.99384	0.99177	0.98969	0.98760	0.98550
350	0.99999	0.99998	0.99983	0.99913	0.99825	0.99650	0.99474	0.99297	0.99120	0.98942	0.98764
375	0.99999	0.99998	0.99985	0.99925	0.99850	0.99699	0.99548	0.99396	0.99244	0.99092	0.98939
400	0.99999	0.99999	0.99987	0.99935	0.99870	0.99740	0.99609	0.99478	0.99347	0.99215	0.99084
425	0.99999	0.99999	0.99989	0.99944	0.99887	0.99774	0.99660	0.99547	0.99433	0.99319	0.99205
450	0.99999	0.99999	0.99990	0.99951	0.99901	0.99803	0.99704	0.99605	0.99506	0.99406	0.99307
475	0.99999	0.99999	0.99991	0.99957	0.99914	0.99827	0.99741	0.99654	0.99567	0.99480	0.99394
500	1.00000	0.99999	0.99992	0.99962	0.99924	0.99848	0.99772	0.99696	0.99620	0.99544	0.99468
525	1.00000	0.99999	0.99993	0.99967	0.99933	0.99866	0.99799	0.99733	0.99665	0.99598	0.99531
550	1.00000	0.99999	0.99994	0.99971	0.99941	0.99882	0.99823	0.99764	0.99705	0.99645	0.99586
575	1.00000	0.99999	0.99995	0.99974	0.99948	0.99896	0.99843	0.99791	0.99739	0.99686	0.99634
600	1.00000	1.00000	0.99995	0.99977	0.99954	0.99907	0.99861	0.99815	0.99768	0.99722	0.99675
625	1.00000	1.00000	0.99996	0.99979	0.99959	0.99918	0.99877	0.99835	0.99794	0.99753	0.99712
650	1.00000	1.00000	0.99996	0.99982	0.99963	0.99927	0.99890	0.99854	0.99817	0.99780	0.99744
675	1.00000	1.00000	0.99997	0.99984	0.99967	0.99935	0.99902	0.99870	0.99837	0.99804	0.99772
700	1.00000	1.00000	0.99997	0.99985	0.99971	0.99942	0.99913	0.99884	0.99855	0.99826	0.99797
725	1.00000	1.00000	0.99997	0.99987	0.99974	0.99948	0.99922	0.99897	0.99871	0.99845	0.99819
750	1.00000	1.00000	0.99998	0.99988	0.99977	0.99954	0.99931	0.99908	0.99885	0.99862	0.99839
775	1.00000	1.00000	0.99998	0.99990	0.99979	0.99959	0.99938	0.99918	0.99897	0.99877	0.99856
800	1.00000	1.00000	0.99998	0.99991	0.99982	0.99963	0.99945	0.99927	0.99908	0.99890	0.99872

[a] The horizontal lines in the columns indicate the transition from the liquid phase to the gas phase.

Table 7 Compression factor z [–] [a] – Continued

t [°C]	p [bar] 8	9	10	15	20	25	50	75	100	150	200
0	0.00634	0.00714	0.00793	0.01189	0.01585	0.01981	0.03957	0.05928	0.07894	0.11812	0.15712
5	0.00623	0.00701	0.00779	0.01168	0.01557	0.01945	0.03886	0.05822	0.07753	0.11601	0.15432
10	0.00612	0.00689	0.00765	0.01147	0.01530	0.01911	0.03818	0.05721	0.07619	0.11402	0.15168
15	0.00602	0.00677	0.00752	0.01128	0.01504	0.01879	0.03755	0.05625	0.07492	0.11212	0.14917
20	0.00592	0.00666	0.00740	0.01110	0.01480	0.01849	0.03694	0.05535	0.07371	0.11032	0.14678
25	0.00583	0.00656	0.00729	0.01093	0.01457	0.01820	0.03636	0.05448	0.07257	0.10861	0.14450
30	0.00574	0.00646	0.00718	0.01076	0.01435	0.01793	0.03581	0.05366	0.07147	0.10698	0.14233
35	0.00566	0.00636	0.00707	0.01060	0.01414	0.01767	0.03529	0.05288	0.07043	0.10542	0.14026
40	0.00558	0.00627	0.00697	0.01045	0.01394	0.01742	0.03479	0.05213	0.06943	0.10393	0.13828
45	0.00550	0.00619	0.00687	0.01031	0.01374	0.01718	0.03431	0.05142	0.06848	0.10250	0.13638
50	0.00543	0.00611	0.00678	0.01017	0.01356	0.01695	0.03386	0.05073	0.06757	0.10114	0.13457
60	0.00529	0.00595	0.00661	0.00992	0.01322	0.01652	0.03300	0.04945	0.06586	0.09858	0.13116
70	0.00516	0.00581	0.00646	0.00968	0.01290	0.01613	0.03222	0.04827	0.06429	0.09623	0.12803
80	0.00505	0.00568	0.00631	0.00946	0.01262	0.01577	0.03150	0.04719	0.06285	0.09407	0.12515
90	0.00494	0.00556	0.00618	0.00927	0.01235	0.01543	0.03083	0.04620	0.06152	0.09208	0.12249
100	0.00485	0.00545	0.00606	0.00908	0.01211	0.01513	0.03022	0.04528	0.06030	0.09024	0.12004
125	0.00463	0.00521	0.00579	0.00869	0.01158	0.01447	0.02890	0.04330	0.05765	0.08626	0.11472
150	0.00447	0.00502	0.00558	0.00837	0.01116	0.01394	0.02784	0.04170	0.05552	0.08303	0.11039
175	0.94237	0.00488	0.00542	0.00812	0.01083	0.01353	0.02701	0.04045	0.05384	0.08048	0.10695
200	0.95569	0.94959	0.94337	0.90974	0.01059	0.01323	0.02640	0.03952	0.05258	0.07855	0.10432
225	0.96483	0.96012	0.95534	0.93027	0.90296	0.87269	0.02601	0.03892	0.05175	0.07724	0.10248
250	0.97147	0.96772	0.96393	0.94430	0.92346	0.90127	0.02588	0.03869	0.05140	0.07660	0.10150
275	0.97647	0.97342	0.97034	0.95454	0.93804	0.92075	0.81902	0.03894	0.05166	0.07679	0.10152
300	0.98033	0.97780	0.97526	0.96229	0.94888	0.93501	0.85714	0.75826	0.05285	0.07816	0.10291
325	0.98338	0.98126	0.97913	0.96832	0.95722	0.94584	0.88376	0.81069	0.72009	0.08173	0.10656
350	0.98584	0.98405	0.98224	0.97311	0.96380	0.95430	0.90354	0.84627	0.78033	0.59879	0.11578
375	0.98785	0.98632	0.98477	0.97699	0.96909	0.96106	0.91879	0.87242	0.82106	0.69713	0.51316
400	0.98951	0.98819	0.98686	0.98018	0.97341	0.96656	0.93087	0.89250	0.85102	0.75663	0.64051
425	0.99090	0.98976	0.98861	0.98283	0.97699	0.97110	0.94064	0.90838	0.87410	0.79869	0.71231
450	0.99207	0.99107	0.99007	0.98505	0.97999	0.97488	0.94867	0.92123	0.89243	0.83047	0.76225
475	0.99306	0.99219	0.99132	0.98694	0.98252	0.97808	0.95537	0.93179	0.90730	0.85543	0.79975
500	0.99391	0.99315	0.99238	0.98854	0.98468	0.98079	0.96101	0.94061	0.91957	0.87557	0.82913
525	0.99464	0.99397	0.99329	0.98992	0.98652	0.98311	0.96580	0.94804	0.92984	0.89213	0.85284
550	0.99527	0.99467	0.99408	0.99110	0.98811	0.98511	0.96990	0.95437	0.93853	0.90595	0.87236
575	0.99581	0.99529	0.99476	0.99213	0.98949	0.98684	0.97344	0.95981	0.94595	0.91764	0.88868
600	0.99629	0.99582	0.99536	0.99303	0.99069	0.98834	0.97651	0.96450	0.95234	0.92761	0.90249
625	0.99670	0.99629	0.99588	0.99381	0.99174	0.98966	0.97918	0.96858	0.95787	0.93620	0.91430
650	0.99707	0.99670	0.99634	0.99450	0.99265	0.99081	0.98152	0.97214	0.96269	0.94364	0.92448
675	0.99739	0.99707	0.99674	0.99510	0.99346	0.99182	0.98358	0.97527	0.96692	0.95013	0.93332
700	0.99768	0.99739	0.99709	0.99564	0.99418	0.99272	0.98539	0.97802	0.97063	0.95582	0.94104
725	0.99793	0.99767	0.99741	0.99611	0.99482	0.99352	0.98700	0.98046	0.97392	0.96083	0.94782
750	0.99815	0.99792	0.99769	0.99654	0.99538	0.99422	0.98843	0.98263	0.97683	0.96526	0.95381
775	0.99836	0.99815	0.99794	0.99692	0.99589	0.99486	0.98971	0.98456	0.97942	0.96920	0.95911
800	0.99854	0.99835	0.99817	0.99725	0.99634	0.99542	0.99085	0.98629	0.98174	0.97271	0.96383

[a] The horizontal lines in the columns indicate the transition from the liquid phase to the gas phase.

Table 7 Compression factor z [–] – Continued

t [°C]	p [bar] 250	300	350	400	450	500	600	700	800	900	1000
0	0.19593	0.23456	0.27302	0.31131	0.34943	0.38739	0.46284	0.53769	0.61196	0.68568	0.75888
5	0.19246	0.23042	0.26822	0.30586	0.34333	0.38066	0.45485	0.52847	0.60153	0.67406	0.74609
10	0.18917	0.22650	0.26367	0.30068	0.33754	0.37426	0.44725	0.51968	0.59158	0.66296	0.73386
15	0.18605	0.22277	0.25934	0.29576	0.33203	0.36816	0.43999	0.51129	0.58207	0.65235	0.72216
20	0.18307	0.21922	0.25522	0.29107	0.32677	0.36234	0.43307	0.50327	0.57298	0.64219	0.71095
25	0.18024	0.21583	0.25128	0.28659	0.32175	0.35678	0.42645	0.49560	0.56427	0.63246	0.70021
30	0.17754	0.21260	0.24752	0.28231	0.31695	0.35147	0.42011	0.48826	0.55593	0.62314	0.68990
35	0.17496	0.20951	0.24393	0.27821	0.31236	0.34638	0.41405	0.48122	0.54793	0.61419	0.68001
40	0.17249	0.20656	0.24049	0.27429	0.30797	0.34151	0.40823	0.47447	0.54025	0.60559	0.67051
45	0.17012	0.20373	0.23720	0.27054	0.30375	0.33684	0.40265	0.46800	0.53289	0.59734	0.66137
50	0.16786	0.20102	0.23404	0.26694	0.29971	0.33236	0.39730	0.46178	0.52581	0.58941	0.65259
60	0.16361	0.19593	0.22812	0.26018	0.29212	0.32394	0.38723	0.45006	0.51246	0.57444	0.63602
70	0.15970	0.19124	0.22266	0.25394	0.28511	0.31616	0.37792	0.43923	0.50011	0.56058	0.62066
80	0.15610	0.18692	0.21762	0.24819	0.27864	0.30898	0.36931	0.42919	0.48866	0.54772	0.60639
90	0.15278	0.18293	0.21296	0.24287	0.27266	0.30233	0.36133	0.41989	0.47804	0.53578	0.59314
100	0.14971	0.17925	0.20866	0.23795	0.26712	0.29617	0.35394	0.41126	0.46817	0.52468	0.58080
125	0.14304	0.17122	0.19928	0.22721	0.25501	0.28269	0.33771	0.39229	0.44644	0.50019	0.55354
150	0.13760	0.16467	0.19160	0.21839	0.24505	0.27159	0.32429	0.37653	0.42833	0.47972	0.53070
175	0.13325	0.15940	0.18539	0.21124	0.23695	0.26252	0.31326	0.36352	0.41331	0.46266	0.51160
200	0.12990	0.15530	0.18053	0.20560	0.23051	0.25527	0.30436	0.35292	0.40098	0.44858	0.49574
225	0.12751	0.15232	0.17694	0.20137	0.22563	0.24972	0.29741	0.34453	0.39110	0.43717	0.48277
250	0.12613	0.15051	0.17465	0.19858	0.22230	0.24583	0.29235	0.33822	0.38349	0.42822	0.47245
275	0.12591	0.14999	0.17378	0.19731	0.22060	0.24367	0.28919	0.33397	0.37810	0.42163	0.46462
300	0.12720	0.15109	0.17462	0.19784	0.22077	0.24344	0.28807	0.33188	0.37496	0.41739	0.45924
325	0.13079	0.15450	0.17778	0.20069	0.22327	0.24555	0.28931	0.33216	0.37423	0.41560	0.45636
350	0.13898	0.16199	0.18467	0.20701	0.22903	0.25077	0.29347	0.33524	0.37620	0.41647	0.45611
375	0.16531	0.17970	0.19910	0.21948	0.24009	0.26069	0.30155	0.34178	0.38136	0.42033	0.45872
400	0.48320	0.27003	0.23721	0.24600	0.26124	0.27857	0.31537	0.35293	0.39046	0.42768	0.46453
425	0.61184	0.49349	0.37315	0.31500	0.30548	0.31169	0.33811	0.37045	0.40458	0.43926	0.47401
450	0.68728	0.60567	0.52003	0.44257	0.39306	0.37265	0.37477	0.39684	0.42520	0.45600	0.48783
475	0.74042	0.67803	0.61404	0.55174	0.49780	0.45939	0.42922	0.43446	0.45371	0.47880	0.50659
500	0.78063	0.73063	0.68007	0.63054	0.58444	0.54500	0.49630	0.48316	0.49055	0.50804	0.53057
525	0.81234	0.77112	0.72987	0.68949	0.65117	0.61643	0.56395	0.53841	0.53418	0.54310	0.55945
550	0.83805	0.80345	0.76906	0.73548	0.70341	0.67365	0.62460	0.59389	0.58121	0.58222	0.59221
575	0.85933	0.82992	0.80082	0.77247	0.74534	0.71992	0.67626	0.64511	0.62800	0.62301	0.62733
600	0.87719	0.85197	0.82710	0.80292	0.77975	0.75793	0.71967	0.69046	0.67173	0.66320	0.66312
625	0.89237	0.87059	0.84919	0.82841	0.80848	0.78966	0.75625	0.72978	0.71129	0.70098	0.69812
650	0.90538	0.88648	0.86796	0.85001	0.83279	0.81649	0.78734	0.76371	0.74638	0.73559	0.73100
675	0.91662	0.90016	0.88407	0.86849	0.85356	0.83941	0.81397	0.79305	0.77728	0.76686	0.76159
700	0.92641	0.91203	0.89801	0.88446	0.87147	0.85916	0.83696	0.81854	0.80442	0.79480	0.78955
725	0.93498	0.92240	0.91015	0.89833	0.88702	0.87630	0.85694	0.84080	0.82828	0.81960	0.81470
750	0.94253	0.93150	0.92079	0.91048	0.90062	0.89128	0.87442	0.86032	0.84934	0.84163	0.83717
775	0.94920	0.93953	0.93017	0.92116	0.91257	0.90444	0.88978	0.87753	0.86798	0.86125	0.85727
800	0.95512	0.94665	0.93846	0.93060	0.92312	0.91605	0.90333	0.89276	0.88453	0.87876	0.87535

Table 8 Specific isochoric heat capacity c_v

http://avibert.blogspot.com

For the single-phase region, this table contains values for the

- Specific isochoric heat capacity c_v

for temperatures from 0 °C to 800 °C and pressures from 0.006 112 127 bar to 1000 bar (regions 1 to 3 of IAPWS-IF97). The values for c_v were calculated from the IAPWS-IF97 basic equations, Eqs. (2.3), (2.6), and (2.11).

The horizontal lines in the columns indicate the transition from the liquid phase to the vapour phase.

Values for the specific isochoric heat capacity for temperatures above 800 °C up to 2000 °C and pressures up to 500 bar can be calculated with the program "IAPWS-IF97 Electronic Steam Tables" in Part D.

Table 8 Specific isochoric heat capacity c_v [kJ kg^{-1} K^{-1}] [a]

t	p [bar]										
[°C]	0.006112127	0.01	0.1	0.5	1	2	3	4	5	6	7
0	4.2174	4.2174	4.2174	4.2172	4.2170	4.2165	4.2160	4.2156	4.2151	4.2146	4.2141
5	1.4118	4.2052	4.2052	4.2050	4.2048	4.2044	4.2039	4.2035	4.2031	4.2026	4.2022
10	1.4077	1.4186	4.1912	4.1911	4.1908	4.1904	4.1900	4.1896	4.1892	4.1888	4.1884
15	1.4063	1.4124	4.1754	4.1752	4.1750	4.1747	4.1743	4.1739	4.1735	4.1731	4.1728
20	1.4062	1.4100	4.1578	4.1576	4.1574	4.1571	4.1567	4.1564	4.1560	4.1557	4.1553
25	1.4066	1.4093	4.1385	4.1384	4.1382	4.1379	4.1375	4.1372	4.1368	4.1365	4.1362
30	1.4073	1.4095	4.1178	4.1176	4.1175	4.1172	4.1168	4.1165	4.1162	4.1159	4.1156
35	1.4082	1.4100	4.0958	4.0957	4.0955	4.0952	4.0949	4.0946	4.0943	4.0940	4.0937
40	1.4093	1.4108	4.0728	4.0726	4.0725	4.0722	4.0719	4.0717	4.0714	4.0711	4.0708
45	1.4104	1.4117	4.0489	4.0488	4.0486	4.0484	4.0481	4.0478	4.0476	4.0473	4.0470
50	1.4117	1.4129	1.4510	4.0242	4.0241	4.0239	4.0236	4.0233	4.0231	4.0228	4.0226
60	1.4145	1.4154	1.4397	3.9738	3.9736	3.9734	3.9732	3.9730	3.9727	3.9725	3.9723
70	1.4176	1.4184	1.4366	3.9222	3.9221	3.9219	3.9217	3.9215	3.9213	3.9211	3.9209
80	1.4211	1.4217	1.4361	3.8704	3.8703	3.8701	3.8700	3.8698	3.8696	3.8694	3.8692
90	1.4248	1.4253	1.4371	1.4945	3.8187	3.8186	3.8184	3.8182	3.8181	3.8179	3.8178
100	1.4288	1.4293	1.4389	1.4838	1.5514	3.7676	3.7674	3.7673	3.7671	3.7670	3.7668
125	1.4399	1.4401	1.4461	1.4736	1.5100	1.5962	3.6436	3.6435	3.6434	3.6433	3.6432
150	1.4520	1.4522	1.4561	1.4738	1.4969	1.5467	1.6030	1.6742	3.5264	3.5263	3.5262
175	1.4650	1.4652	1.4678	1.4796	1.4949	1.5274	1.5624	1.6001	1.6414	1.6879	1.7431
200	1.4788	1.4788	1.4806	1.4888	1.4992	1.5213	1.5447	1.5696	1.5959	1.6235	1.6528
225	1.4930	1.4931	1.4943	1.5001	1.5075	1.5229	1.5392	1.5563	1.5742	1.5929	1.6124
250	1.5077	1.5077	1.5086	1.5129	1.5183	1.5294	1.5411	1.5533	1.5659	1.5790	1.5926
275	1.5227	1.5227	1.5234	1.5266	1.5307	1.5390	1.5476	1.5566	1.5658	1.5753	1.5851
300	1.5380	1.5380	1.5386	1.5411	1.5442	1.5506	1.5572	1.5639	1.5709	1.5780	1.5853
325	1.5536	1.5536	1.5541	1.5560	1.5585	1.5636	1.5687	1.5740	1.5794	1.5849	1.5904
350	1.5695	1.5695	1.5699	1.5715	1.5735	1.5776	1.5817	1.5859	1.5902	1.5945	1.5990
375	1.5856	1.5856	1.5859	1.5872	1.5889	1.5923	1.5957	1.5991	1.6026	1.6062	1.6097
400	1.6019	1.6019	1.6022	1.6033	1.6047	1.6076	1.6104	1.6133	1.6162	1.6191	1.6221
425	1.6185	1.6185	1.6187	1.6197	1.6209	1.6233	1.6257	1.6282	1.6306	1.6331	1.6356
450	1.6353	1.6353	1.6354	1.6363	1.6373	1.6394	1.6415	1.6436	1.6457	1.6478	1.6500
475	1.6522	1.6522	1.6524	1.6531	1.6540	1.6558	1.6577	1.6595	1.6613	1.6632	1.6650
500	1.6694	1.6694	1.6695	1.6701	1.6709	1.6725	1.6741	1.6758	1.6774	1.6790	1.6806
525	1.6867	1.6867	1.6868	1.6874	1.6881	1.6895	1.6909	1.6923	1.6937	1.6951	1.6966
550	1.7041	1.7041	1.7042	1.7047	1.7053	1.7066	1.7078	1.7091	1.7104	1.7116	1.7129
575	1.7216	1.7216	1.7217	1.7222	1.7227	1.7239	1.7250	1.7261	1.7272	1.7283	1.7295
600	1.7393	1.7393	1.7393	1.7397	1.7402	1.7412	1.7422	1.7432	1.7442	1.7452	1.7462
625	1.7569	1.7569	1.7570	1.7574	1.7578	1.7587	1.7596	1.7605	1.7614	1.7623	1.7632
650	1.7746	1.7747	1.7747	1.7750	1.7754	1.7762	1.7771	1.7779	1.7787	1.7795	1.7803
675	1.7924	1.7924	1.7924	1.7927	1.7931	1.7938	1.7945	1.7952	1.7960	1.7967	1.7974
700	1.8101	1.8101	1.8102	1.8104	1.8107	1.8114	1.8120	1.8127	1.8133	1.8140	1.8146
725	1.8278	1.8278	1.8278	1.8281	1.8284	1.8289	1.8295	1.8301	1.8307	1.8313	1.8318
750	1.8455	1.8455	1.8455	1.8457	1.8460	1.8465	1.8470	1.8475	1.8481	1.8486	1.8491
775	1.8631	1.8631	1.8632	1.8633	1.8636	1.8640	1.8645	1.8650	1.8654	1.8659	1.8664
800	1.8808	1.8808	1.8808	1.8810	1.8812	1.8816	1.8820	1.8824	1.8828	1.8832	1.8837

[a] The horizontal lines in the columns indicate the transition from the liquid phase to the gas phase.

Table 8 Specific isochoric heat capacity c_v [kJ kg^{-1} K^{-1}] [a] – Continued

t	p [bar]										
[°C]	8	9	10	15	20	25	50	75	100	150	200
0	4.2137	4.2132	4.2127	4.2104	4.2081	4.2057	4.1942	4.1829	4.1717	4.1500	4.1290
5	4.2018	4.2013	4.2009	4.1987	4.1966	4.1944	4.1838	4.1733	4.1630	4.1430	4.1235
10	4.1880	4.1876	4.1872	4.1852	4.1832	4.1812	4.1713	4.1615	4.1519	4.1332	4.1151
15	4.1724	4.1720	4.1716	4.1697	4.1679	4.1660	4.1567	4.1476	4.1386	4.1210	4.1039
20	4.1549	4.1546	4.1542	4.1525	4.1507	4.1489	4.1402	4.1316	4.1231	4.1065	4.0904
25	4.1358	4.1355	4.1352	4.1335	4.1318	4.1302	4.1219	4.1138	4.1058	4.0901	4.0748
30	4.1153	4.1149	4.1146	4.1130	4.1115	4.1099	4.1021	4.0944	4.0868	4.0720	4.0575
35	4.0934	4.0931	4.0928	4.0913	4.0898	4.0883	4.0810	4.0737	4.0665	4.0524	4.0387
40	4.0705	4.0702	4.0699	4.0685	4.0671	4.0657	4.0587	4.0518	4.0450	4.0316	4.0186
45	4.0468	4.0465	4.0462	4.0449	4.0435	4.0422	4.0356	4.0291	4.0226	4.0099	3.9975
50	4.0223	4.0221	4.0218	4.0206	4.0193	4.0180	4.0118	4.0056	3.9994	3.9874	3.9756
60	3.9720	3.9718	3.9716	3.9705	3.9693	3.9682	3.9626	3.9570	3.9515	3.9406	3.9300
70	3.9207	3.9205	3.9203	3.9193	3.9183	3.9173	3.9122	3.9072	3.9023	3.8925	3.8829
80	3.8690	3.8689	3.8687	3.8678	3.8669	3.8660	3.8614	3.8570	3.8525	3.8437	3.8351
90	3.8176	3.8174	3.8173	3.8165	3.8156	3.8148	3.8108	3.8068	3.8028	3.7948	3.7870
100	3.7667	3.7665	3.7664	3.7657	3.7649	3.7642	3.7606	3.7569	3.7533	3.7462	3.7391
125	3.6431	3.6430	3.6429	3.6423	3.6417	3.6411	3.6383	3.6355	3.6327	3.6271	3.6216
150	3.5261	3.5261	3.5260	3.5255	3.5250	3.5246	3.5223	3.5200	3.5178	3.5133	3.5089
175	1.8129	3.4171	3.4170	3.4166	3.4162	3.4158	3.4138	3.4119	3.4100	3.4062	3.4026
200	1.6837	1.7168	1.7526	2.0209	3.3167	3.3163	3.3144	3.3126	3.3108	3.3075	3.3043
225	1.6327	1.6538	1.6757	1.7988	1.9604	2.2207	3.2259	3.2240	3.2223	3.2190	3.2159
250	1.6067	1.6212	1.6362	1.7179	1.8113	1.9195	3.1504	3.1484	3.1464	3.1427	3.1395
275	1.5951	1.6055	1.6161	1.6735	1.7376	1.8084	2.3262	3.0888	3.0861	3.0812	3.0770
300	1.5927	1.6003	1.6081	1.6497	1.6955	1.7454	2.0615	2.5772	3.0496	3.0395	3.0315
325	1.5961	1.6019	1.6078	1.6389	1.6727	1.7090	1.9289	2.2271	2.6626	3.0325	3.0121
350	1.6034	1.6080	1.6126	1.6366	1.6622	1.6894	1.8498	2.0514	2.3073	3.1323	3.0508
375	1.6133	1.6170	1.6207	1.6397	1.6598	1.6808	1.8016	1.9475	2.1202	2.5770	3.3234
400	1.6251	1.6281	1.6311	1.6466	1.6627	1.6795	1.7731	1.8830	2.0085	2.3113	2.7010
425	1.6381	1.6406	1.6432	1.6561	1.6693	1.6830	1.7576	1.8428	1.9380	2.1575	2.4158
450	1.6521	1.6543	1.6564	1.6674	1.6785	1.6899	1.7508	1.8185	1.8929	2.0597	2.2488
475	1.6669	1.6687	1.6706	1.6800	1.6895	1.6992	1.7500	1.8051	1.8646	1.9953	2.1394
500	1.6822	1.6838	1.6854	1.6936	1.7019	1.7102	1.7533	1.7992	1.8477	1.9526	2.0657
525	1.6980	1.6994	1.7008	1.7080	1.7152	1.7225	1.7596	1.7984	1.8389	1.9248	2.0159
550	1.7141	1.7154	1.7167	1.7230	1.7293	1.7357	1.7680	1.8013	1.8356	1.9074	1.9824
575	1.7306	1.7317	1.7328	1.7384	1.7440	1.7497	1.7781	1.8070	1.8364	1.8973	1.9602
600	1.7472	1.7482	1.7492	1.7542	1.7592	1.7642	1.7893	1.8146	1.8402	1.8925	1.9461
625	1.7641	1.7650	1.7659	1.7703	1.7748	1.7792	1.8015	1.8238	1.8462	1.8917	1.9379
650	1.7811	1.7819	1.7827	1.7866	1.7906	1.7946	1.8144	1.8342	1.8540	1.8938	1.9341
675	1.7981	1.7988	1.7995	1.8031	1.8067	1.8102	1.8279	1.8455	1.8630	1.8982	1.9336
700	1.8152	1.8159	1.8165	1.8197	1.8229	1.8261	1.8419	1.8576	1.8732	1.9044	1.9356
725	1.8324	1.8330	1.8336	1.8364	1.8393	1.8421	1.8563	1.8703	1.8842	1.9120	1.9397
750	1.8496	1.8501	1.8506	1.8532	1.8558	1.8583	1.8710	1.8835	1.8960	1.9208	1.9455
775	1.8668	1.8673	1.8677	1.8700	1.8723	1.8746	1.8860	1.8972	1.9084	1.9306	1.9527
800	1.8841	1.8845	1.8849	1.8870	1.8890	1.8911	1.9012	1.9113	1.9214	1.9413	1.9612

[a] The horizontal lines in the columns indicate the transition from the liquid phase to the gas phase.

Table 8 Specific isochoric heat capacity c_v [kJ kg^{-1} K^{-1}] – Continued

t [°C]	p [bar] 250	300	350	400	450	500	600	700	800	900	1000
0	4.1087	4.0891	4.0702	4.0518	4.0341	4.0170	3.9846	3.9543	3.9261	3.8998	3.8754
5	4.1047	4.0866	4.0690	4.0519	4.0355	4.0195	3.9892	3.9607	3.9341	3.9092	3.8858
10	4.0975	4.0805	4.0640	4.0480	4.0326	4.0175	3.9889	3.9620	3.9367	3.9128	3.8904
15	4.0874	4.0714	4.0558	4.0407	4.0261	4.0119	3.9847	3.9590	3.9348	3.9119	3.8903
20	4.0748	4.0596	4.0449	4.0306	4.0166	4.0031	3.9772	3.9526	3.9294	3.9073	3.8865
25	4.0600	4.0456	4.0316	4.0180	4.0047	3.9918	3.9670	3.9434	3.9211	3.8998	3.8796
30	4.0434	4.0297	4.0164	4.0034	3.9907	3.9783	3.9546	3.9319	3.9104	3.8899	3.8704
35	4.0253	4.0122	3.9995	3.9871	3.9749	3.9631	3.9403	3.9186	3.8978	3.8780	3.8592
40	4.0058	3.9934	3.9813	3.9694	3.9578	3.9465	3.9246	3.9037	3.8837	3.8646	3.8464
45	3.9854	3.9735	3.9619	3.9506	3.9395	3.9287	3.9077	3.8876	3.8683	3.8499	3.8323
50	3.9640	3.9527	3.9417	3.9309	3.9203	3.9099	3.8898	3.8705	3.8519	3.8342	3.8171
60	3.9195	3.9093	3.8992	3.8894	3.8797	3.8702	3.8517	3.8339	3.8167	3.8003	3.7845
70	3.8734	3.8642	3.8550	3.8460	3.8372	3.8285	3.8115	3.7951	3.7793	3.7641	3.7495
80	3.8265	3.8181	3.8098	3.8016	3.7935	3.7856	3.7700	3.7550	3.7404	3.7264	3.7129
90	3.7793	3.7717	3.7641	3.7567	3.7493	3.7420	3.7278	3.7140	3.7006	3.6877	3.6753
100	3.7321	3.7252	3.7184	3.7116	3.7049	3.6982	3.6852	3.6725	3.6602	3.6483	3.6370
125	3.6161	3.6107	3.6053	3.5999	3.5945	3.5892	3.5788	3.5685	3.5586	3.5490	3.5400
150	3.5045	3.5002	3.4959	3.4916	3.4873	3.4831	3.4746	3.4663	3.4583	3.4507	3.4437
175	3.3990	3.3956	3.3921	3.3887	3.3852	3.3818	3.3750	3.3683	3.3618	3.3558	3.3504
200	3.3013	3.2984	3.2956	3.2929	3.2901	3.2874	3.2820	3.2766	3.2714	3.2667	3.2627
225	3.2132	3.2106	3.2083	3.2060	3.2039	3.2018	3.1975	3.1933	3.1891	3.1854	3.1825
250	3.1366	3.1341	3.1319	3.1299	3.1281	3.1264	3.1230	3.1196	3.1162	3.1132	3.1113
275	3.0733	3.0703	3.0677	3.0655	3.0636	3.0620	3.0589	3.0559	3.0528	3.0502	3.0488
300	3.0253	3.0202	3.0160	3.0127	3.0100	3.0078	3.0039	3.0004	2.9970	2.9941	2.9929
325	2.9951	2.9843	2.9763	2.9696	2.9642	2.9602	2.9540	2.9487	2.9439	2.9400	2.9384
350	3.0007	2.9598	2.9387	2.9281	2.9184	2.9099	2.8990	2.8915	2.8849	2.8799	2.8786
375	3.1896	3.0108	2.9522	2.9216	2.9019	2.8877	2.8681	2.8550	2.8461	2.8402	2.8366
400	3.2013	3.4045	3.0546	2.9515	2.9027	2.8732	2.8378	2.8171	2.8046	2.7977	2.7950
425	2.7074	3.0080	3.1370	3.0409	2.9464	2.8891	2.8252	2.7906	2.7707	2.7602	2.7567
450	2.4540	2.6593	2.8385	2.9363	2.9343	2.8936	2.8184	2.7718	2.7445	2.7303	2.7258
475	2.2941	2.4515	2.5978	2.7167	2.7856	2.8125	2.7851	2.7442	2.7157	2.7002	2.6958
500	2.1850	2.3075	2.4266	2.5330	2.6204	2.6775	2.7087	2.6955	2.6764	2.6646	2.6625
525	2.1103	2.2062	2.3013	2.3912	2.4698	2.5334	2.6120	2.6269	2.6253	2.6222	2.6249
550	2.0592	2.1363	2.2123	2.2858	2.3542	2.4144	2.5000	2.5486	2.5664	2.5747	2.5841
575	2.0242	2.0881	2.1507	2.2112	2.2686	2.3220	2.4106	2.4681	2.5016	2.5304	2.5414
600	2.0004	2.0546	2.1078	2.1592	2.2082	2.2544	2.3363	2.4014	2.4482	2.4789	2.4892
625	1.9846	2.0313	2.0773	2.1221	2.1651	2.2060	2.2798	2.3412	2.3892	2.4264	2.4613
650	1.9747	2.0153	2.0555	2.0949	2.1331	2.1698	2.2369	2.2939	2.3384	2.3694	2.3917
675	1.9691	2.0047	2.0401	2.0749	2.1088	2.1415	2.2024	2.2552	2.2980	2.3292	2.3491
700	1.9670	1.9984	2.0296	2.0604	2.0905	2.1196	2.1740	2.2218	2.2623	2.2954	2.3233
725	1.9675	1.9954	2.0231	2.0505	2.0773	2.1033	2.1518	2.1946	2.2314	2.2641	2.2976
750	1.9703	1.9952	2.0199	2.0445	2.0686	2.0921	2.1360	2.1749	2.2086	2.2394	2.2732
775	1.9750	1.9972	2.0196	2.0418	2.0638	2.0853	2.1263	2.1632	2.1954	2.2242	2.2544
800	1.9812	2.0014	2.0216	2.0420	2.0624	2.0827	2.1222	2.1590	2.1914	2.2184	2.2410

Table 9 Isobaric cubic expansion coefficient α_v

For the single-phase region, this table contains values for the

- Isobaric cubic expansion coefficient $\alpha_v = v^{-1}(\partial v/\partial T)_p$

for temperatures from 0 °C to 800 °C and pressures from 0.006 112 127 bar to 1000 bar (regions 1 to 3 of IAPWS-IF97). The values for α_v were calculated from the IAPWS-IF97 basic equations, Eqs. (2.3), (2.6), and (2.11).

The horizontal lines in the columns indicate the transition from the liquid phase to the vapour phase.

Values for the isobaric cubic expansion coefficient for temperatures above 800 °C up to 2000 °C and pressures up to 500 bar can be calculated with the program "IAPWS-IF97 Electronic Steam Tables" in Part D.

Partial derivatives of thermodynamic properties can be calculated with values of α_v as described in Sec. 2.4.4.

Table 9 Isobaric cubic expansion coefficient α_v [10^{-6} K^{-1}] [a]

t	p [bar]										
[°C]	0.006112127	0.01	0.1	0.5	1	2	3	4	5	6	7
0	−68.073	−68.071	−68.037	−67.884	−67.694	−67.313	−66.932	−66.551	−66.171	−65.790	−65.410
5	3608.9	15.989	16.017	16.140	16.293	16.600	16.907	17.213	17.519	17.825	18.131
10	3542.1	3551.4	87.910	88.009	88.132	88.377	88.623	88.869	89.114	89.359	89.604
15	3478.8	3485.3	150.68	150.76	150.86	151.05	151.25	151.44	151.64	151.83	152.03
20	3418.3	3423.3	206.47	206.53	206.61	206.76	206.91	207.06	207.22	207.37	207.52
25	3360.1	3364.2	256.81	256.85	256.91	257.03	257.14	257.26	257.37	257.49	257.60
30	3304.0	3307.5	302.80	302.84	302.88	302.96	303.05	303.13	303.21	303.30	303.38
35	3249.8	3252.9	345.30	345.32	345.35	345.40	345.46	345.51	345.57	345.62	345.68
40	3197.5	3200.1	384.92	384.93	384.95	384.98	385.01	385.04	385.07	385.10	385.13
45	3146.8	3149.2	422.16	422.17	422.17	422.18	422.19	422.19	422.20	422.21	422.22
50	3097.8	3099.9	3153.7	457.41	457.41	457.39	457.38	457.37	457.36	457.34	457.33
60	3004.2	3005.9	3045.9	523.16	523.13	523.08	523.03	522.98	522.93	522.88	522.83
70	2916.3	2917.6	2949.2	584.12	584.08	583.99	583.91	583.83	583.74	583.66	583.58
80	2833.4	2834.5	2860.0	641.72	641.66	641.55	641.43	641.32	641.20	641.09	640.97
90	2755.1	2756.0	2776.9	2877.1	697.00	696.85	696.71	696.56	696.42	696.27	696.13
100	2681.0	2681.8	2699.1	2780.6	2897.3	750.84	750.66	750.49	750.31	750.14	749.96
125	2512.4	2512.9	2524.1	2575.9	2645.6	2807.5	884.85	884.60	884.34	884.08	883.82
150	2363.7	2364.1	2371.7	2406.5	2452.4	2552.7	2666.3	2800.3	1026.3	1025.9	1025.6
175	2231.8	2232.0	2237.4	2261.8	2293.6	2361.5	2435.3	2515.5	2603.1	2699.7	2808.5
200	2113.8	2113.9	2117.9	2135.6	2158.5	2206.6	2257.9	2312.4	2370.3	2431.8	2497.1
225	2007.6	2007.8	2010.7	2024.1	2041.1	2076.5	2113.6	2152.4	2193.2	2235.8	2280.4
250	1911.7	1911.8	1914.0	1924.3	1937.3	1964.1	1991.9	2020.7	2050.6	2081.5	2113.5
275	1824.4	1824.5	1826.3	1834.4	1844.6	1865.4	1886.8	1908.8	1931.4	1954.6	1978.5
300	1744.8	1744.9	1746.3	1752.8	1760.9	1777.4	1794.3	1811.5	1829.1	1847.0	1865.4
325	1671.9	1672.0	1673.1	1678.3	1684.9	1698.2	1711.8	1725.5	1739.5	1753.7	1768.1
350	1604.8	1604.9	1605.8	1610.1	1615.5	1626.4	1637.4	1648.5	1659.8	1671.3	1682.9
375	1542.9	1542.9	1543.7	1547.3	1551.8	1560.7	1569.8	1579.0	1588.2	1597.6	1607.0
400	1485.6	1485.6	1486.3	1489.3	1493.0	1500.5	1508.0	1515.7	1523.3	1531.1	1538.9
425	1432.4	1432.4	1433.0	1435.5	1438.6	1444.9	1451.3	1457.7	1464.1	1470.6	1477.1
450	1382.9	1382.9	1383.4	1385.5	1388.2	1393.5	1398.9	1404.3	1409.7	1415.2	1420.7
475	1336.7	1336.7	1337.1	1338.9	1341.2	1345.7	1350.3	1354.9	1359.5	1364.2	1368.8
500	1293.4	1293.4	1293.8	1295.4	1297.3	1301.2	1305.1	1309.1	1313.0	1317.0	1321.0
525	1252.9	1252.9	1253.2	1254.6	1256.3	1259.6	1263.0	1266.4	1269.8	1273.2	1276.6
550	1214.9	1214.9	1215.1	1216.3	1217.8	1220.7	1223.6	1226.5	1229.5	1232.4	1235.4
575	1179.1	1179.1	1179.3	1180.3	1181.6	1184.1	1186.6	1189.2	1191.7	1194.3	1196.9
600	1145.3	1145.3	1145.5	1146.4	1147.5	1149.7	1151.9	1154.1	1156.4	1158.6	1160.9
625	1113.4	1113.4	1113.6	1114.4	1115.3	1117.3	1119.2	1121.2	1123.1	1125.1	1127.0
650	1083.3	1083.3	1083.4	1084.1	1085.0	1086.7	1088.4	1090.1	1091.8	1093.5	1095.3
675	1054.7	1054.7	1054.8	1055.4	1056.2	1057.7	1059.2	1060.7	1062.2	1063.8	1065.3
700	1027.6	1027.6	1027.7	1028.3	1028.9	1030.3	1031.6	1032.9	1034.3	1035.6	1037.0
725	1001.9	1001.9	1002.0	1002.4	1003.0	1004.2	1005.4	1006.6	1007.8	1009.0	1010.2
750	977.38	977.38	977.48	977.90	978.43	979.49	980.56	981.62	982.68	983.75	984.82
775	954.07	954.07	954.16	954.54	955.01	955.96	956.91	957.86	958.81	959.77	960.72
800	931.84	931.84	931.92	932.26	932.69	933.54	934.39	935.24	936.10	936.95	937.81

[a] The horizontal lines in the columns indicate the transition from the liquid phase to the gas phase.

Table 9 Isobaric cubic expansion coefficient α_v [$10^{-6}\,K^{-1}$] [a] – Continued

t [°C]	p [bar] 8	9	10	15	20	25	50	75	100	150	200
0	−65.031	−64.651	−64.272	−62.379	−60.492	−58.611	−49.296	−40.127	−31.102	−13.483	3.5753
5	18.436	18.742	19.047	20.571	22.089	23.604	31.106	38.495	45.770	59.988	73.767
10	89.849	90.094	90.339	91.560	92.778	93.993	100.01	105.94	111.79	123.23	134.33
15	152.22	152.42	152.61	153.58	154.55	155.51	160.30	165.02	169.68	178.80	187.67
20	207.67	207.82	207.98	208.73	209.49	210.24	213.99	217.68	221.34	228.50	235.49
25	257.72	257.83	257.95	258.52	259.10	259.67	262.52	265.34	268.13	273.61	278.98
30	303.46	303.55	303.63	304.05	304.47	304.88	306.95	309.00	311.04	315.06	319.01
35	345.74	345.79	345.85	346.12	346.40	346.68	348.06	349.44	350.81	353.54	356.24
40	385.16	385.19	385.22	385.37	385.53	385.68	386.45	387.23	388.00	389.58	391.16
45	422.22	422.23	422.24	422.28	422.32	422.36	422.58	422.81	423.05	423.57	424.14
50	457.32	457.30	457.29	457.23	457.17	457.10	456.81	456.54	456.29	455.86	455.50
60	522.78	522.73	522.68	522.43	522.19	521.94	520.74	519.58	518.45	516.30	514.28
70	583.49	583.41	583.33	582.91	582.50	582.09	580.08	578.11	576.20	572.51	569.01
80	640.86	640.74	640.63	640.06	639.50	638.93	636.16	633.45	630.80	625.69	620.81
90	695.98	695.84	695.70	694.98	694.26	693.55	690.04	686.61	683.26	676.78	670.58
100	749.79	749.61	749.44	748.57	747.70	746.84	742.59	738.44	734.38	726.53	719.02
125	883.56	883.30	883.04	881.76	880.48	879.21	872.94	866.82	860.85	849.34	838.34
150	1025.2	1024.8	1024.5	1022.7	1020.8	1019.0	1010.2	1001.6	993.19	977.09	961.80
175	2934.9	1186.3	1185.8	1183.2	1180.6	1178.0	1165.4	1153.2	1141.4	1119.0	1097.8
200	2566.7	2640.9	2720.5	3251.6	1375.4	1371.6	1353.2	1335.5	1318.5	1286.3	1256.4
225	2327.1	2375.9	2427.0	2721.1	3105.9	3667.6	1596.5	1569.5	1543.7	1495.8	1452.0
250	2146.7	2181.0	2216.5	2413.9	2649.1	2933.7	1938.9	1894.0	1852.0	1775.6	1707.7
275	2003.0	2028.2	2054.1	2194.5	2355.3	2540.0	4113.3	2398.0	2319.6	2183.1	2067.6
300	1884.1	1903.2	1922.7	2026.9	2142.7	2271.9	3203.2	5220.2	3169.9	2865.0	2633.2
325	1782.8	1797.7	1812.9	1892.6	1979.4	2074.0	2699.0	3752.2	5893.7	4366.2	3714.0
350	1694.6	1706.5	1718.5	1781.2	1848.3	1920.1	2367.6	3027.8	4080.4	10855.0	6982.1
375	1616.6	1626.2	1636.0	1686.3	1739.4	1795.5	2130.2	2584.4	3222.1	5717.2	16818.5
400	1546.8	1554.7	1562.7	1603.8	1646.7	1691.5	1950.1	2280.8	2710.8	4079.1	7051.9
425	1483.7	1490.3	1496.9	1530.9	1566.1	1602.6	1807.6	2058.1	2367.4	3243.0	4719.9
450	1426.2	1431.7	1437.3	1465.7	1495.0	1525.1	1691.0	1886.6	2118.9	2729.2	3625.9
475	1373.5	1378.2	1382.9	1406.9	1431.5	1456.7	1593.1	1749.5	1929.8	2379.0	2983.4
500	1325.0	1329.0	1333.0	1353.4	1374.2	1395.5	1509.2	1636.7	1780.2	2123.9	2559.3
525	1280.1	1283.5	1287.0	1304.4	1322.2	1340.3	1436.1	1541.7	1658.2	1928.9	2257.3
550	1238.3	1241.3	1244.3	1259.4	1274.7	1290.2	1371.7	1460.1	1556.3	1774.4	2030.3
575	1199.5	1202.0	1204.6	1217.7	1230.9	1244.3	1314.1	1389.1	1469.5	1648.5	1852.9
600	1163.1	1165.3	1167.6	1179.0	1190.5	1202.1	1262.4	1326.4	1394.5	1543.4	1710.0
625	1129.0	1131.0	1133.0	1142.9	1152.9	1163.1	1215.4	1270.6	1328.7	1454.2	1592.1
650	1097.0	1098.7	1100.5	1109.2	1118.0	1126.9	1172.5	1220.4	1270.4	1377.3	1492.9
675	1066.8	1068.3	1069.9	1077.6	1085.3	1093.1	1133.2	1174.9	1218.3	1310.1	1408.1
700	1038.3	1039.7	1041.0	1047.8	1054.7	1061.6	1096.9	1133.5	1171.4	1250.7	1334.6
725	1011.4	1012.6	1013.8	1019.8	1025.9	1032.0	1063.3	1095.5	1128.7	1197.9	1270.3
750	985.89	986.96	988.03	993.41	998.82	1004.3	1032.0	1060.5	1089.8	1150.4	1213.3
775	961.68	962.63	963.59	968.40	973.23	978.10	1002.8	1028.1	1054.1	1107.4	1162.4
800	938.67	939.53	940.38	944.69	949.02	953.38	975.47	998.05	1021.1	1068.3	1116.7

[a] The horizontal lines in the columns indicate the transition from the liquid phase to the gas phase.

Table 9 Isobaric cubic expansion coefficient α_v [$10^{-6}\,K^{-1}$] – Continued

t	p [bar]										
[°C]	250	300	350	400	450	500	600	700	800	900	1000
0	20.086	36.061	51.517	66.466	80.925	94.908	121.51	146.40	169.71	191.59	212.16
5	87.118	100.05	112.57	124.70	136.44	147.80	169.45	189.74	208.76	226.62	243.43
10	145.10	155.54	165.68	175.50	185.02	194.25	211.87	228.41	243.96	258.58	272.35
15	196.29	204.67	212.81	220.72	228.40	235.85	250.11	263.54	276.20	288.13	299.38
20	242.29	248.92	255.37	261.66	267.77	273.71	285.12	295.91	306.11	315.75	324.86
25	284.22	289.34	294.34	299.22	303.98	308.63	317.57	326.07	334.14	341.79	349.04
30	322.89	326.69	330.42	334.08	337.66	341.16	347.94	354.42	360.61	366.50	372.11
35	358.91	361.55	364.15	366.72	369.25	371.74	376.59	381.27	385.77	390.08	394.21
40	392.75	394.34	395.93	397.52	399.10	400.68	403.79	406.84	409.81	412.70	415.48
45	424.75	425.40	426.07	426.77	427.49	428.23	429.76	431.32	432.89	434.46	436.00
50	455.21	454.99	454.82	454.70	454.63	454.60	454.67	454.85	455.13	455.48	455.87
60	512.38	510.59	508.91	507.32	505.83	504.43	501.86	499.56	497.50	495.63	493.93
70	565.67	562.49	559.46	556.57	553.81	551.18	546.25	541.73	537.58	533.73	530.14
80	616.15	611.68	607.41	603.31	599.39	595.62	588.53	581.97	575.88	570.21	564.89
90	664.64	658.95	653.48	648.24	643.21	638.37	629.22	620.74	612.84	605.45	598.51
100	711.82	704.92	698.30	691.93	685.81	679.92	668.80	658.45	648.80	639.77	631.27
125	827.82	817.75	808.10	798.83	789.94	781.39	765.24	750.24	736.27	723.20	710.93
150	947.26	933.41	920.18	907.54	895.44	883.85	862.06	841.94	823.30	805.95	789.74
175	1077.9	1059.0	1041.1	1024.1	1007.9	992.49	963.73	937.40	913.21	890.88	870.17
200	1228.6	1202.5	1178.0	1155.0	1133.2	1112.7	1074.7	1040.4	1009.2	980.67	954.48
225	1411.8	1374.8	1340.4	1308.5	1278.8	1250.9	1200.2	1155.1	1114.6	1078.1	1045.0
250	1646.9	1592.0	1542.1	1496.5	1454.6	1415.9	1346.8	1286.6	1233.6	1186.5	1144.4
275	1968.3	1881.7	1805.3	1737.1	1675.9	1620.4	1523.6	1441.8	1371.3	1310.0	1255.9
300	2448.8	2297.5	2170.5	2061.8	1967.3	1884.2	1744.0	1629.8	1534.5	1453.5	1383.5
325	3280.2	2966.4	2724.8	2531.9	2373.7	2240.8	2028.1	1863.7	1731.9	1623.3	1531.8
350	5171.0	4259.5	3694.1	3293.4	2990.3	2754.1	2407.8	2160.9	1973.5	1825.3	1704.2
375	16388	8017.7	5799.9	4700.2	4023.3	3556.7	2944.1	2552.0	2275.2	2067.4	1904.5
400	17054	37835	12907	7963.4	5983.6	4898.9	3716.9	3069.3	2652.2	2357.2	2135.5
425	7496.9	13441	20591	15069	9789.6	7186.2	4835.1	3753.6	3124.0	2706.5	2406.0
450	4992.0	7117.1	10239	12818	12133	9691.5	6226.8	4579.0	3675.7	3106.4	2711.8
475	3804.8	4917.1	6364.6	8024.4	9160.2	9203.7	7172.4	5346.4	4223.3	3510.8	3023.8
500	3108.6	3794.9	4626.7	5565.8	6486.6	7107.8	6877.9	5684.7	4610.6	3840.4	3294.1
525	2651.1	3116.7	3654.3	4248.5	4854.5	5391.0	5855.7	5438.7	4695.6	4012.1	3472.3
550	2326.5	2663.6	3038.8	3443.8	3860.6	4257.4	4809.1	4843.0	4481.2	3988.4	3526.3
575	2083.4	2338.8	2615.8	2908.6	3207.6	3498.8	3978.2	4180.7	4077.6	3801.2	3457.1
600	1893.9	2093.7	2306.5	2527.9	2752.1	2971.1	3354.7	3593.8	3632.5	3509.9	3294.9
625	1741.7	1901.7	2069.8	2242.9	2416.9	2586.8	2892.5	3113.1	3211.2	3181.2	3062.1
650	1616.6	1747.2	1882.8	2021.3	2159.8	2295.0	2541.7	2733.6	2848.1	2875.5	2821.2
675	1511.7	1619.9	1731.3	1844.2	1956.5	2066.2	2268.1	2432.0	2544.0	2598.0	2595.8
700	1422.4	1513.2	1606.0	1699.4	1792.1	1882.5	2050.0	2189.5	2291.6	2352.2	2373.1
725	1345.3	1422.4	1500.6	1578.9	1656.5	1732.0	1872.6	1992.0	2083.0	2141.6	2168.4
750	1278.0	1344.0	1410.6	1477.0	1542.6	1606.4	1725.8	1828.6	1909.4	1964.2	1991.7
775	1218.7	1275.6	1332.8	1389.6	1445.5	1499.9	1602.0	1691.1	1762.9	1814.1	1842.4
800	1165.8	1215.3	1264.7	1313.7	1361.7	1408.3	1495.9	1573.2	1637.2	1685.5	1716.4

Table 10 Isothermal compressibility κ_T

For the single-phase region, this table contains values for the

- Isothermal compressibility $\kappa_T = -v^{-1}(\partial v/\partial p)_T$

for temperatures from 0 °C to 800 °C and pressures from 0.006 112 127 bar to 1000 bar (regions 1 to 3 of IAPWS-IF97). The values for κ_T were calculated from the IAPWS-IF97 basic equations, Eqs. (2.3), (2.6), and (2.11).

The horizontal lines in the columns indicate the transition from the liquid phase to the vapour phase.

Values for the isothermal compressibility for temperatures above 800 °C up to 2000 °C and pressures up to 500 bar can be calculated with the program "IAPWS-IF97 Electronic Steam Tables" in Part D.

Partial derivatives of thermodynamic properties can be calculated with values of κ_T as described in Sec. 2.4.4.

Table 10 Isothermal compressibility κ_T [10^{-6} kPa^{-1}] [a]

t [°C]	p [bar] 0.006112127	0.01	0.1	0.5	1	2	3	4	5	6	7
0	0.50895	0.50895	0.50894	0.50888	0.50881	0.50867	0.50852	0.50838	0.50824	0.50810	0.50795
5	1636924	0.49180	0.49179	0.49174	0.49167	0.49154	0.49141	0.49127	0.49114	0.49101	0.49088
10	1636798	1000752	0.47801	0.47796	0.47790	0.47778	0.47765	0.47753	0.47741	0.47728	0.47716
15	1636709	1000638	0.46702	0.46697	0.46691	0.46679	0.46668	0.46656	0.46644	0.46632	0.46620
20	1636641	1000559	0.45835	0.45831	0.45825	0.45814	0.45802	0.45791	0.45780	0.45768	0.45757
25	1636585	1000498	0.45167	0.45163	0.45157	0.45146	0.45135	0.45124	0.45113	0.45102	0.45091
30	1636538	1000448	0.44670	0.44666	0.44660	0.44649	0.44639	0.44628	0.44617	0.44606	0.44595
35	1636496	1000406	0.44323	0.44319	0.44314	0.44303	0.44292	0.44281	0.44270	0.44260	0.44249
40	1636460	1000369	0.44109	0.44105	0.44100	0.44089	0.44078	0.44067	0.44057	0.44046	0.44035
45	1636428	1000337	0.44015	0.44011	0.44005	0.43994	0.43984	0.43973	0.43962	0.43951	0.43940
50	1636400	1000309	100324	0.44025	0.44020	0.44008	0.43997	0.43986	0.43975	0.43964	0.43953
60	1636352	1000261	100267	0.44347	0.44341	0.44330	0.44318	0.44306	0.44295	0.44283	0.44272
70	1636314	1000223	100226	0.45021	0.45014	0.45002	0.44990	0.44977	0.44965	0.44953	0.44940
80	1636283	1000192	100194	0.46016	0.46010	0.45996	0.45983	0.45969	0.45956	0.45943	0.45930
90	1636258	1000166	100168	20177	0.47311	0.47297	0.47282	0.47268	0.47253	0.47238	0.47224
100	1636237	1000145	100147	20153	10163	0.48901	0.48885	0.48868	0.48852	0.48836	0.48820
125	1636198	1000107	100108	20111	10115	5124.8	0.54291	0.54270	0.54249	0.54227	0.54206
150	1636173	1000081	100082	20083	10086	5090.1	3428.5	2601.1	0.62014	0.61984	0.61954
175	1636155	1000064	100064	20065	10066	5068.4	3404.3	2573.7	2076.5	1746.3	1511.7
200	1636142	1000051	100051	20051	10052	5053.6	3388.4	2556.5	2058.1	1726.3	1489.9
225	1636133	1000041	100041	20042	10042	5043.0	3377.2	2544.7	2045.6	1713.2	1476.0
250	1636126	1000034	100034	20034	10035	5035.1	3369.0	2536.1	2036.7	1703.9	1466.4
275	1636120	1000028	100029	20029	10029	5029.1	3362.8	2529.7	2030.1	1697.1	1459.3
300	1636116	1000024	100024	20024	10024	5024.4	3357.9	2524.8	2025.0	1691.9	1454.0
325	1636112	1000020	100020	20020	10021	5020.7	3354.1	2520.9	2021.1	1687.9	1449.9
350	1636109	1000017	100017	20017	10018	5017.6	3351.1	2517.8	2017.9	1684.7	1446.7
375	1636107	1000015	100015	20015	10015	5015.1	3348.5	2515.3	2015.3	1682.1	1444.0
400	1636105	1000013	100013	20013	10013	5013.1	3346.5	2513.2	2013.2	1679.9	1441.9
425	1636103	1000011	100011	20011	10011	5011.4	3344.7	2511.4	2011.5	1678.2	1440.1
450	1636102	1000010	100010	20010	10010	5009.9	3343.3	2509.9	2010.0	1676.7	1438.6
475	1636100	1000009	100009	20009	10009	5008.7	3342.0	2508.7	2008.7	1675.4	1437.3
500	1636099	1000008	100008	20008	10008	5007.6	3341.0	2507.6	2007.6	1674.3	1436.2
525	1636098	1000007	100007	20007	10007	5006.7	3340.0	2506.7	2006.7	1673.4	1435.3
550	1636098	1000006	100006	20006	10006	5005.9	3339.3	2505.9	2005.9	1672.6	1434.5
575	1636097	1000005	100005	20005	10005	5005.2	3338.6	2505.2	2005.3	1671.9	1433.8
600	1636096	1000005	100005	20005	10005	5004.6	3338.0	2504.6	2004.7	1671.3	1433.2
625	1636096	1000004	100004	20004	10004	5004.1	3337.5	2504.1	2004.1	1670.8	1432.7
650	1636095	1000004	100004	20004	10004	5003.7	3337.0	2503.7	2003.7	1670.3	1432.2
675	1636095	1000003	100003	20003	10003	5003.3	3336.6	2503.3	2003.3	1669.9	1431.8
700	1636095	1000003	100003	20003	10003	5002.9	3336.2	2502.9	2002.9	1669.6	1431.5
725	1636094	1000003	100003	20003	10003	5002.6	3335.9	2502.6	2002.6	1669.3	1431.2
750	1636094	1000002	100002	20002	10002	5002.3	3335.6	2502.3	2002.3	1669.0	1430.9
775	1636094	1000002	100002	20002	10002	5002.1	3335.4	2502.1	2002.1	1668.7	1430.6
800	1636093	1000002	100002	20002	10002	5001.8	3335.2	2501.8	2001.8	1668.5	1430.4

[a] The horizontal lines in the columns indicate the transition from the liquid phase to the gas phase.

Table 10 Isothermal compressibility κ_T [10^{-6} kPa^{-1}] [a] – Continued

t [°C]	p [bar] 8	9	10	15	20	25	50	75	100	150	200
0	0.50781	0.50767	0.50753	0.50682	0.50611	0.50540	0.50187	0.49837	0.49490	0.48802	0.48126
5	0.49075	0.49062	0.49048	0.48983	0.48917	0.48851	0.48525	0.48200	0.47878	0.47242	0.46614
10	0.47703	0.47691	0.47679	0.47617	0.47555	0.47494	0.47187	0.46883	0.46581	0.45983	0.45394
15	0.46609	0.46597	0.46585	0.46526	0.46468	0.46409	0.46118	0.45829	0.45541	0.44973	0.44413
20	0.45746	0.45734	0.45723	0.45667	0.45610	0.45554	0.45273	0.44995	0.44719	0.44172	0.43633
25	0.45080	0.45069	0.45058	0.45003	0.44948	0.44893	0.44620	0.44349	0.44081	0.43549	0.43025
30	0.44584	0.44574	0.44563	0.44509	0.44455	0.44401	0.44132	0.43866	0.43602	0.43080	0.42566
35	0.44238	0.44227	0.44217	0.44163	0.44109	0.44056	0.43790	0.43526	0.43264	0.42746	0.42237
40	0.44024	0.44013	0.44003	0.43949	0.43895	0.43842	0.43575	0.43311	0.43050	0.42533	0.42024
45	0.43929	0.43918	0.43907	0.43853	0.43799	0.43745	0.43477	0.43211	0.42947	0.42427	0.41916
50	0.43942	0.43931	0.43920	0.43865	0.43810	0.43756	0.43483	0.43214	0.42947	0.42420	0.41904
60	0.44260	0.44249	0.44237	0.44180	0.44122	0.44065	0.43780	0.43498	0.43220	0.42672	0.42136
70	0.44928	0.44916	0.44904	0.44842	0.44781	0.44720	0.44417	0.44118	0.43822	0.43242	0.42676
80	0.45916	0.45903	0.45890	0.45823	0.45757	0.45691	0.45364	0.45042	0.44725	0.44102	0.43496
90	0.47209	0.47195	0.47180	0.47108	0.47035	0.46963	0.46607	0.46256	0.45911	0.45236	0.44580
100	0.48804	0.48788	0.48772	0.48692	0.48612	0.48533	0.48140	0.47755	0.47376	0.46637	0.45922
125	0.54185	0.54163	0.54142	0.54036	0.53930	0.53825	0.53307	0.52800	0.52305	0.51348	0.50429
150	0.61924	0.61894	0.61865	0.61717	0.61569	0.61423	0.60705	0.60007	0.59330	0.58030	0.56798
175	1337.2	0.72879	0.72835	0.72617	0.72401	0.72187	0.71139	0.70129	0.69155	0.67306	0.65577
200	1313.0	1176.0	1066.8	746.21	0.88083	0.87750	0.86130	0.84582	0.83102	0.80328	0.77774
225	1298.4	1160.5	1050.4	722.80	563.36	473.80	1.0857	1.0603	1.0363	0.99191	0.95189
250	1288.4	1150.1	1039.6	709.48	546.53	450.90	1.4454	1.3993	1.3565	1.2793	1.2117
275	1281.1	1142.6	1031.9	700.49	536.00	438.44	258.09	1.9974	1.9079	1.7540	1.6261
300	1275.7	1137.0	1026.2	694.06	528.74	430.22	240.26	194.07	3.0590	2.6612	2.3668
325	1271.5	1132.8	1021.8	689.28	523.48	424.41	230.28	172.92	157.57	4.9953	4.0057
350	1268.2	1129.4	1018.4	685.61	519.52	420.12	223.79	162.23	136.61	149.04	10.004
375	1265.5	1126.7	1015.7	682.72	516.44	416.85	219.24	155.66	126.42	107.83	149.15
400	1263.4	1124.5	1013.5	680.39	513.99	414.27	215.88	151.19	120.29	94.041	91.024
425	1261.6	1122.7	1011.6	678.48	512.01	412.21	213.32	147.97	116.18	86.816	76.061
450	1260.1	1121.2	1010.1	676.90	510.38	410.52	211.30	145.54	113.22	82.319	68.768
475	1258.8	1119.9	1008.8	675.58	509.02	409.12	209.68	143.65	111.01	79.243	64.393
500	1257.7	1118.8	1007.7	674.46	507.87	407.95	208.36	142.14	109.29	77.005	61.468
525	1256.8	1117.9	1006.8	673.51	506.90	406.96	207.26	140.92	107.93	75.308	59.373
550	1256.0	1117.1	1006.0	672.69	506.07	406.11	206.34	139.91	106.82	73.980	57.797
575	1255.3	1116.4	1005.3	671.98	505.35	405.38	205.55	139.06	105.90	72.916	56.572
600	1254.7	1115.8	1004.7	671.37	504.73	404.75	204.88	138.35	105.14	72.047	55.595
625	1254.1	1115.3	1004.1	670.84	504.19	404.21	204.31	137.73	104.49	71.326	54.801
650	1253.7	1114.8	1003.7	670.37	503.72	403.73	203.80	137.21	103.94	70.721	54.144
675	1253.3	1114.4	1003.3	669.96	503.30	403.31	203.37	136.75	103.46	70.207	53.594
700	1252.9	1114.0	1002.9	669.59	502.94	402.94	202.98	136.35	103.05	69.766	53.128
725	1252.6	1113.7	1002.6	669.27	502.61	402.62	202.65	136.00	102.69	69.385	52.730
750	1252.3	1113.4	1002.3	668.99	502.32	402.33	202.35	135.70	102.37	69.054	52.386
775	1252.1	1113.2	1002.1	668.73	502.07	402.07	202.08	135.42	102.10	68.765	52.088
800	1251.8	1112.9	1001.8	668.50	501.84	401.84	201.84	135.18	101.85	68.510	51.827

[a] The horizontal lines in the columns indicate the transition from the liquid phase to the gas phase.

Table 10 Isothermal compressibility κ_T [10^{-6} kPa^{-1}] – Continued

t [°C]	*p* [bar] 250	300	350	400	450	500	600	700	800	900	1000
0	0.47460	0.46805	0.46161	0.45528	0.44906	0.44296	0.43109	0.41969	0.40877	0.39834	0.38842
5	0.45997	0.45389	0.44790	0.44201	0.43623	0.43054	0.41946	0.40880	0.39856	0.38875	0.37938
10	0.44813	0.44242	0.43679	0.43125	0.42580	0.42044	0.40999	0.39991	0.39021	0.38090	0.37198
15	0.43861	0.43317	0.42782	0.42255	0.41736	0.41225	0.40229	0.39267	0.38339	0.37447	0.36592
20	0.43103	0.42580	0.42065	0.41557	0.41058	0.40566	0.39607	0.38680	0.37786	0.36925	0.36098
25	0.42509	0.42001	0.41501	0.41008	0.40523	0.40045	0.39113	0.38212	0.37343	0.36506	0.35701
30	0.42060	0.41561	0.41070	0.40587	0.40112	0.39644	0.38730	0.37848	0.36996	0.36176	0.35389
35	0.41736	0.41243	0.40758	0.40280	0.39810	0.39348	0.38446	0.37576	0.36736	0.35928	0.35152
40	0.41525	0.41033	0.40550	0.40074	0.39607	0.39147	0.38251	0.37386	0.36553	0.35752	0.34983
45	0.41414	0.40921	0.40436	0.39960	0.39492	0.39032	0.38136	0.37272	0.36441	0.35642	0.34878
50	0.41397	0.40899	0.40410	0.39930	0.39458	0.38995	0.38094	0.37227	0.36394	0.35595	0.34830
60	0.41610	0.41095	0.40590	0.40095	0.39610	0.39135	0.38212	0.37326	0.36478	0.35667	0.34894
70	0.42122	0.41581	0.41051	0.40533	0.40027	0.39531	0.38571	0.37653	0.36777	0.35943	0.35152
80	0.42905	0.42329	0.41767	0.41218	0.40682	0.40159	0.39148	0.38186	0.37271	0.36404	0.35585
90	0.43944	0.43324	0.42721	0.42133	0.41561	0.41003	0.39930	0.38911	0.37947	0.37037	0.36181
100	0.45229	0.44558	0.43905	0.43271	0.42655	0.42056	0.40906	0.39820	0.38796	0.37833	0.36932
125	0.49547	0.48698	0.47880	0.47090	0.46327	0.45589	0.44186	0.42873	0.41647	0.40508	0.39454
150	0.55627	0.54510	0.53443	0.52421	0.51442	0.50501	0.48727	0.47086	0.45569	0.44174	0.42898
175	0.63953	0.62423	0.60977	0.59605	0.58302	0.57061	0.54745	0.52629	0.50696	0.48937	0.47345
200	0.75412	0.73219	0.71173	0.69257	0.67457	0.65760	0.62635	0.59824	0.57289	0.55006	0.52964
225	0.91558	0.88246	0.85207	0.82407	0.79813	0.77399	0.73032	0.69178	0.65756	0.62717	0.60030
250	1.1519	1.0987	1.0509	1.0078	0.9685	0.93267	0.86919	0.81459	0.76708	0.72556	0.68938
275	1.5179	1.4251	1.3445	1.2737	1.2110	1.1548	1.0584	0.97819	0.91026	0.85216	0.80240
300	2.1387	1.9554	1.8047	1.6783	1.5705	1.4772	1.3230	1.2003	1.1000	1.0167	0.94689
325	3.3701	2.9288	2.5991	2.3420	2.1363	1.9678	1.7055	1.5090	1.3557	1.2329	1.1331
350	6.6947	5.1132	4.1942	3.5748	3.1182	2.7714	2.2837	1.9511	1.7071	1.5208	1.3753
375	33.019	13.002	8.3808	6.2650	5.0355	4.2260	3.2177	2.6106	2.2033	1.9109	1.6909
400	119.94	120.34	27.471	14.186	9.5131	7.1608	4.8062	3.6285	2.9214	2.4498	2.1130
425	75.587	84.782	80.870	41.143	21.477	13.659	7.6248	5.2286	3.9681	3.1964	2.6774
450	62.822	61.221	61.247	54.754	39.131	25.317	12.380	7.6755	5.4612	4.2115	3.4191
475	56.479	52.081	49.382	46.613	41.023	32.908	18.360	10.985	7.4431	5.5212	4.3532
500	52.649	47.151	43.385	40.317	37.064	32.802	22.428	14.398	9.7231	7.0635	5.4524
525	50.083	44.060	39.803	36.481	33.526	30.511	23.552	16.789	11.835	8.6536	6.6326
550	48.240	41.943	37.438	33.961	31.052	28.404	23.142	17.839	13.358	10.047	7.7670
575	46.852	40.400	35.763	32.203	29.295	26.776	22.273	18.018	14.177	11.088	8.7348
600	45.771	39.225	34.514	30.911	28.006	25.549	21.401	17.774	14.498	11.712	9.4469
625	44.907	38.302	33.548	29.924	27.024	24.607	20.657	17.382	14.518	12.023	9.9329
650	44.204	37.561	32.781	29.145	26.253	23.865	20.040	16.979	14.382	12.143	10.235
675	43.622	36.954	32.159	28.518	25.635	23.268	19.530	16.608	14.185	12.124	10.379
700	43.135	36.451	31.646	28.005	25.129	22.779	19.105	16.281	13.977	12.039	10.405
725	42.722	36.028	31.219	27.578	24.709	22.373	18.748	15.997	13.781	11.935	10.384
750	42.369	35.669	30.857	27.218	24.356	22.032	18.444	15.749	13.602	11.830	10.350
775	42.064	35.361	30.548	26.913	24.057	21.742	18.185	15.532	13.439	11.729	10.312
800	41.800	35.095	30.283	26.651	23.801	21.494	17.961	15.342	13.291	11.630	10.265

Table 11 Saturation state: Kinematic viscosity ν, Prandtl number Pr, Dielectric constant ε, Surface tension σ

This table contains values on the saturated liquid ($'$) and saturated vapour ($''$) lines for the following properties for temperatures from 0 °C up to the critical temperature t_c = 373.946 °C:

- Kinematic viscosity $\nu = \eta\rho^{-1}$
- Prandtl number $Pr = \eta c_p \lambda^{-1}$
- Dielectric constant ε

Furthermore, values for the

- Surface tension σ

are also listed.

For given temperatures, the saturation pressures p_s were calculated from the IAPWS-IF97 saturation-pressure equation, Eq. (2.13).

For temperatures $t \leq$ 350 °C and input values of t and p_s, the required *thermodynamic* properties ρ', ρ'', c_p' and c_p'' on the saturated-liquid and saturated-vapour lines were determined from the basic equations for regions 1 and 2, Eqs. (2.3) and (2.6).

For $t >$ 350 °C and input values of t and p_s, the saturation densities ρ' and ρ'' were calculated by iterating the basic equation for region 3, Eq. (2.11). With the values of (ρ', t) and (ρ'', t), the isobaric heat capacities c_p' and c_p'' were determined from the basic equation, Eq. (2.11).

With (ρ', t) and (ρ'', t), the values for the transport properties η' and η'', and λ' and λ'' were determined from Eq. (3.1) and Eq. (3.4), respectively. The values for the dielectric constants, ε' and ε'', were calculated from Eq. (3.9).

The values for the surface tension σ of saturated water were calculated from Eq. (3.8) for the given temperature values.

Table 11 Saturation state: Kinematic viscosity ν, Prandtl number Pr, Dielectric constant ε, Surface tension σ

t [°C]	ν' [10^{-6} m^2 s^{-1}]	ν''	Pr' [–]	Pr''	ε' [–]	ε''	σ [10^{-3} N m^{-1}]
0	1.7923	1844.0	13.456	1.0241	87.899	1.0001	75.648
0.01[a]	1.7917	1842.8	13.451	1.0241	87.895	1.0001	75.646
1	1.7315	1727.0	12.941	1.0233	87.498	1.0001	75.508
2	1.6739	1618.4	12.455	1.0226	87.098	1.0001	75.367
3	1.6193	1517.5	11.998	1.0218	86.701	1.0001	75.226
4	1.5676	1423.7	11.566	1.0211	86.305	1.0001	75.084
5	1.5184	1336.4	11.157	1.0204	85.911	1.0001	74.942
6	1.4718	1255.2	10.771	1.0197	85.520	1.0001	74.799
7	1.4274	1179.6	10.405	1.0191	85.130	1.0001	74.655
8	1.3851	1109.1	10.059	1.0185	84.741	1.0001	74.511
9	1.3448	1043.4	9.7293	1.0179	84.355	1.0001	74.366
10	1.3064	982.13	9.4166	1.0174	83.970	1.0001	74.221
11	1.2698	924.92	9.1193	1.0168	83.588	1.0001	74.075
12	1.2348	871.51	8.8363	1.0163	83.207	1.0001	73.929
13	1.2013	821.59	8.5668	1.0159	82.827	1.0001	73.782
14	1.1693	774.93	8.3098	1.0154	82.450	1.0002	73.634
15	1.1387	731.29	8.0647	1.0150	82.074	1.0002	73.486
16	1.1094	690.44	7.8306	1.0146	81.699	1.0002	73.337
17	1.0812	652.19	7.6070	1.0142	81.327	1.0002	73.188
18	1.0542	616.36	7.3931	1.0138	80.956	1.0002	73.038
19	1.0283	582.77	7.1885	1.0135	80.586	1.0002	72.887
20	1.0035	551.28	6.9926	1.0132	80.219	1.0002	72.736
22	0.95659	493.99	6.6250	1.0126	79.488	1.0002	72.432
24	0.91320	443.46	6.2868	1.0121	78.764	1.0003	72.126
25	0.89271	420.45	6.1276	1.0119	78.405	1.0003	71.972
26	0.87296	398.81	5.9748	1.0117	78.047	1.0003	71.818
28	0.83556	359.28	5.6864	1.0113	77.336	1.0003	71.507
30	0.80074	324.22	5.4193	1.0110	76.631	1.0004	71.194
32	0.76826	293.06	5.1715	1.0107	75.932	1.0004	70.879
34	0.73790	265.33	4.9411	1.0105	75.239	1.0004	70.562
36	0.70949	240.61	4.7265	1.0104	74.553	1.0005	70.242
38	0.68286	218.53	4.5264	1.0103	73.872	1.0005	69.920
40	0.65786	198.78	4.3394	1.0102	73.198	1.0006	69.596
42	0.63436	181.08	4.1645	1.0102	72.529	1.0007	69.270
44	0.61224	165.20	4.0006	1.0102	71.867	1.0007	68.942
46	0.59139	150.92	3.8468	1.0102	71.210	1.0008	68.611
48	0.57172	138.07	3.7024	1.0103	70.559	1.0009	68.279
50	0.55314	126.49	3.5666	1.0104	69.914	1.0009	67.944
52	0.53556	116.03	3.4387	1.0105	69.274	1.0010	67.607
54	0.51892	106.58	3.3182	1.0106	68.641	1.0011	67.268
56	0.50316	98.022	3.2045	1.0108	68.012	1.0012	66.927
58	0.48820	90.264	3.0970	1.0110	67.390	1.0013	66.584

[a] Triple-point temperature.

Table 11 Saturation state: Kinematic viscosity ν, Prandtl number Pr, Dielectric constant ε, Surface tension σ – Continued

t	ν'	ν''	Pr'	Pr''	ε'	ε''	σ
[°C]	[10^{-6} m^2 s^{-1}]		[–]		[–]		[10^{-3} N m^{-1}]
60	0.47400	83.221	2.9955	1.0113	66.773	1.0014	66.238
62	0.46050	76.820	2.8994	1.0115	66.161	1.0015	65.891
64	0.44767	70.994	2.8083	1.0118	65.555	1.0017	65.541
66	0.43545	65.686	2.7221	1.0122	64.954	1.0018	65.190
68	0.42382	60.843	2.6402	1.0126	64.359	1.0020	64.836
70	0.41272	56.419	2.5625	1.0130	63.769	1.0021	64.481
72	0.40214	52.373	2.4886	1.0134	63.184	1.0023	64.123
74	0.39203	48.668	2.4183	1.0139	62.605	1.0024	63.764
76	0.38238	45.272	2.3515	1.0144	62.030	1.0026	63.402
78	0.37315	42.156	2.2878	1.0150	61.461	1.0028	63.038
80	0.36433	39.293	2.2272	1.0156	60.897	1.0030	62.673
82	0.35588	36.660	2.1693	1.0163	60.338	1.0033	62.305
84	0.34778	34.236	2.1141	1.0170	59.784	1.0035	61.936
86	0.34003	32.002	2.0615	1.0177	59.235	1.0037	61.565
88	0.33260	29.942	2.0111	1.0186	58.691	1.0040	61.191
90	0.32546	28.039	1.9630	1.0195	58.152	1.0043	60.816
92	0.31862	26.279	1.9170	1.0204	57.617	1.0046	60.439
94	0.31205	24.652	1.8730	1.0214	57.088	1.0049	60.060
96	0.30573	23.144	1.8309	1.0225	56.563	1.0052	59.679
98	0.29966	21.747	1.7905	1.0237	56.043	1.0055	59.296
100	0.29382	20.450	1.7519	1.0249	55.527	1.0059	58.912
105	0.28017	17.597	1.6620	1.0284	54.259	1.0069	57.943
110	0.26775	15.214	1.5810	1.0324	53.018	1.0079	56.962
115	0.25640	13.211	1.5077	1.0370	51.806	1.0092	55.970
120	0.24603	11.521	1.4413	1.0423	50.620	1.0105	54.968
125	0.23652	10.088	1.3810	1.0481	49.460	1.0121	53.955
130	0.22778	8.8673	1.3262	1.0547	48.326	1.0138	52.932
135	0.21974	7.8225	1.2762	1.0619	47.216	1.0156	51.899
140	0.21233	6.9248	1.2306	1.0696	46.131	1.0177	50.856
145	0.20548	6.1504	1.1890	1.0780	45.069	1.0200	49.803
150	0.19914	5.4798	1.1510	1.0869	44.030	1.0225	48.741
155	0.19326	4.8970	1.1162	1.0963	43.013	1.0252	47.670
160	0.18781	4.3886	1.0844	1.1062	42.018	1.0282	46.591
165	0.18275	3.9437	1.0552	1.1164	41.043	1.0315	45.503
170	0.17803	3.5531	1.0286	1.1270	40.088	1.0350	44.406
175	0.17364	3.2090	1.0043	1.1379	39.153	1.0389	43.302
180	0.16954	2.9051	0.98210	1.1491	38.236	1.0431	42.190
185	0.16571	2.6358	0.96187	1.1608	37.337	1.0476	41.071
190	0.16214	2.3965	0.94347	1.1728	36.456	1.0525	39.945
195	0.15879	2.1834	0.92680	1.1852	35.591	1.0578	38.813

Table 11 Saturation state: Kinematic viscosity ν, Prandtl number Pr, Dielectric constant ε, Surface tension σ – Continued

t [°C]	ν' [10^{-6} m^2 s^{-1}]	ν'' [10^{-6} m^2 s^{-1}]	Pr' [–]	Pr'' [–]	ε' [–]	ε'' [–]	σ [10^{-3} N m^{-1}]
200	0.15565	1.9931	0.91175	1.1982	34.742	1.0636	37.675
205	0.15271	1.8227	0.89823	1.2116	33.909	1.0698	36.530
210	0.14995	1.6698	0.88617	1.2257	33.091	1.0765	35.381
215	0.14736	1.5322	0.87551	1.2404	32.286	1.0837	34.226
220	0.14493	1.4081	0.86619	1.2558	31.496	1.0915	33.067
225	0.14264	1.2961	0.85817	1.2720	30.718	1.0999	31.903
230	0.14048	1.1946	0.85142	1.2890	29.952	1.1089	30.736
235	0.13845	1.1025	0.84593	1.3069	29.198	1.1187	29.566
240	0.13654	1.0188	0.84167	1.3258	28.455	1.1292	28.394
245	0.13474	0.94254	0.83867	1.3457	27.722	1.1405	27.219
250	0.13304	0.87297	0.83693	1.3667	26.999	1.1527	26.043
255	0.13144	0.80937	0.83648	1.3891	26.285	1.1659	24.866
260	0.12992	0.75113	0.83736	1.4129	25.579	1.1802	23.689
265	0.12850	0.69770	0.83965	1.4384	24.881	1.1957	22.512
270	0.12715	0.64860	0.84342	1.4659	24.190	1.2124	21.337
275	0.12588	0.60341	0.84879	1.4959	23.504	1.2306	20.163
280	0.12469	0.56175	0.85590	1.5286	22.824	1.2505	18.993
285	0.12356	0.52329	0.86492	1.5647	22.148	1.2721	17.826
290	0.12250	0.48771	0.87610	1.6046	21.475	1.2958	16.664
295	0.12150	0.45474	0.88972	1.6489	20.805	1.3217	15.508
300	0.12056	0.42416	0.90613	1.6982	20.135	1.3504	14.360
305	0.11968	0.39572	0.92581	1.7531	19.466	1.3820	13.219
310	0.11886	0.36925	0.94935	1.8145	18.794	1.4172	12.089
315	0.11810	0.34456	0.97753	1.8836	18.119	1.4566	10.970
320	0.11739	0.32148	1.0114	1.9623	17.439	1.5010	9.8644
325	0.11674	0.29986	1.0527	2.0537	16.751	1.5514	8.7744
330	0.11615	0.27956	1.1036	2.1625	16.053	1.6091	7.7026
335	0.11563	0.26044	1.1682	2.2957	15.340	1.6762	6.6518
340	0.11517	0.24238	1.2524	2.4621	14.607	1.7552	5.6255
345	0.11479	0.22525	1.3658	2.6724	13.844	1.8499	4.6282
350	0.11449	0.20893	1.5229	2.9362	13.043	1.9663	3.6654
355	0.11431	0.19329	1.7693	3.3547	12.183	2.1138	2.7448
360	0.11427	0.17807	2.1780	4.0021	11.233	2.3107	1.8772
365	0.11450	0.16284	3.0195	5.2331	10.130	2.5975	1.0801
370	0.11533	0.14639	5.8465	8.9326	8.6722	3.1076	0.38822
371	0.11569	0.14260	7.4854	10.955	8.2784	3.2794	0.26921
372	0.11622	0.13836	10.684	14.830	7.8019	3.5119	0.16007
373	0.11717	0.13313	20.105	26.191	7.1501	3.8834	0.064757
373.946 [a]	0.12214 [b]		∞ [c]		5.3606		0

[a] Critical temperature.

[b] In the near-critical region, the use of the industrial equation for η, Eq. (3.1), does not yield accurate values for ν. If more accurate values are needed in this region, the scientific equation for η [31] should be used.

[c] In the near-critical region, the use of IAPWS-IF97 for c_p and the use of the industrial equations for η and λ, Eqs. (3.1) and (3.4), do not yield accurate values for Pr.

Table 12 Kinematic viscosity ν

For the single-phase region, this table contains values for the

- Kinematic viscosity $\nu = \eta\rho^{-1}$

for temperatures from 0 °C to 800 °C and pressures from 0.006 112 127 bar to 1000 bar.

For given pressures and temperatures, the needed density ρ was calculated from the IAPWS-IF97 basic equations, Eqs. (2.3), (2.6), and (2.11).

The dynamic viscosity η was determined from the equation for industrial applications, Eq. (3.1), where the density ρ needed in this equation results from the IAPWS-IF97 basic equations, see above.

The horizontal lines in the columns indicate the transition from the liquid phase to the vapour phase.

Table 12 Kinematic viscosity ν [10^{-6} m^2 s^{-1}] [a]

t [°C]	p [bar] 0.006112127	0.01	0.1	0.5	1	2	3	4	5	6	7
0	1.7923	1.7923	1.7923	1.7922	1.7920	1.7917	1.7914	1.7911	1.7908	1.7905	1.7901
5	1908.5	1.5184	1.5184	1.5183	1.5182	1.5180	1.5178	1.5176	1.5174	1.5171	1.5169
10	1974.8	1206.5	1.3064	1.3064	1.3063	1.3061	1.3060	1.3058	1.3057	1.3055	1.3054
15	2043.0	1248.2	1.1387	1.1386	1.1386	1.1385	1.1384	1.1383	1.1382	1.1381	1.1379
20	2113.0	1291.1	1.0035	1.0034	1.0034	1.0033	1.0032	1.0032	1.0031	1.0030	1.0029
25	2184.8	1335.0	0.89271	0.89269	0.89266	0.89260	0.89255	0.89250	0.89244	0.89239	0.89233
30	2258.5	1380.0	0.80074	0.80072	0.80070	0.80067	0.80063	0.80059	0.80055	0.80052	0.80048
35	2333.9	1426.2	0.72346	0.72345	0.72344	0.72341	0.72339	0.72336	0.72334	0.72331	0.72329
40	2411.1	1473.4	0.65786	0.65785	0.65785	0.65783	0.65781	0.65780	0.65778	0.65776	0.65775
45	2490.1	1521.7	0.60166	0.60166	0.60166	0.60165	0.60164	0.60163	0.60162	0.60161	0.60160
50	2570.9	1571.1	156.42	0.55314	0.55313	0.55313	0.55313	0.55312	0.55312	0.55311	0.55311
60	2737.9	1673.1	166.69	0.47400	0.47400	0.47400	0.47401	0.47401	0.47401	0.47402	0.47402
70	2911.8	1779.5	177.38	0.41272	0.41273	0.41274	0.41274	0.41275	0.41276	0.41277	0.41278
80	3092.8	1890.1	188.50	0.36433	0.36433	0.36434	0.36435	0.36436	0.36437	0.36439	0.36440
90	3280.7	2005.0	200.03	39.577	0.32547	0.32548	0.32549	0.32551	0.32552	0.32553	0.32554
100	3475.7	2124.2	211.98	42.002	20.748	0.29384	0.29385	0.29386	0.29388	0.29389	0.29390
125	3993.2	2440.5	243.69	48.411	23.998	11.785	0.23653	0.23655	0.23656	0.23658	0.23659
150	4553.6	2783.1	278.00	55.324	27.487	13.565	8.9212	6.5966	0.19914	0.19916	0.19917
175	5156.7	3151.7	314.90	62.742	31.221	15.458	10.202	7.5729	5.9941	4.9405	4.1868
200	5801.8	3546.1	354.37	70.667	35.203	17.470	11.558	8.6007	6.8258	5.6420	4.7959
225	6488.8	3966.0	396.39	79.096	39.433	19.601	12.990	9.6837	7.6996	6.3765	5.4311
250	7217.2	4411.1	440.93	88.025	43.911	21.853	14.501	10.824	8.6175	7.1465	6.0955
275	7986.4	4881.3	487.97	97.450	48.635	24.227	16.090	12.022	9.5809	7.9533	6.7907
300	8796.2	5376.3	537.48	107.37	53.603	26.720	17.759	13.279	10.590	8.7979	7.5175
325	9646.0	5895.7	589.44	117.77	58.813	29.334	19.507	14.594	11.646	9.6805	8.2766
350	10535	6439.3	643.81	128.66	64.263	32.066	21.334	15.967	12.748	10.601	9.0679
375	11464	7006.7	700.56	140.02	69.950	34.916	23.238	17.399	13.896	11.560	9.8915
400	12431	7597.7	759.68	151.85	75.872	37.883	25.220	18.888	15.089	12.556	10.747
425	13436	8212.0	821.12	164.15	82.025	40.964	27.277	20.434	16.328	13.591	11.635
450	14478	8849.3	884.85	176.90	88.407	44.160	29.411	22.036	17.612	14.662	12.555
475	15558	9509.3	950.86	190.11	95.015	47.468	31.619	23.695	18.940	15.770	13.506
500	16674	10192	1019.1	203.76	101.85	50.887	33.901	25.408	20.312	16.915	14.489
525	17827	10896	1089.5	217.86	108.90	54.417	36.256	27.176	21.728	18.096	15.502
550	19015	11622	1162.2	232.39	116.17	58.054	38.684	28.998	23.187	19.313	16.546
575	20239	12370	1237.0	247.35	123.65	61.799	41.182	30.874	24.689	20.565	17.620
600	21497	13139	1313.9	262.74	131.34	65.649	43.751	32.801	26.232	21.852	18.724
625	22789	13929	1392.9	278.54	139.25	69.604	46.389	34.781	27.817	23.174	19.857
650	24115	14740	1473.9	294.76	147.36	73.662	49.096	36.813	29.443	24.530	21.020
675	25475	15571	1557.0	311.38	155.67	77.821	51.870	38.895	31.109	25.919	22.212
700	26868	16422	1642.2	328.41	164.19	82.081	54.712	41.027	32.816	27.342	23.432
725	28293	17293	1729.3	345.84	172.91	86.441	57.619	43.208	34.562	28.797	24.680
750	29750	18184	1818.4	363.66	181.82	90.898	60.592	45.439	36.347	30.286	25.956
775	31240	19094	1909.4	381.86	190.92	95.453	63.629	47.718	38.171	31.806	27.260
800	32760	20023	2002.3	400.45	200.22	100.10	66.730	50.044	40.032	33.358	28.591

[a] The horizontal lines in the columns indicate the transition from the liquid phase to the gas phase.

Table 12 Kinematic viscosity ν $[10^{-6}\ m^2\ s^{-1}]$ [a] – Continued

t [°C]	*p* [bar] 8	9	10	15	20	25	50	75	100	150	200
0	1.7898	1.7895	1.7892	1.7876	1.7861	1.7845	1.7769	1.7694	1.7621	1.7479	1.7344
5	1.5167	1.5165	1.5163	1.5152	1.5141	1.5130	1.5078	1.5026	1.4975	1.4877	1.4783
10	1.3052	1.3051	1.3049	1.3042	1.3034	1.3027	1.2989	1.2953	1.2918	1.2849	1.2783
15	1.1378	1.1377	1.1376	1.1371	1.1366	1.1360	1.1334	1.1308	1.1283	1.1234	1.1188
20	1.0029	1.0028	1.0027	1.0023	1.0020	1.0016	0.99971	0.99789	0.99610	0.99265	0.98934
25	0.89228	0.89223	0.89217	0.89190	0.89164	0.89137	0.89005	0.88877	0.88751	0.88508	0.88277
30	0.80044	0.80040	0.80036	0.80018	0.79999	0.79981	0.79889	0.79800	0.79713	0.79545	0.79386
35	0.72326	0.72324	0.72321	0.72308	0.72296	0.72283	0.72222	0.72162	0.72103	0.71992	0.71886
40	0.65773	0.65772	0.65770	0.65762	0.65754	0.65746	0.65707	0.65669	0.65632	0.65562	0.65497
45	0.60159	0.60158	0.60157	0.60153	0.60148	0.60143	0.60121	0.60100	0.60080	0.60042	0.60008
50	0.55311	0.55310	0.55310	0.55308	0.55306	0.55304	0.55295	0.55287	0.55279	0.55266	0.55256
60	0.47403	0.47403	0.47403	0.47405	0.47407	0.47408	0.47417	0.47427	0.47437	0.47458	0.47481
70	0.41278	0.41279	0.41280	0.41284	0.41288	0.41292	0.41312	0.41333	0.41353	0.41396	0.41439
80	0.36441	0.36442	0.36443	0.36448	0.36454	0.36459	0.36486	0.36514	0.36541	0.36597	0.36653
90	0.32556	0.32557	0.32558	0.32565	0.32571	0.32577	0.32609	0.32641	0.32672	0.32736	0.32800
100	0.29392	0.29393	0.29395	0.29401	0.29408	0.29415	0.29450	0.29484	0.29519	0.29588	0.29657
125	0.23661	0.23662	0.23664	0.23671	0.23679	0.23686	0.23724	0.23762	0.23799	0.23874	0.23949
150	0.19919	0.19920	0.19922	0.19930	0.19937	0.19945	0.19984	0.20022	0.20061	0.20137	0.20212
175	3.6206	0.17364	0.17366	0.17373	0.17381	0.17389	0.17428	0.17466	0.17505	0.17581	0.17656
200	4.1608	3.6664	3.2705	2.0777	0.15572	0.15580	0.15619	0.15658	0.15697	0.15773	0.15847
225	4.7217	4.1698	3.7280	2.4000	1.7324	1.3277	0.14303	0.14342	0.14382	0.14458	0.14534
250	5.3071	4.6937	4.2029	2.7288	1.9897	1.5444	0.13321	0.13362	0.13403	0.13482	0.13559
275	5.9186	5.2402	4.6973	3.0680	2.2520	1.7613	0.76838	0.12616	0.12659	0.12743	0.12824
300	6.5572	5.8102	5.2126	3.4191	2.5216	1.9824	0.89758	0.52465	0.12084	0.12177	0.12263
325	7.2236	6.4046	5.7493	3.7832	2.7997	2.2092	1.0244	0.62369	0.41590	0.11738	0.11837
350	7.9179	7.0235	6.3079	4.1610	3.0872	2.4427	1.1515	0.71794	0.49771	0.26300	0.11532
375	8.6403	7.6671	6.8885	4.5526	3.3846	2.6836	1.2804	0.81086	0.57434	0.33241	0.19900
400	9.3906	8.3354	7.4911	4.9584	3.6920	2.9321	1.4117	0.90391	0.64915	0.39206	0.26005
425	10.169	9.0283	8.1158	5.3785	4.0098	3.1885	1.5458	0.99790	0.72355	0.44830	0.30966
450	10.975	9.7457	8.7625	5.8127	4.3379	3.4530	1.6833	1.0933	0.79830	0.50314	0.35557
475	11.808	10.487	9.4309	6.2612	4.6764	3.7256	1.8241	1.1905	0.87384	0.55749	0.39982
500	12.669	11.253	10.121	6.7238	5.0253	4.0063	1.9685	1.2896	0.95046	0.61187	0.44335
525	13.556	12.043	10.832	7.2004	5.3846	4.2951	2.1166	1.3909	1.0284	0.66662	0.48666
550	14.470	12.856	11.565	7.6910	5.7541	4.5920	2.2684	1.4943	1.1077	0.72193	0.53005
575	15.411	13.693	12.319	8.1954	6.1339	4.8970	2.4239	1.6000	1.1885	0.77797	0.57372
600	16.378	14.553	13.093	8.7135	6.5238	5.2101	2.5831	1.7080	1.2710	0.83482	0.61780
625	17.370	15.436	13.888	9.2451	6.9238	5.5311	2.7461	1.8184	1.3550	0.89258	0.66240
650	18.388	16.341	14.703	9.7902	7.3338	5.8600	2.9129	1.9312	1.4407	0.95129	0.70758
675	19.431	17.269	15.539	10.349	7.7536	6.1967	3.0834	2.0463	1.5282	1.0110	0.75340
700	20.499	18.219	16.394	10.920	8.1833	6.5412	3.2577	2.1638	1.6173	1.0717	0.79990
725	21.592	19.190	17.269	11.505	8.6226	6.8934	3.4357	2.2837	1.7081	1.1335	0.84710
750	22.709	20.184	18.163	12.102	9.0715	7.2533	3.6174	2.4060	1.8007	1.1963	0.89504
775	23.850	21.198	19.077	12.712	9.5299	7.6207	3.8027	2.5306	1.8950	1.2602	0.94372
800	25.015	22.234	20.009	13.335	9.9977	7.9956	3.9917	2.6576	1.9910	1.3252	0.99317

[a] The horizontal lines in the columns indicate the transition from the liquid phase to the gas phase.

Table 12 Kinematic viscosity ν [10^{-6} m^2 s^{-1}] – Continued

t	p [bar]										
[°C]	250	300	350	400	450	500	600	700	800	900	1000
0	1.7214	1.7090	1.6972	1.6860	1.6752	1.6651	1.6462	1.6292	1.6140	1.6005	1.5887
5	1.4693	1.4607	1.4525	1.4447	1.4372	1.4301	1.4170	1.4052	1.3947	1.3854	1.3772
10	1.2719	1.2659	1.2601	1.2546	1.2494	1.2444	1.2352	1.2270	1.2197	1.2132	1.2076
15	1.1143	1.1100	1.1060	1.1021	1.0984	1.0949	1.0885	1.0827	1.0777	1.0733	1.0695
20	0.98619	0.98318	0.98032	0.97761	0.97503	0.97259	0.96812	0.96417	0.96073	0.95778	0.95529
25	0.88056	0.87846	0.87648	0.87460	0.87282	0.87115	0.86811	0.86547	0.86321	0.86133	0.85980
30	0.79235	0.79092	0.78958	0.78831	0.78713	0.78603	0.78405	0.78237	0.78099	0.77990	0.77908
35	0.71787	0.71694	0.71608	0.71527	0.71453	0.71385	0.71267	0.71172	0.71100	0.71050	0.71021
40	0.65437	0.65382	0.65332	0.65287	0.65246	0.65210	0.65152	0.65112	0.65090	0.65085	0.65097
45	0.59978	0.59952	0.59929	0.59910	0.59895	0.59884	0.59872	0.59874	0.59890	0.59920	0.59963
50	0.55249	0.55245	0.55244	0.55245	0.55250	0.55257	0.55281	0.55315	0.55361	0.55418	0.55485
60	0.47506	0.47532	0.47561	0.47591	0.47622	0.47656	0.47729	0.47808	0.47895	0.47988	0.48089
70	0.41483	0.41529	0.41575	0.41623	0.41671	0.41721	0.41824	0.41931	0.42043	0.42158	0.42279
80	0.36709	0.36767	0.36824	0.36883	0.36942	0.37002	0.37123	0.37247	0.37374	0.37503	0.37636
90	0.32865	0.32929	0.32994	0.33059	0.33125	0.33191	0.33324	0.33458	0.33594	0.33731	0.33871
100	0.29726	0.29795	0.29864	0.29934	0.30003	0.30073	0.30213	0.30353	0.30494	0.30636	0.30779
125	0.24023	0.24097	0.24171	0.24244	0.24317	0.24390	0.24536	0.24681	0.24826	0.24970	0.25114
150	0.20287	0.20361	0.20435	0.20509	0.20582	0.20655	0.20799	0.20942	0.21084	0.21226	0.21366
175	0.17730	0.17804	0.17877	0.17949	0.18021	0.18092	0.18233	0.18372	0.18510	0.18646	0.18781
200	0.15921	0.15994	0.16066	0.16137	0.16207	0.16277	0.16414	0.16549	0.16682	0.16813	0.16943
225	0.14608	0.14680	0.14751	0.14822	0.14891	0.14959	0.15094	0.15225	0.15354	0.15481	0.15605
250	0.13634	0.13707	0.13779	0.13849	0.13918	0.13986	0.14118	0.14247	0.14372	0.14495	0.14615
275	0.12901	0.12976	0.13049	0.13120	0.13189	0.13256	0.13388	0.13515	0.13637	0.13757	0.13874
300	0.12345	0.12423	0.12498	0.12570	0.12640	0.12708	0.12839	0.12964	0.13085	0.13202	0.13315
325	0.11926	0.12008	0.12085	0.12159	0.12230	0.12298	0.12428	0.12552	0.12670	0.12784	0.12895
350	0.11630	0.11715	0.11794	0.11867	0.11937	0.12004	0.12131	0.12251	0.12365	0.12475	0.12582
375	0.11543	0.11583	0.11642	0.11703	0.11763	0.11822	0.11937	0.12048	0.12154	0.12258	0.12358
400	0.17586	0.12361	0.11807	0.11750	0.11756	0.11782	0.11857	0.11943	0.12032	0.12122	0.12212
425	0.22574	0.17013	0.13644	0.12438	0.12102	0.11985	0.11930	0.11954	0.12006	0.12071	0.12142
450	0.26735	0.20950	0.17036	0.14566	0.13275	0.12679	0.12246	0.12123	0.12097	0.12114	0.12152
475	0.30596	0.24446	0.20211	0.17266	0.15296	0.14073	0.12929	0.12511	0.12340	0.12271	0.12254
500	0.34315	0.27743	0.23180	0.19918	0.17575	0.15917	0.14024	0.13173	0.12770	0.12567	0.12464
525	0.37965	0.30936	0.26031	0.22480	0.19858	0.17910	0.15417	0.14104	0.13406	0.13018	0.12795
550	0.41589	0.34079	0.28818	0.24981	0.22108	0.19924	0.16969	0.15242	0.14230	0.13626	0.13253
575	0.45213	0.37202	0.31574	0.27447	0.24332	0.21933	0.18590	0.16510	0.15205	0.14373	0.13833
600	0.48854	0.40325	0.34319	0.29898	0.26542	0.23937	0.20241	0.17855	0.16283	0.15234	0.14521
625	0.52521	0.43460	0.37066	0.32347	0.28749	0.25939	0.21908	0.19244	0.17432	0.16178	0.15297
650	0.56225	0.46616	0.39826	0.34802	0.30959	0.27947	0.23587	0.20660	0.18628	0.17184	0.16141
675	0.59971	0.49800	0.42604	0.37270	0.33180	0.29963	0.25278	0.22098	0.19857	0.18236	0.17040
700	0.63763	0.53017	0.45406	0.39755	0.35414	0.31991	0.26983	0.23554	0.21111	0.19322	0.17983
725	0.67607	0.56272	0.48236	0.42263	0.37666	0.34035	0.28702	0.25027	0.22387	0.20434	0.18957
750	0.71503	0.59566	0.51097	0.44795	0.39939	0.36096	0.30437	0.26516	0.23681	0.21568	0.19955
775	0.75455	0.62904	0.53992	0.47355	0.42235	0.38178	0.32189	0.28023	0.24994	0.22722	0.20975
800	0.79463	0.66285	0.56922	0.49944	0.44556	0.40281	0.33959	0.29546	0.26324	0.23895	0.22016

Table 13 Prandtl number *Pr*

For the single-phase region, this table contains values for the

- Prandtl number $Pr = \eta c_p \lambda^{-1}$

for temperatures from 0 °C to 800 °C and pressures from 0.006 112 127 bar to 1000 bar.

For given pressures and temperatures, the required values for the specific isobaric heat capacity c_p were calculated from the IAPWS-IF97 basic equations, Eqs. (2.3), (2.6), and (2.11).

The transport properties dynamic viscosity η and thermal conductivity λ were calculated from the equations for industrial applications, Eq. (3.1), and industrial use, Eq. (3.4), where the values for the density ρ needed in these equations result from the IAPWS-IF97 basic equations, see above.

The values for the thermal conductivity beyond the range of validity of the λ equation for industrial use were obtained by extrapolating Eq. (3.4) as described in Sec. 3.2 under the subpoint "Range of Validity."

The horizontal lines in the columns indicate the transition from the liquid phase to the vapour phase.

Table 13 Prandtl number *Pr* [–] [a]

t	*p* [bar]										
[°C]	0.006112127	0.01	0.1	0.5	1	2	3	4	5	6	7
0	13.456	13.456	13.456	13.454	13.452	13.447	13.442	13.438	13.433	13.428	13.423
5	1.0123	11.157	11.157	11.156	11.154	11.151	11.148	11.144	11.141	11.138	11.134
10	1.0048	1.0116	9.4164	9.4154	9.4142	9.4118	9.4094	9.4070	9.4046	9.4022	9.3998
15	0.99932	1.0031	8.0645	8.0638	8.0629	8.0611	8.0593	8.0575	8.0557	8.0539	8.0521
20	0.99487	0.99734	6.9925	6.9920	6.9913	6.9899	6.9886	6.9872	6.9859	6.9845	6.9831
25	0.99106	0.99284	6.1276	6.1272	6.1266	6.1256	6.1245	6.1235	6.1224	6.1214	6.1203
30	0.98769	0.98910	5.4193	5.4189	5.4185	5.4177	5.4169	5.4160	5.4152	5.4144	5.4136
35	0.98467	0.98583	4.8319	4.8316	4.8313	4.8306	4.8300	4.8293	4.8286	4.8280	4.8273
40	0.98192	0.98292	4.3394	4.3392	4.3389	4.3384	4.3378	4.3373	4.3368	4.3362	4.3357
45	0.97941	0.98029	3.9225	3.9223	3.9221	3.9217	3.9212	3.9208	3.9204	3.9199	3.9195
50	0.97712	0.97789	1.0008	3.5665	3.5663	3.5659	3.5656	3.5652	3.5649	3.5645	3.5641
60	0.97309	0.97370	0.98844	2.9954	2.9953	2.9950	2.9948	2.9946	2.9943	2.9941	2.9938
70	0.96967	0.97016	0.98125	2.5624	2.5623	2.5622	2.5620	2.5618	2.5616	2.5615	2.5613
80	0.96674	0.96713	0.97596	2.2272	2.2271	2.2270	2.2269	2.2267	2.2266	2.2265	2.2264
90	0.96422	0.96453	0.97169	1.0023	1.9630	1.9629	1.9628	1.9627	1.9626	1.9625	1.9624
100	0.96201	0.96227	0.96812	0.99249	1.0239	1.7518	1.7517	1.7517	1.7516	1.7515	1.7514
125	0.95753	0.95769	0.96131	0.97667	0.99474	1.0320	1.3810	1.3809	1.3809	1.3809	1.3808
150	0.95399	0.95409	0.95640	0.96641	0.97853	1.0019	1.0255	1.0542	1.1510	1.1509	1.1509
175	0.95092	0.95099	0.95251	0.95918	0.96742	0.98372	0.99989	1.0161	1.0328	1.0510	1.0727
200	0.94806	0.94811	0.94914	0.95372	0.95941	0.97085	0.98240	0.99408	1.0059	1.0179	1.0300
225	0.94526	0.94529	0.94601	0.94923	0.95327	0.96141	0.96970	0.97815	0.98676	0.99553	1.0044
250	0.94240	0.94243	0.94295	0.94529	0.94822	0.95415	0.96019	0.96636	0.97266	0.97909	0.98566
275	0.93947	0.93949	0.93988	0.94162	0.94380	0.94822	0.95272	0.95731	0.96199	0.96676	0.97163
300	0.93644	0.93645	0.93675	0.93809	0.93976	0.94313	0.94656	0.95005	0.95359	0.95720	0.96087
325	0.93332	0.93333	0.93357	0.93461	0.93592	0.93856	0.94124	0.94394	0.94669	0.94948	0.95230
350	0.93013	0.93014	0.93033	0.93116	0.93221	0.93432	0.93645	0.93860	0.94078	0.94297	0.94520
375	0.92689	0.92690	0.92705	0.92773	0.92858	0.93030	0.93203	0.93377	0.93553	0.93730	0.93909
400	0.92362	0.92363	0.92375	0.92432	0.92502	0.92644	0.92786	0.92929	0.93073	0.93218	0.93364
425	0.92035	0.92035	0.92046	0.92093	0.92152	0.92271	0.92389	0.92509	0.92628	0.92749	0.92869
450	0.91709	0.91710	0.91719	0.91759	0.91809	0.91909	0.92009	0.92109	0.92210	0.92311	0.92412
475	0.91387	0.91388	0.91395	0.91429	0.91472	0.91557	0.91642	0.91727	0.91813	0.91898	0.91984
500	0.91070	0.91071	0.91077	0.91106	0.91143	0.91216	0.91288	0.91361	0.91434	0.91507	0.91580
525	0.90760	0.90760	0.90766	0.90791	0.90822	0.90885	0.90947	0.91010	0.91072	0.91135	0.91198
550	0.90456	0.90456	0.90461	0.90483	0.90510	0.90564	0.90618	0.90672	0.90726	0.90780	0.90834
575	0.90161	0.90161	0.90165	0.90184	0.90207	0.90254	0.90300	0.90347	0.90394	0.90440	0.90487
600	0.89874	0.89874	0.89878	0.89894	0.89914	0.89954	0.89995	0.90035	0.90075	0.90115	0.90155
625	0.89596	0.89596	0.89599	0.89613	0.89630	0.89665	0.89700	0.89735	0.89770	0.89805	0.89839
650	0.89327	0.89327	0.89330	0.89342	0.89357	0.89387	0.89417	0.89448	0.89478	0.89508	0.89538
675	0.89068	0.89068	0.89071	0.89081	0.89094	0.89120	0.89146	0.89172	0.89198	0.89224	0.89250
700	0.88819	0.88820	0.88822	0.88831	0.88842	0.88864	0.88887	0.88909	0.88931	0.88954	0.88976
725	0.88582	0.88582	0.88584	0.88591	0.88601	0.88620	0.88639	0.88659	0.88678	0.88697	0.88716
750	0.88356	0.88356	0.88357	0.88364	0.88372	0.88388	0.88405	0.88421	0.88438	0.88454	0.88470
775	0.88142	0.88142	0.88143	0.88149	0.88156	0.88170	0.88184	0.88198	0.88212	0.88226	0.88240
800	0.87943	0.87943	0.87944	0.87949	0.87954	0.87966	0.87978	0.87990	0.88002	0.88013	0.88025

[a] The horizontal lines in the columns indicate the transition from the liquid phase to the gas phase.

Table 13 Prandtl number *Pr* [–][a] – Continued

t [°C]	p [bar] 8	9	10	15	20	25	50	75	100	150	200
0	13.419	13.414	13.410	13.386	13.363	13.340	13.227	13.117	13.009	12.802	12.606
5	11.131	11.128	11.124	11.108	11.092	11.076	10.995	10.917	10.841	10.694	10.553
10	9.3974	9.3950	9.3926	9.3807	9.3688	9.3570	9.2987	9.2416	9.1859	9.0781	8.9750
15	8.0504	8.0486	8.0468	8.0379	8.0290	8.0202	7.9767	7.9341	7.8924	7.8117	7.7344
20	6.9818	6.9804	6.9791	6.9723	6.9656	6.9589	6.9257	6.8933	6.8615	6.7998	6.7406
25	6.1192	6.1182	6.1171	6.1119	6.1067	6.1015	6.0758	6.0507	6.0260	5.9781	5.9321
30	5.4127	5.4119	5.4111	5.4070	5.4029	5.3988	5.3786	5.3588	5.3394	5.3016	5.2653
35	4.8267	4.8260	4.8253	4.8221	4.8188	4.8156	4.7995	4.7837	4.7682	4.7381	4.7091
40	4.3352	4.3346	4.3341	4.3315	4.3288	4.3262	4.3133	4.3006	4.2881	4.2638	4.2404
45	3.9191	3.9186	3.9182	3.9161	3.9139	3.9118	3.9013	3.8909	3.8807	3.8610	3.8420
50	3.5638	3.5634	3.5631	3.5613	3.5596	3.5578	3.5492	3.5407	3.5324	3.5161	3.5005
60	2.9936	2.9933	2.9931	2.9919	2.9907	2.9895	2.9835	2.9777	2.9719	2.9608	2.9500
70	2.5611	2.5610	2.5608	2.5599	2.5591	2.5582	2.5540	2.5499	2.5458	2.5379	2.5304
80	2.2262	2.2261	2.2260	2.2254	2.2247	2.2241	2.2211	2.2181	2.2151	2.2095	2.2040
90	1.9623	1.9623	1.9622	1.9617	1.9612	1.9608	1.9585	1.9563	1.9541	1.9499	1.9459
100	1.7514	1.7513	1.7512	1.7509	1.7505	1.7502	1.7484	1.7467	1.7451	1.7419	1.7389
125	1.3808	1.3807	1.3807	1.3805	1.3802	1.3800	1.3790	1.3779	1.3770	1.3751	1.3733
150	1.1508	1.1508	1.1508	1.1506	1.1504	1.1502	1.1493	1.1484	1.1476	1.1460	1.1446
175	1.1011	1.0043	1.0043	1.0040	1.0038	1.0036	1.0025	1.0014	1.0004	0.99856	0.99688
200	1.0425	1.0556	1.0694	1.1778	0.91145	0.91111	0.90949	0.90795	0.90649	0.90379	0.90137
225	1.0135	1.0227	1.0321	1.0821	1.1458	1.2561	0.85558	0.85310	0.85076	0.84647	0.84264
250	0.99235	0.99917	1.0061	1.0426	1.0822	1.1267	0.83506	0.83073	0.82671	0.81946	0.81310
275	0.97659	0.98165	0.98679	1.0139	1.0433	1.0749	1.3075	0.84357	0.83583	0.82239	0.81109
300	0.96460	0.96840	0.97226	0.99254	1.0144	1.0379	1.1837	1.4492	0.89589	0.86590	0.84287
325	0.95517	0.95807	0.96102	0.97641	0.99287	1.0104	1.1151	1.2616	1.5143	0.99847	0.93568
350	0.94745	0.94972	0.95203	0.96395	0.97658	0.98994	1.0678	1.1660	1.2980	1.9348	1.2364
375	0.94089	0.94272	0.94456	0.95404	0.96402	0.97452	1.0356	1.1121	1.2077	1.5015	2.2777
400	0.93511	0.93659	0.93808	0.94569	0.95360	0.96183	1.0082	1.0641	1.1303	1.3075	1.6084
425	0.92991	0.93113	0.93235	0.93859	0.94500	0.95162	0.98810	1.0309	1.0805	1.2041	1.3764
450	0.92514	0.92616	0.92718	0.93236	0.93765	0.94306	0.97227	1.0056	1.0435	1.1337	1.2480
475	0.92070	0.92156	0.92242	0.92678	0.93119	0.93568	0.95946	0.98588	1.0152	1.0831	1.1639
500	0.91654	0.91727	0.91800	0.92169	0.92542	0.92918	0.94882	0.97009	0.99325	1.0454	1.1049
525	0.91260	0.91323	0.91386	0.91701	0.92017	0.92336	0.93975	0.95713	0.97568	1.0164	1.0615
550	0.90887	0.90941	0.90995	0.91265	0.91536	0.91807	0.93188	0.94625	0.96131	0.99364	1.0285
575	0.90533	0.90579	0.90626	0.90858	0.91090	0.91322	0.92493	0.93692	0.94929	0.97530	1.0027
600	0.90196	0.90236	0.90276	0.90476	0.90675	0.90874	0.91871	0.92879	0.93905	0.96019	0.98200
625	0.89874	0.89909	0.89943	0.90115	0.90287	0.90458	0.91310	0.92160	0.93016	0.94750	0.96502
650	0.89567	0.89597	0.89627	0.89776	0.89923	0.90071	0.90798	0.91519	0.92236	0.93667	0.95084
675	0.89276	0.89301	0.89327	0.89455	0.89582	0.89708	0.90331	0.90942	0.91544	0.92729	0.93880
700	0.88998	0.89020	0.89042	0.89152	0.89261	0.89370	0.89901	0.90419	0.90926	0.91909	0.92846
725	0.88735	0.88754	0.88773	0.88867	0.88961	0.89053	0.89506	0.89945	0.90371	0.91185	0.91947
750	0.88487	0.88503	0.88519	0.88599	0.88679	0.88758	0.89143	0.89513	0.89870	0.90545	0.91162
775	0.88253	0.88267	0.88281	0.88349	0.88417	0.88484	0.88810	0.89121	0.89420	0.89976	0.90473
800	0.88037	0.88048	0.88060	0.88118	0.88175	0.88231	0.88505	0.88766	0.89014	0.89470	0.89868

[a] The horizontal lines in the columns indicate the transition from the liquid phase to the gas phase.

Table 13 Prandtl number Pr [–][a] – Continued

t [°C]	p [bar] 250	300	350	400	450	500	600	700	800	900	1000
0	12.419	12.241	12.073	11.912	11.760	11.616	11.349	11.109	10.893	10.700	10.528
5	10.419	10.292	10.170	10.054	9.9443	9.8394	9.6446	9.4684	9.3093	9.1660	9.0371
10	8.8766	8.7826	8.6928	8.6071	8.5252	8.4471	8.3016	8.1693	8.0494	7.9407	7.8426
15	7.6603	7.5895	7.5217	7.4568	7.3948	7.3354	7.2246	7.1234	7.0313	6.9476	6.8717
20	6.6839	6.6295	6.5774	6.5274	6.4795	6.4337	6.3478	6.2692	6.1974	6.1320	6.0724
25	5.8879	5.8455	5.8048	5.7657	5.7282	5.6923	5.6248	5.5629	5.5062	5.4545	5.4073
30	5.2305	5.1969	5.1647	5.1337	5.1040	5.0755	5.0219	4.9726	4.9274	4.8860	4.8482
35	4.6813	4.6544	4.6286	4.6039	4.5800	4.5571	4.5141	4.4745	4.4381	4.4047	4.3743
40	4.2179	4.1963	4.1754	4.1554	4.1361	4.1176	4.0827	4.0506	4.0211	3.9940	3.9693
45	3.8236	3.8060	3.7890	3.7726	3.7569	3.7418	3.7134	3.6872	3.6631	3.6410	3.6209
50	3.4855	3.4710	3.4570	3.4436	3.4307	3.4183	3.3950	3.3735	3.3537	3.3356	3.3191
60	2.9397	2.9297	2.9201	2.9109	2.9021	2.8936	2.8776	2.8629	2.8495	2.8373	2.8261
70	2.5231	2.5161	2.5094	2.5029	2.4968	2.4908	2.4798	2.4696	2.4604	2.4521	2.4445
80	2.1988	2.1938	2.1890	2.1844	2.1800	2.1759	2.1681	2.1610	2.1547	2.1490	2.1439
90	1.9421	1.9384	1.9350	1.9317	1.9285	1.9255	1.9200	1.9151	1.9107	1.9069	1.9035
100	1.7360	1.7333	1.7307	1.7283	1.7260	1.7239	1.7199	1.7165	1.7135	1.7109	1.7087
125	1.3717	1.3702	1.3689	1.3676	1.3664	1.3653	1.3635	1.3620	1.3608	1.3600	1.3594
150	1.1433	1.1421	1.1411	1.1401	1.1393	1.1385	1.1373	1.1364	1.1358	1.1355	1.1354
175	0.99538	0.99402	0.99280	0.99171	0.99074	0.98989	0.98849	0.98745	0.98674	0.98633	0.98618
200	0.89918	0.89722	0.89545	0.89386	0.89243	0.89116	0.88901	0.88734	0.88608	0.88517	0.88457
225	0.83922	0.83614	0.83338	0.83089	0.82865	0.82664	0.82319	0.82041	0.81819	0.81645	0.81511
250	0.80750	0.80253	0.79811	0.79415	0.79060	0.78741	0.78195	0.77750	0.77387	0.77090	0.76851
275	0.80143	0.79309	0.78580	0.77940	0.77372	0.76867	0.76010	0.75316	0.74748	0.74281	0.73895
300	0.82447	0.80937	0.79670	0.78591	0.77659	0.76845	0.75496	0.74425	0.73559	0.72850	0.72262
325	0.89291	0.86136	0.83684	0.81715	0.80096	0.78734	0.76563	0.74905	0.73598	0.72544	0.71680
350	1.0708	0.98319	0.92625	0.88501	0.85362	0.82896	0.79245	0.76637	0.74671	0.73134	0.71900
375	2.0542	1.3451	1.1374	1.0289	0.95984	0.91107	0.84561	0.80300	0.77273	0.75003	0.73239
400	2.3805	3.4752	1.7513	1.3428	1.1599	1.0527	0.92892	0.85777	0.81091	0.77752	0.75253
425	1.6380	2.0900	2.4611	1.9569	1.5216	1.2880	1.0552	0.93794	0.86617	0.81734	0.78189
450	1.3944	1.5815	1.8057	1.9197	1.7805	1.5445	1.2128	1.0392	0.93670	0.86912	0.82113
475	1.2596	1.3698	1.4886	1.5985	1.6312	1.5748	1.3323	1.1371	1.0103	0.92538	0.86517
500	1.1714	1.2442	1.3197	1.3897	1.4432	1.4557	1.3506	1.1960	1.0687	0.97526	0.90668
525	1.1098	1.1604	1.2114	1.2595	1.2986	1.3222	1.3001	1.2038	1.0984	1.0093	0.93898
550	1.0649	1.1016	1.1373	1.1705	1.1990	1.2197	1.2234	1.1765	1.1006	1.0244	0.95857
575	1.0307	1.0583	1.0844	1.1079	1.1279	1.1432	1.1543	1.1310	1.0808	1.0241	0.96583
600	1.0039	1.0252	1.0449	1.0622	1.0765	1.0871	1.0959	1.0851	1.0540	1.0108	0.96320
625	0.98235	0.99890	1.0140	1.0271	1.0377	1.0452	1.0507	1.0426	1.0211	0.98853	0.95272
650	0.96461	0.97757	0.98925	0.99919	1.0070	1.0124	1.0154	1.0080	0.99089	0.96508	0.93219
675	0.94979	0.95993	0.96891	0.97638	0.98204	0.98570	0.98661	0.97925	0.96476	0.94442	0.91895
700	0.93721	0.94514	0.95198	0.95748	0.96143	0.96366	0.96274	0.95494	0.94151	0.92418	0.90446
725	0.92644	0.93259	0.93773	0.94168	0.94427	0.94539	0.94298	0.93467	0.92152	0.90523	0.88767
750	0.91713	0.92185	0.92564	0.92836	0.92991	0.93018	0.92676	0.91823	0.90537	0.88948	0.87217
775	0.90904	0.91260	0.91531	0.91708	0.91782	0.91749	0.91350	0.90516	0.89295	0.87763	0.86016
800	0.90201	0.90463	0.90648	0.90750	0.90764	0.90690	0.90267	0.89486	0.88366	0.86925	0.85172

[a] The Pr values below the dashed lines were calculated with λ values that are beyond the official range of validity of the λ equation for industrial use, Eq. (3.4); for details of this extrapolation, see Sec. 3.2. If more accurate Pr values are needed, the λ equation for scientific use [35] should be applied.

Table 14 Dielectric constant ε

For the single-phase region, this table contains values for the

- Dielectric constant ε

for temperatures from 0 °C to 800 °C and pressures from 0.006 112 127 bar to 1000 bar. The dielectric constant was calculated from Eq. (3.9). For given pressures and temperatures, the density needed in Eq. (3.9) was determined from the IAPWS-IF97 basic equations, Eqs. (2.3), (2.6), and (2.11).

For temperatures $t \geq 600$ °C, the values for ε were obtained by extrapolating Eq. (3.9) as described in Sec. 3.4 under the subpoint "Range of Validity."

The horizontal lines in the columns indicate the transition from the liquid phase to the vapour phase.

Table 14 Dielectric constant ε [–] [a,b]

t [°C]	***p*** [bar] 0.006112127	0.01	0.1	0.5	1	2	3	4	5	6	7
0	87.899	87.899	87.900	87.901	87.903	87.908	87.912	87.916	87.920	87.924	87.929
5	1.0001	85.911	85.912	85.913	85.915	85.920	85.924	85.928	85.932	85.936	85.940
10	1.0001	1.0001	83.971	83.972	83.974	83.978	83.982	83.986	83.990	83.994	83.998
15	1.0001	1.0001	82.074	82.075	82.077	82.081	82.085	82.089	82.093	82.097	82.101
20	1.0001	1.0001	80.219	80.221	80.222	80.226	80.230	80.234	80.238	80.241	80.245
25	1.0001	1.0001	78.405	78.407	78.408	78.412	78.416	78.420	78.423	78.427	78.431
30	1.0001	1.0001	76.631	76.632	76.634	76.638	76.642	76.645	76.649	76.653	76.656
35	1.0001	1.0001	74.895	74.897	74.899	74.902	74.906	74.910	74.913	74.917	74.920
40	1.0000	1.0001	73.198	73.199	73.201	73.205	73.208	73.212	73.216	73.219	73.223
45	1.0000	1.0001	71.538	71.539	71.541	71.544	71.548	71.552	71.555	71.559	71.562
50	1.0000	1.0001	1.0008	69.915	69.917	69.921	69.924	69.928	69.931	69.935	69.938
60	1.0000	1.0001	1.0007	66.774	66.776	66.779	66.783	66.786	66.790	66.793	66.797
70	1.0000	1.0001	1.0007	63.770	63.771	63.775	63.778	63.782	63.785	63.789	63.792
80	1.0000	1.0001	1.0006	60.897	60.899	60.902	60.906	60.909	60.913	60.916	60.920
90	1.0000	1.0001	1.0006	1.0030	58.153	58.156	58.160	58.163	58.166	58.170	58.173
100	1.0000	1.0001	1.0006	1.0029	1.0058	55.531	55.534	55.538	55.541	55.545	55.548
125	1.0000	1.0001	1.0005	1.0025	1.0051	1.0103	49.462	49.466	49.470	49.473	49.477
150	1.0000	1.0000	1.0004	1.0022	1.0045	1.0091	1.0139	1.0187	44.031	44.035	44.039
175	1.0000	1.0000	1.0004	1.0020	1.0040	1.0081	1.0123	1.0166	1.0209	1.0253	1.0299
200	1.0000	1.0000	1.0004	1.0018	1.0036	1.0073	1.0110	1.0148	1.0187	1.0226	1.0266
225	1.0000	1.0000	1.0003	1.0016	1.0033	1.0066	1.0100	1.0134	1.0168	1.0203	1.0238
250	1.0000	1.0000	1.0003	1.0015	1.0030	1.0060	1.0091	1.0121	1.0152	1.0184	1.0216
275	1.0000	1.0000	1.0003	1.0014	1.0027	1.0055	1.0083	1.0111	1.0139	1.0167	1.0196
300	1.0000	1.0000	1.0002	1.0013	1.0025	1.0050	1.0076	1.0101	1.0127	1.0153	1.0179
325	1.0000	1.0000	1.0002	1.0012	1.0023	1.0046	1.0070	1.0093	1.0117	1.0141	1.0165
350	1.0000	1.0000	1.0002	1.0011	1.0021	1.0043	1.0064	1.0086	1.0108	1.0130	1.0152
375	1.0000	1.0000	1.0002	1.0010	1.0020	1.0040	1.0060	1.0080	1.0100	1.0120	1.0141
400	1.0000	1.0000	1.0002	1.0009	1.0018	1.0037	1.0056	1.0074	1.0093	1.0112	1.0131
425	1.0000	1.0000	1.0002	1.0009	1.0017	1.0034	1.0052	1.0069	1.0087	1.0104	1.0122
450	1.0000	1.0000	1.0002	1.0008	1.0016	1.0032	1.0048	1.0065	1.0081	1.0097	1.0114
475	1.0000	1.0000	1.0002	1.0008	1.0015	1.0030	1.0045	1.0061	1.0076	1.0091	1.0107
500	1.0000	1.0000	1.0001	1.0007	1.0014	1.0028	1.0043	1.0057	1.0071	1.0086	1.0100
525	1.0000	1.0000	1.0001	1.0007	1.0013	1.0027	1.0040	1.0054	1.0067	1.0081	1.0094
550	1.0000	1.0000	1.0001	1.0006	1.0013	1.0025	1.0038	1.0051	1.0063	1.0076	1.0089
575	1.0000	1.0000	1.0001	1.0006	1.0012	1.0024	1.0036	1.0048	1.0060	1.0072	1.0084
600	1.0000	1.0000	1.0001	1.0006	1.0011	1.0023	1.0034	1.0045	1.0057	1.0068	1.0080
625	1.0000	1.0000	1.0001	1.0005	1.0011	1.0021	1.0032	1.0043	1.0054	1.0065	1.0076
650	1.0000	1.0000	1.0001	1.0005	1.0010	1.0020	1.0031	1.0041	1.0051	1.0061	1.0072
675	1.0000	1.0000	1.0001	1.0005	1.0010	1.0019	1.0029	1.0039	1.0049	1.0058	1.0068
700	1.0000	1.0000	1.0001	1.0005	1.0009	1.0018	1.0028	1.0037	1.0046	1.0056	1.0065
725	1.0000	1.0000	1.0001	1.0004	1.0009	1.0018	1.0026	1.0035	1.0044	1.0053	1.0062
750	1.0000	1.0000	1.0001	1.0004	1.0008	1.0017	1.0025	1.0034	1.0042	1.0051	1.0059
775	1.0000	1.0000	1.0001	1.0004	1.0008	1.0016	1.0024	1.0032	1.0040	1.0048	1.0057
800	1.0000	1.0000	1.0001	1.0004	1.0008	1.0015	1.0023	1.0031	1.0039	1.0046	1.0054

[a] The horizontal lines in the columns indicate the transition from the liquid phase to the gas phase.

[b] The ε values below the dashed line were calculated from Eq. (3.9) by extrapolating this equation. This extrapolation is in accordance with the IAPWS release [40], see also Sec. 3.4.

Table 14 Dielectric constant ε [–] [a,b] – Continued

t	***p*** [bar]										
[°C]	8	9	10	15	20	25	50	75	100	150	200
0	87.933	87.937	87.941	87.962	87.983	88.004	88.108	88.212	88.315	88.521	88.725
5	85.944	85.948	85.952	85.972	85.993	86.013	86.114	86.215	86.315	86.515	86.714
10	84.002	84.006	84.010	84.030	84.050	84.069	84.168	84.266	84.364	84.559	84.753
15	82.104	82.108	82.112	82.132	82.151	82.170	82.267	82.363	82.458	82.649	82.838
20	80.249	80.253	80.257	80.276	80.295	80.313	80.408	80.502	80.596	80.783	80.968
25	78.435	78.438	78.442	78.461	78.479	78.498	78.591	78.683	78.775	78.959	79.141
30	76.660	76.664	76.667	76.686	76.704	76.722	76.814	76.905	76.996	77.176	77.356
35	74.924	74.928	74.931	74.949	74.968	74.986	75.076	75.166	75.255	75.434	75.611
40	73.226	73.230	73.234	73.251	73.269	73.287	73.376	73.465	73.554	73.730	73.905
45	71.566	71.569	71.573	71.591	71.608	71.626	71.715	71.803	71.890	72.065	72.238
50	69.942	69.945	69.949	69.966	69.984	70.002	70.089	70.177	70.264	70.437	70.608
60	66.800	66.804	66.807	66.825	66.842	66.859	66.946	67.033	67.119	67.290	67.459
70	63.796	63.799	63.803	63.820	63.837	63.855	63.941	64.027	64.112	64.282	64.450
80	60.923	60.927	60.930	60.947	60.965	60.982	61.068	61.154	61.239	61.408	61.576
90	58.177	58.180	58.184	58.201	58.219	58.236	58.322	58.408	58.493	58.663	58.830
100	55.552	55.555	55.559	55.576	55.593	55.611	55.698	55.784	55.870	56.039	56.207
125	49.480	49.484	49.488	49.506	49.524	49.541	49.631	49.719	49.807	49.980	50.152
150	44.043	44.046	44.050	44.069	44.088	44.107	44.200	44.292	44.384	44.564	44.742
175	1.0345	39.153	39.157	39.177	39.197	39.217	39.317	39.415	39.513	39.704	39.892
200	1.0306	1.0347	1.0389	1.0610	34.762	34.784	34.893	35.001	35.107	35.315	35.517
225	1.0274	1.0310	1.0347	1.0539	1.0747	1.0975	30.839	30.961	31.080	31.312	31.535
250	1.0248	1.0280	1.0313	1.0482	1.0663	1.0855	27.059	27.202	27.342	27.610	27.867
275	1.0225	1.0254	1.0284	1.0436	1.0595	1.0763	1.1788	23.616	23.789	24.118	24.426
300	1.0206	1.0232	1.0259	1.0396	1.0539	1.0688	1.1556	1.2763	20.271	20.714	21.111
325	1.0189	1.0213	1.0238	1.0363	1.0492	1.0626	1.1382	1.2348	1.3705	17.165	17.761
350	1.0174	1.0197	1.0219	1.0333	1.0451	1.0573	1.1244	1.2060	1.3099	1.6860	13.956
375	1.0161	1.0182	1.0203	1.0308	1.0416	1.0527	1.1131	1.1840	1.2696	1.5207	2.1126
400	1.0150	1.0169	1.0188	1.0285	1.0385	1.0487	1.1036	1.1664	1.2397	1.4347	1.7589
425	1.0140	1.0157	1.0175	1.0265	1.0358	1.0452	1.0954	1.1518	1.2160	1.3774	1.6108
450	1.0130	1.0147	1.0164	1.0248	1.0333	1.0421	1.0883	1.1394	1.1967	1.3349	1.5199
475	1.0122	1.0138	1.0153	1.0232	1.0312	1.0393	1.0820	1.1288	1.1804	1.3016	1.4557
500	1.0115	1.0129	1.0144	1.0217	1.0292	1.0368	1.0765	1.1196	1.1665	1.2745	1.4069
525	1.0108	1.0122	1.0135	1.0204	1.0274	1.0345	1.0716	1.1114	1.1545	1.2518	1.3680
550	1.0102	1.0115	1.0128	1.0193	1.0258	1.0325	1.0672	1.1042	1.1439	1.2325	1.3360
575	1.0096	1.0108	1.0121	1.0182	1.0244	1.0307	1.0632	1.0978	1.1345	1.2158	1.3091
600	1.0091	1.0103	1.0114	1.0172	1.0231	1.0290	1.0596	1.0919	1.1262	1.2012	1.2860
625	1.0086	1.0097	1.0108	1.0163	1.0219	1.0275	1.0563	1.0867	1.1187	1.1882	1.2660
650	1.0082	1.0092	1.0103	1.0155	1.0207	1.0260	1.0533	1.0819	1.1120	1.1767	1.2485
675	1.0078	1.0088	1.0098	1.0147	1.0197	1.0247	1.0506	1.0776	1.1058	1.1664	1.2329
700	1.0074	1.0084	1.0093	1.0140	1.0188	1.0235	1.0481	1.0736	1.1003	1.1571	1.2190
725	1.0071	1.0080	1.0089	1.0134	1.0179	1.0224	1.0457	1.0700	1.0952	1.1486	1.2066
750	1.0068	1.0076	1.0085	1.0128	1.0171	1.0214	1.0436	1.0666	1.0905	1.1409	1.1953
775	1.0065	1.0073	1.0081	1.0122	1.0163	1.0205	1.0416	1.0635	1.0862	1.1339	1.1850
800	1.0062	1.0070	1.0078	1.0117	1.0156	1.0196	1.0398	1.0606	1.0822	1.1274	1.1757

[a] The horizontal lines in the columns indicate the transition from the liquid phase to the gas phase.

[b] The ε values below the dashed line were calculated from Eq. (3.9) by extrapolating this equation. This extrapolation is in accordance with the IAPWS release [40], see also Sec. 3.4.

Table 14 Dielectric constant ε [–] [a] – Continued

t	*p* [bar]										
[°C]	250	300	350	400	450	500	600	700	800	900	1000
0	88.929	89.131	89.332	89.531	89.730	89.927	90.318	90.704	91.086	91.464	91.838
5	86.912	87.108	87.303	87.497	87.690	87.881	88.261	88.636	89.007	89.374	89.736
10	84.945	85.137	85.327	85.516	85.703	85.890	86.260	86.625	86.986	87.343	87.696
15	83.026	83.213	83.399	83.583	83.767	83.949	84.310	84.667	85.019	85.367	85.712
20	81.152	81.336	81.517	81.698	81.878	82.056	82.410	82.759	83.103	83.444	83.781
25	79.322	79.502	79.680	79.858	80.034	80.209	80.556	80.898	81.236	81.570	81.900
30	77.534	77.711	77.886	78.061	78.234	78.406	78.747	79.083	79.415	79.743	80.067
35	75.786	75.961	76.134	76.306	76.477	76.646	76.982	77.313	77.640	77.962	78.281
40	74.079	74.251	74.422	74.592	74.760	74.928	75.259	75.585	75.907	76.225	76.539
45	72.410	72.580	72.749	72.917	73.084	73.249	73.577	73.899	74.217	74.531	74.840
50	70.779	70.948	71.115	71.282	71.447	71.610	71.934	72.253	72.568	72.878	73.184
60	67.627	67.794	67.959	68.123	68.285	68.446	68.765	69.078	69.387	69.691	69.990
70	64.617	64.782	64.945	65.107	65.268	65.427	65.742	66.051	66.355	66.655	66.950
80	61.742	61.906	62.068	62.229	62.389	62.547	62.859	63.165	63.466	63.762	64.054
90	58.996	59.160	59.322	59.482	59.641	59.799	60.109	60.413	60.712	61.006	61.295
100	56.373	56.537	56.700	56.860	57.019	57.176	57.486	57.789	58.086	58.378	58.665
125	50.320	50.487	50.651	50.814	50.974	51.132	51.443	51.747	52.044	52.335	52.620
150	44.916	45.088	45.257	45.424	45.588	45.749	46.066	46.374	46.674	46.967	47.254
175	40.075	40.255	40.432	40.605	40.775	40.943	41.269	41.585	41.892	42.191	42.481
200	35.714	35.906	36.093	36.277	36.456	36.632	36.974	37.303	37.620	37.927	38.225
225	31.752	31.962	32.165	32.363	32.556	32.744	33.107	33.454	33.786	34.106	34.414
250	28.112	28.347	28.574	28.793	29.004	29.209	29.601	29.973	30.326	30.663	30.986
275	24.715	24.989	25.249	25.498	25.736	25.964	26.397	26.802	27.182	27.542	27.885
300	21.473	21.808	22.119	22.412	22.688	22.950	23.439	23.888	24.304	24.694	25.062
325	18.264	18.706	19.103	19.465	19.799	20.109	20.675	21.184	21.648	22.076	22.474
350	14.850	15.527	16.086	16.569	16.996	17.382	18.060	18.650	19.175	19.651	20.087
375	10.231	11.888	12.864	13.593	14.189	14.697	15.547	16.250	16.855	17.391	17.874
400	2.5035	5.9302	8.9146	10.313	11.254	11.981	13.094	13.953	14.663	15.274	15.814
425	1.9904	2.7299	4.3712	6.5334	8.0894	9.1766	10.679	11.746	12.586	13.287	13.893
450	1.7823	2.1820	2.8348	3.8823	5.2152	6.4760	8.3525	9.6462	10.629	11.427	12.103
475	1.6582	1.9343	2.3228	2.8759	3.6278	4.5285	6.3155	7.7334	8.8284	9.7108	10.451
500	1.5725	1.7842	2.0592	2.4190	2.8843	3.4609	4.8153	6.1344	7.2504	8.1759	8.9583
525	1.5084	1.6804	1.8930	2.1567	2.4819	2.8757	3.8480	4.9291	5.9555	6.8613	7.6491
550	1.4580	1.6029	1.7761	1.9831	2.2299	2.5209	3.2365	4.0811	4.9569	5.7865	6.5402
575	1.4169	1.5421	1.6880	1.8581	2.0557	2.2835	2.8340	3.4948	4.2152	4.9401	5.6301
600	1.3826	1.4928	1.6187	1.7627	1.9268	2.1127	2.5535	3.0811	3.6712	4.2877	4.8999
625	1.3534	1.4517	1.5624	1.6870	1.8269	1.9832	2.3477	2.7797	3.2671	3.7887	4.3211
650	1.3282	1.4168	1.5155	1.6252	1.7468	1.8812	2.1901	2.5521	2.9607	3.4035	3.8650
675	1.3061	1.3868	1.4757	1.5735	1.6809	1.7984	2.0653	2.3747	2.7227	3.1015	3.5012
700	1.2867	1.3607	1.4414	1.5296	1.6255	1.7298	1.9640	2.2327	2.5334	2.8609	3.2085
725	1.2694	1.3376	1.4116	1.4917	1.5783	1.6717	1.8798	2.1164	2.3797	2.6661	2.9709
750	1.2539	1.3171	1.3853	1.4586	1.5374	1.6220	1.8088	2.0193	2.2525	2.5057	2.7754
775	1.2399	1.2988	1.3619	1.4295	1.5017	1.5788	1.7479	1.9371	2.1455	2.3714	2.6122
800	1.2273	1.2823	1.3410	1.4036	1.4702	1.5409	1.6952	1.8666	2.0544	2.2574	2.4739

[a] The ε values below the dashed line were calculated from Eq. (3.9) by extrapolating this equation. This extrapolation is in accordance with the IAPWS release [40], see also Sec. 3.4.

Table 15 Refractive index *n*
(Saturation state)

This table contains values on the saturated liquid ($'$) and saturated vapour ($''$) lines for the

- Refractive index n

for temperatures from 0 °C up to the critical temperature t_c = 373.946 °C and for the common wavelengths of $\bar{\lambda}$ = 0.2265 µm, 0.40466 µm, 0.5893 µm, and 0.70652 µm.

For given temperatures, the values for the refractive index n were calculated from Eq. (3.10). The densities of the saturated liquid and saturated vapour needed in Eq. (3.10) were calculated from the IAPWS-IF97 basic equations, Eqs. (2.3), (2.6), and (2.11), after calculating the saturation pressures p_s from the saturation-pressure equation, Eq. (2.13).

Table 15 Refractive index n [–]
(Saturation state)

	$\bar{\lambda} = 0.2265$ μm		$\bar{\lambda} = 0.40466$ μm		$\bar{\lambda} = 0.5893$ μm		$\bar{\lambda} = 0.70652$ μm	
t [°C]	n'	n''	n'	n''	n'	n''	n'	n''
0	1.3945	1.0000	1.3441	1.0000	1.3343	1.0000	1.3313	1.0000
0.01[a]	1.3945	1.0000	1.3441	1.0000	1.3343	1.0000	1.3313	1.0000
10	1.3942	1.0000	1.3439	1.0000	1.3340	1.0000	1.3311	1.0000
20	1.3933	1.0000	1.3431	1.0000	1.3333	1.0000	1.3304	1.0000
25	1.3928	1.0000	1.3426	1.0000	1.3328	1.0000	1.3299	1.0000
30	1.3921	1.0000	1.3420	1.0000	1.3323	1.0000	1.3293	1.0000
40	1.3905	1.0000	1.3406	1.0000	1.3309	1.0000	1.3280	1.0000
50	1.3885	1.0000	1.3390	1.0000	1.3294	1.0000	1.3264	1.0000
60	1.3864	1.0000	1.3371	1.0000	1.3276	1.0000	1.3247	1.0000
70	1.3839	1.0001	1.3350	1.0001	1.3256	1.0001	1.3227	1.0001
80	1.3813	1.0001	1.3328	1.0001	1.3234	1.0001	1.3206	1.0001
90	1.3785	1.0002	1.3304	1.0001	1.3211	1.0001	1.3183	1.0001
100	1.3755	1.0002	1.3278	1.0002	1.3186	1.0002	1.3158	1.0002
110	1.3723	1.0003	1.3251	1.0003	1.3159	1.0003	1.3132	1.0003
120	1.3689	1.0004	1.3222	1.0004	1.3132	1.0004	1.3105	1.0004
130	1.3654	1.0005	1.3192	1.0005	1.3103	1.0005	1.3076	1.0005
140	1.3616	1.0007	1.3160	1.0006	1.3072	1.0006	1.3046	1.0006
150	1.3578	1.0009	1.3127	1.0008	1.3040	1.0008	1.3014	1.0008
160	1.3537	1.0012	1.3092	1.0011	1.3007	1.0010	1.2981	1.0010
170	1.3495	1.0015	1.3056	1.0013	1.2972	1.0013	1.2947	1.0013
180	1.3451	1.0019	1.3019	1.0017	1.2936	1.0016	1.2911	1.0016
190	1.3406	1.0023	1.2980	1.0021	1.2898	1.0020	1.2873	1.0020
200	1.3358	1.0029	1.2939	1.0026	1.2858	1.0025	1.2834	1.0025
210	1.3308	1.0035	1.2896	1.0031	1.2817	1.0030	1.2794	1.0030
220	1.3256	1.0042	1.2852	1.0038	1.2774	1.0037	1.2751	1.0036
230	1.3202	1.0051	1.2805	1.0045	1.2729	1.0044	1.2706	1.0044
240	1.3145	1.0061	1.2756	1.0054	1.2682	1.0053	1.2660	1.0053
250	1.3086	1.0073	1.2705	1.0065	1.2632	1.0063	1.2611	1.0063
260	1.3023	1.0087	1.2651	1.0077	1.2580	1.0075	1.2559	1.0074
270	1.2957	1.0103	1.2594	1.0091	1.2525	1.0089	1.2504	1.0088
280	1.2887	1.0121	1.2534	1.0107	1.2466	1.0105	1.2446	1.0104
290	1.2813	1.0143	1.2469	1.0127	1.2404	1.0124	1.2384	1.0123
300	1.2732	1.0169	1.2400	1.0149	1.2336	1.0146	1.2318	1.0145
310	1.2646	1.0199	1.2325	1.0177	1.2264	1.0172	1.2246	1.0171
320	1.2551	1.0236	1.2243	1.0209	1.2184	1.0204	1.2167	1.0203
330	1.2446	1.0282	1.2151	1.0250	1.2095	1.0243	1.2079	1.0242
340	1.2325	1.0339	1.2047	1.0301	1.1994	1.0293	1.1978	1.0291
350	1.2183	1.0417	1.1923	1.0369	1.1873	1.0360	1.1858	1.0357
360	1.1998	1.0529	1.1761	1.0469	1.1716	1.0457	1.1703	1.0454
370	1.1694	1.0746	1.1495	1.0661	1.1457	1.0644	1.1446	1.0640
373.946[b]	1.1200		1.1061		1.1035		1.1027	

[a] Triple-point temperature.
[b] Critical temperature.

Table 16 Refractive index *n*

For the single-phase region, this table contains values for the

- Refractive index n.

The table covers temperatures from 0 °C up to 500 °C, pressures from 0.006 112 127 bar up to 1000 bar and for the common wavelengths of $\bar{\lambda}$ = 0.2265 μm, 0.40466 μm, 0.5893 μm, and 0.70652 μm.

The refractive index was calculated from Eq. (3.10). For given pressures and temperatures, the densities needed for Eq. (3.10) were determined from the IAPWS-IF97 basic equations, Eqs. (2.3), (2.6), and (2.11).

The horizontal lines in the columns indicate the transition from the liquid phase to the vapour phase.

Table 16 Refractive index n [–] [a]

t [°C]	p [bar] 0.006112127	0.01	0.1	1	2	5	10	25	50	75	100
$\bar{\lambda} = 0.2265\ \mu m$											
0	1.3945	1.3945	1.3945	1.3945	1.3945	1.3946	1.3947	1.3950	1.3955	1.3960	1.3965
25	1.0000	1.0000	1.3928	1.3928	1.3928	1.3929	1.3929	1.3932	1.3937	1.3941	1.3945
50	1.0000	1.0000	1.0000	1.3885	1.3886	1.3886	1.3887	1.3890	1.3894	1.3898	1.3903
75	1.0000	1.0000	1.0000	1.3827	1.3827	1.3827	1.3828	1.3831	1.3835	1.3840	1.3844
100	1.0000	1.0000	1.0000	1.0002	1.3755	1.3755	1.3756	1.3759	1.3764	1.3768	1.3773
125	1.0000	1.0000	1.0000	1.0002	1.0004	1.3672	1.3673	1.3676	1.3681	1.3686	1.3691
150	1.0000	1.0000	1.0000	1.0002	1.0004	1.3578	1.3579	1.3582	1.3588	1.3593	1.3599
175	1.0000	1.0000	1.0000	1.0002	1.0004	1.0009	1.3474	1.3478	1.3484	1.3490	1.3497
200	1.0000	1.0000	1.0000	1.0002	1.0003	1.0009	1.0018	1.3361	1.3368	1.3376	1.3383
225	1.0000	1.0000	1.0000	1.0002	1.0003	1.0008	1.0017	1.0046	1.3239	1.3248	1.3256
250	1.0000	1.0000	1.0000	1.0002	1.0003	1.0008	1.0016	1.0042	1.3091	1.3102	1.3113
275	1.0000	1.0000	1.0000	1.0001	1.0003	1.0007	1.0015	1.0039	1.0088	1.2932	1.2947
300	1.0000	1.0000	1.0000	1.0001	1.0003	1.0007	1.0014	1.0037	1.0080	1.0136	1.2745
325	1.0000	1.0000	1.0000	1.0001	1.0003	1.0007	1.0013	1.0035	1.0075	1.0122	1.0184
350	1.0000	1.0000	1.0000	1.0001	1.0003	1.0006	1.0013	1.0033	1.0070	1.0112	1.0162
375	1.0000	1.0000	1.0000	1.0001	1.0002	1.0006	1.0012	1.0032	1.0066	1.0104	1.0148
400	1.0000	1.0000	1.0000	1.0001	1.0002	1.0006	1.0012	1.0030	1.0063	1.0098	1.0137
425	1.0000	1.0000	1.0000	1.0001	1.0002	1.0006	1.0011	1.0029	1.0060	1.0093	1.0129
450	1.0000	1.0000	1.0000	1.0001	1.0002	1.0005	1.0011	1.0028	1.0057	1.0088	1.0121
475	1.0000	1.0000	1.0000	1.0001	1.0002	1.0005	1.0011	1.0027	1.0055	1.0084	1.0115
500	1.0000	1.0000	1.0000	1.0001	1.0002	1.0005	1.0010	1.0026	1.0052	1.0081	1.0110
$\bar{\lambda} = 0.40466\ \mu m$											
0	1.3441	1.3441	1.3441	1.3442	1.3442	1.3442	1.3443	1.3446	1.3450	1.3454	1.3458
25	1.0000	1.0000	1.3426	1.3426	1.3426	1.3427	1.3428	1.3430	1.3434	1.3437	1.3441
50	1.0000	1.0000	1.0000	1.3390	1.3390	1.3390	1.3391	1.3393	1.3397	1.3401	1.3404
75	1.0000	1.0000	1.0000	1.3340	1.3340	1.3340	1.3341	1.3343	1.3347	1.3350	1.3354
100	1.0000	1.0000	1.0000	1.0002	1.3278	1.3279	1.3279	1.3282	1.3286	1.3290	1.3294
125	1.0000	1.0000	1.0000	1.0002	1.0004	1.3207	1.3208	1.3211	1.3215	1.3219	1.3224
150	1.0000	1.0000	1.0000	1.0002	1.0003	1.3127	1.3128	1.3131	1.3136	1.3140	1.3145
175	1.0000	1.0000	1.0000	1.0002	1.0003	1.0008	1.3038	1.3041	1.3047	1.3052	1.3057
200	1.0000	1.0000	1.0000	1.0001	1.0003	1.0008	1.0016	1.2941	1.2948	1.2954	1.2960
225	1.0000	1.0000	1.0000	1.0001	1.0003	1.0007	1.0015	1.0040	1.2836	1.2844	1.2852
250	1.0000	1.0000	1.0000	1.0001	1.0003	1.0007	1.0014	1.0037	1.2709	1.2719	1.2728
275	1.0000	1.0000	1.0000	1.0001	1.0003	1.0006	1.0013	1.0035	1.0078	1.2573	1.2585
300	1.0000	1.0000	1.0000	1.0001	1.0002	1.0006	1.0013	1.0033	1.0071	1.0121	1.2411
325	1.0000	1.0000	1.0000	1.0001	1.0002	1.0006	1.0012	1.0031	1.0066	1.0108	1.0163
350	1.0000	1.0000	1.0000	1.0001	1.0002	1.0006	1.0011	1.0029	1.0062	1.0099	1.0144
375	1.0000	1.0000	1.0000	1.0001	1.0002	1.0005	1.0011	1.0028	1.0058	1.0092	1.0131
400	1.0000	1.0000	1.0000	1.0001	1.0002	1.0005	1.0010	1.0027	1.0055	1.0087	1.0122
425	1.0000	1.0000	1.0000	1.0001	1.0002	1.0005	1.0010	1.0026	1.0053	1.0082	1.0114
450	1.0000	1.0000	1.0000	1.0001	1.0002	1.0005	1.0010	1.0025	1.0051	1.0078	1.0108
475	1.0000	1.0000	1.0000	1.0001	1.0002	1.0005	1.0009	1.0024	1.0048	1.0075	1.0102
500	1.0000	1.0000	1.0000	1.0001	1.0002	1.0004	1.0009	1.0023	1.0046	1.0071	1.0097

[a] The horizontal lines in the columns indicate the transition from the liquid phase to the gas phase.

Table 16 Refractive index n [–] [a] – Continued

t [°C]	p [bar] 150	200	250	300	400	500	600	700	800	900	1000
						$\bar{\lambda} = 0.2265\ \mu m$					
0	1.3975	1.3985	1.3995	1.4004	1.4023	1.4041	1.4059	1.4077	1.4094	1.4111	1.4127
25	1.3954	1.3963	1.3972	1.3980	1.3997	1.4013	1.4030	1.4045	1.4061	1.4076	1.4091
50	1.3911	1.3919	1.3928	1.3936	1.3952	1.3968	1.3984	1.3999	1.4014	1.4029	1.4043
75	1.3853	1.3861	1.3869	1.3878	1.3894	1.3910	1.3926	1.3941	1.3956	1.3971	1.3985
100	1.3782	1.3791	1.3800	1.3808	1.3825	1.3842	1.3858	1.3874	1.3890	1.3905	1.3920
125	1.3701	1.3710	1.3720	1.3729	1.3747	1.3765	1.3783	1.3799	1.3816	1.3832	1.3847
150	1.3610	1.3620	1.3631	1.3641	1.3661	1.3680	1.3699	1.3717	1.3735	1.3752	1.3769
175	1.3509	1.3521	1.3533	1.3544	1.3566	1.3588	1.3608	1.3628	1.3647	1.3666	1.3684
200	1.3397	1.3411	1.3424	1.3438	1.3463	1.3487	1.3510	1.3532	1.3553	1.3574	1.3593
225	1.3273	1.3290	1.3306	1.3321	1.3350	1.3378	1.3404	1.3429	1.3452	1.3475	1.3497
250	1.3134	1.3154	1.3174	1.3192	1.3227	1.3259	1.3289	1.3318	1.3345	1.3371	1.3395
275	1.2975	1.3001	1.3025	1.3048	1.3091	1.3130	1.3166	1.3199	1.3230	1.3259	1.3287
300	1.2786	1.2822	1.2855	1.2885	1.2939	1.2988	1.3031	1.3070	1.3107	1.3141	1.3173
325	1.2541	1.2601	1.2650	1.2694	1.2767	1.2829	1.2883	1.2931	1.2975	1.3015	1.3051
350	1.0319	1.2285	1.2382	1.2455	1.2565	1.2650	1.2719	1.2779	1.2832	1.2879	1.2923
375	1.0262	1.0478	1.1909	1.2114	1.2315	1.2440	1.2535	1.2612	1.2677	1.2734	1.2786
400	1.0232	1.0367	1.0612	1.1334	1.1976	1.2188	1.2324	1.2426	1.2509	1.2579	1.2640
425	1.0212	1.0317	1.0463	1.0693	1.1473	1.1874	1.2079	1.2219	1.2325	1.2412	1.2486
450	1.0196	1.0286	1.0397	1.0543	1.1001	1.1501	1.1800	1.1990	1.2127	1.2235	1.2324
475	1.0184	1.0263	1.0355	1.0467	1.0771	1.1167	1.1510	1.1747	1.1918	1.2049	1.2155
500	1.0173	1.0245	1.0326	1.0418	1.0650	1.0946	1.1255	1.1512	1.1708	1.1860	1.1983
						$\bar{\lambda} = 0.40466\ \mu m$					
0	1.3467	1.3475	1.3483	1.3491	1.3507	1.3523	1.3538	1.3552	1.3567	1.3581	1.3595
25	1.3448	1.3456	1.3463	1.3470	1.3484	1.3498	1.3512	1.3525	1.3538	1.3551	1.3564
50	1.3411	1.3418	1.3425	1.3432	1.3446	1.3459	1.3473	1.3485	1.3498	1.3510	1.3522
75	1.3361	1.3369	1.3376	1.3383	1.3397	1.3410	1.3423	1.3436	1.3449	1.3461	1.3473
100	1.3301	1.3309	1.3316	1.3324	1.3338	1.3352	1.3366	1.3379	1.3392	1.3405	1.3418
125	1.3232	1.3240	1.3248	1.3256	1.3271	1.3286	1.3301	1.3315	1.3329	1.3343	1.3356
150	1.3154	1.3163	1.3172	1.3181	1.3198	1.3214	1.3230	1.3245	1.3260	1.3275	1.3289
175	1.3068	1.3078	1.3088	1.3098	1.3117	1.3135	1.3152	1.3169	1.3185	1.3201	1.3216
200	1.2972	1.2984	1.2996	1.3007	1.3028	1.3049	1.3068	1.3087	1.3105	1.3122	1.3139
225	1.2866	1.2880	1.2894	1.2907	1.2932	1.2955	1.2977	1.2999	1.3019	1.3038	1.3057
250	1.2747	1.2764	1.2780	1.2796	1.2826	1.2853	1.2879	1.2904	1.2927	1.2949	1.2970
275	1.2609	1.2632	1.2653	1.2672	1.2709	1.2742	1.2773	1.2801	1.2828	1.2853	1.2877
300	1.2446	1.2477	1.2506	1.2532	1.2578	1.2620	1.2657	1.2691	1.2722	1.2751	1.2779
325	1.2234	1.2286	1.2329	1.2366	1.2430	1.2483	1.2530	1.2571	1.2608	1.2643	1.2674
350	1.0282	1.2011	1.2096	1.2159	1.2255	1.2328	1.2388	1.2440	1.2485	1.2526	1.2563
375	1.0232	1.0423	1.1684	1.1863	1.2037	1.2146	1.2228	1.2295	1.2351	1.2401	1.2445
400	1.0206	1.0325	1.0542	1.1179	1.1742	1.1927	1.2045	1.2133	1.2205	1.2266	1.2319
425	1.0188	1.0281	1.0410	1.0614	1.1301	1.1652	1.1832	1.1953	1.2046	1.2121	1.2185
450	1.0174	1.0253	1.0352	1.0480	1.0885	1.1325	1.1588	1.1753	1.1873	1.1967	1.2044
475	1.0163	1.0233	1.0315	1.0414	1.0682	1.1032	1.1333	1.1541	1.1690	1.1804	1.1897
500	1.0154	1.0217	1.0288	1.0370	1.0575	1.0837	1.1109	1.1335	1.1506	1.1639	1.1747

[a] The horizontal lines in the columns indicate the transition from the liquid phase to the gas phase.

Table 16 Refractive index *n* [–] [a] – Continued

t [°C]	*p* [bar] 0.006112127	0.01	0.1	1	2	5	10	25	50	75	100
						$\bar{\lambda} = 0.5893\ \mu m$					
0	1.3343	1.3343	1.3343	1.3343	1.3344	1.3344	1.3345	1.3347	1.3351	1.3356	1.3360
25	1.0000	1.0000	1.3328	1.3329	1.3329	1.3329	1.3330	1.3332	1.3336	1.3339	1.3343
50	1.0000	1.0000	1.0000	1.3294	1.3294	1.3294	1.3295	1.3297	1.3301	1.3304	1.3308
75	1.0000	1.0000	1.0000	1.3245	1.3245	1.3246	1.3246	1.3249	1.3252	1.3256	1.3259
100	1.0000	1.0000	1.0000	1.0002	1.3186	1.3186	1.3187	1.3189	1.3193	1.3197	1.3201
125	1.0000	1.0000	1.0000	1.0002	1.0004	1.3118	1.3119	1.3121	1.3125	1.3129	1.3133
150	1.0000	1.0000	1.0000	1.0002	1.0003	1.3040	1.3041	1.3044	1.3048	1.3053	1.3057
175	1.0000	1.0000	1.0000	1.0002	1.0003	1.0008	1.2954	1.2957	1.2963	1.2968	1.2973
200	1.0000	1.0000	1.0000	1.0001	1.0003	1.0007	1.0015	1.2861	1.2867	1.2873	1.2879
225	1.0000	1.0000	1.0000	1.0001	1.0003	1.0007	1.0014	1.0039	1.2759	1.2766	1.2774
250	1.0000	1.0000	1.0000	1.0001	1.0003	1.0007	1.0014	1.0036	1.2636	1.2645	1.2655
275	1.0000	1.0000	1.0000	1.0001	1.0003	1.0006	1.0013	1.0034	1.0076	1.2504	1.2516
300	1.0000	1.0000	1.0000	1.0001	1.0002	1.0006	1.0012	1.0032	1.0069	1.0118	1.2347
325	1.0000	1.0000	1.0000	1.0001	1.0002	1.0006	1.0012	1.0030	1.0064	1.0106	1.0159
350	1.0000	1.0000	1.0000	1.0001	1.0002	1.0005	1.0011	1.0029	1.0060	1.0097	1.0140
375	1.0000	1.0000	1.0000	1.0001	1.0002	1.0005	1.0011	1.0027	1.0057	1.0090	1.0128
400	1.0000	1.0000	1.0000	1.0001	1.0002	1.0005	1.0010	1.0026	1.0054	1.0085	1.0119
425	1.0000	1.0000	1.0000	1.0001	1.0002	1.0005	1.0010	1.0025	1.0052	1.0080	1.0111
450	1.0000	1.0000	1.0000	1.0001	1.0002	1.0005	1.0009	1.0024	1.0049	1.0076	1.0105
475	1.0000	1.0000	1.0000	1.0001	1.0002	1.0005	1.0009	1.0023	1.0047	1.0073	1.0100
500	1.0000	1.0000	1.0000	1.0001	1.0002	1.0004	1.0009	1.0022	1.0045	1.0070	1.0095
						$\bar{\lambda} = 0.70652\ \mu m$					
0	1.3313	1.3313	1.3313	1.3313	1.3314	1.3314	1.3315	1.3317	1.3321	1.3325	1.3330
25	1.0000	1.0000	1.3299	1.3299	1.3299	1.3300	1.3300	1.3302	1.3306	1.3310	1.3313
50	1.0000	1.0000	1.0000	1.3265	1.3265	1.3265	1.3266	1.3268	1.3271	1.3275	1.3278
75	1.0000	1.0000	1.0000	1.3217	1.3217	1.3217	1.3218	1.3220	1.3224	1.3227	1.3231
100	1.0000	1.0000	1.0000	1.0002	1.3158	1.3159	1.3160	1.3162	1.3166	1.3169	1.3173
125	1.0000	1.0000	1.0000	1.0002	1.0004	1.3091	1.3092	1.3094	1.3098	1.3102	1.3106
150	1.0000	1.0000	1.0000	1.0002	1.0003	1.3014	1.3015	1.3018	1.3022	1.3027	1.3031
175	1.0000	1.0000	1.0000	1.0002	1.0003	1.0008	1.2929	1.2932	1.2938	1.2943	1.2948
200	1.0000	1.0000	1.0000	1.0001	1.0003	1.0007	1.0015	1.2837	1.2843	1.2849	1.2855
225	1.0000	1.0000	1.0000	1.0001	1.0003	1.0007	1.0014	1.0039	1.2736	1.2744	1.2751
250	1.0000	1.0000	1.0000	1.0001	1.0003	1.0007	1.0013	1.0036	1.2615	1.2624	1.2633
275	1.0000	1.0000	1.0000	1.0001	1.0002	1.0006	1.0013	1.0034	1.0076	1.2484	1.2496
300	1.0000	1.0000	1.0000	1.0001	1.0002	1.0006	1.0012	1.0032	1.0069	1.0117	1.2328
325	1.0000	1.0000	1.0000	1.0001	1.0002	1.0006	1.0012	1.0030	1.0064	1.0105	1.0158
350	1.0000	1.0000	1.0000	1.0001	1.0002	1.0005	1.0011	1.0028	1.0060	1.0096	1.0139
375	1.0000	1.0000	1.0000	1.0001	1.0002	1.0005	1.0011	1.0027	1.0057	1.0090	1.0127
400	1.0000	1.0000	1.0000	1.0001	1.0002	1.0005	1.0010	1.0026	1.0054	1.0084	1.0118
425	1.0000	1.0000	1.0000	1.0001	1.0002	1.0005	1.0010	1.0025	1.0051	1.0080	1.0110
450	1.0000	1.0000	1.0000	1.0001	1.0002	1.0005	1.0009	1.0024	1.0049	1.0076	1.0104
475	1.0000	1.0000	1.0000	1.0001	1.0002	1.0004	1.0009	1.0023	1.0047	1.0072	1.0099
500	1.0000	1.0000	1.0000	1.0001	1.0002	1.0004	1.0009	1.0022	1.0045	1.0069	1.0094

[a] The horizontal lines in the columns indicate the transition from the liquid phase to the gas phase.

Table 16 Refractive index n [–] [a] – Continued

t [°C]	p [bar] 150	200	250	300	400	500	600	700	800	900	1000
						$\bar{\lambda} = 0.5893\,\mu m$					
0	1.3368	1.3376	1.3383	1.3391	1.3407	1.3421	1.3436	1.3450	1.3464	1.3478	1.3491
25	1.3350	1.3357	1.3364	1.3371	1.3385	1.3398	1.3411	1.3424	1.3437	1.3449	1.3461
50	1.3314	1.3321	1.3328	1.3335	1.3348	1.3361	1.3373	1.3386	1.3398	1.3410	1.3421
75	1.3266	1.3273	1.3280	1.3287	1.3300	1.3313	1.3326	1.3338	1.3351	1.3362	1.3374
100	1.3208	1.3215	1.3223	1.3230	1.3244	1.3257	1.3270	1.3283	1.3296	1.3308	1.3320
125	1.3141	1.3149	1.3157	1.3165	1.3180	1.3194	1.3208	1.3222	1.3235	1.3248	1.3261
150	1.3066	1.3075	1.3084	1.3092	1.3108	1.3124	1.3139	1.3154	1.3169	1.3183	1.3196
175	1.2983	1.2993	1.3002	1.3012	1.3030	1.3048	1.3064	1.3081	1.3096	1.3112	1.3126
200	1.2891	1.2902	1.2913	1.2924	1.2945	1.2964	1.2983	1.3001	1.3019	1.3036	1.3052
225	1.2788	1.2801	1.2814	1.2827	1.2851	1.2874	1.2896	1.2916	1.2936	1.2954	1.2972
250	1.2672	1.2689	1.2705	1.2720	1.2749	1.2776	1.2801	1.2824	1.2847	1.2868	1.2888
275	1.2539	1.2561	1.2581	1.2600	1.2636	1.2668	1.2698	1.2725	1.2751	1.2775	1.2798
300	1.2381	1.2411	1.2439	1.2464	1.2509	1.2549	1.2585	1.2618	1.2649	1.2677	1.2703
325	1.2176	1.2225	1.2267	1.2304	1.2365	1.2417	1.2462	1.2502	1.2538	1.2572	1.2602
350	1.0275	1.1959	1.2041	1.2103	1.2195	1.2266	1.2325	1.2375	1.2419	1.2458	1.2495
375	1.0227	1.0413	1.1640	1.1815	1.1984	1.2090	1.2170	1.2234	1.2289	1.2337	1.2380
400	1.0201	1.0317	1.0528	1.1150	1.1697	1.1877	1.1992	1.2078	1.2147	1.2206	1.2258
425	1.0183	1.0274	1.0400	1.0599	1.1268	1.1610	1.1785	1.1903	1.1993	1.2066	1.2128
450	1.0169	1.0247	1.0343	1.0469	1.0863	1.1292	1.1547	1.1708	1.1825	1.1916	1.1991
475	1.0159	1.0227	1.0307	1.0403	1.0665	1.1006	1.1299	1.1502	1.1647	1.1758	1.1848
500	1.0150	1.0211	1.0281	1.0361	1.0561	1.0816	1.1081	1.1301	1.1468	1.1598	1.1702
						$\bar{\lambda} = 0.70652\,\mu m$					
0	1.3337	1.3345	1.3353	1.3361	1.3376	1.3391	1.3405	1.3419	1.3433	1.3446	1.3459
25	1.3320	1.3327	1.3334	1.3341	1.3355	1.3368	1.3381	1.3393	1.3406	1.3418	1.3430
50	1.3285	1.3292	1.3299	1.3305	1.3318	1.3331	1.3343	1.3356	1.3368	1.3379	1.3391
75	1.3238	1.3244	1.3251	1.3258	1.3271	1.3284	1.3297	1.3309	1.3321	1.3333	1.3344
100	1.3180	1.3187	1.3195	1.3202	1.3215	1.3229	1.3242	1.3255	1.3267	1.3279	1.3291
125	1.3114	1.3122	1.3130	1.3137	1.3152	1.3166	1.3180	1.3194	1.3207	1.3220	1.3233
150	1.3040	1.3049	1.3057	1.3066	1.3082	1.3097	1.3112	1.3127	1.3141	1.3155	1.3169
175	1.2958	1.2968	1.2977	1.2986	1.3004	1.3022	1.3038	1.3055	1.3070	1.3085	1.3100
200	1.2867	1.2878	1.2889	1.2899	1.2920	1.2939	1.2958	1.2976	1.2993	1.3010	1.3026
225	1.2765	1.2778	1.2791	1.2804	1.2828	1.2850	1.2871	1.2892	1.2911	1.2930	1.2948
250	1.2650	1.2667	1.2683	1.2698	1.2726	1.2753	1.2778	1.2801	1.2823	1.2844	1.2864
275	1.2519	1.2540	1.2560	1.2579	1.2615	1.2646	1.2676	1.2703	1.2729	1.2753	1.2776
300	1.2362	1.2392	1.2419	1.2444	1.2489	1.2529	1.2565	1.2597	1.2627	1.2655	1.2682
325	1.2159	1.2208	1.2249	1.2285	1.2347	1.2398	1.2443	1.2482	1.2518	1.2551	1.2581
350	1.0273	1.1944	1.2026	1.2087	1.2178	1.2249	1.2307	1.2356	1.2400	1.2439	1.2475
375	1.0225	1.0410	1.1628	1.1801	1.1969	1.2074	1.2153	1.2217	1.2271	1.2319	1.2361
400	1.0199	1.0315	1.0524	1.1141	1.1684	1.1863	1.1977	1.2062	1.2131	1.2190	1.2240
425	1.0182	1.0272	1.0397	1.0594	1.1258	1.1598	1.1771	1.1888	1.1978	1.2050	1.2112
450	1.0168	1.0245	1.0341	1.0465	1.0857	1.1282	1.1536	1.1696	1.1811	1.1902	1.1976
475	1.0158	1.0225	1.0305	1.0400	1.0660	1.0999	1.1290	1.1491	1.1635	1.1745	1.1834
500	1.0149	1.0210	1.0279	1.0359	1.0557	1.0810	1.1074	1.1291	1.1457	1.1586	1.1690

[a] The horizontal lines in the columns indicate the transition from the liquid phase to the gas phase.

Part C

Diagrams of the Properties of Water and Steam

Overview Diagrams

The first three diagrams of Part C are overview diagrams, namely:

Diagram 1: Mollier *h*-*s* diagram
Diagram 2: *T*-*s* diagram
Diagram 3: $\log(p)$-*h* diagram

The diagrams were calculated from the IAPWS-IF97 basic equations, Eqs. (2.3), (2.6), (2.11), and (2.15), and plotted using the software FluidDIA [45].

In addition, Part E contains the Mollier *h*-*s* diagram and the *T*-*s* diagram as coloured wall charts.

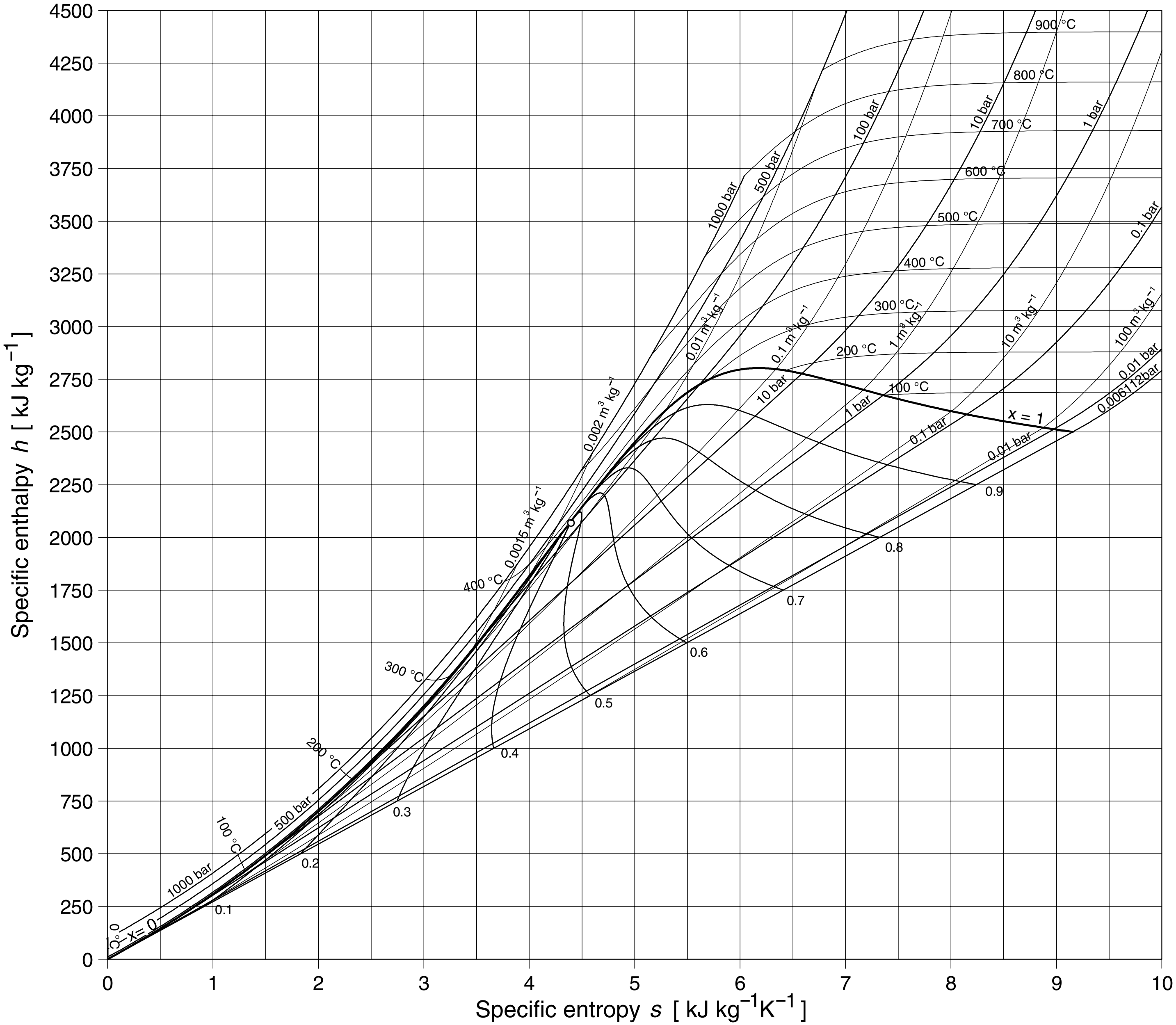

Diagr. 1 Mollier enthalpy-entropy diagram with lines of constant pressure, temperature, and specific volume.

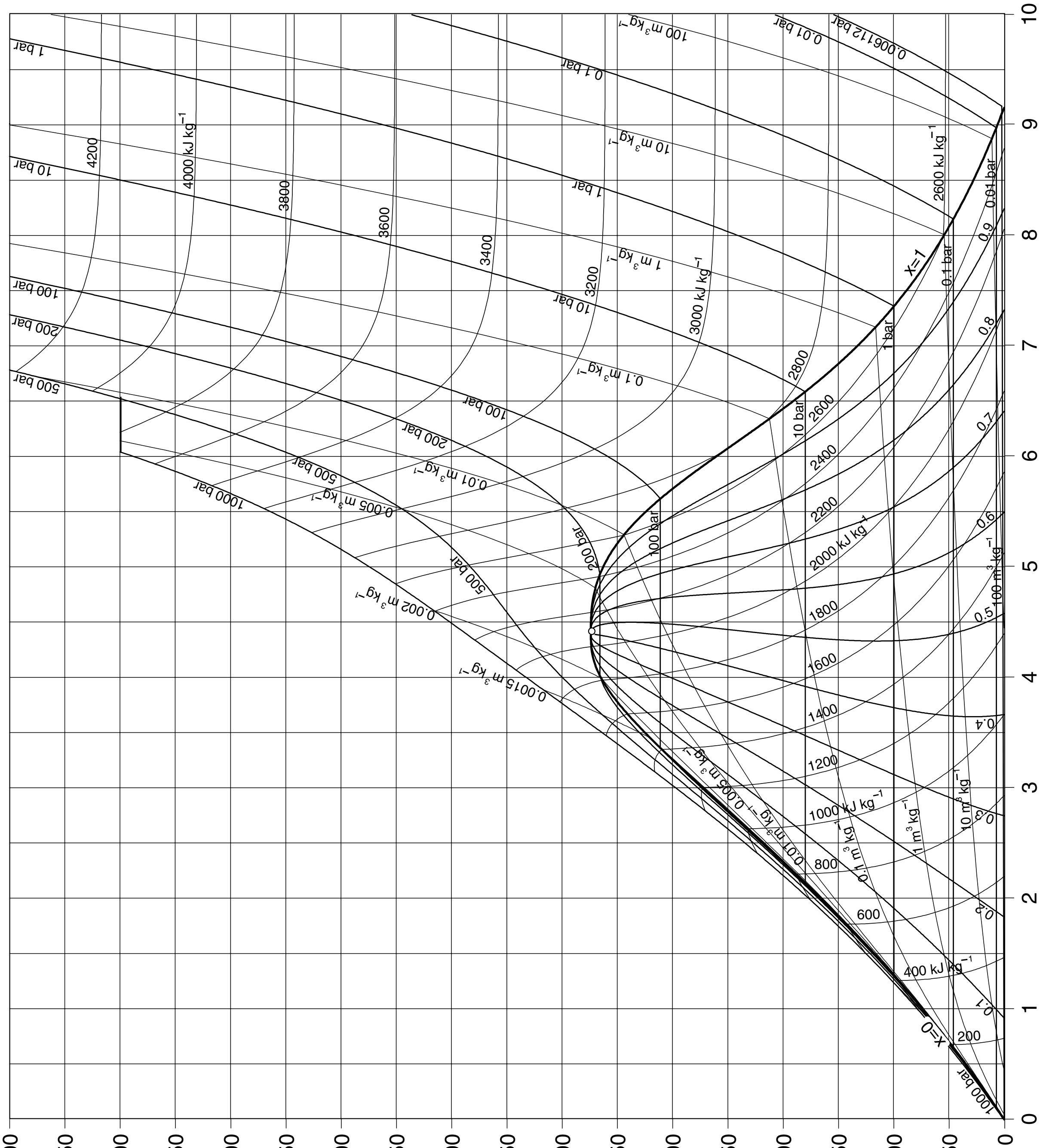

Diagr. 2 Temperature-entropy diagram with lines of constant pressure, specific enthalpy, and specific volume.

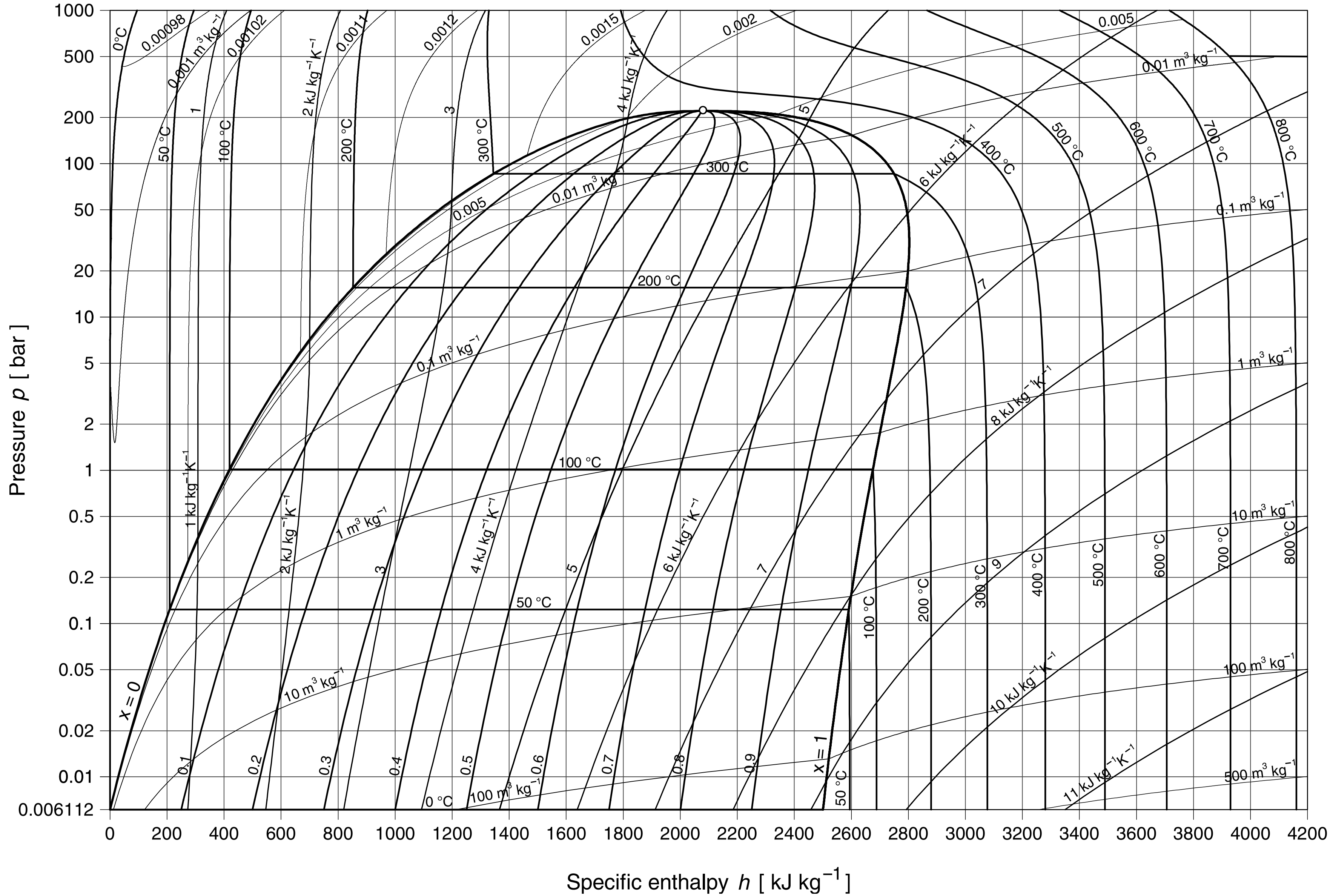

Diagr. 3 Logarithm pressure-enthalpy diagram with lines of constant specific entropy, temperature, and specific volume.

Pressure-Temperature Diagrams with Lines of Constant Properties

Additional diagrams contained in Part C are pressure-temperature diagrams with isolines of the following properties:

Diagram 4: Specific volume v
Diagram 5: Density ρ
Diagram 6: Compression factor z
Diagram 7: Specific enthalpy h
Diagram 8: Specific internal energy u
Diagram 9: Specific entropy s
Diagram 10: Specific Gibbs free energy g
Diagram 11: Specific Helmholtz free energy f
Diagram 12: Specific isobaric heat capacity c_p
Diagram 13: Specific isochoric heat capacity c_v
Diagram 14: Speed of sound w
Diagram 15: Isentropic exponent κ
Diagram 16: Isobaric cubic expansion coefficient α_v
Diagram 17: Isothermal compressibility κ_T
Diagram 18: Relative pressure coefficient α_p
Diagram 19: Isothermal stress coefficient β_p
Diagram 20: Joule-Thomson coefficient μ
Diagram 21: Isothermal throttling coefficient δ_T
Diagram 22: Fugacity f^*
Diagram 23: Dynamic viscosity η
Diagram 24: Kinematic viscosity v
Diagram 25: Thermal conductivity λ
Diagram 26: Prandtl number Pr
Diagram 27: Thermal diffusivity a
Diagram 28: Dielectric constant ε
Diagram 29: Refractive index n

The thermodynamic properties in the diagrams were calculated from the IAPWS-IF97 basic equations, Eqs. (2.3), (2.6), and (2.11), with the exception of c_p, c_v, w, κ_T, δ_T and μ. Since the small inconsistencies for these properties at the region boundaries are visible in such diagrams, they were calculated from the scientific formulation IAPWS-95 [8, 9].

The dynamic viscosity η was calculated from the equation for industrial applications, Eq. (3.1). The thermal conductivity λ was calculated from the scientific equation [35] to avoid visible discontinuities at the critical temperature in the enlarged critical region below the critical pressure. The properties ε and n were calculated from Eqs. (3.9) and (3.10). The densities needed in these equations were determined from the IAPWS-IF97 basic equations, see above.

All of the diagrams were plotted using the software FluidDIA [45].

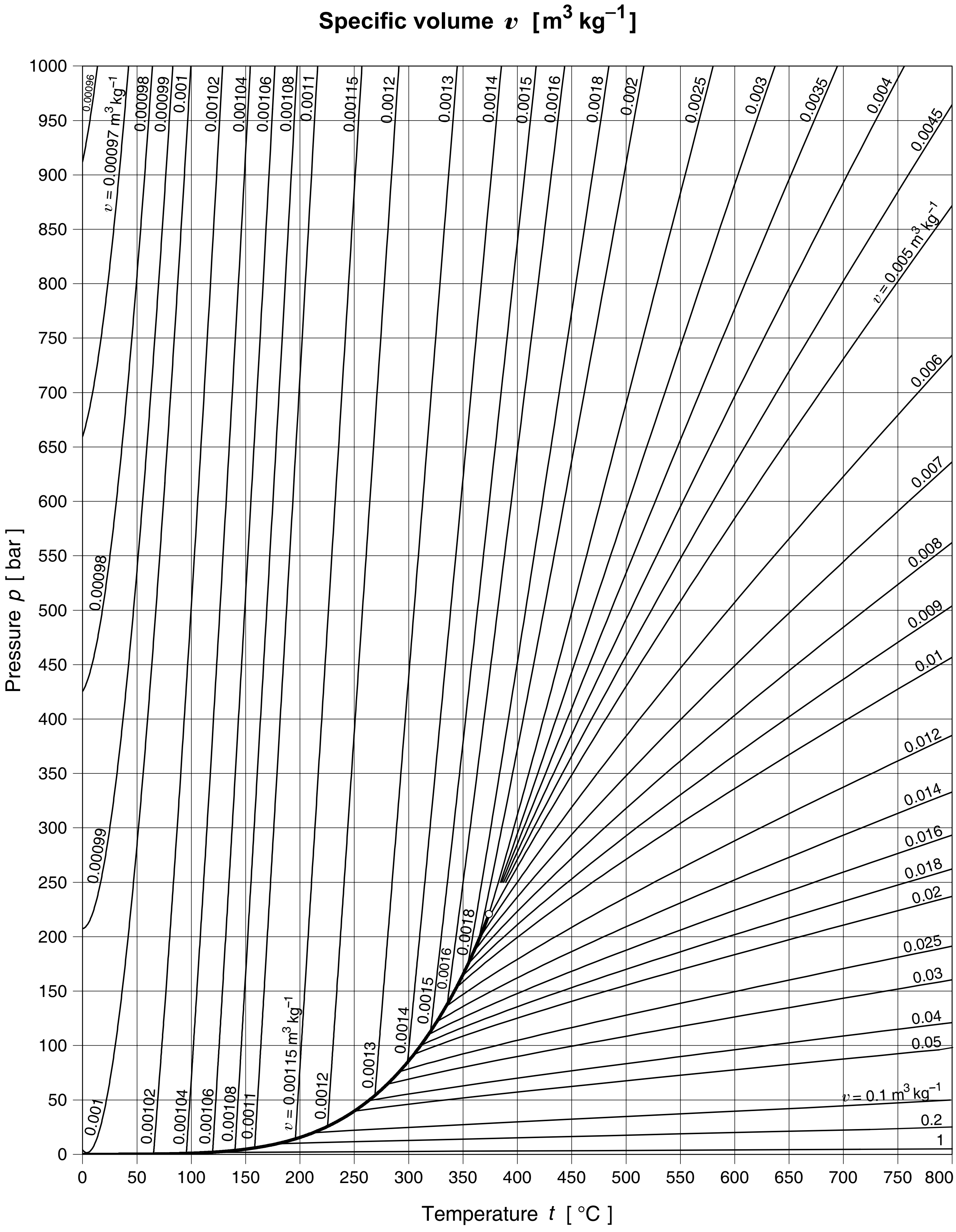

Diagr. 4 Pressure-temperature diagram with lines of constant specific volume.

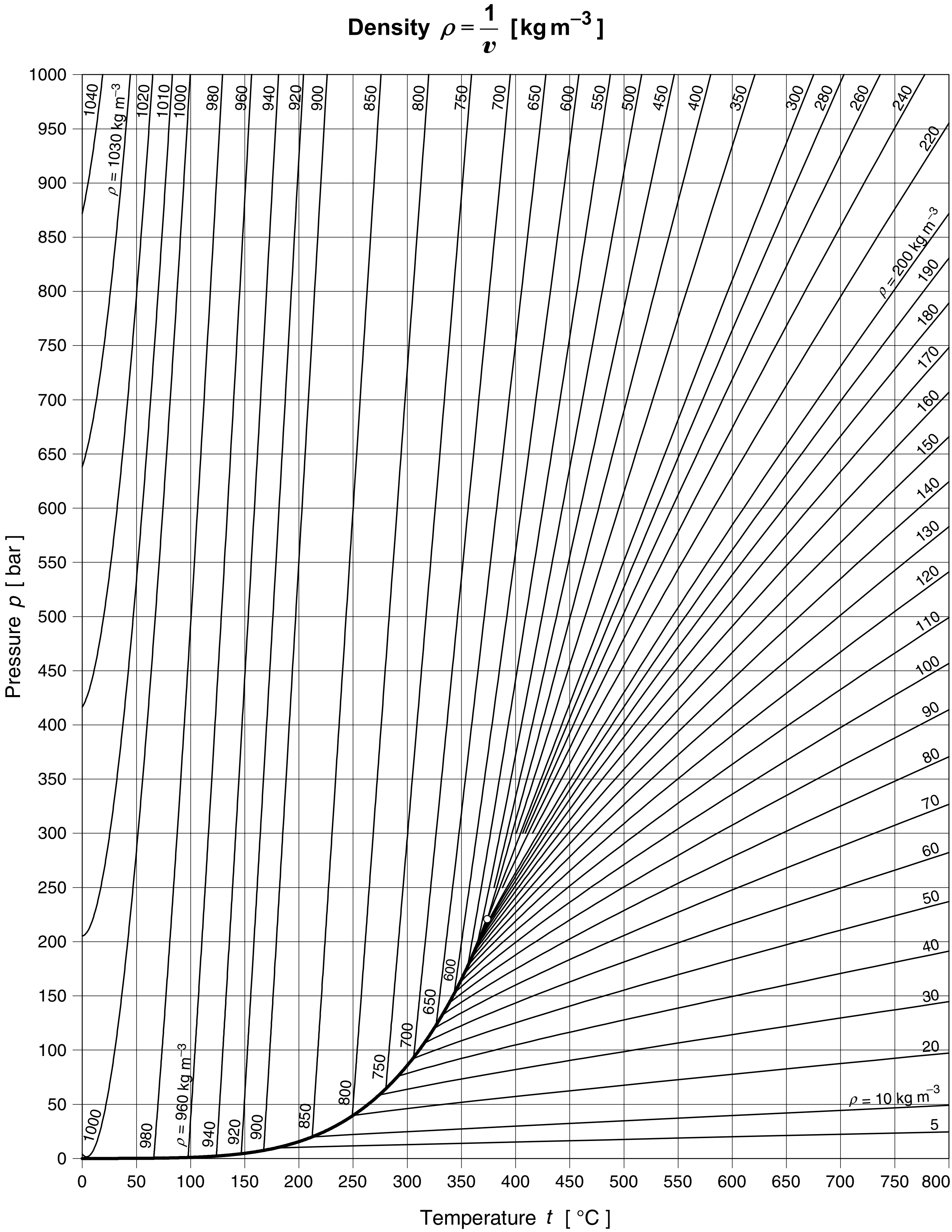

Diagr. 5 Pressure-temperature diagram with lines of constant density.

Compression factor $z = \dfrac{p\,v}{R\,T}$ **[–]**

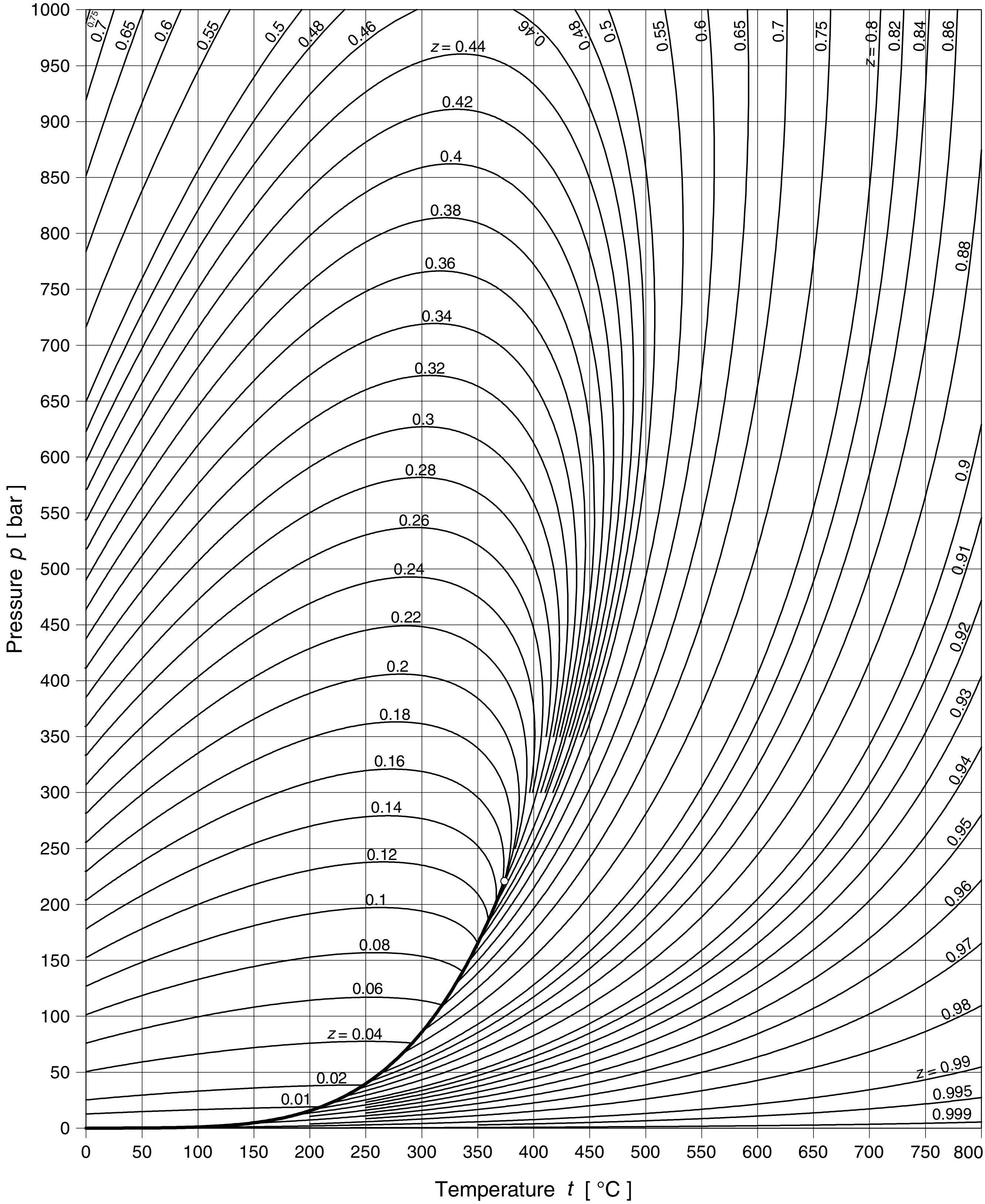

Diagr. 6 Pressure-temperature diagram with lines of constant compression factor.

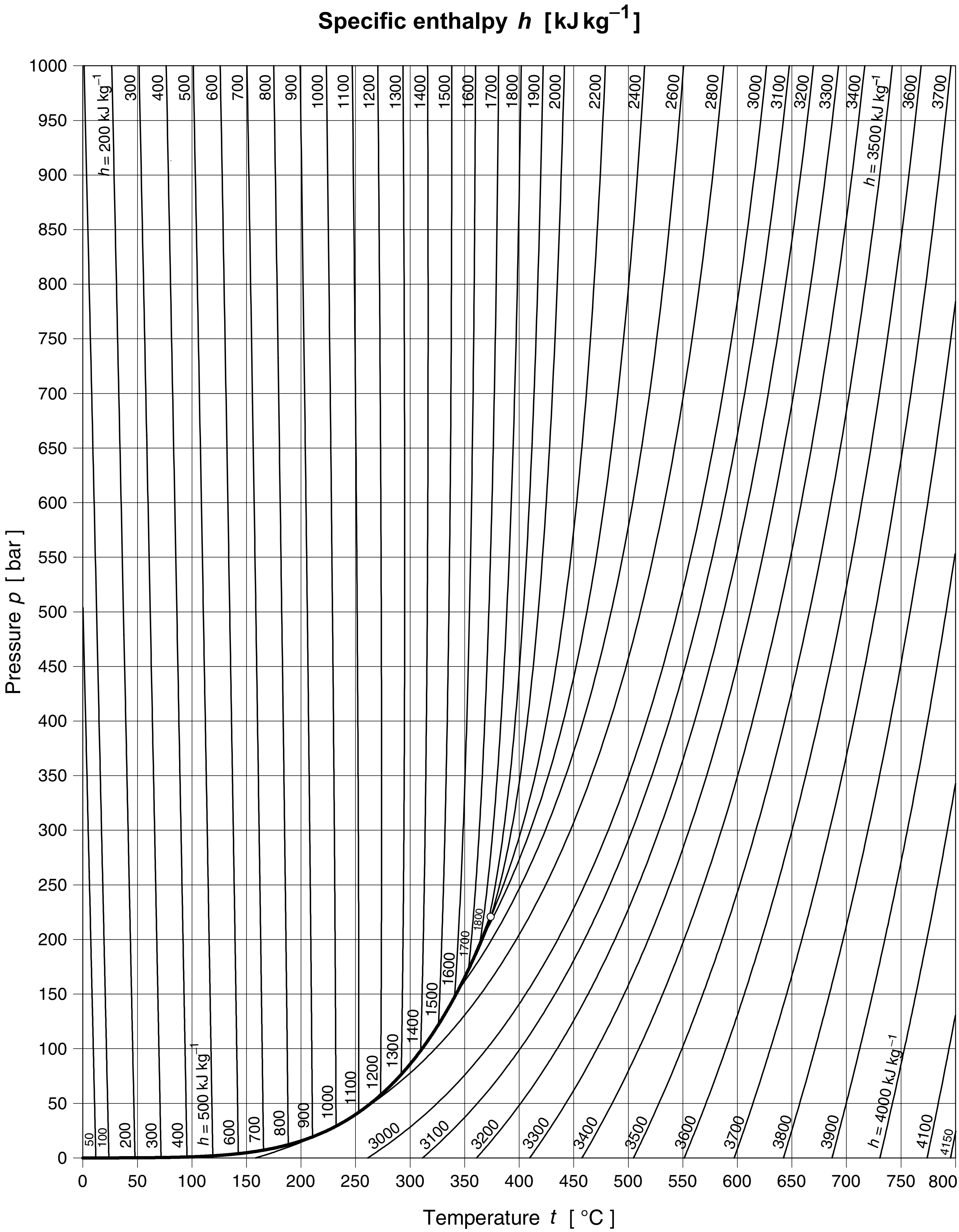

Diagr. 7 Pressure-temperature diagram with lines of constant specific enthalpy.

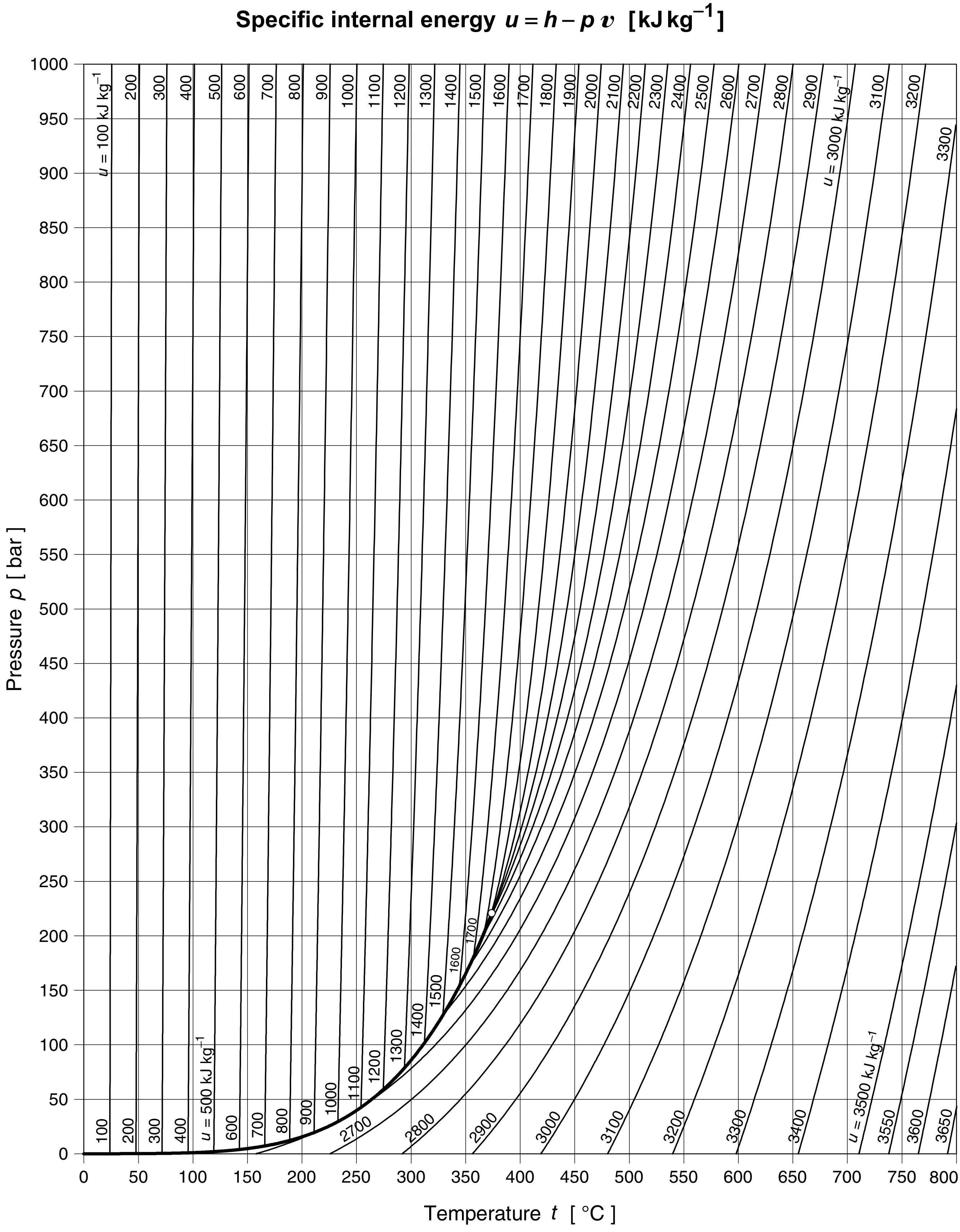

Diagr. 8 Pressure-temperature diagram with lines of constant specific internal energy.

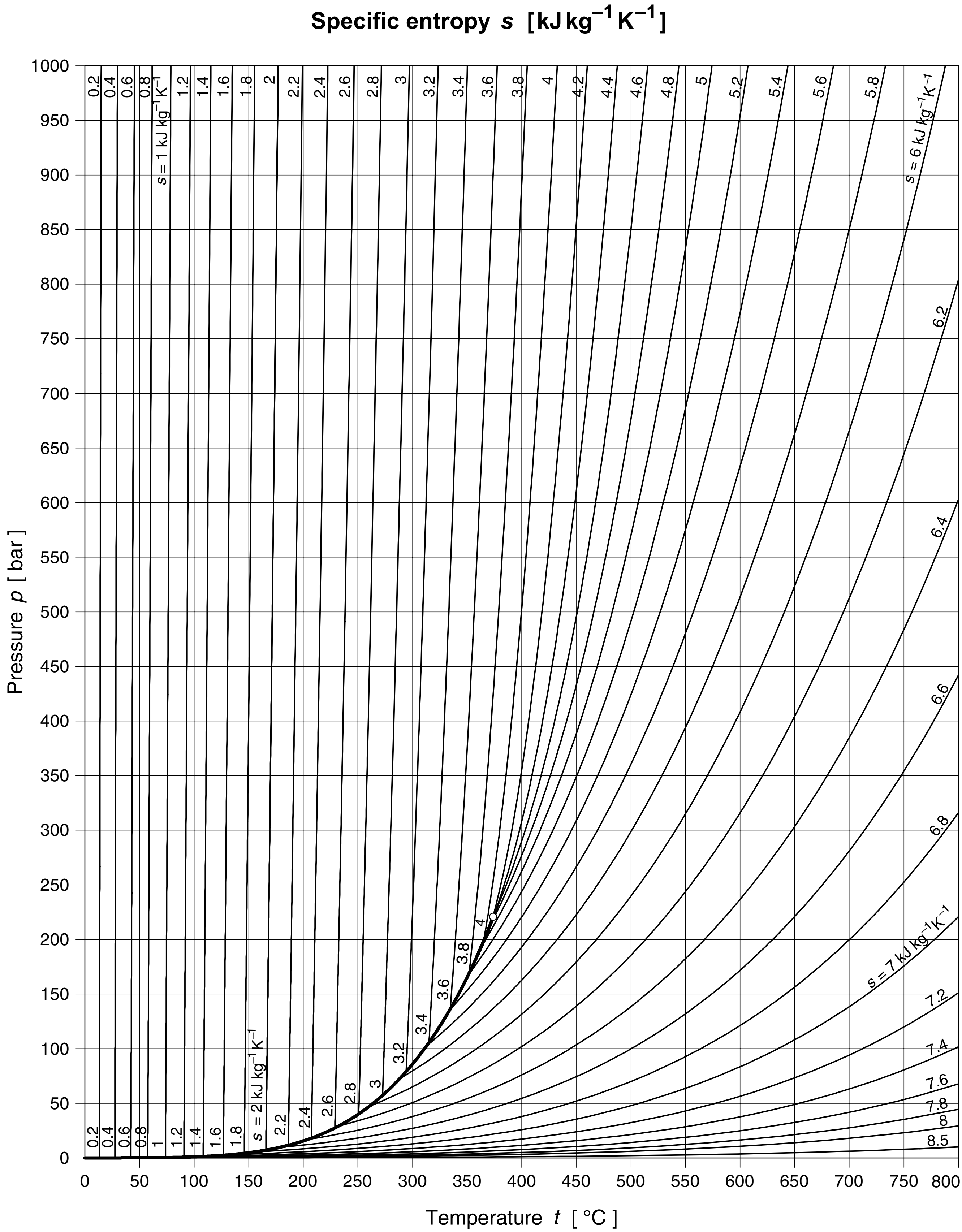

Diagr. 9 Pressure-temperature diagram with lines of constant specific entropy.

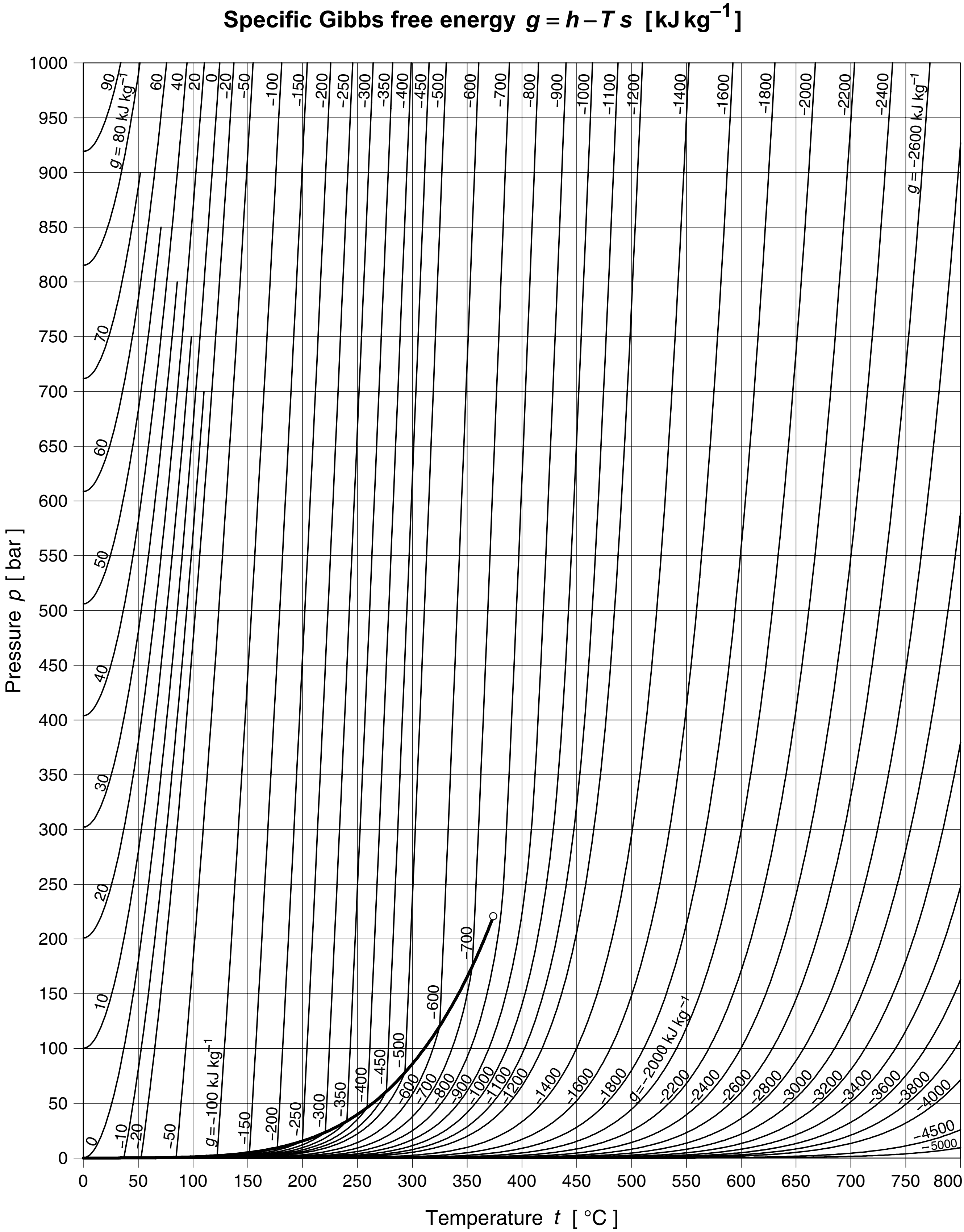

Diagr. 10 Pressure-temperature diagram with lines of constant specific Gibbs free energy.

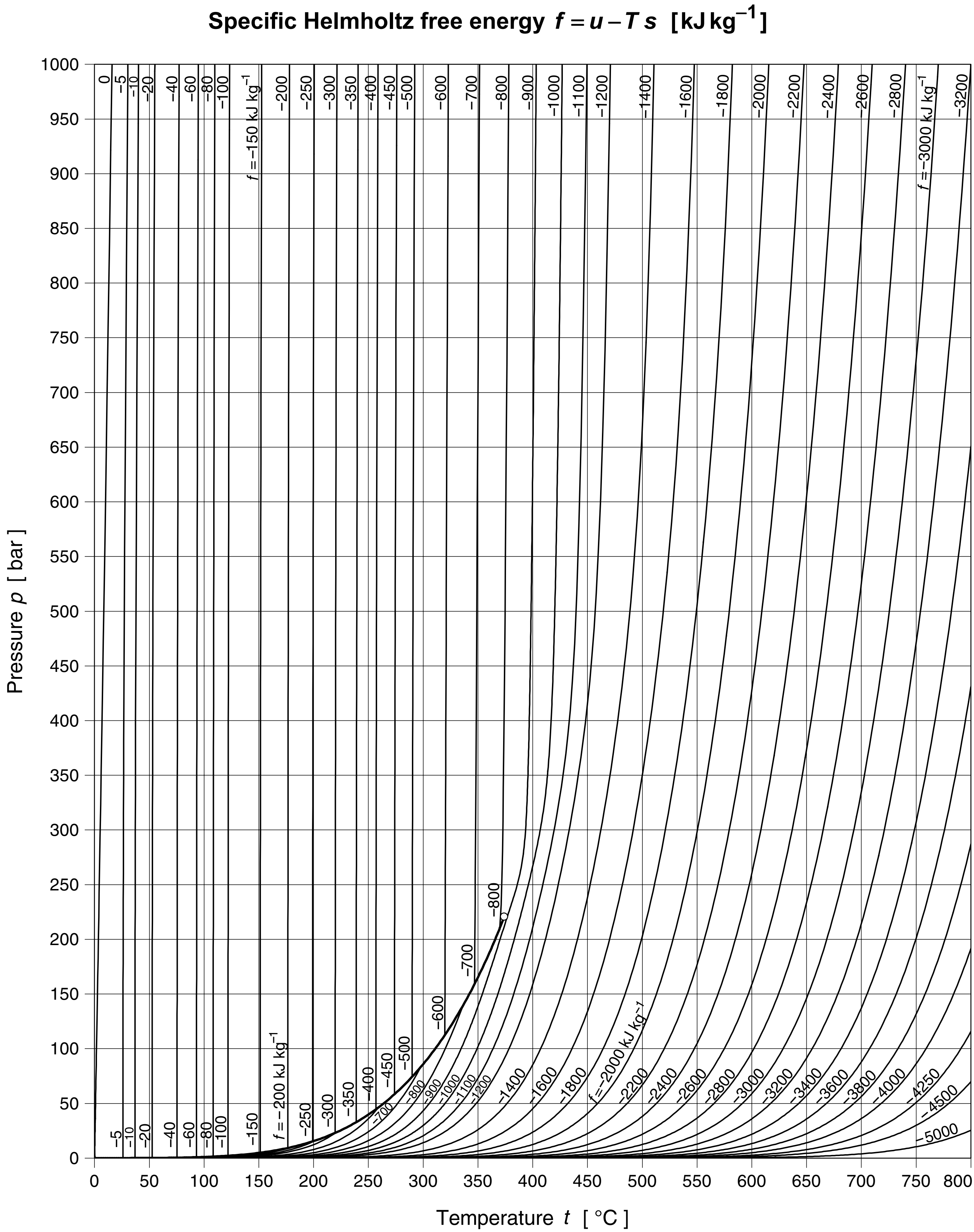

Diagr. 11 Pressure-temperature diagram with lines of constant specific Helmholtz free energy.

Specific isobaric heat capacity $c_p = \left(\frac{\partial h}{\partial T}\right)_p$ [kJ kg^{-1} K^{-1}]

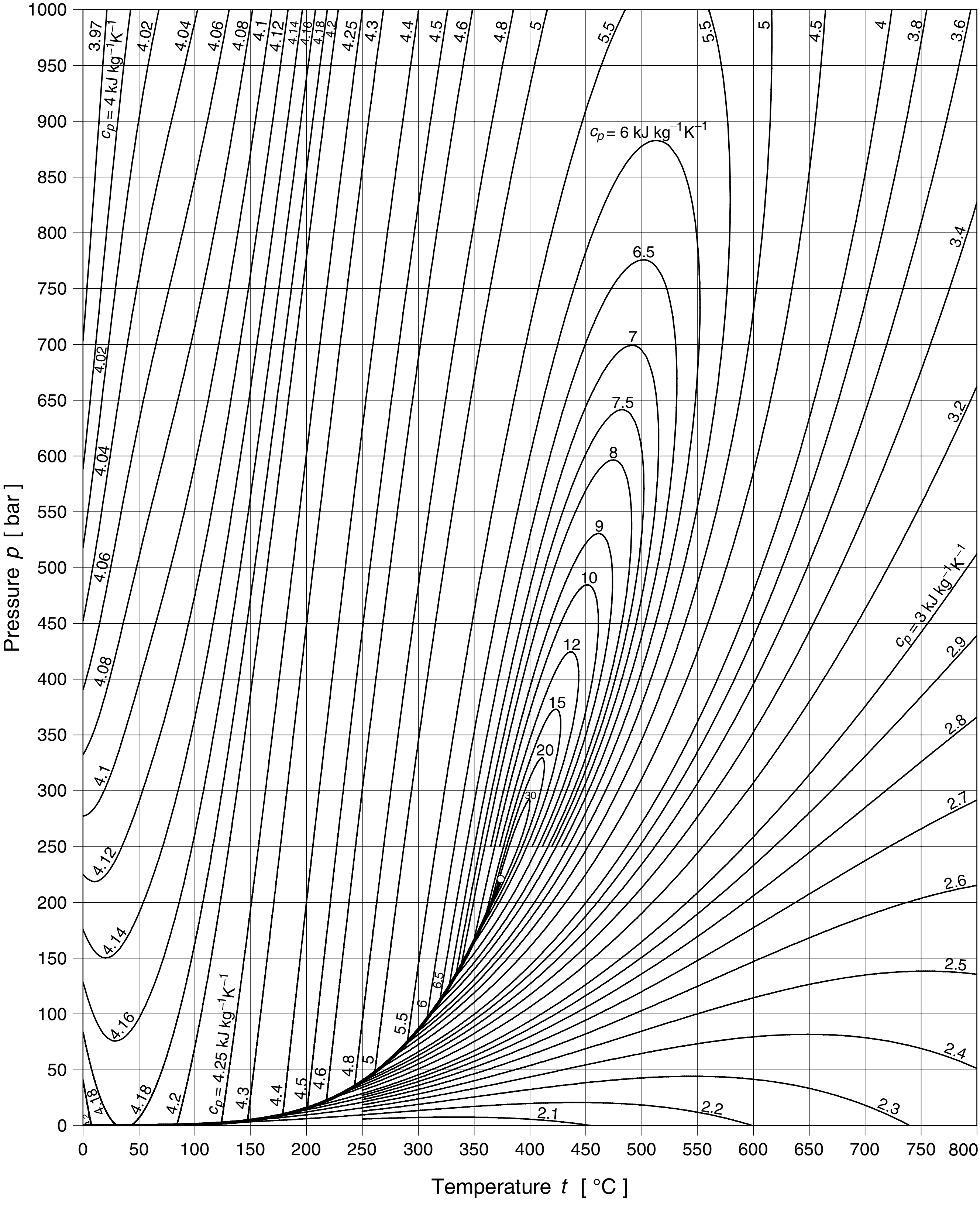

Diagr. 12 Pressure-temperature diagram with lines of constant specific isobaric heat capacity.

Specific isochoric heat capacity $c_v = \left(\frac{\partial u}{\partial T}\right)_v$ **[kJ kg^{-1} K^{-1}]**

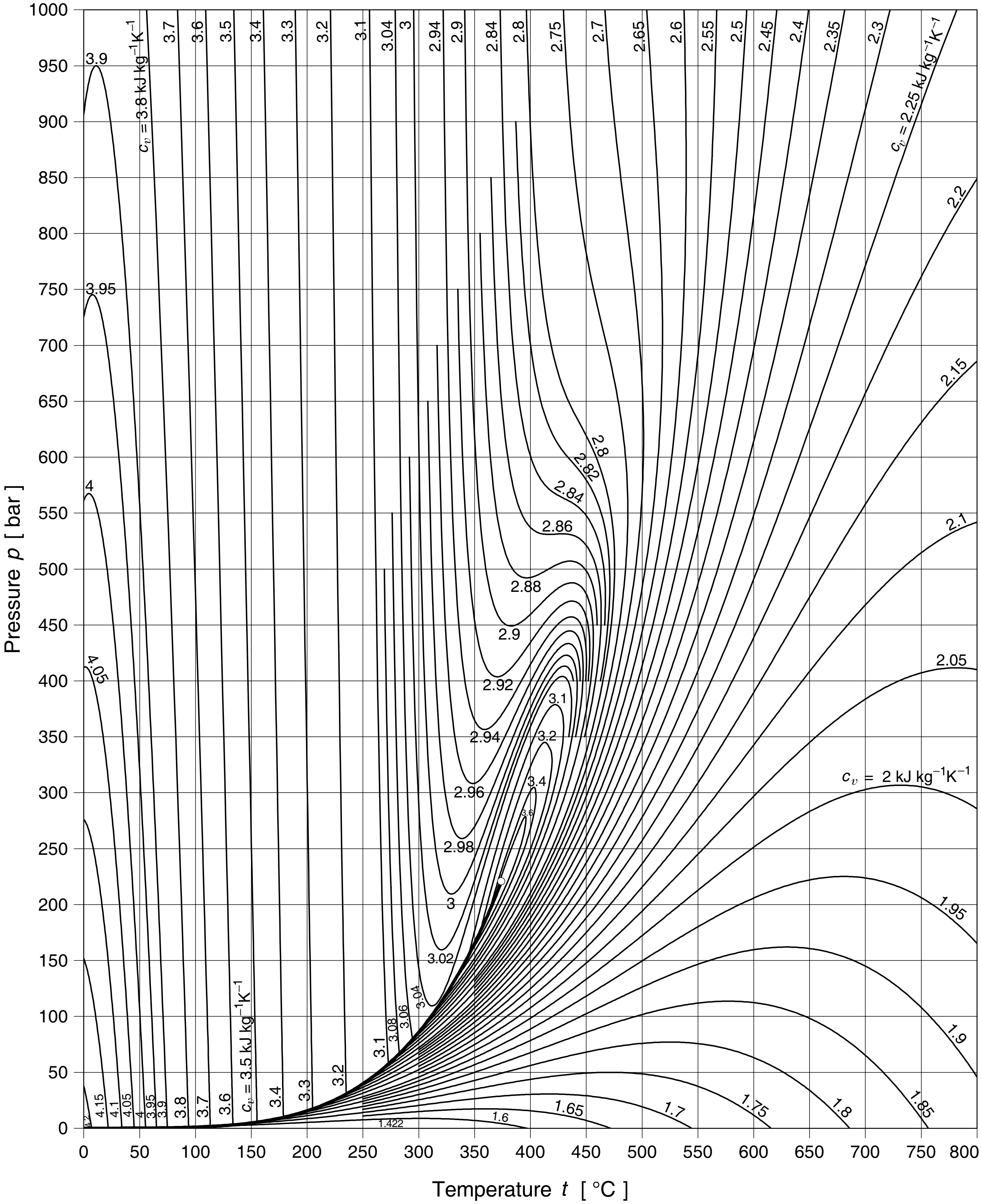

Diagr. 13 Pressure-temperature diagram with lines of constant specific isochoric heat capacity.

Speed of sound $w = v\left(-\left(\frac{\partial p}{\partial v}\right)_s\right)^{0.5}$ **[m s^{-1}]**

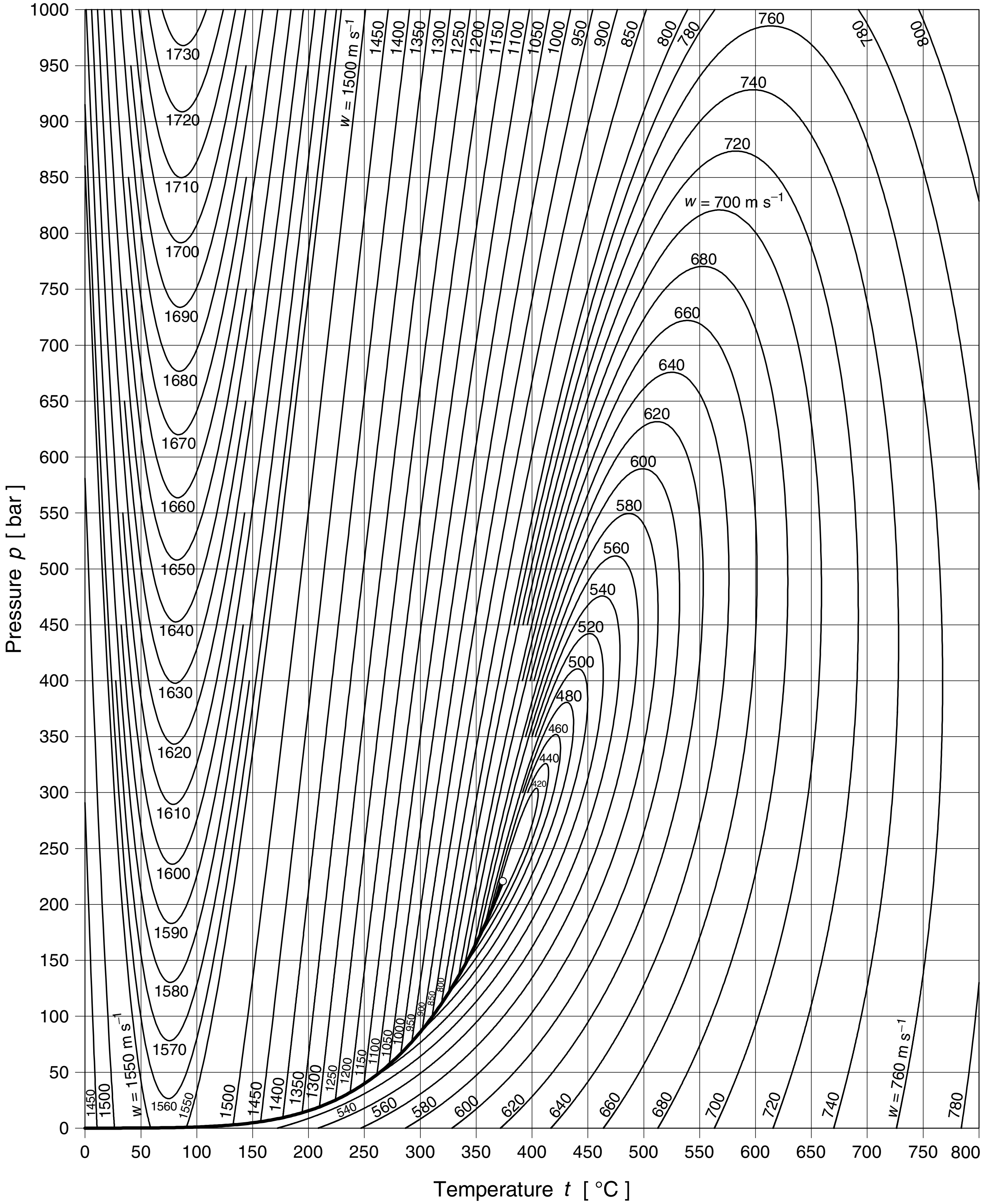

Diagr. 14 Pressure-temperature diagram with lines of constant speed of sound.

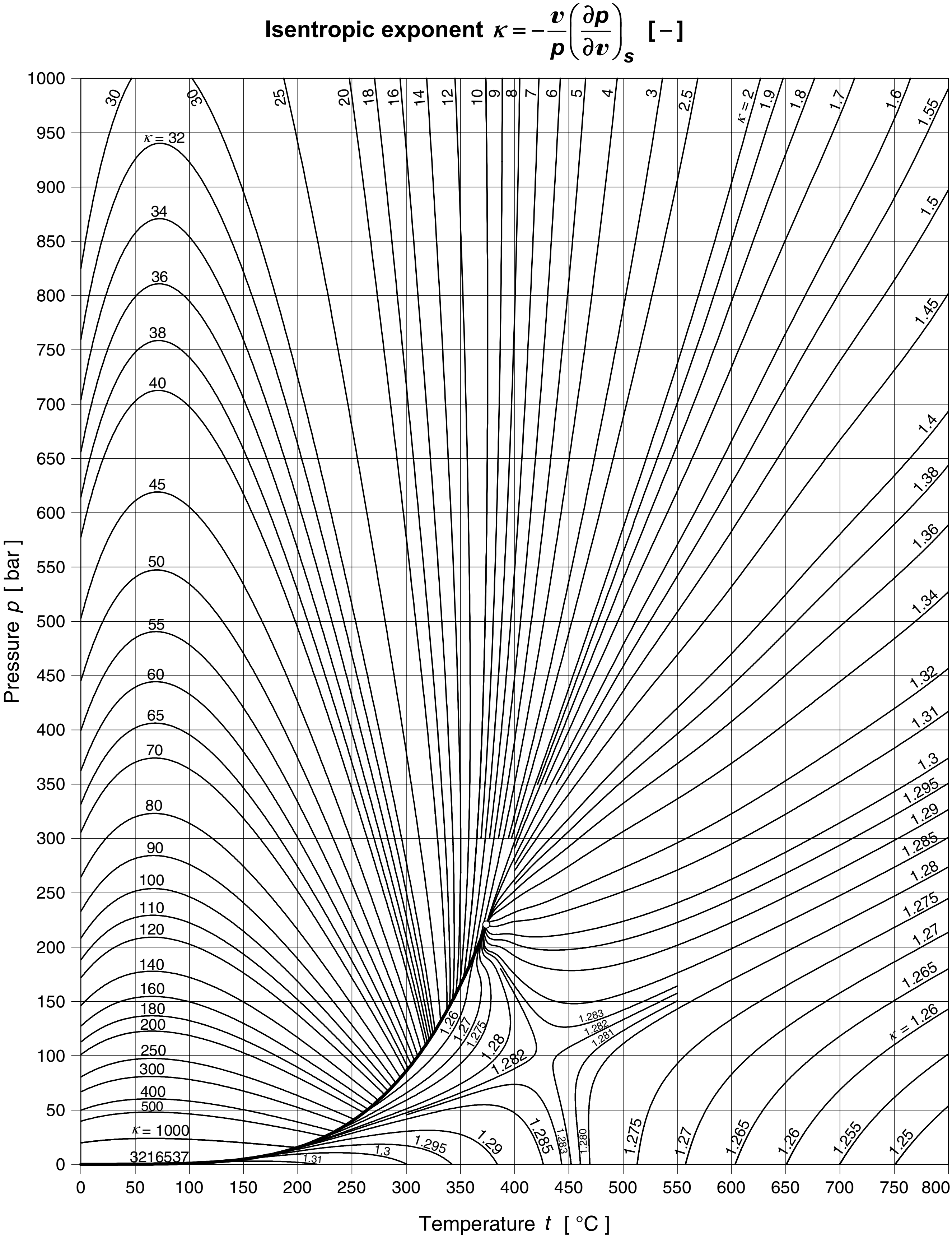

Diagr. 15 Pressure-temperature diagram with lines of constant isentropic exponent.

Isobaric cubic expansion coefficient $\alpha_v = \frac{1}{v}\left(\frac{\partial v}{\partial T}\right)_p$ [10^{-6} K^{-1}]

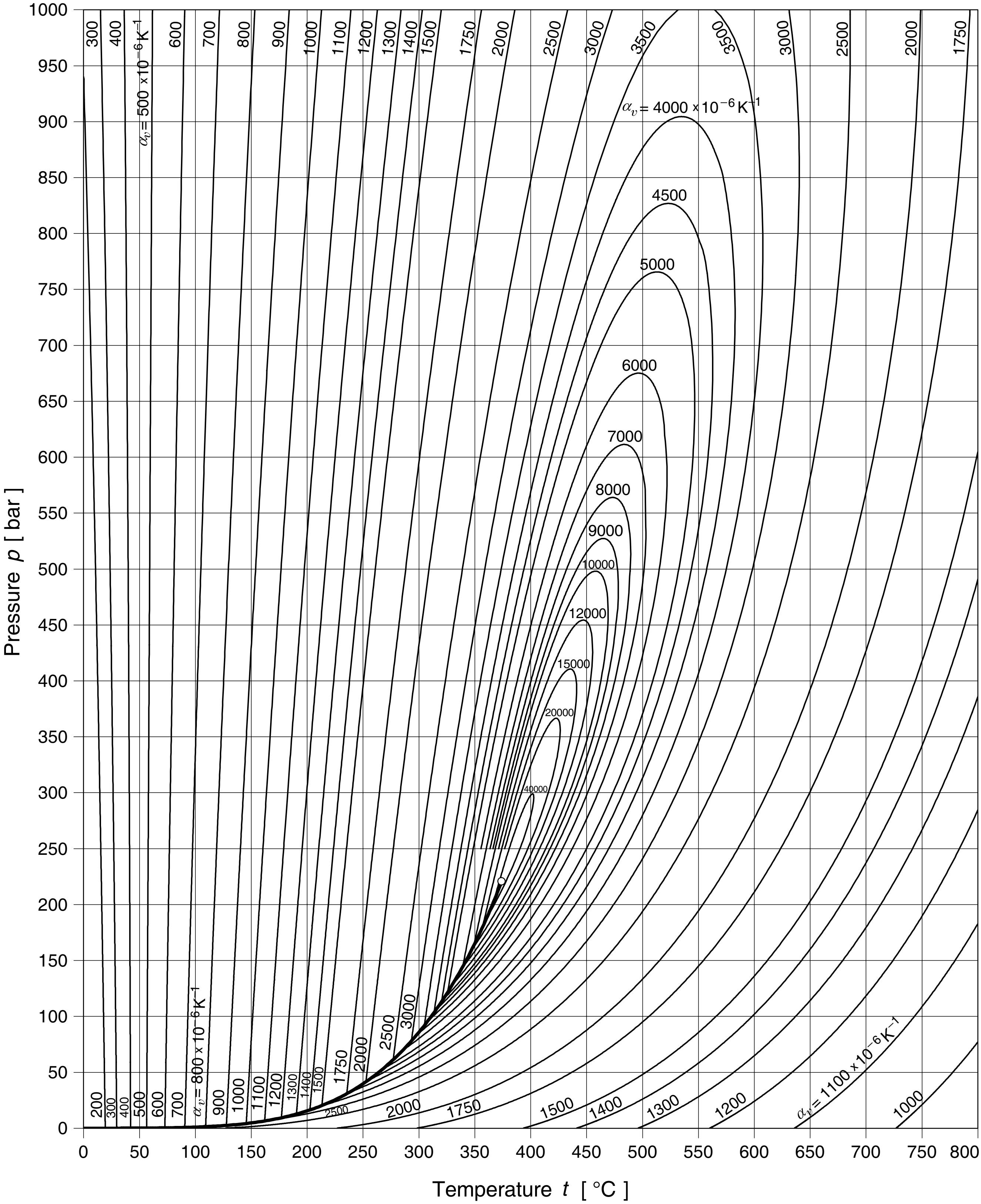

Diagr. 16 Pressure-temperature diagram with lines of const. isobaric cubic expansion coefficient.

Isothermal compressibility $\kappa_T = -\frac{1}{v}\left(\frac{\partial v}{\partial p}\right)_T$ **[10^{-6} kPa^{-1}]**

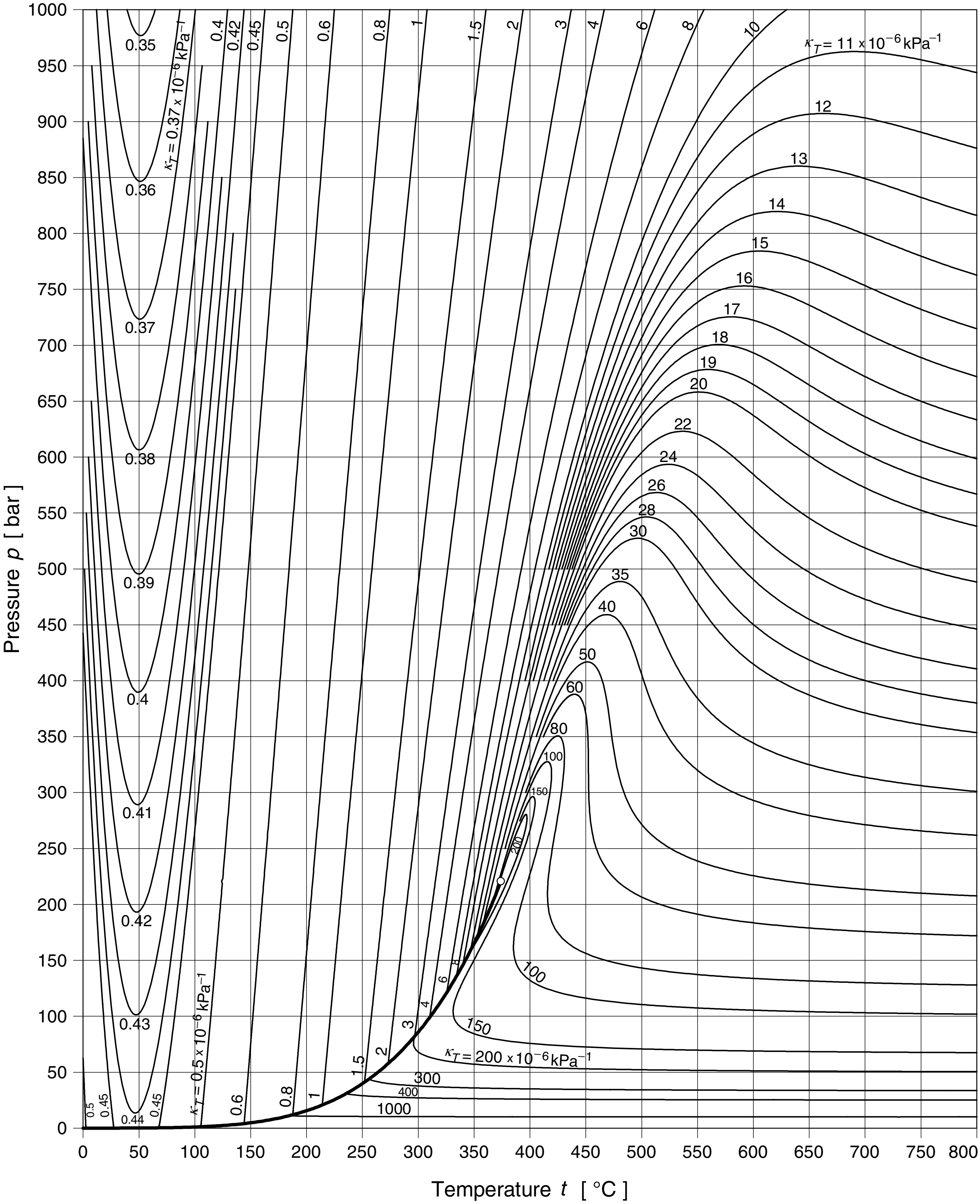

Diagr. 17 Pressure-temperature diagram with lines of constant isothermal compressibility.

Relative pressure coefficient $\alpha_p = \frac{1}{p}\left(\frac{\partial p}{\partial T}\right)_v$ [10^{-3} K^{-1}]

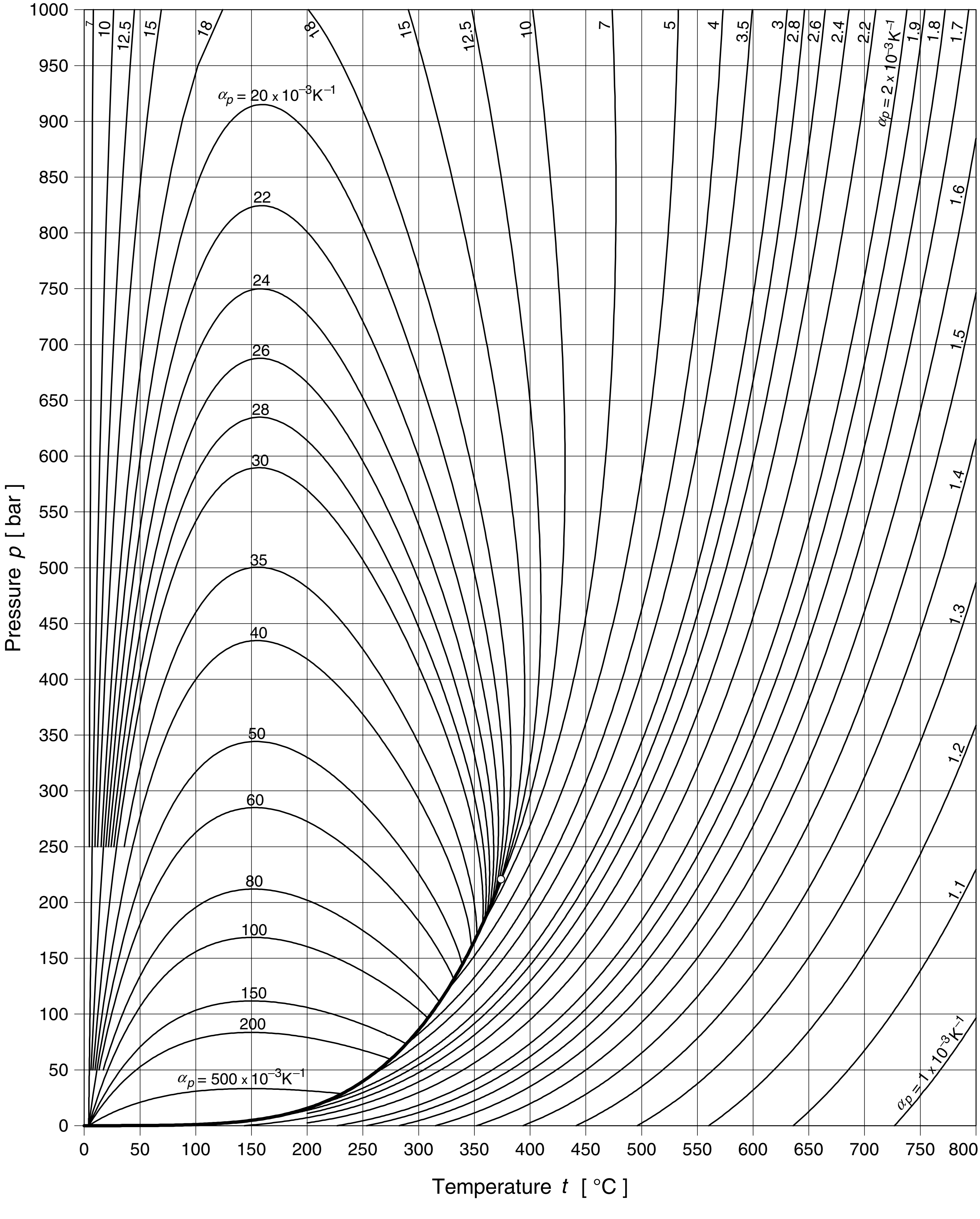

Diagr. 18 Pressure-temperature diagram with lines of constant relative pressure coefficient.

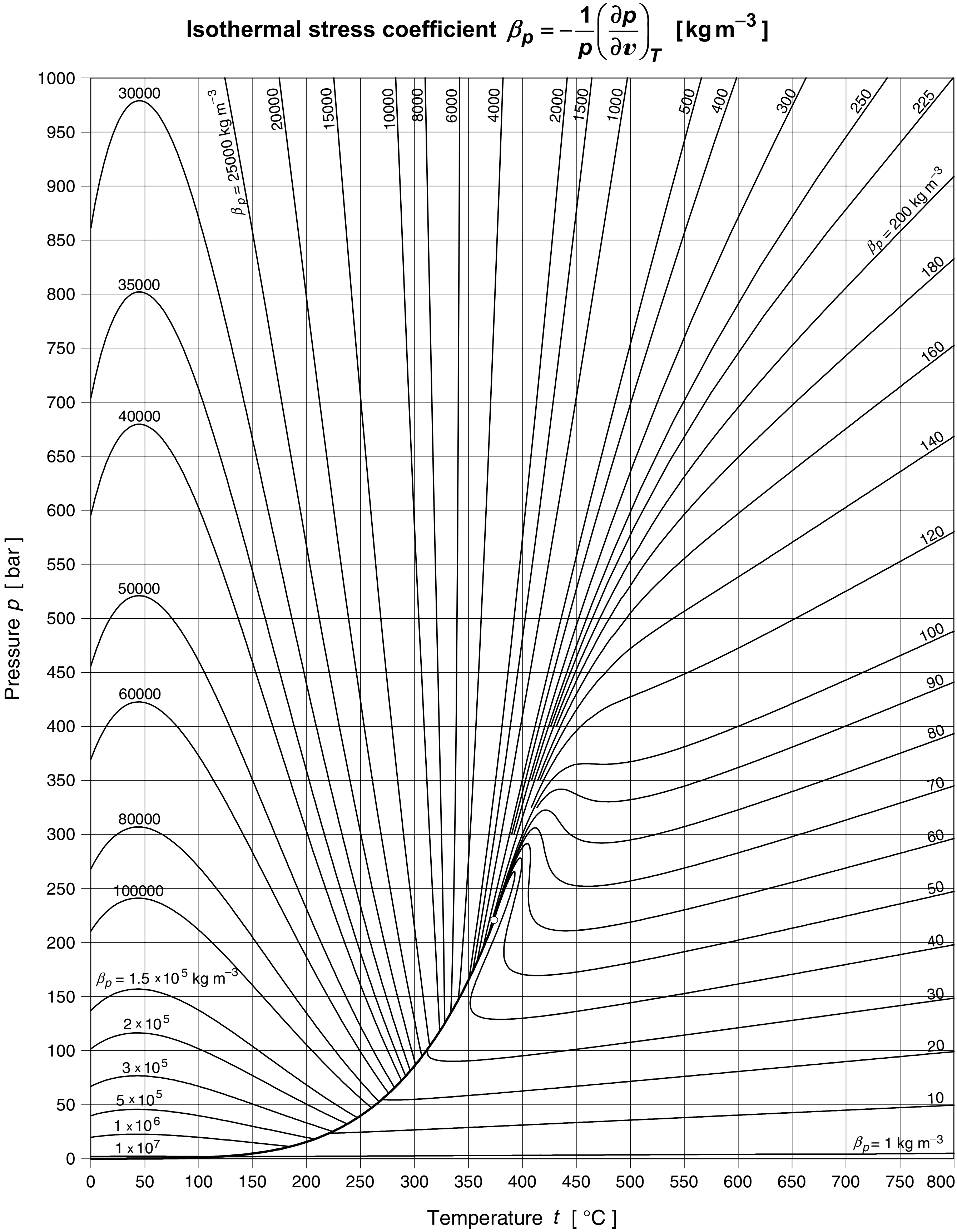

Diagr. 19 Pressure-temperature diagram with lines of constant isothermal stress coefficient.

Joule-Thomson coefficient $\mu = \left(\frac{\partial T}{\partial p}\right)_h$ **[10^{-3} K kPa^{-1}]**

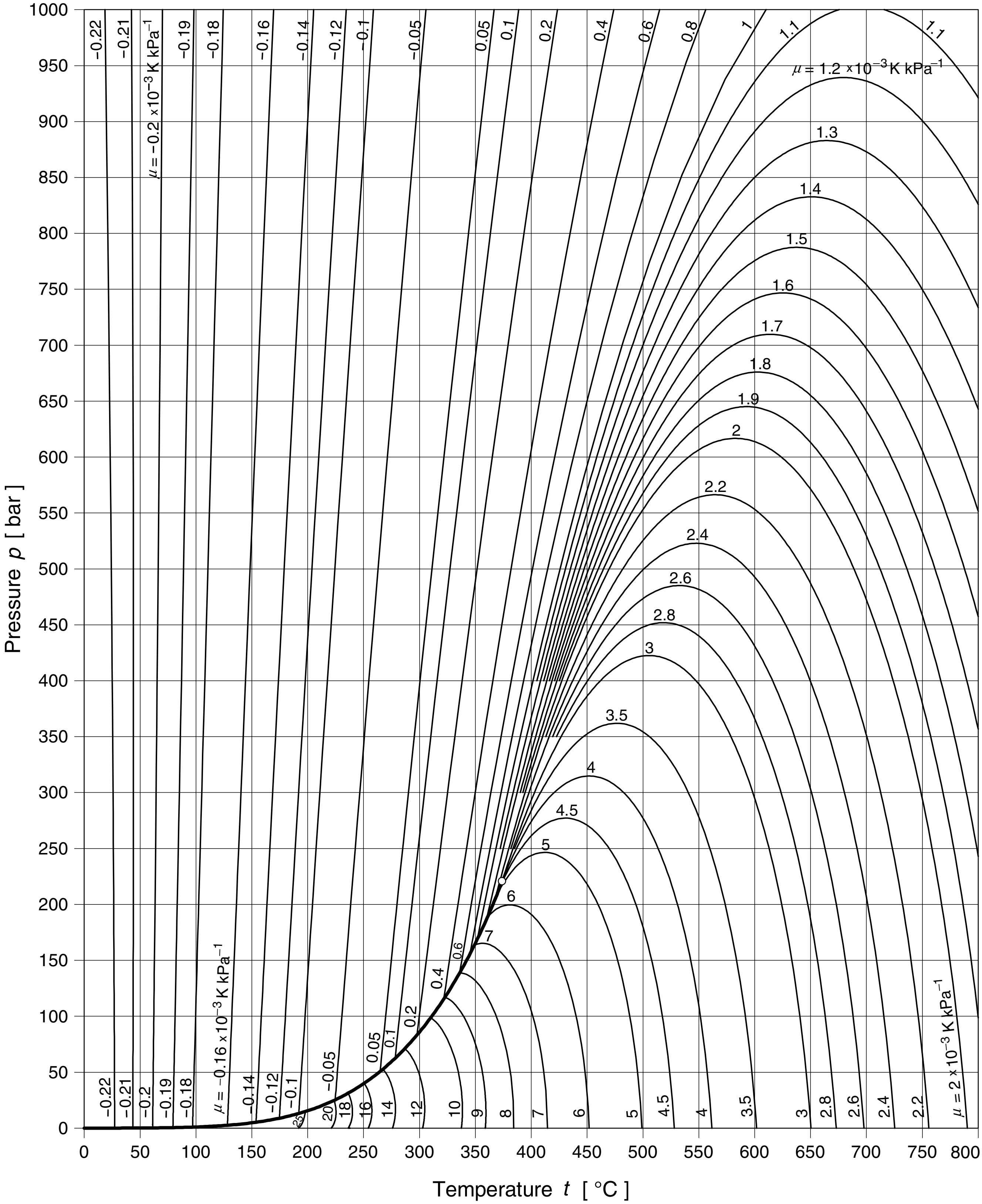

Diagr. 20 Pressure-temperature diagram with lines of constant Joule-Thomson coefficient.

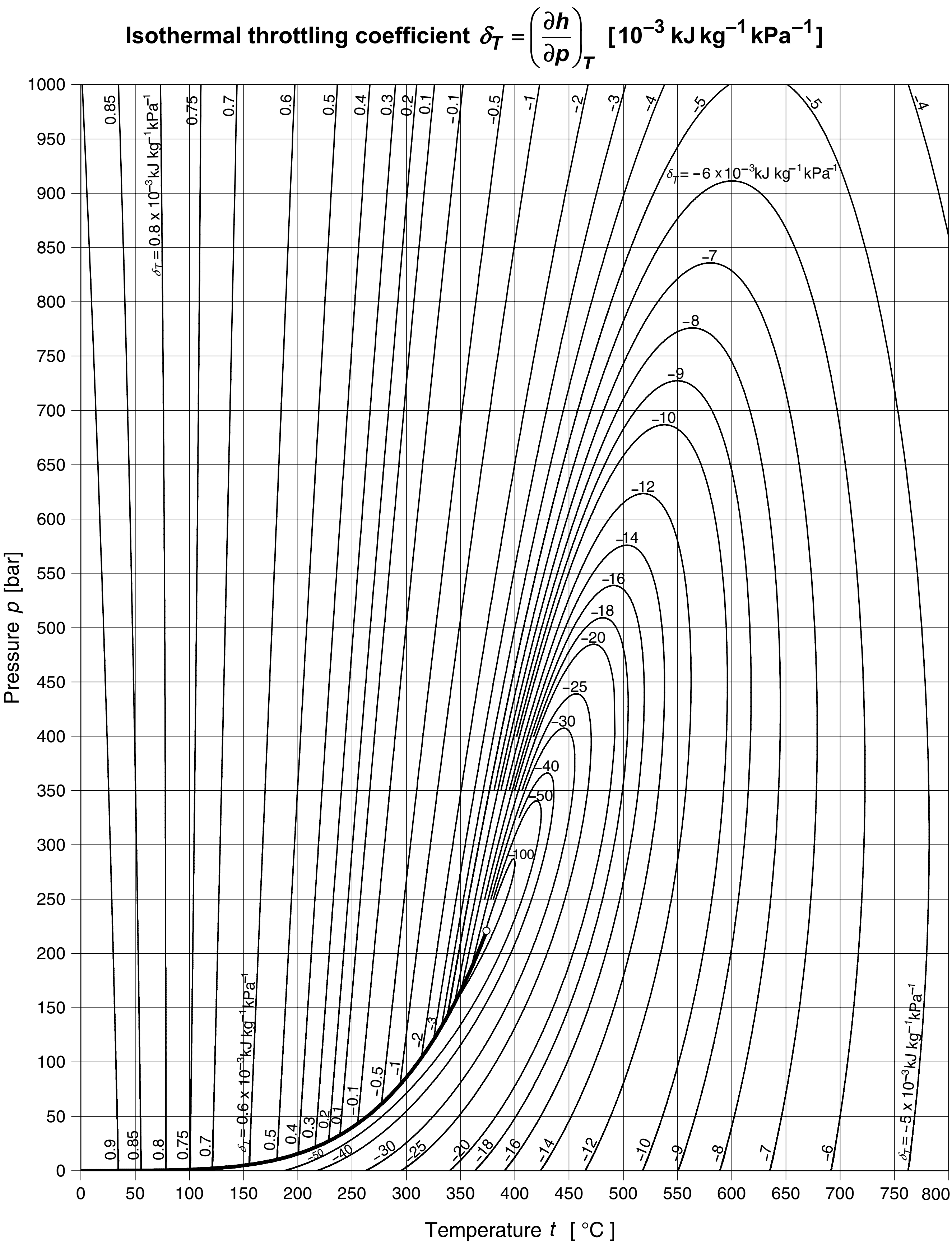

Diagr. 21 Pressure-temperature diagram with lines of constant isothermal throttling coefficient.

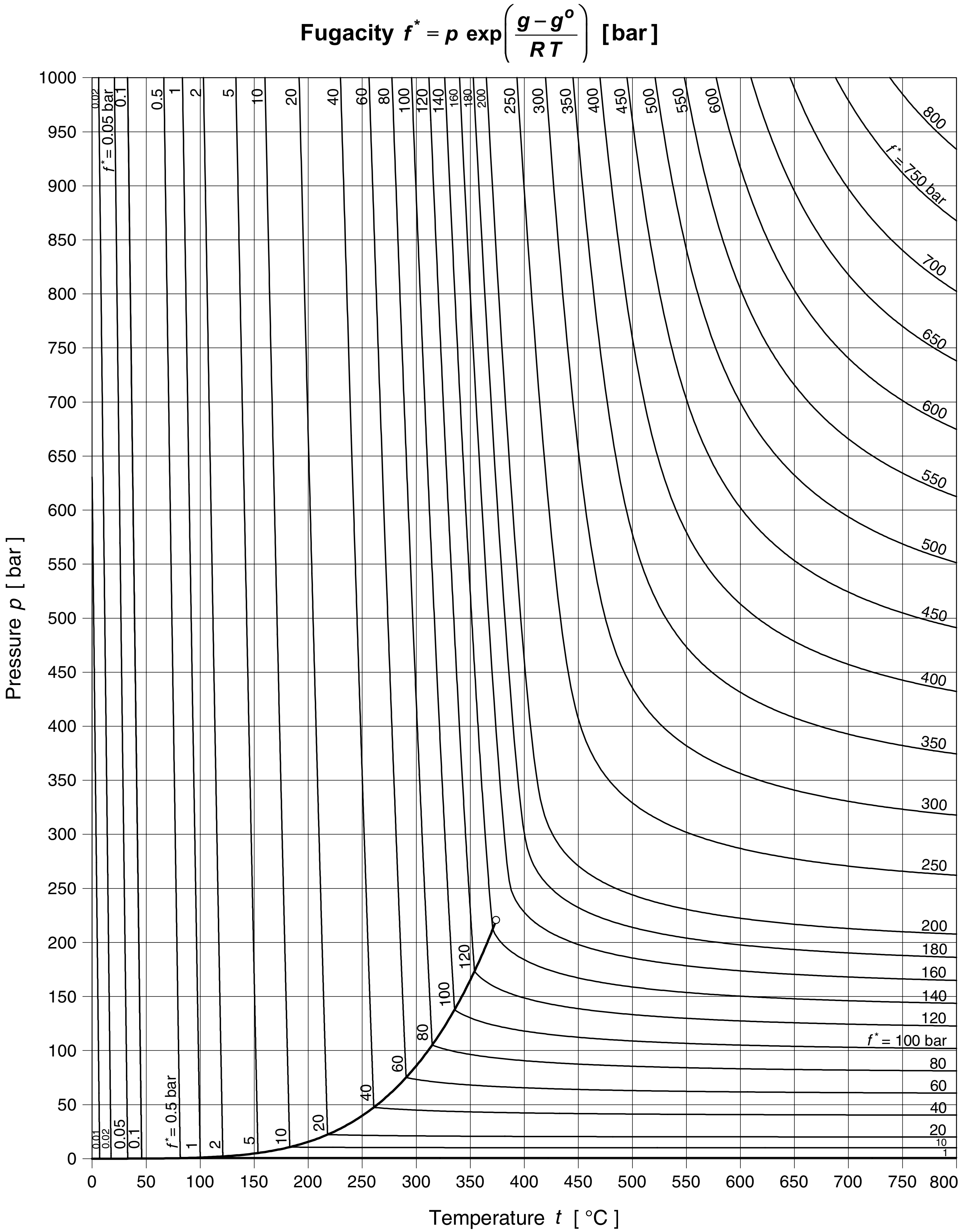

Diagr. 22 Pressure-temperature diagram with lines of constant fugacity.

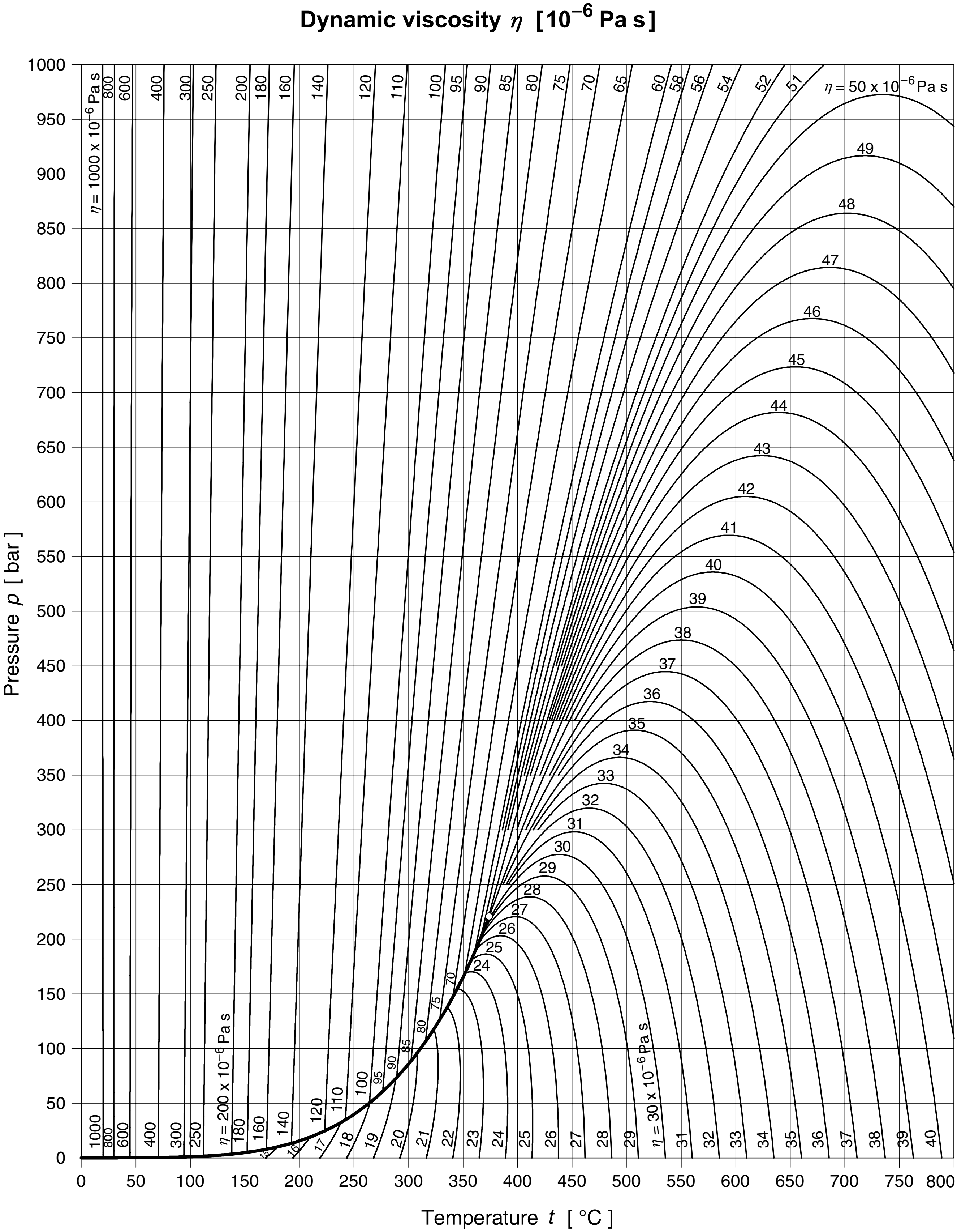

Diagr. 23 Pressure-temperature diagram with lines of constant dynamic viscosity.

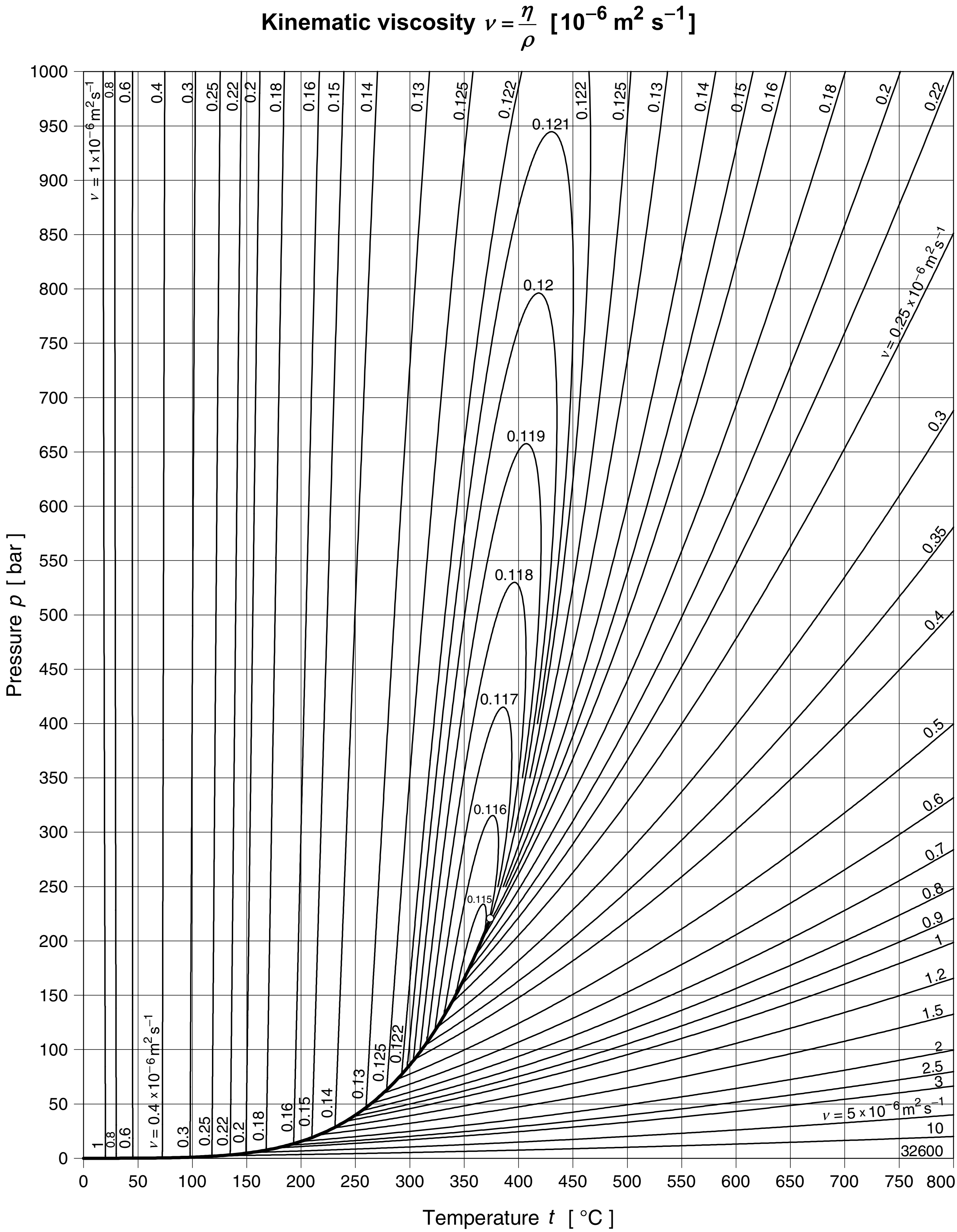

Diagr. 24 Pressure-temperature diagram with lines of constant kinematic viscosity.

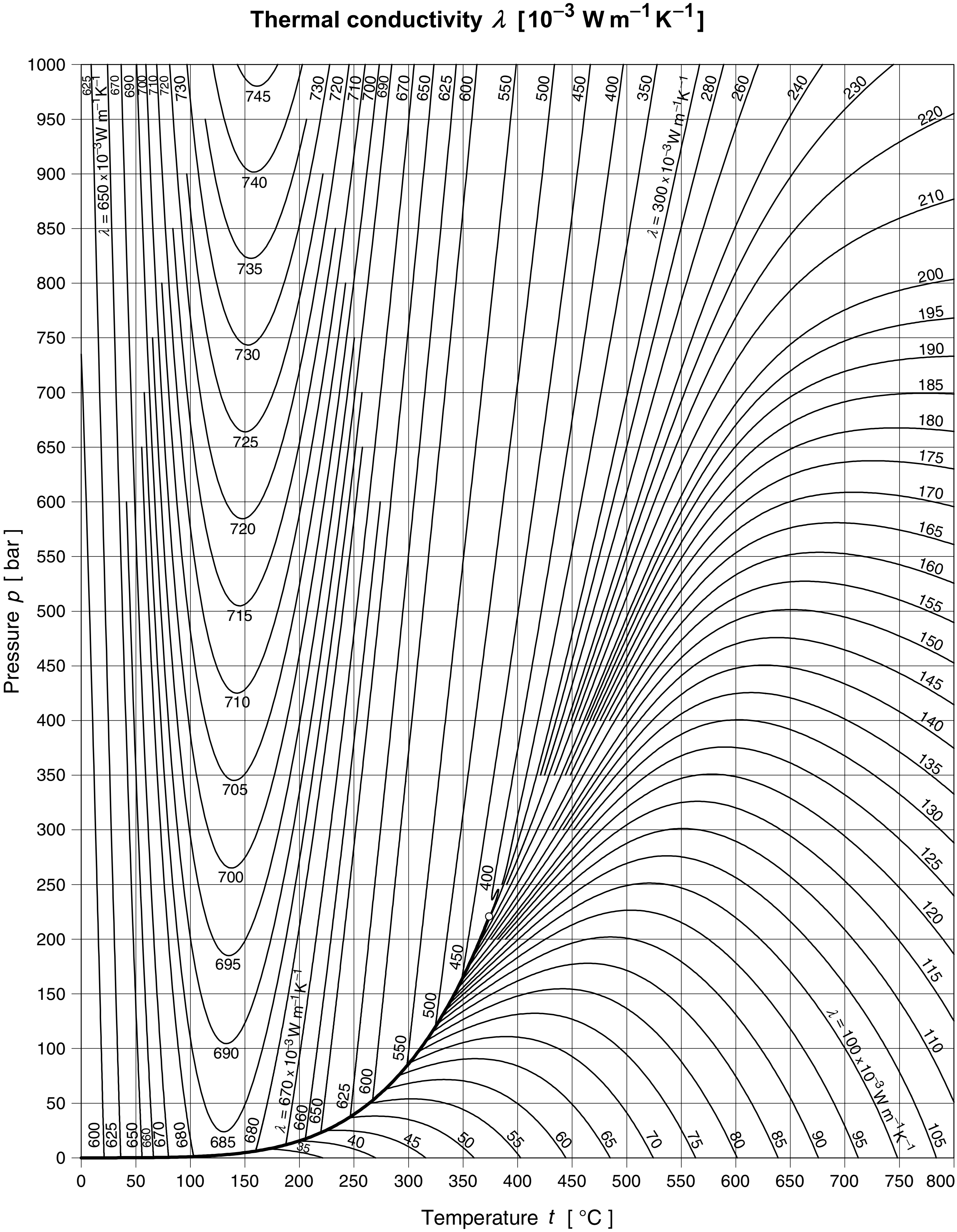

Diagr. 25 Pressure-temperature diagram with lines of constant thermal conductivity.

Prandtl number $Pr = \frac{\eta c_p}{\lambda}$ **[–]**

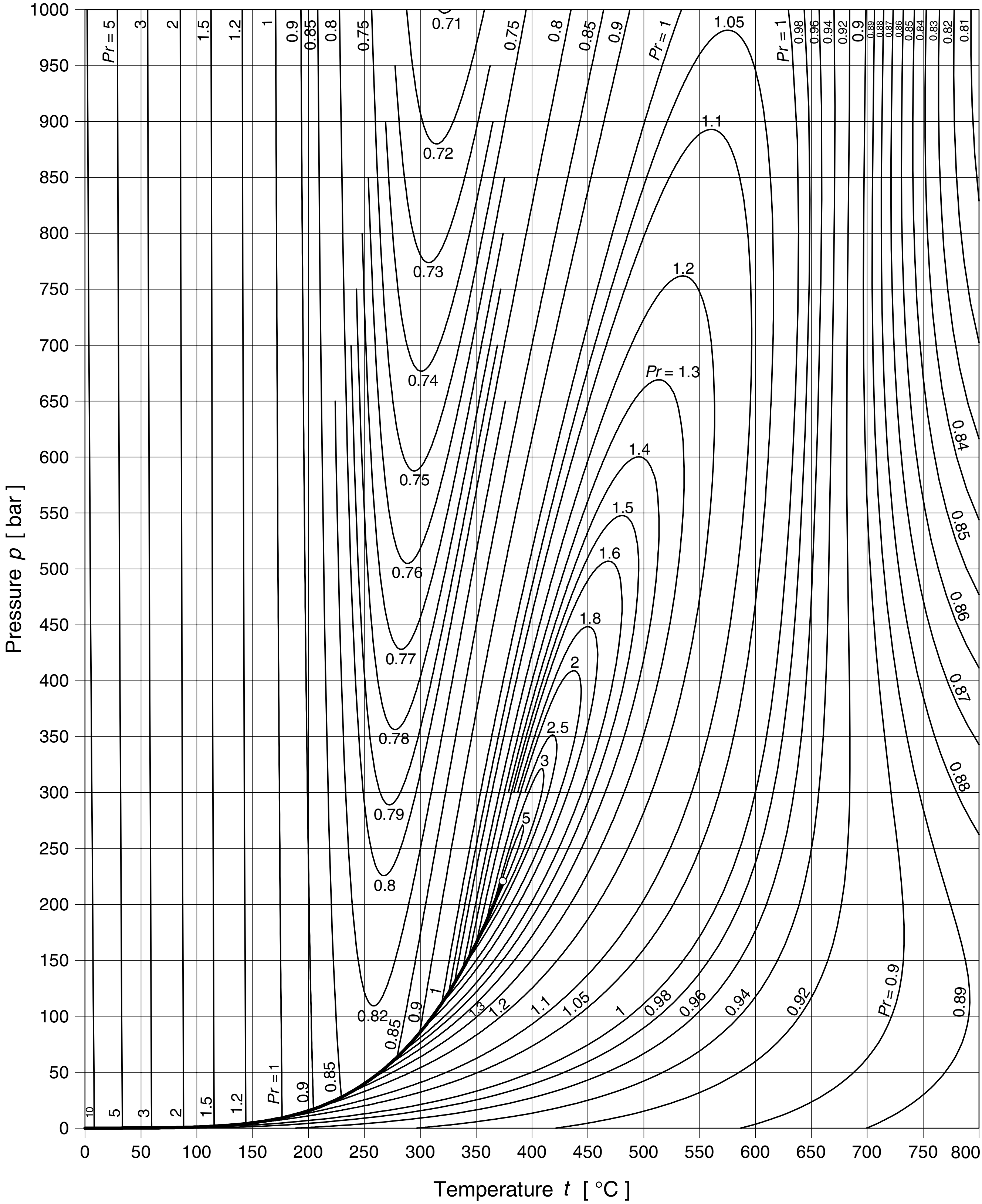

Diagr. 26 Pressure-temperature diagram with lines of constant Prandtl number.

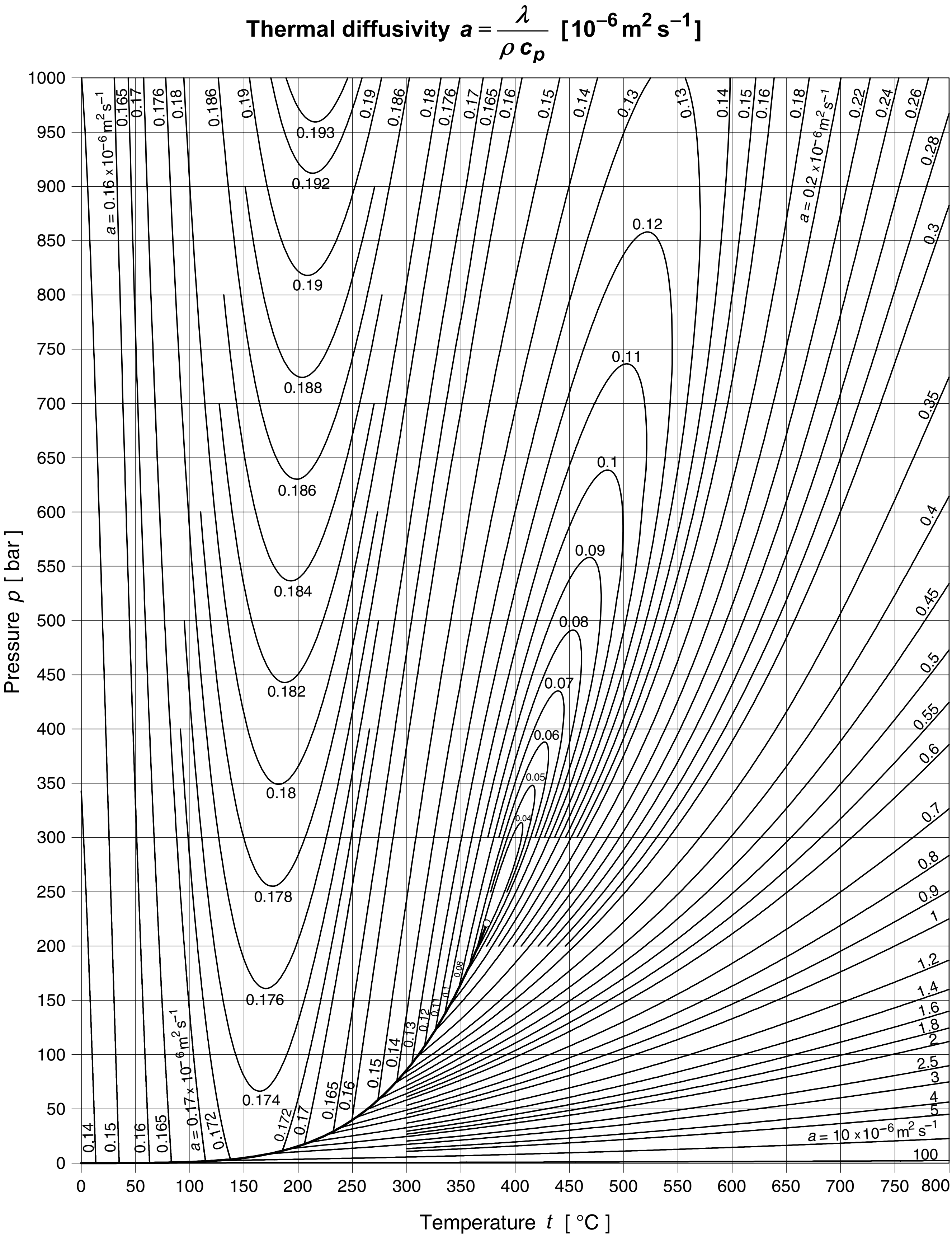

Diagr. 27 Pressure-temperature diagram with lines of constant thermal diffusivity.

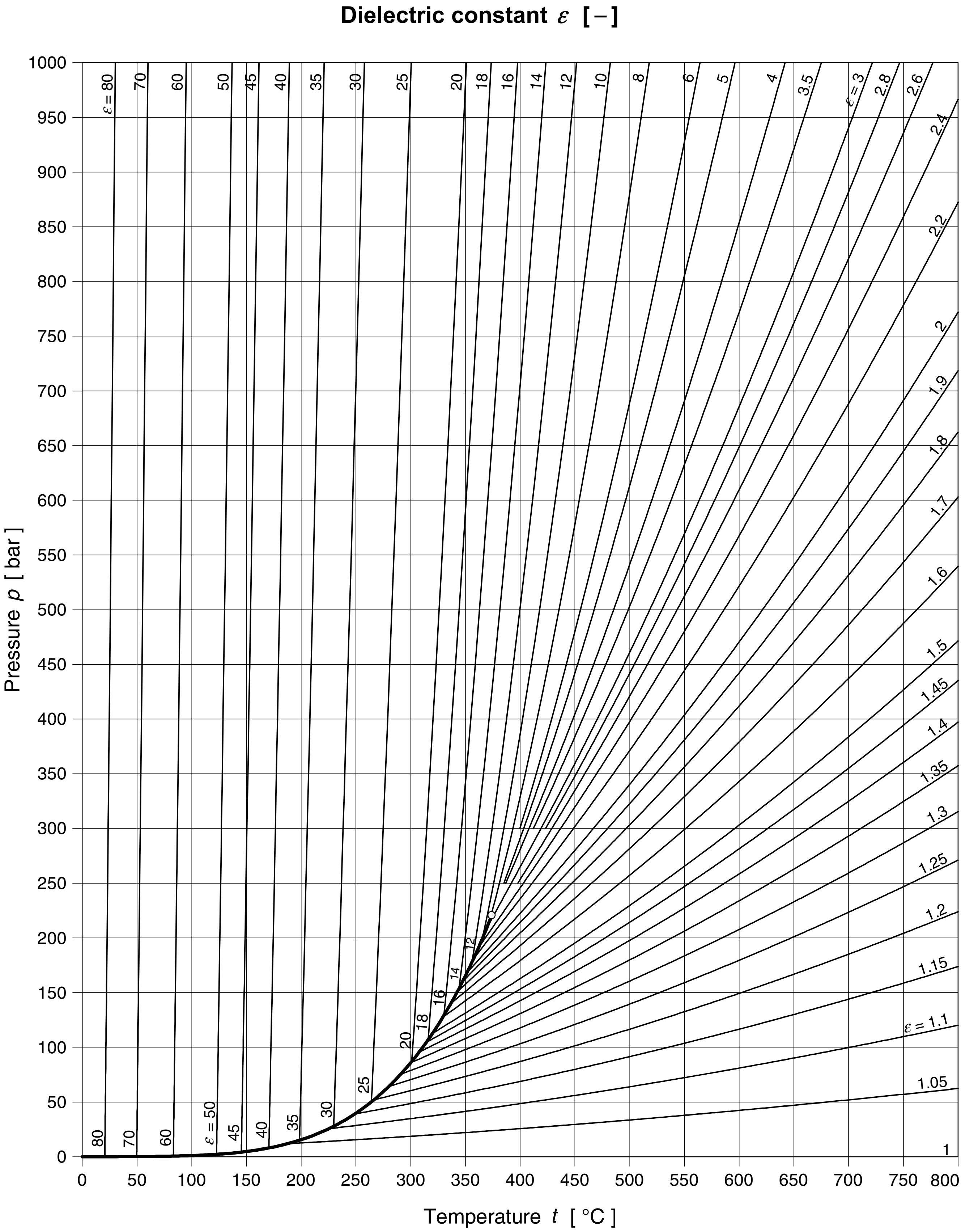

Diagr. 28 Pressure-temperature diagram with lines of constant dielectric constant.

Refractive index *n* [−] (for $\bar{\lambda} = 0.5893\ \mu m$)

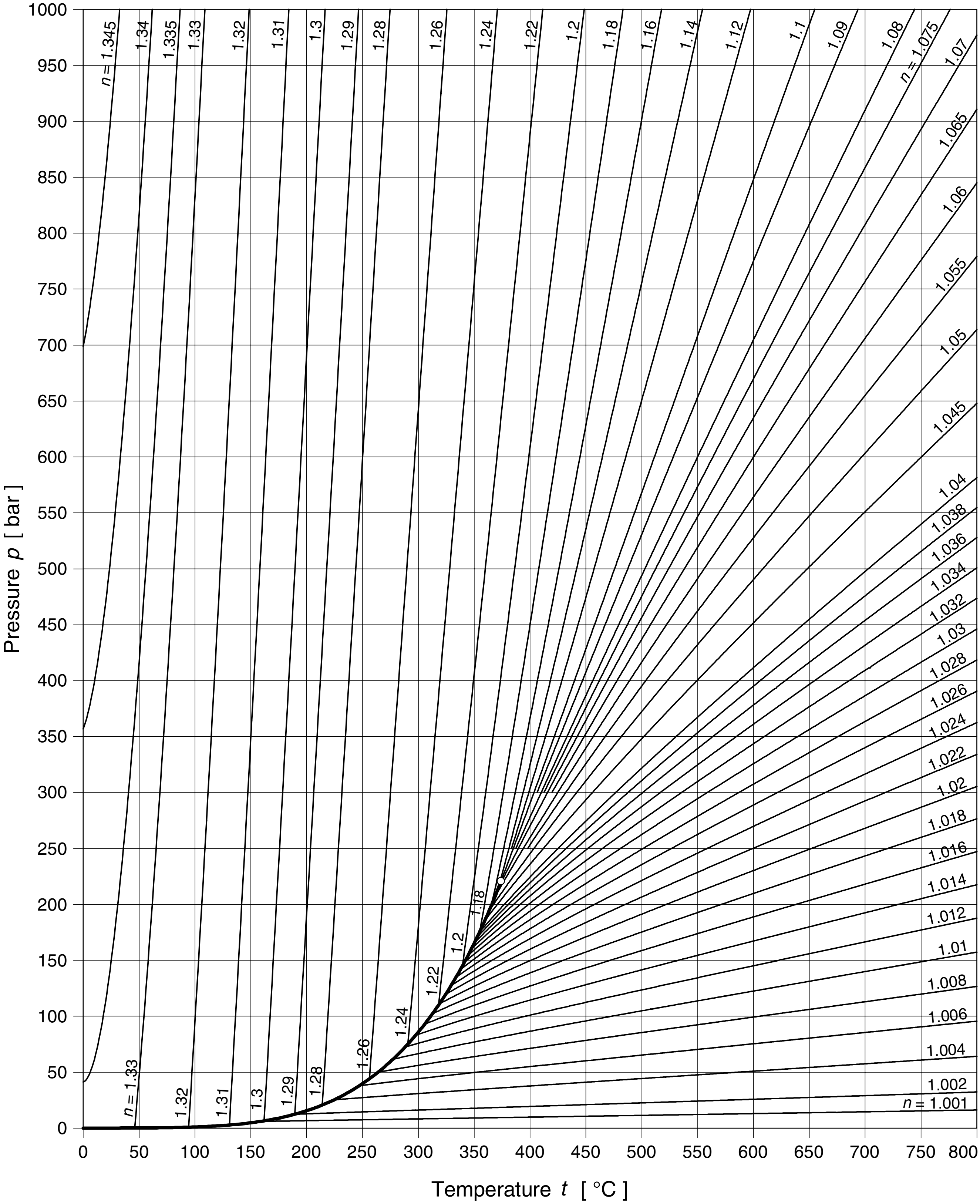

Diagr. 29 Pressure-temperature diagram with lines of constant refractive index.

Part D

IAPWS-IF97 Electronic Steam Tables on CD-ROM

1 Contents of the CD-ROM

The CD-ROM accompanying this book contains an interactive program that enables the user to calculate all of the properties for water and steam that are contained in the book. This program is called "IAPWS-IF97 Electronic Steam Tables" and has the following features:

- The properties in the single-phase region (liquid, vapour, and supercritical region) can be calculated for any value of pressure p and temperature T. In contrast, the tables in Part B only contain values with a fixed pressure-temperature grid.
- The properties on the saturated-liquid and saturated-vapour lines can be calculated for any value of temperature T or pressure p. Those properties for which it is reasonable can also be calculated *within* the two-phase region for given values of p or T and vapour fraction x. The tables in Part B contain only property values for the saturated liquid and saturated vapour at discrete temperatures or pressures.
- The properties cannot be calculated only for single points, but also along isolines, namely along isotherms, isobars, the saturated-liquid line, and the saturated-vapour line. Thus, users can produce their "personal" steam tables.
- Apart from the calculation of specific properties, the program also allows to calculate molar properties. In the book only values for specific properties are given.
- Different units can be chosen for the properties to be calculated. In addition to the units used in the book that are based on SI units, several other units, including U.S. customary units, can be selected.

2 Hardware and Software Requirements

Basically, the requirements for the use of the "IAPWS-IF97 Electronic Steam Tables" are met by a PC with a standard configuration.

The following minimum configuration is required:

- Intel Pentium, AMD Duron, or AMD Athlon processor with 500 MHz
- 256 MB RAM
- Graphics card with 800 x 600 pixels
- 50 MB free hard disc space
- Operating system: Windows 98, NT 4.0 SP 6, Windows 2000, Windows XP, Windows 2003 Server

An update for the operating system Windows Vista will be made available, see item 5 "Updates."

3 Installation

The installation of the Electronic Steam Tables should start automatically when the CD-ROM is inserted into the CD-ROM drive. If the installation program does not start after a few seconds,

the user needs to execute the file setup.exe on the CD-ROM to begin the installation. A guide will lead the user through the installation process.

A comprehensive help file included with the "IAPWS-IF97 Electronic Steam Tables" gives further information on the use of the program.

4 Details about the Calculations

This section gives details about the calculations of thermodynamic, transport, and other properties with the Electronic Steam Tables for the single-phase region, two-phase region, saturated-liquid line, saturated-vapour line, and the ideal-gas state. The calculations can be performed for single points and along isolines.

4.1 Calculable Properties

The following properties can be calculated:

- Saturation pressure p_s
- Saturation temperature T_s
- Specific volume v
- Density ρ
- Compression factor (real-gas factor) $z = pv/(RT)$
- Specific enthalpy h
- Specific internal energy u
- Specific entropy s
- Specific Gibbs free energy g
- Specific Helmholtz free energy f
- Specific isobaric heat capacity c_p
- Mean specific isobaric heat capacity $c_{p,\mathrm{m}}^{\mathrm{o}}$ in the ideal-gas state
- Specific isochoric heat capacity c_v
- Speed of sound w
- Isentropic exponent κ
- Isobaric cubic expansion coefficient $\alpha_v = v^{-1}(\partial v/\partial T)_p$
- Isothermal compressibility $\kappa_T = -v^{-1}(\partial v/\partial p)_T$
- Relative pressure coefficient $\alpha_p = p^{-1}(\partial p/\partial T)_v$
- Isothermal stress coefficient $\beta_p = -p^{-1}(\partial p/\partial v)_T$
- Joule-Thomson coefficient $\mu = (\partial T/\partial p)_h$
- Isothermal throttling coefficient $\delta_T = (\partial h/\partial p)_T$
- Fugacity f^*
- Dynamic viscosity η
- Kinematic viscosity $\nu = \eta\rho^{-1}$
- Thermal conductivity λ
- Prandtl number $Pr = \eta c_p \lambda^{-1}$
- Thermal diffusivity $a = \lambda/(\rho c_p)$
- Dielectric constant ε

- Refractive index n
- Surface tension σ (only in the saturation state)

The specific properties v, h, u, s, g, f, c_p, $c_{p,\mathrm{m}}$, c_v, and the mass-based density ρ can also be calculated as molar properties.

In addition, the number of the region where the given state point is located (liquid region 1, vapour region 2, critical and supercritical region 3, two-phase region 4, or high-temperature region 5) is displayed.

4.2 Calculations in the Single-Phase Region

In the single-phase region (in the program "Range of state: Single-phase region"), properties can be calculated for given values of pressure and temperature (p, T).

The thermodynamic properties v, ρ, z, h, u, s, g, f, c_p, c_v, w, κ, α_v, κ_T, α_p, β_p, μ, δ_T, and f^* can be calculated within the range of validity of IAPWS-IF97, i.e. within

$$\begin{array}{rl} 0 < p \leq \ \ 500 \text{ bar} & 0\ °\mathrm{C} \leq t \leq 2000\ °\mathrm{C} \\ 500 \text{ bar} < p \leq 1000 \text{ bar} & 0\ °\mathrm{C} \leq t \leq \ \ 800\ °\mathrm{C}. \end{array}$$

Values can be calculated for the dynamic viscosity η and kinematic viscosity v in the range

$$\begin{array}{rl} 0 < p \leq \ \ 500 \text{ bar} & 0\ °\mathrm{C} \leq t \leq 1000\ °\mathrm{C} \\ 500 \text{ bar} < p \leq 1000 \text{ bar} & 0\ °\mathrm{C} \leq t \leq \ \ 800\ °\mathrm{C}, \end{array}$$

and for the thermal conductivity λ, Prandtl number Pr, and thermal diffusivity a in the range

$$0 < p \leq 1000 \text{ bar} \qquad 0\ °\mathrm{C} \leq t \leq \ \ 800\ °\mathrm{C}.$$

Values can be determined for the dielectric constant ε in the range

$$\begin{array}{rl} 0 < p \leq \ \ 500 \text{ bar} & 0\ °\mathrm{C} \leq t \leq \ \ 926.85\ °\mathrm{C} \\ 500 \text{ bar} < p \leq 1000 \text{ bar} & 0\ °\mathrm{C} \leq t \leq \ \ 800\ °\mathrm{C}, \end{array}$$

and for the refractive index n in the range

$$\begin{array}{c} 0 < p \leq 1000 \text{ bar} \qquad 0\ °\mathrm{C} \leq t \leq \ \ 500\ °\mathrm{C} \\ 0.2\ \mu\mathrm{m} \leq \bar{\lambda} \leq 1.1\ \mu\mathrm{m}. \end{array}$$

The thermodynamic properties v, ρ, z, h, u, s, g, f, c_p, c_v, w, κ, α_v, κ_T, α_p, β_p, μ, δ_T, and f^* are calculated from the IAPWS-IF97 basic equations, Eqs. (2.3), (2.6), (2.11), or (2.15), given in Sec. 2.2. The transport properties η and λ are determined from the equations for industrial applications, Eq. (3.1), and industrial use, Eq. (3.4), given in Secs. 3.1 and 3.2. The calculation of the quantities c_p, ρ, η, and λ needed for determining the properties v, Pr, and a is performed with the equations mentioned above. The properties ε and n are determined from Eqs. (3.9) and (3.10) given in Secs. 3.4 and 3.5. For the calculation of n, the wavelength of light, which is marked with λ^* in the program, is needed as a further input value. The density ρ required in all of these equations is calculated from the IAPWS-IF97 basic equations, see above.

When calculating properties in the single-phase region, the saturation properties are automatically calculated as well, namely p_s, v', and v'' for given values of t (if $0\ °\mathrm{C} \leq t \leq t_\mathrm{c} = 373.946\ °\mathrm{C}$), and t_s for given values for p (if $0.006\,112\,127 \leq p \leq p_\mathrm{c} = 220.64$ bar). The procedure used to determine these properties is described in the next section.

All of these properties can be calculated for single points or along isolines, namely along isobars and isotherms.

Directly at the critical point some properties are not calculated, because IAPWS-IF97 does not yield physically meaningful values for these properties at this point.

4.3 Calculations in the Two-Phase Region

In the two-phase region (in the program "Range of state: Two-phase region"), the properties can be calculated for input values of vapour fraction x ($0 \le x \le 1$) and either temperature T or pressure p. The calculations can be carried out over the entire two-phase region, defined by the ranges of temperature and vapour fraction

$$0\ \text{°C} \le t \le 373.946\ \text{°C} \qquad 0 \le x \le 1,$$

or by the ranges of pressure and vapour fraction

$$0.006\,112\,126\,77\ \text{bar} \le p \le 220.64\ \text{bar} \qquad 0 \le x \le 1.$$

For given temperatures, the saturation pressures p_s are calculated from the IAPWS-IF97 saturation-pressure equation, Eq. (2.13).

For temperatures $t \le 350$ °C and input values for t and p_s, all of the thermodynamic properties on the saturated-liquid and saturated-vapour lines are determined from the basic equations for regions 1 and 2, Eqs. (2.3) and (2.6), given in Sec. 2.2.

For $t > 350$ °C and input values for t and p_s, the densities ρ' and ρ'' (and thus also the specific volumes v' and v'') are calculated by iterating the basic equation for region 3, Eq. (2.11). With the values for (ρ', t) and (ρ'', t), the other thermodynamic properties are determined from the basic equation, Eq. (2.11).

For given pressures, the saturation temperatures t_s are calculated from the IAPWS-IF97 saturation-temperature equation, Eq. (2.14).

For pressures $p \le 165.292$ bar and input values for p and t_s, the properties on the saturated-liquid and saturated-vapour lines are determined from the basic equations for regions 1 and 2, Eqs. (2.3) and (2.6).

For $p > 165.292$ bar and input values for p and t_s, the densities ρ' and ρ'' (and thus also the specific volumes v' and v'') are calculated by iterating the basic equation for region 3, Eq. (2.11). With the values for (ρ', t_s) and (ρ'', t_s), the other thermodynamic properties are determined from the basic equation, Eq. (2.11).

The transport properties η and λ are determined from the equations for industrial applications, Eq. (3.1), and industrial use, Eq. (3.4), given in Secs. 3.1 and 3.2. For determining the properties ν, Pr, and a, apart from η and λ, the thermodynamic properties c_p and ρ are needed and are calculated from the IAPWS-IF97 basic equations as described above. The properties ε and n are determined from Eqs. (3.9) and (3.10) given in Secs. 3.4 and 3.5. For the calculation of n, the wavelength of light, which is marked with λ^* in the program, is needed as a further input value. The density ρ required in Eqs. (3.1), (3.4), (3.9), and (3.10) is calculated from the IAPWS-IF97 basic equations, see above.

The calculation of the surface tension σ is based on Eq. (3.8) given in Sec. 3.3.

The values of the thermodynamic properties *within* the two-phase region ($0 < x < 1$) are calculated from the relation $y = y' + x(y'' - y')$, where y stands for v, h, u, s, g, and f. The values on the saturated-liquid and saturated-vapour line are calculated as described above.

The values for the properties z, c_p, c_v, w, κ, α_v, κ_T, α_p, β_p, μ, δ_T, f^*, η, ν, λ, Pr, a, ε, and n can only be calculated for the saturated liquid ($x = 0$, superscript $'$) and for the saturated vapour ($x = 1$, superscript $''$), because they are not defined or not reasonable *within* the two-phase region.

Directly at the critical point some properties are not calculated, because IAPWS-IF97 does not yield physically meaningful values for these properties at this point.

4.4 Calculations Along the Saturated-Liquid and Saturated-Vapour Lines

Along the saturated-liquid line (in the program "Range of state: Saturated-liquid line") and the saturated-vapour line (in the Electronic Steam Tables "Range of state: Saturated-vapour line"), all of the properties listed in Sec. 4.1 can be calculated for the input values of temperature or pressure. These calculations are performed in the same manner as described in Sec. 4.3 for the saturated liquid (properties marked by a single prime) and the saturated vapour (properties marked by a double prime). Here, however, the properties are not marked by any prime, because it is clear for which branch of the phase boundary the calculations are performed.

In contrast to the calculations for the two-phase region, here calculations cannot be performed only for single points, but in the modus "Isolines" also along the entire saturated-liquid or the saturated-vapour line.

Directly at the critical point some properties are not calculated, because IAPWS-IF97 does not yield physically meaningful values for these properties at this point.

4.5 Calculations in the Ideal-Gas State

In the ideal-gas state (in the program "Range of state: Ideal-gas state"), the thermodynamic properties v^o, ρ^o, h^o, s^o, u^o, c_p^o, c_v^o, w^o, κ^o, and $c_{p,\mathrm{m}}^\mathrm{o}$ can be calculated for pressures and temperatures within the range of validity of IAPWS-IF97, see Sec. 4.2 of this Part D.

Except for the specific volume v^o, density ρ^o, and specific entropy s^o, all the other ideal-gas properties are a function of temperature only. The calculation of v^o, ρ^o, and s^o requires, in addition to temperature, input values for pressure as well.

The properties mentioned above are calculated from Eq. (2.7) for temperatures $0\ °\mathrm{C} \le t \le 800\ °\mathrm{C}$, and from Eq. (2.16) for temperatures $800\ °\mathrm{C} < t \le 2000\ °\mathrm{C}$.

The mean specific isobaric heat capacity $c_{p,\mathrm{m}}^\mathrm{o}$ between the reference temperature $t_0 = 0\ °\mathrm{C}$ and the temperature t of the given state point is defined and calculated by the relation

$$c_{p,\mathrm{m}}^\mathrm{o} = c_p^\mathrm{o}\Big|_{t_0}^{t} = \frac{1}{t - t_0}\int_{T_0}^{T} c_p^\mathrm{o}(T)\,\mathrm{d}T\,.$$

The values for the specific enthalpy h^o, the specific entropy s^o, and the mean specific isobaric heat capacity $c_{p,\mathrm{m}}^\mathrm{o}$ relate to the reference temperature $t_0 = 0\ °\mathrm{C}$, and for s^o, in addition, to the reference pressure $p_0 = 0.006\,112\,127$ bar. The reference values for $h^\mathrm{o}(t_0)$ and $s^\mathrm{o}(p_0, t_0)$ are in

accordance with the zero points of the specific internal energy and specific entropy given by Eq. (2.4).

4.6 Units

The program "IAPWS-IF97 Electronic Steam Tables" allows the use of different units for all of the properties. There are three versions of default settings for the units: "Units used in the book," "SI units," (International System of Units) and "U.S. customary units." The only difference between the "Units used in the book" and the "SI units" are the use of °C for temperature and bar for pressure, instead of K and MPa. Table D1 shows for the various properties the "Units used in the book" and the "U.S. customary units" and the units that can be selected instead of the default units.

Table D1 Default units and selectable units for the various properties

Property	Default units used in the book	Default U.S. customary units	Selectable units [a]
Pressure p Fugacity f^*	bar	psia	bar, mbar, N/m^2 = Pa, kPa, MPa, kp/cm^2 = at, atm, mm Hg = Torr, m H_2O, psia, in Hg, ft H_2O
Temperature T	°C	°F	°C, K, °F, °R
Wavelength of light λ^* ($\bar{\lambda}$ in the book)	µm	µft	µm, mm, cm, µft, in
Specific volume v	m^3/kg	ft^3/lb_m	m^3/kg, cm^3/g, ℓ/kg, ℓ/g, mℓ/g, ft^3/lb_m, in^3/lb_m, gal(US)/lb_m, gal(UK)/lb_m
Density ρ Isothermal stress coefficient β_p	kg/m^3	lb_m/ft^3	kg/m^3, g/cm^3, kg/ℓ, g/ℓ, g/mℓ, lb_m/ft^3, lb_m/in^3, lb_m/gal (US), lb_m/gal (UK)
Specific enthalpy h Specific internal energy u Specific Helmholtz free energy f Specific Gibbs free enthalpy g	kJ/kg	Btu/lb_m	kJ/kg, J/kg, J/g, kcal/kg, cal/kg, cal/g, Btu/lb_m, ft lb_f/lb_m
Specific entropy s Specific isobaric heat capacity c_p Specific isochoric heat capacity c_v Specific gas constant R	kJ/(kg K)	Btu/(lb_m °R)	kJ/(kg K), J/(kg K), J/(g K), kcal/(kg K), cal/(kg K), cal/(g K), Btu/(lb_m °R), ft lb_f/(lb_m °R)
Speed of sound w	m/s	ft/s	m/s, km/h, ft/s, mile/h, in/s

Continued on next page.

Table D1 – Continued

Property	Default units used in the book	Default U.S. customary units	Selectable units
Isobaric cubic expansion coefficient α_v Relative pressure coefficient α_p	1/K	1/°R	1/K, 1/°R
Isothermal compressibility κ_T	1/kPa	1/psia	1/kPa, 1/MPa, 1/bar, 1/psia
Joule-Thomson coefficient μ	K/kPa	°R/psia	K/kPa, K/MPa, K/bar, °R/psia
Isothermal throttling coefficient δ_T	kJ/(kg kPa)	Btu/(lb_m psia)	kJ/(kg kPa), kJ/(kg MPa), kJ/(kg bar), kcal/(kg bar), Btu/(lb_m psia)
Dynamic viscosity η	Pa s	lb_m/(ft s)	Pa s, mPa s, μPa s, g/(cm s) = poise, kg/(m s), poise (P), cP, mP, N s/m^2, mN s/m^2, μN s/m^2, lb_m/(ft s), lb_m/(ft h)
Kinematic viscosity v	m^2/s	ft^2/s	m^2/s, cm^2/s = stoke, mm^2/s, m^2/h, stoke (St), cSt, ft^2/s, ft^2/h
Thermal conductivity λ	W/(m K)	Btu/(ft h °R)	W/(m K), kcal/(m h K), cal/(cm s K), Btu/(ft h °R)
Thermal diffusivity a	m^2/s	ft^2/s	m^2/s, cm^2/s, mm^2/s, m^2/h, ft^2/s, ft^2/h
Surface tension σ	N/m	lb_f/ft	N/m, mN/m, lb_f/ft
Molar mass M	kg/kmol	lb_m/lbmol	kg/kmol, kg/mol, g/mol, lb_m/lbmol
Compression factor z Isentropic exponent κ Prandtl number Pr Dielectric constant ε Refractive index n	–	–	–

[a] lb_m = pound (mass), lb_f = pound (force), ℓ = liter.

The unit of a property can be chosen by clicking on the unit displayed for the respective property. A menu bar showing the units that can be selected will be opened and the desired unit can be clicked.

5 Updates

Updates will be released as soon as they become necessary. It is advisable to check from time to time whether an update is available. Please follow the steps below to update your software.

The user should first check whether an update is available or not. To do this, please click in the menu bar of the main form of the Electronic Steam Tables on "?" and after that on "Update check." The program will check for an update if the computer is connected to the internet. If an update is available, a corresponding message will appear in the window. To download this update, click on the link located in the upper right corner of the window, which will lead you to the download website of the International Steam Tables: http://www.international-steam-tables.com. On this website click "Update" and download the update. The downloaded file has to be executed to install the update automatically. The program should be closed before starting the installation process.

6 Extended Software Packages for IAPWS-IF97 and IAPWS-95

The authors' groups have developed extended software for calculating values for the thermodynamic properties of water and steam based on the industrial formulation IAPWS-IF97 and on the scientific formulation IAPWS-95 [8, 9]. These software packages can calculate not only the thermodynamic and transport properties for the input variables (p, T), but also for (p, h), (p, s), (h, s), etc.

The software packages comprise the following sorts of software:

- Interactive programs that can also generate thermodynamic diagrams.
- Libraries that can be integrated into user specific programs written, for example, in Fortran, Pascal (Delphi), C++, or Visual Basic under the operating systems Windows®, Unix®/ Linux®, and Mac OS®. The libraries contain functions to calculate more than 20 thermodynamic and transport properties, but also thermodynamic derivatives and backward functions. These functions can be used for calculating heat cycles, boilers, steam turbines, etc.
- Dynamic-Link Libraries (DLLs) that can be integrated into user specific programs under the operating system Windows®.
- Add-Ins to add the functions of the DLL to Excel®.
- Add-Ins to combine the DLL with Mathcad® and MATLAB®.
- Programs that can be used as electronic steam tables for some types of pocket calculators from Texas Instruments, Hewlett-Packard, and Casio.

Further information on these software packages is given on the website:

http://www.international-steam-tables.com

Part E

Wall Charts of the Properties of Water and Steam

Mollier *h*-*s* Diagram and *T*-*s* Diagram

Part E of this book contains wall charts of the following diagrams:

- Mollier *h*-*s* diagram
- *T*-*s* diagram

The diagrams were calculated from the IAPWS-IF97 basic equations Eqs. (2.3), (2.6), (2.11), and (2.15) and plotted using the software FluidDIA [45].

In addition, Part C contains the Mollier *h*-*s* diagram and the *T*-*s* diagram as overview charts.